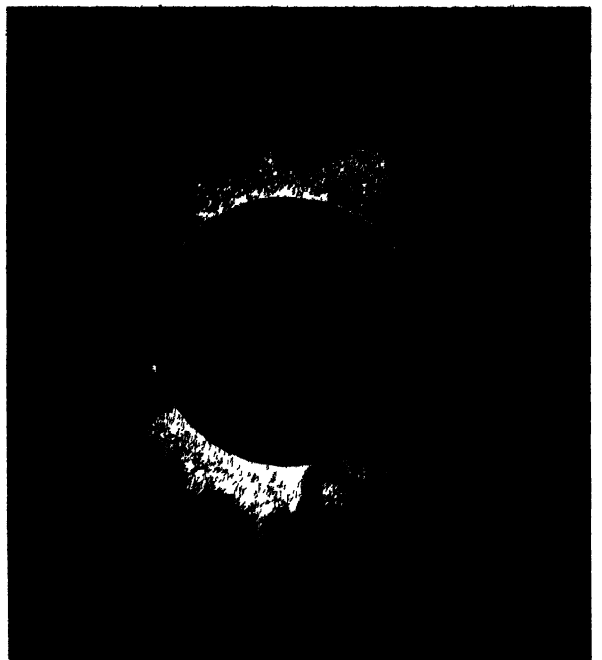
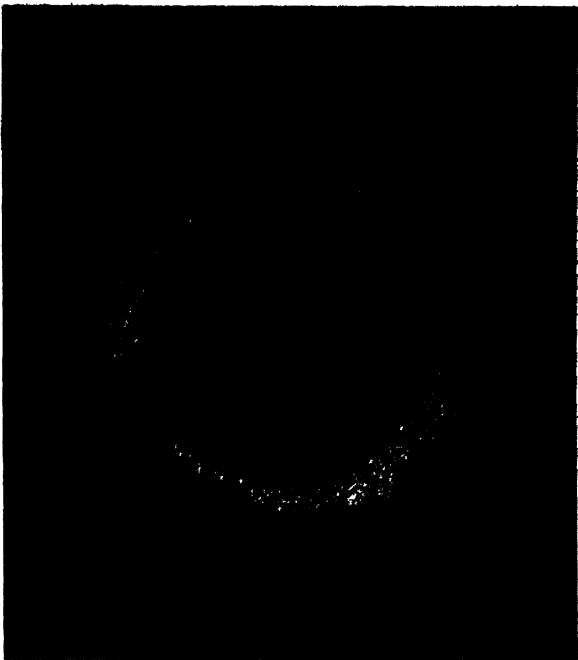


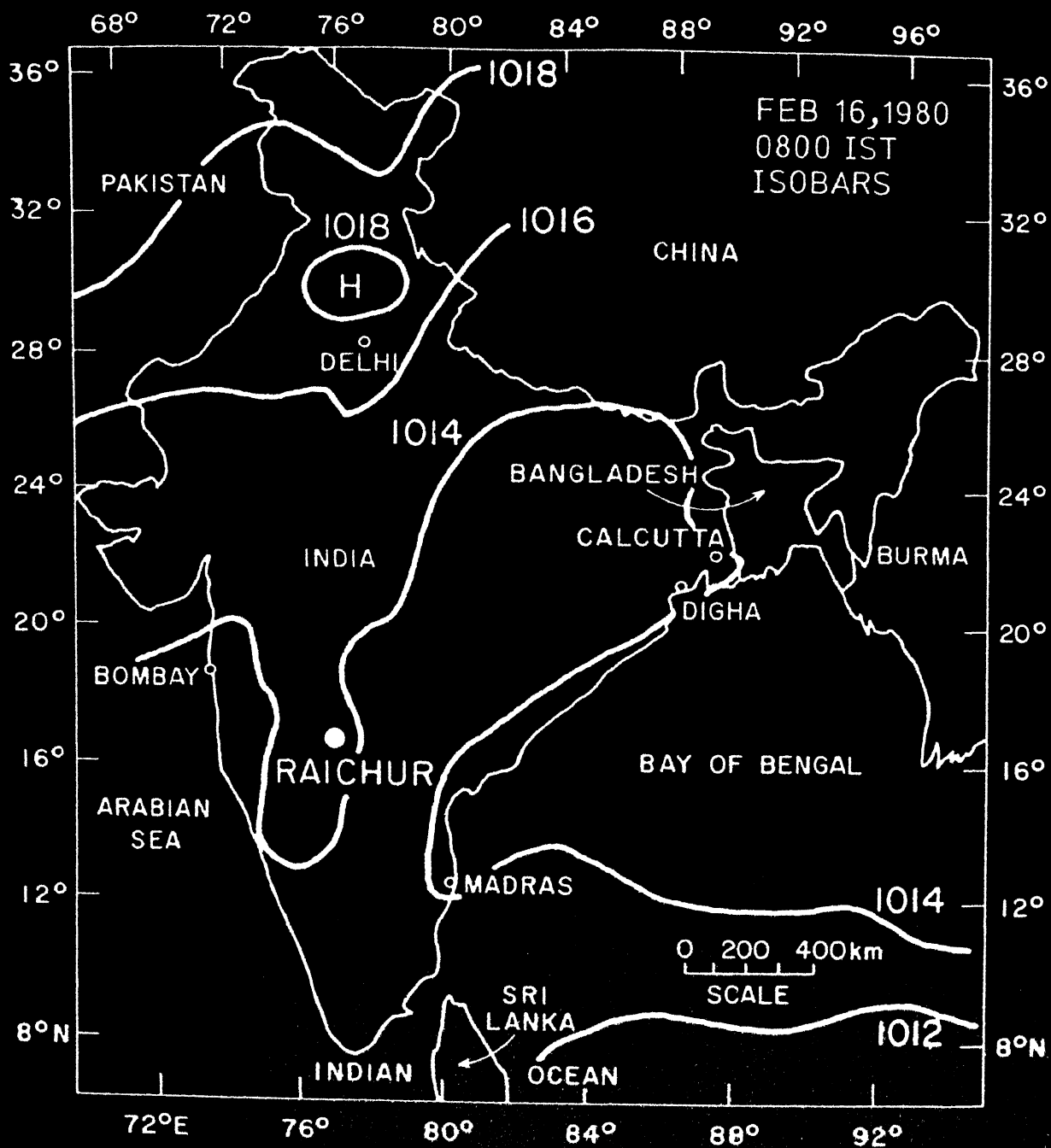
# TOTAL SOLAR ECLIPSE

of

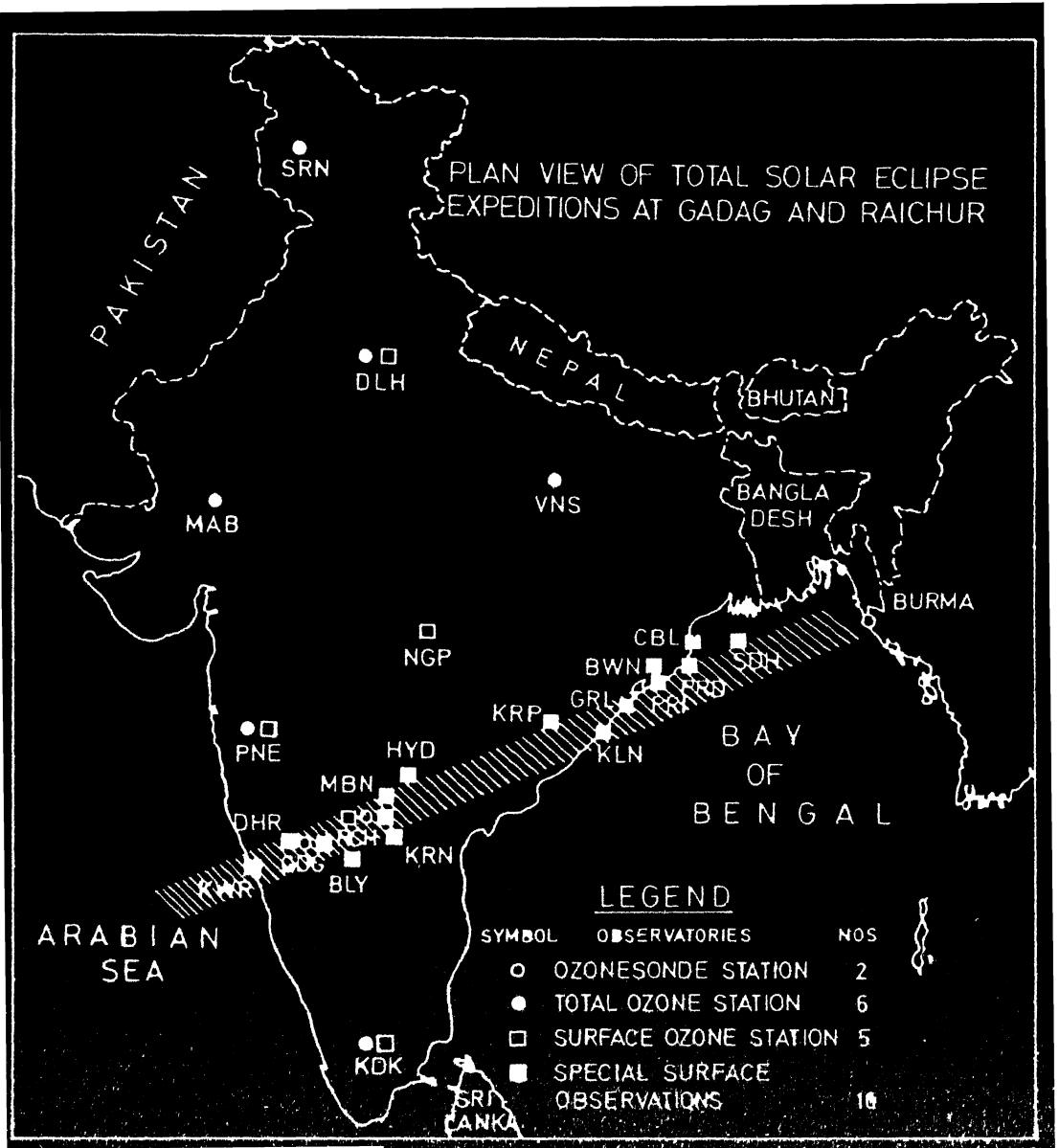
## 16 February 1980



INDIAN NATIONAL SCIENCE ACADEMY  
NEW DELHI









# **TOTAL SOLAR ECLIPSE OF 16 FEBRUARY 1980**

## **RESULTS OF OBSERVATIONS**

*(A Special Supplement to Proceedings of INSA,  
Part A, Physical Sciences, Vol. 48, carrying  
Research Papers presented at the  
International Symposium on the  
Total Solar Eclipse of 16 February 1980  
during January 27–31, 1981  
held at INSA, New Delhi)*



1982

**INDIAN NATIONAL SCIENCE ACADEMY  
NEW DELHI**

Indian National Science Academy  
All rights reserved.

*Editor of Publications* : PROFESSOR S. K. TREHAN, FNA  
*Assistant Executive Secretary* : DR M. DHARA  
*Associate Editor (Publications)*  
*Assistant Editor* : J. SAKETHARAMAN

First published in October 1982

Price: Rs. 225.00     \$ 75.00

Published by A. K. Bose, Executive Secretary,  
Indian National Science Academy, New Delhi  
Printed at Indraprastha Press (CBT), Nehru House,  
4, Bahadur Shah Zafar Marg, New Delhi-110 002



*Dedicated to the Memory  
of  
Dr Manali Kallat Vainu Bappu  
(10-08-1927 to 19-08-1982)*



DR M K V BAPPU

*Dr Manali Kallat Vainu Bappu, Fellow of the Indian National Science Academy (elected in 1968) passed away at Munich on 19 August 1982. He went there on a research assignment in May this year, and subsequently developed cardiac complaints which necessitated a heart surgery. Further complications after the successful bypass operation could not be overcome and he succumbed ten days later. The death of this Indian astronomer has cut short a brilliant scientific career at its peak. Dr Bappu was Director, Indian Institute of Astrophysics, Bangalore and President, International Astronomical Union at the time of his death. He had actively participated in the Total Solar Eclipse experiments in 1980.*

## Foreword

THE total solar eclipse of 16 February 1980 over India occurred at a particularly opportune moment. Over the last few decades research in the fields of astronomy and atmospheric science has grown to a significant extent, and new major facilities have emerged, including the rocket ranges in Thumba and Sriharikota, the balloon facility in Hyderabad, large optical telescopes at Kavalur, Nainital and Rangapur, ionospheric stations at Ahmedabad, Delhi, Trivandrum, the radiotelescope at Ootacamund etc. Consequently, a wide variety of experiments could be carried out, fortunately with considerable success, during the eclipse. A new feature was the undertaking of systematic observations of plant, bird and animal behaviour during the eclipse.

The International Symposium organized at the end of January 1981 to report on the results of the experiments carried out during this event was attended by meteorologists and ionospheric scientists, by astronomers, by botanists and zoologists and by medical scientists, providing an important interdisciplinary forum. The present volume consists of the papers in physical sciences. We expect to bring out shortly the second volume on observations in the life sciences.

It is tragic that Dr Vainu Bappu, who shouldered much of the responsibility of the successful eclipse campaign, is no longer with us. He died unexpectedly in Munich on August 19, creating a loss for astronomical science in this country that will be difficult to fill.

The Indian National Science Academy dedicates this volume to the memory of Dr Vainu Bappu

*Dated : 7 October 1982*

M. G. K. MENON  
*President, INSA*  
*and*  
*Member, Planning Commission*  
*New Delhi*





## Introductory Remarks

THE total solar eclipse of 16 February 1980 occurred at a time when the Sun was at its peak solar activity, and amongst the countries through which the path of totality passed, India was very favourably placed, from the point of view of observing conditions, availability of trained and experienced scientists, and special facilities. The special facilities included the use of rockets from three ranges: Trivandrum, Sriharikota and Bangalore; a large number of ground stations receiving radio signals from the Japanese satellite ETS II; use of micrometeorological towers and balloons; Dicke radiometers at GHz regions including some at the water vapour absorption line at 22.3GHz; telemetry receiver stations of ISRO's Tracking Network (ISTRAC) operating at 136MHz at Trivandrum, Sriharikota and Car Nicobar; and astronomical measurements of a high order by Indian and Foreign Scientists in the path of totality.

The observations carried out covered a wide variety of disciplines: optical and radio astronomy, atmospheric physics, ionospheric physics, atmospheric electricity, geomagnetism, animal, bird and insect behaviour. Several hundred scientists were involved in India alone, and a satisfying feature was the involvement of a large number of young scientists from institutions with limited facilities. The area of astronomy attracted scientists from the USA, Switzerland, Japan, West Germany, Yugoslavia, Czechoslovakia. In ionospheric and atmospheric physics and in observations involving life processes, participation was primarily from Indian scientists. However, there was collaboration with US scientists on satellite beacon measurements and on boundary layer studies (which worked well), and Dr Ogawa from Japan included a Nitric Oxide payload along with several Indian packages in a rocket flown from Thumba.

We are pleased that several of the U.S. astronomers who participated in the observational programme were present here, and the three Astronomy sessions were exciting. We are glad that Sri Granville Beynon from U. K. agreed on our request to participate in this Symposium. Sir Granville, in his long eventful career, have had opportunities to participate in many eclipse programmes and also was one of the main architects of the exceedingly valuable Solar Eclipse Symposium held in Brussels in 1955. He pointed out that some of the measurements carried out during this eclipse were also carried out at that time and that the summarising remarks made at that time by Professor Ratcliffe for ionospheric programme continue to be relevant today. We are glad that Dr Kenneth Davies who had a pioneering role in ATS-6 satellite beacon programme was also present; we had a Satellite Beacon Workshop as a part of this Symposium on 16 and 17 February 1981 at NPL, New Delhi.

The response of the Indian scientists was overwhelming. We have had about 100 presentations covering all disciplines. An unconventional step we decided to take

was to include observations on plant, bird and animal behaviour. Although on some views such observations did not provide "hard" facts that could be considered physically consistent, introduction of such results in the context of many observations relating to atmosphere and to radiation, and bringing together physical and life scientists in a common forum for a programme that have areas of overlap was considered to be important. In this context, observations on stratospheric ozone were important. As expected no change in ozone occurred at stratospheric levels. This means that the ultraviolet radiation at the erythemally important wavelengths around 300nm varied only in accordance with the obscuration of the solar disc modified by the location of any UV spots—there is no possibility of any increase in the radiation which could have occurred in the event of a large decrease in ozone. This is important to emphasise since in several papers in the area of life sciences, enhancements in ionizing radiation were looked for.

Another interesting set of measurements concerns the study of atmospheric boundary layer. Instrumented micrometeorological towers were used at Gadag by IMD, at Raichur by Indian Institute of Science and a combination of instrumented tower and Sodar at BARC in Trombay. The results of this campaign are discussed in one of the sessions.

There were some surprising results. At Gadag, the Meteorological Department observed a very large decrease in soil temperature of about 20 °C, the decrease following approximately the rate of obscuration with a delay of about 20 minutes. Such a large decrease and at this rate was unexpected. The drop in air temperature, on the other hand, was only about 2 °C; here again the atmosphere seemed to respond quickly with a delay of about 15 minutes.

The other surprising feature was that the atmosphere seemed to have atleast three different time scales: (a) a few minutes; (b) about half an hour; and (c) a few hours. The eerie feeling of a pervading stillness came, it appears, from a decrease in the wind velocity as well as in temperature over the entire thickness of the boundary layer.

On a normal day, the atmosphere has a certain amount of turbulence. We expected the turbulence to gradually die out during the eclipse. Actually, it did not quite die out, but was substantially damped as the Sodar observations showed. There was a fall of the height of the thermal plumes. There were temperature inversions of about 1.5 °C near the earth's surface and an appearance of double tropopause and the cooling of the entire atmosphere from ground to 30km.

On ozone, as we have mentioned before, we had not expected any change at stratospheric heights. This is because the time constant of ozone at these heights is on the order of a few days, certainly much larger than the duration of the eclipse. This has also been confirmed during the solar eclipse of 26 February 1979 over the American continent by instruments carried in an U-2 Aircraft that flew at a height of 19.8km. There was no evidence of ozone change; however, nitric oxide changed by very large amount during this period.

In the Indian observations also no measurable change in stratospheric ozone was observed. However, there were changes at other levels. Near the surface, the Meteorological Department observed a *decrease* in ozone. This has been attributed to damping of all mixing, convection and transport processes due to the cooling of the atmos-

phere. There may have been other causes. It is important to point out that the amount of ozone in the troposphere under normal conditions is larger than can be produced locally. One suggestion attributes this excess of ozone in the troposphere to a transfer of ozone from stratosphere to troposphere. The observed decrease could then be interpreted as a result of shutting off of this exchange path. The second interesting result concerns changes in the mesosphere (above 50km). Here an *increase* in ozone concentration was observed. This is not surprising. Increase in ozone under eclipse conditions have been reported in the past for such heights. In a general way, we also understand how this can happen. At these heights while ozone *production* rate decreases as the ultraviolet radiation is decreased, so does the ozone *destruction* rate. This destruction is partly through dissociation of ozone again by ultraviolet radiation (but in a different wavelength band) and also through a number of other minor species such as CO, OH and HO<sub>2</sub>. A quantitative examination of this increase is now in progress. We believe that this will provide some interesting information on atmospheric chemistry.

I have referred earlier to the questions that were posed by Professor Ratcliffe some 35 years ago. Some of these questions still remain outstanding and some new ones can now be added such as the following:

1. Does the lowest part of the ionosphere collapse during totality?
2. Are there any gravity waves generated by solar eclipse at any level in the ionosphere and how are these caused? Is the ozone cooling the only mechanism for the production of these gravity waves and if so, what is the actual degree of cooling required? What is the role played by other minor species of climatic interest such as NO<sub>2</sub> which has absorption in the visible region?
3. Do we really have any change in the main constituents of the atmosphere (N<sub>2</sub> and O ) and of the neutral temperature?
4. If there is an increase in ozone in the mesosphere, what are its consequences? It must affect other minor species and also ions, but to what extent?
5. Have we properly estimated the relative contributions from the sun's disc, from the active centres of the disc and outside the disc in the production of ions in the ionosphere? Should we not integrate the observed changes in both ionization and of solar radiation to arrive at a quantitative picture?
6. Are the response times of the ionosphere at various levels consistent with our current ideas of atmospheric chemistry?

These are only some of the questions posed. There can be many other questions. On the matter of gravity waves, it appeared that there was no convincing evidence of any gravity wave that could be ascribed to the eclipse at heights around 300km. However, these were apparently observed near the ground and around 150–200km. One possible cause was the cooling of ozone around 45km level as the heating source was being switched off. Thumba rocket measurements recorded a cooling by 10 °C. There was also evidence of heating around 15km. An important conclusion that emerged is that the classical concept of the production of eclipse-generated gravity waves in terms of a decrease in ozone heating around 45km is perhaps an over-simplification. Ozone is not the only constituent of climatic interest and consequently we should look for changes in heating or cooling not only around 45km but over the entire environment. A satisfying feature of the Indian observations was that simultaneously

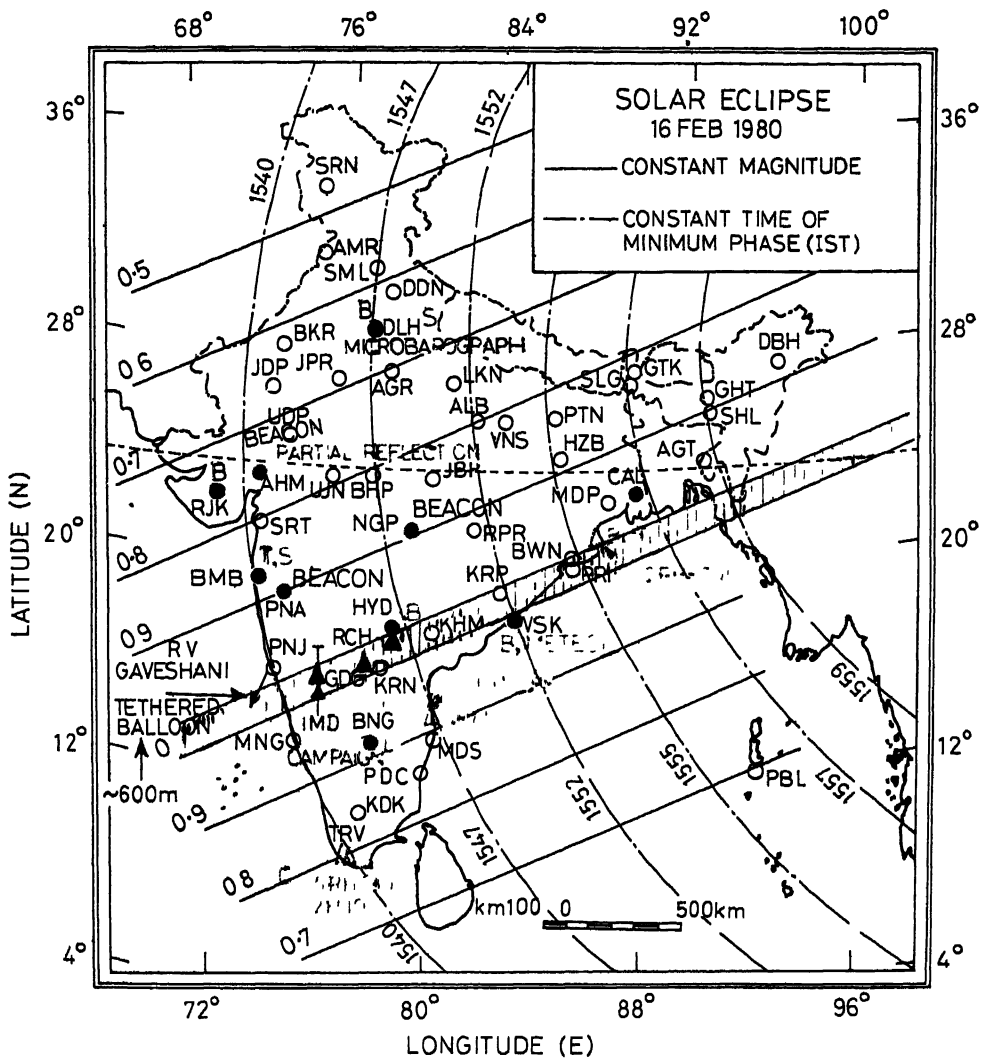
with observations on the response of the atmosphere at various levels there was also observation with meteorological rockets of how temperature changed during the eclipse at different heights. This has provided the basis on which a proper theory on eclipse generated gravity waves can be built.

The totality on Indian peninsula began at the West Coast at 15<sup>h</sup>39<sup>m</sup> IST near Gokarn (in Karnataka). The shadow then moved in a northeasterly direction and after sweeping over Andhra Pradesh and Orissa finally left the East Coast near Puri at 15<sup>h</sup>56<sup>m</sup> IST and again touched a small stretch in Mizoram. The width of the path of totality was nearly 130km. Along the central line the duration of totality for various places in India exceeded 2min, the maximum being 2<sup>m</sup>50<sup>s</sup> at the West Coast and 2<sup>m</sup>09<sup>s</sup> at Japal-Rangapur near Hyderabad. The following table gives the relevant data at some of the important observation sites (also see map on facing page)

# SOLAR ECLIPSE 16 FEBRUARY 1980

## Local circumstances relating to certain places in India

Place	Geog Co-ordinates	Eclipse timing (hr IST)			Magnitude (Maximum obscuration)
		Beg	Max	End	
Ahmedabad	23°02'N, 72°36'E	1423	1541	1651	0.75
Balasore	21°30'N, 86°56'E	1444	1555	1700	0.96
Bangalore	12°58'N, 77°36'E	1423	1544	1654	0.92
Bombay	18°58'N, 72°50'E	1419	1540	1652	0.87
Calcutta	22°32'N, 88°20'E	1447	1557	1700	0.96
Dehra Dun	30°19'N, 78°03'E	1439	1548	1650	0.61
Delhi	28°38'N, 77°13'E	1436	1547	1651	0.65
Gadag	15°26'N, 75°38'E	1421	1542	1654	1.04
Goa	15°25'N, 73°47'E	1417	1540	1652	0.99
Gauribidanur	13°36'N, 77°26'E	1424	1545	1654	0.93
Hyderabad	17°21'N, 78°28'E	1428	1547	1656	0.99
Jaipur	26°55'N, 75°49'E	1432	1546	1651	0.68
Japal Rangapur	17°06'N, 78°44'E	1429	1547	1656	1.04
Kandla	23°01'N, 70°13'E	1415	1538	1647	0.50
Karwar	14°49'N, 74°08'E	1417	1540	1652	1.04
Kodaikanal	10°14'N, 77°28'E	1422	1542	1652	0.84
Nagpur	29°09'N, 79°05'E	1432	1549	1656	0.89
Palem	16°32'N, 78°15'E	1427	1546	1656	1.02
Pune	18°31'N, 73°53'E	1420	1541	1652	0.90
Puri	19°48'N, 85°50'E	1442	1555	1700	1.03
Rajkot	22°19'N, 72°44'E	1419	1543	1649	0.75
Raichur	16°22'N, 77°21'E	1425	1545	1655	1.04
Sriharikota (SHAR)	13°47'N, 80°15'E	1429	1548	1656	0.91
Srinagar	34°06'N, 74°48'E	1440	1544	1642	0.47
Trivandrum (THUMBA)	8°31'N, 77°00'E	1420	1540	1650	0.80
Udaipur	24°35'N, 73°42'E	1428	1542	1649	0.72
Varanasi	25°19'N, 83°01'E	1441	1553	1657	0.81
Visakhapatnam	17°43'N, 83°18'E	1437	1552	1658	0.99





In the editing of the papers and in the preparation of this volume considerable assistance has been rendered by Dr A. K. Saha and Dr R. Venkatachari of the National Physical Laboratory, New Delhi. Indian National Science Academy wishes to express its gratitude to them

I would also personally like to express my appreciation of the dedicated efforts put in by Mr J Saketharaman, Assistant Editor, Indian National Science Academy

*Dated· 1 October 1982*

A. P. MITRA  
*Secretary, INSA*  
*Director*  
*National Physical Laboratory*  
*New Delhi*

*Dedicated to the Memory  
of  
Dr Manali Kallat Vainu Bappu  
(10-08-1927 to 19-08-1982)*



DR M K V BAPPU

*Dr Manali Kallat Vainu Bappu, Fellow of the Indian National Science Academy (elected in 1968) passed away at Munich on 19 August 1982. He went there on a research assignment in May this year, and subsequently developed cardiac complaints which necessitated a heart surgery. Further complications after the successful bypass operation could not be overcome and he succumbed ten days later. The death of this Indian astronomer has cut short a brilliant scientific career at its peak. Dr Bappu was Director, Indian Institute of Astrophysics, Bangalore and President, International Astronomical Union at the time of his death. He had actively participated in the Total Solar Eclipse experiments in 1980.*



# CONTENTS

	<i>Page</i>
<b>Session A: ASTRONOMY</b>	
Scientific Objectives of the Observations	<b>J. C. Bhattacharyya . 1</b>
Solar Physics at Future Solar Eclipses	<b>J. B. Zirker . . 6</b>
A Rocket Borne Solar Eclipse Experiment to measure the Temperature ... Structure of the Solar Corona <i>via</i> Lyman- $\alpha$ Line Profile Observations <b>Harold V. Argo, John G. Laros, William C. Feldman, Jacques M. Beckers, and Elmo C. Bruner</b>	<b>11</b>
Preliminary Results from Eclipse Coronal Velocity Observation	<b>. . 18</b>
<b>W. Livingston and J. Harvey</b>	
Observations for Coronal Velocity Field and Colour Movie of Flash Spectrum . . during Total Solar Eclipse of 16 February 1980 <b>A. Bhatnagar, D. B. Jadhav, R. M. Jain, R. N. Shelke and S. P. Purohit</b>	<b>29</b>
Airborne Eclipse Expedition A Description of Five Experiments to determine . Temperature, Density and Structure in the Corona	<b>33</b>
<b>C. F. Keller</b>	
Multicolour Photometry of the Corona	<b>J. Dürst . 53</b>
Optical Study of the Solar Corona during the Total Solar Eclipse of . 16 February 1980 <b>J. N. Desai, T. Chandrasekhar, K. C. Sahu, H. C. Bhatt, N. M. Ashok, P. D. Angreji, D. B. Vaidya and V. B. Kamble</b>	<b>57</b>
A Search for Optical Modulation of the Solar Corona during the 16 February 1980 Total Solar Eclipse	<b>64</b>
<b>E. J. Seykora</b>	
Detection of Variations in the Solar Radius through Observations of Baily's Beads at the Edge of the Path of Totality <b>A. D. Fiala, D. W. Dunham and J. B. Dunham</b>	<b>70</b>
High Resolution Microwave Brightness Temperature Measurements during Total Solar Eclipse on 16 February 1980 <b>R. V. Bhonsle, S. K. Alurkar, S. S. Degaonkar, O. P. N. Calla, G. Raju, S. S. Rana and B. Lokanadham</b>	<b>75</b>
High Resolution Coronal Intensity and Polarization Measurement	<b>81</b>
<b>John L. Streete and Leon B. Lacey</b>	
Effect of seeing Plus Scattering on the observed Intensity Distribution in Solar Corona	<b>85</b>
<b>K. D. Abhyankar and P. V. Subrahmanyam</b>	

	<i>Page</i>
Eclipse Studies of Dust Motion in the F-Corona W. I. Beavers, P. H. Carr and J. J. Eitter	.. 89
Two Colour Photometry of the Solar Corona K. Anthony Raju and K. D. Abhyankar	91
Interferometric Eclipse Observations of the Fe XIV Inner Corona R. N. Smartt, J. B. Zirker and H. A. Maunder	. 102
 <b>Session B: ATMOSPHERIC PHYSICS</b>	
Solar Radiation and Relevance of Eclipse Studies A. K. Saha	.. 109
Rocket Measurement of Ozone Concentrations during the Solar Eclipse of 16 February 1980 B. H. Subbaraya and Shyam Lal	. 115
Total Ozone, Surface Ozone and Vertical Distribution of Atmospheric Ozone Measurements conducted at Gadag and other Stations in India during the Total Solar Eclipse of 16 February 1980 Kalipada Chatterjee and Harbans Singh Ahuja	. 125
Measurement of Solar UV Radiation over Delhi during Solar Eclipse of 16 February 1980 B. N. Srivastava, M. C. Sharma and R. S. Tanwar	. 131
Atmospheric Ozone and Solar Eclipse S. Devanarayanan and K. Mohanakumar	135
Ozone Concentration Measurements near the ground at Raichur during the Total Solar Eclipse of 1980 G. P. Srivastava, P. M. Pakkiri Mohammad and R. R. Balwalli	138
Solar and Earth's Radiation and Radiometersonde Measurements at Gadag C. K. Chandrasekharan, A. B. Sarkar and Kalipada Chatterjee	143
Radiation Flux Measurements over India during the Total Solar Eclipse of 16 February 1980 V. Desikan, C. K. Chandrasekharan, C. G. Rahalkar and G. P. Srivastava	150
Shadow Impressions of 16 February 1980 Total Solar Eclipse as viewed by the Scanner of a Meteorological Polar Orbiting Satellite K. R. Rao and R. K. Gupta	159
Changes in Tidal Character during Total Solar Eclipse of 16 February 1980 R. Suseel Reddy, B. K. Mukherjee and Bh. V. Ramana Murty	168
Atmospheric Boundary Layer Experiment R. Narasimha, A. Prabhu, K. Narahari Rao and C. R. Prasad	175

	<i>Page</i>
Dynamics of the Atmospheric Boundary Layer during the 1980 Total Solar Eclipse S. Sethu Raman	187
Total Solar Eclipse of 16 February 1980 and the Vertical Profiles of Atmospheric Parameters in the Lowest 200M V. Ramesh Babu and J. S. Sastry	196
Meteorological Parameters near the Earth's Surface along the Path of Totality during the Total Solar Eclipse of 16 February 1980 S. K. Das, S. M. Kulshrestha, Kalipada Chatterjee and C. K. Chandrasekharan	202
Solar Eclipse of 16 February 1980—Its Effect on Meteorological Parameters K. Mohanakumar and S. Devanarayanan	209
Measurements of Meteorological Parameters at the Lowest Layers of the Atmosphere during Total Solar Eclipse of 1980 R. K. Kankane, B. K. Hazra and A. B. Sarkar	217
A Study of Change in the Atmospheric Properties During Solar Eclipse of ... 16 February 1980 R. K. Kapoor, B. B. Adiga, S. P. Singal, S. K. Aggarwal and B. S. Gera	224
Radiometric Observations of Solar Eclipse over New Delhi on 16 February 1980 M. K. Raina, G. S. Uppal and R. Chadha	234
Atmospheric Pressure Perturbation during Total Solar Eclipse on 16 February 1980 P. K. Kunhikrishnan and B. V. Krishna Murthy	238
Boundary Layer Studies conducted at Gadag during the Total Solar Eclipse of 16 February 1980 Kalipada Chatterjee, C. K. Chandrasekharan and V. P. Verma	254
Photoelectric Observations of Shadow Bands during 16 February 1980 Total Solar Eclipse from Japal-Rangapur Observatory A. Bhatnagar, D. B. Jadhav, R. M. Jain, R. N. Shelke, S. P. Purohit, R. V. Bhonsle and R. Pratap	260
Variations in Atmospheric Electrical Parameters during Solar Eclipse S. Nizamuddin, R. Ramanadham, A. M. Rao, M. K. Khera B. A. Makhdoumi, A. R. Rafiqi, B. N. Raina, Venkatanarayana Reddy Mukku, R. K. Goel, P. P. Pathak, J. Rai and N. C. Varshneya	263
Measurements of Atmospheric Electricity Parameters during the Total Solar Eclipse of 16 February 1980 G. P. Srivastava, V. Srinivasan and A. K. De	271

Variation in Solar Energy Intensity during Total Solar Eclipse of 16 February 1980	280
U. K. Chaturvedi, S. K. Agrawal, N. Rajan, R. Bhanja and A. K. Singh	

# Session C: IONOSPHERIC PHYSICS

Determination of Ozone from Eclipse Observations of O <sub>2</sub> (a' Δ <sub>g</sub> ) Dayglow	284
V. V. Agashe and S. M. Rathi	
VLF/LF Detection of Ionization Changes and Wave Motions in the Middle Atmosphere associated with the February 1980 Total Solar Eclipse	293
Y. V. Ramanamurty, S. C. Garg, M. V. S. N. Prasad and A. Hamid	
Changes in the Field Intensity of Radio Signals and Noise during the Total Solar Eclipse of 16 February 1980 in Relation to Ionospheric Radio Wave Propagation	302
A. K. Sen, B. Saha, S. K. Trehan, S. Sekhar Dey, S. K. Saha, R. N. Dutta, S. K. Chatterjee, J. S. Sehra and M. K. Das Gupta	
Multi-station Monitoring of Short and Medium Wave Broadcast Circuits during Solar Eclipse of 16 February 1980	308
D. R. Lakshmi, B. M. Reddy, R. Chakravarthy and Mangal Sain	
Ionospheric Radio Effects of the Solar Eclipse on 16 February 1980	316
K. G. Jani, G. Datta, D. B. Patel and K. M. Kotadia	
Effects of Solar Eclipse on Shortwave Transmission	325
E. P. Radhakrishnan, N. Balan, A. A. Sridhar and K. Usha Devi	
Ionospheric Absorption Changes in 11.8 MHz Radio Propagation during the Total Solar Eclipse of 16 February 1980	334
Girija Rajaram, T. R. Rao and D. D. Patil	
Atmospheric Gravity Waves produced by Solar Eclipses—A Review	342
Kenneth Davies	
Atmospheric Pressure Waves generated by Solar Eclipses	356
C. A. Reddy	
Evidence of Atmospheric Gravity Waves in the Wake of the Eclipse Shadow	370
R. Venkatachari, A. K. Saha, C. V. Subrahmanyam and S. K. Chatterjee	
Solar Eclipse Effects on the Lower Ionosphere	375
R. Venkatanarayana and T. S. N. Somayaji	
AI Absorption Measurements during the Total Solar Eclipse of 16 February 1980	380
U. V. Girish Kumar and K. V. V. Ramana	

	<i>Page</i>
Multifrequency Ionospheric Absorption Results during the Solar Eclipse of . . 16 February 1980 over Udaipur B. L. Acharya, H. K. Yagnik, T. C. Bansal, S. K. Vijayvergia and R. K. Rai	388
Phase Height and Absorption Measurements during Solar Eclipse N. N. Purkait and M. K. Das Gupta	396
Phase Path and Group Path Variations during the Solar Eclipse of 16 February 1980 P. Ernest Raj, M. Srirama Rao, C. Jogulu and B. Madhusudhana Rao	400
Ionospheric Disturbances during the Total Solar Eclipse on 16 February 1980 ... N. Balan, B. V. Krishna Murthy, C. Raghava Reddi P. B. Rao and K. S. V. Subbarao	406
Ionospheric Electron Content Variation observed at Delhi during Total Solar Eclipse of 16 February 1980 Lakha Singh, T. R. Tyagi, P. N. Vijayakumar and Y. V. Somayajulu	416
Total Electron Content Studies during 16 February 1980 Solar Eclipse by ... Differential Doppler Method M. R. Deshpande, H. Chandra, Banshidhai, H. O. Vats, G. Sethia, N. Vadher, C. L. Jain, M. R. Sivaraman, S. K. Kothari and Sheela S. Goyal	420
Effects of the Total Solar Eclipse of 16 February 1980 on TEC Low Latitudes M. R. Deshpande, H. Chandra, G. Sethia, H. O. Vats and G. D. Vyas	427
TEC Observations at Waltair during the Total Solar Eclipse of 16 February 1980 P. V. S. Rama Rao, B. V. P. S. Rao, D. Nru and K. Niranjan	434
Ionospheric Electron Content Changes near the Crest of the Equatorial Anomaly during the Total Solar Eclipse of 16 February 1980 A. Maitra, S. K. Day, A. Das Gupta and M. K. Das Gupta	439
Response of the Total Electron Content of the Ionosphere over North America to the Total Solar Eclipse of 26 February 1979 E. A. Essex, J. A. Klobuchar and C. R. Philbrick	444
Horizontal Drift Measurements over Udaipur during the Solar Eclipse of 16 February 1980 D. V. Sardesai, M. Agrawal, S. Mathur and R. K. Rai	458
Solar Eclipse effects on Geomagnetism R. G. Rastogi	464

Magnetic Observations at Hyderabad and Etaiyapuram during the Solar ... Eclipse of 16 February 1980 B. J. Srivastava, D. Pandurangam, T. S. Sastry and Habiba Abbas	473
Geomagnetic Field Observations in the Indian Zone during the Total Solar .. Eclipse of 16 February 1980 R. G. Rastogi, G. K. Rangarajan and A. K. Agarwal	482
Magnetometer Array Study and Total Solar Eclipse of 16 February 1980 .. N. K. Thakur, M. V. Mahashabde, B. R. Arora, B. P. Singh, B. J. Srivastava and S. N. Prasad	489
The Indian Rocket Programme for the 16 February 1980 Solar Eclipse ... B. H. Subbaraya	494
Stratospheric and Mesospheric Winds over Thumba during the Solar Eclipse .. of 16 February 1980 K. S. Appu and V. Narayanan	502
Thermal Structure of the Atmosphere—Surface to Mesosphere—during the .. Solar Eclipse of 16 February 1980 K. S. Appu, B. V. Krishna Murthy, V. Narayanan, C. A. Reddy and K. Sen Gupta	506
D-Region Electron Loss Coefficients during Solar Eclipse of 16 February 1980 . Y. V. Somayajulu, K. S. Zalpuri and P. Subrahmanyam	511
On Variation of $\lambda$ and $\alpha_{\text{eff}}$ in the Mesosphere during the Solar Eclipse of 16 February 1980 over India S. P. Gupta and D. K. Chakrabarty	518
Rocket Measurement of Photoelectron Flux during the Solar Eclipse Campaign on 16 February 1980 at Low Latitudes B C. N Rao, A. Banerjee and Y. V. Somayajulu	523

Printed in India.

# Overview

## Session A: ASTRONOMY

### SCIENTIFIC OBJECTIVES OF THE OBSERVATIONS

J. C. BHATTACHARYYA, F.N.A.

*Indian Institute of Astrophysics, Bangalore-560 034, India*

*(Received 18 September 1981)*

THE umbral shadow track of the eclipse event on 16 February 1980 crossed the earth's surface from sunrise over the Atlantic Ocean to sunset over China three and half hours later. The width of the path varied from 86km to 150km and the duration of totality upto a maximum 4m 8s. Although this was not the longest eclipse in recent times, it was long enough for several important observations to be attempted. I shall concentrate on the experiments which sought to find answers to the riddles of the solar atmosphere. The effects and repercussions on our planet earth will be dealt by more competent persons in later sessions of this symposium.

The reason why total eclipses are valuable in studies of the Sun is explained here. Many interesting processes are happening in the outer envelope of the solar

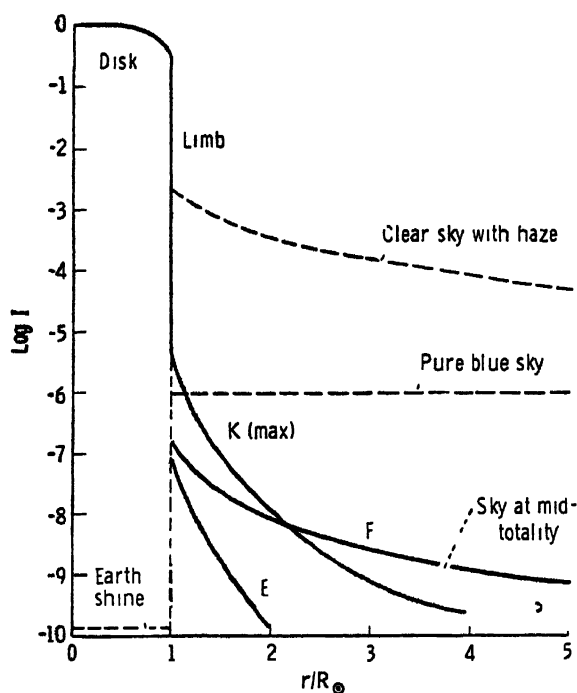


FIG. 1.

atmosphere, which goes undetected. The scattered light from the photosphere drowns every faint feature surrounding the solar disc. From the earth's surface, the only time these are visible is, when the brilliant disc of the sun is completely covered. Otherwise, even at locations on high mountain tops with perfectly blue skies, special instruments using scatter-free optics, can just read the brightest part of the inner corona at favourable times. This is illustrated in Fig. 1. The problem of detailed studies of this outer feature of the sun is possible only during totality. The information holds the key to answers for many questions of very fundamental importance.

Let us try to have a quick glance over the problems which confront the solar physicists of today. The next figure (Fig. 2) shows a section through the sun; showing

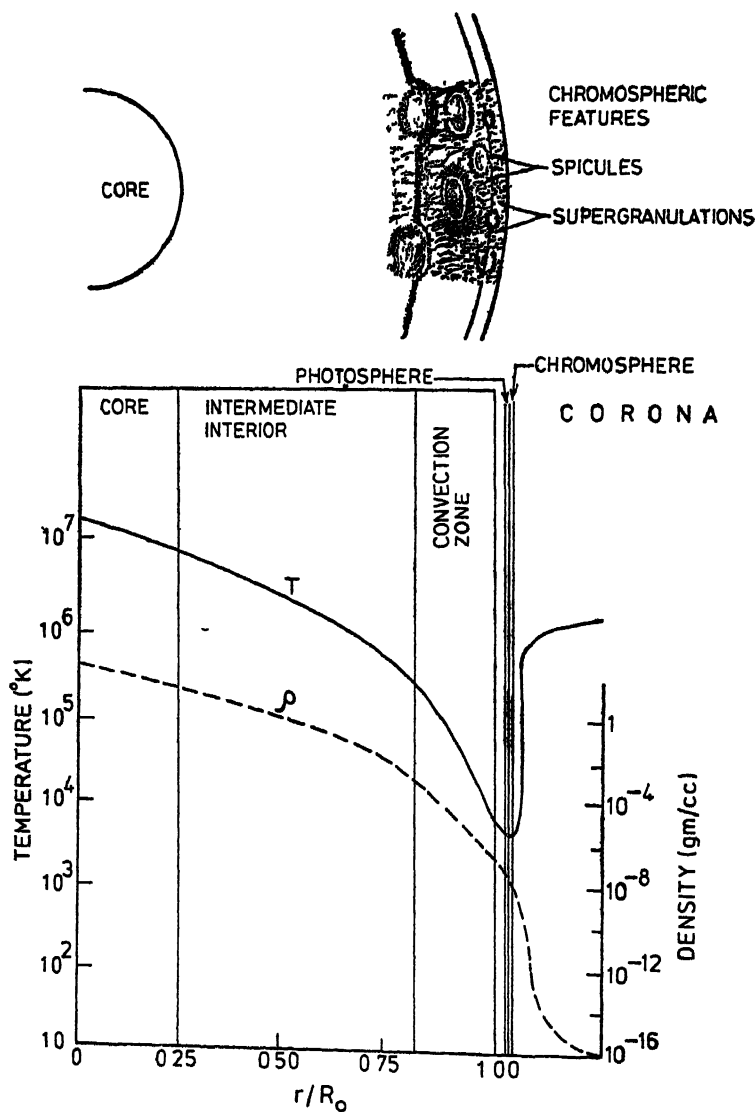


FIG. 2



a somewhat idealised structure which could be derived from various observations. At the centre, we have the core, where thermonuclear reactions at extreme high temperatures and pressures release the energy, which flows outwards through a series of complex processes of absorption and re-emission. Surrounding the core are the different layers of the solar interior, and the three visible outer layers. The photosphere, chromosphere and the corona.

I would like to draw your attention to the temperature structure. High temperatures at the core fall rapidly outwards, but just beyond the visible photosphere the trend is reversed. In the chromosphere, the temperature starts rising again, slowly at first and then rapidly until reaching a value exceeding a million degree Kelvin in the corona. The mode of energy transport at the outer layers is really complex, there are observational indications, suggesting an unusual type of energy transport mechanisms near the visible solar surface, which are of immense importance in understanding the



FIG. 3

© Big Bear Solar Observatory, U S A

physics of the visible layers of the sun. Some of the detectable features in this zone are shown here; the supergranulation, the spicules etc., all these impart a highly dynamic aspect to the ever changing scenery of the solar atmosphere.

The picture of the sun taken through a narrow pass band filter through  $H_{\alpha}$  display majestic views of the chromosphere, in active areas, the interplay between the turbulent solar material and the magnetic field gives rise to violent events (Fig. 3). Such pictures can be taken every day using very narrow pass band filters. But during a total solar eclipse a much finer and detailed polychromatic picture flashes into view. Fig. 4 shows the glimpse of such a view.

Questions for which answers were sought for in the present eclipse concerned almost all outer layers of the sun, let me start from the photosphere. In one experiment, aim was to obtain an accurate value of the limb darkening coefficient, by measuring the intensities of the slowly disappearing and reappearing crescent at different spectral regions. In another experiment, the times of the last view of the solar crescent or the first reappearance—the so called second and third contacts were determined from several locations, an information which may unfold the possible accurately slow change in the solar radius or oblateness.

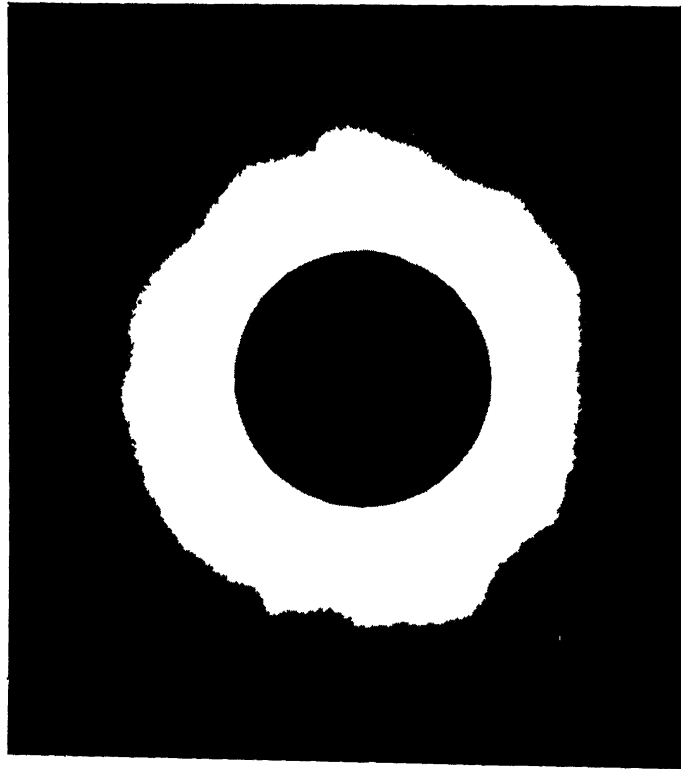


FIG 4

In the chromosphere, the experiments aimed at measurement of the temperature and density structure, dynamics etc. Several experiments employed new devices to get

better data by using modern developments in instrumentation. A number of papers listed in the programme may throw new light on this thin layer of the sun

Majority of the solar physics experiments concerned the outer crown of the solar envelope—the corona, a number of experiments aimed towards studying the temperature structure and dynamics of this region. We know that the structure of the corona is not spherically symmetric, and it varies from eclipse to eclipse. In order to understand the physics of this hot plasma envelope it is necessary to know to what extent the density and temperature structure and dynamics of the solar corona is dependent on the underlying features on the normally visible photosphere. The experiments utilised many innovations to attain high sensitivity and resolution. The ensuing presentations will no doubt give us a clearer view of the solar corona.

The scope of some of the experiments reached beyond the visible corona. One experiment sought to detect the presence of dust grains in the outer reaches of the corona. A second experiment looked for a ring like structure surrounding the sun. We are looking forward to obtain the details of these interesting experiments in this symposium.

This eclipse was not ideal for search for faint bodies near the Sun, because the corona was very bright, much brighter compared to some of the earlier total eclipses. This may have something to do with the phase of the activity cycle. As far as my information goes, no detection of faint asteroids or comets has been reported.

The results of measurements during the last eclipse have given a clearer insight in many areas of investigation about nature. I have just briefly covered some of the aims of experiments in the field of solar physics

Printed in India.

Invited Review (Astronomy)

## SOLAR PHYSICS AT FUTURE SOLAR ECLIPSES

J. B. ZIRKER\*

*Sacramento Peak Observatory, U.S.A.*

### INTRODUCTION

As we all recognize, experiments at total solar eclipses have advanced solar physics enormously in the past. By taking advantage of the low sky background during a total eclipse, solar astronomers have made tremendous strides in understanding the structure of the corona, the flash spectrum of the chromosphere, and the internal structure of prominences. Taking advantage of the uniform lunar motion across the disc of the Sun, radio astronomers have obtained high resolution maps of active regions in the radio spectrum. However, the use of coronagraphs, especially externally occulted coronagraphs on rockets and satellites, as well as the use of direct X-ray imaging have reduced the importance of total solar eclipses. It is now possible to obtain, with some sacrifice in signal-to-noise, observations that were only obtainable during total eclipse. On the other hand, the use of fast aircraft to extend the total phase of an eclipse to as long as an hour has increased the value of total eclipses. At this moment, after a generally successful series of experiments at the 1980 Indian eclipse, we may well ask: what experiments will be most valuable at future eclipses? Or, another way of putting it: do total eclipses of the Sun have any future value to solar physics?

Any projection like this is, of course, difficult to make. I cannot take into account the ingenuity of experimenters and the advances of technology that will make possible new experiments that we cannot even conceive of at the moment. However, I will hazard a few guesses.

### ALTERNATIVES TO ECLIPSES

It is worthwhile, first of all, to look a little more closely at some of the alternative methods of obtaining information on the outer atmosphere of the Sun. Good coronagraphic sites are rare. Among the best are the Pic-du-Midi, the Soviet station in the Caucasus, Mauna Loa in the Hawaiian Islands, and Sacramento Peak Observatory in the southwestern United States. With the possible exception of the Hawaiian site, these locations enjoy coronagraphic skies for only a few months a year, and at the very best, the sky brightness measured 15 arcseconds above the limb is never smaller than 10-millionths of the disc brightness. In contrast, the sky brightness at mid-totality approaches  $10^{-9}$  of the disc brightness. These factors limit somewhat the value of coronagraphic observations.

---

\* Chairman of Session A

Recent experience at the South Pole suggests that the sky brightness there, close to the limb, may approach 1 to 2-millionths of the disc brightness and remain relatively constant for several successive 24-hour days during the austral Summer. Thus, the South Pole may have advantages for coronagraphic observation, but again, only at the price of mounting a difficult experiment under rigorous weather conditions.

Externally occulted coronagraphs have been used on orbiting solar observatories (OSO 5 and 7), Spacelab, and most recently the Solar Maximum Mission. In general, the region inside two solar radii is unobservable, but such experiments are irreplaceable for studies in the extreme ultraviolet or white light beyond two radii and as far out as six solar radii. Unfortunately satellites cost  $\$10^8$ , and rockets are extremely expensive per hour of observation. "The U.S. Space Program" will offer relatively few opportunities to solar experimenters during the coming decade. NASA's International Solar-Polar Mission is the only approved free-flying satellite that will study the corona during this period.

Direct imaging of the chromosphere in the extreme ultraviolet or of the corona in soft X-rays has produced an enormous wealth of information during the past decade. Such experiments must be carried either by rockets or by satellites and suffer from the same limitation of high expense and limited opportunities.

Solar astronomers must pursue their science aggressively by whatever route is open to them. Despite the increasing cost of space experiments, they must and will continue to compete for them. However, total solar eclipses offer a relatively inexpensive means of undertaking some kinds of research and, despite the vagaries of the weather, are often successful.

Let's examine some possible future experiments, then, that may prove helpful in addressing some of the scientific problems in solar physics concerned with the outer atmosphere of the Sun.

#### CORONAL EXPERIMENTS

##### *A. Evolution*

Observations of the changing structure of the corona are important for their relevance to the understanding of the solar sun-spot cycle and, at once remove, the solar dynamo. Moreover, they serve to guide studies of the structure of the solar wind. For this reason, the High Altitude Observatory (HAO) at Boulder will continue observations from its Mauna Loa station in Hawaii for the next decade using a sophisticated coronagraphic instrument. It seems to me that the superb eclipse photographs taken in white light by HAO with a radially graded filter have proved enormously valuable in studying coronal evolution and should be continued. Such photographs are important for comparison with the coronagraphic observations because they afford generally better resolution of the finer details of the corona and thus a better comparison with calculated coronal magnetic fields.

##### *B. Streamers*

There has been a surprising lack of interest in the structure and dynamics of coronal streamers during the past five to ten years. We have been preoccupied instead with loops and coronal holes, which I will discuss in a moment. However, the streamers, particularly at solar maximum, are of the most striking features of the Sun's outer atmosphere and are undoubtedly important to the overall mass balance of the corona.

The airborne experiments of the Los Alamos Scientific Laboratory during a series of eclipses have been successful in recording white light streamers out to 20 solar radii. The most recent of these, during the 1980 eclipse, shows remarkable twisting and deformation of the streamers, as well as an extraordinary white light transient. Such observations are worth continuing in the future, because they give us information on a region of the heliosphere that is almost inaccessible otherwise. I wish there were some ways to measure the radial velocity within the streamers, out to 20 solar radii. The Los Alamos group has suggested an experiment that might obtain such velocity measurements in streamers.

### C *Loops*

Closed magnetic field regions on the Sun, i.e., loops, are stimulating a great deal of theoretical interest today, particularly with regard to the heating of the corona. It is important, therefore, that we have the best possible empirical models of temperature, density, velocity, and if possible, magnetic fields in coronal loops. High resolution optical spectra or narrow-band filter photography can supply such information during total eclipse and should be pursued.

It is still an open question as to whether Joule heating or the dissipation of mechanical waves or both are responsible for the heating of loops. During the 1980 eclipse the Williams College team searched for wave motions with periods as short as one second. Their results are, at best, ambiguous and further work in this direction is sorely needed.

### D *Coronal Holes*

Observations with an externally occulted coronagraph aboard the Skylab suggest that the critical point in the solar wind lies at a distance of two to five radii above a coronal hole. To make further progress in understanding the acceleration of the wind, we badly need measurements of temperature and velocity in this region. The High Altitude Observatory and Center for Astrophysics have flown two successful rocket experiments to measure the profile of chromospheric Lyman- $\alpha$  scattered from coronal hydrogen atoms. Assuming spherical symmetry, they are able to derive the temperature and temperature gradient in the region between two and six radii.

Another rocket experiment, flown by the Laboratory for Atmospheric and Space Physics at the University of Colorado, has measured the doppler shift of the coronal magnesium lines at 625Å above a coronal hole in order to determine the velocity and mass flux in the inner corona. These experiments show great promise in giving us the information we need. There are other possibilities, however.

The Los Alamos group, for example, has constructed an experiment to be flown on a fast aircraft during the eclipse to measure the residual intensity of the Calcium K line in the electron-scattered coronal continuum. The intensity is determined by Doppler broadening by thermal electrons, as Grotian suggested around 1940. This experiment has interesting prospects for an independent measure of the temperature in streamers and possibly in coronal holes.

## PROMINENCES

During the last decade, spectroscopy of prominences both in and out of eclipse has

improved our knowledge of their temperature and density structure. However, we still have surprisingly little information about the "transition zone" between the cold prominence material and the corona. We know virtually nothing about the gradient of temperature and the velocity and mass flux across this zone. Here we need some really new ingenious ideas, and I am afraid I have nothing specific to suggest. There is no question, however, that the low sky background attainable during the eclipse would help in exploring this unknown region.

Vector magnetic field measurement in prominences have been carried out successfully at Sacramento Peak by the High Altitude Observatory group and their collaborators. Although a good start has been made, it is likely that more refined observations, with higher spatial resolution, will be needed before we have a good understanding of how the prominence material is supported against the force of gravity and how its radiative energy losses are supplied. We need high resolution two-dimensional Stokes measurements. These may be possible during total eclipse using the kind of narrow-band filters being built at the Lockheed Palo Alto Laboratories.

### SMALL PHOTOSPHERIC STRUCTURE

Ground-based observations of the smallest photospheric structures (intergranular lanes, filigree, umbral dots, and the elusive magnetic flux elements) are all limited ultimately by seeing. A number of investigators have attempted to use the sharp moon's limb during a total or partial eclipse to derive the modulation transfer function and so correct their observations for seeing. They find one-dimensional corrected spatial power spectra, but not images. To my knowledge, no one has applied yet speckle interferometry during a total eclipse to obtain two-dimensional images. The lunar profile is known extremely well, and the angular scale of the mountains on the moon are of the same order, i.e., an arcsecond or less, as the structures one would like to resolve. *The moon could thus serve as an extraterrestrial for the speckle observations.* The moon takes 4 to 6 seconds to cross a typical isoplanetic patch of 2 to 3 arcseconds, so that a reasonable time is available to collect images of a fine structure. It seems worth exploring an experiment to record very rapidly speckle photographs with a large aperture telescope or with a Michelson interferometer in order to investigate photospheric structures with a size as small as a tenth of an arcsecond.

### SOLAR DIAMETER MEASUREMENT

The U.S. Naval Observatory group has been successful in measuring the solar diameter to a few hundredths of an arcsecond during the past three solar eclipses. I personally feel that this simple and precise experiment should be repeated for the next decade whenever possible. As S. Sofia and H. Hill have shown, the diameter of the Sun is an indirect measure of the solar luminosity, a quantity which is still very difficult to measure with the requisite precision and which is of vital importance to climatology.

## CONCLUSION

In this short survey, I have tried to sketch some of the areas in solar physics that could benefit from observations at future solar eclipses. On the whole, I think such experiments will continue to attract imaginative experimenters who recognize an opportunity to carry out new and exciting science in a relatively inexpensive and painless way.



Printed in India.

Astronomy

# A ROCKET BORNE SOLAR ECLIPSE EXPERIMENT TO MEASURE THE TEMPERATURE STRUCTURE OF THE SOLAR CORONA VIA LYMAN- $\alpha$ LINE PROFILE OBSERVATIONS

HAROLD V. ARGO

*Principal Investigator, Los Alamos Scientific Laboratory, U. S. A.*

JOHN G. LAROS and WILLIAM C. FELDMAN

*Co-Investigators, Los Alamos Scientific Laboratory, U. S. A.*

JACQUES M. BECKERS

*Co-Investigator, Multiple Mirror Telescope Observatory, U. S. A.*

and

ELMO C. BRUNER

*Co-Investigator, Lockheed Missiles & Space Corporation, U. S. A.*

*(Received 18 July 1981)*

A rocket borne experiment to measure the temperature structure of the inner solar corona via the doppler broadening of the resonance hydrogen Lyman- $\alpha$  ( $\lambda$  1216Å) radiation scattered by ambient neutral hydrogen atoms was attempted during the 16 February 1980 solar eclipse. Two Nike-Black Brant V sounding rockets carrying instrumented payloads were launched into the path of the advancing eclipse umbra from the San Marco satellite launch platform 3 miles off the east coast of Kenya

**Keywords:** Coronal Temperature; Lyman- $\alpha$ ; UV Spectroscopy; Ion Densities

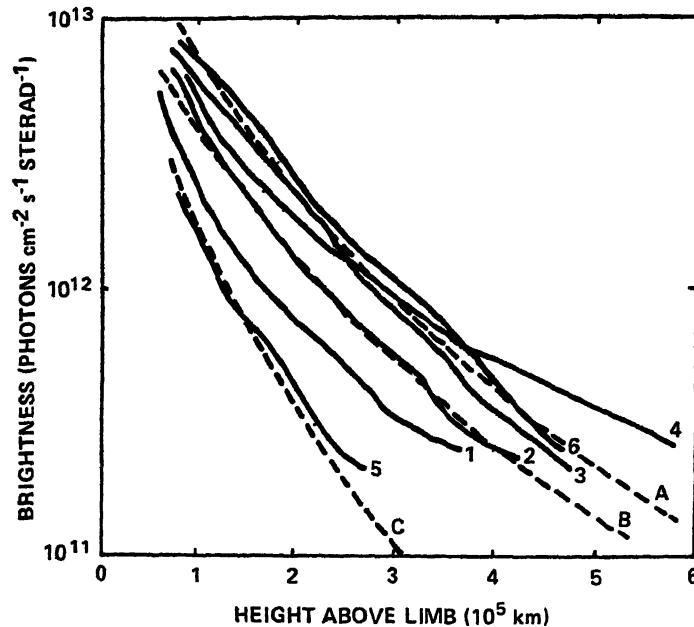
## INTRODUCTION

WITHIN the last several years a wealth of information concerning the physical state of the sun's chromosphere-corona transition region and lower corona have become available primarily as a result of the NASA sponsored Skylab Program. Although much effort has been expended, it is fair to say that very little concrete evidence is presently in hand concerning the basic heating and cooling mechanisms of either the quiet or active solar corona. In particular, the form of the energy flux which maintains the corona and the radial dependence of the divergence of this flux are not understood. The primary cause of our uncertainty is a lack of information concerning the physical state of the coronal plasma beyond about  $2 \times 10^6$  km above the photosphere. Present EUV and X-ray instrumentation literally run out of gas in this region.

Since the coronal temperature is the major uncertain factor in the modelling of the corona and solar wind, a knowledge of the temperature and its variation throughout the corona and solar wind is most important. The other factors—the coronal

density and the magnetic field—are now accessible by ground based observations of the polarisation of both the coronal continuum and coronal emission lines

During the 7 March 1970 solar eclipse it was discovered that the solar corona emits a very intense radiation in the hydrogen Lyman- $\alpha$  line at 1215.7Å (Fig. 1). Gabriel (1971) showed that the main mechanism responsible for this emission was the very efficient resonance scattering of the chromospheric Lyman- $\alpha$  radiation by the few neutral hydrogen atoms left in the hostile environment of the 1–2 million degree coronal plasma. Of secondary importance was the collisional excitation of the neutral atoms followed by photo de-excitation.



RADIAL BRIGHTNESS VARIATION OF THE LYMAN  $\alpha$  CORONA. CURVES 1, 2, AND 3 REPRESENT OBSERVATIONS AT SOLAR N, W, AND E, 4 IS AT AN INTENSE WHITE LIGHT STREAMER, 5 IS A QUIET COOL REGION AND 6 IS AT A CORONAL CONDENSATION

FIG 1 The 7 March 1970 Solar Eclipse Data by Gabriel

This discovery of Gabriel led one of us (Jacques Beckers) to conceive this experiment which measures the coronal temperature and density distributions throughout the inner corona from a determination of the line profiles and intensities of the Lyman- $\alpha$  emission in this region. J. M. Beckers and E. Chipman (1974) subsequently showed that indeed in the inner corona ( $\rho < 2$ ) the line width is a sensitive indicator of the coronal temperature.

In simplified but still applicable terms, if the corona were stationary the width of the emission line for a given atomic species would be proportional to the Doppler component of the mean thermal velocity of that atom, which in turn is inversely proportional to the square root of the mass. Thus the widths of lines of light hydrogen

atoms are much more sensitive as temperature indicators than are those of the usually observed metallic ions. Furthermore, because of the light mass, the thermal velocities of the hydrogen atoms (approximately 300km/sec) are substantially higher than the ever-present nonthermal motions which therefore have little effect on the Lyman- $\alpha$  line width. In contrast, the typical line used for similar studies, Fe XIV  $\lambda$  5303Å, is affected by the unknown nonthermal motions which are believed to be comparable to the thermal motions and are virtually indistinguishable in their effect on line widths. In fact, a comparison of the Lyman- $\alpha$  line width with the heavy ion line widths would give the first direct determination of these turbulent motions of both types of lines originated in the same parts of the corona. It has been argued, however, that the coronal temperatures vary significantly from point to point in the corona, making the comparison between the hydrogen and heavy ion line width more complex. The Fe XIV green line originates for example only in regions of the corona within specific temperature boundaries (1.5 to 2.5 million degrees) corresponding to the temperatures at which most iron atoms are thirteen times ionized. The green line profile would therefore reflect the physical conditions in those regions only. The same is true for the Fe X  $\lambda$  6375Å line. Since the degree of hydrogen ionization is much less sensitive to the coronal temperatures than the degree of ionization of other heavier atoms (Gabriel, 1971), the temperature derived from the Lyman- $\alpha$  line width should represent a very much better, truer average of the temperature than that derived from intensities of other lines. Line intensity methods of deducting plasma temperatures depend also on the accuracy of a host of uncertain complex atomic parameters, their interactions with radiation, and some knowledge of coronal density.

This experiment is the first attempt to obtain a reliable inner corona temperature distribution using the Lyman- $\alpha$  line profile. The experiment can be performed only during a solar eclipse when the scattered light conditions are optimum for probing the inner corona down to the chromosphere, the very region where the greatest temperature gradients exist and no direct measurements have been made.

#### INSTRUMENT DESCRIPTION

Fig 2 is a schematic of the instrument. It utilizes a 125mm diameter cassegrain tele-

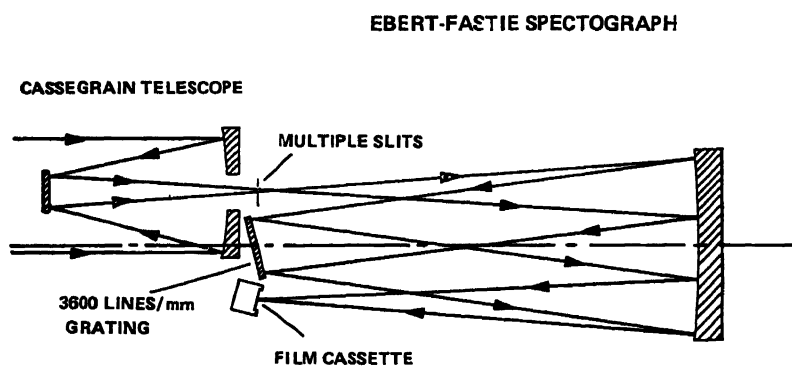


FIG 2 A schematic sketch of the cassegrain telescope—Ebert spectrograph system developed for the Lyman- $\alpha$  Eclipse Experiment. The optics are  $f/8$ .

scope with an effective aperture ratio of  $f/8$  to image the sun with about a 10mm solar diameter. The useful image field is about 25mm square. Fig. 3 shows the spectro-meter slit configuration super-imposed upon the photograph of the corona in white light scattered by free electrons, taken by Dr. Gordon Newkirk during the 7 March 1970 solar eclipse. Since the distributions of free electrons and neutral hydrogen atoms are quite similar, this is a good simulation of the Lyman- $\alpha$  corona. The 21 slits located in the focal plane of the telescope give 21 cross-sections of the corona. Those slits normal to the lunar limb will give very detailed information about the height variation in the corona, and those slits more parallel to the lunar limb will provide more information on the temperature variation across coronal streamers and active regions.

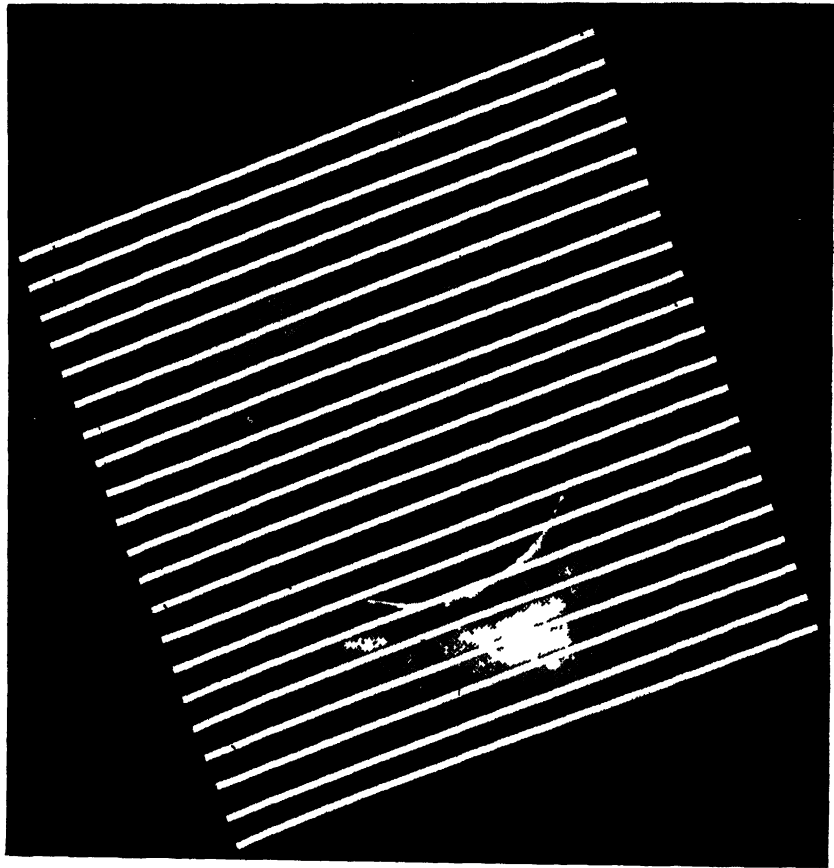


FIG. 3. A superposition of the multiple slit entrance aperture for the spectrograph upon the white light corona photograph. The Lyman- $\alpha$  line profiles will be obtained at all points along the slits.

This slit array in turn provides the entrance aperture for the 500mm focal length modified Ebert-Fastie type spectrograph we have adopted. The Ebert-Fastie optical system was chosen in preference to the asymmetrical Czerny-Turner system both

because of simplicity and ease of alignment and because an analysis of aberrations showed that parabolizing the Ebert mirror would permit both high spectral and spatial resolution over the full  $25 \times 25$  mm square field depicted in Fig 3. A fortunate balance of field distortions between the f/8 cassegrain and the parabolize-Ebert-Fastie spectrograph allows the use of linear slits through the full length of the field, as shown.

A multiple slit system of alternate  $20\mu$  and  $60\mu$  slits was chosen to optimize the inevitable compromise between intensity requirements and the desire for spectral resolution compatible with the expected Lyman- $\alpha$  line widths of about  $1\text{\AA}$  (FWHM) for coronal temperatures near  $1.5(10)^6$  °K. The system will resolve 1/5 to 1/10 of this over nearly all of the field.

The diffraction grating has a ruling frequency of 3600 grooves per mm and used in first order produces an  $18\mu$  image for a wavelength range of  $0.1\text{\AA}$ , a suitable match for the  $20\mu$  slits. The slits have 1mm separation corresponding to  $5.6\text{\AA}$  in a focal plane, which is ample to prevent overlapping of line images in the focal. The nearest coronal line that might interfere with the Lyman- $\alpha$  at  $1216\text{\AA}$  is the  $\text{Si III } \lambda 1206.5\text{\AA}$  which is normally about a factor 50 down in intensity from the Lyman- $\alpha$ .

The instruments recorded the spectral images on Eastman type 101 spectroscopic film carried in water tight motorized film cassettes that took sequences of exposures varying in length from 1s to 60s. On the basis of the 7 March 1970 eclipse data of Gabriel, the anticipated coronal Lyman- $\alpha$  intensities should give usable line intensities near the lunar limb with 1 second exposures and  $20\mu$  slits. The 60 second exposures and  $60\mu$  slits should probe further out into the corona. The overall dynamic range will be the normal film latitude times the factor 180 provided by the slit widths and exposure times. Table I lists the instrument sensitivity and exposure factors.

TABLE I

*Intensity and exposure factors*

- 
- Gabriel (1970) reports a measured brightness at  $1.3 R_{\odot}$  of  $5(10)^{12}$  photons/cm<sup>2</sup> second sterad Lyman- $\alpha$   $\lambda 1216\text{\AA}$
  - This instrument will deliver  $> 1.3(10)^4$  photons/second onto a  $20\mu$  square of film, given  $5(10)^{12}$  photons/cm<sup>2</sup> second sterad input
  - Laboratory calibration of this instrument on 101 film shows  $3(10)^4$  photons/ $20\mu$  element will give image above background
  - On the basis of the above fluxes, a  $20\mu$  slit imaging near the limb should give useable line intensities with a 1 second exposure
- 

Two complete rocket payloads were prepared and launched to improve the overall probability of a successful launch and recovery. Orienting the two slit systems at  $90^\circ$  to each other during the eclipse data taking and combining the resultant images during the data analyses gives a two-dimensional grid of data to assist in interpretation.

Two Nike-Black Brant V rockets carried the instrument payloads to altitudes near 350km. The rockets were launched eastward from the San Marco Satellite Launch Platform 3 miles off the coast of Kenya, near Malindi. Fig 4 is a schematic representation of the rocket payload and the trajectory into the umbral shadow. After nose cone ejection at 60s, the attitude control system (ACS) had about 180s to orient the

optic axes of the telescope toward the eclipsing sun and become stabilized before entering totality. Active control of the pointing was passed over to a stable platform prior to entering totality, and drift was limited to less than one arc sec per sec of time. A nominal trajectory gave over 500s in totality.

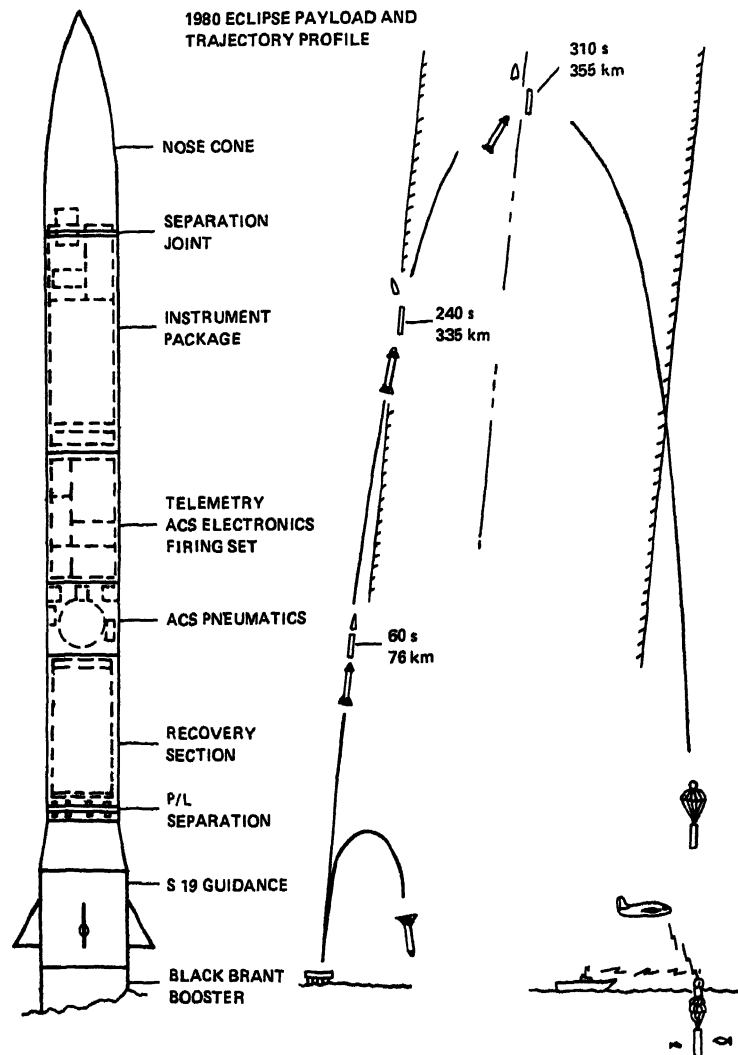


FIG. 4. A schematic drawing of a typical payload trajectory intersection with the umbral shadow.

The recovery was by parachute into the water where a float system with light and radio beacons guided recovery aircraft to the site, and they, in turn, vectored recovery boats to the floating payloads

## RESULTS

The two Nike-Black Brant V rockets were launched precisely on schedule and per-

formed as programmed. Unfortunately, an idiosyncrasy in the complex ACS prevented the system from looking on to the eclipsed sun and no useful data were acquired.

#### DISCUSSION

This attempted measurement remains one of the most important measurements still to be made on the physical characteristics of the inner corona. Current technology restricts it to eclipse conditions. My colleagues and I will be happy to assist any other experimenters who would like to make a successful attempt during a future eclipse.

#### ACKNOWLEDGEMENTS

This experiment was supported by the National Aeronautics and Space Administration, the Department of Energy, and the National Science Foundation.

#### REFERENCES

- Beckers, J. M., and Chipman, E. (1974) The profile and polarization of the coronal Lyman alpha line. *Solar Phys*, 34, 151-161.  
Gabriel, A. H. (1971) Measurements on the Lyman alpha corona. *Solar Phys.*, 21, 392-400.

Printed in India

Astronomy

## PRELIMINARY RESULTS FROM ECLIPSE CORONAL VELOCITY OBSERVATIONS

W LIVINGSTON *and* J HARVEY

*Kitt Peak National Observatory\*, Tucson, Arizona, U.S A*

*(Received 7 August 1981)*

A multislit, high dispersion spectrograph has yielded coronal 5303Å green line spectra, with neon comparisons, along parallels of latitude out to  $1.5 R_{\odot}$  in Mexico (1970), Kenya (1973) and India (1980). K-coronameter synoptic data centered about the eclipse dates have allowed observed line shifts to be identified with discrete coronal features. Results are

- 1) From plane-of-sky features the rest wavelength of Fe XIV is found to be  $5302.81 \pm 0.01 \text{Å}$
- 2) Sidereal rotation rate of the corona, near the equator, is  $13.6 \pm 2.9$  deg/day, or essentially the same as the photosphere
- 3) Systematic radial flows *towards* the sun, 3-15 km/sec, are found in about 30 per cent of our samples. This may be evidence for the "siphon flows" discussed theoretically by Cargill and Priest (1980)
- 4) In terms of small scale random velocities the corona is remarkably quiet. Although line-of-sight velocities up to 12 km/sec are seen, 0.5 km/sec is characteristic of the inner corona at a resolution of 20,000 km
- 5) The width of 5303, if assumed thermal, yields  $1.5-1.7 (10^6) \text{K}$ . The width shows a slight decrease outward except in active regions where there is a slight *increase*

**Keywords:** Solar Eclipse; Solar Corona; Coronal Velocity

### INTRODUCTION

A multislit high dispersion spectrograph has been successfully employed to measure coronal velocities and line profiles using the emission line of Fe XIV at the total eclipses of 1970 (Mexico), 1973 (Kenya) and 1980 (India). The original intent was to deduce a rotation rate for the corona. At present, we are uncertain to what degree the coronal gas co-rotates with the underlying solar surface. Our results do contain information on rotation but an uncertainty of 20 per cent, arising from various other systematic and random flow patterns precludes differentiating between rotation models without observing an impractical number of eclipses. However, these "disturbing" flow patterns have proved even more interesting than rotation. We find that the corona is remarkably quiescent and that most of the sensed motion is towards the sun. The latter observation may be an evidence for hypothetical siphon flows which transport material between the ends of large coronal loops. In this report we describe the instrument,

---

\*Operated by the Association of Universities for Research in Astronomy, Inc., under contract with the National Science Foundation



formed as programmed. Unfortunately, an idiosyncrasy in the complex ACS prevented the system from looking on to the eclipsed sun and no useful data were acquired.

#### DISCUSSION

This attempted measurement remains one of the most important measurements still to be made on the physical characteristics of the inner corona. Current technology restricts it to eclipse conditions. My colleagues and I will be happy to assist any other experimenters who would like to make a successful attempt during a future eclipse.

#### ACKNOWLEDGEMENTS

This experiment was supported by the National Aeronautics and Space Administration, the Department of Energy, and the National Science Foundation.

#### REFERENCES

- Beckers, J. M., and Chipman, E. (1974) The profile and polarization of the coronal Lyman alpha line. *Solar Phys*, 34, 151-161.  
Gabriel, A. H. (1971) Measurements on the Lyman alpha corona. *Solar Phys.*, 21, 392-400.

Frame No.	Position	Exposure	
	Cent. Slit*	Ne	Fe XIV
1	—3°	15s	90s w/graded filter
2	—5°	15	25

\*Heliographic latitude.

The film was hand developed in D76 for 8<sup>m</sup> at 20 °C to produce a gamma of near unity. Examples of these and other spectra taken with this instrument are given in Fig. 2 of Livingston *et al.* (1980)

#### B. Kenya, 29 June 1973

The equipment operated by L. A. Doe and W. Livingston was located at the main American site in Loryengalani on Lake Rudolf (latitude=N 2° 45'; longitude=E 36° 42'). A somewhat hazy sky caused us to reduce the number of slits to three. With the sun at an altitude of 37°, second contact began at 15:57 local time. No graded filter was used.

Frame No.	Position	Exposure	
	Cent Slit	Ne	Fe XIV
1	—2°	10s	90s
2	—2	10	15
3	+17	10	30
4	—25	10	30
5	+33	10	~25

Film was machine processed in a Versamat processor at 5ft/min to yield a gamma near unity.

#### C. India, 16 February 1980

The equipment operated by J. Harvey, G Ladd and W. Livingston, was again located at the main American camp this being at Japal-Rangapur Observatory, Andhra Pradesh (latitude=N 17°6'; longitude=E 78°45'). The sun's altitude was 32° at second contact, 15.46 local time. Five slits were open with the image offset so that one slit passed through a coronal hole in the south

Frame No	Position	Exposure	
	Cent. Slit	Ne	Fe XIV
1	~ —20		1s
2	~ —20	20s	110

The film was again machine processed at 5 ft/min.

formed as programmed. Unfortunately, an idiosyncrasy in the complex ACS prevented the system from looking on to the eclipsed sun and no useful data were acquired.

#### DISCUSSION

This attempted measurement remains one of the most important measurements still to be made on the physical characteristics of the inner corona. Current technology restricts it to eclipse conditions. My colleagues and I will be happy to assist any other experimenters who would like to make a successful attempt during a future eclipse.

#### ACKNOWLEDGEMENTS

This experiment was supported by the National Aeronautics and Space Administration, the Department of Energy, and the National Science Foundation.

#### REFERENCES

- Beckers, J. M., and Chipman, E. (1974) The profile and polarization of the coronal Lyman alpha line. *Solar Phys*, 34, 151-161.  
Gabriel, A. H. (1971) Measurements on the Lyman alpha corona. *Solar Phys.*, 21, 392-400.

TABLE I

*Published wavelengths of the green line*

$\lambda$ (Å.)	eclipse	reference
5303.1	<1893-1918>	Campbell and Moore (1918a)
5302.80	1918	Campbell and Moore (1918b)
5303.0	1918	Slipher (1922)
5302.80	1926	Davidson and Stratton (1927)
5302.9	1929	Grotrian (1934)
5303.0	1930	Moore and Menzel (1930)
5302.91	1930	Mitchell (1932)
5302.85	—	Lyot (1932)
5302.77	1936	Tanaka <i>et al.</i> , (1937)
5303.2	1936	Petrie and Menzel (1942)
5302.86 $\pm$ 0.02	—	Lyot (1939)
5301.9	1952	Aly (1955)
5303.4 $\pm$ 0.4	1965	Jefferies (1969)
5302.775	—	Tsubaki (1975)

principal coronal structures lay outside the sky plane in 1970, making this eclipse unfavourable for rest wavelength measurements. Fortunately, similar data for 1973 (e.g., Poulain, 1974) show that much of the west limb and part of the east limb corona was in the sky plane, and our determinations are confined to these features.

Starting with the rectified wavelengths found above we remove the effect rotation by assuming a rigid coronal rotation at a sidereal rate of 13.6 deg/day. Table II gives the individual values leading to a mean of 5302.91  $\pm$  0.01. This is the solar wavelength on the international scale without an adjustment for gravitational red shift.

TABLE II

*Rest wavelength of the green line from sky-plane features in 1973*

Frame	Slit limb	$\lambda$ (Å.)
4	north both	5302.812
3	south both	.819
2	centre east	806
5	south east	806
5	centre both	.814
	mean	5302.81 $\pm$ 0.01

The dominant error remaining is caused, we believe, by residual coronal motions. Systematic errors due to the limited numbers of reference line measurements give an uncertainty of  $\pm$  0.008 Å. Random error arising from film grain and the fixed pattern noise of the image tube is  $\pm$  0.003 Å.

### *Rotation*

Information on coronal rotation is summarized in Fig. 10 of Bohlin's (1970) review. Probably, the method which produces the most consistent is that of tracers, i.e., timing the consecutive passage of long-lived streamers. We recall, though, that in

formed as programmed. Unfortunately, an idiosyncrasy in the complex ACS prevented the system from looking on to the eclipsed sun and no useful data were acquired.

#### DISCUSSION

This attempted measurement remains one of the most important measurements still to be made on the physical characteristics of the inner corona. Current technology restricts it to eclipse conditions. My colleagues and I will be happy to assist any other experimenters who would like to make a successful attempt during a future eclipse.

#### ACKNOWLEDGEMENTS

This experiment was supported by the National Aeronautics and Space Administration, the Department of Energy, and the National Science Foundation.

#### REFERENCES

- Beckers, J. M., and Chipman, E. (1974) The profile and polarization of the coronal Lyman alpha line. *Solar Phys*, 34, 151-161.  
Gabriel, A. H. (1971) Measurements on the Lyman alpha corona. *Solar Phys.*, 21, 392-400.

longitudinal motions, implies velocities of the order of 0.3 km/s which is small compared to the observed radial components

We have computed the relative intensity of the green line as a function of distance along the LOS using the excitation equilibrium equation given by Billings (p 138, 1966), ionization equilibria given by Landini and Fossi (1972) and a temperature distribution with radius vector  $r$  varying as

$$T(r) = 1.5 (10^6) (r/R_{\odot})^{4/7}$$

following Newkirk (1967). Three-dimensional electron density information was generously provided for 1970 and 1973 by M. Perry, M. Altschuler, D. Brown, R. Hansen and S. Hansen based on K-coronameter observations (see Perry & Altschuler, 1973).

**B. Deduction of Flow Patterns** Figs. 1 and 2 compare our LOS velocities with the white light corona. The only notable correlation is that the highest velocities occur in the ray structure of reduced brightness.

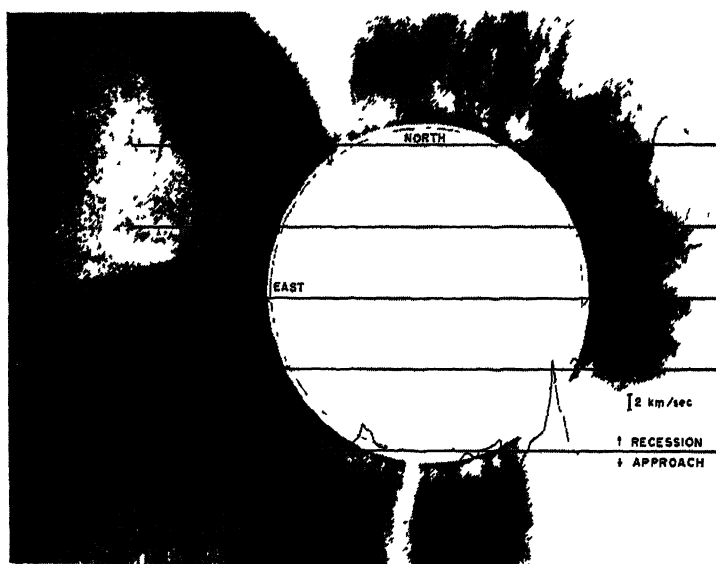


FIG 1 High Altitude Observatory white light photo of 1970 corona with our spectroscopic deduced velocities super-imposed along the multi-slit intercepts

An objective measure of flow direction is obtained from the product of velocity and position of origin as given by the contribution function. Let the residual LOS velocity at each point  $i$  be  $v_i$  km/s, with  $v_i > 0$  for recession. The corresponding sky-plane distance is  $Z_i$ , in units of  $R_{\odot}$ , with  $Z_i > 0$  for material earthward of the sky-plane. Then for each limb chord  $j$  we compute

$$V_j = \frac{1}{n} \sum_{i=1}^n v_i \times Z_i$$

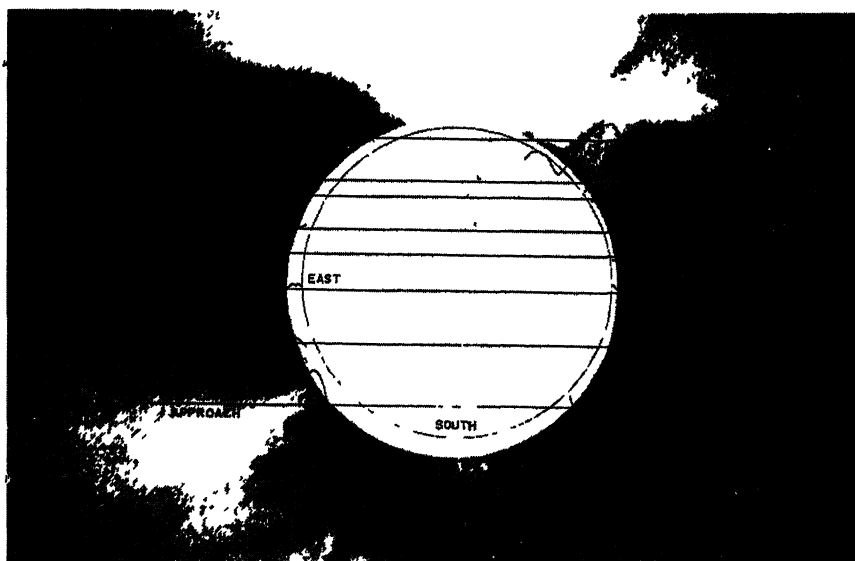


FIG. 2. Same as Fig 1 except for 1973

Here  $n$  is the appropriate number of 20,000km steps along the slit within which  $p \leq v_r < \pm 0.2 \text{ km/s}$ . The  $p \leq v_r$  depends on brightness.

$V_r$  is a weighted indicator of velocity direction, with positive  $V_r$  being inward, negative outward. Table IV tabulates  $V_r$  and identifies the heliographic slit positions. The majority of features have low weight and the direction is uncertain. The interesting point is that the high weight features are directed inward toward the sun.

Excluding the low weight features, we could estimate the sun-directed velocities along the various rays and streamers. From the contribution function we obtained  $\theta$ , the angle between the feature and the sky-plane. Then  $V_r = \bar{V}_r \sin^{-1} \theta$ . Where  $\bar{V}_r$  is the average LOS velocity for chord  $r$ . Table IV also lists these values. The inferred peak velocity is 15.4 km/s inward, the mean is  $3.7 \pm 1.4 \text{ km/s}$  omitting this peak value.

#### *Random Motions*

After removing the effects of solar rotation and what we have termed systematic flows we are left with small scale random motions. Neglecting the very large velocities, identified in the preceding section, an average of 0.5 km/s appears characteristic of random motion at our 20,000km resolution. This conflicts somewhat with the findings of previous studies where a much more turbulent corona is indicated (e.g., see Delone & Makarova, 1969, and Babin & Steshenko, 1973).

#### *Width of Green Line*

Our rectified spectra yield line widths for each position along the slit. Typically the line width, when interpreted as purely thermal, gives temperatures of 2–5 ( $10^6$ )°K. In general, the width decreases outward except over active regions where we see a slight increase with height. Such high temperatures are not consistent with

TABLE IV

*Summary of deduced velocities*

$\phi$	$V_s$	East km/s <sup>-1</sup>			West km/s <sup>-1</sup>			
		$\bar{V}$	$V_p$	V	$V_s$	$\bar{V}$	$V_p$	V
1970								
+64		0.22	4.0	1.2 out	+0.19	-0.33	2.2	2.1 in
+23		-0.19	1.4	1.4 in	+0.17	-0.56	3.0	5.3 in
- 3		-0.43	2.8	2.7 out	+0.71	1.54	3.0	8.1 in
-29		-0.49	2.6	bifurcated	-0.28	0.80	1.2	3.8 in
- 83		-0.15	3.4	bifurcated	+0.35	1.17	12.0	5.2 in
1973								
+68		+1.55	2.0	4.8 in	0.68	-1.48	4.0	6.6 in
+41		+0.24	2.0	1.0 in	-0.23	-1.36	2.3	sky-plane
+33		+0.05	1.4	bifurcated	0.09	0.28	3.4	sky-plane
+20 20, 17	+0.05	-0.04	0.5		0.21	-2.16	3.6	sky-plane
10	-0.03	+0.22	1.0	1.1 Out	0.04	-0.33	1.0	4.7 in
-2 -2 -3	+0.01	-0.11	0.7	bifurcated	0.06	-0.25	1.0	bifurcated
-24, -24, -25	+0.40	+1.21	1.6	5.4 in	-0.07	0.42	1.0	2.2 out
- 53	+3.01	+4.51	5.6	15.4 in	-0.26	1.38	2.2	sky-plane

$\phi$  = solar latitude     $\bar{V}$  = average velocity     $V_p$  = peak velocity    V = deduced vector velocity,  $V_s$  see text  
 Multiple values of  $\phi$  means that the observations from those latitudes have been averaged together



the indicated ionization condition and we can hypothesize either an isotropic turbulence  $\sim 40\text{ km/s}$  or the superposition of unresolved anisotropic flows. If we fix our attention on the regions of minimum line width we deduce a temperature of  $1.5\text{--}1.7 (10^6)^\circ\text{K}$ .

### DISCUSSION

Our finding that most of the reliably detected flows were downward to the surface came as a surprise. One thinks of the corona as serving as the roots for the outward bound solar wind. But either the outward motion is too small very near the sun or, as in the case of coronal holes, the gas may be too tenuous to register on our spectra. Moreover, the brightest regions are magnetically closed, in any case, and would not contribute to an outflow.

The peripheries of helmet structures contribute the most to our spectra because their material cross-section is the greatest. Typically, a helmet lies adjacent to a coronal hole which is a region of weak magnetic flux. Perhaps then we have evidence for the siphon flows discussed by Cargill and Priest (1980). Their model indicates that material may be preferentially siphoned from high field regions (interior to helmets) to the low field's edge outlining the helmet. A more detailed investigation of the siphon flow model and its relation to our data is planned.

### ACKNOWLEDGEMENTS

We wish to thank belatedly the Governments of Mexico and Kenya for the excellent cooperation and for the facilities placed at our disposal that made these eclipse observations possible. More immediate in our memory is the enthusiasm and help of our Indian colleagues in Hyderabad who made the arrangements and solved the day-to-day problems related to our 1980 work at Japal-Rangapur Observatory. We also thank the Department of Science and Technology of the Government of India for their hospitality and the logistic arrangements. Finally, we extend our appreciation to the Indian National Science Academy, and in particular to Professor M. G. K. Menon, Dr A. P. Mitra and Professor S. K. Trehan for sponsoring this symposium.

### REFERENCES

- Aly, M. K. (1955) Preliminary note on measures of coronal emission lines observed at the total solar eclipse, February 25, 1952, by B. Lyot and M. K. Aly. *Astrophys. J.*, **122**, 438.
- Babin, A. N., and Steshenko, N. V. (1973) Physical conditions in two regions of the solar corona on 7 March 1970. *Izv. Krynsk. Astrofiz. Obs.*, **47**, 36.
- Billings, D. E. (1966) In *A Guide to the Solar Corona*. Academic Press, New York, p. 138.
- Bohlin, J. D. (1970) Solar coronal streamers. I. Observed locations, general evolution, and classification. *Solar Phys.*, **12**, 240.
- Brault, J., and White, O. R. (1971) The analysis and restoration of astronomical data via the fast Fourier transform. *Astron. Astrophys.*, **13**, 169.
- Campbell, W. W., and Moore, J. H. (1918a) The spectrum of the solar corona. *Lick Obs. Bull.*, **10**, 8.
- (1918b) The wave length of the green coronium line. *Publ. astron. Soc. Pacific*, **30**, 348.
- Cargill, P. J., and Priest, E. R. (1980) Siphon flows in coronal loops. I. Adiabatic flow. *Solar Phys.*, **65**, 251.

- Davidson, C R., and Stratton, F J. M. (1927) Report on the total solar eclipse of 1926 January 14. *Mem. R. astron. Soc.*, **64**, 105
- Delone, A. B., and Makarova, E A. (1969) Interferometric investigation of the red and green coronal lines during the total solar eclipse of May 30, 1965 *Solar Phys.*, **9**, 116
- Grotian, W (1934) Über das Fraunhofersche spektrum der sonnenkorone. *Z. f. Astrophys.*, **8**, 142
- Hansen, R. T., Hansen, S F., and Garcia, C J (1970) Mauna Loa coronagraph observations around the 7 March 1970 eclipse. *Solar Phys.*, **15**, 387
- Jefferies, J. T (1969) Forbidden lines in the solar corona *Mem. Soc. R. Sci. Liege*, **17**, 213.
- Landini, M., and Fossi, B C. Monsignori (1972) Ionization balance for ions of Na, Al, P, Cl, A, K, Ca, Cr, Mn, Fe and Ni *Astron. Astrophys., Suppl.*, **7**, 291
- Livingston, W., Harvey, J., Doe, L A., Gilespe, B., and Ladd, G (1980) The Kitt Peak coronal velocity experiment *Bull. astron. Soc. Inaa*, **8**, 43.
- Lyot, B (1932) Etude de la couronne solaire en dehors des eclipses. *Z. f. Astrophys.*, **5**, 73
- (1939) A study of the solar corona and prominences without eclipses *Mon. Not. R. astron. Soc.*, **99**, 580.
- Minkowski, R. (1942) Curvature of the lines in plane-grating spectra *Astrophys. J.*, **96**, 306.
- Mitchell, S. A. (1932) The spectrum of the corona *Astrophys. J.*, **75**, 1
- Moore, J H., and Menzel, D H. (1930) The green coronal line at the eclipse of April 28, 1930 *Publ. Astron. Soc. Pacific*, **42**, 182
- Newkirk, G, Jr (1967) Structure of the solar corona. *Ann. Rev. Astron. Astrophys.*, **5**, 213.
- Perry, R. M., and Altschuler, M. D. (1973) Improved three-dimensional mapping of the electron density distribution of the solar corona. *Solar Phys.*, **28**, 435.
- Petrie, W., and Menzel, D H (1942) The wavelengths of new coronal lines *Astrophys. J.*, **96**, 395.
- Poulain, P. (1974) Observations coronographiques avant et apres les eclipses by 10 Juillet 1972 et du Juin 1973 *Solar Phys.*, **36**, 339
- Slipher, V M (1922) The spectrum of the corona as observed by the expedition from the Lowell Observatory at the total eclipse of June 8, 1918 *Astrophys. J.*, **55**, 73
- Tanaka, T., Koana, A., and Kondo, M. (1937) On the spectrum of the solar corona at the total eclipse in 1936 I On the coronal lines *Proc. phys. Soc. Japan*, **19**, 693
- Tsubaki, T. (1975) Line profile analysis of a coronal formation observed near a quiescent prominence intensities, temperatures and velocity fields *Solar Phys.*, **43**, 147

Printed in India.

Astronomy

OBSERVATIONS FOR CORONAL VELOCITY FIELD AND COLOUR  
MOVIE OF FLASH SPECTRUM DURING TOTAL SOLAR  
ECLIPSE OF 16 FEBRUARY 1980

A. BHATNAGAR, D B JADHAV, R. M. JAIN, R N SHELKE\* and S. P. PUROHIT

*Vedhshala, Udaipur Solar Observatory, Udaipur, India*

*(Received 7 August 1981, after Revision 27 September 1981)*

Observations using a multi-slit spectrograph at  $5303\text{\AA}$  Fe XIV line were obtained during the 16 February 1980 total solar eclipse, for velocity field determination in the solar corona. A colour movie film of flash spectrum was obtained using an objective prism coupled with a telephoto lens.

**Keywords:** Coronal Velocity Field; Flash Spectrum; Multi-slit Spectrograph

CORONAL VELOCITY FIELD

AN improved knowledge of the coronal velocity field is basic to an understanding of the dynamics of the sun's atmosphere. Observations made so far indicate that coronal velocity field is made up of two components—a rotational velocity and a random velocity. The picture that emerges is of an inner corona rotating as a solid extension of the photosphere with outward streaming elements. More observations are needed to define the motions and also to determine to what extent the corona co-rotates with the underlying photosphere as a function of height and latitude.

Our experiment conducted during the total solar eclipse of 16 February 1980, was designed to measure the line of sight velocity component of the coronal gases, upto a distance of about 0.5 solar radii from the limb of the sun. A similar attempt had been made earlier during the 1970 and 1973 total eclipse by Livingston *et al* (1973, 1980) of Kitt Peak National Observatory, U S A. They obtained an unexpected result, that instead of outward flow of coronal material, which normally one would expect, an inflow of material towards the sun was observed. This is an interesting result and needs further verification and confirmation, as it is of fundamental importance to understand the dynamics of the solar coronal material.

Our team from the Vedhshala Udaipur Solar Observatory had built a multi-slit Littrow spectrograph having 5 slits for taking simultaneous spectra of the coronal line of Fe XIV at  $5303\text{\AA}$ , so that in a single exposure one could obtain 5 spectra of different regions in the corona and the line of sight component of velocity field in the corona.

The sunlight was directed from a 8'-coelostat to a 150mm aperture f/13 objective lens. This formed a 20mm diameter solar image at the multi-slit. This multi-

---

\*presented by R. N. Shelke

slit comprises of 5 slits, each separated by 10mm. A  $200\text{\AA}$  pass-band filter centered at  $5300\text{\AA}$  was placed before the multislit to act as a blocking filter to isolate the  $5303\text{\AA}$  emission line. Just behind the multislit a field lens of 1 meter focal length was used to decrease the vignetting on to the grating. A Littrow lens of 1.27 meter focal length and a plane reflecting grating having 600 lines/mm and blazed in the second order green was used, to yield a dispersion of  $5.2\text{\AA}/\text{mm}$  in the second order.

The slit positions with respect to solar image is shown in Fig 1. The solar image was centered on the multislit in such a way that one slit crossed the sun's disc near

### DIAGRAM OF SLIT POSITIONS FOR TAKING MULTI-SLIT SPECTRA

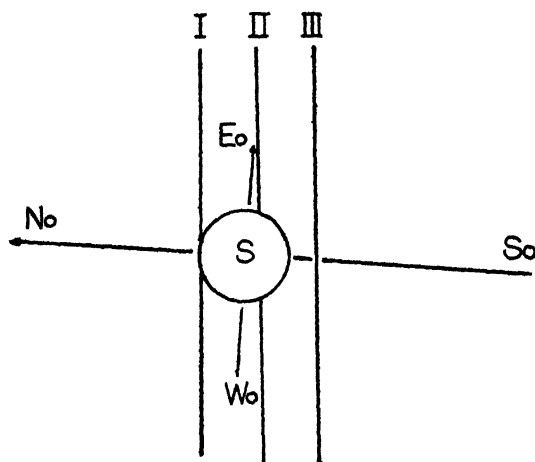


Fig 1 Slit positions I, II and III with respect to the solar image. Sun's north, south, east-west directions are indicated.

the disc centre and one slit near the northern limb and the other beyond the southern limb of the sun in the corona in the hope of determining velocity field in the coronal hole, which was known to be seen near the south pole. The remaining two slits were blocked to decrease the scattered light in the spectrograph. Only one spectrum during the totality with an exposure of 120 seconds was obtained on II-a-D Eastman Kodak plate. A comparison spectrum of mercury lamp was also obtained on the same plate for Doppler shift measurement of the coronal line. Fig 2 shows multislit spectrogram of coronal line  $5303\text{\AA}$  and  $5461\text{\AA}$  mercury comparison line. The coronal emission line  $5303\text{\AA}$  could be recorded only on two slits, the 3rd slit was placed too far out in the corona where the line intensity was low and therefore  $5303\text{\AA}$  line was not recorded. On this spectrum, the coronal line appears upto a maximum of about 0.3 solar radii from the limb of the sun.

Detailed analysis of the multi-slit spectra is in progress, for determination of the coronal velocity field.



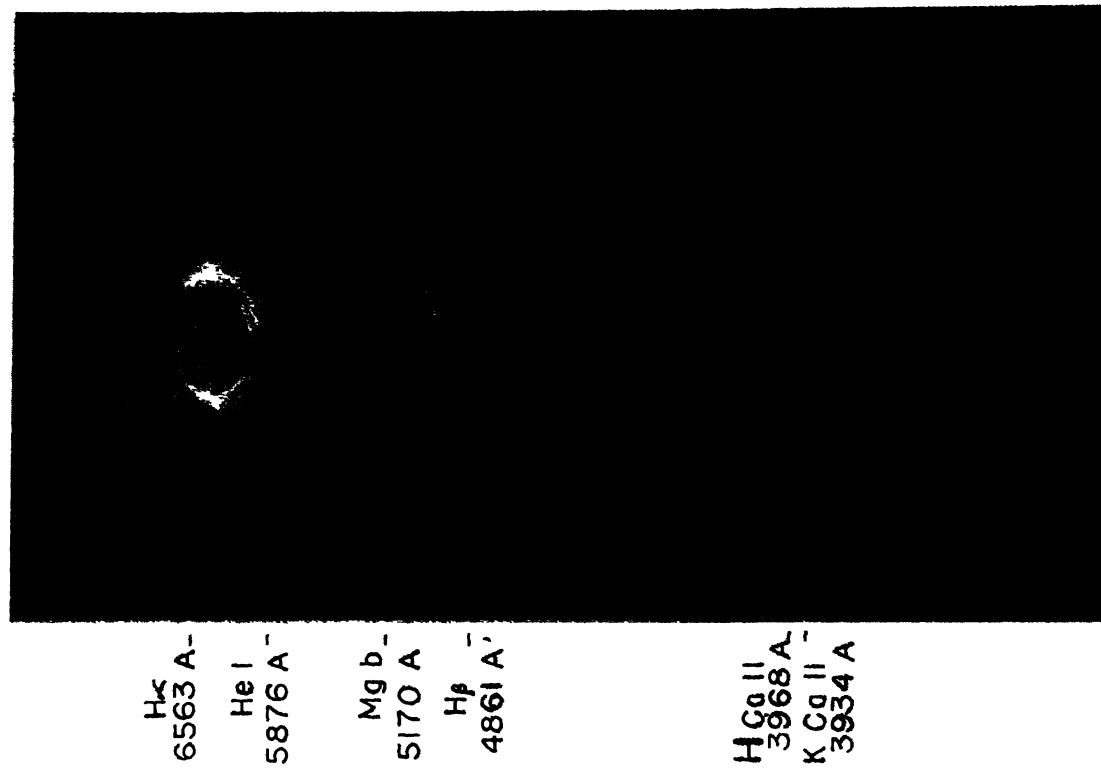


FIG. 3 Colour print of flash spectrum. Brilliant arcs are emission lines due to H $\alpha$ , HeI, Mgb, H $\beta$  and ionized calcium (H&K).

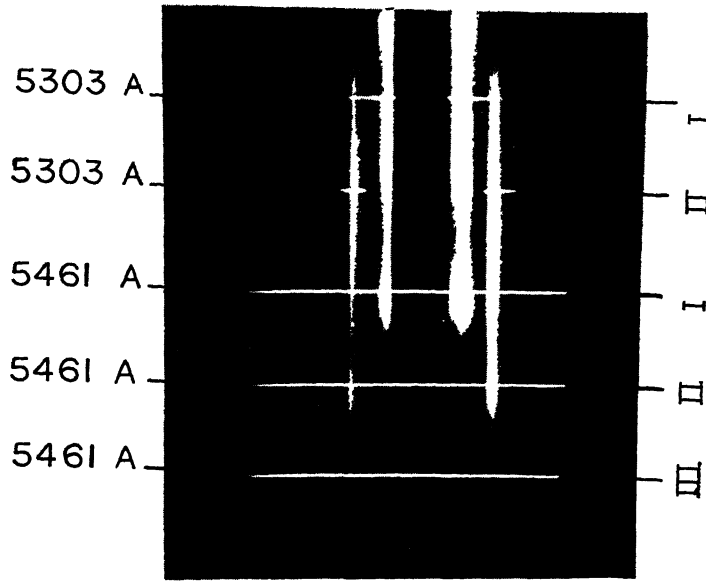


FIG 2 Multi-slit coronal spectra in 5303Å line and comparison spectra of Hg 5461Å. The three slit positions are marked on the top as I, II and III

#### FLASH SPECTRUM COLOUR MOVIE

Our second experiment was to obtain a movie of the flash spectrum in colour

Just before the totality, dark absorption spectrum of the photosphere vanishes and bright emission line spectrum appears. The narrow crescent of the sun and the edge of the moon together act as a slit of spectrograph, thus throwing a brilliant arc-shaped emission line spectrum for a few seconds of the chromosphere, called the "flash spectrum". As the edge of the moon moves a finite distance in front of solar chromosphere, the spectra of radiation from different heights in chromosphere are observed and from these one could determine the distance from which various radiations due to Hydrogen, Helium and metals etc., originate.

For the flash spectrum observations, we used a 60°-objective prism placed in front of a 210mm focal length f/4.0 telephoto lens attached to a 35mm movie camera with Eastman-Colour film and a Kodak 85 filter for proper colour balance. This arrangement gave a dispersion of nearly 80Å/mm at  $H_{\gamma}$  and the flash spectrum in the range from 6563Å upto 3950Å was obtained. The cinematographic observations of the flash spectrum was made at a rate of 24 frames/second. A total of 300 good spectra have been obtained before and around the second contact, but the flash spectrum observations were missed after the 3rd contact, due to delay in starting the movie camera. Fig 3 shows one of the frames of flash spectrum. The arcs are the emission lines due to  $H_{\alpha}$ , HeI, MgB,  $H_{\beta}$  and ionized calcium (H & K). As the time advanced the moon covered higher and higher layers of the chromosphere and resulting decrease in intensity of MgB, HeI and H & K lines in this order. The flash spectrum movie was taken at a rapid rate of 24 frames/second, hence theoretically the spatial

resolution obtained from one frame to next would yield better than 15 kilometers on the sun. A frame by frame analysis of the spectral lines would give information on the heights of various emission lines in the chromosphere. The colour movie sequence of the flash spectrum shows a spectacular view of the disappearance of the chromospheric emission lines and leaves a marvellous visual impression.

#### ACKNOWLEDGEMENTS

The financial support for the total solar eclipse experiments was given by the Department of Space, under the RESPOND programme. Our thanks are also to Professor M. K. Vainu Bappu for kindly giving on loan the 8-inch coelostat and to Professor K. D. Abhyankar for generously providing all facilities at the Japal-Rangapur Observatory.

#### REFERENCES

- Livingson, W., Harvey, J., and Doe, L. (1973) *Final Rep 1973 Solar Eclipse, Bulletin No 5* National Science Foundation, Washington D C 20550, p. 34  
Livingson, W., Harvey, J., Doe, L. A., Gillespie, B., and Ladd, G. (1980) *Bull astron. Soc. India*, 8, Nos. 2 & 3, 43



**AIRBORNE ECLIPSE EXPEDITION:  
A DESCRIPTION OF FIVE EXPERIMENTS TO DETERMINE  
TEMPERATURE, DENSITY AND STRUCTURE IN THE CORONA**

C. F. KELLER

*National Science Foundation, Washington DC 20550, U.S.A.*

*(Received 7 August 1981)*

Los Alamos flew five experiments to Kenya aboard a USAF NC-135 aircraft. Altitude of observations was 11.5km, solar altitude was 81 degrees; totality duration was 7<sup>m</sup> 06<sup>s</sup>.

Four of the experiments were a unified set to determine coronal temperatures and densities

- (1) *Heavy Ion Temperatures* from high resolution emission line profiles to 2.5d  $R_{\odot}$
- (2) *Electron Temperatures* from broadening of absorption features centered on H and K Cell  $\pm 750$  Å using a method due to L. Cramm, to 2.0  $R_{\odot}$
- (3) *Electron Density* from photographic polarimetric photometry to 12  $R_{\odot}$ .
- (4) Images of corona from 500 to 1000mm cameras which reduces radial brightness gradient and from computer enhancement of images taken for (3).

The fifth experiment searched at 0.7 and 2.2 for emission due to circumsolar dust out to 50  $R_{\odot}$ .

**RESULTS**

- (1) Electron temperature experiment failed to record data due to faulty computer storage disc.
- (2) Excellent data on emission line profiles of Fe XIV (530.3nm) and Ca XV (569nm).
- (3) Excellent photographic polarimetry and absolute photometry of inner (limb to 2.6  $R_{\odot}$ ) and outer corona (2-12  $R_{\odot}$ ) as well as absolute photometry to 20  $R_{\odot}$ . Preliminary reduction shows sky background brightness of  $1.5 \times 10^{-10}$  solar mean brightness and that the polar corona was approximately three times brighter than in 1973. Isophotes are essentially circular to 5  $R_{\odot}$  where F-corona begins to contribute extra intensity to equatorial regions.
- (4) Good photographic images to 12  $R_{\odot}$  resulted from electron density photography and to 7  $R_{\odot}$  from radially graded reduction cameras although filters not perfectly centered. At the time of experiment we recorded a complete coronal transient in West limb to 7  $R_{\odot}$ .
- (5) Infrared observations show emission at 7  $R_{\odot}$  but none beyond that to 50  $R_{\odot}$  thus questioning recent observations of 20  $R_{\odot}$  features

**Keywords:** Solar Eclipse; Solar Corona

**INTRODUCTION**

ON 16 February 1980, the moon's shadow raced across our planet from the Atlantic Ocean to China at about 1600 kilometres per hour. Thousands of spectators and

scientists scattered along the shadow's path lifted their heads to glimpse the pearly glow of the solar corona, the sun's outermost atmosphere. Near the midpoint of this path where sun, moon, and earth were aligned for the longest time, a high-altitude United States Air Force jet made its carefully programmed rendezvous with the eclipse shadow. Aboard the aircraft were 18 Los Alamos scientists, observers from Indiana University and Kitt Peak National Observatory, a 12-man Air Force flight and support crew, a Kenyan observer, and two media representatives.

We were intent on recording the conditions in the solar corona during the second highest peak in solar activity in the past century. Five experiments, planned months ahead, were mounted inside the aircraft to make high-resolution measurements of coronal morphology, electron densities, electron temperatures, ion temperatures, and circumsolar dust rings. Our expedition was the seventh in a series of Los Alamos airborne missions that began in 1965 as an outgrowth of the national Test Readiness Program.

During a total eclipse the aircraft provides near ideal conditions for observing the solar corona. At an altitude of 11 kilometers (36,000 feet) we enjoy freedom from cloud cover and reduced sky brightness and, by flying along the eclipse path, we increase the time of totality by 50 per cent or more. In 1980, we had an unobstructed overhead view of the eclipse for 7 minutes and 7 seconds.

#### PROBLEM OF CORONAL TEMPERATURES

The key parameters for modelling energy transport in the corona are the distribution of electrons and ions in the corona and their temperature, or, more precisely, their velocity distribution.

The average values of the particle distribution are fairly well known, but not the temperature distribution. We would like to know not only gross averages but details of temperature distributions in various structural features of the corona since the energy transport will vary from one to another. At present the results from various methods gathered at various times are in disagreement. Although these discrepancies are understandable, given the fact that the various methods for measuring temperature involve different assumptions, the methods are complementary, if done in a coordinated fashion, the separate measurements can be compared to yield more information than any single one can yield alone.

The results of recent temperature measurements shown in Fig. 1 are in obvious disagreement. In coronal holes (Fig. 1a), we see upper and lower limits on kinetic temperatures based on electron density data. The lower limit is  $\approx 1$  MK based on the assumption of a static, isothermal corona. The Skylab electron density data, interpreted through a model that accounts for expansion velocities as described above, results in a steeply rising curve that reaches 3.5 MK by  $3 R_{\odot}$ . The other three observations fall within these bounds but are too sparse to allow determination of the position of the temperature maximum. The single EUV temperature and the single Lyman- $\alpha$ -proton temperature suggest extended magnetic heating. When the Los Alamos iron ion temperatures are included, the temperature maximum moves below  $1.3 R_{\odot}$ .

Fig. 1b shows similar results for relatively quiet regions of the corona (regions

that are devoid of obvious streamers but are not coronal holes). Neglecting the iron ion temperature puts the temperature maximum beyond  $1.4 R_{\odot}$ ; including it moves the maximum below  $1.2 R_{\odot}$ . Preliminary iron ion temperatures from the Los Alamos 1973 eclipse observations show ever increasing temperatures down to  $1.1 R_{\odot}$ . If the electron density and the EUV results in the lower corona can be believed, then the iron ion results must include a large turbulent contribution to line broadening.

Interpretation of the results shown in Fig 1 is further complicated by the fact that the data were obtained at different times and at different places in the corona. To resolve the discrepancies, we need simultaneous observations of ion temperatures, electron temperatures, and electron densities. One of the primary goals of the Laboratory's 1980 solar eclipse expedition was to do just this.

### THE 1980 EXPERIMENTS

The sun's magnetic activity follows a well-known 11-year cycle becoming very active, waning to near total inactivity, and then repeating. The amplitude of this variation is never the same, but by 1979 it was obvious that the 1980 maximum would be one of the highest in history and many experiments were planned to observe the solar corona during the eclipse in February, 1980.

The National Aeronautics and Space Administration (NASA) planned to launch the Solar Maximum Mission, a satellite similar to Skylab's observatory. Aboard it would be experiments to determine electron densities and to obtain a crude estimate of ion temperatures from Fe XIV emission intensities. (Unfortunately, this experiment was not operating by the time of the eclipse.) NASA also funded two rocket experiments, including one from Los Alamos, to measure proton temperatures from the Lyman- $\alpha$  line. The Naval Research Laboratory's orbiting coronagraph was to make hourly recordings of the white light from the outer corona ( $3-10 R_{\odot}$ ). The National Science Foundation (NSF) planned to send to India a large contingent of ground-based observers, who would make a variety of measurements.

In planning the Los Alamos airborne expedition, we were in communication with scientists from NASA projects and some NSF projects. It was apparent that cross-calibration and data comparison would assure maximum confidence in the results.

As discussed above, to answer significant questions about the nature of coronal heating and solar wind acceleration requires simultaneous measurements of the following:

- \* electron density,  $n_e$
- \* ion temperature,  $T_{ion}$
- \* electron temperature,  $T_e$

All these measurements were attempted by our expedition. All were designed to provide a good two-dimensional spatial resolution. We expected to be able to determine all the quantities not only in the relatively uniform portions of the corona, but also within major features such as streamers, condensations, and coronal holes. Table I summarizes the experiments and the information sought.

To determine ion temperatures we measured the Doppler-broadened emission lines from two heavy ions—Fe XIV and Ca XV. We will compare our results with

proton temperatures deduced from rocket measurements of Lyman- $\alpha$  emission at several points in the corona beyond  $1.5 R_{\odot}$  to distinguish thermal from nonthermal contributions to line broadening. We are particularly interested in determining

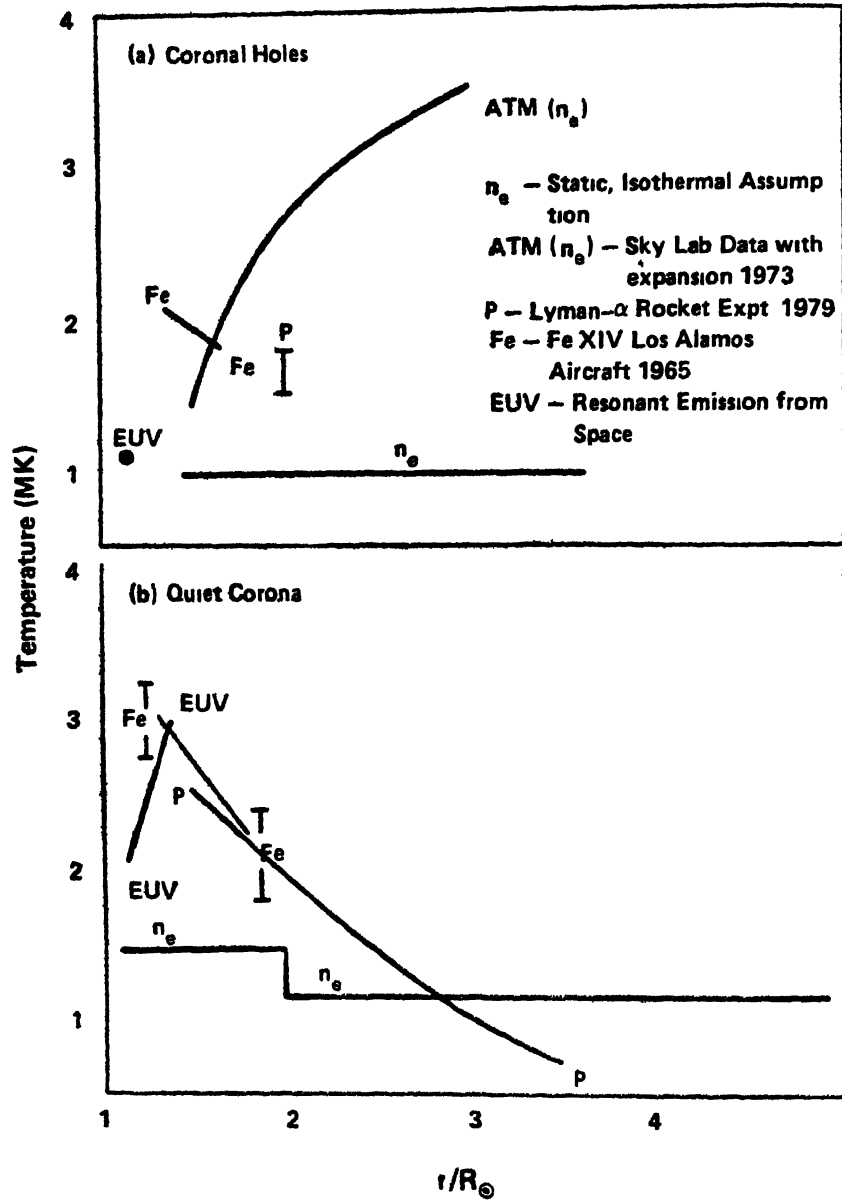


FIG 1 Plots of coronal temperature versus radial distance for (a) coronal holes and (b) a quiet coronal region. As discussed in the text, data are sparse and, when compared, confusing. The main purpose of the Los Alamos expedition was to attempt to reduce some of the sources of disagreement by making contemporaneous and cospatial measurements.

whether the extremely high ion temperatures at the base of the corona deduced from our 1973 results are correct or should be attributed to the effects of turbulence, but we must await data from these low altitudes. We also measured electron densities, recorded high-resolution images of the corona, and attempted to observe electron temperatures by a new, untried method. Finally, we attempted to determine the location of hot dust rings around the sun from their infrared emissions.

TABLE I

*1980 Solar eclipse experiments*

Experiment	Principal Investigators	Information obtained or sought	Resolution
Emission Line Ion Temperature Measurement of coronal Fe XIV and Ca XV emission line profiles with Fabry-Perot interferometer	D H. Liebenberg E A. Brown R N. Kennedy H S. Murray W M. Sanders	Temperatures of Fe XIV and Ca XV, variation of emission line intensity with radial distance, and nonthermal contributions to ion tem- perature from 1 to 3 $R_{\odot}$	0.005 $R_{\odot}$ (3500km)
Electron Temperature Measurement of K coronal spectral intensity with silicon photodiode detector array	M T. Sandford F J. Honey R. K. Honeycutt, Indiana University	Electron temperature and coronal spectra at 1.2, 1.6, and 2.0 $R_{\odot}$	0.067 $R_{\odot}$ (46,000km)
Electron Density Measurement of intensity and polarization of coronal light with camera-polarimeter	C. F. Keller J. A. Montoya B. G. Strait	Electron density, K+Fe corona intensity, and K corona polarization from 1.1 to 5 $R_{\odot}$ in polar regions and from 1.1 to 12 $R_{\odot}$ in equatorial regions and image-enhanced photographs of streamers from 1 to 20 $R_{\odot}$	0.067 $R_{\odot}$ (46,000km)
Photography Coronal photography with radially graded filter and internal occulting disc	W H. Regan C G. Lilliequist	Detailed coronal structure from 1 to 6 $R_{\odot}$	0.033 $R_{\odot}$ (23,000km)
Infrared Emission of Dust Rings Measurement of coronal infrared emission intensity with InSb detector and charge-injection- device television camera	J P. Mutschlecner R R. Brownlee D N. Hall, Kitt Peak National Observatory	Radial location of dust rings and infrared emission intensity from 3 to 50 $R_{\odot}$	0.25 $R_{\odot}$ (175,000km)

Except for the data loss from a mechanical failure in the electron temperature experiment, we obtained excellent data in all areas. And photographs of the corona

taken from the aircraft will enable us to associate our detailed observations with particular spatial structures.

Data reduction and comparison is a long and difficult process that is only beginning. Before we discuss each experiment and give an early estimate of the data it acquired, let us consider some of the general conditions of coronal observation.

#### *Direct Photography—Imaging the Corona*

Good photographic prints of the solar corona are extremely difficult to make because coronal brightness varies by factors of 1000 from  $1.4 R_{\odot}$  and 10,000 from  $1-10 R_{\odot}$ , whereas prints can display only a factor of 10. We use three methods to reduce this radial brightness gradient.

1. A radially graded filter placed just in front of the film transmits light in precisely the desired amount as a function of distance from the sun.
2. An internal occulting disc in the converging light path within the camera also uniformly reduces the brightness gradient.
3. Computer processing reduces the gradient in the digitized photographs from the electron density experiment.

All three methods were used during the 1980 expedition. Because of a slight misalignment of the mirror tracking system aboard the aircraft, the first two gave good photographic records of only two-thirds of the corona. Nevertheless, these pictures give us a remarkably detailed view of the corona during the sun's maximum activity.

Photographs of a huge bubble-like structure extending from the sun's limb to 7 solar radii were a most exciting result of our 1980 expedition. The structure is formed by a hydrodynamic eruptive disturbance that ejects large quantities of mass into interplanetary space. The eruption is very clearly visible on the computer-enhanced image (Fig. 2) processed from 32 digitized photographs. These large and frequent mass eruptions have been recorded since the early 1970s by Naval Research Laboratory satellites and by Skylab, but the bases of the eruptions were always obscured by the oversized occulting discs used in satellite coronagraphs. Thus ours is the first complete record of the phenomenon.

At first glance the structure looks like a tennis racket with its handle in the sun. Closer examination reveals that it is not entirely symmetric about an axis extending radially from the sun. Its polar side is markedly flattened and a density enhancement, which is possibly due to a shock wave ahead of the eruption, is very prominent above and on the equatorial side, but is nearly absent on the polar side. Nearby major streamers that usually extend in a radial direction from the sun are bent toward the disturbance, more so on the equatorial than on the polar side. In addition, the eruption may possibly be bent slightly toward the solar equator. Characteristics similar to these have been reported for eruptions observed from Skylab.

The position of this eruptive disturbance recorded from the aircraft differs markedly from that recorded by the Laboratory's rocket team in Kenya about 15 minutes earlier, from the difference we infer an expansion velocity of about 500 km/s. This value is in agreement with the eruption's absence from photographs taken from the main scientific site in India, where the eclipse occurred about 90 minutes later.

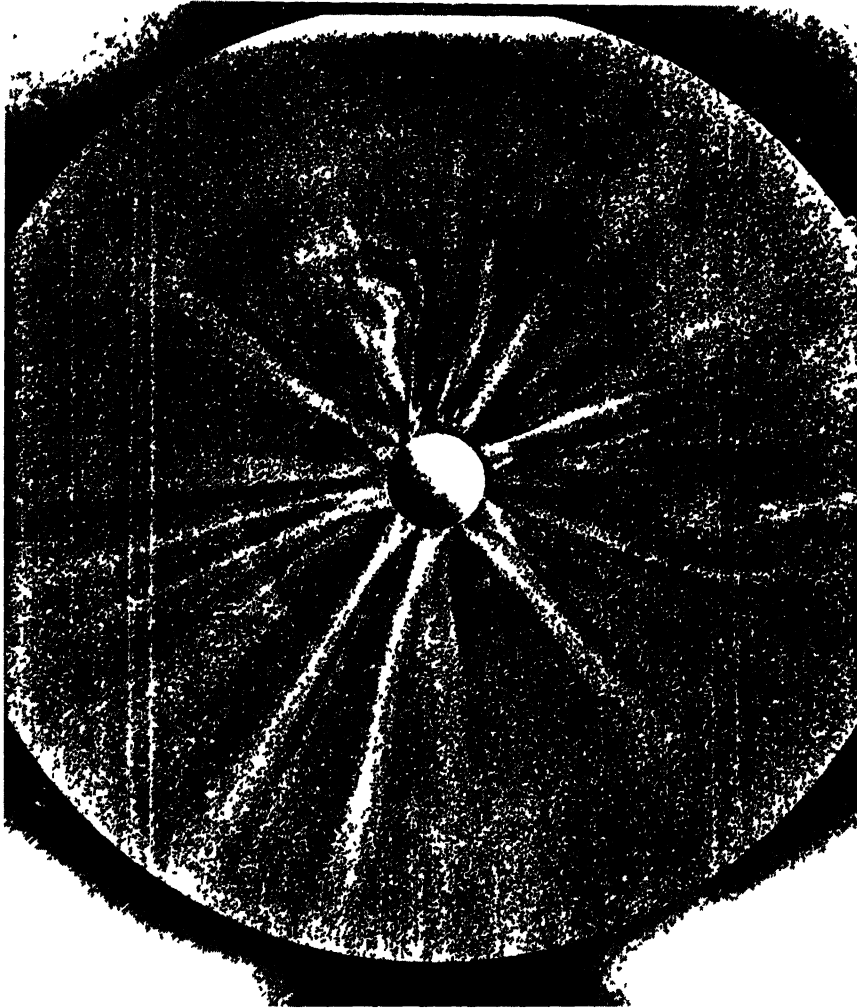


FIG 2 Coronal photograph from the 16 February 1980 Airborne Eclipse Expedition of the Los Alamos National Laboratory, University of California

This is a print of a computer-developed 35mm negative which resulted from addition of thirty two exposures made during the Eclipse from the LANL-USAF NC-135 jet aircraft at an altitude of 11km over the Indian Ocean. Altitude of the sun was  $79^\circ$ .

Heliocentric North is approximately at top. West is at right.

Each of the 32 negatives was digitized into a  $1000 \times 1000$  point matrix. These matrices were then processed by two computer filters. The first evened the large radial density gradient and the smaller azimuthal variation. The second was a high pass Fourier transfer filter which further enhance streamer detail. All bright circles are artifacts of the radial filter. A wealth of complex streamer detail is apparent out to  $12 R_\odot$ . Viewing the print from a distance helps to show low contrast detail such as the possible second outer envelope surrounding the large coronal transient arising from the west limb. Note also a possible outer transient above the south pole. Scale— $8.2 \text{ mm}/R_\odot$ , Lunar mask  $-1.2 D_\odot$ . (Computer generated)

During that time, the eruption would have moved beyond range of observation from the ground. If the velocity of expansion is nearly constant during its lifetime, the disturbance must have begun just as the eclipse was arriving on Africa's west coast, about 90 minutes before we saw it. We are at present trying to obtain good photographs taken from Zaire and Tanzania to study the earlier phases of the event.

Such eruptions are apparently quite common. They are estimated to have occurred at least once a day in 1973 during low solar activity and perhaps three times more frequently during this past year's maximum solar activity. Each one typically ejects a mass of about  $10^{13}$  kg and an energy of  $10^{24}$  J. The apparent rate of occurrence would make them responsible for at least 10 per cent of the entire solar mass efflux!

We also obtained camera-polarimeter images and Fe XIV emission line profiles of the eruption. Its Thompson-scattered light is highly polarized so we will be able to determine electron densities and its base appears to have the most intense green line (Fe XIV) emission in the corona. We anticipate that these measurements and our photographs, which together comprise a wealth of interconnected information, will answer several questions about these important sources of solar wind.

#### ELECTRON DENSITY EXPERIMENT

The scattering process that produces the K corona, namely, Thompson scattering of photospheric light by electrons, is independent of wavelength and depends only on electron density. K coronal intensities are thus a direct measure of electron densities. Since we can measure only total white light intensities (K+F corona), we need a method to subtract the unwanted F coronal light.

Much of the K coronal light we observe during an eclipse has been scattered through angles near  $90^\circ$ . The K corona is therefore highly polarized, whereas the F corona is not. The two components can be separated by measuring both the absolute intensity of the K+F corona (K+F) and the fraction and direction of polarization at each point on digitized images. The measured fractional polarization can be written

$$P_{\text{total}} = \frac{P_K K}{K+F},$$

where  $P_K$  is the fractional polarization of the K corona, and K and (K+F) are the K coronal intensity and total white light intensity, respectively. Data reduction to determine K requires a model of the corona. We assume that the corona has cylindrical symmetry and that its density varies smoothly between polar and equatorial regions. From this model, we calculate  $P_K$  and K and compare them with the measured quantities  $P_{\text{total}}$  and (K+F). Finally, we vary electron densities in the model to obtain consistency between the two measured and two calculated quantities.

Photographs of the K+F corona are taken with a camera-polarimeter through plane polarizing filters oriented at three different angles. A fourth photograph taken without any polarizing filter completes a set. During the 1980 eclipse, we made 10 sets of photographs using high-resolution film for the bright inner corona and very fast low-resolution film for the outer corona. This is the first time we have taken special care to get high-resolution data from the inner corona.

The camera and its centre-of-mass, three-axis gyro-stabilized tracking system were designed and built at Los Alamos. With this tracking system, motion during a



3-second exposure was less than 20 arc seconds. Our polarization data extend out to  $12 R_{\odot}$  in the equatorial region of the corona—much greater distances than have been achieved from ground observations during an eclipse or from Skylab observations outside of eclipse. In the 1979 and 1980 eclipses we were able to make two exposures out to  $20 R_{\odot}$ .

We have made similar measurements using the same instrument at five times during the sun's 11-year magnetic activity cycle (1970, 1972, 1973, 1979, and 1980). We thus have a very uniform set of data with which to compare variations in coronal structures, brightness, electron density, and material distribution as a function of solar activity.

For instance, standard observational models of coronal brightness indicate a marked variation between maximum and minimum solar activity. We are unique in being able to verify this variation for the inner corona (out to 3 or 4  $R_{\odot}$ ) and to extend it reliably to  $12 R_{\odot}$ .

#### Results of 1973 Electron Density Experiments

In recent years, the 1973 eclipse was the most widely observed both from the ground and in space. Figs. 3a and b show plots of absolute intensity of the corona

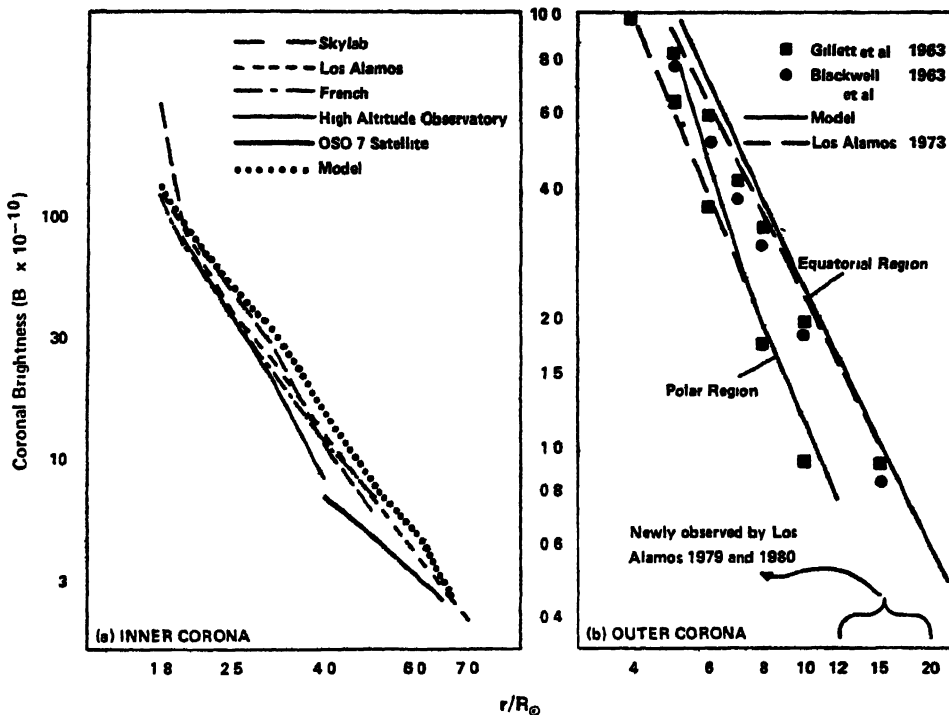


FIG 3 Various observations of coronal brightness versus intensity for (a) the inner Polar corona and (b) the outer corona. Also shown in both cases is the brightness calculated from a consensus model [Blackwell *et al* (1976)]. Figure 3a is a unique comparison of cospatial, cotemporal observations from two ground-based, one airborne, and two space experiments. Only the Los Alamos data cover the entire range of comparison, and the Los Alamos 1980 data, when reduced, will extend observations to  $20 R_{\odot}$  for the first time since 1963.

(K+F) as a function of radial distance in the inner and outer corona, respectively. Also included in these plots is the consensus model K+F brightness based on pre-1965 eclipse data. Fig 3a is a comparison of results from five independent observations of the 1973 eclipse: two from the ground, two from space coronagraphs, and one from the Los Alamos airborne expedition. Only the Los Alamos data extend over the entire range shown and beyond.

In comparing our results for the 1973 eclipse with those of Skylab's Apollo Telescope Mount, we were puzzled to find the Skylab values of coronal brightness disturbingly higher than ours. Upon careful examination of Skylab reduction pro-

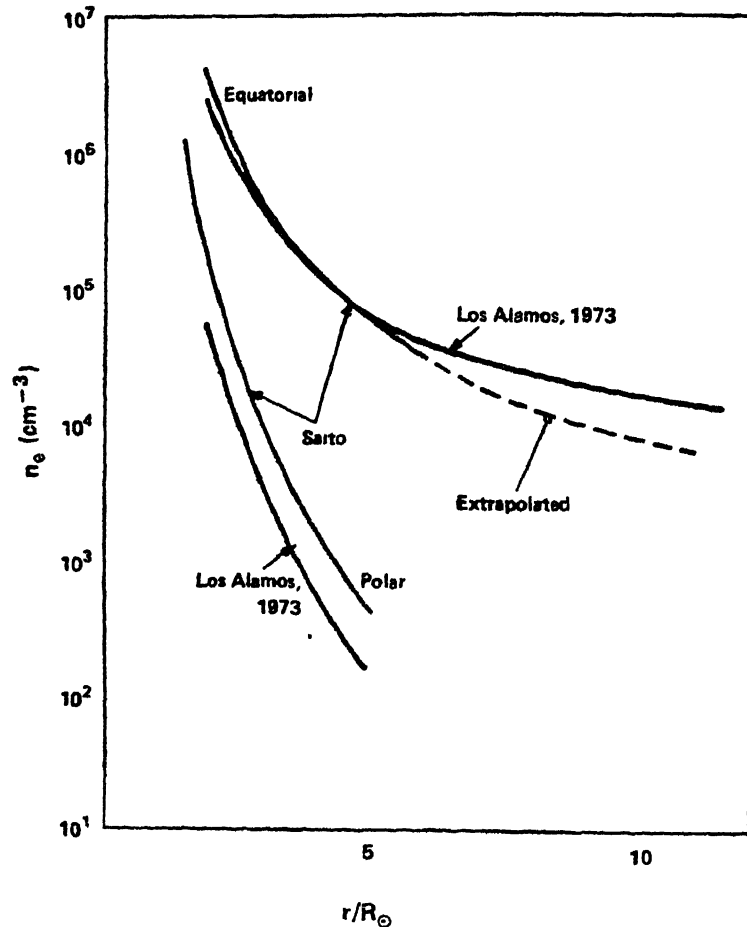


FIG. 4 Electron density as a function of radial distance determined from photographic polarization data gathered during the Los Alamos airborne expedition of 1973. The results of K. Saito, a respected ground-based observer, are shown for comparison. Photographic polarization data for the polar regions are reliable only to about  $3-4 R_{\odot}$ , whereas absolute intensity data (see Fig 3) are good beyond  $10 R_{\odot}$ . We differ from Saito's results in equatorial regions beyond  $4 R_{\odot}$  primarily because the reduction in atmospheric contamination realized by our airborne expedition permitted us to acquire good polarization data to  $12 R_{\odot}$ , as compared with the limit of  $5 R_{\odot}$  for ground-based observations.

cedure, we discovered an error in absolute calibration that resulted in a 9 per cent reduction of all Skylab values of coronal brightness. This transfers roughly to a similar reduction in all published results prior to 1978. The intensities plotted in Fig. 3a have been corrected for this error.

Fig. 3b compares Los Alamos data for the outer corona with the two best recent observations of that region.

Fig. 4 shows our 1973 results compared with those from K. Saito's ground-based observations (Saito, 1972). Because of sky background brightness, ground-based observations seldom are reliable beyond  $5 R_{\odot}$  in equatorial regions and  $3 R_{\odot}$  in polar regions, but the Los Alamos intensity data appear excellent beyond  $10 R_{\odot}$ . Polarization measurements in the equatorial regions are also good to this distance, but over the sun's poles the K corona is so faint that polarization falls below the limit of photographic detectability at  $4 R_{\odot}$ . We measure a fainter corona in polar regions than Saito does and therefore conclude that electron densities in polar coronal holes are lower than previously thought.

In equatorial regions the situation is more complicated. We find coronal intensity to be lower, but we measure higher polarization beyond  $4 R_{\odot}$ . Our measurements suggests that in equatorial regions electron densities beyond  $4 R_{\odot}$  are higher and, more significantly for solar wind models, do not fall off as fast as we proceed outward from the sun. We also observed this significant result at the 1970 and 1972 eclipses.

We look forward to comparing electron densities from the 1973 eclipse with those of the 1980 eclipse as soon as our 1980 data have been reduced and evaluated.

Preliminary analysis of our 1980 intensity data shows that the corona was about three times brighter than it was in 1973, and that polar regions are as bright as equatorial regions out to  $5 R_{\odot}$ , where the F corona begins to dominate (*see* Fig. 5).

#### *Emission Line Experiment*

We consider the coronal emission line experiment to be the most important aboard the aircraft because the measured line profiles contain a wealth of information on the state of the coronal plasma. The shape of the line profiles can be analyzed to yield ion temperatures and nonthermal components of the velocity distribution. The variations of line intensity with position, or with time, contain information about the mechanisms that excite the emitting ions. Bright features in or near the plane of the sky (plane through the sun's centre perpendicular to the line of sight) easily contribute the major portion of our measured signal along a line of sight because emission line intensities fall off very rapidly with distance from the sun. Therefore, we can attribute measured signals to specific coronal features with a fair degree of confidence.

Since 1965, we have made airborne measurements of the Fe XIV green line intensity and wavelength broadening using a Fabry-Perot interferometer to obtain spectral (wavelength) resolution. We chose an interferometer for several reasons. It is a relatively small instrument well suited to the space constraints aboard the aircraft. It also has a high spatial resolution, in part because it preserves a two-dimensional image rather than the one-dimensional images obtained from grating spectrographs and other instruments that pass the incoming light through a slit. Perhaps most important, spectral distortions introduced by the interferometer can be calculated

quite accurately and subtracted from the measured line profiles, enabling us to achieve very high spectral resolution.

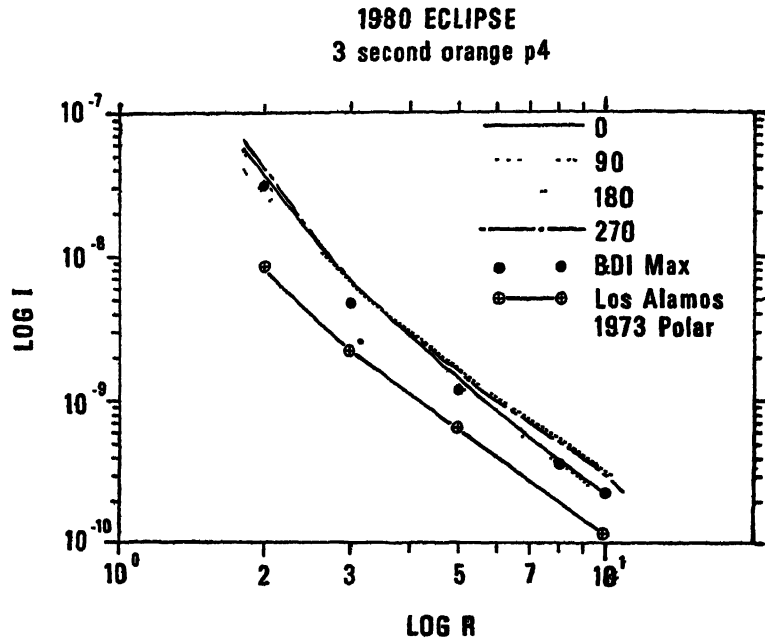


FIG 5 Preliminary results from 16 February 1980, plotted in the same way as Fig. 3. (Numbers on graph denote heliocentric azimuth)

In 1973, we scanned the entire corona out to  $2.5 R_{\odot}$  with a spatial resolution of 15–20 arc seconds. We measured very weak polarization of the green line along radial vectors from the sun. Weak polarization implies that green line emission is excited by electron collisions rather than the absorption of photons. This result confirms expectations that electron collisions are the dominant mechanism by which energy is distributed in the inner corona. We also observed that Ca XV yellow line emission occurred over a much larger region of the lower corona than previously expected. The presence of the yellow line was thought to signify very hot regions of the corona, corresponding to the 4–5 MK ionization potential maximum of the Ca XV ionization state, but the 1973 line widths indicate that the yellow line is produced in cooler regions as well, and thus that coronal temperatures may be much more uniform on a scale of arc minutes than had been guessed from other emission line measurements.

Our 1980 data are much more extensive and have a much higher spatial resolution than that from previous eclipses.

Light from the 1980 experiment was collected by the "Rube Goldberg," a massive 10-inch telescope with an 80-inch focal length that has been used aboard the aircraft since our 1965 expedition. Emission line signals, imaged by the telescope and interferometer, were amplified and recorded on videotape at 16ms intervals from an image-intensified vidicon detector. This rapid data acquisition system, a dramatic improvement over the 30-second exposure times required by photographic techniques, collect-



Data from the 1980 measurements are much easier to reduce than those from previous eclipses. Preliminary results show wide variations in line shapes and are suggestive of the turbulent conditions that may be present during a solar maximum. We also see many details within small regions of high activity. However, data reduction must be completed before we can make definitive interpretations.

### *Interpreting Emission Line Profiles*

Both line shapes and line intensities are analyzed to learn about the conditions in the coronal plasma. Since the intrinsic line widths (from ions at rest) are extremely narrow, the observed Doppler-broadened line profiles are identical in shape to the velocity distribution of the emitting ions.

For ions in thermal equilibrium, both the velocity distribution and the emission line profile would be Gaussian in shape. The width of the line profile would then be proportional to the kinetic temperature of the emitting ions. However, ion temperatures deduced directly from observed Gaussian line profiles (for example, the ion temperatures shown in Fig. 1) may be too high because nonthermal effects, such as macroscopic turbulence and magnetic wave acceleration of the solar wind, may add to the velocities of the ions and, in turn, to the line broadening.

An approximate expression for the line width in terms of the kinetic temperature  $T$  and the average turbulent macroscopic velocity  $v_t$  is given by

$$\frac{\Delta\lambda}{\lambda} \propto \left( \frac{T}{m} + v_t^2 \right)^{1/2}$$

where  $\Delta\lambda$  is the full width of the line profile at half-maximum intensity and  $m$  is the mass of the emitting ion. Note that the kinetic temperature contribution depends on the mass of the ion, whereas the contribution from macroscopic turbulence is mass independent. Therefore, it is possible to separate thermal and turbulent contributions to the line broadening by measuring emission line profiles of two ions with widely differing masses. But these measurements must be made at the same time and at the same place in the corona so that we can assume that the two ions have the same kinetic temperature and average turbulent velocity  $v_t$ .

Our Ca XV data from the 1980 eclipse may be appropriate for comparison with our Fe XIV measurements, but the emission was weaker than expected and so the profiles may not be accurate enough. However, the Lyman- $\alpha$  data recorded by rocket experiments at several places in the corona will certainly be useful in determining nonthermal contributions to our Fe XIV line profiles.

Variations in line shape are also indications of nonthermal velocities. For example, calculations show that large expansion velocities from solar wind flow tend to flatten and extend what would have been a Gaussian line shape. Although these departures are not significant until expansion velocities are 40 km/s or greater, such velocities are predicted by some models of solar wind flow at distances of 2–3  $R_\odot$ . The line profile shapes are also altered by large-scale turbulent motion or significant magnetic wave acceleration of the plasma.

Fig. 7 illustrates the variety of line shapes that were actually measured in 1980. We see asymmetries, as well as departures from Gaussian shapes. Interpretation of these line shapes depends on theoretical assumptions and supporting data, except

perhaps for the case of split lines, which clearly indicate relative bulk motion of the emitting material.

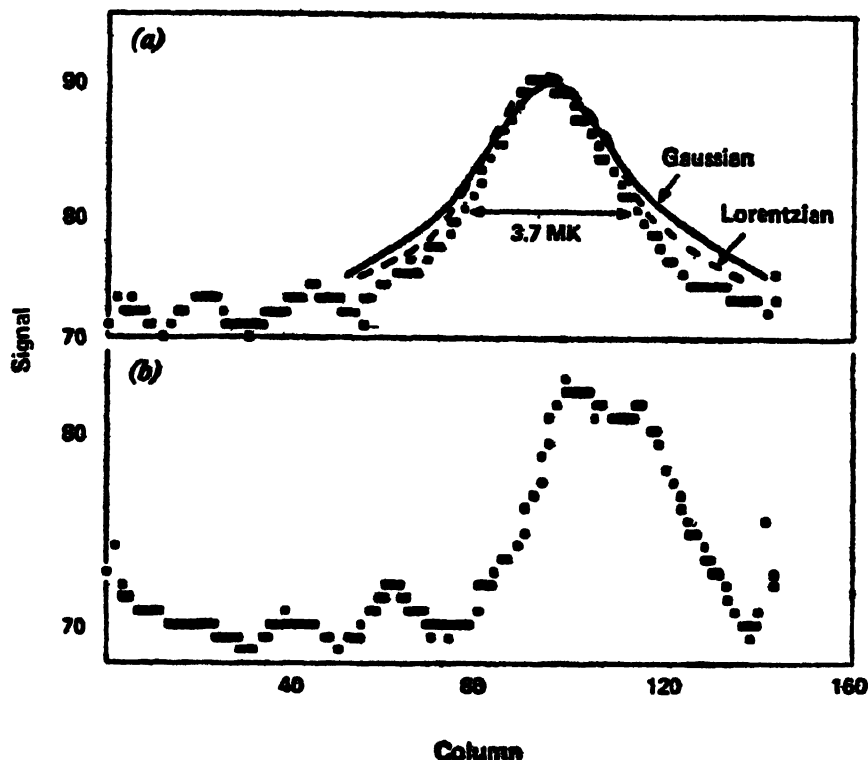


FIG. 7. These preliminary 1980 Fe XIV emission line profiles were obtained by digitizing a sequence of video frames and reordering the data to give a signal versus frame number (or wavelength) profile of the intensity at a single pixel (corresponding to a single spatial location in the corona). In (a) we have fitted both a Gaussian and a Lorentzian profile to the emission line such that the full width at half-maximum intensity and the peak intensity agree with observations. The wings of the observed line are not fitted by either profile. In (b) an example of a more complicated emission line is shown. This profile could represent coronal material with significantly different velocities along the line of sight. A relative velocity of about 15 km/s would fit this profile. Some further corrections for intensity and wavelength calibration will be applied to these data before our analysis is complete.

Analysis of line intensities can also be quite revealing. Since emission intensity depends on density and temperature, comparison with independent electron density measurements is helpful in deciding whether bright regions are due to high temperatures or, alternatively, to high densities. We can also analyse intensity variations as a function of radial distance to infer excitation mechanisms. If ions are excited by electron collisions, intensities are proportional to the square of the electron density ( $n_e$ )<sup>2</sup> and thus should decrease as  $1/r^{12}$ . On the other hand if photon excitation is the dominant mechanism, then line intensities are proportional to  $n_e$  and thus decrease as  $1/r^6$ .

## ELECTRON TEMPERATURE EXPERIMENT

Coronal electron temperatures as a function of radial distance are badly needed to determine whether electrons and ions are in thermal equilibrium. In 1976, L. E. Cram suggested a method to determine these temperatures from spectral intensities of the K corona. Our 1980 attempt to perform the measurement used a much more sensitive technique than has been tried before and, although we failed to record data, we did confirm the feasibility of the technique.

The principle behind the experiment is based on Cram's analysis of the K coronal spectrum. This spectrum is formed as light coming from the photosphere (the Fraunhofer spectrum) is scattered by energetic coronal electrons. The Doppler shifts suffered by these scattered photons broaden the absorption lines in the original Fraunhofer spectrum to produce the diffuse spectrum known as the K corona.

Cram's calculated spectra for a spherically symmetric, isothermal corona at four electron temperatures are shown in Fig. 8. His results display two very interesting

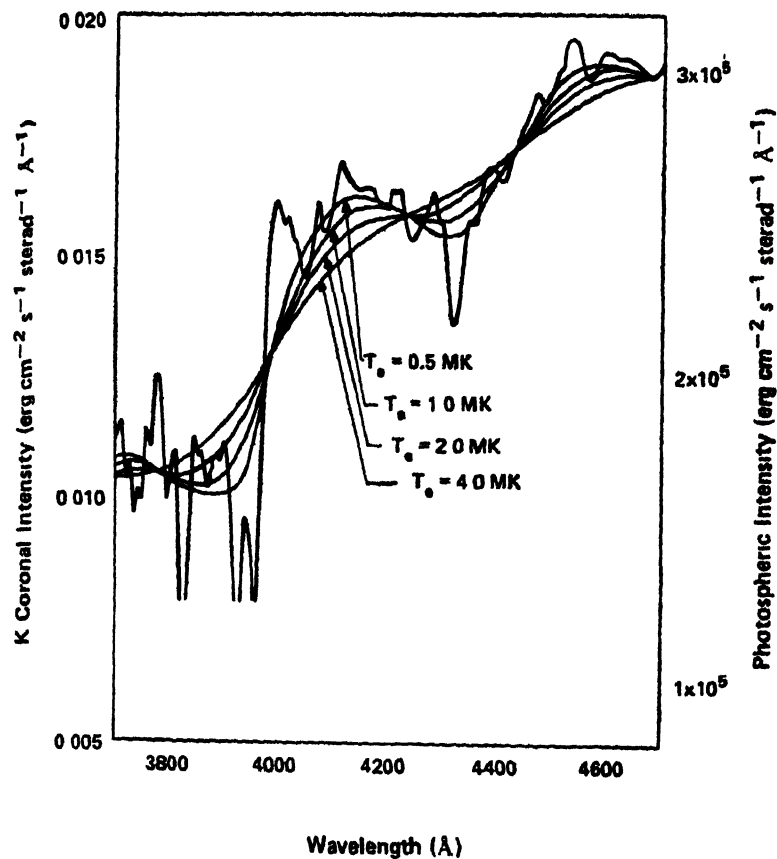


FIG. 8. Absolute intensity of the K coronal spectrum for four coronal electron temperatures, as calculated by Cram. The absolute intensity of the photospheric spectrum from the centre of the sun's disc is shown for comparison.



features. First, there exist spectral "nodes," that is, wavelengths at which the intensity is independent of the assumed electron temperature. These nodes occur on either side of the H and K absorption lines of Ca II and near other absorption features of the Fraunhofer spectrum. Second, the spectra undulate about these nodes with an amplitude that is related to the electron temperature. Thus, the ratio of two measured intensities, one at a nodal wavelength and one at a wavelength nearby, should determine the electron temperature uniquely.

Although such an experiment is very simple in principle, in practice it is quite difficult because the intensities must be measured with great precision. An error of  $\pm 0.2$  per cent in the intensity ratio translates to an uncertainty of  $\pm 0.1$  MK in coronal electron temperature. The 5–10 per cent errors common in standard photometric techniques would obliterate the information sought [as learned by Menzel and Pasachoff (1968) who searched without success for residual depressions from the H and K absorption lines of CA II in photographic records of absorption spectra from the 1936 total eclipse].

To achieve the required sensitivity, we built our instrument around the only type of detector suitable for the task—an array of silicon photodiodes. These solid-state photosensitive devices have very high quantum efficiency in the spectral range of interest.

A commercially available detector, consisting of a linear array of 512 silicon photodiodes on a single integrated circuit, served as the main component of our K corona spectrograph (Fig. 9). This large array enabled us to look not just at two wavelengths but at wavelengths of the K coronal spectrum over a  $1500\text{\AA}$  range with  $3\text{\AA}$  resolution.

The experiment was in some sense a fishing expedition. We set out to observe the entire spectrum with high precision and search for Cram's predicted undulation patterns at three radial distances from the sun.

During the eclipse, the spectrograph appeared to function well, and we were able to confirm that its sensitivity is adequate to measure the shape of the K coronal spectrum and, in principle, to determine electron temperatures. The data that appeared on our monitoring screen were not recorded by our computerized data-acquisition system because both the computer disc drive and the back-up drive failed to function.

Indeed the equipment failure was a tremendous disappointment, but we did prove that the experiment was feasible, and are now redesigning some of the electronics with hopes of flying again during the 1983 solar eclipse.

#### *Infrared Observations of Dust Rings*

The F corona and the zodiacal light, a zone of scattered light symmetric about the approximate plane of the planetary orbits, give clear evidence of the presence of dust throughout much of the solar system. These observations also indicate that the dust particles are very fine—only a few micrometers in diameter. Their presence may be a remnant of the formation of the solar system but probably wandering comets have also left a contribution.

Whatever the source, theorists have modelled the fate of the dust once it is deposited in the solar system. The dynamics of the dust particles is influenced by four factors: the sun's gravity, radiation pressure, the Poynting-Robertson effect, and

particle evaporation. Calculations including these factors indicate that the dust will spiral in toward the sun but may ultimately settle at particular distances and form broad rings about the sun. Evaporation of the dust may also lead to its being blown outward once again. By determining the radial location of these rings we learn something about the dust's composition because its location depends on its reflectivity and evaporation temperature. Likely compositions include obsidian, silicate-type rock, iron, and perhaps water-ice.

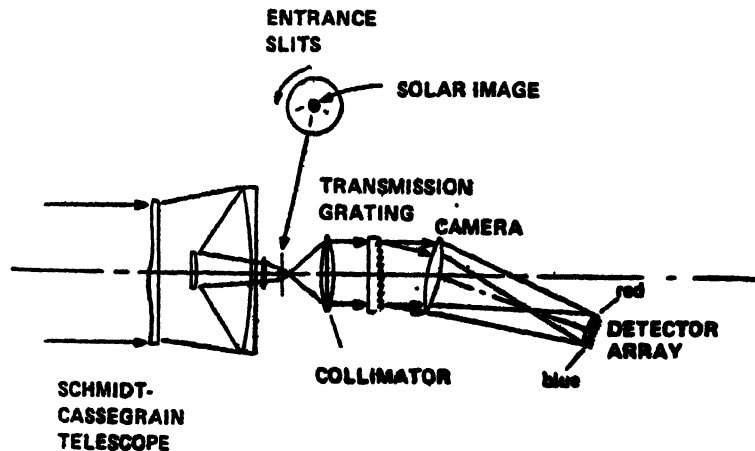


FIG 9. The K corona spectrograph for the electron temperature experiment consists of a telescope, entrance slit assembly, a transmission grating spectrograph, a silicon photodiode detector array, and electronics for data acquisition and storage. The  $f/2.0$ , 400-mm focal length telescope maximizes the light at the detector. Three entrance slits, corresponding to radial distances from the sun of 1.2, 1.6 and  $2.0 R_{\odot}$ , were formed by photolithographic techniques on a glass disc. A computer-controlled lever-arm and motor-drive assembly positions the selected entrance slit in the telescope focal plane. The entrance slit length is magnified by the spectrograph to match and thereby utilize the entire photodiode length. The spectrograph covers  $1500\text{\AA}$  and its resolution is  $3\text{\AA}$  per channel. Exposure times range from 10 seconds at  $1.2 R_{\odot}$  to 40 seconds at  $2.0 R_{\odot}$ . Satisfactory data can therefore be obtained only during eclipses of relatively long duration or from aircraft whose flight path lengthens the duration of totality.

The presence of glowing dust rings at 4, 9, and  $20 R_{\odot}$  and elsewhere has been deduced from observations of infrared emission features. These emission features are presumably produced as dust particles heat up and evaporate, emitting radiation corresponding to black-body temperatures between 500 and 2000 K. These observations are difficult to make from the ground and, with the exception of the features at  $4 R_{\odot}$ , the existence of these features is in dispute.

From aboard the aircraft during the 1980 eclipse, we made a new attempt to determine the spatial distribution of infrared emission features.

Infrared intensity as a function of distance from the sun was measured at  $2.2\text{ }\mu\text{m}$  with an InSb detector, a standard technique, and at  $\sim 0.7\text{ }\mu\text{m}$  with a charge-injection-device television camera.

The corona was scanned along the ecliptic (plane of the earth's orbit) out to

50  $R_{\odot}$  east and west of the sun and at several angles to the ecliptic. The scan pattern was designed to determine the radial location and approximate extent of any dust rings.

Both detection systems worked well and yielded high quality data. However, tracking errors during totality will severely compromise interpretation of data close to the sun, so we will not be able to confirm the existence of the feature at 4  $R_{\odot}$ . At greater distances, however, these errors have less effect.

Our analyses to date strongly suggest the existence of a dust ring at 9  $R_{\odot}$ , but indicate no other features at greater distances from the sun. Thus we find no feature at about 20  $R_{\odot}$ . A feature at this location, which corresponds to a temperature of  $\sim 800$  K, had been suggested by E. P. Nye on the basis of ground-level observations at the 26 February 1979 and 16 February 1980 eclipses; however, at both eclipses his observations may have been contaminated by the effects of clouds. Existence of such a feature would be of interest because dust shells with temperatures of  $\sim 800$  K have been found about some other stars.

### CONCLUSIONS

Most scientists studying the solar corona believe that a temperature maximum exists near 2  $R_{\odot}$ . Our results indicate that the maximum might be closer to the limb, although some of the Fe XIV emission line broadening can always be attributed to large-scale turbulence or to expansion velocities. However, comparison with proton temperature values from the rocket-borne coronagraph at a few positions in the corona will allow us to determine such velocities if they exist. We can then interpret the rest of our iron emission line data in the light of these findings. The fact that many of our 1980 profiles are actually double-peaked indicates large differential mass motions that are probably due to the extremely complex nature of coronal features during maximum solar activity.

Ion temperature gradients measured in 1965 indicated that coronal holes could support solar wind flow. We now have high-resolution data from our 1980 measurements of the residual coronal hole above the sun's south pole to compare with the 1965 results. We will also be able to analyze temperature gradients and velocity distributions in streamer structures, to determine whether these structures also contribute to solar wind flow.

Our emission line intensity data from several previous solar eclipse observations suggested that collisional mechanisms dominate energy transport in the lower corona out to 2  $R_{\odot}$ . Our high-resolution 1980 data from several streamer structures and one coronal condensation, when combined with electron densities determined from camera-polarimeter measurements, will be a better test of this model.

The possibility of extended wave heating in the corona has become increasingly significant. Our emission line intensity data from the 1973 Concorde flight, which gave 74 minutes of totality, provided tentative evidence for periodic temperature variations, and in 1980 we looked for temporal changes on the sun's west limb by taking a sequence of intensity measurements at 30-second intervals over the 7 minutes of totality. But a more extensive search will be required to establish the dynamics and the extent of plasma heating.

Comparison of the computer-enhanced coronal photographs from five eclipses shows that the corona at the 1980 eclipse exhibited features never before seen, including the umbilical connection of the hydrodynamic eruptive disturbance to the solar surface. This observation calls into question previous speculation, based on Skylab photographs down to  $1.5 R_{\odot}$ , that the connection to the surface was quite broad. Evidently, the energy source for some mass eruptions is localized and concentrated. We may learn more about the dynamics at the base of this disturbance once our electron density and Fe XIV data have been reduced.

Our photographic record also shows that nearby streamers respond to the eruption by bending around it, an effect also seen on Skylab photographs but only out to  $6 R_{\odot}$ . The curious shape of long streamers above the sun's south pole suggests that a second eruptive disturbance may also have been in progress at the same time.

Electron densities resulting from our observations agree with other studies in the inner corona, but beyond  $4 R_{\odot}$  in equatorial regions the density decrease with radial distance is much more gradual than indicated previously. This could have a marked effect on theoretical models of the solar wind.

In summary, we now have collected ion temperature and electron density data at all phases of solar activity except during a deep minimum. Our 1980 data combined with proton temperatures from rocket experiments will provide a focal point for all future analysis. For the first time, we will have an accurate determination of material density, ion temperatures, and nonthermal velocities at several places in the corona. We hope these results will be a basis for more meaningful interpretation of our data throughout the rest of the inner corona.

#### REFERENCES

- Blackwell, D., Denhurst, D., and Ingham, M. (1976) The zodiacal light. In: *Advances in Astronomy and Astrophysics*, 1.
- Cram, L. E. (1976) Determination of the temperature of the solar corona from the spectrum of the electron-scattering continuum *Solar Phys.*, 48, 3-19.
- Menzel, D. H., and Pasachoff, J. M. (1968) On the obliteration of strong Fraunhofer lines by electron scattering in the solar corona *Publ. astron. Soc. Pacific*, 80, 458.
- Saito, K. (1972) *Ann. Tokyo Astron. Observ.*, 13, 93.

Printed in India.

Astronomy

## MULTICOLOUR PHOTOMETRY OF THE CORONA

J. DÜRST

*Institut für Astronomie ETH, CH-8092, Zürich, Switzerland*

*(Received 7 August 1981)*

During the eclipse of 16 February 1980, colour photos were taken in order to determine the colour of the F-corona and to detect concentrations of dust located a few solar radii from the Sun. Such concentrations would scatter the sunlight at high scattering angles giving rise to colour differences compared to the normal F-corona. The advantages and disadvantages of colour films for eclipse photometry are discussed and a new type of eclipse camera is described.

**Keywords:** Solar corona; Interplanetary Dust; Eclipse Photography; Colour Films

### INTRODUCTION

MULTICOLOUR photometry of the corona gives information mainly about the dust-corona because the physical processes giving rise to the dust-corona are wavelength dependent. These processes are thermal radiation and scattering of sunlight. On the other hand, the electron corona is produced by Thomson scattering and therefore shows no or only small colour effects. Nevertheless multicolour photometry can also be a useful tool to distinguish between coronal and chromospheric features (Koutchmy & Stellmacher, 1976).

### SCIENTIFIC PURPOSE

The following well-known observations gave rise to the present experiment: At the 1970 eclipse several groups have observed diffuse enhancements in the outer corona at  $R \sim 4 R_{\odot}$  (Koomen *et al.*, 1970; Lilliequist & Schmahl, 1970; and Koutchmy, 1972), and at the 1966 eclipse maxima of thermal radiation were detected again at  $R \sim 4 R_{\odot}$  (Peterson, 1967; and Mac Queen, 1968). For a smooth distribution of the dust, calculations of F-corona radiation (Peterson, 1963) predict no large colour effects in the visible light and for  $R < 4 R_{\odot}$ . On the other hand, calculations about dust dynamics (Lamy, 1974) and colour observations during the 1970 eclipse (Ajmanov & Nikolsky, 1980) show evidence for dust concentrations. If such concentrations at  $R \sim 4 R_{\odot}$  exist, they would scatter the sunlight at scattering angles  $60^{\circ}$ – $90^{\circ}$ , in contrast to the light of the normal F-corona which is scattered at small angles. These two components may be detected by colour differences. The purpose of the eclipse experiment is therefore to derive a map of colour indices of the corona, in order to find a correlation between colour and intensity of the F-corona at a certain distance from the Sun's centre. At present, definitive results are not available

## OBSERVATIONAL METHOD

From previous observations (Koutchmy, 1972) one can expect that the brightness of diffuse enhancements is about 15–20 per cent of the total light observed at  $R=4R_{\odot}$ . Hence, photographic photometry with an accuracy of 1–2 per cent is a useful observing method. The dynamic range of the film, assuming such an accuracy, is only about 1 to 10 and consequently, a radial gradient filter has to be used, reducing the bright inner parts of the corona.

Photometry of the outer corona does not require high resolution, but to bring out interesting features that may occur in the inner corona, the camera should have a resolution of 1–2" in the inner parts. Colour films are sensitive from 400nm up to 700nm which means that achromatic doublet lenses, widely used for eclipse photography, are not suitable for colour photography and so an apochromatic triplet lens  $f=1.9\text{m}$ ,  $N=15$  was selected. The most disturbing defects of such a lens (as of all "thin" lenses) are astigmatism and field curvature producing elliptical image points with long axis in radial direction. Field curvature can be corrected by a plane concave lens at the focal plane reducing the errors by a factor 4 in radial direction. In our camera this lens is cemented to the radial-gradient filter and placed against the film during exposure (Fig. 1).

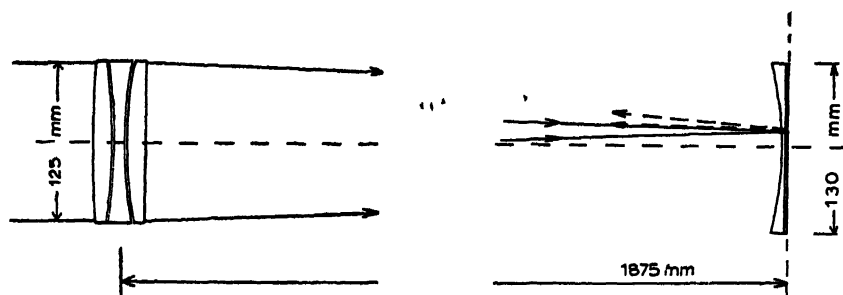


Fig. 1. Eclipse camera consisting of apochromatic triplet lens ( $F=1875\text{ mm}$ ,  $D=125\text{mm}$ ) and a plane concave field-flattening lens ( $D=130\text{mm}$ ) cemented to the radial gradient-filter. The field-flattening lens has the additional effect to refract the light reflected by the aluminium layer of the gradient-filter, toward the tube of the camera. The gradient-filter is placed against the film during exposure, securing exact position of the film.

## COLOUR FILM FOR THREE COLOUR PHOTOMETRY

Until now colour films have not been widely used for quantitative photometrical work because the 3 layers of the film are not completely independent. In the first place, the sensitivity ranges overlap and secondly, the absorption curves of the dyes in the 3 layers also overlap (Fig. 2). If for instance we would like to determine the amount of cyan dye (produced in the third layer) by measuring the absorption of monochromatic light near the absorption maximum of cyan, magenta and yellow dye give also small contributions. These effects have to be carefully considered by distinguishing between analytical and integral densities.

If at the film element  $(x, y)$  only one film layer is exposed, e.g., in a calibration

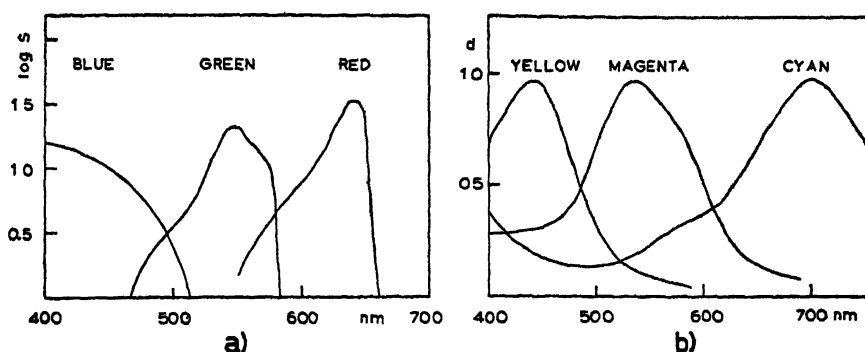


FIG. 2. Relative spectral sensitivity of the three layers of Agfachrome 50 S reversal film (a) and spectral absorption of the dyes produced in the layers of Agfachrome 50 S (b).

spectrum, we measure analytical densities  $d_A$ . From  $d_A$ , the exposure  $E$  can easily be derived as in the case of black and white film:

$$\begin{aligned} d_A^B &= \gamma_B \log E_B + c_1 \\ d_A^G &= \gamma_G \log E_G + c_2 \\ d_A^R &= \gamma_R \log E_R + c_3 \end{aligned} \quad \dots (1)$$

$\gamma_B, \gamma_G, \gamma_R$  are the local slopes of the characteristic curves,  $c_1, c_2, c_3$  are constants. B=blue, G=green, R=red. The simple equations (1) are valid only in a small density range and in every case the connection between  $d_A$  and  $E$  has to be derived carefully.

If we have different colours at the film element  $(x, y)$ , e.g., in a coronal picture, we measure integral densities  $d_I$ . This is done by measuring the absorption of light having wavelengths near the absorption maxima of the dyes. The integral densities are composed of the analytical densities as follows:

$$\begin{aligned} d_I^B &= d_A^B + k_{12} d_A^G + k_{13} d_A^R \\ d_I^G &= k_{21} d_A^B + d_A^G + k_{23} d_A^R \\ d_I^R &= k_{31} d_A^B + k_{32} d_A^G + d_A^R \end{aligned} \quad (2)$$

$k_{ij}$  are the so-called interimage coefficients and they have to be measured for every film (Kovalisky, 1977; and Koutchmy, 1978). For instance,  $k_{12}$  is determined by measuring blue integral densities  $d_I^B$  for constant blue exposure and varying green exposure. Having determined the interimage coefficients and the integral densities, we have [for each filmelement  $(x, y)$ ] 3 equations for the 3 unknown analytical densities  $d_A^B, d_A^G$  and  $d_A^R$ . Again equations (2) are valid only in a small density range and hence, a radial-gradient filter is necessary for coronal photometry with colour films.





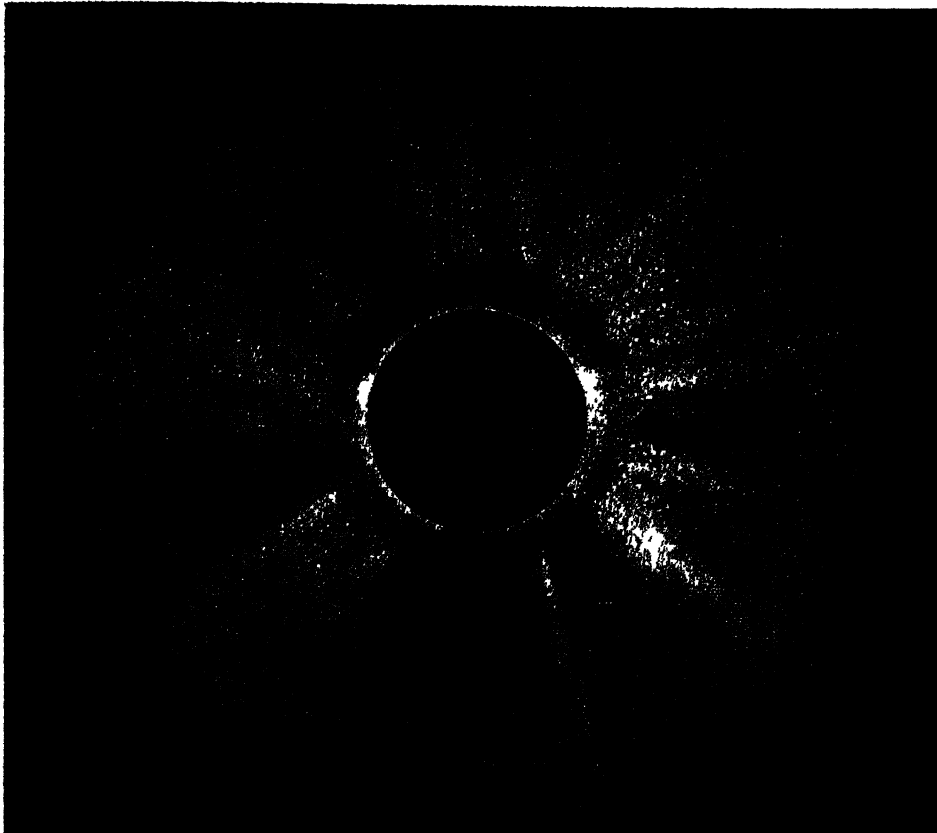


FIG 3 The corona of 16 February 1980 photographed on Agfachrome 50S reversal film with the camera described in section II. Exposure time 10s. The bright circle on the moon's disc is due to a central hole in the radial-gradient filter. This hole is useful in determining the exact position of the filter relative to the sun and measuring scattered light and sky background. The original features on the moon's disc, illuminated by earthlight, can easily be seen. This indicates that scattered light level is low. The colour difference in the innermost corona is an effect of the radial gradient-filter because at high densities the aluminium layer absorbs blue light more than red light.



Printed in India

Astrophysics

## OPTICAL STUDY OF THE SOLAR CORONA DURING THE TOTAL SOLAR ECLIPSE OF 16 FEBRUARY 1980

J N DESAI, T. CHANDRASEKHAR, K. C SAHU, H C BHATT *and*  
N M. ASHOK

*Physical Research Laboratory, Ahmedabad-380 009, India*

P D ANGREJI

*Vedhshala, Ahmedabad, India*

D B VAIDYA

*Gujarat College, Ahmedabad, India*

*and*

V B. KAMBLE

*Vikram Sarabhai Community Science Centre, Ahmedabad, India*

*(Received 7 August 1981)*

The Physical Research Laboratory, Ahmedabad, in collaboration with Vedhshala, Ahmedabad, and the Vikram Sarabhai Community Science Centre, Ahmedabad, conducted three optical experiments to study the solar corona during the total solar eclipse of 16 February 1980. The main experiment involved Fabry-Perot interferometry in the green coronal line  $\lambda 5303\text{\AA}$  to obtain Doppler temperature mapping of the corona. The other two experiments consisted of photography of the corona in

a)  $\lambda 5303\text{\AA}$  through a  $10\text{\AA}$  bandwidth filter and

b) white light photography with different orientations of a polaroid filter

Detailed microphotometry has been carried out on all the negatives. Coronal temperatures so obtained are between 2 to 4 million degrees Kelvin. There is an indication of a local temperature peak at  $1.1 R_{\odot}$  on several azimuths. The photometry of the monochromatic green line coronal brightness shows systematic though weak departures from linearity in  $\log I$  vs  $R/R_{\odot}$  plots which have a tentative explanation in magnetohydrodynamic wave propagation. The white light pictures have yielded polarisation values along several azimuths as a first step in the evaluation of electron density distribution of the corona.

**Keywords** Corona; Line-Width Temperature; Green Line; Fabry-Perot Interferometry

### INTRODUCTION

THE Physical Research Laboratory, Ahmedabad, conducted three optical experiments during the total solar eclipse of 16 February 1980, in collaboration with the

Vedhshala, Ahmedabad and the V A S Community Science Centre, Ahmedabad

These experiments were carried out at Gadag ( $15^{\circ}25'N$ ,  $75^{\circ}37'E$ ) in Karnataka close to the central line of totality, under the perfect sky conditions.

The experiments were

- 1 Fabry-Perot interferometry in the green coronal line ( $\lambda 5303\text{\AA}$ ) to obtain the Doppler temperature mapping of the corona
- 2 Photography of the corona in  $5303\text{\AA}$  through a  $10\text{\AA}$  bandwidth filter to construct a monochromatic intensity distribution of the corona in this line
- 3 Photography of the corona in white light with and without linear polariser to construct a polarisation map of the corona, and hence to determine the electron density distribution

#### DOPPLER TEMPERATURE MAPPING

Optically contacted Fabry-Perot etalon ( $300\mu\text{m}$  spacer) coupled with a  $7\text{\AA}$  bandwidth interference filter centred at  $\lambda 5303\text{\AA}$  produced fringes of the green line, which were subsequently photographed on precalibrated Kodak Tri X (400 ASA) 35mm film. A 15cm aperture f/15 lens served as the light collector. The centre of the Fabry-Perot fringe system was kept off centred with respect to the centre of the solar disc by  $\sim 20$  arc min to ensure some near radial fringes along certain azimuths and increased spatial resolution along other azimuths. Instrumental spectral resolution, as determined from the mercury green line fringes was  $0.23\text{\AA}$  in excellent agreement

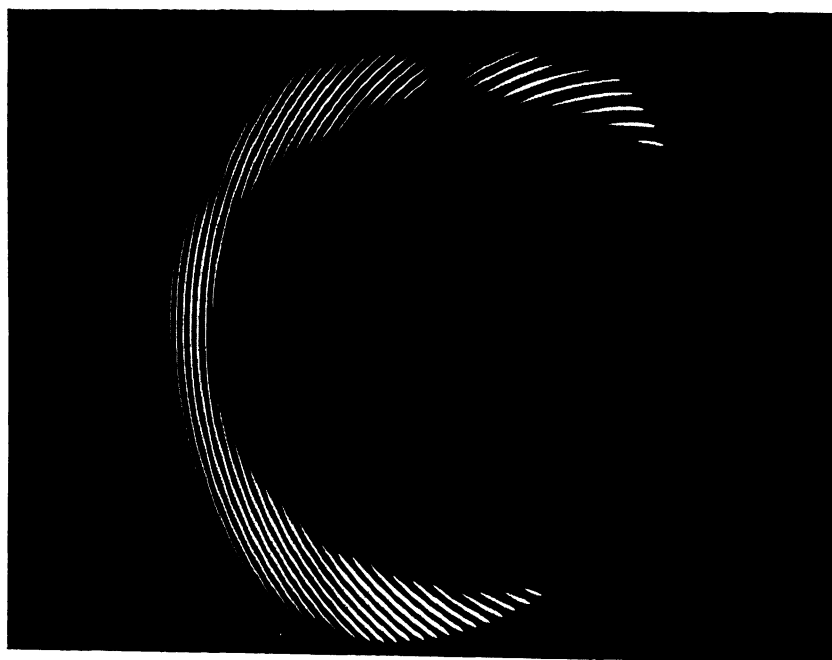


FIG 1 Coronal Interferogram (90 seconds)

with the theoretical one based on manufacturers specifications for the etalon (IC Optical Systems).

Four exposures viz., 10 sec., 90 sec., 30 sec., and 40 sec. respectively, were during the 2 minutes and 46 seconds of totality. A detailed microphotometer analysis of the coronal interferograms has yielded temperature map of the solar maximum corona covering  $270^\circ$  in azimuth ( $210^\circ\text{W}$  to  $120^\circ\text{E}$ ). For obtaining the temperatures, observed linewidths were deconvoluted using the experimentally measured instrument width with Hg green calibration. Fig. 1 shows the coronal interferogram (90 sec exposure) and Fig. 2 shows the temperature map.

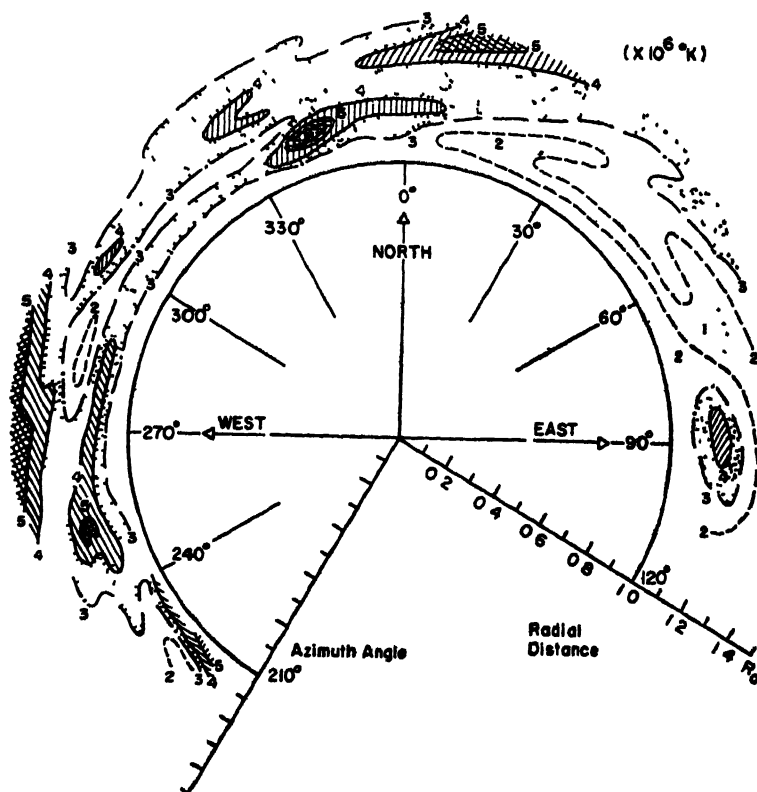


FIG. 2 Coronal temperature map.

The temperatures lie mainly in the range two to four million degrees Kelvin, though a few high values going upto five million Kelvin are noted. Along many azimuths, coronal temperatures rise upto a local peak value at  $1.1R_\odot$  before dropping off again.

#### MONOCHROMATIC ( $\lambda 5303\text{\AA}$ ) INTENSITY DISTRIBUTION IN THE SOLAR CORONA

The green line corona was photographed through a  $10\text{\AA}$  bandwidth filter centred at  $5303\text{\AA}$  using f/10 Celestron-8 telescope. Exposures of 5, 15, 15, 45 and 45sec. respectively were taken on a precalibrated Tri X film. Careful microphotometry was

carried out on the negatives to study the radial variation of the brightness of corona at that wavelength.

In general, the slope of  $\log I$  vs.  $R/R_{\odot}$  plot ( $I$ , brightness of corona in arbitrary units) was consistent with a mean temperature of about 2.4 million  $^{\circ}\text{K}$ .

A very interesting feature was observed at a specific azimuth ( $316^{\circ}$ ) where plot is shown in Fig. 3. Here, a wave like modulation, though weak is apparent on the general linear plot.

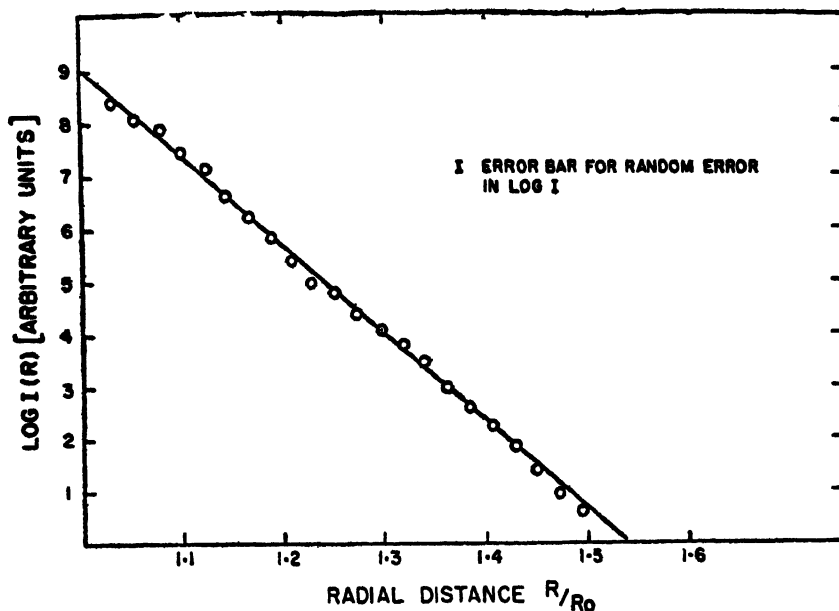


FIG. 3. Plot of  $I$  vs.  $R/R_{\odot}$  for  $\lambda 5303\text{\AA}$  corona at azimuth  $316^{\circ}$ .

The mean wavelength ( $\lambda$ ) observed is of the order of  $0.22 R_{\odot}$ . If one associates these oscillations with the known 5 minute periodicity photospheric oscillations of the Sun (Leighton *et al.*, 1962), then by putting  $T = \frac{\lambda}{V} = 300$  sec, one gets  $V \sim 500\text{ km/sec}$ . Since the phase velocity of the fast mode acoustic wave is given by

$$V > \frac{B}{\sqrt{4\pi\rho}}$$

where

$B$  = magnetic field in gauss

$\rho$  = plasma density in  $\text{gm-cm}^{-3}$ .

Putting  $N_e = 10^8 \text{ cm}^{-3}$  and assuming hydrogen plasma, one finds  $B \sim 2.3$  gauss. So one may conclude that within the reasonable uncertainty of coronal magnetic field values our observations are consistent with a hydromagnetic wave of 300 sec periodicity.

During the totality, successive exposures of 5sec, 15sec, 15sec, 45sec and 45sec were taken. Further, analysis of all these frames is in progress to ascertain the phase velocity and periodicity of the observed wave. Preliminary analysis shows that

the wave pattern is evident on all 5sec and 15sec exposures but not on 45sec exposures. This would imply a periodicity 90sec which is much less than the stipulated 300sec.

#### WHITE LIGHT CORONA WITH POLARISER

An 8.75cm f/16 Questar telescope was used to photograph the white light corona on a precalibrated plus X 35mm film. Photographs were taken at polaroid orientations of  $0^\circ$ ,  $45^\circ$ ,  $90^\circ$ ,  $135^\circ$  measured from a suitable reference plane. At each orientation 3 photographs were obtained with exposure times of  $\frac{1}{4}$ , 1 and 3 sec. respectively. Further photographs without the polariser were also taken with the same exposure times. The corona is seen to extend upto  $2 R_\odot$  from the limb in these photographs.

An extensive programme of digital microdensitometry has been carried out on all the Questar pictures. The resolution on the film is  $50 \mu\text{m}$  corresponding to  $0.07 R_\odot$  at the corona. Each frame has been divided into  $600 \times 500$  squares giving 300,000 grey levels. A computer analysis to separate the unpolarised F-corona contribution from the pictures and hence to construct a polarisation map of the corona is under way. The ultimate goal of the experiment is to determine by an iterative analysis, the electron density distribution and to use it for a study of the inhomogenities in the corona.

In the preliminary analysis, radial plots of degree of polarisation have been obtained for a few azimuths. Fig. 4 (a, b) shows these plots for the two azimuths, viz.,  $316^\circ$  and  $241^\circ$ , compared against mean solar maximum values given by van de Hulst (1952). Rather low values of polarisation in S-W direction is notable and probably implies depleted electron densities.

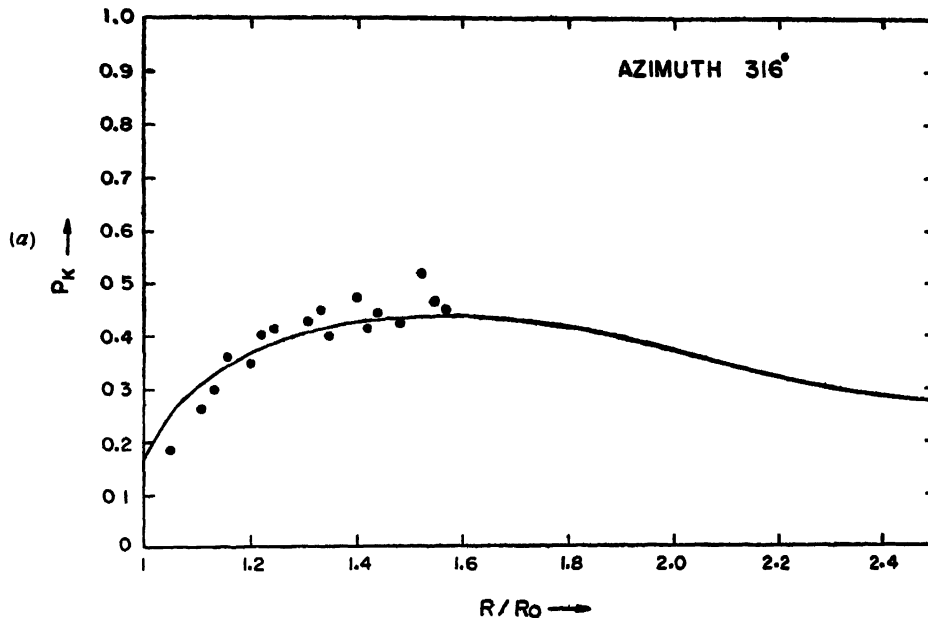


Fig. 4 a). Polarisation  $P_K$  vs.  $R/R_\odot$  at  $316^\circ$  azimuth.

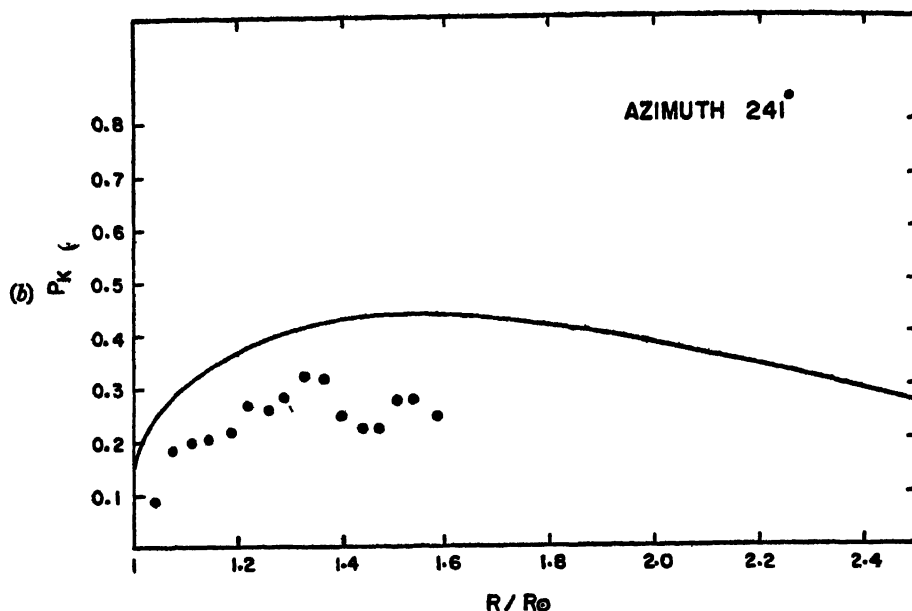


FIG. 4b). Polarisation  $P_k$  vs.  $R/R_\odot$  at  $241^\circ$  azimuth.

#### DISCUSSION

The coronal interferogram has yielded a high spatial resolution temperature map of the corona. Temperatures range from 2–4 million °K with a few spots having temperatures as high as 5 million °K. The inversion height of about  $1.1R_\odot$  observed in the temperature map is consistent with the theoretical calculations of Kuperus (1969) on the heating of the corona. Correlation between the “hot” regions in the corona and X-ray bright points as well as their interrelationships with coronal magnetic fields remain to be studied.

At a specific azimuth, we see the evidence of a hydromagnetic wave modulating the brightness of  $5303\text{\AA}$  corona. Exact periodicity remains to be established but could be 100 sec which is much smaller than the periodicity of 360sec reported earlier in the temporal variations (Liebenberg & Hoffmann, 1973) and 300sec periodicity of photospheric oscillations.

Under the assumption that for monochromatic corona, the brightness  $\propto$  (electron density)<sup>2</sup>; one gets a mean scale height temperature of  $2.82 \pm 0.14$  million °K from the mean slope of Fig. 3.

#### ACKNOWLEDGEMENTS

Our thanks are due to Professor J. Pasachoff for making available the precalibrated films. Thanks are also due to amateur astronomers P. Pandya, P. Patel and P. Panchal



for their valuable assistance in conducting the experiments. The work was financially supported by Department of Space, Government of India.

## REFERENCES

- Leighton R. B *et al* (1962) Velocity fields in the solar atmosphere *Ap. J.*, 135, 474.  
Van de Hulst (1952) *The SUN*, Ch 5, pp 262 (*Ed.* G. Kuiper) The Univ of Chicago Press, Chicago.  
Kuperus, M (1969) The heating of the solar corona, *Space Sci. Rev.*, 9, 713  
Liebenberg D H, and Hoffmann, N. M. (1973) *Coronal Disturbances*, IAU Symp. No 57, pp. 485  
(*Ed* Gordon Newkirk Jr).

Printed in India

Astrophysics

# A SEARCH FOR OPTICAL MODULATION OF THE SOLAR CORONA DURING THE 16 FEBRUARY 1980 TOTAL SOLAR ECLIPSE\*

E. J. SEYKORA

*East Carolina University, Greenville North Carolina 27834, U.S.A.*

*(Received 7 August 1981)*

Results of a search for optical modulation, or fast variations of the optical intensity, of the solar corona during the 16 February 1980 total solar eclipse are presented. Equipment is described which was developed to record variations in the frequency range from 20Hz to 15kHz and to 15 MHz. The detection sensitivity is discussed and limits on the modulation or fluctuation have been determined to be less than a luminous flux variation of 10 picolumens in the frequency range from 5MHz to 15MHz. The detection of a number of atmospheric phenomena in the frequency range from 20Hz to 15kHz are discussed along with recordings of eclipse shadow bands.

**Keywords:** Optical Modulation; Solar Corona; Optical Intensity; Luminous Flux Variation; Shadow Bands

## INTRODUCTION

THE objective of this project was primarily concerned with setting limits on, or detecting very fast optical variations or fluctuations originating from the solar corona. Although a number of mechanisms by which such optical variations can be excited exist, the major excitation mechanism is thought to be associated with transient puffs of high speed particles that move through the coronal gas and excite plasma oscillations. Such transients have been associated with Type II and Type III bursts of radio noise in the decameter range. The existence of harmonics in the radio-frequency noise suggests a microscopic non-linear oscillation of the coronal gas in a region above a flare location (Aller, 1963). The continuity and force equations of electrodynamics can be drawn to yield a wave equation for the plasma, or density fluctuation, of the form:

$$\frac{d^2n}{dt^2} + \frac{4\pi e^2 n_0}{m} n = 0$$

where  $n$  is the charge density and  $\frac{4\pi e^2 n_0}{m}$  is the Plasma frequency  $\omega_p$  (Jackson, 1975). As a result of this equation the charge density, velocity and electric field all oscillate with the plasma frequency  $\omega_p$ . As a result of such charge density variations, the resultant optical emission is modulated at the plasma frequency

\*This material is based upon work supported by the National Science Foundation.

## EQUIPMENT

The instrumentation used, in this search for optical modulation of the solar corona, included two separate detection systems one system for detection of modulation frequencies in the range from 20Hz to 15kHz, and a second system for 3MHz to 6MHz.

For the modulation band from 20Hz to 15kHz, three solid state photodetector systems with high gain AC coupled amplifiers were used. The detector-amplifier outputs were recorded directly on magnetic tape. Each detector consisted of a silicon solar cell with a 1.0 cm aperture stop at the cell. The cells were operated in the current mode, being shunted by the 5 ohm primary winding of a 100X step-up transformer. Small optical variations result in an AC coupled voltage variation at the secondary winding of the transformer, which was recorded *via* the high gain AC amplifier. This system can record changes in the light intensity amounting to a one part per million variation in background illumination. As a result of this sensitivity, this detector system is capable of detecting and recording light fluctuations from a number of terrestrial-atmospheric phenomena. Several of these phenomena which compete or add background noise to the coronal modulation are listed here.

- 1) Atmospheric striae resulting from turbulent mixing of regions of warm and cold air refract light from the sun and give rise to light fluctuations at the surface of the earth. Previous measurements in this frequency range have indicated a turbulent atmospheric change following a solar eclipse (Seykora, 1979).

- 2) Individual insects at altitudes in the kilometer range are recorded. As high flying insects cross the solar disc the background light is modulated by the beat frequency of the insects' wings. Furthermore, it is now believed that specific species of insects can be detected by their characteristic wing beat frequency.

- 3) Sound waves in the atmosphere may be recorded optically over a very great range. That is, the refraction of light from the solar disc by sound waves is detected at the surface of the earth, as a modulation of the solar disc. The largest range at which such waves have been detected to date is  $\sim 35,000$  ft, the sound originating from a high altitude aircraft.

Because the light fluctuations from atmospheric turbulence and other terrestrial phenomena are spatially local (several meters), the fluctuations resulting from the solar corona would be coincident at three widely separated detectors ( $\sim 10$  meters).

For the modulation band from 3-16MHz a photomultiplier (10 stage S11 spectral response) and radio receiver were used. The radio receiver frequency was swept, in time, (1MHz/sec) and the receiver output was recorded both on magnetic tape and paper chart. The resultant recording represents the light modulation intensity vs frequency.

## RESULTS

*(1) Optical Modulation Band for 20Hz to 15kHz:*

A recording of one of the three solid state detectors (20Hz to 15kHz) is shown in Fig. 1. The majority of the fluctuations and scintillations recorded are of atmospheric origin. The numerous spikes recorded that form a background on all recordings

have been shown to be high flying insects crossing the solar disc. Each signal can be heard on reviewing the tape as an insect which modulated the background light by the beat frequency of the insect's wings. The large number of scintillations recorded from four minutes before totality to totality was a result of eclipse shadow bands. During this time period shadow bands were seen visually and no band was seen or recorded after totality at the location of the detectors. The recordings from each of the three detectors were analyzed for coincident events which would be indicative of optical modulation or fluctuations originating at the solar corona. In no instance were there any coincident events recorded at the three detectors. Although no modulation or variation of the solar corona was detected, it was concluded that any variation of the corona in the band from 20Hz to 15kHz was less than  $10^{-8}$  times the static coronal intensity.

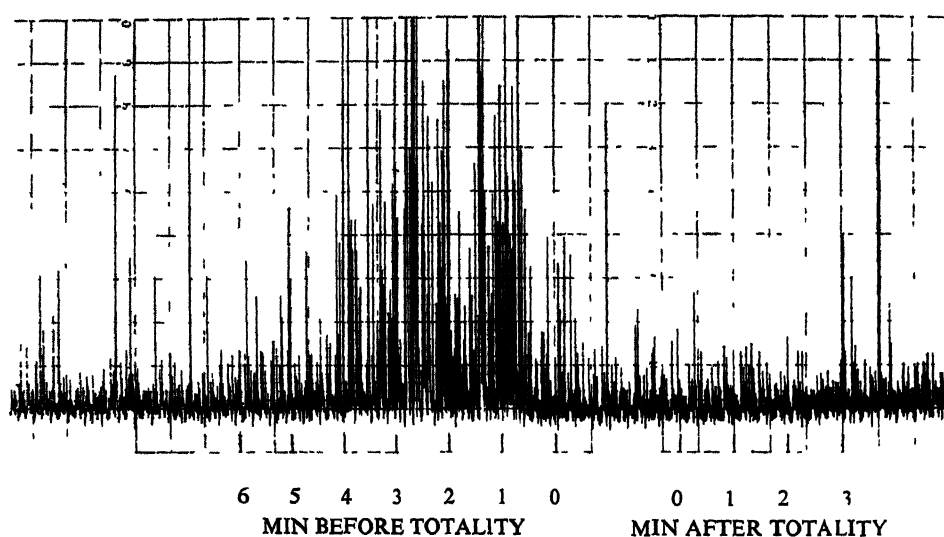


FIG 1 Solar scintillations recorded during the 16 February 1980 total solar eclipse, at the Japal-Rangapur Observatory. Full-scale amplitude  $10^{-5} \times$  static background illumination.

(2) *Optical Modulation Band from 3MHz to 16MHz*

The upper pen recording shown in Fig 2 represents the photomultiplier output as scanned by the radio receiver from 16MHz to 3MHz and back to 16MHz during totality. For comparison, the dark photomultiplier and receiver noise is shown in the lower recording of Fig. 2. The cyclic variation recorded in both recordings was a result of a uniform variation in the receiver sensitivity with frequency. As shown in Fig 2 the photomultiplier output during totality did not show any narrow band optical variations or fluctuations in the frequency range from 3-16MHz. The overall noise throughout this frequency range was larger because of the photomultiplier shot noise generated by the photomultiplier current. During the 20 second time period before the end of totality the noise level increased at a larger rate. This increased noise level is believed to be a result of an increase in light level toward the end of totality. If the light level during this period was increasing the photomultiplier current

would increase proportionately. An increase of the photomultiplier's current would then result in an increase in the shot noise recorded at radio frequencies.

An upper limit on the luminous flux of the optical fluctuations in this frequency range can be placed at 10 picolumens as calculated from the photomultiplier current, and shot noise level recorded at the receiver.

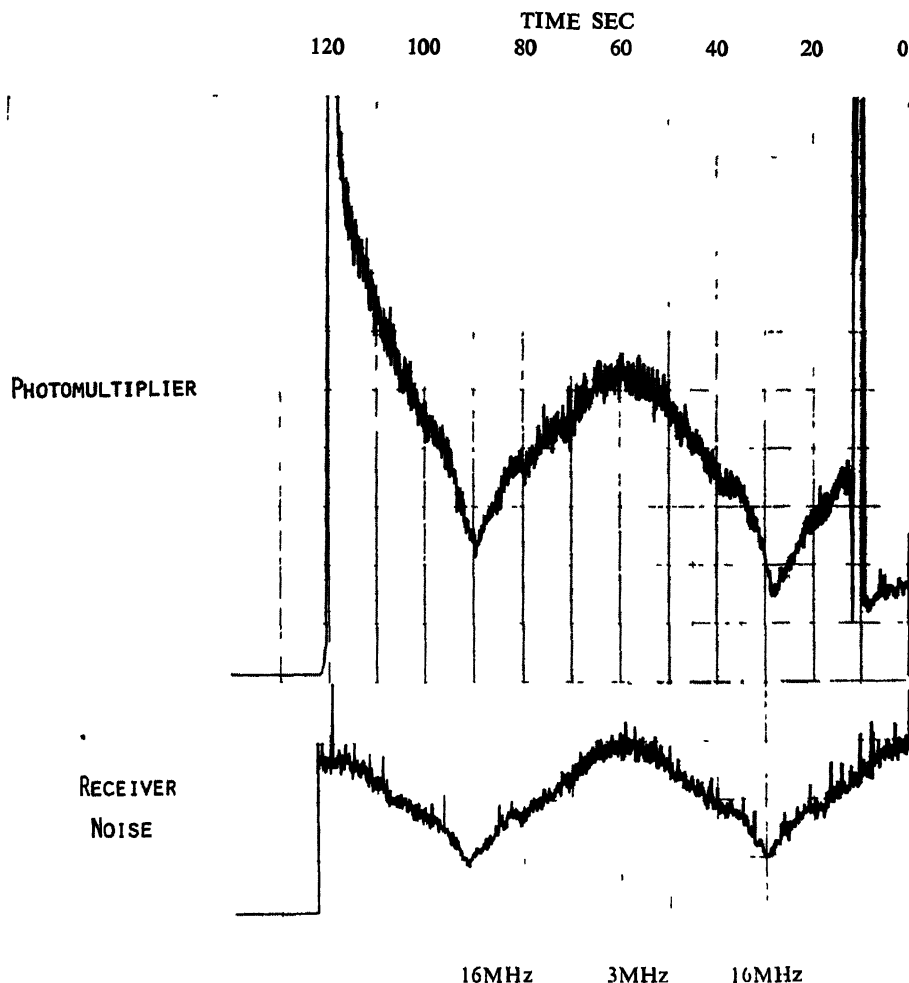


FIG. 2 The upper pen recording represents the photomultiplier output as scanned by the radio receiver, from 16MHz to 3MHz and back to 16MHz, during totality at the Japal-Rangapur Observatory. The lower recording represents the dark photomultiplier and receiver noise over the same frequency interval.

### (3) Shadow Band Recordings

The recordings of the eclipse shadow bands shown in Fig. 2, represent rather unique recordings of this phenomena. That is unique in that the ground level wind and turbulence was low at the time of the eclipse and the optical fluctuations associated with this type of disturbance was minimal.

Several conclusions can be drawn from the shadow band recordings analyzed to date. First, they do appear as true atmospheric scintillations. The correlation from one scintillation to the next is random in time and amplitude. Furthermore, a large variation in the intensity of the shadow band phenomena was seen at the three detectors separated by  $\sim 10$  meters.

It is important to note that the shadow band phenomena can be recorded at times other than solar eclipses (Seykora, 1979), because the scintillations result from upper atmospheric waves or turbulence. The turbulent mixing of small regions of warm and cold air produce striae that deform plane waves of light passing through the atmosphere, from the very thin solar crescent, producing the observed system of shadow bands. For a larger solar disc every point on the disc produces a system of shadow bands of its own, which tend to overlap in position, reducing the intensity of the fluctuations.

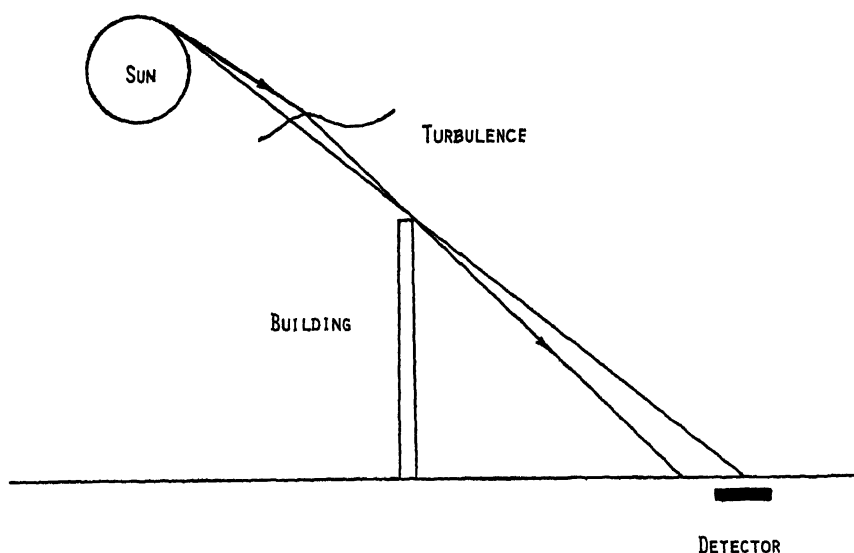


FIG. 3. Ray diagram showing the refraction of light from the solar disc by atmospheric turbulence and striae. The refracted rays may be displaced into or away from the shadow edge during the time interval the sun is occulted by the building. This results in solar scintillations at the detector.

If the sun is artificially eclipsed, as shown in Fig. 3, by a distant building the shadow edge fluctuates because of distant striae. The striae in the upper atmosphere refract the rays to a greater or lesser degree, distorting the apparent position of the solar disc at the edge of the building. Under conditions of very low ground level wind and turbulence, scintillations may be recorded during the time any portion of the solar disc is occulted by the building. Fig. 4 is a pen recording of the light fluctuations on a clear day when the sun was artificially eclipsed by a building 30m away. The detector was placed in the shadow of the building and aligned such that the motion

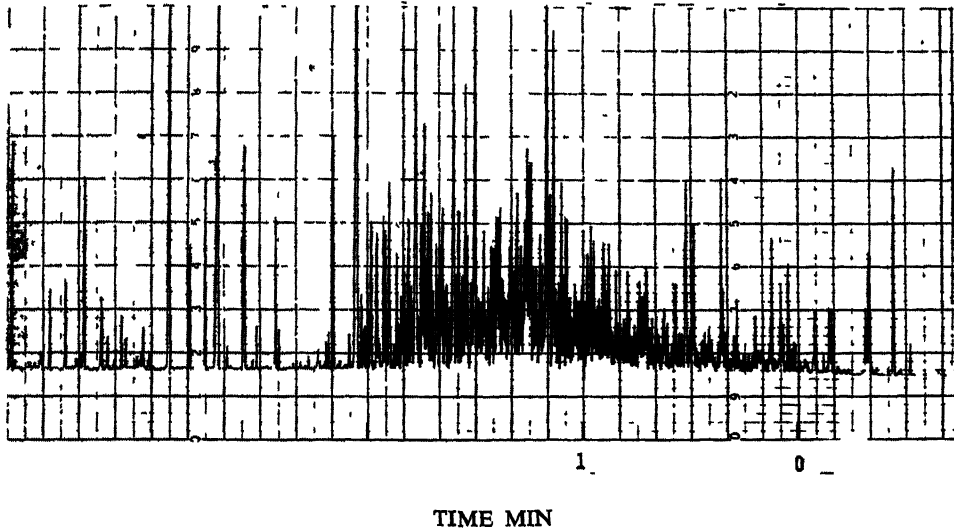


FIG 4 Solar scintillations recorded during an artificial eclipse. The solar disc was occulted by a distant building during the time interval from 0 to 2 minutes.

of the sun caused illumination of the detector. As shown in Fig 4, scintillations were recorded in the time interval from time zero to two minutes, the time interval the sun was occulted by the building. It should be noted that there is a remarkable similarity between the recorded eclipse shadow bands (Fig 1) and the scintillations recorded during artificial eclipses (Fig 4). Preliminary spectral analyses have also shown an equally strong correlation, indicating that the shadow band phenomena can be investigated at times other than solar eclipses.

#### ACKNOWLEDGEMENTS

The author wishes to thank Mr R. LaCount, the National Science Foundation Eclipse Coordinator, Mrs K. Crouch and Mr G. Prantner, the field support managers for their special efforts and support during this project. The special efforts of Professor K. D. Abhyankar and colleagues at the Astronomy Department of Osmania University, and the use of their facilities, was greatly appreciated. The assistance of Miss R. A. Gray, Miss P. A. Harrell and Mr M. H. Cobb with the observations is gratefully acknowledged.

#### REFERENCES

- Aller, L. H. (1963) *The Atmospheres of the Sun and Stars*. The Ronald Press Company, New York, p. 571.
- Jackson, J. D. (1975) *Classical Electrodynamics*. John Wiley and Sons, Inc., New York.
- Seykora, E. I. (1979) Observations of eclipse shadow bands and related phenomena. *Appl. Opt.* **18**, 21, 3538.

Printed in India

Astrophysics

# DETECTION OF VARIATIONS IN THE SOLAR RADIUS THROUGH OBSERVATIONS OF BAILY'S BEADS AT THE EDGE OF THE PATH OF TOTALITY

A. D FIALA

*U.S Naval Observatory, U S A*

*and*

D W DUNHAM *and* J B DUNHAM

*Computer Sciences Corporation, U.S A.*

*(Received 7 August 1981)*

During a central solar eclipse, the Moon acts as an occulting disc passing in front of the Sun. Observing the phenomenon of Baily's Beads from the edges of the path provides multiple precise timings of events which can be analyzed to detect small corrections to the assumed solar radius.

This paper gives a summary of the theory, the conditions under which it can be applied, and the results through 1980. This was the third eclipse observed by this method in modern times and the fifth to be reduced in a historical series. Assuming a solar radius of 959.63, we find corrections as follows:

1715	$+0.52 \pm 0.2$
1925	$+0.62 \pm 0.08$
1976	$-0.23 \pm 0.14$
1979	$-0.08 \pm 0.09$
1980	$-0.03 \pm 0.04$

**Keywords** Solar Radius; Solar Eclipse; Baily's Beads

## INTRODUCTION

ANALYSIS of meridian circle observations made at Greenwich during 1836-1953 has indicated that the Sun is shrinking at an alarming rate, i.e., 0.1 per cent per century (Eddy & Boornazian, 1979). On the other hand, analyses of transits of Mercury over an even longer period, 1736-1973, show little or no variation (Shapiro, 1980, and Parkinson *et al*, 1980). All of the observing methods for these observations require that the observers judge when the bright solar limb is apparently tangent to a dark narrow wire or small disc, under high magnification. Thus there are severe personal and systematic errors.

Consider then the observation of a total or annular solar eclipse, in which the Moon is regarded as a large occulting disk whose radius is known exactly, and the



separation of the two centers is also known precisely. In that case, recording the contacts of the limbs gives measures of points in space on the solar limb. Furthermore, it is an observation fairly easy to make, for one need only judge whether light is present or not.

### ECLIPSE TIMINGS

#### *Theory and Criteria for Usability*

Assuming that the distances of the Sun and the Moon from the Earth are accurately known, and that the size and rotation of both the Earth and the Moon are accurately known, then if the Sun and the Moon were perfectly spherical, timed observations of the contacts of a solar eclipse from anywhere within the central path would yield information on the solar radius by mapping the length of a chord of the disc (Sofia *et al.*, 1980). The relative rate of motion between the two limbs is about  $0''.5$  per second hence timing accuracy of 0.2 seconds yields precision of  $0''.1$ .

Unfortunately, the Moon has a rough surface and hence a rough limb. At the mean distance,  $0''.1$  corresponds to approximately 190m. Consequently, the precision of the timing is lost unless the limb features are known to better than accuracy than 190m for all orientations of the Moon (liberations). This is not in general the case except near the lunar poles, as described in a following section.

When eclipses occur, the lunar latitude is near zero, hence the lunar polar regions cast the parts of the shadow which form the edges of the path. It is necessary to observe from both edges in order to separate a change in the path width from a longitudinal shift of the entire path. If observers can establish their positions within 100m of precision, it is then possible to determine a correction to the solar radius with an accuracy approaching  $0''.05$ . There is no systematic error, and the method may be applied to past eclipses for which similar observations were made. So far, we have been able to achieve the accuracy of position by obtaining various national survey maps. In the future, we may be able to use Doppler navigation receivers.

#### *Corrections to the Ideal Spherical Predictions*

Refinements to the location of the predicted northern and southern limits of the path include lunar profile corrections and corrections to the lunar and solar ephemerides based upon modern observations. The path limits are operationally defined by the bottoms of particular valleys in the polar regions of the Moon.

The best source for lunar limb information is Watts' limb charts (Watts, 1963). Approximate profile information can be obtained from U.S.N.O. Circular 141 (Duncombe, 1973). For our project, we obtained detailed limb data automatically for a given time and location by reading the chart data from a computer file. Then the corrections to the predicted limits to take into account the profile could be calculated. The details of this procedure are found in Sofia *et al.* (1980).

Accurate ephemerides of the Sun and the Moon which incorporate fits to spacecraft radio tracking and lunar laser ranging data are preferred (e.g., Jet Propulsion Laboratory, *Current Development Ephemeris*). The location of the centre of Watts' reference datum with respect to the center of mass, and corrections to reduce the ephemeris to the FK4 system, have been derived by T. C. van Flandern

of U.S. Naval Observatory through comprehensive analyses of thousands of lunar occultation timings

All of these factors are combined into overall corrections to the coordinates of the Moon with respect to the Sun, resolved into along-path and cross-path components, and applied to the predicted limits.

#### *Accuracy of Results*

A detailed theoretical analysis of the effect of errors in the individual components of these calculations as carried through to the final predictions is not practical. It is more illuminating to consider what observational experience indicates about these errors.

It was noted in a previous section that making use of the full precision of the timing of contacts depends on knowing the linear size of lunar features to within 200m. This is the main reason why it is only useful to observe near the path limits. Eclipses only occur when the Moon's ecliptic latitude is near zero. As a consequence, the polar regions of the lunar disc cast the shadow along the edges of the path. An examination of the range of profiles given in Duncombe (1973) by overlaying the extremes in libration shows quite clearly that in the polar regions there is very little change in the profiles, whereas along the east and west limbs there are variations far exceeding 1 arc second. Furthermore, the polar regions tend to show many of the same features to be observed along the edges of the paths of all central eclipses.

Let us now consider occultations of stars by the Moon, which occur much more frequently than solar eclipses, yet are subject to many of the same sources of error. It is useful to apply knowledge gained from occultation observations to estimating the accuracy of eclipse observations.

An occultation of a star by the Moon is visible along a path whose width is comparable to the lunar diameter. Along the edges of this path, the star may appear to be occulted several times in quick succession over a few minutes time as the rough polar limb passes in front of it. If several observers time these events at several stations spread across the edge of the path, a very accurate profile of the lunar limb can be mapped. Since 1963, over a thousand such grazing occultations have been observed. Other information obtained includes determination of the ecliptic latitude of the Moon relative to the star with an accuracy an order of magnitude better than we are considering for eclipses. Also, it is noted that the effect of diffraction at the limb of the Moon is even smaller than that.

Observing a central solar eclipse from the edges of the path is similar in principle (Dunham & Dunham, 1973). The difference is that instead of a moving point source, one observes an extended source which is cut into small pieces and then reforms (Baily's Beads). This has the advantage of providing multiple events on which statistical analysis can be performed to find the best fit for the radius to match predictions to observations. It has been found by experience that the intensity gradient at the edge of the solar limb drops off so rapidly that there is no observational difficulty in identifying the appearance or disappearance of a Bead.

We are confident that our analytic procedure yields positional accuracy for points on the solar limb of  $\pm 0''.05$ . For remote past epochs we, argue that the upper bound is  $\pm 0''.2$  (Dunham *et al.*, 1980).

### Application and Results

The observational technique we employed has been described elsewhere (Fiala *et al.*, 1980). Once observations have been taken, the next step is to match the timed events to identified features on the calculated lunar limb profile, and then perform the statistical analysis (Herald, 1976).

So far we have reduced observations from 5 eclipses using this method of analysis. The corrections deduced for the solar radius are shown in the first column of Table I. These numbers are based on observations of Bead events occurring within  $30^\circ$  of a pole. The second column of deduced corrections shows similar results obtained by analyzing only specific lunar limb features which were observed at 3 different eclipses.

TABLE I

*Solar radius corrections determined from observations near eclipse path edges*

Date	Timings within $30^\circ$ of lunar axis			Timings using features determining 1925 events			Lunar librations	
	No.	$\Delta r_\odot$		No.	$\Delta r_\odot$		long.	lat.
1715 May 3	4	+0.52	$\pm 0.2$	0	—	—	+1.8	-0.2
1925 Jan 24	4	+0.62	0.08	4	+0.62	0.08	+2.5	-0.2
1976 Oct 23	15	-0.23	0.14	0	—	—	-1.4	+0.1
1979 Feb. 26	33	-0.08	0.09	3	+0.11	0.23	+1.7	-0.3
1980 Feb. 16	55	-0.03	0.04	3	-0.05	0.35	-3.0	-0.1

### CONCLUDING REMARKS

While no significant change in the solar radius is deduced from the observations of recent eclipses, there is a significant decrease of at least  $0''.5$  from 1925 to 1979. These two eclipses were separated by exactly three *Saros* cycles and had similar geometries and librations. Overall, from only 5 eclipses, the pattern of behavior cannot yet be identified (secular, cyclic, or random). We plan to continue observing more eclipses in the future by the same method, including annular as well as total eclipses. Also, we have found in the literature and the archives unused observations from the eclipses of 1869, 1878, 1900, and additionally from 1925, all of which can be analysed in the same way. Up until now, the enormity of the labour and the uncertainty of the errors have been too great for anyone to finish the analysis. The resolution of the Sun's variability is of such significance to the physical structure that we are encouraged to keep trying.

### ACKNOWLEDGMENTS

This work has been supported by NSF Grant ATM-77-23757, NASA Grant NAS-5-24350, and the U.S. Naval Observatory.

## REFERENCES

- Duncombe, J S. (1973) Lunar limb profiles for solar eclipses. U S. Naval Observatory Circular No. 141.
- Dunham, D W., and Dunham, J B (1973) Observing total solar eclipses from near the edge of the predicted path. *The Moon*, 8, 546-547.
- Dunham, D W., Sofia, S, Fiala, A D, Herald, D, and Muller, P. M (1980) Observations of a probable change in the solar radius between 1715 and 1979 *Science*, 210, 1243-1245 (12 Dec)
- Eddy, J A, and Boornazian, A. A (1979) Secular decrease in the solar diameter, 1863-1953 *Bull. Am. astron. Soc*, 11, 437 (*Abstr*)
- Fiala, A D, Dunham, D. W., and Dunham, J B. (1980) Observations of Baily's beads from the edges of the path of the total solar eclipse of 16 February 1980. *Bull. Indian astron Soc.*, 8, Nos 2 & 3, 81-82
- Herald, D (1976) Observations of Baily's beads from near the northern limit of the total solar eclipse of June 20, 1974. *The Moon*, 16, 91-100
- Parkinson, J H, Morrison, L. V, and Stephenson, F. R. (1980) The constancy of the solar diameter over the past 250 years. *Nature*, 288, 548-551.
- Shapiro, I. I. (1980) Is the Sun shrinking? *Science*, 208, 51-53 (4 April)
- Sofia, S, Dunham, D. W., and Fiala, A D. (1980) Determination of variations of the solar radius from solar eclipse observations In. *Proc. Conf Ancient Sun*, 147-157 (Eds. R O Pepin, J. A Eddy and R. H Merrill)
- Watts, G. B. (1963) The marginal zone of the moon. *Astron Papers Am. Ephem.*, 17.

Printed in India

Astrophysics

HIGH RESOLUTION MICROWAVE BRIGHTNESS TEMPERATURE  
MEASUREMENTS DURING TOTAL SOLAR ECLIPSE ON  
16 FEBRUARY 1980

R. V. BHONSLE, S. K. ALURKAR, S. S. DEGAONKAR

*Physical Research Laboratory  
Ahmedabad-380 009, India*

O P. N. CALLA, G. RAJU, S. S. RANA

*Space Applications Centre (ISRO)  
Ahmedabad-380 053, India*

and

B LOKANADHAM

*Centre of Advanced Study in Astronomy  
Osmania Univeristy  
Hyderabad-500 007, India*

*(Received 7 August 1981)*

Simultaneous observations of solar fluxes using total power radiometers at 2.8, 10, 19.3 and 22.2 GHz were made at Japal-Rangapur Observatory, Hyderabad in the path of totality during the solar eclipse on 16 February 1980. Residual fluxes of 23, 3.5 and 3 per cent of the uneclipsed values were observed 2 to 7 minutes prior to the totality at 2.8, 10 and 19.3 GHz respectively. Analog data were digitized with 5 seconds interval. Using the slopes of the eclipse curves, radial brightness temperature distribution across the solar disc was derived at different frequencies. Enhancements of radio brightness ranging from 25 to nearly 100 per cent and half-power widths of 2-4 arc were observed corresponding to two major bright regions seen in H-alpha photographs of the Sun. Spectra of brightness temperature over different regions of the Sun indicate 1-10 minute periodicities, while the spectra of bright regions show a dominant periodicity of about 5 minutes.

**Keywords:** High Resolution Microwave; Solar Fluxes; Solar Brightness Temperature; Maximum Entropy; Supergranular cells

EXPERIMENTAL SET-UP AND OBSERVATIONS

MULTI-FREQUENCY observations of radio emissions from the Sun were made at the Japal-Rangapur Observatory (Long. 78°, 43'.7E; Lat 17°, 05'.9N) of the Osmania University, Hyderabad during the total solar eclipse on 16 February 1980. Dicke-type

total power radiometers at 2.8, 10 and 19.3 & 22.2GHz were operated by the Physical Research Laboratory (PRL) Astronomy Department, Osmania University and the Space Applications Centre (SAC) respectively. Table I summarizes some important characteristics of the radiometers:

TABLE I  
*Characteristics of microwave radiometers*

Frequency (GHz)	2.8	10.0	19.3	22.2
Sensitivity ( $^{\circ}$ K)	1.3	0.4	0.16	0.6
Integration time (sec)	1	1	1	1
Halfpower beamwidth ( $^{\circ}$ )	5	0.8	1.5	1.5

The 2.8, 19.3 and 22.2GHz parabolic antennas were equatorially mounted and continuously tracked the Sun, while the 10GHz antenna was manually adjusted periodically to obtain transits of the Sun. Calibration levels corresponding to equivalent radio brightness temperatures of the earth, sky and Sun were marked on the strip charts before and after the eclipse. Except for a few minutes around totality in the case of the 22.2GHz radiometer, the overall stability of all the radiometers was quite satisfactory.

## RESULTS AND DISCUSSION

The observed eclipse curves for all the four frequencies are shown in Fig 1, where the solar fluxes (normalised to their pre-eclipsed values) are plotted as a function of time. It is interesting to note that the residual fluxes of 23, 3.5 and 3 per cent at 2.8, 10 and 19.3GHz occurred some 2 to 7 minutes earlier than the time of the optical totality. This implies that the centroid of the radio Sun in each case was shifted towards the south-west limb of the Sun indicating the presence of an active centre at that limb.

Comparing the observed eclipse curves with those obtained by artificially eclipsing uniformly bright radio discs of the Sun of appropriate diameters, one can obtain departures of the slope of the observed flux curves from those of the theoretical eclipse curves. One example is shown in Fig 2, in which the observed eclipse curve at 2.8GHz is compared with the corresponding computed curve for an uniformly bright solar disk of radius 18.2 arc minutes. The radius is assumed at this frequency as measured by Furst *et al.* (1979). The changes in the slope of the observed eclipse curves are a result of the variations in the radio brightness of the solar disc in the presence of bright radio regions scanned by the moon's edge.

The observed flux values were then corrected for atmospheric absorption, antenna beam shape, cable attenuation, moon's microwave brightness temperature, etc., and the analog data on 2.8, 19.3 and 22.2GHz were digitized to obtain solar flux

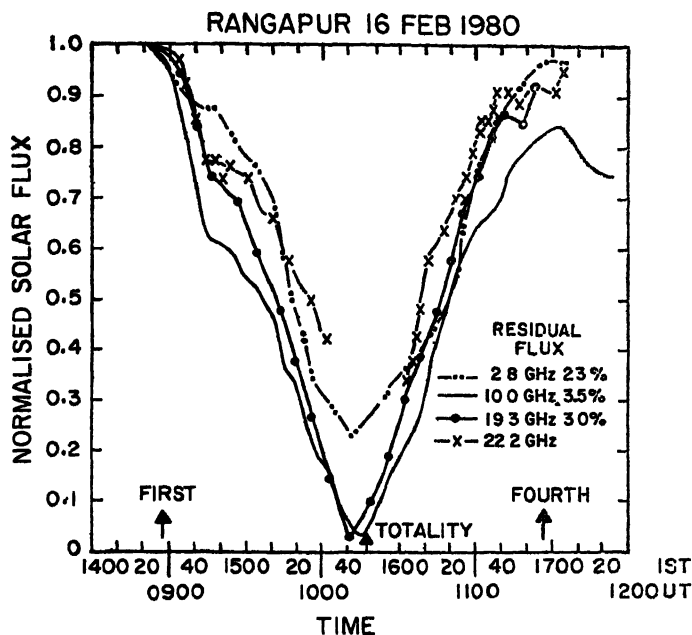


FIG. 1. Observed eclipse curves at 2.8, 10, 19.3 and 22.2GHz for the total solar eclipse on 16 February 1980. Times of first contact, totality and fourth contact are indicated by arrows

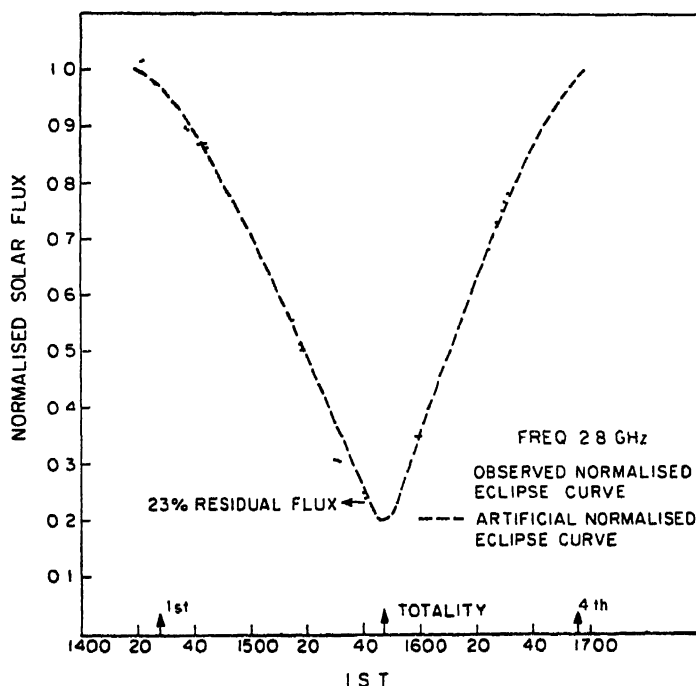


FIG. 2 Comparison of observed eclipse curve at 2.8GHz with artificial eclipse curve for a uniformly bright radio sun with radius of 18.2 arc minutes

values at an interval of 5sec, thus yielding high spatial resolution ( $\sim 3\text{--}4$  arc seconds) in one-dimension scan of the solar disc. Three-point moving averages of the large number of data points were taken a number of times to filter out high frequency fluctuations arising due to the system noise. The radial distribution of brightness temperatures across the solar disc was then computed using the method of Hagen and Swanson (1975).

Fig 3 shows one sample of the brightness temperature variation at 2.8, 19.3 and 22.2GHz as a function of radial distance from the centre of solar disc toward its north-east limb. The dashed horizontal line indicates the brightness temperature (normalised to unity) of the uniformly bright solar disc and the continuous line shows the variations of brightness temperature as the moon scans the solar disc. The fluctuations of brightness temperature at 2.8GHz are seen to occur more rapidly than those at the higher frequencies. Further, two specific radio bright regions are seen centred at about  $0.15$  and  $0.4 R_{\odot}$  from the centre of the disc. These were identified with calcium plage regions seen on the H-alpha photograph of the Sun taken on that day. Another important aspect to be noted in Fig 3 is that the limb-brightening was observed on all the three frequencies around  $1.25 R_{\odot}$  at 2.8GHz and  $1.2 R_{\odot}$  at 19.3 and 22.2GHz.

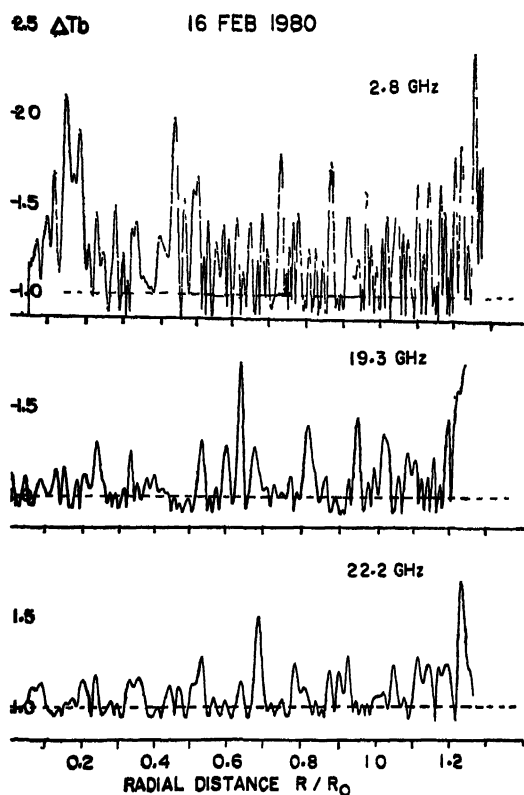


FIG. 3. Radial distribution of brightness temperatures at 2.8, 19.3 and 22.2GHz from the centre toward the north-east limb of the Sun.



Using Burg's (1967) maximum entropy method (MEM), spectra of the fluctuations in the brightness temperature were obtained over different regions of the Sun. The spectra showed oscillatory features at all the three frequencies, with dominant periodicities in the range 1–10 min. More interestingly, spectra of the bright radio regions mentioned earlier, indicated a dominant periodicity of about 5min. These values were subjected to various statistical tests and were found to be significant. Hence, these statistically significant periodicities indicate that they are of solar origin. Broadly speaking, the periodicities smaller than about 200sec seem to correspond to scale sizes of supergranular cells which have diameters of  $\sim 30,000\text{km}$  (Tanenbaum *et al.*, 1969) but those observed around 300sec may or may not be connected with the well-known photospheric velocity oscillations having similar periodicities (Leighton *et al.*, 1962). This ambiguity may be resolved if it could be known *a priori* whether the observed periodicity of 300sec in our case is a result of spatial variation or of temporal variation of the radio brightness temperature.

### CONCLUSIONS

Multi-frequency microwave observations were made successfully during total solar eclipse of 16 February 1980. Eclipse curve at each frequency was obtained. The minimum flux at these frequencies occurred about 2 to 7 minutes earlier than the optical totality. Radial brightness temperature distribution was calculated. Enhancements of radio brightness ranged from 25 to 100 per cent over the uniformly bright disc of the Sun. The MEM spectra of the brightness temperature fluctuations revealed statistically significant periodicities in the 1–10 min range and around 5 min. The periodicities below 200sec correspond well to the scale sizes of supergranular cells but that at 300sec may also be connected with spatial variations corresponding to active regions.

### ACKNOWLEDGEMENTS

The authors express their sincere thanks to Professor D. Lal, F.R.S., Director PRL; Professor Yash Pal, Director, SAC (ISRO); and Professor K. D. Abhyankar, Director, Centre for Advanced Study in Astronomy and Japal-Rangapur Observatory, Osmania University, Hyderabad for their keen interest and support. Technical assistance rendered by Shri N. S. Nirman in fabrication of 10GHz radiometer and overall operation of eclipse campaign is very much appreciated. M/s. H. T. Ali, N. V. Dalal, A. H. Desai and G. H. Patel from PRL and Shri Kevalia from SAC also helped in taking eclipse observations and maintenance of radiometers. Dr D. R. Kulkarni, M/s. S. K. Shah and K. J. Shah assisted in the data analysis.

Financial support for 2.8, 19 and 22GHz radiometers came from the Department of Space, Government of India and for 10GHz radiometer from the University Grants Commission.

### REFERENCES

- Burg, J. P. (1967) Maximum entropy spectral analysis, paper presented at 37th Meeting, Soc. Explor. Geophys., Oklahoma, Oct. 1967.

- Furst, E., Hirth, W., and Lantos, P. (1979) *Solar Phys.*, **63**, 257.  
Hagen, J. P., and Swanson, P. N. (1975) *Ap J*, **198**, 219.  
Leighton, R. B., Noyes, R. W., and Simon, G. W. (1962) *Ap. J.*, **135**, 474.  
Tanenbaum, A. S., Wilcox, J. M., Frazier, E. N., and Howard, R. (1969) *Solar Phys.*, **9**, 328

Printed in India.

**Astrophysics**

## HIGH RESOLUTION CORONAL INTENSITY AND POLARIZATION MEASUREMENTS

JOHN L. STREETE\*

*South Western at Memphis, Memphis, Tennessee, U S A*

*and*

LEON B. LACEY

*High Altitude Observatory (HAO) National, Center for Atmospheric Research,  
Boulder, Colorado, U.S.A*

*(Received 7 August 1981)*

The total eclipse of 16 February 1980 was successfully photographed with the High Altitude Observatory's coronal camera from a site in Palam, India. The purpose of the experiment was to obtain, with high spatial resolution, polarization and intensity measurements of the corona to about  $3.5 R_{\odot}$ . The exposures are now processed, raster scanned, digitized and stored on magnetic tape. Sky background corrected radial plots of K + F coronal brightness are given for polar and equatorial directions.

**Keywords.** High Resolution Coronal Intensity; Polarization; K and F Corona

### INTRODUCTION

THE experiment was designed to record, with high spatial resolution, the total intensity and polarization of the corona from the limb to about  $3.5 R_{\odot}$ . The intensity, percent polarization, and polarization direction will ultimately be used in electron density and temperature models. The results will also be available for cross calibration with other measurements such as those obtained with the ground based HAO Mark III K-coronameter instrument at Mauna Loa, Hawaii, the joint Harvard/HAO Lyman-alpha/White Light Coronagraph Rocket Flight and the Naval Research Laboratory's coronagraph on satellite P78-1.

### DESCRIPTION

The instrument used in the experiment was the High Altitude Observatory's coronal camera (Newkirk *et al*, 1970). It was slightly modified during the summer of 1979 by the installation of heat shields to prevent temperature produced changes in focus. The format of the calibration step wedge was also modified. A Goetz 178cm focal

---

\*Currently on leave-of-absence to HAO

length,  $f/16$ , objective lens, which forms a coronal image on 70mm film, is the primary optical element of the instrument. Inserted in the light path directly in front of the film plane is a filter wheel containing the four filters required for the measurement of intensity and polarization and a fifth filter used to obtain a single-exposure photograph of the entire corona. The former four filters consist of three HN-38 polaroid filters sandwiched between a clear cover glass and a Schott OG-3 filter and a fourth, identical filter without a polaroid. The three polaroid filters are oriented at  $60^\circ$  intervals. The fifth filter is a radially graded neutral density filter constructed to com-

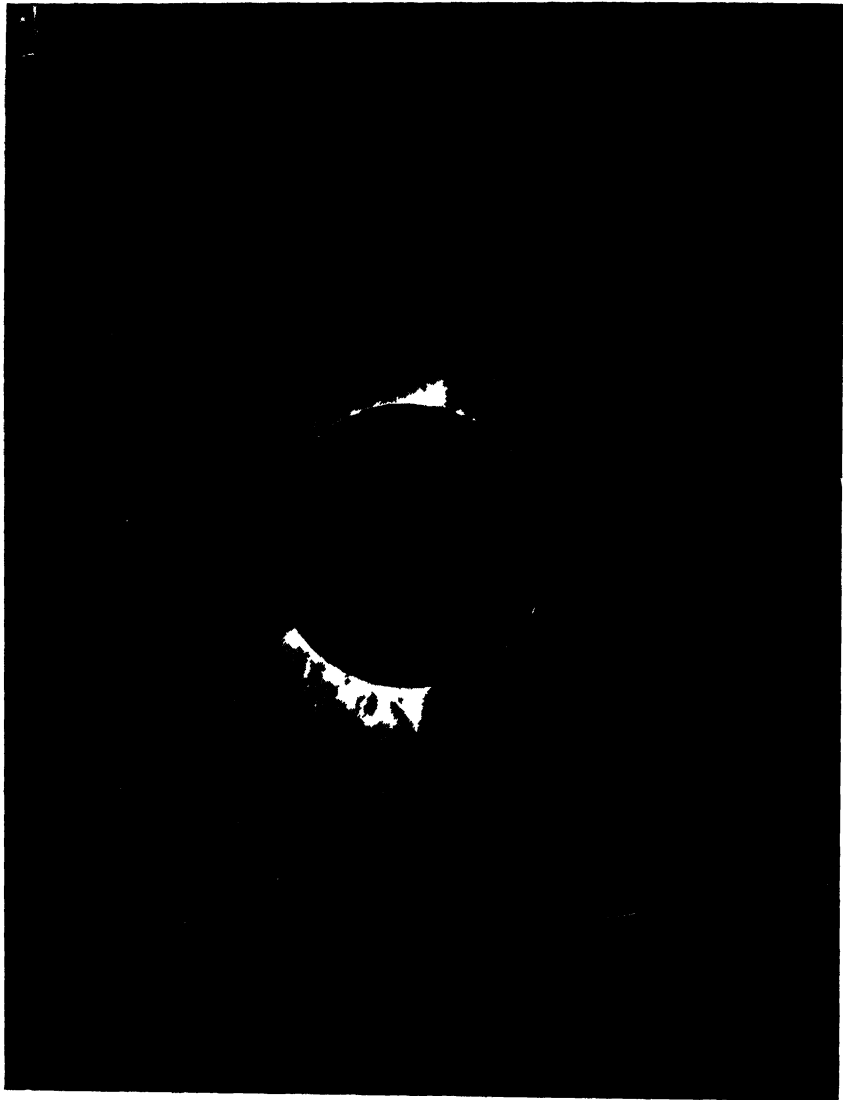


FIG 1 The solar corona of 16 February 1980 photographed through a radially-graded, focal plane filter with an exposure time of 24s

pensate for the sharp radial decrease in coronal intensity. The Schott filters and spectral sensitivity of the Kodak Linagraph Shellburst film produce a spectral band-pass of about  $1400\text{\AA}$  centered at  $6500\text{\AA}$ .

On the edge of each frame is focused an image of a 20-step wedge which is illuminated by a stabilized strip filament lamp. These images were standardized to the photosphere by recording exposures through calibrated opal filters on clear days when the sun was at eclipse elevation. In an attempt to obtain maximum photometric accuracy the exposure times for the calibration exposures were produced with the same programme cam as used during the eclipse (Lilliequist, 1977).

In order to determine the sky contribution to the recorded intensity and polarization values, an image from an  $8.5^\circ$  sky field  $10^\circ$  from the sun was formed on the edge of appropriate frames. These exposures were also made through three polaroids oriented at  $60^\circ$  intervals.

### RESULTS

A total of thirteen exposures, including one radially-graded photograph, three clear filter and nine polaroid exposures were obtained during the 160 seconds of totality. These are now processed and the latter twelve raster scanned and digitized as are all of the calibration exposures. The eclipse photograph recorded through the radially-graded focal plane filter, using an exposure time of 24 seconds, is seen in Fig. 1. Data from the clear filter have been analyzed and we are in the process of completing the analysis of the polaroid data. The sky background contribution as determined from the sky channel exposures was found to be  $7.4 \pm 1.1 \times 10^{-10} B_\odot$ . It has been found (Lilliequist, 1977) that a plot of  $\log B/B_\odot$  vs.  $\log R/R_\odot$  with the

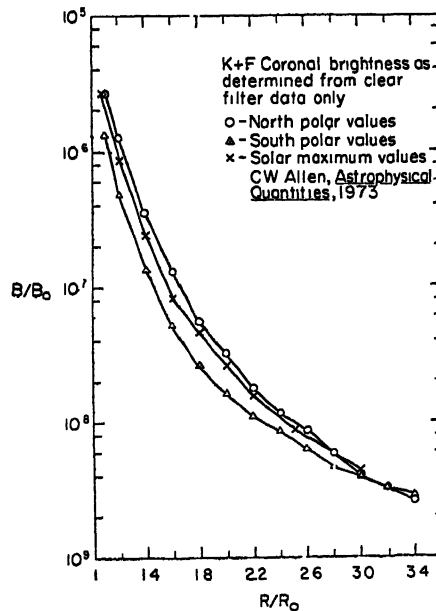


FIG. 2. Polar radial plots of K+F coronal brightness with sky background contribution subtracted

correct amount of sky background subtracted should yield a uniform slope through  $3R_{\odot}$ . This is indeed the case when the above value of sky background is used.

In Figs. 2 and 3 the sky background contribution has been subtracted from the measured K+F coronal brightness values. Shown in these figures is the radial decrease in intensity respectively for the two polar directions and equatorial directions. These curves are obtained by merging the brightness values from the  $0.15^{\circ}$  and  $1.5^{\circ}$  exposures from the limb to  $1.8R_{\odot}$  and the  $1.5^{\circ}$  and  $10^{\circ}$  exposures from  $1.8R_{\odot}$  to  $2.4R_{\odot}$ . Average discrepancies of about 15 per cent from  $1.4R_{\odot}$  to  $1.8R_{\odot}$  existed while from  $1.8R_{\odot}$  to  $2.4R_{\odot}$  the average discrepancy fell to about 12 per cent. Also for comparison on each graph is a standard brightness curve for the corona at solar maximum (Allen, 1973). A simple average of the two polar and two equatorial curves changes from slightly above the standard curve to slightly below at about  $1.8R_{\odot}$ .

Location Palem, India.

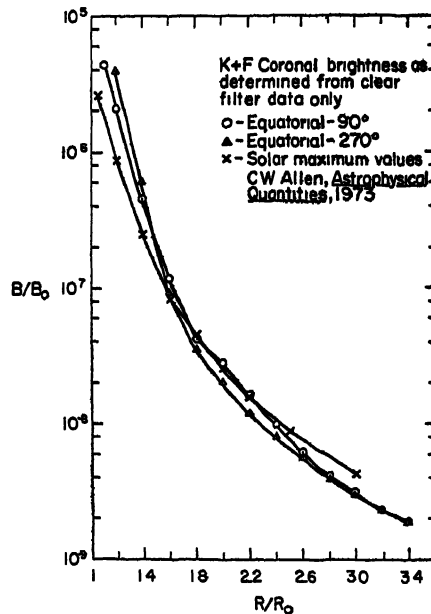


FIG 3 Equatorial radial plots of K+F coronal brightness with sky background contribution subtracted

#### ACKNOWLEDGEMENTS

National Center for Atmospheric Research, which is operated by the University Corporation for Atmospheric Research under contract to the National Science Foundation.

#### REFERENCES

- Allen C W. (1973) *Astrophysical Quantities*, third edition. Althone, London, 176  
 Lilliequist, C. (1977) Photometry and polarimetry of the solar corona of 30 June 1973. *NCAR Tech. Note*, 128-STR  
 Newkirk, Jr., G, Dupree, R., and Schmahl, E. (1970) *Solar Phys.*, 15, 15.

Printed in India

Astrophysics

## EFFECT OF SEEING PLUS SCATTERING ON THE OBSERVED INTENSITY DISTRIBUTION IN SOLAR CORONA

K. D. ABHYANKAR *and* P. V. SUBRAHMANYAM

*Centre of Advanced Study in Astronomy, Osmania University, Hyderabad 500 007  
India*

*(Received 7 August 1981)*

A method for estimating the broadening of the intensity profile of the solar corona caused by atmospheric turbulence, scattering in the photographic emulsion, focussing errors etc, is suggested.

**Keywords:** Plus Scattering; Intensity Distribution; Solar Corona; Atmospheric Turbulence; Photographic Emulsion

### INTRODUCTION

THE total solar eclipse gives a unique opportunity for measuring the coronal intensity which, in turn, gives the electron density distribution as a function of the radial distance above the photosphere. The observed intensity distribution is obviously affected by atmospheric seeing, scattering in the photographic emulsion and other effects of the same kind. The problem is similar to what one encounters in measuring the photospheric intensity distribution close to the solar limb. The seeing etc., blur the sharp boundary of the limb by spreading the photospheric radiation into the outer regions occupied by the sky background. In the same way, the coronal light is thrown into the regions of the photographic plate that are occupied by the moon's disc at the time of the total solar eclipse. There is no mention in the literature regarding the estimation of and correction for these effects in the case of coronal observations. So we have attempted here to outline a method which is based on the procedure originally suggested by Wanders (1934) and improved by Minnaert *et al* (1940) for correcting the influence of atmospheric scintillation and other apparatus effects on the measured intensity near the solar limb.

### COMPUTED THEORETICAL EFFECT

It is assumed that the seeing caused by atmospheric turbulence, scattering in the photographic emulsion, focussing errors, etc, together cause a blur in the intensity profile according to a Gaussian function

$$F(x, y) = \frac{a}{\pi} \exp[-a(x^2 + y^2)] \quad (1)$$

where  $x$  and  $y$  are expressed in the units of solar radius. As the sun has an angular

radius of  $960''$ , the broadening function of equation (1) has a width of  $(960/\sqrt{a})$  seconds of arc. For points along a diameter ( $x$ -axis) we can integrate over  $y$  and write

$$F(x) = \sqrt{\frac{a}{\pi}} \cdot e^{-ax^2} \quad \dots (2)$$

Accordingly, if  $J(x)$  is the true intensity distribution, then the observed intensity distribution  $I(x)$  will be given by

$$I(x) = \sqrt{\frac{a}{\pi}} \int_{-\infty}^{+\infty} J(\xi) \exp[-a(x-\xi)^2] d\xi \quad \dots (3)$$

Now, in the case of the photospheric radiation  $J(x)$  is represented by a cosine or other appropriate limb darkening function. In the present case, we shall take the following expression given by Baumbach (1937) for the mean corona:

$$J(\rho) = \frac{A}{\rho^{2.5}} + \frac{B}{\rho^7} + \frac{C}{\rho^{17}} \quad \dots (4)$$

where  $\rho = (r/R_{\odot}) \geq 1$  and  $A = 0.0532$ ,  $B = 1.425$ ,  $C = 2.565$  when  $J$  is expressed in units of  $I_0 \times 10^{-6}$ ,  $I_0$  being the intensity at the centre of the solar disc. Measuring the distance  $x$  from the solar limb we have  $x = \rho - 1$  and  $J(x) = 0$  for  $x < 0$ . Then, at the time of the second and third contacts when the limbs of the sun and moon coincide we have along the common diameter

$$I(x) = \sqrt{\frac{a}{\pi}} \int_0^{\infty} \left\{ \frac{A}{(\xi+1)^{2.5}} + \frac{B}{(\xi+1)^7} + \frac{C}{(\xi+1)^{17}} \right\} \times \exp[-a(x-\xi)^2] d\xi \quad \dots (5a)$$

On the other hand, at the time of mid-eclipse of magnitude ' $m$ ' we have to put  $I(x) = 0$  for  $x < (m-1)$  so that the broadened intensity profile will take the form:

$$I(x) = \sqrt{\frac{a}{\pi}} \int_{m-1}^{\infty} \left\{ \frac{A}{(\xi+1)^{2.5}} + \frac{B}{(\xi+1)^7} + \frac{C}{(\xi+1)^{17}} \right\} \exp[-a(x-\xi)^2] d\xi \quad \dots (5b)$$

We have computed  $I(x)$  from equations (5a) and (5b) for various values of ' $a$ ' starting from  $a = \infty$ , which represents perfect seeing and ideal apparatus, to  $a = 60''$  which corresponds to a spread of  $960/60 = 16$  seconds of arc. In (5b), we have taken  $m = 1.008$  corresponding to the magnitude of the eclipse at Japal-Rangapur Observatory. These curves are shown in Figs 1 and 2, respectively. They all have a point of inflexion at  $x=0$  for (5a) and  $x=0.008$  for (5b). This property can be used for identifying the position of the lunar limb on the intensity profile.

#### APPLICATION TO OBSERVATIONS

The position of the lunar limb, observed in the intensity profile can be determined



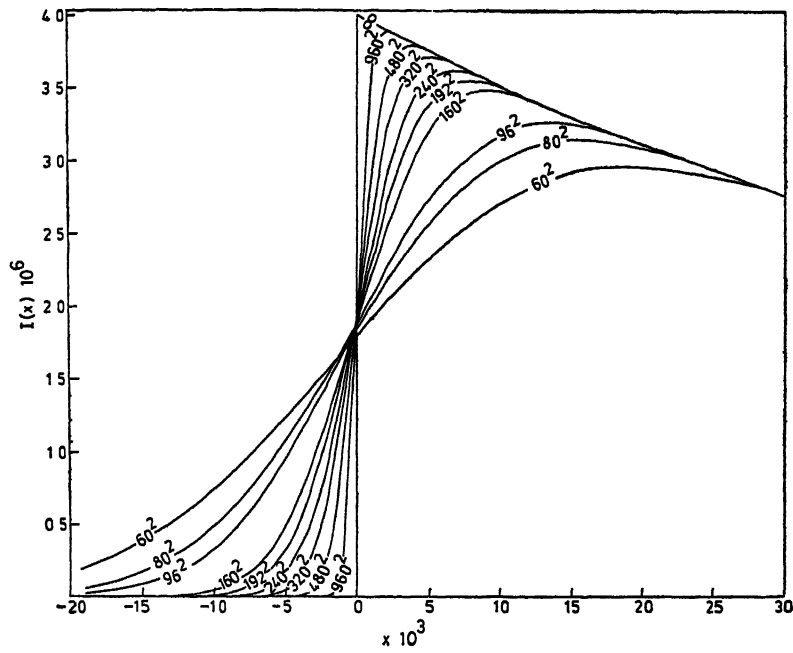


FIG. 1.

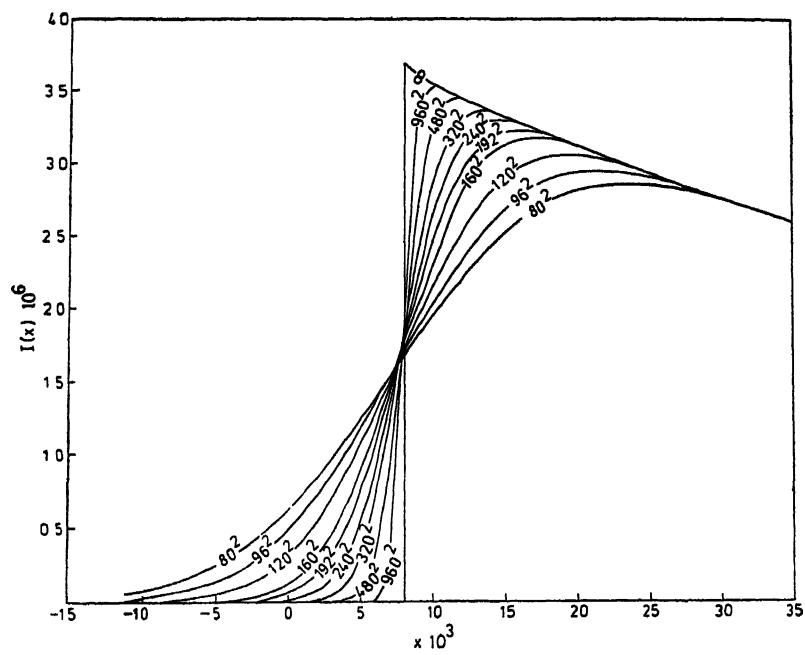


FIG. 2.

by identifying the point of inflection. It can be determined by representing the intensity distribution in its neighbourhood by the cubic equation:

$$I(x) = (ax^3 + bx^2 + cx + d), \quad . (6)$$

which gives

$$x_{\text{inflec}} = -b/3a \quad (7)$$

Finally, the observed intensity has to be scaled by factor  $K$  to bring it to the level of the mean intensity of equation (4) by means of the equation

$$K \int_{x_0}^{\infty} I(x) dx = \int_{x_0}^{\infty} J(x) dx \quad . (8)$$

where  $x_0 = 0$  or  $m-1$  as the case may be.

The scaled and properly positioned intensity profiles can then be compared with the theoretical curves for deriving the broadening parameter  $a$ . Estimate of ' $a$ ' can be by comparing either the observed and computed intensities or the observed and computed slopes at the point of inflection

It is clear that the observed coronal intensity distribution must be corrected for the smearing effect of the broadening function. The serial procedural steps would be:

- i) Use the derived isophotes to obtain the observed radial distribution of intensity at various position angles
- ii) Correct the observed radial intensity distribution by a numerical iteration technique similar to that given by Burger and van Cittert (1932)
- iii) Replot the isophotes on the basis of the corrected intensity profiles.

The computations reported in this paper were performed on the TDC 12 computer of the Osmania University Computer Centre

#### REFERENCES

- Baumbach, S. (1937) *Astron. Nach.*, 263, 121  
 Burger, H. C., and van Cittert, P. H., (1932) *Z. f. Phys.*, 79, 722  
 Minnaert, M., van den Hoven, E., van Genderen and van Diggelen, J. (1940) *B. A. N.*, 11, 55.  
 Wanders, P. (1934) *Z. f. Astrophys.*, 8, 108

Printed in India.

## Astrophysics

### ECLIPSE STUDIES OF DUST MOTION IN THE F-CORONA

W I. BEAVERS, P. H. CARR and J. J. EITTER

*Erwin W. Fick Observatory, I.S U. Ames, Iowa 50011, U.S.A.*

*(Received 7 August 1981)*

The Fick Observatory programme of study of dust motion in the F-Corona is reviewed. A detailed description is given of the photoelectric radial velocity spectrometer instruments which have been employed in both the 1979 Canadian and 1980 Indian total solar eclipses. Two of the measurements in the 1979 eclipse indicate a predominant low velocity blue shift from dust in the corona along lines of sight  $3.2 R_{\odot}$  and  $4.3 R_{\odot}$  west of the sun. Interpretations of these results and future eclipse experiment plans are described.

**Keywords:** Solar Eclipse; Solar Corona; Coronal Dust

ECLIPSE expedition teams from Erwin W. Fick Observatory had employed small portable radial velocity spectrometers at two recent solar eclipses in attempts to detect and measure line-of-sight velocities of the dust in the F-corona. Results of the velocity measurements at the 1979 Canadian eclipse have been reported by Beavers *et al* (1980). Multiple dip velocity profiles with a primary blue shift of about 50 km/sec were recorded at both  $3.2 R_{\odot}$  and  $4.3 R_{\odot}$  west of the sun. Attempts to repeat the measurements at a site in Palem, India during the 1980 solar eclipse were not successful due to difficulties with the mini-computer control of the experiment.

The programme continued with major efforts in the following two directions:

#### A. EQUIPMENT IMPROVEMENTS

1. To increase the effective data collection time in future eclipses similar multiple experiment configurations are being developed. Thus, two systems effectively double the brief eclipse observations period.
2. Each entire portable experiment is self-contained except for the need for a power source of 12 volts. This is consistent with field use anywhere in the world.
3. Experiments are being made with the use of fiber optics to couple the telescope and spectrometers, thus further reducing the size and weight of the equipment.
4. Attempts are being made to put one or more of these experiments aboard aircraft for future eclipses. This would permit obtaining more measurements during the event, provide the opportunity for attempting measurements at greater distances, i.e.,  $\sim 10 R_{\odot}$ , and will avoid clouds.
5. The eclipse spectrometers are being tested for possible applications in Zodiacal light studies.

## B. INTERPRETATION OF THE VELOCITY FEATURES

Attempts have been made to model the dust corona with small, large, or combinations of small and large particles to see what details of particle motion and distribution can produce the observed doppler signatures. So far the best fitting models appear to be those with predominantly large particles in direct eccentric orbits. Some of the models produce doppler features sufficiently narrow that we are considering developing at least one spectrometer system with higher resolution capabilities. Dependence of the doppler profiles on such features as possible inner dust boundary, role of radiation pressure and related features such as color and polarization of the coronal light is also being investigated.

## ACKNOWLEDGEMENTS

This work has received support from the U.S. National Science Foundation under Grant No. AST-7921980. We also wish to express our thanks and appreciation to the Government of India and to the cooperative officials of Andhra Pradesh, Mahabubnagar District, and to the numerous friendly hosts from Palem during our visit for the 1980 eclipse experiment.

## REFERENCE

Beavers, W. I., Carr, P. H., and Eitter, J. J. (1980) *Ap. J.*, 238, 349.

Printed in India

Astronomy

## TWO COLOUR PHOTOMETRY OF THE SOLAR CORONA

K. ANTHONY RAJU *and* K. D. ABHYANKAR

*Centre of Advanced Study in Astronomy, Osmania University, Hyderabad 500 007, India*

*(Received 7 August 1981)*

The analysis of the direct photographs of the corona taken with the double polarigraph, through blue ( $\lambda 3200\text{\AA}$ ) and red ( $\lambda 7000\text{\AA}$ ) filters, is presented. The method adopted for the absolute calibration and reduction is given. Isophote parameters like ellipticity, central shifts and average and effective radii are calculated. The intensities in the two colours are compared with the van de Hulst's model corona after applying corrections for the effect of limb darkening. It is found that in general the blue intensities are less and the red intensities more than the model corona at all radii.

**Keywords:** Corona; Isophotes; Ellipticity; Central Shifts

### INTRODUCTION

It is well established that the coronal light consists of three distinct components (Hulst, 1953) K-corona, F-corona and E-corona. The first component, K-corona, is due to the photospheric light scattered by the free electrons present in the corona. Its spectrum is continuous, without any Fraunhofer lines, since these are washed out by very fast moving electrons. The light due to K-corona is polarized and is independent of the wavelength. The second component, F-corona, is due to the diffraction of sun's light by the interplanetary dust particles. The spectrum of this component shows Fraunhofer lines, because the dust particles are heavy and relatively slow moving so that the Fraunhofer lines are not washed out. This component is unpolarized and dependent on wavelength, although the exact relation is not known accurately. It has been pointed out by van de Hulst (1950) that the F-corona varies as  $\lambda^{1/2}$ . This makes the corona significantly redder at large  $R_{\odot}$ . The third component is revealed by the emission lines in the coronal spectrum caused by the highly ionized atoms present in the coronal gas. This component, E-corona, is very weak and makes negligible contribution to the total intensity of the corona.

Attempts have been made to study the intensity of the corona in the monochromatic light of two strong coronal lines at  $5303\text{\AA}$  and  $6374\text{\AA}$ . But the problem of the colour of the corona and the wave-length dependence of F-corona is not settled yet. Allen, who made the photometric study of the corona, at the eclipse of 30 June 1954 in two colours found no reddening and concluded that there was no severe change of colour in the corona as far as 10 radii (Allen, 1956). On the other hand both theory and observations showed that the F-corona is significantly redder (Hulst, 1947, and Blackwell, 1952). Ney has found a small infrared excess in the corona during the eclipse of 2 October 1959 (Ney *et al*, 1961).

*Instrument*

In order to study the intensity distribution of the corona at two wavelengths during the total eclipse of 16 February 1980 a double polarigraph had been constructed (Anthony Raju, 1980). This instrument enables one to photograph the corona directly and also through polaroids in two colours. Two filters, blue and red, whose peak transmission are at  $4200\text{\AA}$  and  $7000\text{\AA}$  respectively, were used to photograph the corona. Thus the intensity and also the polarization of the corona can be studied at two wavelengths simultaneously.

This instrument was attached to the 48-inch telescope of the Japal-Rangapur Observatory of Osmania University from where the eclipse photographs were taken. The local circumstances of the eclipse at the observatory were (Subrahmanyam & Sreedhar Rao, 1979). Longitude= $-98^{\circ} 43' 7''$ , Latitude= $17^{\circ} 05' 9''$ , Elevation= $695\text{m}$  above msl, Duration of totality= $129\text{s}$ .

Eight photographs of the corona in each colour, of which two are direct ones, were taken during the totality with exposure times of 4s and 10s. The two direct photographs taken through blue and red filters are shown in Figs 1 and 2, respectively.

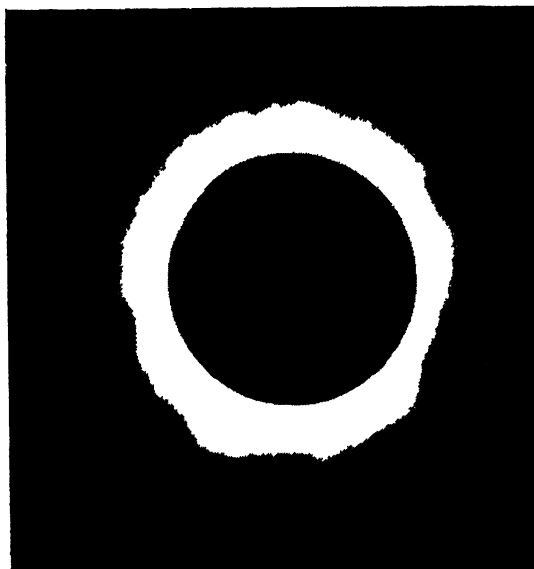


FIG 1 Photograph of the corona in blue

#### CALIBRATION AND REDUCTION

*(a) Calibration*

The calibration in the present work was made in the absolute units in the following manner. Two sources of light, the Sun and another standard source, were photographed through a 20-step optical wedge. The intensity of the sun was reduced by a known amount by using two neutral density filters. The effect of limb darkening was

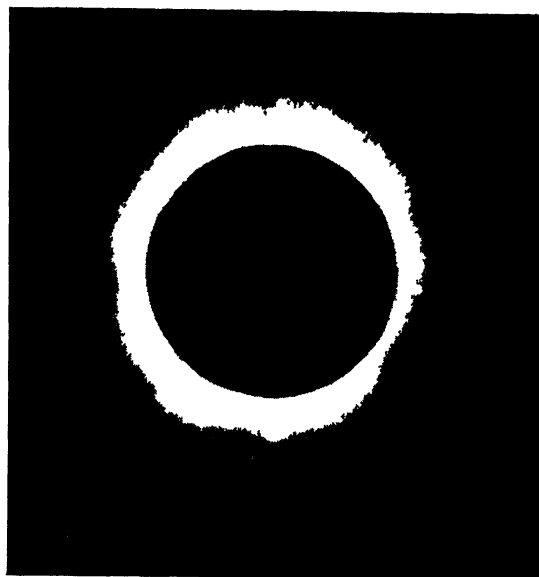


FIG. 2. Photograph of the corona in red.

properly taken into account. The two curves resulting from these were plotted on the same scale and they were found to be parallel. The curve for the sun had only a few points whereas the other curve had 20 points covering the whole range of densities. Since the short curve was in the absolute units, the shift necessary to make both the curves coincide was found out and this was used to put the complete curve in the absolute units. Thus all the intensities are expressed in terms of brightness at the centre of the solar disc. The same optical system and the same exposure times that were used for the corona were used for the calibration also. Separate curves were drawn for both the colours.

(b) *Transmission of ND Filters*

We used Kodak Wratten ND filters of densities 0.9 and 3.0 as specified by the manufacturers. In order to check the neutrality of the filters, we measured their transmissions by observing G stars with the photoelectric photometer attached to the 48-inch telescope of Japal-Rangapur Observatory. The measured densities are given in Table I, from which it is clear that the filters are not strictly neutral. We have used our measured densities for the absolute calibration of the coronal intensities.

(c) *Scanning of the Photographs*

The eclipse negatives were scanned using the Joyce-Loebl microdensitometer of Regional Research Laboratories of Hyderabad. The north-south direction was marked on each of the negatives, which were scanned along this direction and also along parallel sections at intervals of  $\frac{1}{2}$  mm for blue and  $\frac{1}{4}$  mm for red. A slot of 20 microns square was used for scanning.

TABLE I  
*ND filter transmissions*

Filter No	Density given by manufacturer	Measured density	
		Blue	Red
1	3.0	3.446	3.269
2	0.9	1.090	0.904
Total	3.9	4.536	4.173

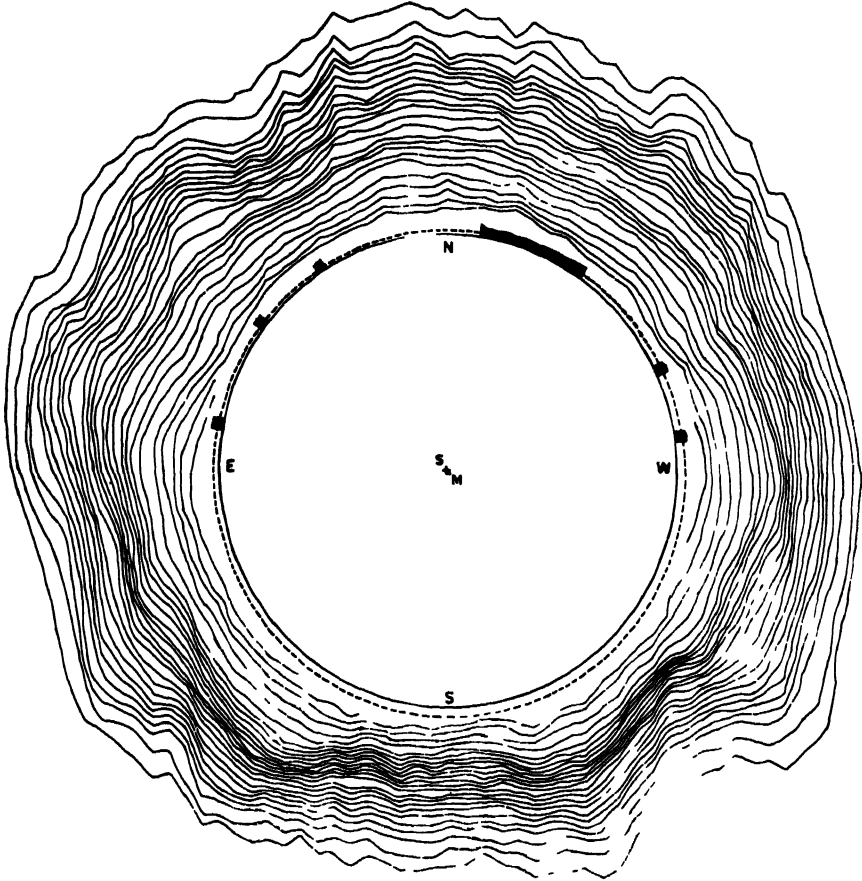


FIG 3 Coronal isophotes in blue



(d) *Drawing of the Isophotes*

The microdensitometer scans were used to plot the contours of equal intensity in the corona. The distances of points having a fixed intensity were found out from the centre of the moon on each tracings. All the points were plotted with the centre of the moon as origin and they were joined to give the isophote of that intensity. This procedure was repeated for all the isophotes, drawn at an interval of 0.075 in log intensity, except for a few inner ones where the interval was 0.15 on the same scale. Both negatives of 10s and 4s exposures were combined for plotting the isophotes. The final isophotes for blue and red wavelengths are shown in Figs. 3 & 4. The intensities of various isophotes are given in Tables II and III where the isophotes are counted from outside in.

(e) *Positions of the Moon and the Sun*

The isophotes thus obtained are centred around the moon. The diameter of the

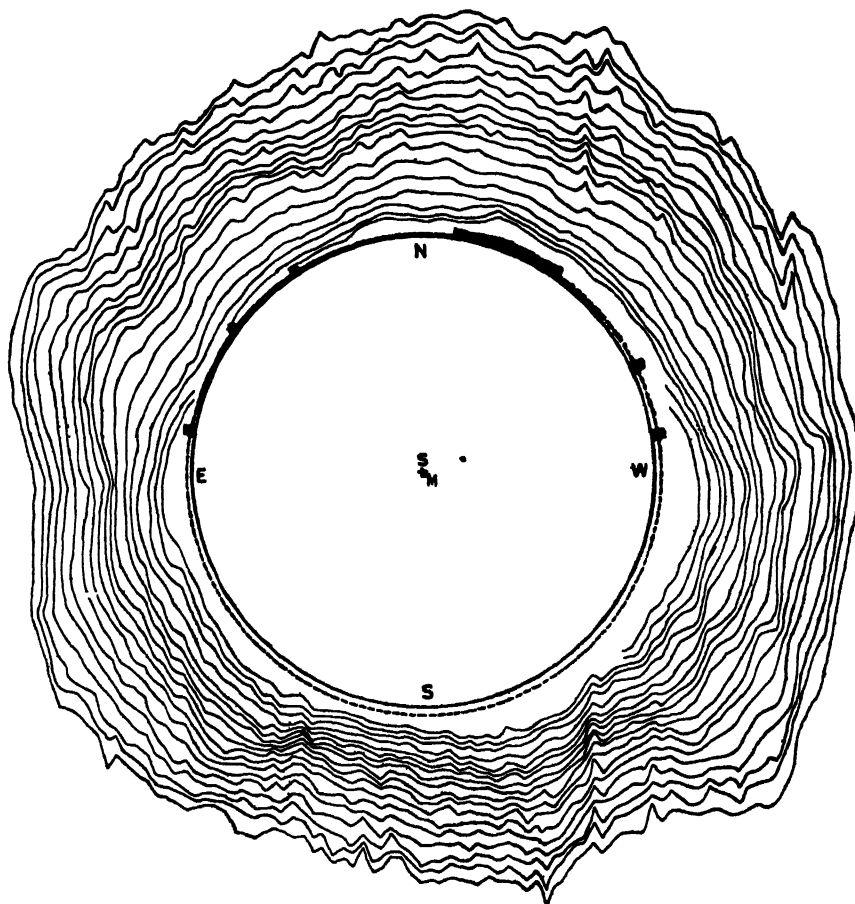


FIG 4 Coronal isophotes in red

TABLE II

*Coronal isophotes in blue*

Isophote No.	Intensity (in $B_{\odot}$ )	Ellipticity	Shifts of Centres Towards North      Towards East		Average radius (in $R_{\odot}$ )	Effective radius (in $R_{\odot}$ )
1	$8.811 \times 10^{-8}$	0.023	0.083	0.062	1.832	1.854
2	$1.047 \times 10^{-8}$	0.030	0.075	0.046	1.762	1.786
3	1.245	0.041	0.054	0.047	1.703	1.733
4	1.479	0.045	0.054	0.051	1.669	1.693
5	1.758	0.040	0.060	0.042	1.638	1.666
6	$2.089 \times 10^{-8}$	0.041	0.062	0.046	1.612	1.640
7	2.484	0.041	0.057	0.038	1.589	1.613
8	2.952	0.042	0.052	0.034	1.563	1.574
9	3.508	0.042	0.050	0.033	1.539	1.550
10	4.168	0.053	0.051	0.015	1.513	1.535
11	$4.954 \times 10^{-8}$	0.039	0.049	0.031	1.483	1.501
12	5.888	0.040	0.049	0.034	1.463	1.477
13	6.999	0.038	0.044	0.029	1.438	1.458
14	8.317	0.048	0.036	0.031	1.413	1.437
15	9.887	0.054	0.028	0.029	1.385	1.402
16	$1.175 \times 10^{-7}$	0.052	0.024	0.029	1.368	1.382
17	1.396	0.051	0.024	0.026	1.343	1.363
18	1.660	0.047	0.011	0.023	1.317	1.335
19	1.973	0.049	0.005	0.021	1.296	1.307
20	2.344	0.045	-0.007	0.026	1.255	1.271
21	$3.312 \times 10^{-7}$	0.038	-0.011	0.021	1.222	1.234
22	4.678	0.026	-0.013	0.015	1.184	1.193
23	6.606	0.032	-0.010	0.016	1.148	1.165
24	9.333	0.024	-0.010	0.016	1.119	1.132

moon's disc was determined by:

- i) measuring the actual diameter on the negative;
- ii) calculating the diameter from the focal length of the lens; and
- iii) measuring the distance between the points of inflection on the tracings

These three values agreed within the experimental errors

To draw the Sun's disc inside the moon, the following procedure was adopted. The values of the semi-diameters of the Sun and the Moon were found out, for the

TABLE III

*Coronal isophotes in red*

Isophote No	Intensity (in $B_{\odot}$ )	Ellipticity	Shifts of Centres		Average radius (in $R_{\odot}$ )	Effective radius (in $R_{\odot}$ )
			Towards North	Towards West		
1	$5.703 \times 10^{-8}$	0.014	0.086	0.063	1.849	1.865
2	6.775	0.021	0.078	0.061	1.801	1.807
3	8.052	0.029	0.065	0.057	1.756	1.762
4	9.570	0.044	0.059	0.063	1.700	1.709
5	$1.137 \times 10^{-7}$	0.040	0.051	0.059	1.647	1.656
6	$1.353 \times 10^{-7}$	0.053	0.051	0.065	1.600	1.619
7	1.607	0.054	0.049	0.067	1.557	1.562
8	1.909	0.054	0.039	0.067	1.511	1.507
9	2.269	0.054	0.039	0.076	1.483	1.494
10	2.697	0.054	0.046	0.072	1.449	1.449
11	$3.206 \times 10^{-7}$	0.047	0.039	0.067	1.415	1.416
12	3.810	0.047	0.023	0.070	1.362	1.368
13	4.528	0.052	0.006	0.079	1.319	1.336
14	5.382	0.057	-0.017	0.072	1.271	1.278
15	7.602	0.046	-0.027	0.070	1.221	1.239
16	$1.074 \times 10^{-6}$	0.076	-0.061	0.070	1.181	1.195
17	1.517	0.056	-0.033	0.066	1.156	1.163
18	1.999	0.052	-0.034	0.064	1.140	1.137

eclipse day, from the ephemeris. The position angles of the second and third contacts for Rangapur site were taken from the General Information on total solar eclipse, 16 February 1980 (Bhattacharyya, 1979). Taking the moon as stationary, the positions of the centre of the sun are found out at second and third contacts using the above values. The line joining these two will give the path of the Sun's centre during totality. The position of the centre of the Sun is found out for the time at which the photograph is taken, and taking this point as the centre, the Sun's disc is drawn. The dashed circles in Figs 3 and 4 show the moon and the inner continuous circle shows the position of the sun. The positions of the prominences, as observed by us are also indicated in them, they coincide with other observations by Durst (1981) and Rybansky (1980).

(f) *General Description of the Isophotes*

The general appearance of the isophotes in the two colours is more or less similar. They are almost circular as they should be for the corona of the maximum phase of the solar cycle (Waldmeier, 1971). The isophotes show a clear asymmetry in the north-south direction. From the positions of the prominences, it appears that the north-south asymmetry is correlated to the high prominence activity on the north side, which has spread out the isophotes in that direction. Several observers have reported

the existence of a coronal hole in the south at the time of the eclipse which also makes the corona less bright in the south (Sivaraman, 1980)

#### ISOPHOTE PARAMETERS

##### (a) *Ellipticity*

For each isophote the ellipticity is calculated using the Ludendorff's (1928, 1934) formula

$$\epsilon = \frac{D_{\text{equ}}}{D_{\text{pole}}} - 1. \quad (1)$$

Here  $D_{\text{equ}}$  is the average of the equatorial diameter and the two diameters that make an angle of  $22^\circ 5'$  with the equator. Similarly  $D_{\text{pole}}$  is the average of the polar diameter and the two diameters that make an angle of  $22^\circ 5'$  with the polar axis.

The values obtained for the corona in blue are given in Table II. They vary between 0.02 and 0.055 with an average about 0.04. The values of the ellipticity for the corona in red are given in Table III, here the average ellipticity is about 0.05. These are expected values for the corona of maximum phase (Bappu *et al.*, 1973). Our values of ellipticity for the present corona are compared, in Table IV, with the other values for the various coronas in different phases of solar cycle (table after Waldmeier, 1971). The ellipticity of the present corona is nowhere zero, which shows that this corona is not perfectly circularly symmetrical.

TABLE IV  
*Ellipticity of the corona*

Eclipse				Ellipticity
1958	October	12		0.07
1959	October	2		0.14
1961	February	15		0.17
1962	February	5		0.28
1963	July	20		0.29
1965	May	30		0.24
1968	September	22		0.06
1970	March	7		0.00
1980	February	16	(present work)	0.045

##### (b) *Central Shifts*

In addition to the ellipticity, the shift of the centre of the isophote from the centre of the Sun is also calculated for each isophote, because they also represent the asymmetry of the corona. These values were calculated using the formulae

$$\begin{aligned} \text{Shift towards north} &= \frac{r_n - r_s}{2}, \\ \text{and} \\ \text{Shift towards east} &= \frac{r_e - r_w}{2}, \end{aligned} \quad (2)$$

where  $r_n$ ,  $r_s$ ,  $r_e$  and  $r_w$  are the radial distances of the isophote in north, south, east and west directions, respectively. The values of the shifts thus calculated are given in Tables II and III, where they are expressed in the units of  $R_\odot$ . In blue, the shift towards east is more or less constant, but the shift towards north is found to increase as the distance from the limb increases. A similar behaviour is observed in red also. But the difference between the corona in two colours is apparent in the east-west direction. In red, the shift is towards west, i.e., the isophotes are more spread out in the west while in the blue the shift is towards east. Thus these shifts not only show the general asymmetry of the corona in a particular colour, but also the differences in isophotes between the two colours. The shifts are obviously related to the structure of the corona in various directions. When more information would become available regarding the differences of temperature, density, magnetic fields etc., in the various parts of the corona, it may become possible to interpret our findings regarding the differences in various isophotes of the same colour and the differences in the blue and red corona.

(c) *Average Radius and Effective Radius*

The average radius for each isophote is found out by taking the average of the 16 radial distances at intervals of  $22^\circ 5'$  in azimuth. Thus

$$r_{\text{ave.}} = \sum_{i=0}^{15} \frac{r(N - 22^\circ 5')}{16} \quad \dots (3)$$

Next, the area of the corona under each isophote is measured and the effective radius is found out by means of the equation:

$$A = \pi r_{\text{eff.}}^2 \quad (4)$$

Both values are given in the Tables II and III; it can be seen that they are nearly the same

#### RADIAL VARIATION OF INTENSITY

Both the average radius and the effective radius can be used to plot the variation of intensity in the corona. However, the effective radius is more representative as it takes into account the extent of the isophote in all directions. Consequently, the plots of intensity against  $r_{\text{eff}}$  shown in Fig. 5 are a good measure of the average variation of coronal intensity with radial distance. The van de Hulst model corona for maximum solar cycle is also shown for comparison.

It can be seen that the corona in red is brighter than the model corona throughout whereas the intensity in blue colour is lower than that of the model. The model corona which is based on a limb darkening coefficient of 0.6 most probably represents the wavelengths of  $\lambda 5500\text{\AA}$ . A part of the difference between the three curves is obviously due to the effect of the limb darkening on the intensity of the corona (Billings, 1966).

In order to compare with the van de Hulst model, our values are converted to  $\lambda 5500\text{\AA}$  after allowing for the limb darkening effect. The two expressions for tan-

gential component,  $I_t$ , and radial component,  $I_r$ , of electric vector of the scattered radiation are (Billings, 1966):

$$I_t = I_0 \frac{N_s \pi \sigma}{2} [(1-u)C + uD] \quad \dots (5)$$

$$I_t - I_r = I_0 \frac{N_s \pi \sigma}{2} \sin^2 \chi [(1-u)A + uB] \quad \dots (6)$$

where  $A, B, C, D$  are functions that depend on  $r$  and are tabulated by Billings

From the above two expressions the total intensity can be written as (taking  $\chi = \pi/2$ )

$$I_t + I_r = I_0 \frac{N_s \pi \sigma}{2} [(1-u)(2C-A) + u(2D-B)] \quad \dots (7)$$

Then the ratio of the intensities in two wavelengths  $\lambda_1$  and  $\lambda_0$  becomes

$$\frac{I(\lambda_1)}{I(\lambda_2)} = \frac{(1-u_1)(2C-A) + u_1(2D-B)}{(1-u_2)(2C-A) + u_2(2D-B)} \quad \dots (8)$$

Putting  $u=0.796, 0.600$  and  $0.485$  for  $\lambda=4200\text{\AA}, 5500\text{\AA}$  and  $7000\text{\AA}$  respectively, the intensities in blue and red can be reduced to those at  $\lambda=5500\text{\AA}$ . They are shown in Fig. 5 with thin lines. We now find that the intensity in the blue merges with the model corona near the limb and is less in the outer region. The intensity in red is however greater than the model corona at all distances

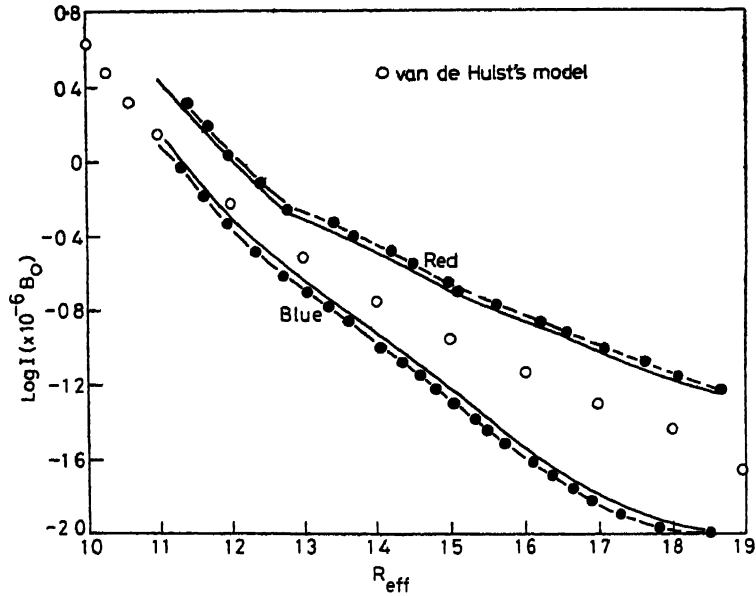


FIG 5 Variation of intensity with  $r_{eff}$

Our analysis has so far given the qualitative behaviour of the corona in two colours separately, which shows that the corona is not similar in the two colours.

The detailed quantitative comparison of the intensities is being made and final results will be available after some time

#### ACKNOWLEDGEMENTS

We thank Mr K. R. Radhakrishnan, for helping us in the calibration of filters. We are also thankful to the Director and staff of Regional Research Laboratory, Hyderabad for their help in making the density tracings K. Anthony Raju thanks the University Grants Commission, New Delhi, for giving Teacher Fellowship under the Faculty Improvement Programme.

#### REFERENCES

- Allen, C W (1956) *Mon Not R astron Soc.*, **116**, 69.  
 Anthony Raju, K (1980) *Bull astron Soc. India*, **8**, 65.  
 Bappu, M K V *et al.* (1973) *Pramana*, **1**, 117.  
 Bhattacharyya, J C (1979) *General Information, Total Solar Eclipse, February 16, 1980*, p. 11  
 Billings, D. E (1966) *A Guide to Solar Corona*, p 150. Academic Press, New York  
 Blackwell, D. E (1952) *Mon Not R astr Soc*, **112**, 652  
 Dürst, J (1981) *Private Commun*  
 Hulst, H C van de (1947) *Astrophys J*, **105**, 471  
 ——— (1950) *Bull astr. Inst Netherl*, **11**, 135.  
 ——— (1953) *The Sun*, p 255 (Ed G P Kuiper) The University of Chicago Press, Chicago.  
 Lundendorff, H (1928) *Sitzber Preuss Akad Wiss*, **16**, 185  
 ——— (1934) *Ibid*, 200  
 Ney, E P *et al*, (1961) *Astrophys J*, **133**, 616  
 Rybansky, M (1980) *Bull astron Inst Czechosl*, **31**, 316  
 Sivaraman, K R (1980) Paper presented at Astr Soc India Sixth Annual meeting  
 Subrahmanyam, P V, and Sreedhar Rao, S (1979) Nizamiah and Japal-Rangapur Observatories, Contr No 11  
 Waldmeier, M. (1971) *Physics of the Solar Corona*, p 130 (Ed C J Macris). Reidel Publishing Company, Dordrecht

Printed in India

Astronomy

## INTERFEROMETRIC ECLIPSE OBSERVATIONS OF THE Fe XIV INNER CORONA

R N SMARTT, J B ZIRKER and H. A. MAUTER

*Sacramento Peak Observatory,\* Sunspot, New Mexico 88349, U.S.A*

*(Received 7 August 1981)*

An experiment carried out during the 16 February 1980 total solar eclipse to measure velocities and intensity distributions associated with coronal loops is described. The optical instrumentation used consisted of a 30cm aperture Cassegrain telescope, a solid Fabry-Perot etalon, ancillary optical components and a motor-driven camera. During totality, the green corona was photographed both with and without the etalon in the system, the first maximum of the etalon beyond the limb was recorded on three frames. A preliminary discussion of the data is presented.

**Keywords:** Solar Eclipse; Inner Corona; Magnetic Loops

### INTRODUCTION

The primary objective of our experiment was to determine the mass flux in magnetic loops associated with active regions in the corona, and the 16 February 1980 solar eclipse presented an attractive opportunity to obtain such observations since it occurred close to the maximum activity phase of the solar cycle. A secondary objective was to study the detailed intensity distribution of the corona in the vicinity of the limb, obtained near second and third contacts, to provide further information about where and how the energy contained in the downward mass flow is dissipated. The observations were carried out at the Japal-Rangapur Observatory, operated by Osmania University, Hyderabad, India.

Observations of coronal and prominence loops, in the EUV and at visible wavelengths, have suggested that there is significant mass motion of the plasma along loop field lines (Kopp & Pneuman, 1976). This concept is supported by calculations (Cheng, 1977) that show that such mass motion can account, at least in part, for the remarkable stability of coronal loops, which, in the absence of such stabilizing factors, would be disrupted in a magnetohydrodynamic time scale of a few seconds. Based on an analysis of the energy and pressure balance of coronal loops, Foukal (1976, 1978) has suggested that material flows from the corona, across field lines at the top of loops, and down both sides to the chromosphere, the downflow resulting either from thermal instability or from fluctuations in the deposition of non-thermal energy.

---

\*Operated by the Association of Universities for Research in Astronomy, Inc. under contract AST-78-17292 with the National Science Foundation, U.S.A.



His conclusions are based on a relatively small sample of optical spectra obtained at Sacramento Peak Observatory in coronal surveys between the years 1971 and 1976. His suggestions, if valid, would prove extremely interesting for the further development of ideas on mass balance, and our experiment was aimed at checking these suggestions.

Eclipse observations have been carried out using Fabry-Perot interferometers (Jarrett & von Klüber, 1955, 1961, Delone & Makarova, 1969; Liebenberg, 1975 and Liebenberg *et al.*, 1975) to obtain emission corona line widths, and the instrumentation used in the experiment described here was similar. A principal difference was that we used a solid Fabry-Perot etalon, which has significantly greater stability than the air-spaced designs used previously. We also were concerned to obtain as high spatial resolution as possible, with interest principally in details of the inner corona. Because of the marked non-uniformities of the corona in this region, reduction of the data is substantially more complex than for data obtained further out in the corona where the distribution tends to be more uniform. We present here details of our experiment and a preliminary summary of the data obtained.

### INSTRUMENTATION

The configuration of the optical system used is illustrated in Fig. 1. The primary imaging system consisted of an  $f/7.7$  field-corrected Cassegrain telescope, 30cm aperture. This system was measured interferometrically and found to have a mean wavefront error  $\sim \lambda/4$  out to a semi-field angle  $\sim 0.5^\circ$ , a value which is almost twice the angular semi field covered in our experiment. Beyond the primary focal plane,

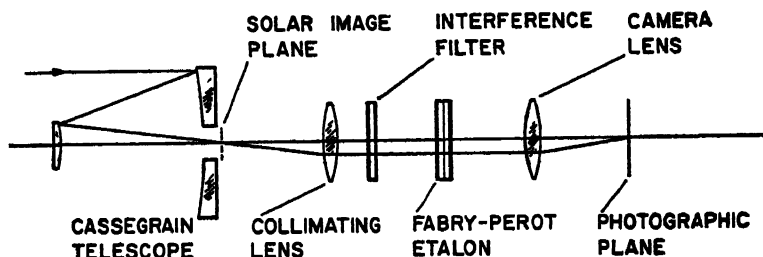


FIG. 1

© Sacramento Peak Observatory, Association of Universities for Research in Astronomy, Inc., U.S.A. — 8101 11

a 17.8cm focal length lens collimated the source rays and formed an image, 23mm diameter, of the objective aperture which was also the entrance pupil. A solid Fabry-Perot etalon, with a finesse  $\sim 20$  and free spectral range  $\sim 2.7\text{\AA}$ , was located in this image plane, with a blocking filter positioned between the collimating lens and the etalon. The filter transmission band,  $12\text{\AA}$  FWHM, was centered, for normally incident light, at  $\sim 5303\text{\AA}$ , with a peak transmittance of 0.71. The etalon was followed by a 35mm motor-driven camera, with an  $f/2.5$ , 135mm lens, located to form a telecentric system. The relayed solar image at the film plane was 17mm diameter. Panatomic-X film, although slow speed (ASA 32), was used because of its relatively high resolving power (100–200 lines/mm, depending on object contrast, exposure and development).

The Fabry-Perot etalon, of crucial importance in such an experiment, consisted of a fused-silica substrate, 0.352mm thick, 44mm diameter, with 8-layer dielectric coatings on each surface. Since such a component is extremely fragile, it was oiled between anti-reflection coated optical glass cover plates, to give a reflectance,  $R \sim 0.97$ . This value for  $R$  was probably slightly high for optimum performance, since some residual parallelism imperfections in the substrate were observed when it was examined at a large tilt angle, in an interferoscope. The finesse was measured using a filtered mercury isotope lamp source, and was found to be  $\sim 20$ , corresponding to a velocity sensitivity of approximately 3km/s, adequate for the aim of our experiment. The etalon sandwich was mounted in a temperature-controlled oven, which, with outer optical-grade windows sealed by o-rings, and internal air gaps  $\sim 1.5$ cm, provided a very stable thermal environment. A solid etalon has a considerable practical advantage for this application of being very stable, since once constructed to the thickness appropriate for the desired form and location of the interference pattern, its stability is a function only of the temperature sensitivity of the substrate. For fused silica, the coefficient of thermal refractive index change dominates the coefficient of the thermal expansion, in terms of optical thickness. Taking both parameters into account results in a sensitivity in the case of this etalon of 0.008 order shift per Celsius degree over normal operating ranges. Therefore, with only the crudest thermal control, the fringe pattern dimension is stable to within the measuring precision. For our experiment, the etalon oven was set at 40 °C.

The entire optical train was mounted on a massive, equatorially-mounted spar. An auxiliary co-aligned telescope, mounted on another spar face, produced a projected solar image, 13cm in diameter; this system was used primarily for monitoring the guiding precision. An advantage of the large-mass mount was high pointing stability, even when adjusting the optical system components. The spar was driven in right ascension, through a gear train, by a synchronous motor. Trimming of the drive rate was then possible by a variable input frequency control. Fast and slow slewing in both right ascension and declination was also possible. The guiding rate tended to drift, due in part to gear errors, and there is some possibility that a non-negligible drift occurred during the period of eclipse observations, although this is not obvious in the recorded images.

### *Calibration*

*Photometric* A telescope cover containing four holes, each 16mm diameter and covered with neutral density glass filters, produced an attenuation of  $2.8 \times 10^{-5}$  of the light transmitted by the uncovered aperture over the spectral range of the interference filter. By recording a range of exposures of the solar disc with the cover in place, exposure values appropriate for typical brightness levels of the inner green-line corona were obtained. As well, a neutral density calibrated step wedge was positioned at the primary image and the image recorded, which provided additional calibration data not only as a check of the method just described, but also to give the characteristic curve of the film.

*Interferometric* Provision was made to insert a mercury lamp, together with a condensing lens, diffusing screen and an appropriate filter for the mercury green

line, into the optical system such that the screen was located in the primary focal plane. This allowed the circular Fabry-Perot fringes characteristic of the etalon parameters and the illumination geometry, at  $\lambda$  5460.7 Å, to be recorded over an angular field identical dimensionally with that of the coronal field, apart from the negligibly small aberration introduced by the Cassegrain telescope. The etalon was designed to produce the first maximum beyond the solar limb (two maxima within the image of the solar disc) at an angular radius of 17.84', for a wavelength of  $\lambda$  5460.7 Å. The value measured was 17.93', the difference presumably due to the phase change on reflection at the dielectric films of the etalon. Any possible dispersion of phase shift between the calibrating and operating wavelengths has not yet been measured.

*Spatial Resolution:* The entire optical system was bench tested using an illuminated resolution target at the focus of a collimating mirror that was coaligned with the optical axis of the Cassegrain telescope. Measurements of the recorded image showed a resolution limit  $< 1$  second of arc, consistent both with the independent measurements of the telescope wavefront aberration, and with the scale of 0.018 mm at the film plane corresponding to a 1 arc sec field angle. Hence, with extremely good atmospheric seeing and an object of modest contrast, we would expect to detect detail down to 1 arc sec.

#### OBSERVATIONS AND PRELIMINARY ANALYSIS

Both photometric and interferometric calibration records were obtained before the first contact and in the partial phases before and after totality. During the total phase, which lasted 128s, a sequence of exposures were obtained according to a set program. Except for exposure times  $\leq 1$ s, the camera was triggered by a remotely located photographic timer. A secondary aim of the experiment was to attempt to trace loops down as close to the photosphere as possible, to gain observational clues as to how the energy, assuming downward mass flow, might be dissipated. Exposures were therefore obtained immediately following second contact and just prior to third contact, without the etalon in the optical path. Fortunately, the most active part of the green-line corona at that time almost coincided in position angle with the first part of the disc to be exposed at third contact. The angular resolution in the recorded images is estimated to be between 2 and 3 arc sec, and some loop structures are clearly evident. To determine if any loops observed were actually at limb passage at the time of observation, it was planned to intercompare the eclipse images with ground-based coronal observations at daylight hours closest to the eclipse time, but cloud precluded obtaining any such observations at Sacramento Peak Observatory except over a period of a few minutes, and the quality was not sufficient to make useful comparisons. One isolated, single loop, extending to a height of  $2.7 \times 10^4$  km, is however clearly recorded in the exposure obtained just prior to third contact and is close to the position angle of the first part of the disc to be exposed at the end of totality. Although microdensitometer tracings are required for confirmation, a visual inspection indicates that one leg of the loop disappears, or almost so, before reaching the limb. While the other leg appears to extend to the surface, there is, of course, no certainty that this is the case. Asymmetry in radiance, if in fact real, differs from the usually accepted form of such loops, but is not inconsistent with

the idea of an electric current flow from one leg to the other, under which circumstance asymmetries are presumably likely to exist

In the intervening period which represented the major part of totality, the main experiment was carried out. For this the etalon was inserted in the optical path, and exposures obtained at 0.07s, 0.13s, 0.25s, 0.5s, 1s, 5s, 15s, 25s, and 45s. Estimates of the required exposure time suggested that 1s would not give useful information, and that proved to be the case. The strategy however was that these several exposures, each  $< 1s$ , together represented only a small fraction of the totality period, and could be useful in the event of an exceptionally bright coronal region. Exposures at 15s, 25s, and 45s reveal the first maximum in the etalon transmission function. Although not crucial to the experiment, it was hoped to record also the next maximum further out in the field. Apparently, a much longer exposure time would have been required for this, since the images obtained without the etalon indicated that the green-line corona was less extensive than usual for this phase in the solar cycle.

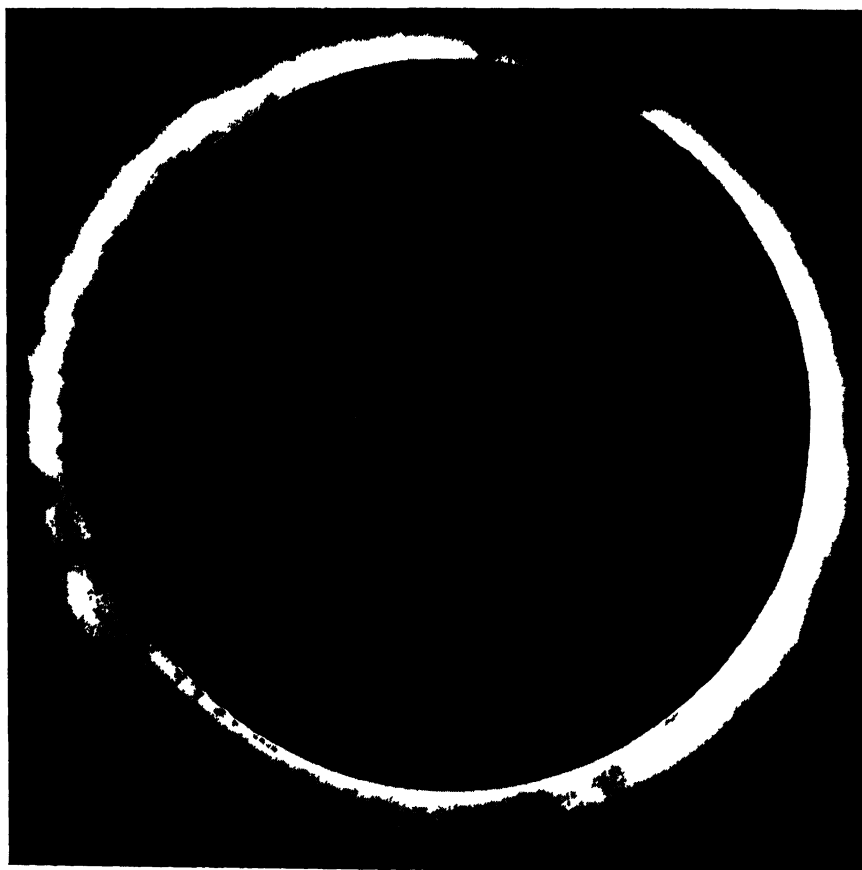


FIG 2

© Sacramento Peak Observatory, Association of Universities for Research in Astronomy, Inc, U S A 8004 15

One of the images obtained with the etalon in the optical path is reproduced in Fig 2 To highlight the maximum region, an image of the corona without the etalon has been subtracted from one with it This subtraction is poor however, due primarily to the different contrast ratio in details in the two images. Although the optical system was adjusted such that the interference pattern was precisely concentric with the solar disc prior to first contact, Fig 2 reveals an eccentric location of the maximum fringe. This is in part only apparent since the occultation by the moon is not symmetrical. But there remains a substantial eccentricity, possibly due to a tracking error, although image smearing during the 45s exposure, for example, is not evident. A further possibility is that the magnitude of the gross radial flow in the corona varied moderately systematically with position angle Since this latter explanation would require radial velocities up to an order of magnitude greater than that from solar rotation, it is regarded as implausible But such a possibility, at least to some extent, cannot be excluded at this time. Further, the diameter of the maximum fringe in the eclipse image is larger than the corresponding fringe in the mercury green pattern, while the opposite situation is to be expected without any gross radial velocity flow of the inner corona and with negligible dispersion of phase shift associated with the etalon Since some dispersion of phase shift in the etalon is likely (previously assumed negligible), while large-scale velocity flow of about  $23\text{ km s}^{-1}$  in the corona is not, we tentatively conclude that the primary cause of the displaced maximum in the eclipse image is of instrumental origin The required calibration measurement is not easily obtained, but will be carried out by recording spectra over the appropriate wavelength interval produced by a spectrograph with the etalon placed over the entrance slit.

Finally, while the eclipse records are rich in structure detail, precise information cannot be simply extracted, since this detail itself complicates the reduction Therefore, to deduce accurate line profiles and line shifts, especially in the vicinity of loops, requires micro-densitometer scans and computer processing of the data. This work is proceeding

#### ACKNOWLEDGEMENTS

We are extremely grateful to the Astronomy Department of Osmania University under the directorship of Professor R. D. Abhyankar for the hospitality and excellent support provided, especially the work carried out at the site by Professor B. K. Sarma, Dr N. B. Sanwal and Mr G. Som Sunder. This experiment was made possible by the National Science Foundation sponsored eclipse expedition, efficiently organized by Ronald R. La Count, coordinator, and effectively executed in India by Gene Prantner, field support manager

#### REFERENCES

- Cheng, C. C. (1977) On the stability of a coronal loop with mass motion (*Submitted*)  
 Delone, A. B., and Makarova, E. A. (1969) Interferometric investigation of the red and green coronal lines during the total solar eclipse of May 30, 1965 *Solar Phys.* **9**, 116–130  
 Foukal, P. V. (1976) The pressure and energy balance of the cool corona over sunspots *Ap J*, **210**, 575–581  
 ——— (1978) Magnetic loops, downflows and convection in the solar corona *Ap J*, **233**, 1046–1057

- Jarrett, A H, and von Klüber, H. (1955) Interferometric measurements of the green coronal line during the total solar eclipse of 1954 June 30. *M N*, **115**, 343–362
- (1961) Interferometric investigation of emission lines of the solar corona during the total solar eclipse of 1958 October 12 *M N*, **122**, 223–238
- Kopp, R A, and Pneuman, G W (1976) Magnetic reconnection in the corona and the loop prominence phenomenon *Solar Phys*, **50**, 85–98
- Lieenberg, D. H (1975) Coronal emission line profile observations at total solar eclipses *Solar Phys*, **44**, 331–344.
- Lieenberg, D H, Bessey, R. J, and Watson, B (1975) Observed coronal temperatures at  $1.37 R_{\odot}$  in the region of a helmet structure *Solar Phys*, **40**, 387–396

## Session B : ATMOSPHERIC PHYSICS

### SOLAR RADIATION AND RELEVANCE TO ECLIPSE STUDIES

A. K. SAHA

*National Physical Laboratory, New Delhi-110012, India*

*(Received 2 September 1981)*

This is a discussion on solar electromagnetic radiation as it impinges on the earth's atmosphere. With a solar eclipse this radiation is obstructed by the moon and consequences of blanking of radiation are felt at various levels of the atmosphere.

**Keywords:** Solar Radiation; Blanking of Radiation

Major part of radiation from the Sun is in the visible and infrared region and is emitted with an equivalent black body temperature of about 5900 °K. There are radiations of lower intensity in the far ultraviolet and in the X-ray region and at metre wavelengths in the radio frequency that correspond to higher temperatures. A sizeable part of the radiation over the whole spectrum range is absorbed at various levels of the atmosphere by various constituent molecules and atoms at their characteristic wavelengths. In Fig. 1, this is illustrated with the level of radiation at the

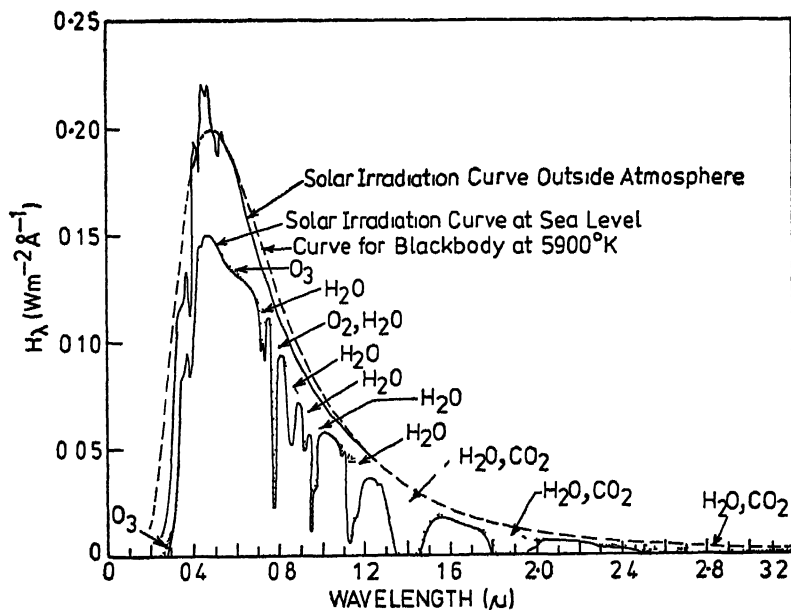


FIG. 1. Spectral distribution of solar irradiation reaching the earth.

top of the atmosphere and the level reaching the ground. This is for the overhead sun. With the inclination of the sun, the mass of intervening atmosphere in the ray path increases and there is a continuing diminution of level at all wavelengths with the zenith angle.

The earth's surface and the atmosphere receive energy from the incident sunlight. Part of the incident light is reflected back from the top of the atmosphere, from the ground surface and from cloud cover, forming the albedo. The earth, constituting the surface and the atmosphere, also re-radiates energy outwards. But this is with a much lower characteristic temperature of about 288 °K, so that the bulk of this energy is in the infrared region. This re-radiation also is possible only in certain windows of the spectrum, where the atmospheric gases (mainly H<sub>2</sub>O and CO<sub>2</sub>) do not have their absorption bands (Fig. 2). The incoming energy and the re-radiation constitute the atmospheric radiation balance, affecting climate and meteorology on the earth.

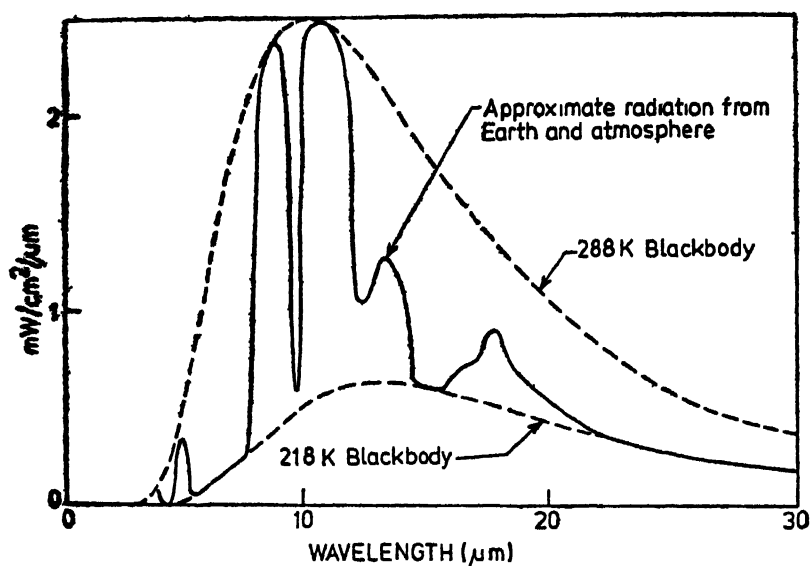


FIG. 2. Spectral radiance curve for thermal radiation leaving the earth. The earth's surface is approximated to 288 °K blackbody and the atmosphere to 218 °K.

In the stratosphere, there are some minor constituents whose concentrations are dependent on photo-chemical processes. For example, nitric oxide at these heights is known to decrease during an eclipse. Of more interest is Ozone, on which several studies have been made. Fig. 3 shows results of some computations of Ozone concentrations at various height levels (Herman, 1979), according to known photo-chemical processes, during day and night periods. A solar eclipse may be considered as onset of night time conditions on a compressed time scale. It may be noted in Fig. 3 that no changes in ozone concentration are expected at heights below 30km. For higher heights there is an increase in ozone. But total ozone change is expected to be less than 1 per cent (increase) as the bulk of ozone is below 30km level. An U-2 flight



at a height of 19.6km in 1979 total solar eclipse over North American continent did not show any change in ozone (Starr *et al*, 1980).

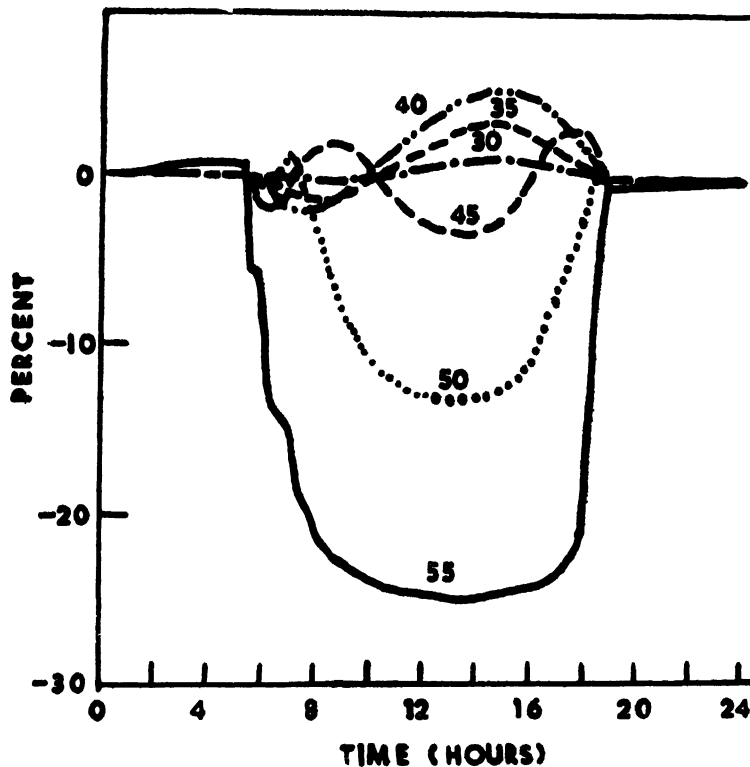


FIG. 3. Theoretical estimate of percentage change in diurnal variation of ozone at altitude of 30, 35, 40, 45, 50 and 55km (after Herman, 1979).

Solar radiation at wavelengths below about 2900Å is absorbed in the upper atmosphere (Friedman, 1960). Ozone in the stratosphere is responsible for the absorption down to about 2000Å. Molecular oxygen absorbs below 2000Å, radiation at wavelengths shorter than 1750Å dissociating  $O_2$  in the height range 85–100km. Below about 850Å all constituents of the upper atmosphere contribute to the absorption (Fig. 4).

Extreme ultraviolet radiation ionizes various constituents of the upper atmosphere to form the ionosphere. Lyman- $\alpha$  radiation at 1216Å ionize NO in the D-region around 70–80km Lyman- $\beta$  at 1025Å, ionizing  $O_2$ , is partly responsible for the E-region. Radiation at wavelengths below about 1000Å cause ionization at upper E and F-regions. Several line radiations like neutral and singly ionized helium at 584Å and 304Å and multiple ionized iron lines at 355Å and 288Å contribute substantially to F-region ionization. Soft X-ray spectrum of 30–100Å are absorbed between 100 and 140km to provide bulk of the E-region ionization. Still shorter X-rays contribute to

ionization in the upper D-region Blocking of the ionizing radiations during a solar eclipse should affect electron density levels at all ionospheric heights.

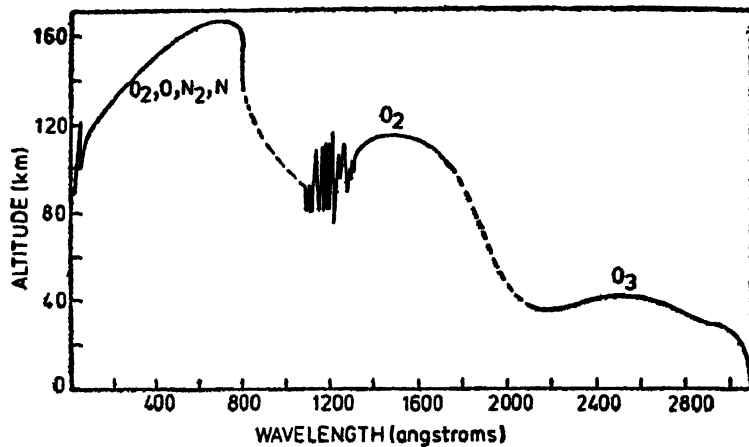


FIG. 4. Penetration of solar radiation into the atmosphere, indicating the level at which the intensity is reduced to  $1/e$ .

The ionizing radiation changes during a solar eclipse will be a combined effect of the diurnal change of the zenith angle of the sun and the obscuration of the sun by the moon. The total insolation pattern would be similar to what is shown in Fig. 5. This will be so if all the radiation came uniformly from the visible solar disc or the photosphere. However, the radiations in both extreme ultraviolet (XUV) and X-rays are from specific areas of the Sun and these are not necessarily limited to the solar disc. Very often they overflow outside. The positions of the active areas are of significance in understanding the ionization changes in the ionospheric layer during a solar eclipse. Satellite observations of the Sun in XUV and X-rays allow predictions of positions of these active areas. Such predictions were provided by the National Physical Laboratory, New Delhi, for the solar eclipse of 16 February 1980, to help timing the launch of rocket payloads from Thumba and SHAR, so that they were in periods when the active areas were eclipsed by the moon.

Radiations from the Sun in the radio ranges are also from selective and active areas and, therefore, their obscurations are also not according to the simple picture given in Fig. 5. These radiations do not affect the atmosphere. But they are observable at ground level and, during an eclipse and solar obscuration, give some information on the distribution of the radio emitting regions on the sun, which are often associated with active regions emitting XUV and X-rays.

Temperature changes during eclipse period, at various heights in the atmosphere, will be dependent on the amount of energy that is being absorbed at those heights and the time variation of the incident radiation. At levels near the surface of the earth, there should be a substantial cooling effect and cooling should be expected at almost all heights, unless there is a change in concentration of the absorbing consti-

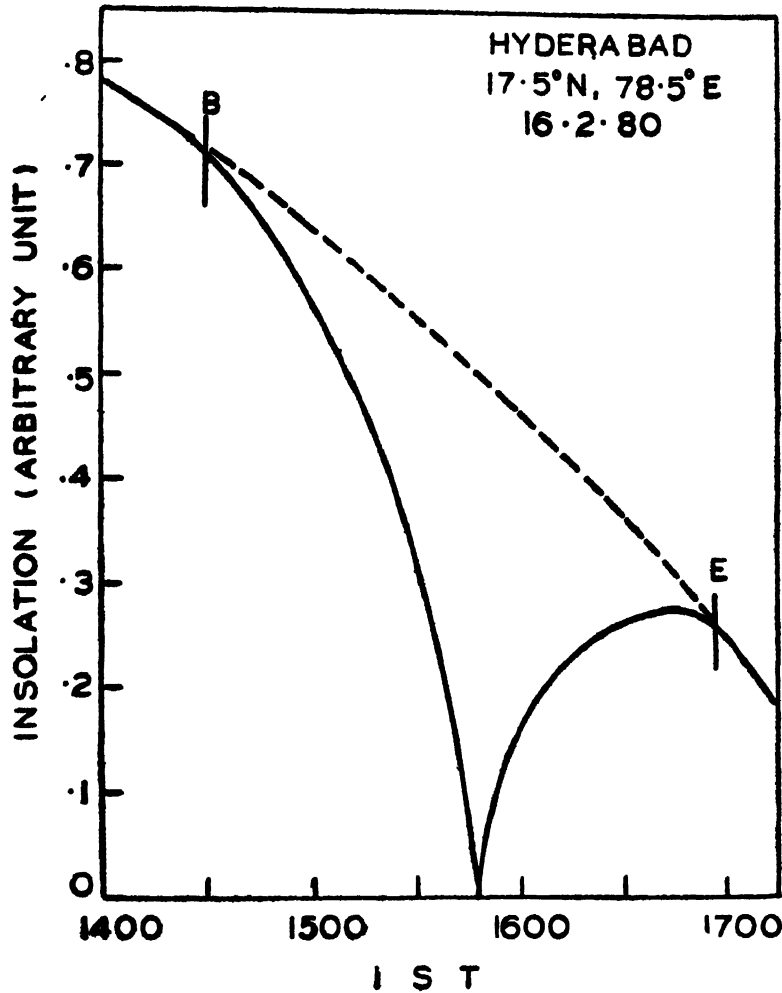


FIG. 5. Variation of solar radiation reaching ground level with progress of solar eclipse, as expected from simple considerations

tuent at that height. Such effects may be felt at heights where ozone level increases during eclipse. Increase in temperature has been observed at heights above 50km, but cooling effects are reported even at 40 or 45km. Sudden decrease of temperature at such heights during eclipse totality have been cited as source of atmospheric gravity waves proceeding outwards from the eclipse path (Chimonas & Hines, 1970). Lowering of temperatures at ionospheric heights have also been inferred, such as in Fig. 6, where temperature estimation has been made by combined analysis of ionosonde and absorption measurements during a previous eclipse (Venkatachari *et al*, 1972).

During a solar eclipse, radiation levels at all wavelengths should decrease with the obscuration of the Sun. Decrease in concentration of some absorbing gas, in the

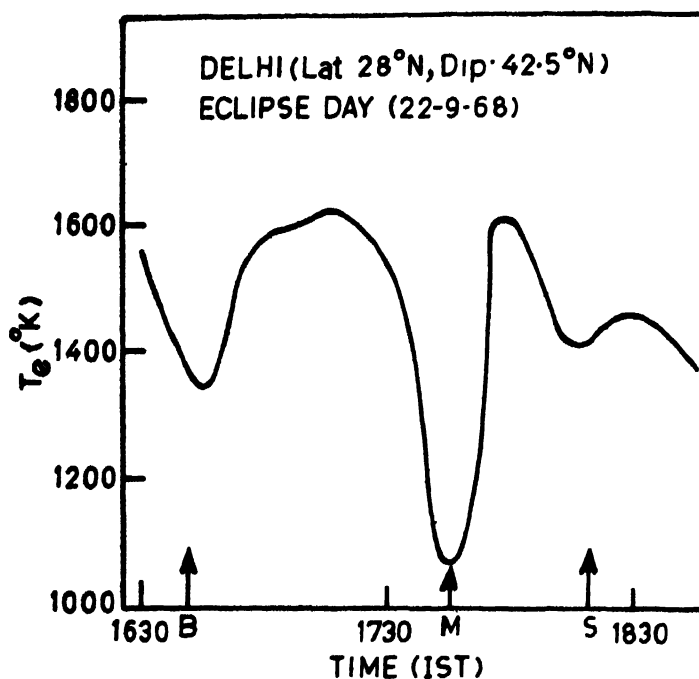


FIG. 6. Variation of electron temperature in the F-region during a solar eclipse, inferred from radio observations

atmosphere, could result in increase of irradiation at ground level, at some wavelengths. This, however, does not occur, even with ozone, that shields solar ultraviolet radiation that is harmful to life. No additional danger from the Sun is therefore expected during eclipse.

#### REFERENCES

- Chimonas, G., and Hines, C. O. (1970) Atmospheric gravity waves induced by a solar eclipse. *JGR*, **75**, 875.
- Friedman, H. (1960) The sun's ionizing radiations. In *Physics of the Upper Atmosphere* (Ed. J. A. Ratcliffe) Academic Press, 133-218.
- Herman, J. R. (1979) The response of stratospheric constituents to a solar eclipse, sunrise, and sunset. *JGR*, **84**, 3701-3710.
- Starr, W. L., Craig, R. A., Loewenstein, M., and McGhan, M. E. (1980) Measurement of NO, O<sub>3</sub>, and temperature at 19.8 km during the total solar eclipse of 26 February, 1979. *Geophys. Res. Lett.*, **7**, 553-555.
- Venkatachari, R., Sharma, L. H., and Chakrabarty, D. K. (1972) Anomalous behaviour of F-region during solar eclipse of September 22, 1968. *Indian J. Radio & Space Phys.*, **1**, 246-248.

Printed in India.

Ozone

## ROCKET MEASUREMENT OF OZONE CONCENTRATIONS DURING THE SOLAR ECLIPSE OF 16 FEBRUARY 1980

B. H. SUBBARAYA *and* SHYAM LAL

*Physical Research Laboratory, Ahmedabad-380 009, India*

*(Received 15 February 1982)*

Three Centaure IIB rockets were launched with a combination of payloads for studying the behaviour of the lower ionosphere, neutral atmosphere and atmospheric ozone during the solar eclipse of 16 February 1980 from Thumba (8.5°N, 77°0'E), India. Two rockets were launched on the eclipse day, the first at 1454hr IST when the sun was obscured by 40 per cent and the second at 1522hr IST when the sun was obscured by 70 per cent. The third rocket was launched as a control flight on 17 February 1980 at 1522hr IST. Ozone concentrations could be estimated from an altitude of 15km to about 65km. It was found that while the ozone concentrations at the peak were nearly same on all the flights, there were some changes in the level of the ozone maximum. Further, below the peak both the profile shape and number densities changed from flight to flight. In the 40-50km region, the ozone values were larger during the eclipse than the normal values, the difference increasing with height and with the progress of the eclipse. In the lower mesosphere, i.e., above about 55km, large increases were observed during the first flight. This was followed by a decrease in ozone from the first flight to the second flight, i.e., from 40 per cent eclipse to 70 per cent eclipse. Results of a theoretical study involving the solution of the time dependent continuity equation with full oxygen and hydrogen chemistry are given.

**Keywords.** Rocket Measurement; Ozone; Profile Shape; Number Density; Time-Dependent Continuity Equation

### INTRODUCTION

OZONE variations caused by a solar eclipse have been of interest not just because ozone is a photochemical product of solar radiation, but, also because it plays a dominant role in the chemistry at stratospheric and lower mesospheric altitudes, influencing a number of other minor constituents of the earth's atmosphere, and the ion chemistry in the D-region. Further, in recent years, there has been an increased interest in ozone studies due to the realisation of the possible adverse effect of certain anthropogenic activities on the total ozone overburden. The time constants for ozone loss in the upper atmosphere at various altitudes have been significantly revised in recent years as a result of the ozone loss processes due to HO<sub>2</sub>, NO<sub>2</sub> and the chloro-fluoromethanes. However, the rate coefficients for some of these reactions are not well known. In some cases there are significant temperature dependences which need to be taken into account and further, the concentrations in the upper atmosphere of these species which are invoked to destroy ozone are not well known. Hence, the

need for an observational study of the ozone life times in the upper atmosphere has been well recognised

#### OZONE STUDIES DURING PREVIOUS SOLAR ECLIPSES

There have been several attempts to monitor the variations in total ozone during an eclipse. Jerlov *et al.* (1954) found a decrease in total ozone during the solar eclipse of 1945 which was later attributed to atmospheric effects. Several workers have found an increase in total ozone by a few per cent (Fournier d'Albe & Rasool, 1956; and Svensson, 1958) during partial as well as total solar eclipses. Bezverkhni *et al.* (1956) have found a considerable increase in total ozone (6–8 per cent) during the February 1952 and June 1954 solar eclipses. Stranz (1961) found an increase of about 4 per cent during the 22 October 1959 eclipse at an equatorial station, Bunia in Belgian Congo. The increase started about twenty minutes before the maximum phase of the eclipse, maximum effect was reached somewhat after the eclipse maximum phase and the higher level of ozone persisted for sometime after the eclipse maximum phase. Since day to day variability in total ozone is believed to be much less in equatorial regions than elsewhere, the 1959 results are considered to be more definite as an eclipse induced ozone change.

A theoretical study by Hunt (1965) predicts a 0.6 per cent increase in total ozone during a total solar eclipse. Most of the variation is contributed by changes at altitudes above about 40 km. Below 40 km, the time constants for ozone loss are large and no eclipse induced changes are predicted. However, Hunt's study is restricted to a consideration of pure oxygen chemistry only and we now know that the pure oxygen chemistry accounts for only 17 per cent of the total ozone loss. Loss mechanisms involving radicals of hydrogen, nitrogen as well as halogens are important additional candidates for ozone loss in the stratosphere and mesosphere. The relative importance of the different loss schemes is altitude-dependent. Since the relative importance of the various ozone loss mechanisms is altitude-dependent, a study of the ozone variations at different altitudes during a solar eclipse is important. The level above which significant changes can occur and the extent of the change produced at different altitudes are not established. Wuebbles and Chang (1979) attempted a treatment of the changes in stratospheric trace constituents for the February 1979 eclipse. Even though the complex chemistry of  $\text{HO}_2$ ,  $\text{NO}_2$  and  $\text{ClO}_2$  was included in their study, it was limited to the region below 40 km and further, ozone was held fixed and the variations of other trace constituents were studied. The variations of stratospheric constituents during a solar eclipse, sunrise and sunset have also been studied. However, no results are available on eclipse induced effects on ozone from this study. Further, some attempts have also been made to study the solar eclipse effects on mesospheric ozone for altitudes above about 65 km. However, there has been a considerable revision of the ozone photochemistry since these studies and a full theoretical treatment of the solar eclipse problem for ozone including the hydrogen and nitrogen chemistry is not yet available for stratospheric and mesospheric altitudes.

The first attempt to study the variations of ozone at different altitudes during a solar eclipse was undertaken by Randhawa (1968) during the total solar eclipse of 12 November 1966 in Argentina, which occurred in the prenoon hours. Two rockets

were launched with chemiluminescent ozonesondes, one on the day prior to the eclipse and one on the eclipse day at the time of totality. The eclipse day ozone concentrations were larger than the previous day values by a factor of 2 at altitudes above about 50km. An increase in ozone was observed when the instrument was under totality and the ozone concentrations started decreasing as the instrument came out of totality indicating a sharp response of ozone at these levels to the solar radiation. At lower altitudes, no eclipse induced changes in ozone were detected. During the partial solar eclipse of 10 July 1972, a well-organised campaign for stratospheric investigations which included measurement of ozone, temperature and winds from rockets as well as balloons was undertaken at Poker flat, Alaska, a subpolar station (Randhawa, 1973). Ozone measurements were made upto an altitude of about 50km under eclipsed and noneclipsed conditions. No appreciable change in ozone was observed at altitudes above 40km during the eclipse. This lack of an eclipse effect was attributed to the fact that at Poker flat in the summer months daylight extends for more than 21 hours while the eclipse lasted for only 2 hours. At altitudes below 40km, however, an increase was seen during the eclipse, the increase being by a factor of 1.5 at 35km. While Randhawa concluded that this increase could not be due to eclipse induced photochemistry, it is interesting to note that the wind measurements made during the eclipse did not show any eclipse induced changes in the local winds. Starr *et al* (1980) made measurements of ozone during the total eclipse of 26 February 1979 from the U-2 aircraft and did not detect any effect due to the eclipse at the aircraft altitude of 19.8km.

#### THE THUMBA CAMPAIGN

A coordinated rocket programme to study the response of the lower ionosphere, variations in neutral atmospheric structure as well as variations in ozone concentration profiles during a solar eclipse was undertaken from Thumba for the 16 February 1980 solar eclipse. Table I shows the details of the rocket launches from

TABLE I  
*Rocket campaign for the solar eclipse—Thumba 8° 5N, 77° E*

Rocket flight	Launch Date	Launch time Hrs (IST)	Eclipse level	Measured Parameters
M-100 B 08 506 (Met)	16.2 1980	1253	Before eclipse	Temperature and winds
Centaure (D1) 05 60	16.2 1980	1454	40%	Ozone, Molecular oxygen and Electron and Ion densities
Centaure (D2) 05 61	16 2.1980	1522	70%	-do-
M-100 B 08 507 (Met)	16 2 1980	1635	After eclipse	Temperature and winds
Centaure 05 63	16 2 1980	1855	Twilight	Winds, Windshears and gravity waves
Centaure (D 3) 05 64	17 2 1980	1522	Control flight	Ozone, Molecular oxygen, Elec- tron and Ion densities

Thumba. The three Centaure rockets designated D1, D2 and D3 carried identical payloads comprising of a Langmuir probe (PRL), a Gerdien condensor (NPL) and a propagation receiver for electron and ion density measurements (NPL), a Lyman-alpha ion chamber for measurement of  $O_2$  concentrations (PRL) and a three channel MUV photometer for ozone concentration measurements (PRL). The MUV photometer is a three channel instrument working at 250nm, 280nm and 310nm wavelengths, each with a bandwidth of about 10nm. Details of the instrument are described in Acharya *et al.* (1979). The photometer is calibrated before flight not only for its spectral response but also for its angular response. The rockets performed well reaching peak altitude of about 140km. The first rocket D1 could not be successfully tracked and the rocket trajectory had to be extrapolated from the trajectories of D2 and D3. Fig. 1 illustrates the eclipse conditions during the trajectory of the flights D1 and D2.

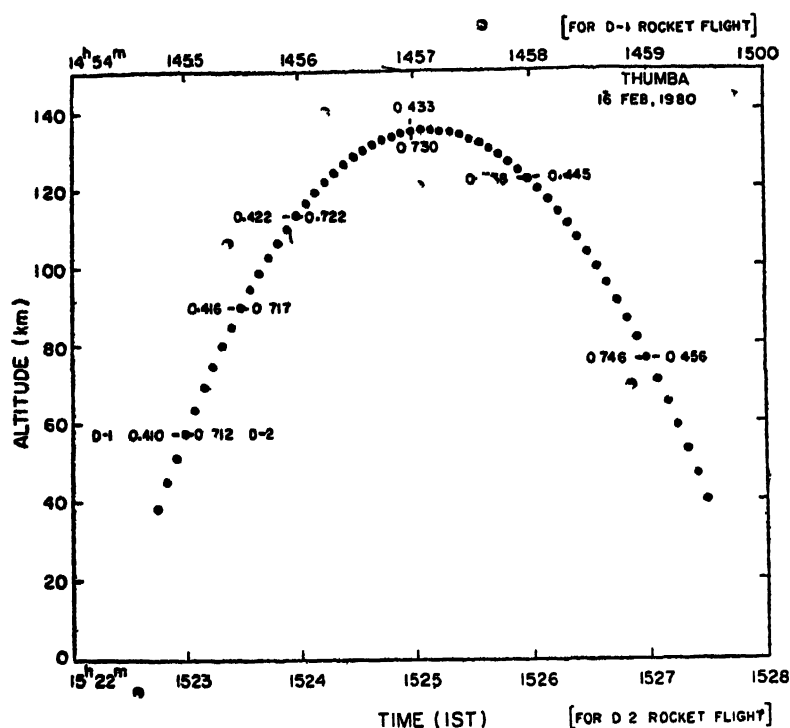


FIG. 1. Flight history of rockets D1 and D2 showing the progress of the eclipse along the rocket trajectory.

### EXPERIMENTAL RESULTS

The MUV photometers functioned well on all the three flights and gave good data. The photometer outputs are read from the telemetry charts, corrected for rocket aspect and smoothed before use in estimation of ozone densities. Fig. 2 shows some samples of such aspect corrected and smoothed profiles. A height-dependent effective absorption cross section is used to estimate the ozone concentrations. A full descrip-



tion of the data analysis procedure is described elsewhere (Subbaraya & Shyam Lal, 1981). Ozone concentrations could be determined for the three flights upto an altitude of about 65km or more. Even though photometer data are available right from the ground, at altitudes below about 15km, the data need to be corrected for atmospheric scattering effects and reliable ozone estimates are not possible at these lower heights. The India Meteorological Department had made arrangements for balloon ascents from Trivandrum with an ozonesonde on the solar eclipse day. Unfortunately, the balloon data turned out to be noisy and the data could not be reduced to give reliable ozone concentrations. A mean model profile constructed by Kundu (*private communication*) based on balloon ascents from Trivandrum has been used for the lower altitudes to extend the experimental profiles down to the ground level. The results are shown in Fig. 3.

Ozone concentrations from the first flight (D1) could be estimated for the altitude region of about 15km to 70km. The profile shows a trough above the tropopause with a minimum concentration of  $1.1 \times 10^{12}$  per cc at 20km above which the ozone concentration steadily increases to reach a broad maximum of  $1.95 \times 10^{12}$  per cc in the 26–28km region. Above this peak, the ozone concentration steadily decreases with a scale height of about 6km upto an altitude of about 50km. But above about 55km there is a sharp change in the profile shape. The data from the second flight (D2) could be used to determine ozone concentrations in the altitude region of 15km to 66km. This profile also shows a minimum above the tropopause around 20km with an ozone concentration of  $8.0 \times 10^{11}$  per cc. The ozone maximum is reached at 28km with a value of  $1.90 \times 10^{12}$  molecules per cc. Above the peak, ozone density decreases with a scale height of about 6km upto about 50km above which the decrease is sharper. This profile does not show the sharp change in profile shape above 50km, which was shown by the D1 profile. The third flight conducted as a control flight on the following day also yielded good data. Ozone concentrations could be estimated from 15km to 65km altitude. The minimum above the tropopause is at a lower altitude, near 17km and is not so well pronounced as on D1 and D2. The ozone maximum is reached at 28km with a peak concentration of  $2.03 \times 10^{12}$  molecules per cc. Above the peak level, the D3 profile follows closely the profile of D2, but the ozone concentrations are everywhere smaller.

A comparison of the eclipse day results from the results of the control flight shows that while the maximum ozone density is nearly same for all the flights, during the first flight of 40 per cent solar obscuration the ozone profile shows a much broader peak than the other two profiles. Below the level of the peak, the ozone concentrations as well as the profile shapes are different for the three flights. There is a systematic decrease in ozone from D1 to D2 as the eclipse progresses and both values are smaller than the normal (D3) values. Since ozone at these altitudes has large photochemical life times, these variations cannot be explained by eclipse induced photochemistry and are likely to be due to dynamical processes. Above the level of the ozone peak, the three profiles agree within experimental errors upto about 38km altitude. Above this altitude, a systematic increase is seen during the eclipse. From D3 to D1, i.e., at 40 per cent eclipse ozone increases by about 20 per cent in the 40–50km range. Above 50km, the increase is larger, becomes 50 per cent at 55km, a factor of 2.8 at 60km. Further, upto about 50km altitude, ozone densities increase

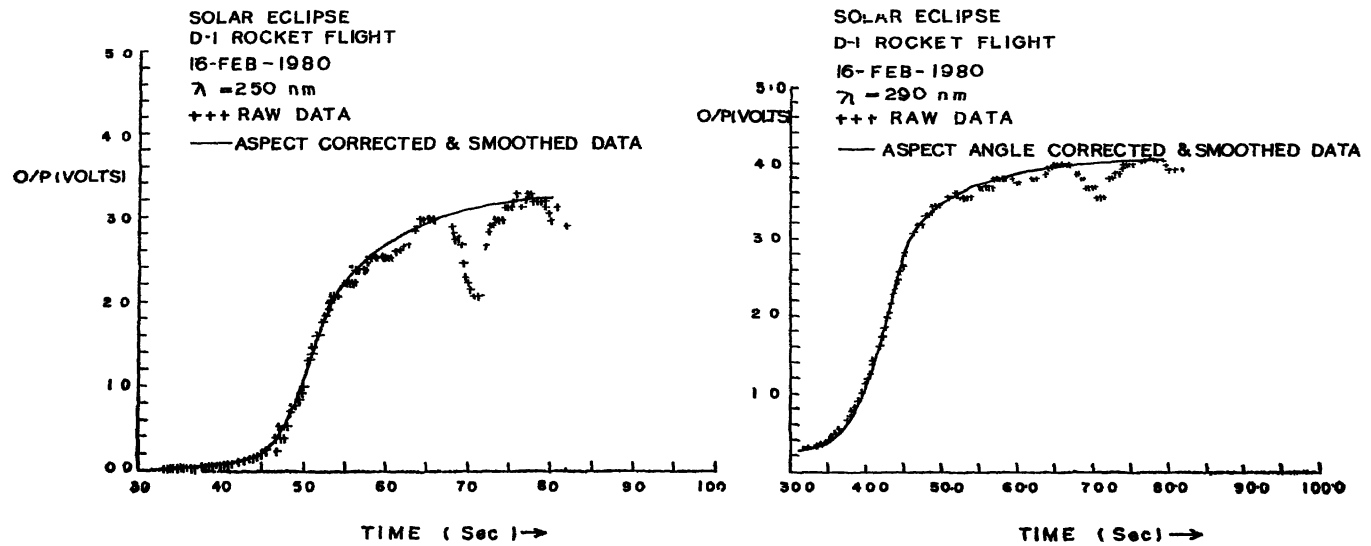


Fig 2 MUV Photometer data for channels 1 and 2 of the first rocket flight D1. Figure shows the raw data (crosses) together with the aspect corrected and smoothed profile which is ultimately used for estimation of ozone concentrations.

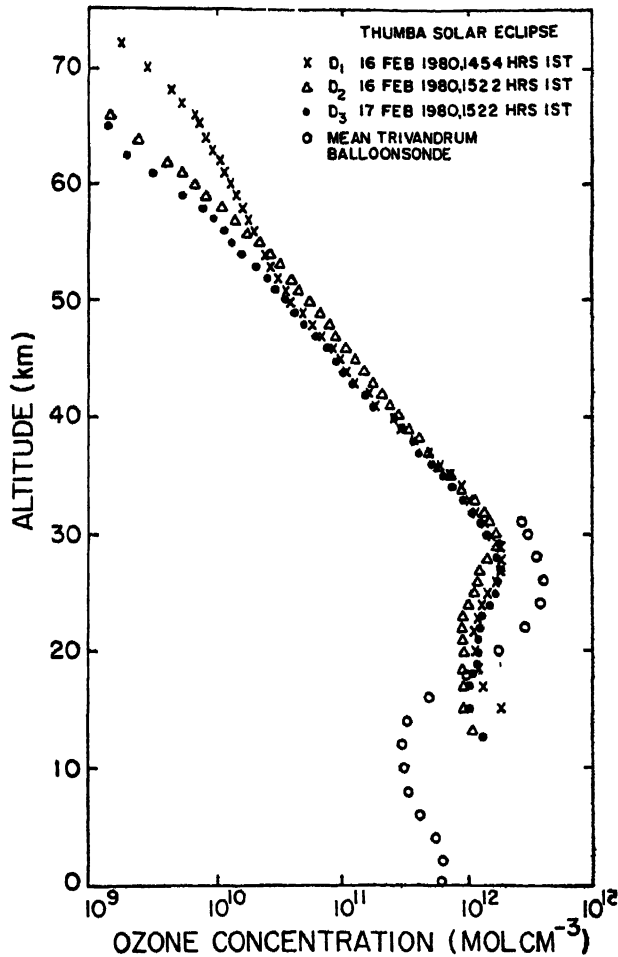


FIG. 3. Ozone concentration profiles for the three rocket flights D1 (16 February 1980,  $\chi=42.5^\circ$  eclipse 40 per cent), D2 (16 February 1980,  $\chi=46.6^\circ$  eclipse 70 per cent) and D3 (17 February 1980  $\chi=46.6$  per cent control flight)

from the 40 per cent obscuration level to the 70 per cent obscuration level (see Table II). Above 50 km, this increase with the progress of the eclipse diminishes, and the two eclipse profiles intersect at 55 km. Above 55 km, ozone values measured at 40 per cent eclipse are larger than those measured at 70 per cent eclipse, even though both are larger than normal values. At 60 km for example, the D1 values are twice the D2 values and 2.8 times the D3 values. At 65 km, the D1 values are 3.8 times the D2 values and 5.5 times the D3 values. The D2 values are larger than the D3 values by a factor of about 1.4 throughout this range of altitudes.

The noise level of the instrument is low except at very low altitudes. The signal to noise ratio of the telemetered data was good on all the flights except for certain portions of the first flight D1. Major sources of error in the estimation of ozone concentrations are (1) error in the reading of the photometer current, (2) error due to

TABLE II

*Ozone concentrations at different altitudes in the upper stratosphere and mesosphere during the solar eclipse and control condition*

Altitude (km)	D1 16 Feb. 1980 40% (cm <sup>-3</sup> )	D2 16 Feb. 1980 70% (cm <sup>-3</sup> )	D3 17 Feb. 1980 Control cm <sup>-3</sup> )
30	1.7(12)	1.8(12)	1.6(12)
35	7.6(11)	7.5(11)	7.3(11)
40	2.8(11)	3.0(11)	2.7(11)
45	1.15(11)	1.4(11)	1.0(11)
50	4.5(10)	6.2(10)	3.8(10)
55	2.5(10)	2.4(10)	1.5(10)
60	1.5(10)	7.5(9)	4.5(9)
65	7.2(9)	1.8(9)	1.3(9)
70	3.4(9)	—	—

1.7(12) means  $1.7 \times 10^{12}$

uncertainties in rocket aspect, and (3) error due to uncertainties in the rocket trajectory. Errors in the estimation of the effective absorption cross section used contribute generally much less than the three errors mentioned above. These are discussed in detail elsewhere (Subbaraya & Shyam Lal, *loc. cit.*). The combined error could be as large as  $\pm 50$  per cent at the lower and the upper ends of the useful altitude range of any given channel. For the rest of the altitude range, the errors are smaller reaching values of  $\pm 5$  per cent or less in the middle of the altitude range. For the ozone concentrations of D1 on the 310nm channel the error is  $\pm 50$  per cent at 14km decreases to  $\pm 20$  per cent at 18km and reaches a value of  $\pm 5$  per cent in the 20–22km, before it increases again to  $\pm 20$  per cent at 24km and  $\pm 50$  per cent at 25km. Similarly for the 280nm channel, the errors are  $\pm 50$  per cent at 20km decrease to  $\pm 20$  per cent in the 22–25km region, reducing to  $\pm 5$  per cent in the 26–35km region before increasing again to  $\pm 20$  per cent in the 38–40km and above 40km, the errors are  $\pm 50$  per cent. For the 250nm channel, the errors are  $\pm 50$  per cent in the 32–35km region,  $\pm 20$  per cent in the 36–40km region and reduce to  $\pm 5$  per cent in the 40 to 50km region. Above 50km, the errors increase reaching values of  $\pm 20$  per cent at 60km and  $\pm 50$  per cent at 65km. At 70km and above, the measurements could be uncertain by a factor of 2 or more.

#### THEORETICAL STUDY

A theoretical study was undertaken to study the effect of a solar eclipse on the ozone concentrations in the altitude region of 50–80km. This study includes in addition to the classical Chapman reactions, important reactions involving hydrogen species (H, OH & HO<sub>2</sub>).

The time-dependent continuity equations are solved for five species (O, O<sub>3</sub>, H, OH and HO<sub>2</sub>) using latest reaction rates for the various chemical reactions and the

integration is carried out for the entire duration of the solar eclipse. The effects of the reactions involving nitrogen species on the loss of odd oxygen ( $O$  and  $O_3$ ) is one to two orders of magnitude less in the 50–55km and even less at higher altitudes, hence reactions involving oxides of nitrogen are not included. Details of the analytical procedure and full results are described elsewhere (Shyam Lal, 1981). The analysis shows that below about 45km altitude the eclipse induced photochemistry does not produce any change in ozone. Eclipse produces an increase in ozone only above this height. The magnitude of the effect increases with increase in altitude and with the progress of the eclipse. Maximum change in ozone is delayed with respect to eclipse totality by an interval which is dependent on the altitude. The experimental results are broadly in agreement with the results of the analysis. However, the sharp change in the slope of the ozone profile above 55km seen on the first flight D1 at 40 per cent obscuration, and the consequent decrease in ozone from 40 per cent eclipse to 70 per cent eclipse (D1 to D2) conditions are not reproduced by the calculations. The results of D1 above 55km are anomalous and cannot be explained by straightforward photochemistry. However, the experimental results are beyond the limits of uncertainty. The combination of photochemistry and dynamics required to produce such changes remain to be explored.

#### ACKNOWLEDGEMENTS

Professors D. Lal, S. P. Pandya, A. P. Mitra and R. Daniel helped in formulating the rocket campaign for the solar eclipse. Fabrication and testing of the MUV photometers was assisted by Messrs S. K. Banerjee, R. I. Patel and J. T. Vinchhi.

The rocket launchings were facilitated by the staff of TERLS, special mention to be made of Messrs V. Sudhakar and A. C. Bahl. Mr K. S. Patel assisted in the data reading and analysis. Acknowledgements are also due to Mr A. Jayaraman for assistance in the preparation of this paper.

#### REFERENCES

- Acharya, Y. B., Misra, R. N., Shyam Lal, and Subbaraya, B. H. (1979) A rocketborne solar MUV photometer for measurement of ozone concentrations in the stratosphere *J. Inst. Elect. Telecom. Engrs.*, **25**, 254–257.
- Beynon, W. J. G., and Brown, G. M. (1956) *Eds. Solar Eclipses and the Ionosphere* Pergamon Press, London.
- Bezverkhniy, S. A., Osherovich, A. L., and Rodinov, S. F. (1956) Electromagnetic investigation of atmospheric ozone during the solar eclipse of 25 February 1952 and 30 June 1954 *Akad. Nauk SSSR Doklady*, **106**, 651–654.
- Fournier d'Albe, E. M., and Rasool, S. I. (1956) Observations de l'ozone atmosphérique Pendant une éclipse du Soleil *Ann. Geophys.*, **12**, 72–74.
- Hunt, B. G. (1965) A theoretical study of the changes occurring in the ozonosphere during a total eclipse of the Sun *Tellus*, **18**, 516–523.
- (1966) Photochemistry of ozone in a moist atmosphere *J. geophys. Res.*, **71**, 1385–1398.
- Jerlov, N., Oson, H., and Schnepf, W. (1954) Measurements of solar radiation at Lovangel in Sweden during the total eclipse of 1945. *Tellus*, **6**, 44–45.
- Krueger, A. J., and Minzner, R. A. (1976) A midlatitude ozone model for the 1976 US standard atmosphere *J. geophys. Res.*, **81**, 4477–4481.

- McElroy, M. B., Wofsy, S. C., Penner, J. E., and McConnell, J. C. (1974) Atmospheric ozone: possible impact of stratospheric aviation *J. atm Sci*, 31, 287
- Randhawa, J. S. (1968) Mesospheric ozone measurements during a solar eclipse. *J. geophys. Res.*, 73, 493-495
- (1973) An investigation of solar eclipse effect on the sub-polar stratosphere. *J. geophys. Res.*, 78, 7139-7144.
- Sevensson, B. (1958) Observations on the amount of ozone by Dobson spectrophotometer during the solar eclipse of June 30, 1954 *Arkiv f Geophys*, 2, 573-594
- Shyam Lal (1981) Studies in the equatorial neutral atmosphere. *Ph D Thesis*, Gujarat Univ.
- Starr, W. L., Craig, R. A., Loewenstein, M., and McGhan, M. E. (1980) Measurements of NO<sub>2</sub>, O<sub>3</sub> and temperature at 19.8km during the total solar eclipse of 26 February 1979. *Geophys. Res Lett.*, 7, 553-555.
- Stranz, D. (1961) Ozone measurements during solar eclipse. *Tellus*, 13, 276-279.
- Subbaraya, B. H., and Shyam Lal (1981) Rocket measurements of ozone concentrations in the stratosphere and mesosphere over Thumba *Proc. Indian Acad Sci. (Earth & Planet. Sci.)*, 90, 173-187.
- Turco, R. P., Whitten, R. C., Poppoff, I. G., and Capone, L. A. (1978) SST's nitrogen fertilizer and stratospheric ozone. *Nature*, 276, 805-807
- Wuebbles, D., and Chang, J. S. (1979) A theoretical study of stratospheric trace species variations during a solar eclipse. *Geophys Res. Lett.*, 6, 179-182.

Printed in India

## Ozone

# TOTAL OZONE, SURFACE OZONE AND VERTICAL DISTRIBUTION OF ATMOSPHERIC OZONE MEASUREMENTS CONDUCTED AT GADAG AND OTHER STATIONS IN INDIA DURING THE TOTAL SOLAR ECLIPSE OF 16 FEBRUARY 1980

KALIPADA CHATTERJEE *and* HARBANS SINGH AHUJA

*National Ozone Centre, India Meteorological Department, New Delhi-110 003, India*

*and*

C K. CHANDRASEKHARAN

*Instruments Division, Meteorological Office, Pune, India*

*(Received 20 March 1982)*

The present study deals with the total ozone, surface ozone and vertical distribution of ozone measurements conducted at Gadag, and from the existing network of ozone stations in India during the period 15-17 February 1980. These ozone data for the days before, during and after the total eclipse have been analysed and the effect of the total solar eclipse on the total ozone, ozone near the earth's surface and the distribution of ozone in the vertical has been presented and discussed in the paper.

**Keywords:** Ozone—Total, Surface and Atmospheric; Ozonesonde; Dobson Ozone Spectrophotometer; Ozonagram

## OBJECTIVE

The main objective of the present study is to investigate if the total solar eclipse that occurred over the Indian Peninsula on 16 February 1980 had any effect on the total ozone, vertical distribution of ozone, and on the ozone concentration near the earth's surface. With this objective total ozone, surface ozone and vertical distribution of ozone measurements were conducted at Gadag during the period 15-17 February 1980. These ozone data along with similar data from the other ozone measuring stations in India for the days before, during and after the total solar eclipse were computed and plotted to study the effect of solar eclipse on the ozone content of the atmosphere.

## OBSERVATIONAL SET-UP

Dobson Ozone Spectrophotometer for measurement of total ozone, Indian Balloon Borne Ozonesonde for measurement of vertical distribution of ozone from ground to 35km, and surface ozone sensors for continuous recording of surface ozone were used at Gadag and other stations in India. These instruments and the present status

of ozone measurements in India have been described earlier by Alexander & Chatterjee (1980).

#### SURFACE OZONE

Surface ozone measurements were carried out from Delhi, Pune, Nagpur and Kodaikanal during the period. In addition to these observations of IMD network, surface ozone sensors were set up at Gadag and Raichur which were in the path of totality, as a part of the total solar eclipse expedition programme of the India Meteorological Department.

#### TOTAL OZONE

Dobson Ozone Spectrophotometer being a very heavy and also a very delicate optical instrument, only one Dobson Spectrophotometer was transported from Delhi and was set up at Gadag for taking total ozone observations and vertical distribution of ozone by Umkehr method, during the period from 14–18 February 1980. In addition, total observations were also made at Srinagar, New Delhi, Varanasi, Pune and Kodaikanal which are the network stations in India for total ozone observations.

#### VERTICAL DISTRIBUTION OF OZONE

Instrument facilities and balloon facilities were set up both at Raichur and Gadag for sending balloon borne ozonesonde instruments operating at 403MHz. Only a limited number of ozone soundings could be taken as other types of soundings at the same frequency were also taken from these two stations during the period.

#### DATA

##### *Surface Ozone*

The surface ozone data from Kodaikanal, Gadag, Raichur, Pune and Nagpur for these days have been plotted in Figs 1A & 1B.

##### *Total Ozone*

The total ozone data from Kodaikanal, Gadag, Pune, Varanasi and New Delhi for these days have been plotted in Figs. 2A & 2B.

##### *Ozonesonde*

Ozonesonde data from Gadag for 15 and 16 February have been plotted in Fig 3.

#### DISCUSSION

##### *Surface Ozone*

Comparison of the data for 15, 16 and 17 February 1980 for the different stations brings out the following salient feature:



- (i) From an analysis of data it is seen that surface ozone decreased from  $41 \mu\text{gm}/\text{m}^3$  to  $37 \mu\text{gm}/\text{m}^3$  during 1500hr to 1630hr on 16 February 1980 over Gadag. This may be due to the cooling of the atmosphere and the damping of all convective processes during the eclipse period which resulted in lowering the ozone concentration at the surface. On a scrutiny of the micromet wind data at Gadag for the same period it is observed that the wind was practically calm from surface to 13.5m above ground.
- (ii) Other than the above feature there was no other detectable change in the surface ozone values around the time of the eclipse which could be attributed to eclipse itself. This is understandable as far as we know, since tropospheric ozone is physically transported from the higher levels due to the various mixing and circulating processes

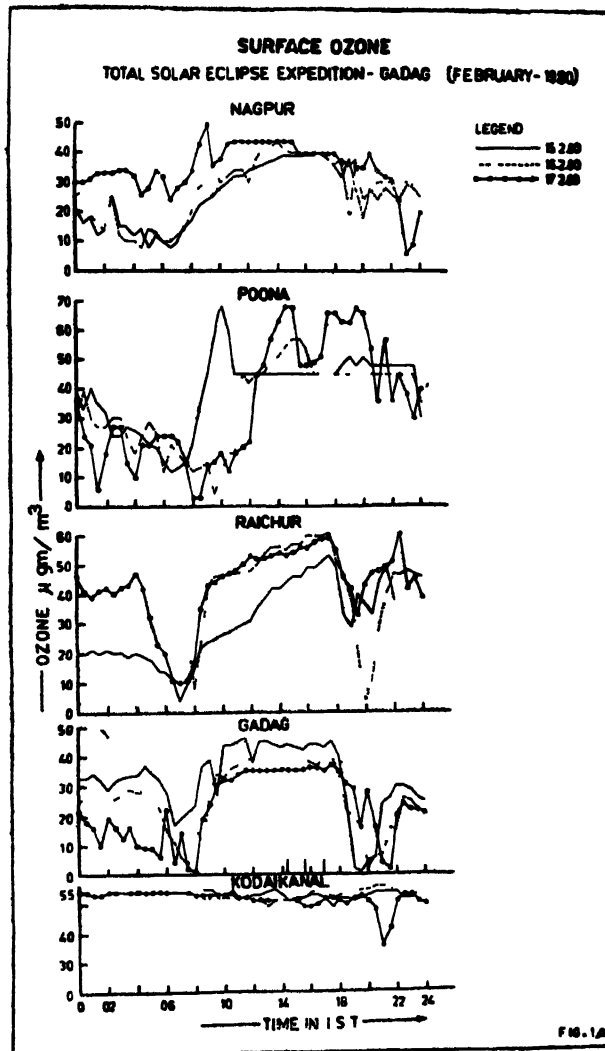


FIG. 1A.

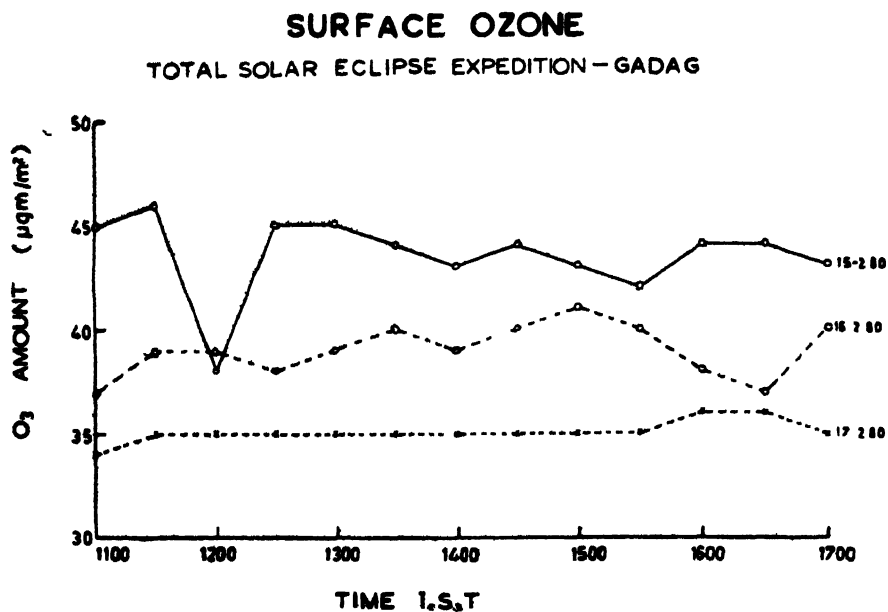


FIG. 1B.

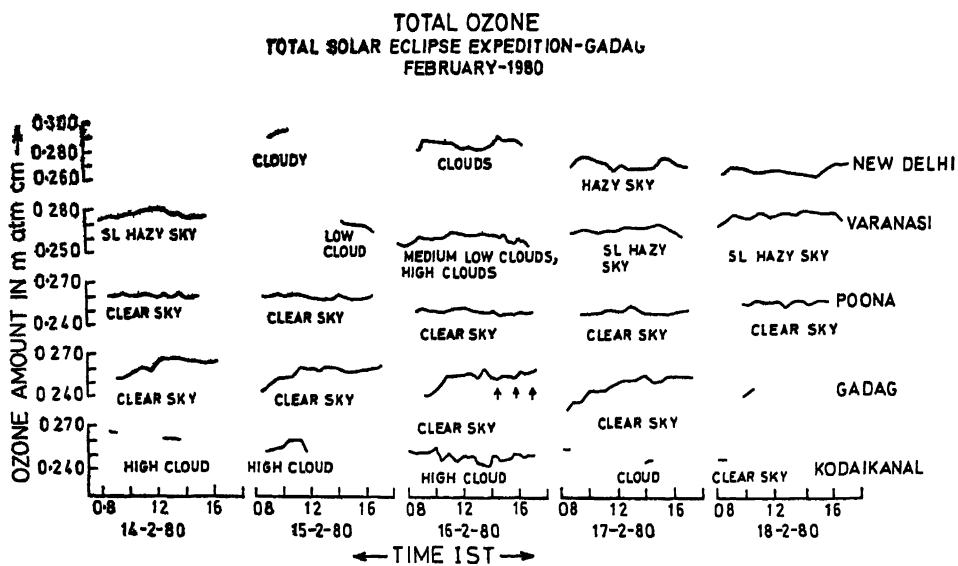


FIG 2A

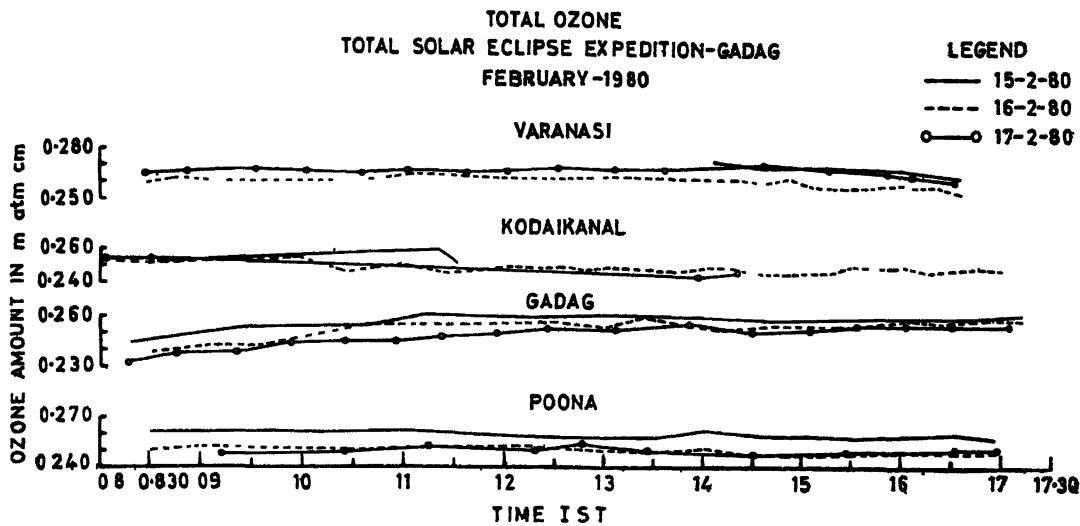


FIG. 2B.

in the atmosphere and is not photochemically produced in the troposphere itself.

(iii) Variations in surface ozone observed in Pune can be attributed to change in the mixing processes in the lower troposphere as well as changes in wind direction.

#### Total Ozone

The analyses of the total ozone data of 14-18 February 1980 from Kodaikanal, Gadag, Pune, Varanasi and New Delhi show that there is no significant change in the total ozone at any of the above stations except a decrease in the total ozone observed at Gadag by 2 per cent on the 17th. The decrease noticed during the first contact is, however, within the instrumental and personal errors and cannot be conclusively attributed to the effect of eclipse itself

#### Vertical Distribution of Ozone (Ozonogram)

On an analysis of the ozonesonde data of 15 and 16 February 1980 over Gadag the following salient features are brought out

There is an increase of ozone mixing ratio above 36mb (22km). At the level of ozone maximum this increase corresponds to about  $3\mu\text{gm/gm}$  i.e., from 10 to  $13\mu\text{gm/gm}$ .

The ozonesonde data tend to suggest that during the eclipse period the mechanism of ozone destruction was less active than during the normal sunshine period. However, there appears to be considerable realignment of the ozone above the tropopause. The ozone amount between 80mbs and 36mbs decreased. This could have happened on account of the horizontal advection of new air mass in the region of the upper atmosphere.



Printed in India.

Radiation

## MEASUREMENT OF SOLAR UV RADIATION OVER DELHI DURING SOLAR ECLIPSE OF 16 FEBRUARY 1980

B N SRIVASTAVA, M. C. SHARMA and R. S. TANWAR

*Radio Science Division  
National Physical Laboratory, New Delhi-110 012, India*

*(Received 21 January 1982)*

A solar UV photometer regularly recording solar UV radiation at wavelengths  $280 \pm 1\text{nm}$ ,  $290 \pm 1\text{nm}$  and  $310 \pm 1\text{nm}$  at the National Physical Laboratory, New Delhi was kept operative during the solar eclipse of 16 February 1980. The photometer during pre- and post-eclipse days was recording at 290nm wavelength in the sun-tracking mode. Also, visible radiation from 330nm to 1.2 micron was recorded by a standard solar cell. Analysis of results have shown that the decrease in UV radiation was not in proportion to the obscurity of the solar disc while the decrease in visible radiation was of the same proportion.

**Keywords:** UV-B Radiation; Solar UV Photometer; Ozone; Solar Eclipse

### INTRODUCTION

EARLIER observations during the total solar eclipse have not clearly shown any effect in the ozone content of the atmosphere. In view of this our solar UV photometer which has been recording regularly UV-B radiation at the National Physical Laboratory (NPL), New Delhi was operated to record the UV-B radiation at 290nm wavelength during the solar eclipse of 16 February 1980.

The optics and other details of the solar UV photometer has been described in RSD Scientific Report No 101 (Srivastava & Sharma, 1979). This UV photometer operates at wavelengths  $280 \pm 1\text{nm}$ ,  $290 \pm 1\text{nm}$  and  $310 \pm 1\text{nm}$  using interference filters and a wide band UG-11 coloured glass filter. The photometer during pre-eclipse and post-eclipse days was operated at 290nm filter in the sun-tracking mode. The output of the photo multiplier tube was fed into a photon counting system and from the rate meter a signal proportionate to the count rate was recorded on a strip chart recorder. On the same sun-tracking system a standard NASA solar cell sensitive in the region 330nm to 1.2 micron was mounted to record the visible radiation. Due to Westerly disturbances during February 1980, weather condition was not good several days before and after the eclipse. In this disturbed weather condition it was difficult to take a control day data of a clear day for the comparison. On 16 February 1980, the atmosphere was hazy and cloudy. During the eclipse period moving patches of clouds passed through the field of view of the solar UV photometer.

### RESULTS

Relative strength of intensity of UV-B radiation at 290nm on the eclipse day and of a

control day are presented in Fig. 1 UV intensity at 290nm is given for the eclipse day and two control days, 18 and 19 February 1980. The dotted line in the figure gives the haze a normalized variation for 18 February 1980. A simple normalization factor has been taken by determining the relative intensity ratio during forenoon hours of 16 and 18 February 1980. From this figure, it is clear that the fall in UV-B radiation during eclipse was steeper compared to the control day data which was

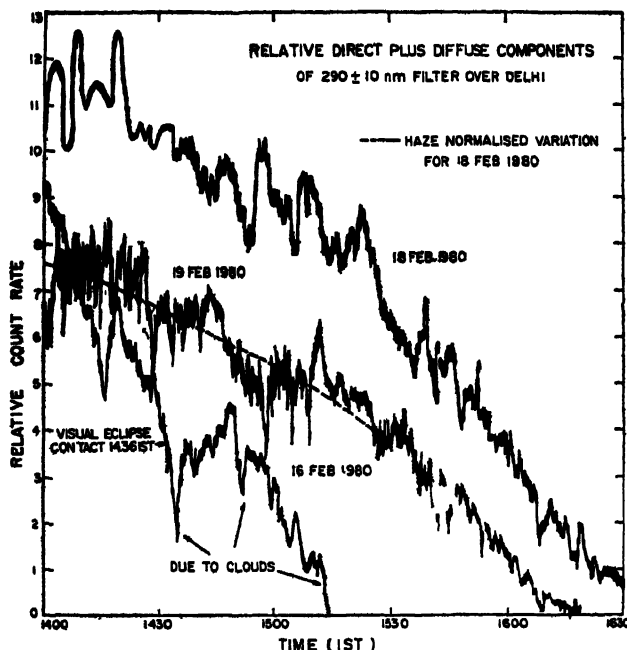


FIG 1. Solar UV-B radiation relative record at  $290 \pm 1 \text{ nm}$  of 16, 18 and 19 February 1980 taken at NPL, New Delhi.

unexpected. In Fig. 2, records of the NASA solar cell which was kept in operation on the same sun-tracking mode for visible radiation for 16 February (eclipse day) and 18 February (control day) are presented. The fall in visible radiation on 16 February 1980 during the eclipse in comparison to the 18 February control day values is nearly proportional to the coverage of solar disc by the moon shadow. In Fig. 3, the UV-B radiation at 290nm and the output of solar cell for visible region are plotted. Both have been normalized to 100 at 1400hr to compare the fall in UV-B radiation and visible radiation during the eclipse period.

#### DISCUSSION

From the observation of 290nm wavelength radiation during the eclipse, it appears that the decrease in UV-B radiation was proportionately more than the observation. This can be attributed to an enhancement of ozone which is unlikely. The observation of total ozone content by the India Meteorological Department Group (private

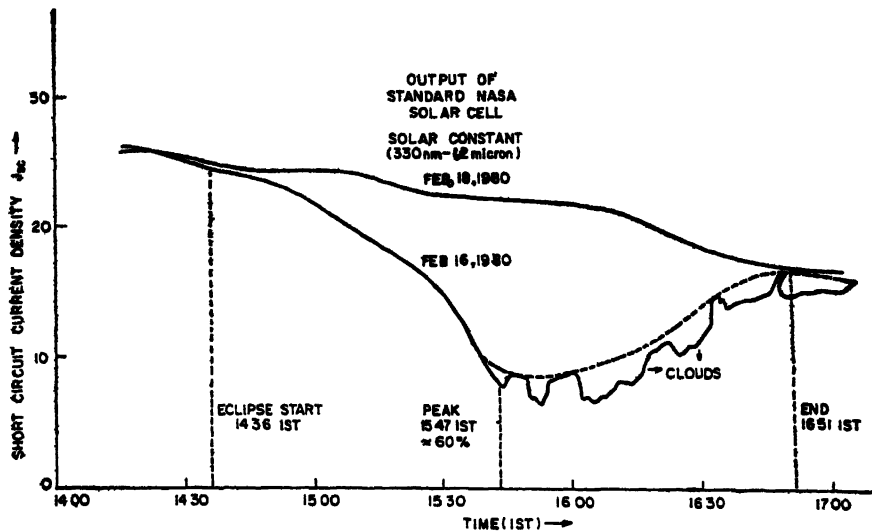


FIG. 2. Output record of a standard NASA solar cell for 16 and 18 February 1980.

communication) shows a large variation in ozone content from 15 February 1980 to 19 February 1980 thereby a suitable control day observation cannot be taken as a normal standard curve. Also due to the Westerly disturbances the fluctuations in ozone and wind pattern makes observation less reliable. The  $290 \pm 1\text{ nm}$  wavelength region is strongly sensitive to small variation in total ozone content and spatial distribution. The eclipse took place when the solar zenith angle was increasing and the effect of scattered component was becoming more predominant in the observations. The scattered component mainly depends on the weather condition, tur-

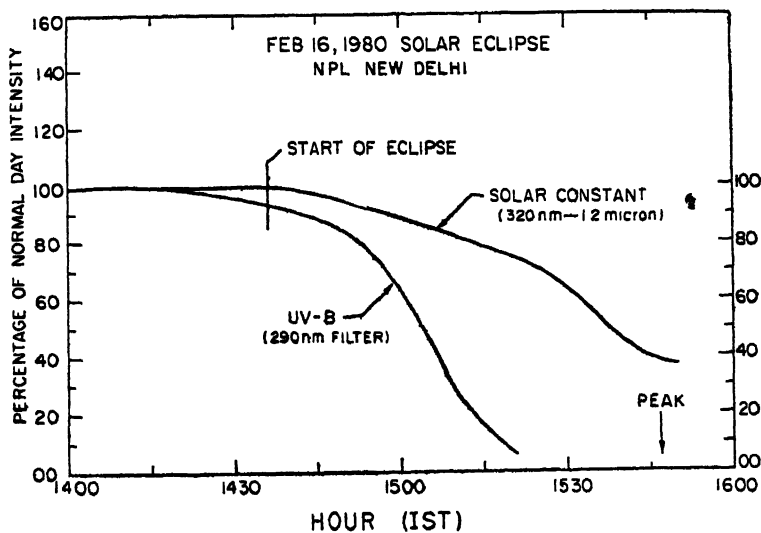


FIG 3 Normalized relative intensity of UV-B radiation and of visible radiation of the solar eclipse day.

idity and wind pattern. Thus, the inclement weather conditions created greater uncertainty in the total radiation recorded at the ground by the solar UV photometer. However, the sudden fall in UV-B radiation before eclipse may be due to obscurity of an intense solar UV-B radiation spot in chromosphere by the moon shadow. This assumption could not be verified after the III contact by observing any fast enhancement in UV-B radiation because no observation was recorded during this phase of eclipse due to clouds. The present observation of UV-B radiation supports the idea that in the short span of a solar eclipse there is very little possibility in decrease of ozone content and any enhancement in UV-B radiation.

#### ACKNOWLEDGEMENTS

Authors are grateful to Dr A. P. Mitra for his constant encouragement and helpful advice in this project of solar UV-B radiation measurement. We are also thankful to Dr Santosh Kumar for providing the NASA solar cell records for comparison.

#### REFERENCES

- Srivastava, B. N., and Sharma, M. C. (1979) Design and development of a solar UV-B photometer, *Scient. Tech. Rep.*, No. 101, Radio Science Division, National Physical Laboratory, New Delhi.



Printed in India

Ozone

## ATMOSPHERIC OZONE AND SOLAR ECLIPSE

S. DEVANARAYANAN *and* K. MOHANAKUMAR

*Department of Physics, University of Kerala, Kariavattom,  
Trivandrum-695 581, India*

*(Received 22 February 1982)*

Effect of 16 February 1980 solar eclipse on the vertical distribution of ozone in the lower atmosphere over Trivandrum ( $8^{\circ}\text{N}$ ,  $77^{\circ}\text{E}$ ) was studied. It was found that at 24km altitude, ozone partial pressure during the eclipse was 173 micromillibars as against the pre-eclipse value of 150 micromillibars at Gadag ( $15^{\circ}25'\text{N}$ )

**Keywords:** Ozone Profile; Lower Atmosphere; Partial Pressure; Photochemical Reaction; Solar Eclipse

### INTRODUCTION

THE balloon borne ozonesonde data recorded at Trivandrum ( $8^{\circ}28'\text{N}$ ,  $76^{\circ}57'\text{E}$ ) during the solar eclipse on 16 February 1980 have been presented. Mark II version of the Indian ozonesonde was used for this purpose. It had a non-reactive sampling airpump and the reaction of ozone with potassium iodide solution took place in the sensor using the Brewer wet chemical cell to detect ozone (Sreedharan, 1971). For the study, special soundings were conducted by the India Meteorological Department (IMD) on the eclipse day (February 16) and two control days (February 15 & 17) at this station. Unfortunately, the ozonesonde ascents on the control days were found to be defective, and, therefore, reliable data were obtained only on the eclipse day at Trivandrum when the obscuration was 46 per cent. The IMD had also conducted similar sounding at Gadag ( $15^{\circ}25'\text{N}$ ,  $75^{\circ}38'\text{E}$ ) and reliable data were obtained only from the sounding at 12 40hr IST, on 15 February 1980. The data used by the present authors have been the corrected ones with reference to standard measurements with the IMD, and the overall accuracy was estimated by the IMD at  $\pm 10$  per cent.

The ozone profile with respect to altitude at the time of 46 per cent obscuration for Trivandrum is as shown in Fig 1 (continuous line). In the absence of the ozone profile of the control day there is no possibility to study the effect of the eclipse on the distribution of ozone. On the other hand, it is well known that there is no noticeable difference among the ozonograms of equatorial tropical and near-equatorial tropical stations. So it may be considered that the ozone profiles over Gadag and Trivandrum are virtually the same, neglecting the small latitude effect. Ozone profiles taken in the previous years endorse this view (Sreedharan, 1975). The dotted curve in Fig. 1 represents the zone distribution over Gadag.

## RESULTS AND DISCUSSION

It appears from Fig. 1 that the eclipse may have affected the vertical distribution of ozone at different altitudes. Below the tropopause the ozone concentration on the eclipse day was lower. But above the tropopause upto 29km altitude, the ozone concentration was higher than that of normal day profiles. The maximum ozone concentration of  $173\mu\text{mbs}$  was observed at 24km during the eclipse time; and this amount is more than the normal days by 15 per cent.

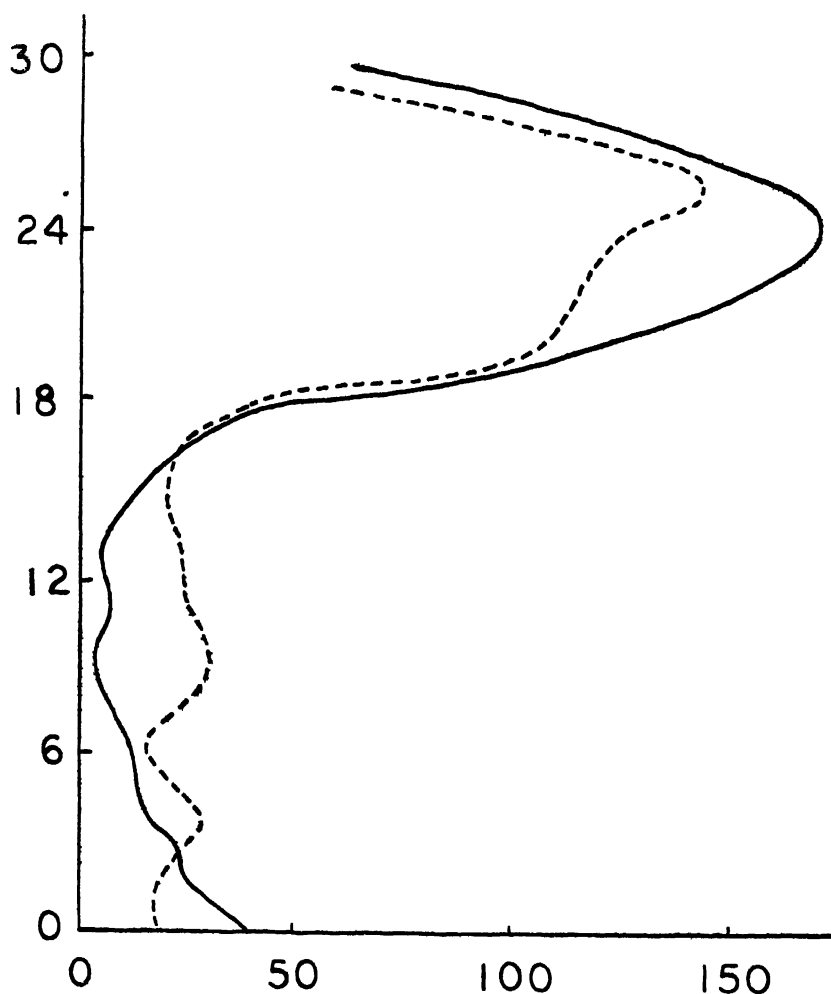


FIG. 1 Vertical distribution of ozone over Trivandrum on 16 February 1980 (continuous line) and Gadag on 15 February 1980 (dotted line)

From a detailed study of the vertical distribution of ozone over Trivandrum, Sreedharan *et al* (1976) arrived at the conclusion that the seasonal variation of ozone concentration at this station is small and the partial pressure of ozone does not exceed  $160\mu\text{mbs}$ . Investigations of ozone in the upper atmosphere over Trivandrum

showed that the contribution to the higher total ozone is from the layers above 28km, where photochemical reaction takes place. Ozone is an optically active gas, which absorbs and emits terrestrial IR radiation in the 8–10 $\mu$ m region and strongly absorbs solar radiation in the UV region. Hence, a change in ozone concentration resulted from the eclipse would have perturbed the radiative energy budget of the earth-atmosphere system; possibly paving the way to perturb the climate.

Hunt (1965) has shown theoretically that an eclipse does not affect the ozonosphere below 45km. Further, the time of half restoration for any departure from photochemical equilibrium is of the order of months for the layers of stratosphere (Stranz, 1961). But the present study of the equatorial stratosphere gives some indication of a possible increase during the eclipse of the maximum ozone concentration.

#### ACKNOWLEDGEMENTS

The authors are thankful to the DDGM, IMD, Poona for the kind supply of corrected ozonesonde data used here. One of us (KM) would like to thank the UGC for awarding a fellowship.

#### REFERENCES

- Hunt, B. G. (1965) *Tellus*, **17**, 516–523.  
Sreedharan, C. R. (1971) *J Phys E Sci Inst*, **4**, 614  
——— (1975) *Ph D Thesis*, Univ Kerala  
Sreedharan, C. R., Jayaraman, K. and Mani, A. (1976) *Proc Jt Symp Atm Ozone, Dresden*  
Stranz, D. (1961) *Tellus*, **13**, 276–279

Printed in India.

Ozone

## OZONE CONCENTRATION MEASUREMENTS NEAR THE GROUND AT RAICHUR DURING THE TOTAL SOLAR ECLIPSE OF 1980

G. P. SRIVASTAVA, P. M. PAKKIR MOHAMMED *and* R. R. BALWALLI

*Instruments Division,  
Meteorological Office, Pune-411 005, India*

*(Received 23 February 1982)*

Continuous recording of surface ozone was made at two levels, 1.5m and 15m above the ground at Raichur ( $77^{\circ}21'E$ ,  $161^{\circ}2'N$ ) during the total solar eclipse on 16 February 1980, the station being situated in the path of totality of the eclipse. The ozone concentrations were recorded for five days from 14 February to 18 February 1980, i.e., two days before and two days after the total solar eclipse. Simultaneous recordings of wind and temperature at both these levels were also made. The results of continuous measurements of ozone concentration at the two levels near the ground are discussed.

**Keywords:** Ozone—Surface, Concentrations of; Radiation Flux

### INTRODUCTION

THE total solar eclipse observed in India on 16 February 1980 had its path of totality sweep over the southern peninsula from the west coast to east coast and the period of totality was almost the longest at Raichur being 2m/43 sec. This gave a rare opportunity to study the short term effects on ozone concentrations near the ground, due to sudden change in the radiation fluxes and almost total absence of ozone producing ultraviolet radiation during the period of totality.

### INSTRUMENTATION AND EXPERIMENTATION SET-UP

The sensor used in this experiment is an electrochemical type based on the well-known principle of reduction of Potassium Iodide (KI) solution. The sensor assembly is similar to the one described by Sreedharan (1973) and consists of a bubbler reservoir, reciprocating piston pump for drawing the atmospheric air through the bubbler, an amplifier to convert the sensor current level and a chart recorder. The instrument gives a continuous recording of surface ozone.

The campus of the Agricultural Research Institute at Raichur was selected for the experiment. Two sensors were installed, one at a height of 1.5m above the ground level and the other at a height of 15m above the ground level on top of a collapsible tower of light weight tubular frame structure. Other sensors for recording wind and temperature were also installed at these levels on specially designed booms and attached to the main frame of the tower ensuring that no sensor was shadowed by any other instrument.

## RESULTS

Fig. 1 shows the hourly values of ozone concentration in  $\text{gm}/\text{metre}^3$  plotted for all days from 14 to 18 February 1980 for both the levels. Dotted line shows the values at 1.5m level and full line, the values at 15m level.

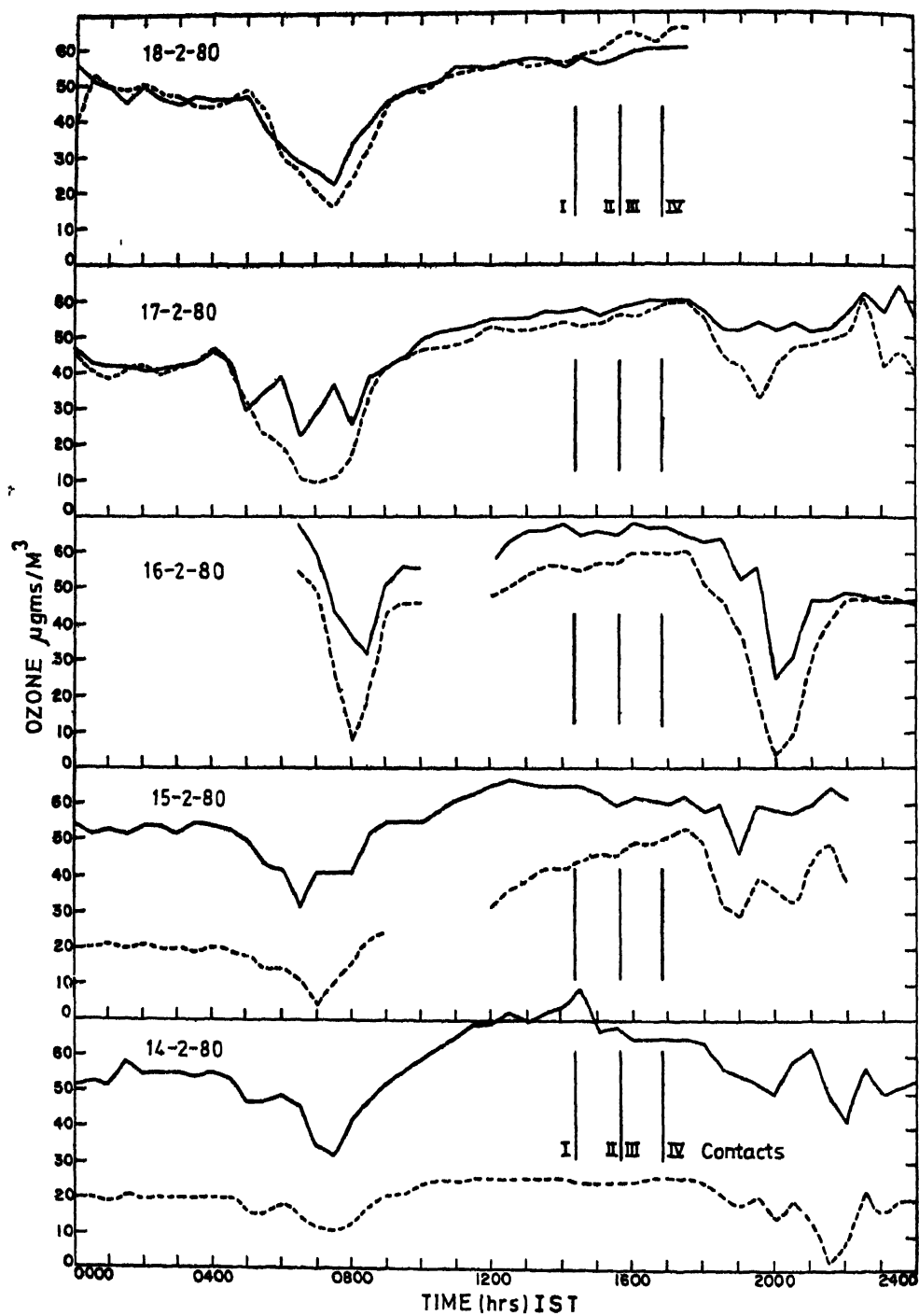
It is seen from the records that the hourly values of ozone concentration at 1.5m level near the ground show a gradual increase day after day from about  $20\text{gm}/\text{m}^3$  on 14 February 1980 to around  $50\text{gm}/\text{m}^3$  on 18 February. The ozone values at the higher level at 15m from the ground, on the other hand, are generally stable and consistent being around  $60$  to  $70\text{gm}/\text{m}^3$  on all the days. The gradual increase in the ozone values at the ground level day after day can be attributed to two factors. Either the instrument at the ground might have developed some trouble or the site of experiment being Agricultural Research Institute, the adjacent experimental farms using large amounts of agricultural chemicals gave rise to other pollutants in the air that reacted with the KI solution in the sensor showing gradual increase in ozone concentration, as the days passed.

It may be mentioned that since the sensor used in this experiment is based on electrochemical principle of reduction of KI solution, it would also react to the presence of other oxidants in the atmosphere (other than ozone). Since the observations are made in the vicinity of the agricultural farms, the measurements of ozone near ground level, were considered not quite reliable due to possible influence of other oxidants on the sensor.

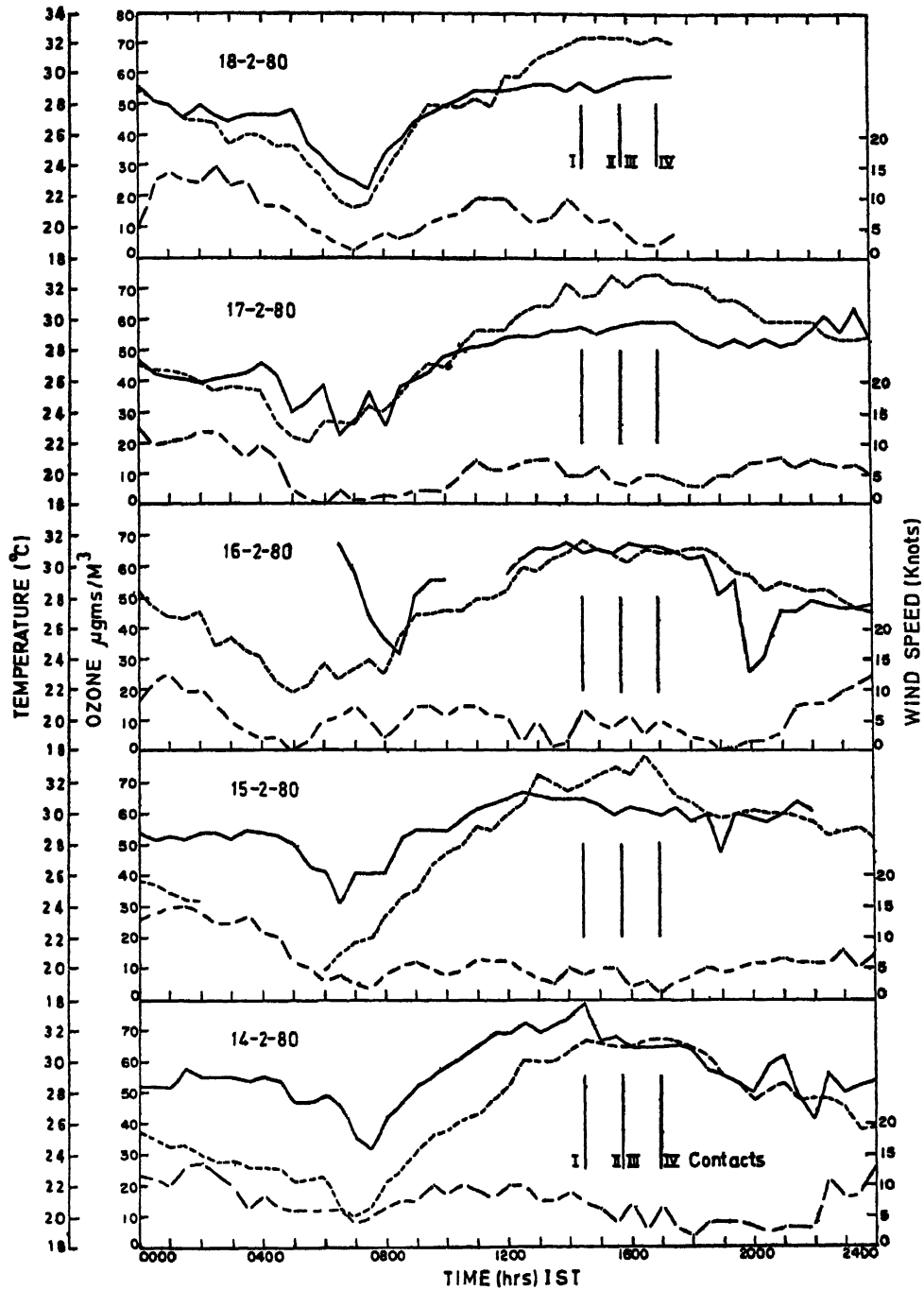
The 15m level ozone values which were more steady throughout the period from 14 to 18 February, are thus considered for studying the effects of total solar eclipse on the surface ozone concentrations. It can be seen that on all days the ozone values exhibit the typical daily variation with a minimum at about 0700hr IST and a maximum at about 1500hr IST. All the days are characterised by a secondary minima around 2000hr IST coinciding with a minima in the wind speed. This dip in ozone concentration is seen to be more pronounced on the day of eclipse. On all days except on 16 February the dip in concentration is of the order of  $10\text{gm}/\text{m}^3$  at this level, whereas on the day of eclipse this decrease was observed to be of the order of  $30\text{gm}/\text{m}^3$ . Also there seems to be no significant change in the ozone concentration during the entire period of the eclipse, nor even during totality.

## DISCUSSION

It is typical of land stations to have an ozone minimum early morning invariably associated with low wind activity as a result of *in-situ* destruction of ozone under near stable conditions of the atmosphere. As the day progresses, the increased mixing gives rise to observed increased maxima around early afternoon. Fig. 2 gives simultaneous records of wind speed, air temperature and ozone concentrations at 15m level above the ground. It would be seen that the air temperature on all the days in the afternoon generally has shown similar variations, with gradual decrease from around 1700hr and more or less afternoon maxima of about  $30$ – $32^\circ\text{C}$ . On 16 February, however, there is a marked decrease from the time of the first contact till the second/third contact and a gradual increase thereafter, before the afternoon fall.



Legend ----- 1.5m Level, — 15m Level  
 FIG. 1. Hourly values of ozone concentration



Legend — OZONE, - - - - - TEMPERATURE, - . - . - WIND SPEED

FIG. 2. Hourly values of ozone temperature and wind speed.

commences. The ozone variations, however, during this period, though somewhat noticeable, are generally of the order of normal perturbations observed even on other days.

The wind speed record, however, shows some very interesting co-relation with ozone variations. As we know ozone concentrations are closely related to wind speed, with larger winds giving rise to better mixing and hence higher values of concentrations. Both the morning and evening minima observed around 0700hr and 2000hr IST on all days can thus be attributed to drop in wind activity at these hours. The records, however, clearly show a definite time lag, with ozone concentration decrease occurring around 30 minutes to 1 hour after the fall in wind speed.

The evening minima on the eclipse day, is, however, significant with concentration decreasing to almost one third of the values normally obtained on days prior or after the eclipse. A comparison with wind records at these hours for all days shows the wind speed to be considerably lower throughout the period on 16 February having dropped down to nearly zero at 1900hr compared to generally 5 to 7 knots on all other days. The observed very low ozone concentrations, at these hours on 16 February obviously thus resulted from low wind activity. The time lag of about one hour between ozone and wind minima is also very clearly noticed.

This trend is also clearly observed on the 1.5m level recorder, even though we may not be very sure of the absolute values (as mentioned earlier).

It is generally believed that there will be reduction in ozone during the period of the solar eclipse due to near absence of sun light. However, this is not borne out by our observations as shown in Fig 2. In fact, the total ozone content as recorded by Dobson spectrophotometer at Gadag—the second observational site in the path of totality of eclipse—and at Pune (85 per cent totality) did not show any recognisable reduction during the eclipse period. It may also be mentioned that a slight increase in Dobson ozone values was observed by Yadav and Sinha (1969) at Delhi during the eclipse on 20 May 1966. Thus we may conclude that the popular belief that ozone concentration decreased during solar eclipse is not substantiated.

#### REFERENCES

- Sreedharan, C. R. (1973) *J pure appl Phys*, **106-108**, (V-VII), 1085-1090  
Yadav, B. R., and Sinha, S. S. (1969) *Indian J Met Geophys*, **20**, 41-46



Printed in India

## Radiation

# SOLAR AND EARTH'S RADIATION AND RADIOMETERSONDE MEASUREMENTS AT GADAG

C. K. CHANDRASEKHARAN, A. B. SARKAR *and* KALIPADA CHATTERJEE\*

*Instruments Divisions, India Meteorological Department, New Delhi & Pune, India*

(Received 31 March 1982)

Results of radiation flux measurements at Gadag (lat. 15°25'N, long. 75°38'E) during the total solar eclipse of 16 February 1980 are presented. Intensity at normal incidence from a pyrheliometer mounted on a heliostat and also the global, diffuse and net radiation were recorded on a number of days before and after the total eclipse. The normal intensity in various spectral bands was also continuously monitored on the day of the eclipse at Gadag.

Whereas the diffuse radiation showed a minimum value a few minutes before the totality, the minima of direct, global and net radiation occurred a few minutes after the totality.

Radiative fluxes were also measured by sending radiometersondes with balloons during the period 15-17 February 1980 from Gadag. These results have also been analysed and presented in the paper.

**Keywords:** Radiation—Solar & Earth; Radiometersonde

## INTRODUCTION

SPECIAL measurements of various components of solar radiation were organised at Gadag (15°25'N, 75°38'E, 655m) located 12.6 km north of the central path of totality of the total solar eclipse of 16 February 1980. The components measured were (i) global solar radiation (ii) diffuse solar radiation (iii) direct solar radiation and (iv) net radiation. In addition to these instantaneous measurements of the direct solar radiation in different spectral ranges and the vertical profile of terrestrial radiation twice in a day were also made. The following are the details of the instruments used.

<i>Parameter</i>	<i>Instrument used</i>	<i>Auxiliary equipment</i>
1 Direct solar radiation	Eppler normal incidence pyrheliometer mounted on a heliostat	Honeywell 4 point potentiometric recorder.
2 Global solar radiation	Thermopile pyranometer	-do-
3 Diffuse solar radiation	Thermopile pyranometer with Schuepp model shading ring	-do-

\*IMD, New Delhi

4. Net radiation	Funk type net pyrradio- meter	-do-
5. Direct solar radiation	Eppley normal incidence pyrheliometer with OG1, RG2 and RG8 filters	Cambridge potentiometer Vernier
6. Upper air terrestrial radiation	Soumı-kuhn radiometer- sonde	401MHz ground equip- ment

The measurements were made in the campus of Jagadguru Tontadarya College. The radiation sensors were installed on the roof of the Science Laboratories and the recorder kept inside the Laboratory below. The net pyrradiometer was installed in the spacious playground of the college. Care was taken that there were no major obstructions cutting off a sizeable sky portion and that no shadow was being cast on the instruments. Measurements were made on two days prior to and two days later than the eclipse day, viz., 16 February 1980.

## RESULTS

### *Direct Solar Radiation*

The direct solar radiation measurements made were used to compute the transmission coefficients for the five days of observations. The mean coefficient obtained for 16 February was used to calculate the direct solar radiation during the eclipse period utilising the observation data received from Calcutta. Necessary corrections have been applied for the water vapour absorption, ozone absorptions and the atmospheric turbidity. It was generally noticed that the observed values were always less than calculated values. The sky was generally clear but there were always some changes in the sky brightness probably due to the presence by the invisible cloud particulates. The variations in the direct solar radiation were thus not smooth as can be seen from Fig. 1.

Fig. 2 gives the spectral distribution of direct solar radiation in the different wavelength ranges viz.

- $I_t$  from 300 to 4000nm
- $I_s$  from 710 to 2700nm
- $I_t - I_1$  from 300 to 525nm
- $I_s - I_8$  from 630 to 710 nm
- $I_t - I_8$  from 300 to 710nm.

Data for 15 February 1980 are not included because of the cloudy sky condition. A study of the spectral distribution shows that there was a small decrease in the blue wavelength just after the first contact. This was however, a temporary one as shortly afterwards the blue wavelengths showed a sudden spurt of more than  $20\text{W/m}^2$  whereas there was a general decrease in all other regions. The decreasing tendency was later on picked up and this continued till 1456hr L A T. when there was a sudden increase giving rise to the darkening of the zenith sky. This may be perhaps due to

the light scattering by very small particles at very high altitudes. This shift of the colour to blue was indeed very dramatic at Gadag.

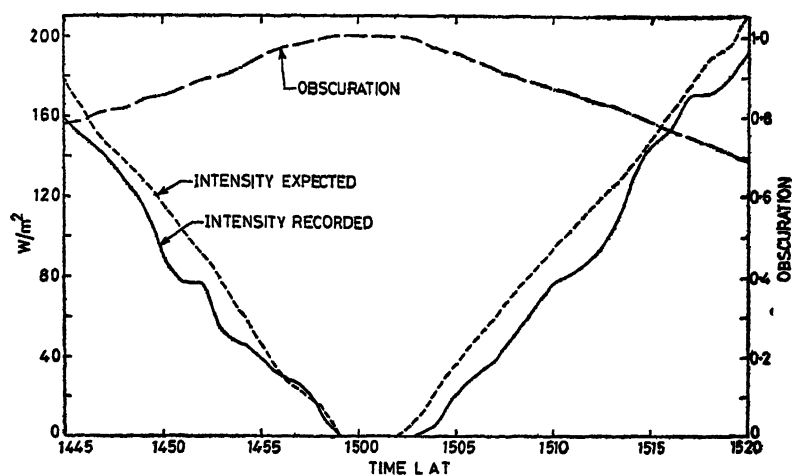


FIG 1. Direct radiation and obscuration of the sun at Gadag on 17 February 1980.

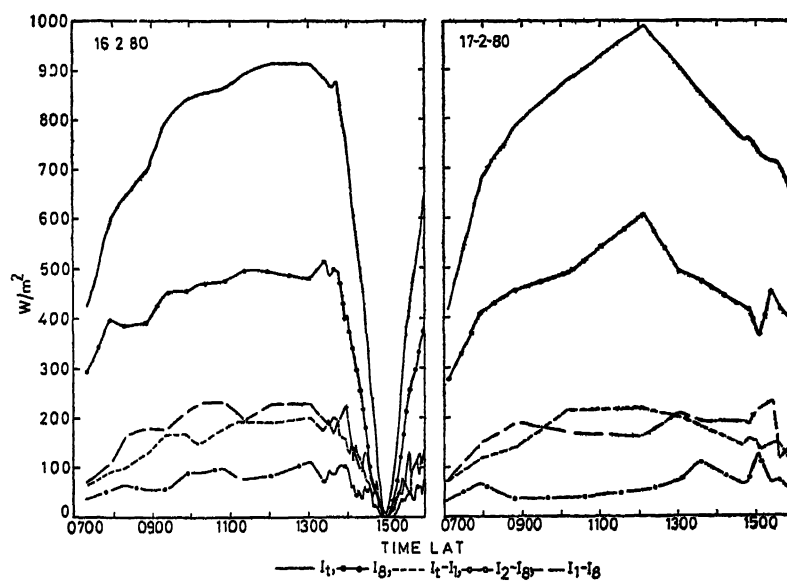


FIG 2 Spectral distribution of solar radiation at Gadag.

*Global Solar Radiation*

Global solar radiation also showed a slight increase after the 1st contact (Fig. 3a) and then it started to decrease as the sun started getting more and more obscured. During the period of totality the value recorded was zero. The values shown in Fig. 3a do not indicate zero and the values plotted are the totals for ten minutes intervals.

*Diffuse Solar Radiation*

Here also there was a small increase in the radiation after the 1st contact (Fig. 3b) which may be ascribed to the more scattering due to dust particles.

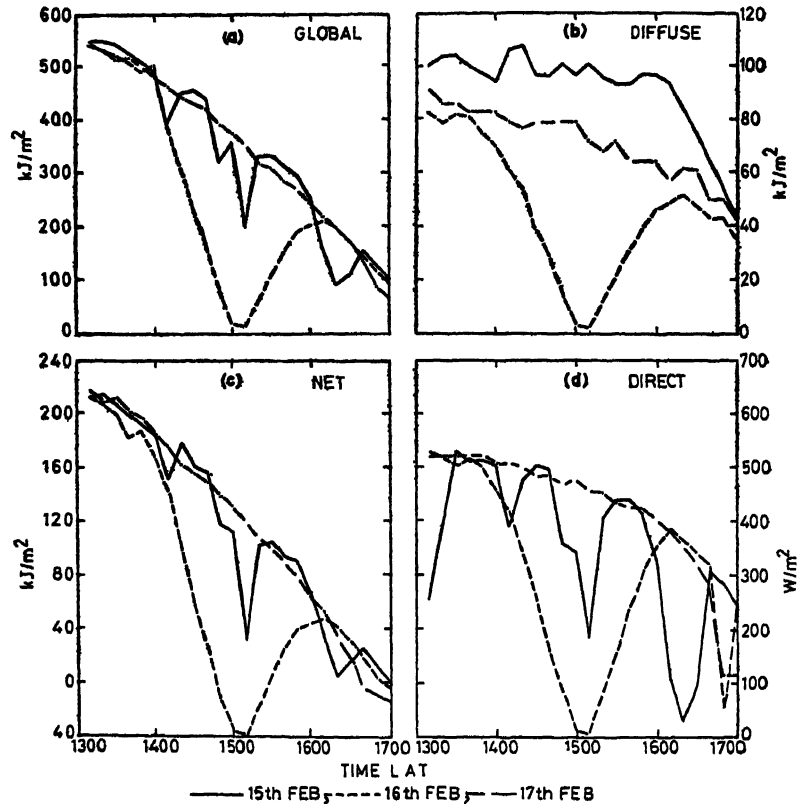


FIG 3 Radiation parameters with and without the effect of eclipse at Gadag.

Fig. 3(d) shows the variation of direct solar radiation on the three successive days 15, 16 and 17 February. 15th was unfortunately cloudy and 17th showed a lot of variations due to changing atmospheric conditions though the sky was free from cloud masses. A slight increase just before the commencement of the eclipse was noticed. This continued for about eleven minutes. The values of direct solar radiation were 40, 20 and 1.5 per cent of the value before the commencement of the eclipse, corresponding to the observation rates of 50, 75 and 90 per cent, before the totality. The corresponding values after the 3rd contact were 55, 25 and 8.1 per cent respec-

tively It was noticed that the restoration of the direct solar radiation was faster than the decreasing rates.

### *Comparative Study of Global and Diffuse Radiation*

A comparative study (Fig. 4) shows that the rate of decrease before the totality and the rate of increase after that was less for diffuse radiation than that for global radiation. However, the rate of decrease was more than the rate of increase. But the rate of increase in global radiation was much more than that for diffuse radiation. The rate of decrease in global and diffuse radiation was slower upto 50 per cent of obscuration—slower than the rate of obscuration. The withdrawal rate was slower upto 50 per cent of obscuration than the rate of increase in the radiation values.

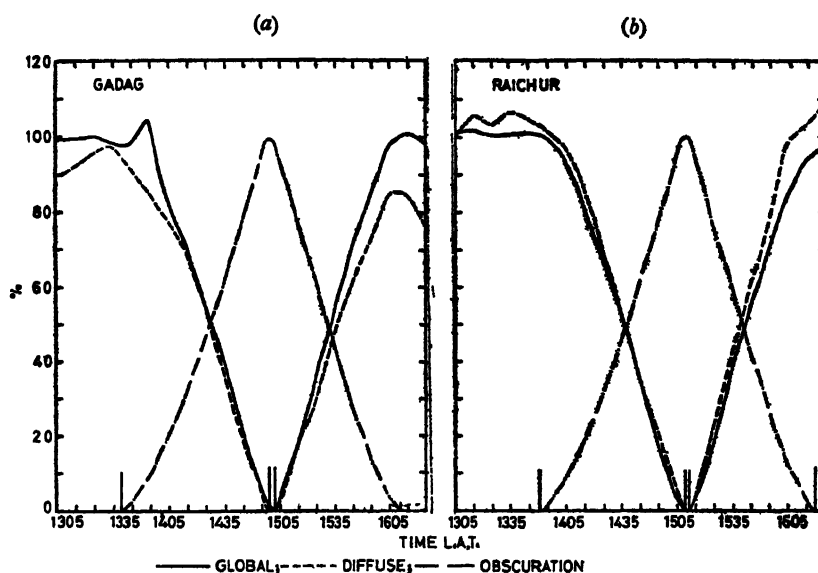


FIG 4 Percentage variation of global and diffuse radiation with progress of the eclipse (w.r.t. values on 17 February 1980)

### *Net Radiation*

The net radiation became zero at 1442hr L A T. when the obscuration was 73 per cent Fig 3(c). It reached a maximum negative value of  $4.6 \text{ MJ/m}^2$  at the time of 3rd contact. The net radiation remained negative upto 1523hr L A T (with 55 per cent obscuration). Thus there had been a delay of above five minutes before the negative value was derived out and the net radiation could become positive. This can be easily explained when the low albedo and high emissivity of the local black cotton soil is taken into account. The fall in surface (top soil) temperature during the eclipse was about  $20^\circ\text{C}$ .

### *Vertical Profile of Terrestrial Radiation*

Every day there were two radiometersonde ascents on 15, 16 and 17 February—one at 0430hr IST and the other around 2100hr or after. One special ascent was also taken at 1528hr IST on 16 Feb 80, few minutes before totality. The balloon was already

near the 500mbs level at the time of 2nd contact. The value as measured at about this time are given below:

Time IST	Pressure level mb.	Terrestrial radiation		
		Upward	Downward	Net
1540.2	550	397.6	245.5	152.5
1542.5	500	376.1	219.7	156.4
1544.5	450	367.9	181.0	186.9

These values are subject to errors due to exposure of the radiation sensors to Sun's rays before the Second contact.

Fig. 5 gives the vertical profile of the terrestrial radiation parameters for both morning and evening radiometersonde ascents. It is seen that there are not much large variations in the different parameters due to the eclipse. However, it is seen that the upward and downward terrestrial radiations were considerably lower on the night of 16-2-80, even after taking into account the slight delay in taking ascent. But by 17th night the normal pattern as given on 15th night was reached. This lowering

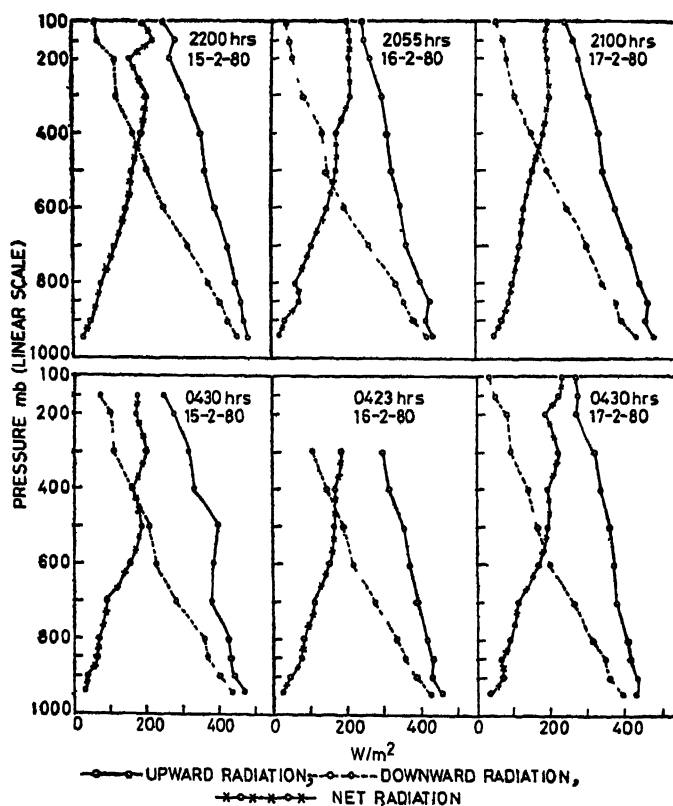


FIG 5 Upper air terrestrial radiation parameters,

of the values is not so much clearly seen from the 17th morning ascent as the upper levels beyond 600mb had already been restored to the normal values.

#### ACKNOWLEDGEMENTS

The authors express their grateful thanks to Dr P. K. Das, F.A Sc , F.N.A., Director-General of Meteorology for providing the facilities, encouragement and for communicating the paper.

The authors also express their grateful thanks to Sri S K. Das, Additional Director-General of Meteorology for providing guidance in the analysis and investigation of the data.

Printed in India

## Radiation

# RADIATION FLUX MEASUREMENTS OVER INDIA DURING THE TOTAL SOLAR ECLIPSE OF 16 FEBRUARY 1980

V. DESIKAN, C K CHANDRASEKHARAN, C. G RAHALKAR and G P. SRIVASTAVA

*Instruments Division  
Meteorological Office, Pune-411 005, India*

*(Received 17 April 1982)*

Special measurements of various components of solar radiation were organised at Gadag (15°25'N, 75°38'E, 655m) and Raichur (16°12'N, 77°21'E, 401m) located 12.6 km and 9 km both north of the central path of totality of the total solar eclipse of 16 February 1980. Continuous recordings of direct, global and diffuse solar radiation and net radiation were made at Gadag besides the measurement of duration of sunshine. At Raichur, global ultraviolet and reflected solar radiation were in addition measured. Continuous records of global and diffuse radiation were also made in all the 15 network stations equipped with these instruments and 8 more stations made only global solar radiation. The magnitude of the eclipse was between 60 and 99 per cent in those locations.

**Keywords:** Radiation Flux; Solar Radiation Pyranometers

## INSTRUMENTATION

### *Exposure*

At Raichur, the measurements were made at the Regional Agricultural Research Station. The sensors were installed on the terrace of the Agricultural Engineering Institute and the recorders kept in the laboratory just below. The reflected solar radiation pyranometer and the net pyrradiometer were installed on the playground adjoining the Institute. At Gadag the instruments were installed at the roof of the J T. College Building. At other stations these were located at respective meteorological stations.

### *Instruments used for Various Measurements*

Direct solar radiation	Kipp & Zonen Moll thermopile pyrheliometer mounted on a heliostat
Global, Diffuse and Reflected solar radiation	Moll-Gorczynski pyranometers
Global ultraviolet radiation	Eppley global ultraviolet radiometer
Net radiation	IMD net pyrradiometer (Funk type)

Besides these, instantaneous measurements of direct solar radiation in different spectral ranges were also made. Linke-Feussner pyrheliometer was used for this purpose at Raichur. Portable vernier potentiometers were used to read out the outputs



Continuous records were obtained on potentiometric recorders. A sunphotometer with interference filters at four wavelengths was also used to measure direct solar radiation.

## RESULTS

### *Direct Solar Radiation*

The mean transmission coefficient obtained from the pyrheliometric measurements was used to compute the expected values of direct solar radiation on 16 February. Allowances were made for the effect of water vapour and ozone contents of the atmosphere. The progress of obscuration obtained from Director, Positional Astronomy Centre, Calcutta was used to calculate the expected values during the eclipse. The observed values were always lower than the computed ones both at Raichur and Gadag. The departures were more fluctuating at Gadag than those at Raichur. The departures were more near the totality period perhaps due to the time constants and other inherent instrumental factors. The departure is of the order of 80 per cent before the totality and it increased to 90 per cent after the event (Fig. 1).

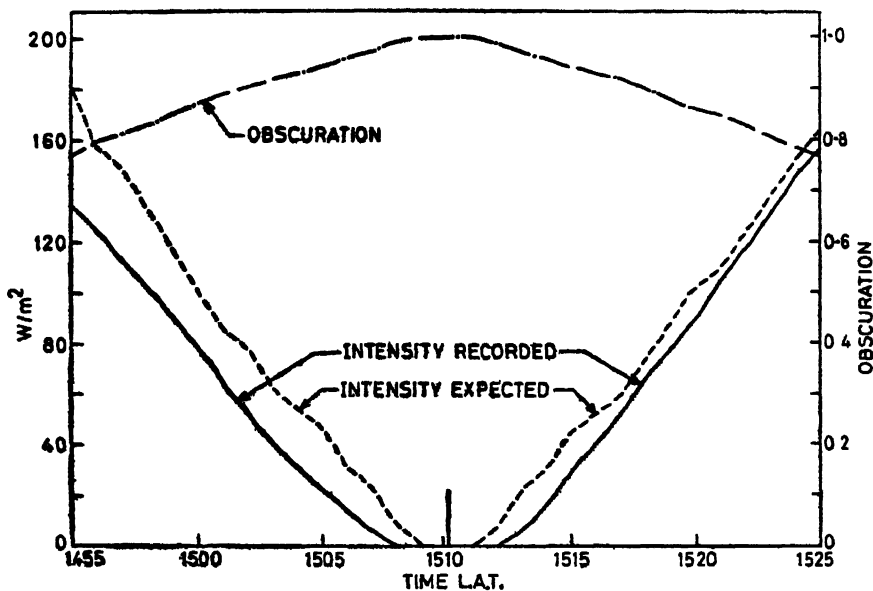


FIG. 1. Direct solar radiation and obscuration of the sun at Raichur on 16 February 1980

A slight increase in direct radiation was noticed at Gadag (Fig. 2) just before the commencement of the eclipse and it continued for about eleven minutes. The decrease in the intensities generally correspond to the rate of obscuration or magnitude of the eclipse at different stages of the eclipse. At Raichur, the values were 45, 25 and 6.6 per cents of the value at the time of first contact, the corresponding obscuration values were 50, 75 and 90 per cent before the totality. The values for the corresponding obscurations after the totality were 60, 29 and 11 per cent of the values after the eclipse. The corresponding values for Gadag were 40, 20 and 1.5 per cents before

totality and 55, 25 and 8.1 per cent after that. The restoration of the direct solar radiation is faster than the rate of decrease of the value.

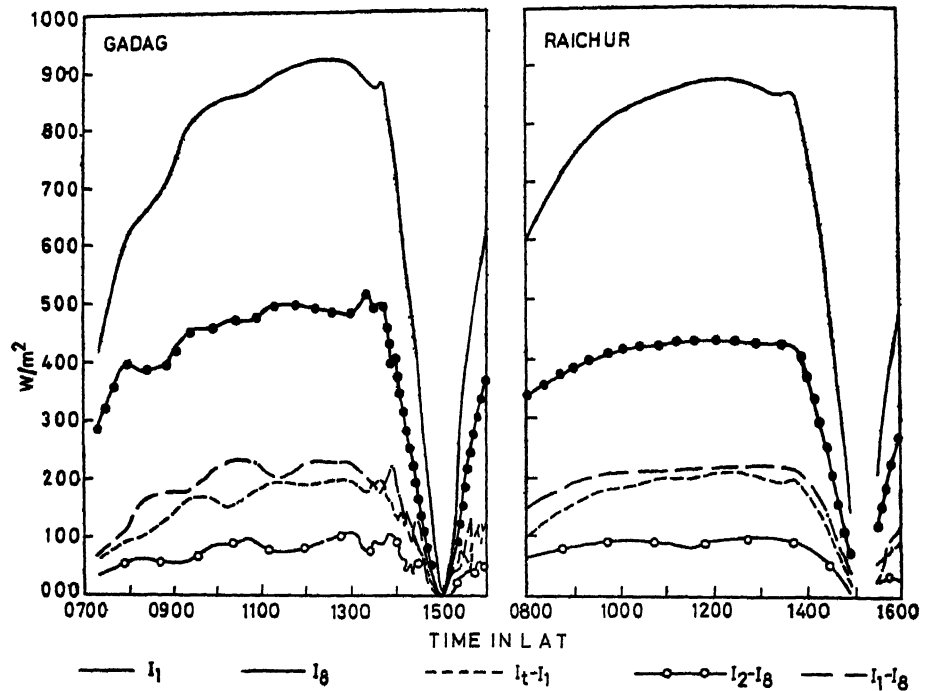


FIG. 2. Spectral distribution of direct solar radiation at Gadag & Raichur

The Red/Blue ratio initially showed a tendency to increase (Fig. 3) but started decreasing as the eclipse progresses till about 1456hr L.A.T. The percentage of radiation in blue wavelengths decreased with the commencement of the eclipse perhaps leading to the more yellowish tinge. The decreasing tendency continued upto about 1456h L.A.T. and then it abruptly increased. Thus the colour started becoming bluer giving rise to the darkening of the zenith sky. This may be due to the fact that the scattered light emanates from the high altitudes where dust loading is small and the Rayleigh scattering dominates. Thus the sky colour, can and does, shift to the blue during the totality. The percentage of radiation in the red wavelengths decreases from 1415hr L.A.T. onwards and reaches a very low value near about the 2nd contact. This shift of the colour toward the blue would become more dramatic when the lower atmosphere contains more dust as had happened at Gadag.

#### Global Solar Radiation

Global solar radiation started to decrease along with the progress of the eclipse at most of the stations except at Gadag, Hyderabad and Visakhapatnam where it increased slightly after the commencement of the eclipse and later it followed the progress of the eclipse. The locations represented in the diagram are located just outside the path of totality. The rate of decrease of radiation was generally smooth.

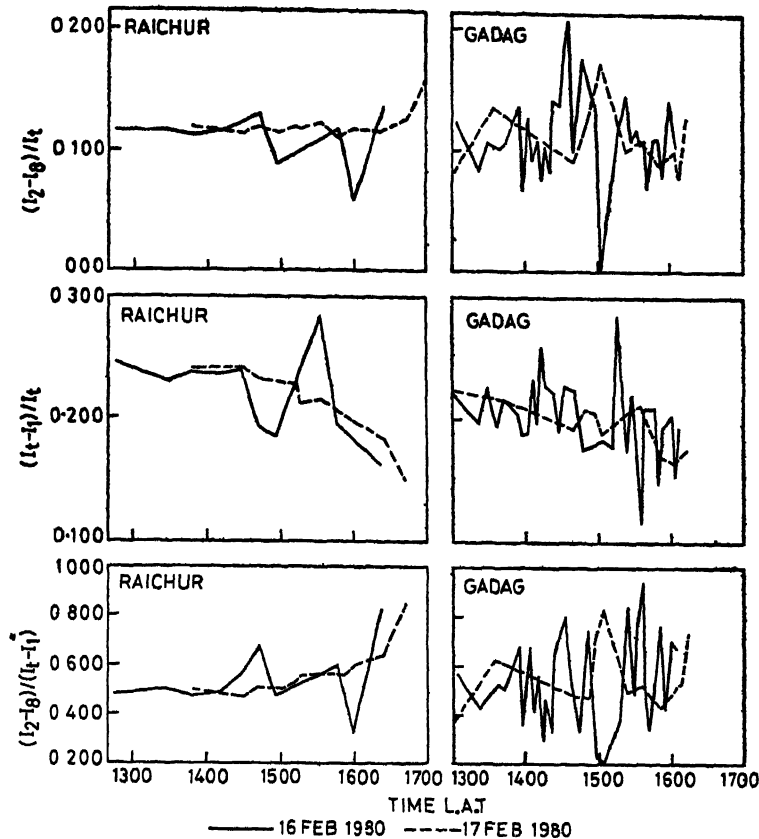


FIG 3 Variation in spectral distribution of direct solar radiation

initially perhaps due to the higher percentage contribution of the diffuse radiation. The recovery in the global radiation after the maximum did not have the same slope perhaps due to the decreasing altitude of the sun as well. The lowest values recorded generally coincided with the peak value of magnitude. The maximum values of global radiation were recorded not at or after the fourth contact but slightly earlier. Pune recorded this as early as 19 minutes. It was 9 and 7 minutes for Raichur and Gadag whereas it was hardly a minute for Hyderabad (Fig 4).

#### *Global and Diffuse Solar Radiation*

A study of the global and diffuse radiation values shows (Fig 5) that the diffuse values at Raichur were always lower than those at Gadag and that global radiation was always more than those at Gadag. Pune records showed that the global radiation at the maximum (91 per cent) was also 91 per cent of the pre-eclipse values ( $102.0 \text{ kJ/m}^2$ ). On the other hand diffuse radiation became almost zero. Like Gadag, Visakhapatnam also registered a small increase of 2.7 per cent in global radiation. Diffuse radiation was very uniform. The global radiation is 99 per cent corresponding to the magnitude of the eclipse. The diffuse value however was 90 per cent only.

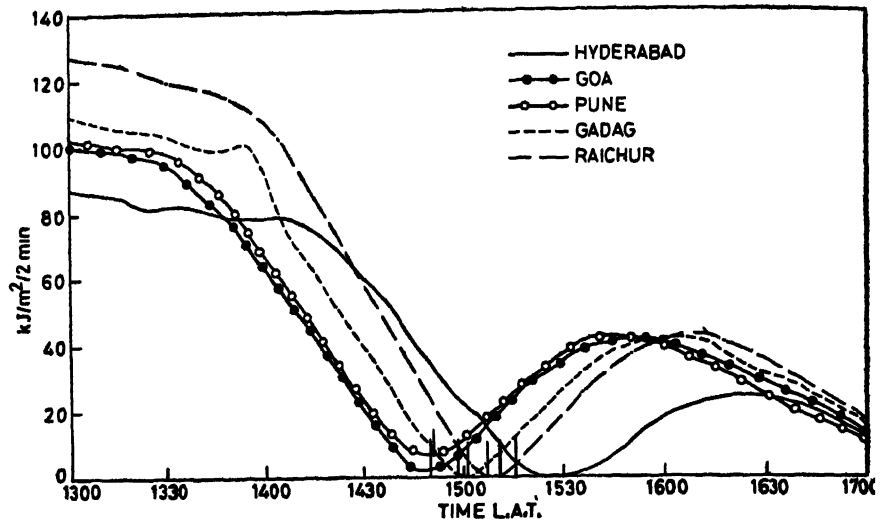


FIG 4 Global solar radiation on 16 February 1980

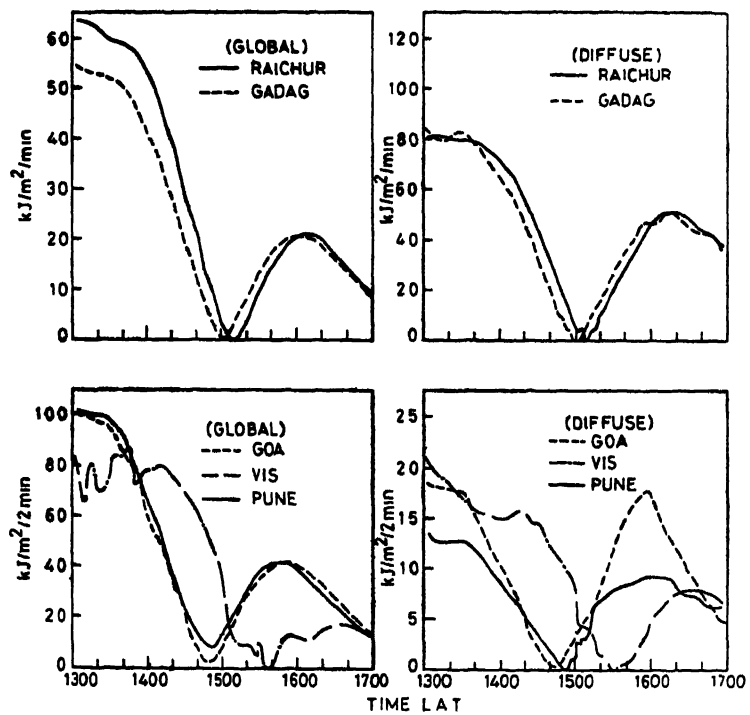


FIG 5 Variation of global and diffuse radiation on 16 February 1980

A detailed study of the percentage of the global and diffuse radiation on 16 February at Raichur and Gadag with reference to the values at the corresponding times on 17 February shows interesting results. (Fig. 6)

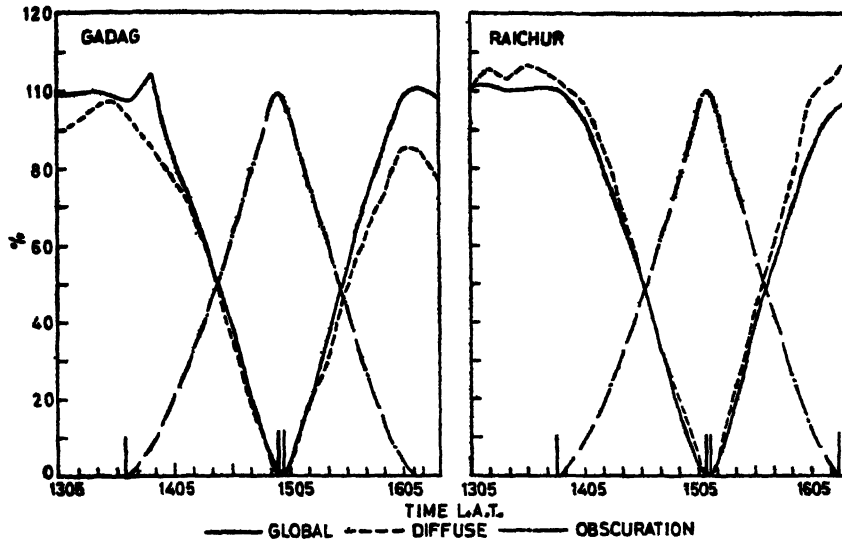


FIG 6 Percentage variation of global and diffuse radiation with the progress of the eclipse (w.r t. values on 17 February 1980)

#### *Raichur*

- (1) Increase in G(Global) and D(Diffuse) was always more than the decreasing values before the eclipse. They are of the order of 3.5 per cent.
- (2) The rate of decrease and increase of diffuse radiation was more than that for global radiation.
- (3) The rate of increase of diffuse radiation after totality was more than the rate of decrease before totality.
- (4) The rate of decrease in G and D was faster than the rate of obscuration, but the withdrawal was faster than the rate of increase in G and D.

#### *Gadag*

- (1) Increase was slower than the decrease of values before the eclipse.
- (2) The rate was less for diffuse radiation than that for global radiation.
- (3) The rate of decrease in diffuse radiation was more than the rate of increase.
- (4) The rate of decrease was slower than the rate of obscuration till 50 per cent is reached. After this rate was more than the rate of obscuration. Similarly, the rate of increase was more than the withdrawal rate till 50 per cent was reached. The withdrawal rate was then faster than the rate of increase in G and D.

- (5) The rates of fall or rise in G and D were more or less of the same order. The rates for D were slightly more than those for G.
- (6) There was only a marginal increase in G (of the order of 1 per cent) before the time of first contact
- (5) The rates of fall were more or less the same for both G and D but the rate of increase for global were much more than those for diffuse
- (6) The increase was relatively more (3–5 per cent) in G before the first contact.

#### *Variations in Radiation Components at Raichur and Gadag*

**Raichur**—The direct solar radiation I was always ahead of the eclipse stages. They had already attained 45, 24.5 and 6.6 per cent of the value ( $805 \text{ W m}^{-2}$ ) obtained before the time of first contact as compared with the corresponding obscuration values of 50, 75 and 90 per cent. For the same rates of obscuration after the third contact, the corresponding first values were 60, 29 and 11 per cents. These variations were more in the case of global radiation the percentages being 40, 21 and 4.7 before the totality and 65, 31 and 11 after the totality respectively. The rates were similar

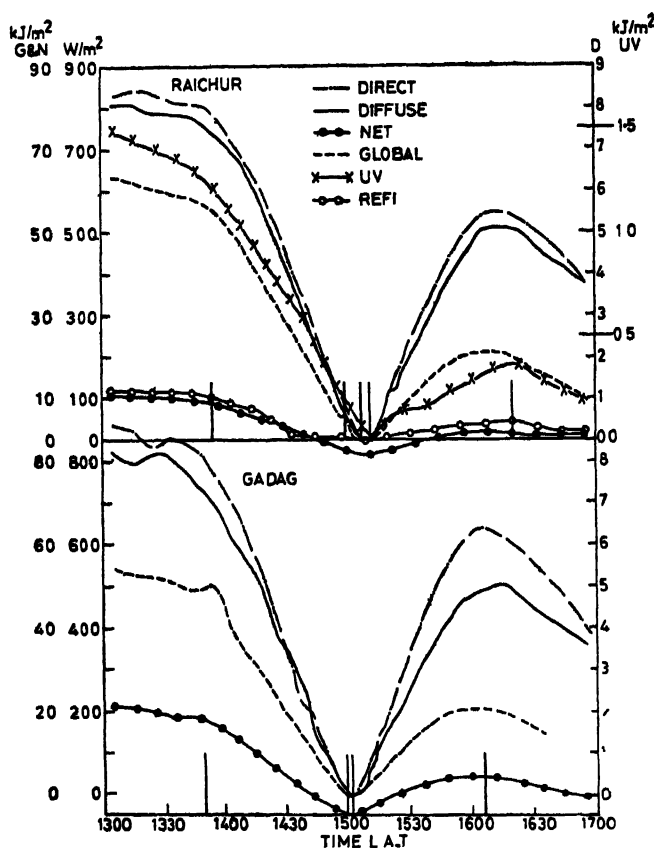


FIG 7 Progress of parameters at Raichur and Gadag.

for diffuse radiation except that they were much closer to the rates of obscuration, viz 47, 23 and 6 before the totality and 10, 27 and 56 after the totality.

Ultraviolet radiation in the range 290–390nm also showed similar tendency. It was 48, 30 and 6 per cent when the obscuration values were 50, 75 and 90 per cent but unlike other parameters it did not reach zero during totality. The global ultraviolet radiation was  $0.02 \text{ kJ/m}^2$ , about 1.6 per cent of the value before the first contact ( $11.0 \text{ kJ/m}^2$ ). During the withdrawal period however, the slope of the increase was rather very steep initially being 21 and 37 per cent for 90 and 75 per cent coverage. After this (75 per cent) this rate slowed down and it was only 47 per cent at 50 per cent obscuration.

Reflected solar radiation showed drastic decrease, 90 per cent even when the obscuration was only 50 per cent. It became 4.6 per cent for 90 per cent coverage. A similar pattern was seen after the totality. Net radiation reached zero from  $9.3 \text{ kJ/m}^2$  at the time of third contact. Net radiation remained negative upto 1537hr L.A.T. (55 per cent obscuration). The delay in reaching zero and then becoming positive is to be attributed to the fall in the soil temperature (of the order of  $20^\circ \text{C}$ ).

The maximum in each of the parameters after the third contact was reached about 7 minutes earlier than the fourth contact except in the case of ultraviolet which attained maximum at the time of fourth contact (1619hr L.A.T.). The net radiation reached the maximum about 15 minutes prior to the fourth contact.

*Gadag* — The rate of decrease for direct, global and diffuse solar radiation was more than the rate of increase when the obscuration became 90 per cent, the values of direct, global and diffuse radiation were 1.5, 1.0 and 1.6 per cent of the values at the time of first contact. The values at the same coverage after the totality were 8.1, 9.7 and 3.9 per cent.

Net radiation became zero at 1442hr L.A.T. (73 per cent coverage) and attained a negative maximum of  $4.6 \text{ kJ/m}^2$  at the time of third contact. It became zero again at 1523hr L.A.T. being quicker than that at Raichur. The lowest temperature of the soil recorded at Gadag is about  $38^\circ \text{C}$  due to the eclipse and it was  $32^\circ \text{C}$  at Raichur. This temperature difference may perhaps be the cause for the delayed zero at Raichur.

The maximum in direct, global and net radiation were reached 6–7 minutes prior to the time of fourth contact (1611hr L.A.T.). The diffuse radiation attained the maximum at 1615hr L.A.T. only.

### *Direct Fluxes of Illumination*

The direct fluxes of illumination were computed using the pyrheliometric data in different spectral regions by using the relationships given by A. J. Drummond and A. Angstrom. The formulae are

$$\begin{aligned}\rho &= 0.58 (1 + 0.235m + 1.19m\beta) \text{ for OG1 filters} \\ &= 0.39 (1 + 0.073m + 0.305m\beta) \text{ for RG2 filters} \\ &= 0.315 (1 + 0.032m) \text{ for RG8 filters}\end{aligned}$$

where  $\rho$  = luminous efficiency

$m$  = the airmass and

$\beta$  = the Angstrom turbidity coefficient

The direct fluxes of illumination  $E$  (in kiloluxes) in different spectral bands is then given by

$E = 0.6812W$  where  $W$  is the spectral value of intensity of direct radiation in the relevant band and expressed in Watt per square metre

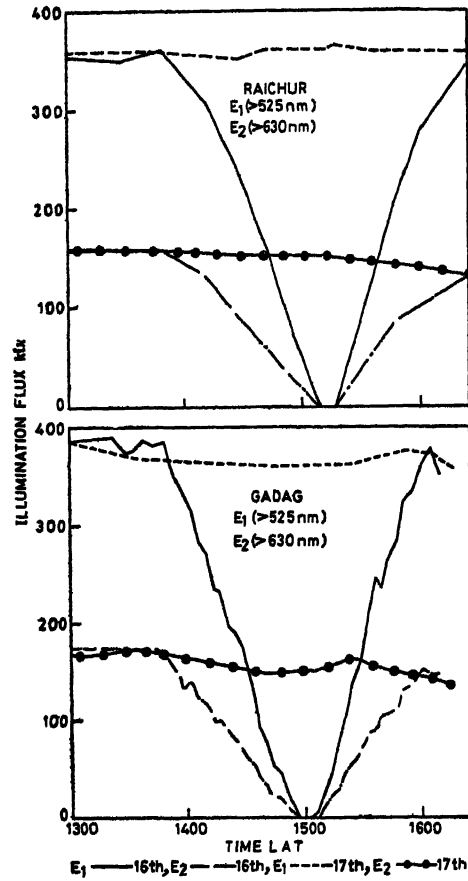


FIG. 8 Direct fluxes of illumination in kilolux

The values indicate that the rate of fall of intensities is more for RG2 wavelengths than that for OG1 wavelengths. After the totality the rates are more or less the same for both the wavelengths. The Gadag values indicate a faster decrease in RG2 wavelengths than those at Raichur, possibly due to the prevalent higher turbidity content of the atmosphere.



Printed in India

Eclipse Shadow

## SHADOW IMPRESSIONS OF 16 FEBRUARY 1980 TOTAL SOLAR ECLIPSE AS VIEWED BY THE SCANNER OF A METEOROLOGICAL POLAR ORBITING SATELLITE\*

K R RAO and R K GUPTA

*National Remote Sensing Agency, No 4 Sardar Patel Road,  
Secunderabad-500 003, India*

*(Received 18 July 1981)*

Coinciding of TIROS-N 10 00 28-10 15 33 GMT pass over NRSA Earth Station at Shadnagar (17 03N, 78 18E), 55km south of Hyderabad, covering Indian Mainland, Arabian Sea and Southern Bay of Bengal, with total solar eclipse duration over Arabian Sea enabled planning and successful execution of the experiment. The 10-bit Advanced Very High Resolution Radiometer (AVHRR) digital data received in 0.55-0.90 (B1), 0.725-1.1 (B2), 3.55-3.93 (B3) and 10.5-11.5 (B4)  $\mu\text{m}$  bands was converted into enhanced imageries. The bands 1 and 2 imageries depicted shadow zones of varying intensity and the effect was more pronounced in B1. The enhanced imageries for B3 and B4 did not have such modulations. Using the data on solar eclipse visibility and other physical informations on soil etc., the authors have attempted an explanation to the observed variations in shadow intensity within a zone and among different zones of enhanced B1 imagery. The explanation to the observed shadow geometry has also been attempted. To make the data useful for further studies, approximate computed values of scan time, latitude and longitude coordinates for shadow boundary discriminating points have also been included.

**Keywords** Total Solar Eclipse Shadows; Satellite Scanning; High Resolution Pictures

### INTRODUCTION

By virtue of the location of National Remote Sensing Agency (NRSA) Earth Station (Fig 1) the TIROS-N 10 00 28-10 15 33 GMT pass of 16 February 1980 was in the microwave visibility of the Earth Station and this was coinciding with the Total Solar Eclipse event period. Incidentally, the Earth Station, located at Shadnagar (17 03N, 78 18E)—55km south of Hyderabad, was also lying in the Total Solar Eclipse path. NRSA availed of this opportunity and successfully conducted an experiment to capture the Solar Eclipse shadow impressions in the visible band enhanced imagery using the digital data of Advanced Very High Resolution Radiometer (AVHRR) system on-board the TIROS-N.

---

\*Similar base analysis of the data has appeared in the "Remote Sensing of Environment."

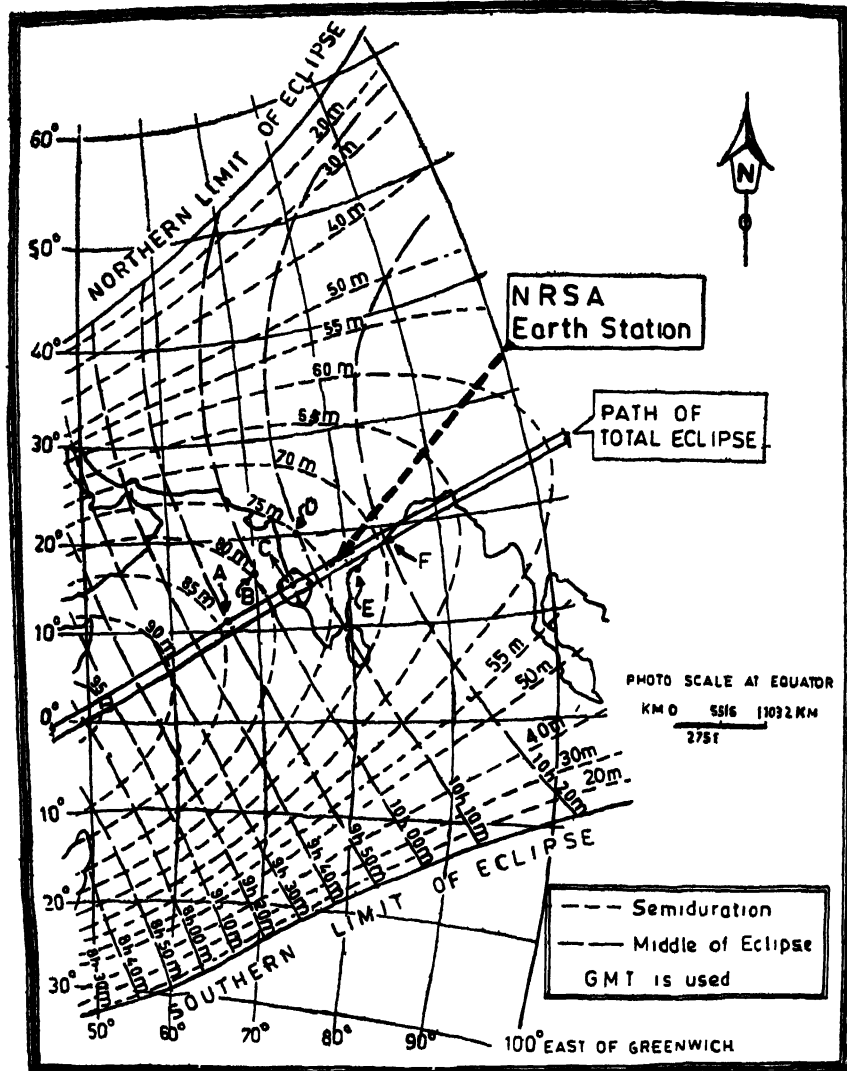


FIG 1 Eclipse geometry for the duration of interest

## SENSING SYSTEM AND DATA PROCESSING DETAILS

NRSA Landsat Earth Station receives real-time digital data from TIROS-N series of US Polar Orbiting meteorological satellites in High Resolution Picture Transmission (HRPT) format and processes the 10-bit AVHRR data to produce radiometrically and geometrically corrected (for earth rotation, panoramic distortions etc) black and white imageries in the four AVHRR bands Table I depicts the spectral characteristics and instrument parameters of TIROS-N/AVHRR

The AVHRR 10-bit data is resampled to 8-bit data using Look-UP Table (LUT) and the 0 to 225 count values of thus resampled 8-bit data are used to produce 17-

steps gray scales for Black and White imageries of the individual band data Channel 1 is useful for day time surface and cloud mapping while the near IR channel (band 2) is good for discriminating water and soil masses Band 3 and Band 4 refer to thermal IR data

TABLE I

*Spectral characteristics and instrument parameters of TIROS-N/AVHRR*

AVHRR	CH1	CH2	CH3	CH4	CH5
	0.55–0.9 μm	0.725–1.1 μm	3.55–3.93 μm	10.5–11.5 μm	Data from CH4 repeated. Kept for future growth
Cross track scan			± 55.4° from Nadir		
Line Rate			360 lines per minute		
Optical field of view			1.3 milliradians		
Ground Resolution (IFOV) <sup>1</sup>			1.1 km at Nadir		
Infrared Channel (NEΔT) <sup>2</sup>			0.12 K at 300 K		
Visible channel S/N <sup>3</sup>			3.1 at 0.5 per cent albedo		
(1) Instantaneous field of view					
(2) NEΔT—Noise Equivalent differential temperature					
(3) Signal to Noise Ratio					
HRPT Transmission					
Carrier Modulation			Digital split phase, phase modulated		
Transmit Frequency			1707.0 MHz, RHC polarization		
EIRP (approx )			39.0 dBm		
Transmit Power			5 watts		
Spectrum Bandwidth			less than 3 MHz		
TIROS-N	Satellite name standing for Television Infrared Operational Satellite-N Series				
AVHRR	Advanced Very High Resolution Radiometer				
HRPT	Data Transmission Format standing for High Resolution Picture Transmission				

There are 2048 data pixels for a swath width of 3000.0591 km. With 1.1 km (spatial resolution at sub-satellite point) data points we should have 2727 pixels and to affect geometric and panoramic correction the 2048 actual data pixels are resampled to 2727 data pixels using either Nearest Neighbour (NN) or Cubic Convolution (CC) method. The image format consists of 3600 pixels. 248 square pixels (191 are actually needed) are kept reserved for applying earth rotation offset to the filmed data. Thus we have a total number of 2975 pixels available for imaging the data and rotation offset. As the film format consists of 3600 pixels we further scale the film by 1.2101210 (3600/2975). Thus we have 3300 rescaled and resampled AVHRR data pixels per line. To satisfy aspect ratio criteria a line repeat ratio of 1.508633 is practised.

#### DATA DESCRIPTION

As the data obtained in AVHRR CH1 and CH2 pertains to the amount of solar radiation reflected by the upper boundary of various natural terrestrial surfaces, clouds etc.,

the eclipse shadow impressions, and the variations of the reflectivity of the earth's surface in and around the shadow impressions were observed in the enhanced imageries for bands 1 and 2. Unenhanced imageries for these bands were having very less brightness in general and few of the shadow zones were impressible even in these imageries. Enhancement of the imageries in all the four bands was obtained by suitably adjusting the gain and bias controls and using a mapping algorithm corresponding to a saw tooth wave type. As the phenomenon of totality of eclipse was only of a few minutes duration and because of the high thermal inertia of earth, these variations were not so much observable in the pictures for bands 3 and 4. As expected, a general reduction in the emission intensity in the thermal IR bands was observed. Even enhancement of data in these IR bands did not give any shadow zones. The shadow zones were more remarkably discriminative in band 1 enhanced imagery as compared to that for band 2. Fig 2 refers to the band 1 image. In an overlay to Fig 2, approximate boundaries for few shadow levels over the oceanic region have been marked. Approximate coast line of the Indian Continent have also been transferred to Fig 2. The figure also depicts fifty seven shadow boundary discriminating points. The time, latitude and longitude coordinates for these points have been computed to make the data useful for further studies (Table II). Points 39, 43, 44 and 48 refer to points on the periphery of clouds.



FIG 2 Picture in visible spectrum using TIROS-N AVHRR data for 100510-101221 GMT

During this TIROS-N pass, the subsatellite point track moved from 10 24 S, 81 88 E (10 00 28 GMT, 0 71° elevation) to 43 61 N, 67.79 E (10 15 53 GMT, 0 37°

elevation) The antenna elevation angle during the period of data presented in Fig. 2 ranged between  $27^{\circ}23'$  to  $16^{\circ}01'$  and had its maximum value of  $69.92^{\circ}$  at 10 07:58 GMT (16 07 N, 75 78 E). Due to good elevation, the data is of substantially high quality.

TABLE II

*Computed coordinates and time of scanning for the shadow boundary discriminating points located on the overlay for Fig 2.*

Point Identification No.	Scan time in GMT (HH MM SS S)	Coordinates of the point	
		Lat. (N)	Long. (E)
(1)	(2)	(3)	(4)
1	10 05 54.2	8.31	75 52
5	10 06 21.2	10 11	75.95
10	10 06 52.6	13.76	83.09
15	10 07 10.6	11 97	69.50
20	10 07 36	14 92	72.55
25	10 07 42 9	17.18	87.53
30	10 08 03 5	16 02	73.83
35	10 08 24 9	17 24	73.23
40	10.08 46.8	21 27	87.74
45	10 09 28 2	21	72.52
50	10:10 00 2	20 18	62.33
55	10:10 35	22 12	61.52

Table III (after Bhattacharyya, 1978) gives the data for the central line of 16 February 1980 Total Solar Eclipse.

TABLE III

*Total Solar Eclipse of 16 February 1980  
Central Line*

Ephemeris Time		Latitude		Ephemeris Longitude		Duration		Width of path	Altitude of the Sun
H	M	(°)	(')	(°)	(')	M	S	miles	(°)
10	00	N 11	47.0	E 63	33 0	3	10 0	84	48
	05	13	02 4	70	55 7	3	01 3	82	44
	10	14	23 3	73	35 1	2	51 9	80	40
	15	15	51 3	76	37 3	2	41 6	78	36
	20	17	28 8	80	12 7	2	30 2	75	31
	25	19	20 7	84	41 3	2	17 2	72	25
10	30	21	39 0	90	54 6	2	01 3	68	18

From Table III, one could approximately infer that during the period of Fig. 2 data, the total solar eclipse was taking place between  $13^{\circ}\text{N}$ ,  $71^{\circ}\text{E}$  and  $15^{\circ}\text{N}$ ,  $75^{\circ}\text{E}$ . Sun altitude during this period was between  $44^{\circ}$  and  $36^{\circ}$ . The satellite speed and the eclipse path speed over the Indian west coast and the adjacent Arabian Sea could be approximated to  $385\text{km/min}$  and  $68\text{km/min}$  respectively and the ratio (say  $R$ ) of these works out to be  $5.66$ —approximated as  $5.7$ . The eclipse path was subtending an angle of  $104.5^{\circ}$  (measured westward) to sub-satellite point track. It should be noted that the satellite picture is not a snap-shot i.e., taken at an instant of time; it is a line-scan generated picture. Since the scanning is at  $90^{\circ}$  to subsatellite point track the angle between scan lines on the ground and the eclipse path works out to be  $14.5^{\circ}$ .

Fig. 1, drawn using the picture published by Fiala and Lukac (1978), depicts the eclipse map over the region of interest. Though the legend states that GMT is used, the authors have written to treat this as Ephemeris Time (ET) and therefore, while using Fig. 1 one has to subtract one minute from the depicted value to get the correct GMT. Since most of the areas of Fig. 2 got covered during 095000–102000 ET middle of eclipse time, the authors have marked cardinal points (A through F) in Fig. 1 and the first and last contact times alongwith the middle of eclipse times for these points have been presented in Table IV. The location of NRSA Landsat Earth Station has also been marked therein. In addition to this the closed curve corresponding to shadow zone defined in Fig. 2 by points 30, 21, 16 and 20 has also been marked in Fig. 1 for the ease of comparison.

TABLE IV

*Middle of eclipse, first and last contact times for few points marked in Fig. 1*

Point Identification mark	Time for first contact (HH MM:SS GMT)	Time for middle of Eclipse (as labelled in fig. 1) (HH MM SS GMT)	Time for last contact (HH MM SS GMT)
A	08:25 45	09 50 00	11 14 15
B	08 39 00	09 59 00	11 19 00
C	08 47 45	10 05 00	11 22 15
D	08 54 00	10 10 00	11 24 00
E	09 02 50	10 15 20	11 27 50
F	09 08 08	10 20 00	11 29 32

#### DISCUSSION AND CONCLUSIONS

The picture at Fig. 2 is the result of a complex inter-relationship of satellite dynamics, satellite scanning geometry, eclipse kinematics and eclipse geometry. The analysis of such an image gets further complicated due to scanning of different areas at different times (Table II). In the following paragraphs, authors have attempted to provide a broad analysis of the picture presented at Fig. 2.

The first noticeable point in Fig. 2 is that the shadow appears to be more intense over sea surface compared to that over land area. This intensity variation could be assigned to poor scattering properties of sea surface due to specular reflection as

compared to that over land areas where light is scattered because of surface irregularities

In Fig 2, the shadow zones demarcated by points 5, 9, 15, 19, 23 and 31 (Zone I), 7, 12, 24 and 32 (Zone II) were scanned during 100620–100812 GMT while the middle of eclipse during this period was between points C and D (Fig. 1), one could easily understand the shadows to be more intense in Zone I as compared to those in Zone II. With reference to data received in the field of view of satellite radiometers, the Gulf of Mexico is reported to have 9 per cent albedo while Pacific Ocean contributes only 7 per cent (Anderson *et al*, 1973). For this reason, authors feel that warmer bay of Bengal will reflect more in band 1 as compared to that from Arabian sea. Of course, this factor must have only slightly contributed to variations in shadow intensity over regions I and II.

Barrett and Curtis (1976) have mentioned albedo values, in visible spectrum, of 16–23 per cent for winter wheat, 17 per cent for deciduous forest, 14 per cent for moist ploughed fields, 8 per cent for moist black soil and of 37 per cent for fine soil. The region 'Y' consists dominantly of alluvial and deltaic soils and is rich in forest and vegetation. The arc 'X' could also be considered equally rich in vegetative coverage. In Fig 2, one finds that area 'X' had more shadow intensity compared to area 'Y' in contrast to albedo impressions observed on non-eclipse days. In the light of above discussion, the observations could be explained by taking into consideration the increased eclipse magnitude over area 'X' as compared to that over area 'Y' by virtue of its nearness to total solar eclipse path. The area little far right of point 53 refers to Rajasthan desert where near 37 per cent albedo could be expected and this happens to be much higher than the expected albedo of 7–9 per cent over Arabian Sea. This accounts, within the same shadow zone, for the observed very much less shadow intensity over land area (right of point 53) compared to its counterpart over Arabian Sea. In nearly 60 per cent of the land region right of points 30, 35, 42, the podzolized soils with patches of black, mixed red and black soils, and shallow black soils are noticed. Land surface further east of this area upto Indian east coast mainly consists of mixed red and yellow soils, and red soils. In addition to the effect of different magnitudes of eclipse over these zones, the variations in albedo due to different types of soils should have substantially contributed to the observed finer shadow intensity variations over these two regions.

The authors have attempted to explain the geometry of shadow impressions by taking up an ideal case to visualize how a circular moving shadow would be registered by the scanner of a progressing satellite. The width of total eclipse path over the ground could be approximated to 127 km and this would have been scanned by the satellite in  $(127 \times \sec(14.5^\circ) \times 60) / 385 = 20.44$  seconds. As the ratio of satellite speed to eclipse speed ( $R$ ) is 5.7, a circle drawn with a diameter of  $20.44 \times 5.7 = 116.5$  mm (it could be any unit of distance) with 'C' as centre (Fig 3) would depict the zone of shadow at zero reference time. Taking into account the  $104.5^\circ$  angle between sub-satellite point and eclipse track, the line drawn to depict sub-satellite point track passing through 'C' cuts the lower semicircle segment of the drawn circle at point P which has been considered as the initial time position for scanner to visualize the impressions of scanning dynamics and moving eclipse shadow when the whole circular image has been scanned in 20.44 seconds. Now, if we move the circular shadow zone

at the rate of 1mm/sec along its X-axis by drawing circles of 116.5mm diameter with centre (marked 'C' for initial zero reference time shadow) drifted by 1mm after every second and move the scanner path (which will be perpendicular to satellite subpoint track) by 5.7mm starting from zero reference time scan position *P*, the points of intersection of scanner path after a particular time interval with the shadow circle corresponding to the same time will give the limiting points for the intercepted portion of moving circular eclipse impressions at that instant. Thus these limiting points could be obtained for 1, 2, 3 ... 20 and 20.44 seconds. A line drawn through these points of intersections depicts the shadow geometry as recorded by the scanner of the satellite and Fig 3 is a result of such an exercise. It is seen that the boundary is nearly circular in shape at 'a' and 'd', elongated at 'b' and 'c', discontinuous at 'e' and 'f' because the scan line has moved out from the actual shadow zone. This region (e-f) can also be noticed in Fig 2. The step like structures (e.g., between points 35 and 42, 5 and 13) seen within a shadow zone (Fig 2) are due to sudden variation of reflectivity characteristics over coastal boundaries. The returns from the sea are less than that from the land. Thus two contiguous points situated on either side of the coast (one on the sea and the other on the land) appear with different tones in the picture. Taking note of this, the picture from the sea and contiguous part of the land can be combined into a single shadow boundary as appearing in Fig 2. The shape of this boundary compares very well with the computed shape shown in Fig 3.

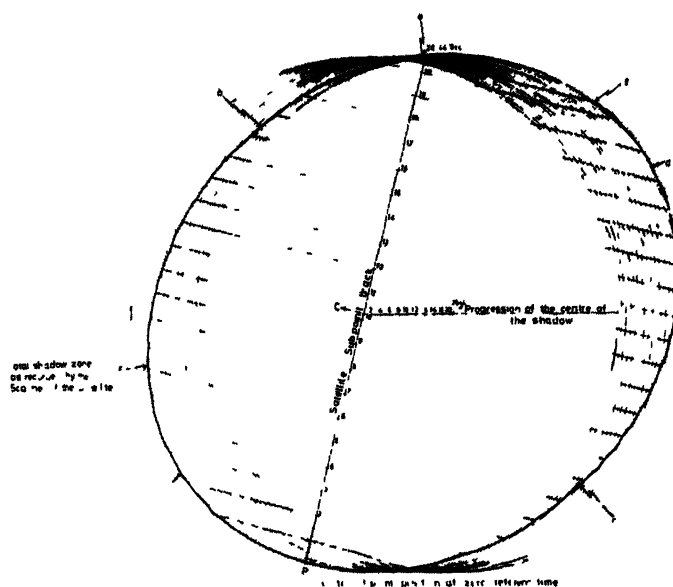


FIG 3 Final shape of a moving circular shadow as scanned by a moving satellite.

Looking within the shadow zone I, a geometric structure (encircled by points 30, 21, 16 and 20 in Fig 2) somewhat similar to Fig 3 though of a little less shadow intensity was observed. The data encompassed within this structure (say Zone III)





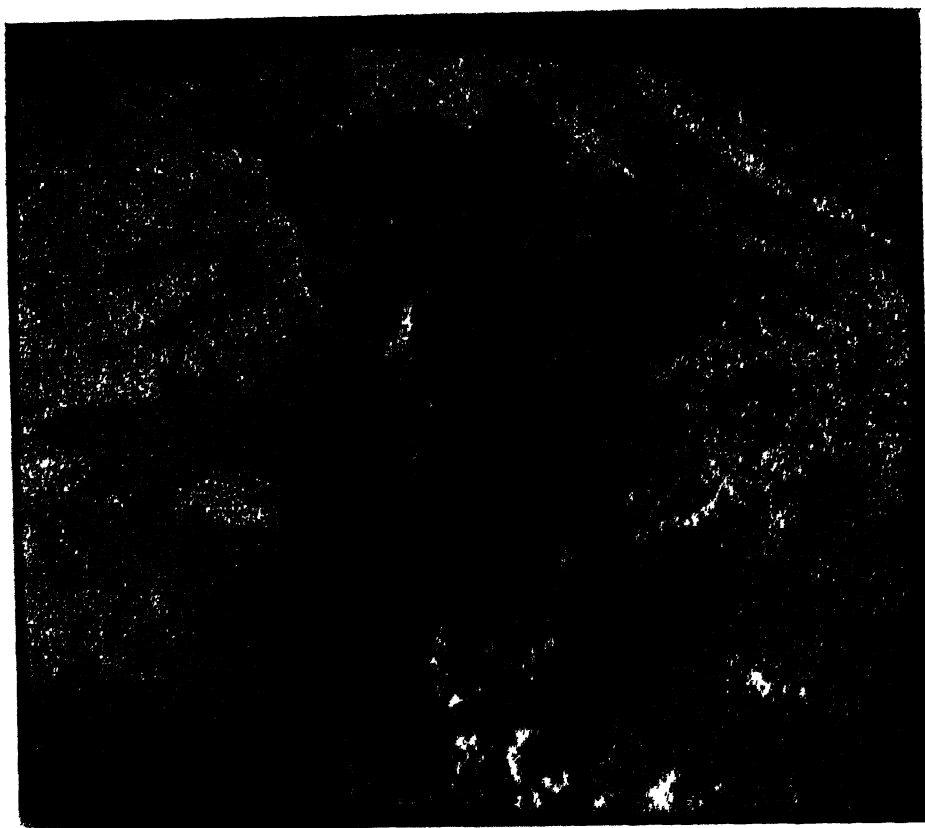


FIG 4 Colour composite of visible—, near IR and thermal IR band images made using digital data obtained during 16 February 1980 total solar eclipse time (100510–101221 GMT) through TIROS-N/Advanced Very High Resolution Radiometer

was scanned during 100710–100803 GMT. The closed curve passing through these points (on Indian west coast) depicts the area enclosed by these points. It could be seen that total solar eclipse path passes through the Zone III (Fig. 1). As per Fiala and Lukac (1978), the total solar eclipse touched the Indian west coast around 101000 GMT. With the suggested consideration of this time as ET (as mentioned earlier) the figure could be put as 100900 GMT. Therefore, the Zone III, except at its western boundary, could not be expected to observe the total solar eclipse as the scanning was during 100710–100803 GMT. However, it could easily be considered that the central strip of Zone III was under near total solar eclipse condition while the region west of this zone was experiencing comparatively more pronounced total solar eclipse effect and this explains for the decrease of shadow intensity in Zone III compared to that of west of the zone. It is obvious to expect decrease in shadow intensity north and south of central total solar eclipse path strip in Zone III.

Fig. 4 refers to colour composite of Eclipse data using enhanced imageries in bands 1, 2 and 4. This gives a composite view of data taken in visible, near IR and thermal IR atmospheric window regions.

#### ACKNOWLEDGEMENTS

The authors are thankful to NRSA authorities for providing the facility to conduct the experiment. The authors are thankful to Mr D. V. Raju, Head and Engineers of NRSA earth station division for taking pains to acquire valuable data. The authors are thankful to Ms I. S. Neelaveni for the strains taken by her in typing the manuscript of this paper.

#### REFERENCES

- Anderson, R. K., Ashman, J. P., Farr, G. R., Ferguson, E. W., Isayeva, G. N., Oliver, V. J., Paramenter, F. C., Popova, T. P., Skidmore, R. W., Smith, A. H., and Veltushchve, N. F. (1973) *The Use of Satellite Pictures in Weather Analysis and Forecasting*. World Meteorological Organisation, Geneva, *Tech. Note*, No. 124.
- Barrett, E. C., and Curtis, L. F. (1976) *Introduction to Environmental Remote Sensing*. Chapman and Hall, London, 23 pp.
- Bhattacharyya, J. C. (1978) *The Eclipse of February 16, 1980—Path of Totality in India*. Report of Indian Institute of Astrophysics, Bangalore.
- Champion, Sir Harry G., and Seth, S. K. (1968) *A Revised Survey of the Forest Types of India*, Government of India Publication, 15 pp.
- Fiala, A. D., and Lukac, R. L. (1978) *Total Solar Eclipse of 16 February 1980*. U.S. Naval Observatory, Washington D.C., Circular No. 158.

Printed in India

Tides

## CHANGES IN TIDAL CHARACTER DURING TOTAL SOLAR ECLIPSE OF 16 FEBRUARY 1980

R. SUSEEL REDDY, B. K. MUKHERJEE and BH. V. RAMANA MURTY

*Indian Institute of Tropical Meteorology, Pune-411 005, India*

*(Received 18 July 1981)*

The changes in tidal character during total solar eclipse of 16 February 1980, for the three stations, Kandla (50 per cent eclipse), Bombay (90 per cent eclipse) and Karwar (100 per cent eclipse), have been investigated making use of superposed-epoch and  $T/C$  ratio methods. An increase in high tide of 2 days and a decrease in low tide 0 to 2 days have been observed after the phase of the new moon. Karwar has exhibited maximum changes in tidal activity as compared to Kandla and Bombay. The possible association of changes in tidal activity during the total solar eclipse would be the nearness of the moon to the earth and the secular acceleration of the moon and the sun.

**Keywords:** Tide; Phase of the New Moon; Solar Eclipse-1980

### INTRODUCTION

THE eclipse of 16 February 1980 has opened another opportunity to research workers for studies in the field of Solar-Terrestrial Physics and Meteorology (STP-M). Also, the study on tides during eclipse is important for better understanding of some of the gravitational laws with respect to sun, moon and earth. Many studies have been reported on the possible effects of solar eclipse on various parameters of the earth's atmosphere, but the studies on tides are few. The authors have, therefore, undertaken the present study to examine changes in tidal character during the eclipse of 16 February 1980.

### TIDES

The regular rise and fall of the sea, known as tide, can be observed on any shore. The tides are caused principally due to combined gravitational forces of the sun and the moon on the earth. When the sun and the moon are lined up with the earth, the tidal effects of the bodies reinforce each other and the tides are at their maximum height. When the gravitational forces exerted by the sun and the moon on the earth are pulling at right angles to each other, they do not reinforce each other, and the tides become the weakest. The tides follow generally the phase of the moon. There are additional effects due to variable distances between the moon and the earth, as well as the more important effect of varying lunar and solar declination.

## DATA

The data considered in the present study pertain to tides (high and low) and dates of the phases of the new moon for the period 10 to 24 January; 9 to 23 February; 9 to 23 March 1980. The dates of the phases of the new moon are 17 January, 16 February and 16 March of which solar eclipse has occurred on 16 February 1980. The data were extracted from the Indian Tide Tables for the year 1980 published by the Surveyor General of India. The details of the stations and the details of the solar eclipse are given in Table I. A brief history, predictions and general remarks of tides are described in the above report of *Indian Tide Tables*. Table I also gives the  $T/C$  ratio values for high and low tides that have been calculated for Kandla, Bombay and Karwar during January-March, 1980. The values of the tidal range are also provided.

TABLE I

*Details of the stations, eclipse and the  $T/C$  ratio for tides  
(high and low range)*

Sl No	Name of the Station	Latitude	Longitude	Maximum eclipse in percentage	Date of the phases of new moon including eclipse	( $T/C$ ) High	( $T/C$ ) Low	Range
1.	Kandla	23° 01' N	70° 13' E	50	17.1.1980	1.01	0.71	0.30
					16.2.1980*	1.01	0.71	0.30
					16.3.1980	1.01	0.71	0.30
2.	Bombay	18° 55' N	72° 50' E	90	17.1.1980	1.00	0.72	0.28
					16.2.1980*	1.02	0.50	0.42
					16.3.1980	1.00	0.70	0.30
3	Karwar	14° 48' N	74° 07' E	100	17.1.1980	0.95	0.66	0.21
					16.2.1980*	1.03	0.44	0.59
					16.3.1980	0.98	0.75	0.23

\* the day on which solar eclipse occurred during the phase of the new moon

## METHOD OF ANALYSIS

To find the height of the tide at any time, the method is used as given in the *Indian Tide Tables*. The heights of the tides are then calculated at 1600hr for the period considered above and the values so obtained have been analysed by the superposed epoch method.

The variations in the amplitudes of the tidal wave are more in high and small in low tides 0 to 2 days following the dates of the phases of the new moon and it is difficult to bring out the changes in tides during the eclipse from this analysis. For the evaluation of the changes in the tidal activity during the total solar eclipse, the

value of the tide on the day of new moon (Target,  $T$ ) is compared to the average value of 4 days (Control,  $C$ ) consisting of 2 days before and 2 days after the day of the new moon. The ratio values of  $T/C$  were computed and used in the study. If the value is  $>1$ , it is taken as increase in tidal activity, if it is  $<1$ , it is taken as decrease and if it is  $=1$ , it is taken as zero change. The  $T/C$  ratio method is widely used in the evaluation of weather modification experiments (Brier, 1974)

## RESULTS

### *Superposed-Epoch Method*

The values of tides (high and low separately) for the three stations, Kandla, Bombay and Karwar, for the period (a) 10–24 January 1980 (17–1–1980: phase of the new moon), (b) 9–23 February 1980 (16–2–1980: phase of the new moon and the day on which solar eclipse occurred), (c) 9–23 March 1980 (16–3–1980: phase of the new moon) have been analysed by a superposed-epoch method considering even days before and seven days after the dates of the phases of the new moon (17 January, 16 February and 16 March during which total solar eclipse occurred on 16 February).

The values obtained by this method are shown in Figs 1, 2 and 3 for the above three stations respectively. It is noticed from the figures that generally all the three stations have exhibited an increase in high tide, 2 days after the phase of the new moon. The increase is significant at 99 per cent level. They have also exhibited a decrease in low tide 0 to 2 days after the phase of the new moon. The decrease is significant at 99 per cent level. Similar features are noticed even during totality.

From Table I it is noticed that Kandla has exhibited no change in tidal activity; but, Bombay has exhibited a small increase by 2 per cent in high tide and decrease by 29 per cent in low tide and an increase in the tidal range by 40 per cent during eclipse when compared to the other months. Karwar has exhibited an increase in high tide by 8 per cent and decrease in low tide by 35 per cent and increase in tidal range by 190 per cent during eclipse period when compared to the other months. It is also seen that the changes are more in low tide than in high tide during eclipse period. Also, Karwar, which is low in tidal activity as compared to Kandla and Bombay, has exhibited almost three times more variation in the tidal range than the other two months during totality.

## DISCUSSION

The moon rarely plays an important part in the affairs of the earth, but in its influence on the tidal phenomena of the oceans and seas it is of fundamental importance. It is well known that the gravitational forces of the earth, moon and sun on one another is the basic cause of the tides. The movements of these bodies are complex, but regular and well known, which enable the tides to be predicted with some accuracy. According to McLellan (1965), the equilibrium tide due to the moon is 35.4 cm at the maxima and  $-17.7$  cm at the minima; and due to the sun it is 16.2 cm and  $-8.2$  cm. Nevertheless, other factors are also involved which are not so well understood; the response of the oceans and seas to the tide producing forces has, in the past, given rise to a number of different theories to account for the observed tidal phenomena,

while unusual meteorological conditions can cause considerable differences between the predicted and actual tidal conditions.

The statistical method (superposed-epoch) used in the present study does not clearly depict the real tide character as seen from the Figs. 1, 2 and 3. However, an increase in high tide of 2 days and a decrease in low tide 0 to 2 days after total solar eclipse are found to be significant at 99 per cent level according to student 't'. As it is difficult to bring out the changes in tidal character from the analysis of superposed-epoch method, the authors have designed 'T/C' ratio method for the evaluation of the changes in tidal character. This method depicts better the changes in tidal character for the stations Bombay and Karwar after the total solar eclipse (Table I). The observed changes in tidal activity of the present study, 0 to 2 days after the phase of the new moon require explanation. During times of new and full moon (actually 1 or 2 days later because the tidal bulges are not aligned with the moon), the tidal

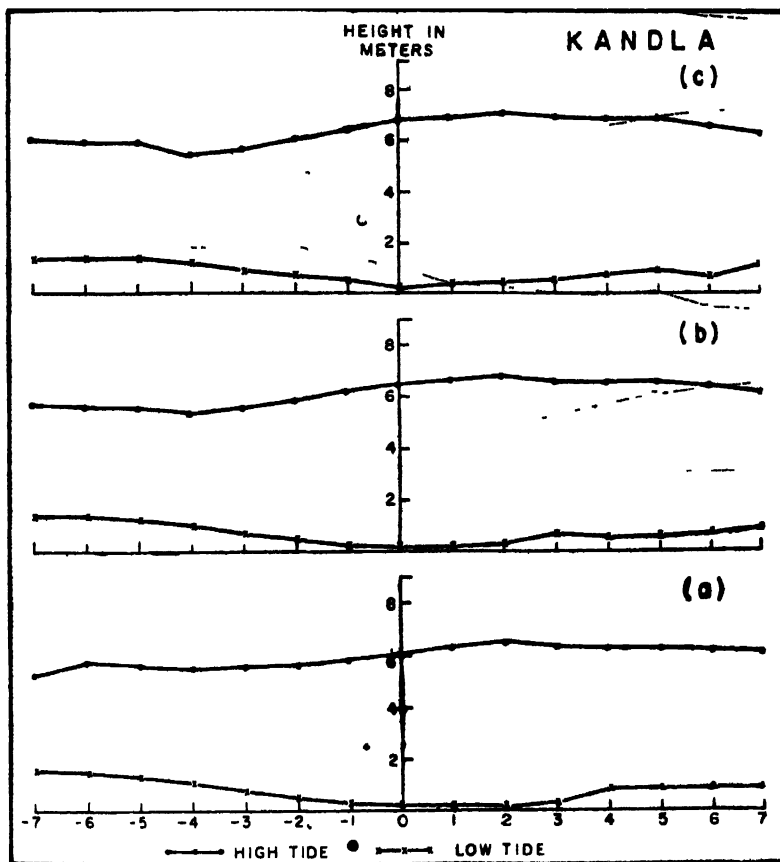


FIG 1 Superposed-epoch analysis of tides (high and low) for Kandla seven days before and after the date of phase of the new moon (a) 10-24 January 1980 (17-1-1980 phase of the new moon), (b) 9-23 February 1980 (16-2-1980 phase of the new moon and the day on which solar eclipse occurred), (c) 9-23 March 1980 (16-3-1980 phase of the new moon)

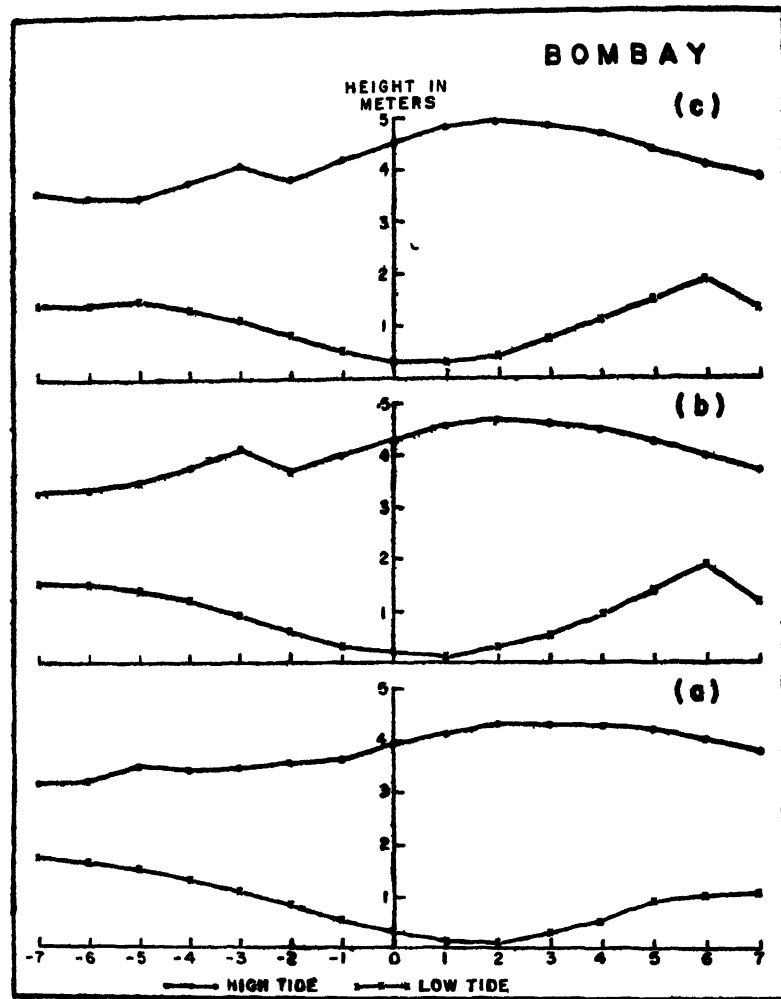


FIG. 2. Superposed-epoch analysis of tides (high and low) for Bombay seven days before and after the date of phase of the new moon: (a) 10-24 January 1980 (17-1-1980 phase of the new moon); (b) 9-23 February 1980 (16-2-1980: phase of the new moon and the day on which solar eclipse occurred), (c) 9-23 March 1980 (16-3-1980: phase of the new moon)

effects of the moon and the sun reinforce each other and cause exceptionally great tides (Ordway, 1966). The observed changes in tidal activity during totality can be attributed to the force of gravitational attraction between the earth and the moon and it is well known that during totality, the moon is closer to the earth. Although this phenomenon is well established, an opportunity has arisen to further verify such relationships during the present eclipse. The force of gravitational coupling between the earth and the moon is  $GME/R^2$ , where  $G$  = the gravitational constant,  $M$  = mass of the moon,  $E$  = mass of the earth and  $R$  is distance between the centres. The average gravitational attraction, which is equal to the centrifugal acceleration, is then



proportional to  $ME/R^2$ , since the gravitational attraction is proportional to the mass and inversely proportional to the square of the distance.

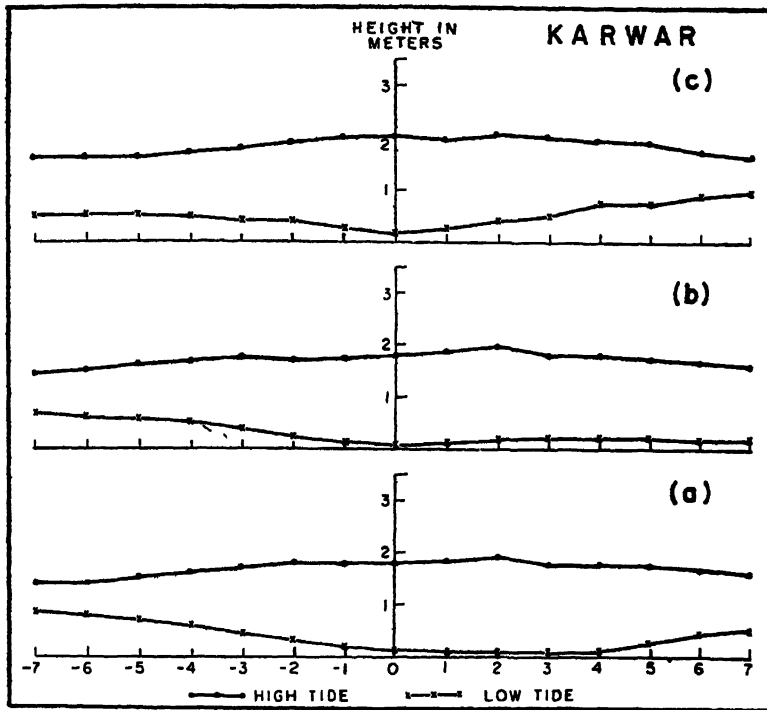


FIG 3 Superposed-epoch analysis of tides (high and low) for Karwar seven days before and after the date of phase of the new moon (a) 10-24 January 1980 (17-1-1980 phase of the new moon), (b) 9-23 February 1980 (16-2-1980 phase of the new moon and the day on which solar eclipse occurred), (c) 9-23 March 1980 (16-3-1980 phase of the new moon)

In the present study, we have observed that Karwar (100 per cent eclipse) has exhibited maximum changes in tidal activity compared to Bombay (90 per cent eclipse) and Kandla (50 per cent eclipse) during total solar eclipse. The centres of the three bodies, sun, moon and earth are almost along a straight line during total eclipse. Tidal friction in the Irish Sea during solar eclipse was much greater than previous days and attributed to the secular acceleration of the moon and the sun, where the acceleration of the moon might be accounted greater for changes in tidal friction than that of the sun (Dyson & Woolley, 1937). We, therefore, infer from the present study the possible association of changes in tidal activity during the total solar eclipse would be the nearness of the moon to the earth and the acceleration of the moon and the sun. The total gravitational attraction between the sun and the earth exceeds that between the moon and the earth by about 175 times. However, tides are caused by a difference in gravitational attraction on the near and far sides of a body, not by the total pull on it. Quantitatively, the creation of tides varies inversely as the cube of the distance. Thus the relatively short distance separating

the earth and the moon makes its tide-raising force more than double that of the distant sun. The size of the tides is also affected by the moon's varying distance from the earth. Tides are greatest when the distance is least (Ordway, 1966).

Also, the study of the tides during total solar eclipse is important for better understanding of the aerosols of sea origin and their role in cloud physics. Recently, Khemani *et al.* (1980) have observed an increase in the concentration of aerosols of sea origin by 27 per cent during the period of the total solar eclipse. Also, the giant size hygroscopic and non-hygroscopic particles increased by 43 and 23 per cent respectively during the period of totality. Such studies of possible association between tidal activity and aerosols of sea origin require further investigation.

#### ACKNOWLEDGEMENTS

The authors are grateful to Professor J. C. Bhattacharyya, Associate Professor, Indian Institute of Astrophysics, Bangalore, for his valuable suggestions. The authors express their sincere thanks to Dr A. S. R. Murty for the help received from him during the preparation of the paper.

#### REFERENCES

- Brier, G. W. (1974) Design and evaluation of weather modification experiments. In *Weather and Climate Modification* (Ed. W. N. Hess) John Wiley and Sons, New York.
- Dyson, F., and Woolley, R. V. D. R. (1937) *Eclipses of the Sun and Moon*. Clarendon Press, Oxford.
- Khemani, L. T., Momin, G. A., Naik, M. S., Ramachandra Murty, A. S., Mary Selvam, A., and Ramana Murty, Bh. V. (1980) *Proc Symp Atm Ozone*, Boulder, Colorado, USA, 4-9 August 1980.
- McLellan, H. J. (1965) *Elements of Physical Oceanography*. Pergamon Press, Oxford.
- Ordway, R. J. (1966) *Earth Sciences* van Nostrand Reinhold Company, New York.

Printed in India.

Atmospheric Boundary Layer

## ATMOSPHERIC BOUNDARY LAYER EXPERIMENT

R. NARASIMHA, A. PRABHU, K. NARAHARI RAO and C. R. PRASAD

*Indian Institute of Science, Bangalore-560 012, India*

*(Received 30 December 1981)*

A micrometeorological tower of 12m height, with five instrumented booms at different heights carrying wind, temperature and radiation sensors, was set up at Raichur to study the effects of the total solar eclipse on the atmospheric surface layer. The observed effects are rather complex, and at least three different time-scales can be distinguished in the variations of measured parameters. At a height of 1.3m above the surface, the mean and r.m.s. fluctuation of the air temperature start decreasing in a time of the order of minutes from the beginning of the eclipse. About  $\frac{1}{2}$ -1hr thereafter, velocity fluctuations tend to decrease, and, possibly as a consequence, the mean wind speed tends to increase. There is, however, an interestingly delayed response on a third time scale: about 3hr after the end of the eclipse, temperatures are lower than normal by about 3 °C at 1.3m above ground, and wind speeds are lower by an order of magnitude. Possible explanations for these phenomena are suggested.

**Keywords:** Micrometeorology; Local Winds; Effects of Total Solar Eclipse; Atmospheric Boundary Layer

### INTRODUCTION

THE motion of air in the atmosphere, and in particular also the atmospheric boundary layer, is maintained in the final analysis by solar radiation. The relatively sudden cut-off in the radiant energy flux that occurs during a solar eclipse may therefore be expected to result in unusual changes in atmospheric motion. Such changes should be particularly pronounced in the surface layer, as the temperature of the ground responds faster than the air above it to changes in the incident energy flux.

There is of course a well-known diurnal cycle in the atmospheric boundary layer (e.g., Wyngaard, 1973). The corresponding day-night transitions are however the result of a relatively gradual diminution in the solar insolation (we shall present below quantitative comparisons of the insolation on normal and eclipse days). Clouding of the skies does not produce conditions comparable to those during an eclipse either, because of complex reflection and scattering phenomena in the presence of clouds. In fact, a solar eclipse provides a unique opportunity for a relatively clean atmospheric boundary layer experiment, when the response of the layer to a sudden switching-off of its major driving force may be observed: a situation that is otherwise so difficult to produce in nature. The result of such observations should offer a severe test, if not a challenge, to numerical models of the atmospheric boundary layer.

In view of all this, and the general mystery that still surrounds the effects of a total solar eclipse, it is surprising how few detailed observations exist of micro-meteorological phenomena associated with such an eclipse. Indeed, the only attempt comparable to the present experiment was made by Antonia *et al.* (1979), who reported some interesting measurements made during the solar eclipse of 23 October 1976 experienced in parts of Australia. Unfortunately, at the site of these measurements the eclipse was only partial (80 per cent); furthermore, the final stages of this eclipse (which lasted roughly from 1500–1700hr) gradually merged into the normal sunset period, so that the effect of the eclipse could not be unambiguously isolated, especially as the results on the eclipse day were not compared with those on other days.

This paper reports preliminary results from an experiment conducted during the total solar eclipse of 16 February 1980 in India. A brief announcement of these results was made in December 1980 at the First Asian Congress of Fluid Mechanics (Prabhu *et al.*, 1980).

#### THE ECLIPSE AND THE SITE OF MEASUREMENTS

The path of totality in India covered a track of about 120km width, with line of maximum duration going from just south of Karwar on the West Coast to Puri on the East Coast (IMD, 1979). After considering several possible sites, it was decided to set up the experiment at Raichur, which was almost right on the line of maximum duration, would experience totality not too late in the afternoon, recorded reasonable winds on a normal day (IMD, 1979), and offered the required logistic support. Table I gives some details regarding the eclipse at this site. Fortunately, synoptic conditions during the week including the day of the eclipse were very favourable, with clear skies and no appreciable pressure gradients over most of the country, the experiment carried out was therefore gratifyingly clean.

TABLE I

*Total solar eclipse at Raichur*

Coordinates of Raichur	16°12'N	77°21'E
Elevation above mean sea level	400m	
Beginning of eclipse	14 25 13h*	
Beginning of totality	15 43 40hr	
Greatest phase	15 45 hr	
End of totality	15 46 22hr	
End of eclipse	16 55 hr	
Magnitude of eclipse**	1 04	

\* All times in Indian Standard Time

\*\*Fraction of the sun's diameter obscured by the moon at time of the greatest phase

A 40ft (12.2m) mast to carry the sensors was set up in an open field on the campus of the University of Agricultural Sciences at Raichur (Fig. 1). The nearest obstruction was a building about 200m away. The general direction of wind at the site during afternoons was towards the buildings, as indicated in the diagram.

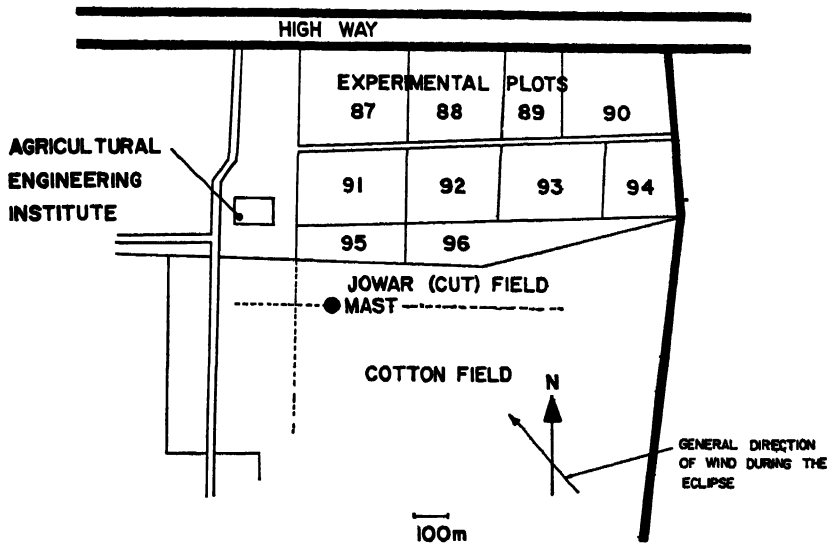


FIG 1. Location of instrumented mast in the campus of the University of Agricultural Sciences at Raichur. The mast was in an essentially flat open field, as the jowar crop had all been cut, the cotton plants were about 0.5 m tall.

#### EXPERIMENTAL SET-UP

A photograph of the mast with sensors is shown in Fig. 2. A total of five booms were attached to the mast, at levels and with sensors as shown in Table II. The Instrumentation System used for the experiment, and in particular the characteristics of the velocity and temperature sensors used, have been described by Prabhu *et al* (1981), the radiation sensors, which measured the energy flux in the visible spectrum, respectively across the horizontal and a surface normal to the direction of the Sun at totality, have been described by Prasad (1981). In general, the frequency response was always adequate to measure fluctuations upto at least 5 Hz. All five levels carried light cup anemometers (using ping pong ball rotors) to measure horizontal wind speed  $u$ ; the vertical velocity  $w$  was measured at four levels using a Gill-type propeller Vanes at three levels provided flow direction ( $\theta$ ) in the horizontal plane. The temperature  $T$  was measured at four levels using a platinum-wire thermometer.

TABLE II  
*Experimental set-up at Raichur*

Level	Sensor height above ground (m)	Sensors				
		Cup ( $u$ )	Vane ( $\theta$ )	Propeller ( $w$ )	Temperature ( $T$ )	Radiant flux ( $q$ )
$z_1$	1.3	X		X		X
$z_2$	2.25	X	X	X	X	
$z_3$	4.25	X	X			
$z_4$	6.8	X		X	X	
$z_5$	10.25	X	X	X	X	

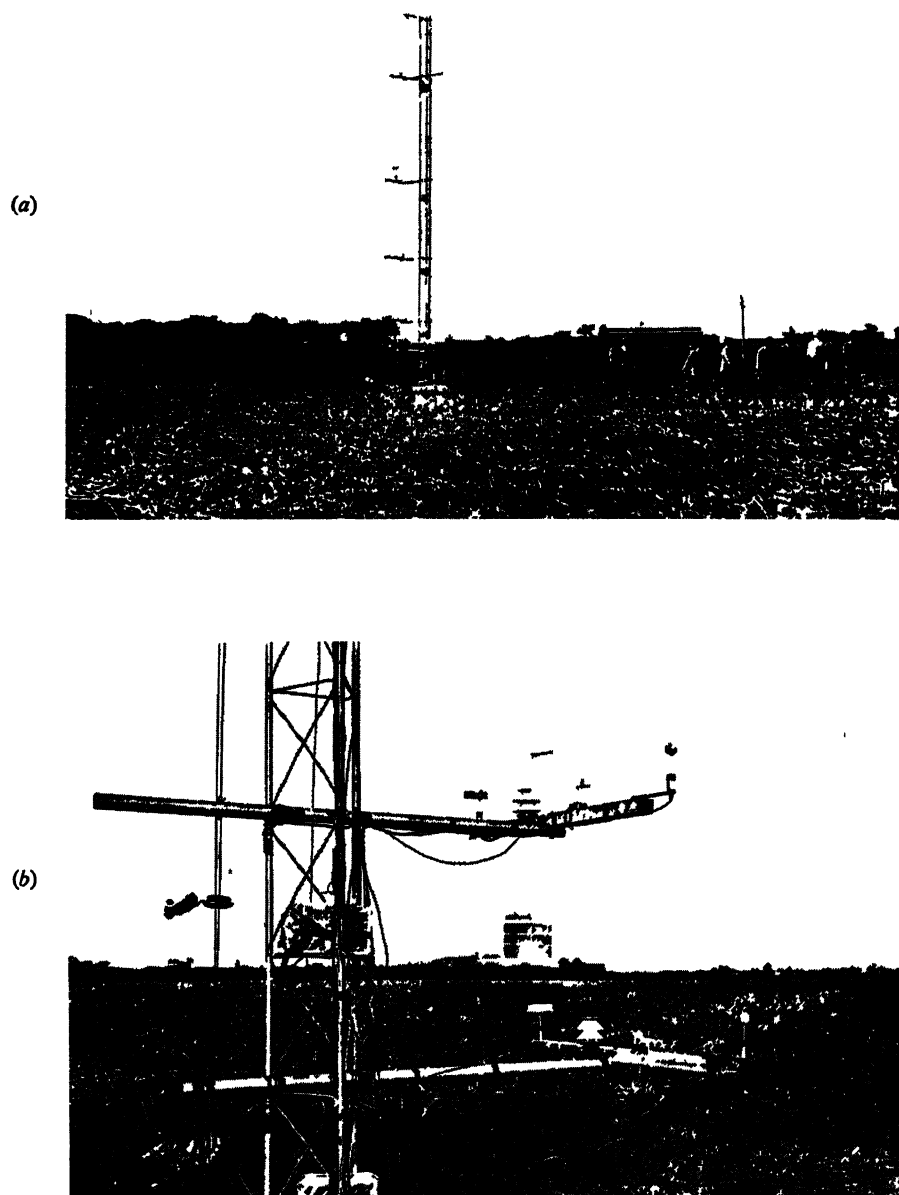


FIG 2 Photograph of (a) mast and (b) sensors. On the lowest boom, in (b), can be seen (from left to right) a Gill propeller, thermometer, radiation sensors and cup anemometer. The next level has a vane as well. At left, suspended on a string for traversing up and down, is a mini-radio-sonde, for measuring temperature.

The outputs from the sensors were digitized, multiplexed and transmitted through a twisted pair of wires to a receiving station, where the data were recorded on cassette tapes controlled by a PSI Z/80 microcomputer; data on each channel could also be monitored in analog or digital form. Fig. 3 is a block diagram of the data system; a complete description of the system is given by Prabhu *et al.* (1981), and Adiga *et al.* (1981). The surface supporting the microcomputer has been developed by Rao and Venkataraman (1981).

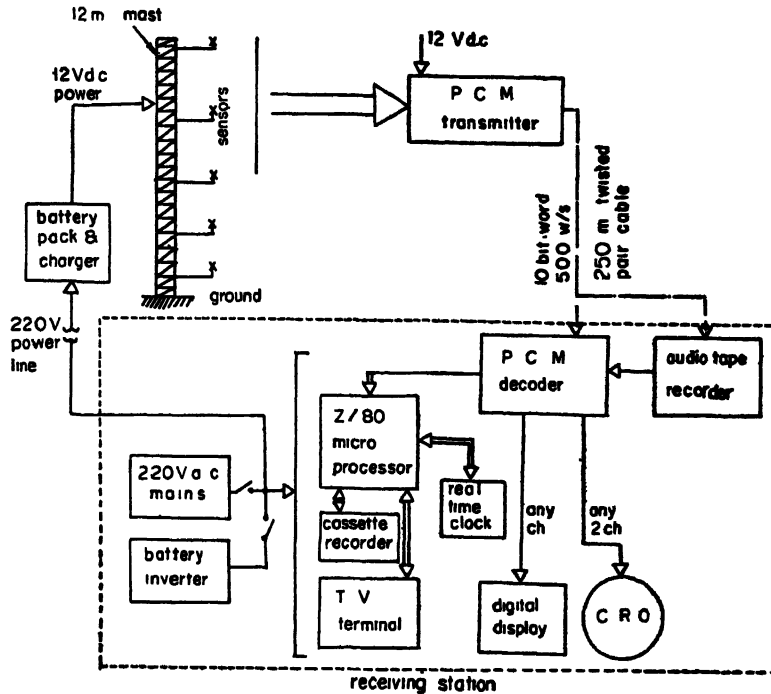


FIG 3 Block diagram of IISc Atmospheric Surface Layer Instrumentation System (Prabhu *et al.*, 1981). The data receiving station was set up in a shed about 250m away from the mast.

## RESULTS

### Radiation

Fig. 4 shows the solar flux on a horizontal surface, as deduced from the present measurements taken on 16 and 17 February. Data were taken almost continuously on the 16th, and at a limited number of periods on the 17th. It is clear from Fig. 4 that, except during the eclipse, the solar flux at any given time of day was the same on both days. Taking time-derivatives of the flux curves shown, it is found that during the eclipse, the rate at which solar insolation fell reached a maximum of about  $0.21 \text{ W/m}^2\text{s}$  at about 1500hr IST. The insolation increased after totality, reaching a maximum rate of about  $0.17 \text{ W/m}^2\text{s}$ . After the eclipse ended insolation decreased at the normal rate, reaching a maximum value of only  $0.07 \text{ W/m}^2\text{s}$ . It is therefore clear that the rate at which radiation was switched off during the eclipse at Raichur was three times higher than during normal sunset.

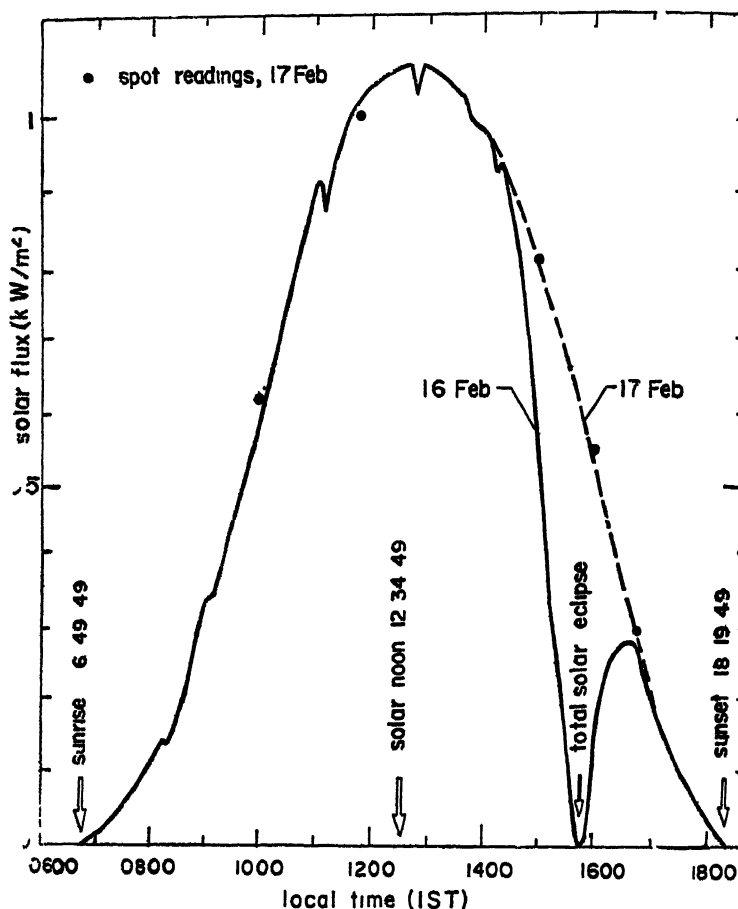


FIG. 4. Solar flux on a horizontal surface at Raichur. On the day of the eclipse (16 February), measurements were recorded almost continuously, and are shown by the full line. On the next day (17 February) measurements were recorded at less frequent intervals, and are shown by filled circles and the dashed line

### Temperature

Fig. 5 shows the temperature variation on 16 and 17 February at a height  $z = z_2 = 2.25\text{m}$ , above ground, corresponding to the second lowest instrumented level on the mast. These temperatures are 5-min. averages; this averaging period corresponds to a third of the length of the cassette tape used for recording data. Fig. 5 also shows the r.m.s. value of the temperature fluctuations, averaged over the same period.

It is seen from data for the 17th that the general diurnal temperature variation indicates a peak of about  $34^\circ\text{C}$  around 1530–1600hr; thereafter, the temperature drops at a rate of about  $1^\circ\text{C/hr}$ . On the day of the eclipse, the temperature increases as on a normal day up to the time of first contact (1425hr), shortly thereafter, the temperature starts falling, at a rate of about  $2^\circ\text{C/hr}$ , reaches a minimum of  $30.5^\circ\text{C}$



at approximately the time of totality, and starts increasing again. By the end of the eclipse the temperature has almost reached the normal value.

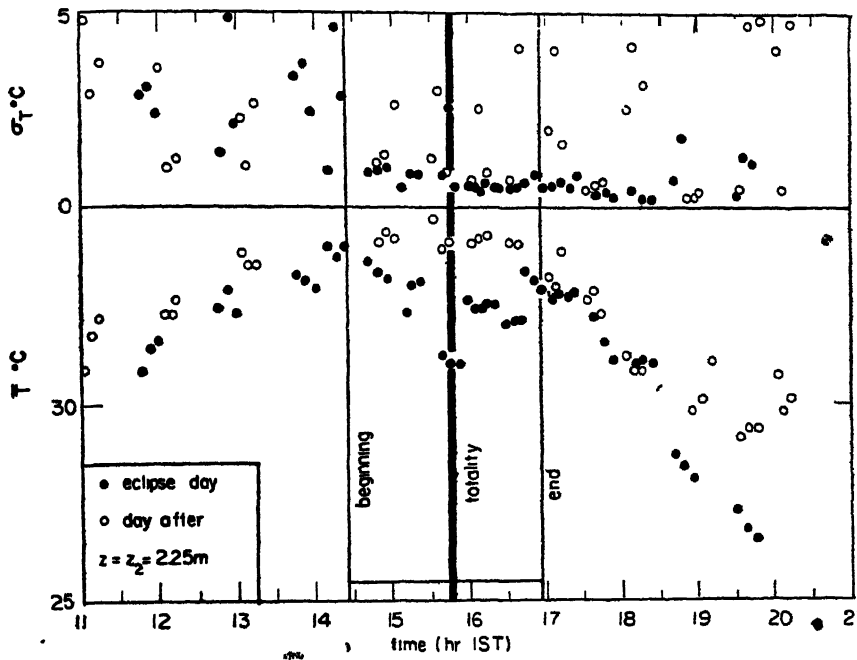


FIG 5. Mean and standard deviation of the air temperature at the level  $z = z_2 = 225\text{m}$   $\bar{T}_2 = \sigma_T$  at  $z_2$ . Averaging period is 5min

Interestingly, the temperature starts decreasing steeply (about  $2.5^\circ\text{C/hr}$ ) after fourth contact (normal sunset rates are seen to be about  $1.5^\circ\text{C/hr}$  from Fig. 5). At 2000hr, three hours after fourth contact, the temperature is lower than normal (for that time of day) by about  $3^\circ\text{C}$

It is seen that, while the air temperature at this level starts responding to the eclipse in a time of the order of minutes, there is also a delayed response a few hours after the eclipse is over.

The r.m.s. value of the temperature fluctuations,  $\sigma_T$ , decreased rapidly after first contact, and remains low thereafter, till about 2000hr

#### Wind Velocity

Fig. 6 shows  $7\frac{1}{2}$ -min averages of the horizontal wind speed, at  $z = 1025\text{m}$ . There are appreciable variations in these average with time of day, but it may be noted that around 1200hr and 2030hr, observed wind speeds are about the same on all three days (15, 16 and 17 February). This agreement is reassuring, and enables us to assert that the other changes observed must be attributed to the eclipse.

These changes are intriguing, and do not appear to have been noticed before. The most striking feature is the spectacular drop in wind speed beginning around 1800hr on eclipse day, compared to its value on the previous or succeeding day. We again see the delayed response mentioned in the previous section

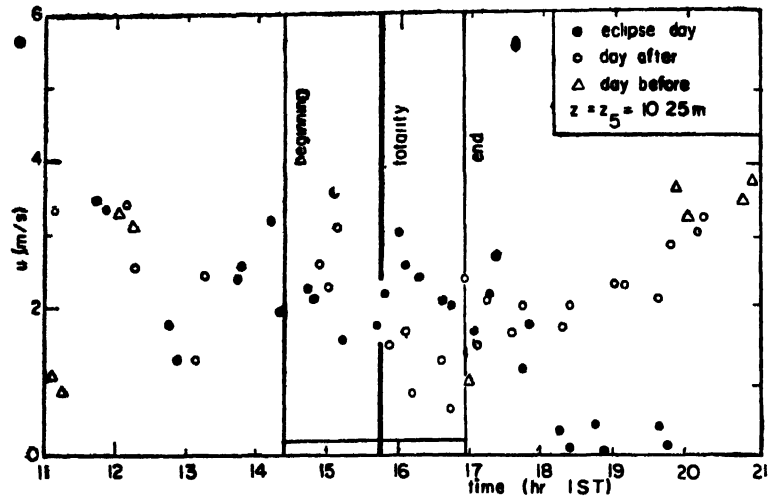


FIG. 6. Mean horizontal wind speed at the top of the mast,  $z=z_5=10.25\text{m}$ .  $\bar{U}_5=\bar{u}_m$  at  $z_5$ . Averaging period is 7.5min.

Fig. 7 shows the r.m.s. value of the horizontal speed fluctuations,  $\sigma_u$ . In general, the 7½-min. average value for  $\sigma_u$  itself shows strong fluctuations on a normal day; on the day of the eclipse, the value of  $\sigma_u$  itself as well as its range of variation come down after the beginning of the eclipse, particularly after totality. This suppression of turbulence must be a result of the stabilization of the surface layer following the drop in temperature discussed under 'Temperature'.

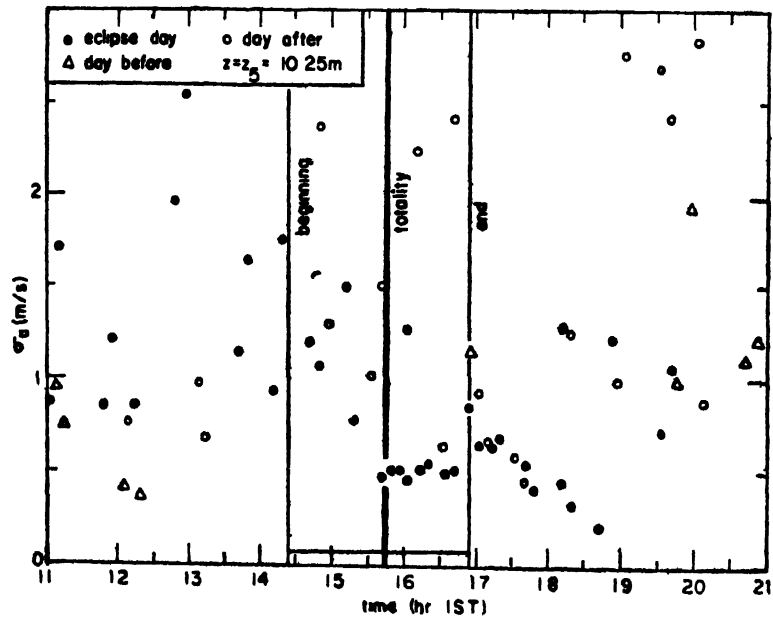


FIG. 7. Standard deviation of horizontal wind speed at the top of the mast,  $z=z_5=10.25\text{m}$ .  $\hat{U}_5=\sigma_u$  at  $z_5$ . Averaging period 7.5min.]

Fig. 8 shows the mean wind speeds at certain times of day on the three days: the averaging period has now been increased to 15 to 30 min, in order to suppress the masking effect of fluctuations at lower periods. (It was not possible to adopt a uniform averaging period because of the different frequencies at which data were recorded on the three days.) At 1200hr, 1515hr and 2400hr, there is essentially no change in wind speeds; at 1600hr and 1700hr, between third and fourth contact, the mean wind changes; slightly higher on eclipse day; at 2000hr, as already mentioned, the wind speed is lower by almost an order of magnitude.

Note that, on non-eclipse days,  $\sigma_u$  reaches values of the order of the mean velocity itself ( $\sim 2-3\text{m/s}$ ) around 2000hr. This is characteristic of a transition in the flow regime, of the type discussed by Lenschow *et al.* (1979). It was found that, at the site of measurement, the wind velocities that are seen to reach values of  $3.4\text{m/s}$  in Fig. 8 remain comparably high during much of the night. We suspect that these winds are of katabatic origin, and can be attributed to the presence of low hills  $3\text{km}$  east of the site of measurement. This suspicion is reinforced by a change in the direction of wind, beginning around 2000hr, to easterly. The switch to the katabatic regime could well be marked by the high values of  $\sigma_u$  noted above.

It appears therefore that the eclipse is responsible for suppression of the onset of katabatic winds at the site; as these winds had picked up by about midnight (Fig. 8) their onset is apparently delayed by 3-4hr because of the eclipse

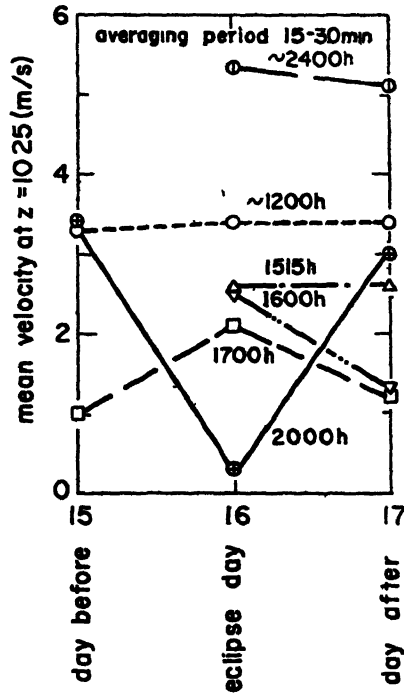


FIG. 8. Mean wind velocity at  $z_s = 10.25\text{m}$  on eclipse day (16th) and on the previous and succeeding days, at selected times of day

### Clouds

A curious visual observation of clouds must be reported here. As has already been mentioned, the skies were very clear at Raichur all through the experiment, but there were a few wisps of small fair weather clouds. One of these, of angular dimension slightly larger than the sun itself and located at about the same elevation as the sun but  $15^\circ$  to the north in azimuth, dissipated around 1530hr, but started reforming around 1537hr (about 6min. before totality). This intriguing qualitative observation suggests that there was an appreciable subsidence about 15min. before totality, but that rising motion resumed less than 10min. later. This implies that there are significant changes in boundary layer processes even well away from the surface when the radiation has been diminished for a period of about an hour; but these changes are not monotonic in time, at least at cloud level.

## DISCUSSION

It is clear from the present results that a total solar eclipse has significant micro-meteorological effects. The most spectacular one that was observed at Raichur was that the wind velocity, compared to its value at the same time of day on other days, showed a remarkable drop (by an order of magnitude), beginning about three hours after the end of the eclipse (i.e., after 4th contact) and extending over a further period of 3–4 hr. It is likely that this drop in wind is related to the drop in temperature observed at about the same time; and that this in turn is a response to the net diminution in radiation (amounting to about 15 per cent) on the day of the eclipse. The observed time lag of a few hours is comparable to the value that characterizes the lag between *maximum* temperature and *maximum* insolation on a normal day, and is probably determined chiefly by the thermal conductivity of the soil.

This delayed-action response to the eclipse can be (and we believe has been) missed if attention is confined to what happens during the eclipse!

The disappearance and reappearance of small clouds is also very intriguing. A possible explanation may be based on the realization that the eclipse results in a moving cold spot (i.e., shadow) on the surface of the earth. This cold spot may be expected to set up a circulation like a land-sea breeze, because of the temperature contrast across the band of totality. Such a circulation would normally lead to subsidence over the region experiencing totality, and would explain the observed disappearance of clouds. Their *reappearance*, however, must imply a change in the sign of the vertical velocity. Such a change is possible if the circulation is double-celled. It is interesting here to note that in some studies of sea breeze on a circular island [Neumann & Mahrer (1974); *see also* Pearson (1980)] it is found that on a 'large' island (of 102 km diameter) a double-cell structure was predicted. In this circulation, the flow is downward over the centre of the island *and* over the sea, but is upward in a 20 km ring toward the edge of the island (No such double cell was found on a smaller island of 52 km diameter.) Such double-cell circulation could explain our observations regarding clouds during the solar eclipse.

We have earlier suggested that the drop in wind velocities that followed the eclipse could have been due to the suppression of local katabatic winds. This raises a question about whether the phenomenon is restricted to sites like the one chosen for the present experiment, or whether similar significant effects on the wind were observed widely: if the latter is true, it is possible that the temperature contrasts caused by the eclipse affect the circulation on a larger scale. This cannot be ruled out, as there was a significant diminution in total insolation over scales of order  $10^3$  km on the day of the eclipse.

The observations from the present experiment are summarized in Table III. It is seen that we can distinguish the response of the atmospheric surface layer on at least three time scales. Within minutes of the beginning of the eclipse, both mean air temperature and its fluctuation intensity near the surface start dropping. On a time scale of half to one hour, the turbulent velocity fluctuations become lower, the increase in mean wind speed noticed after totality may be the result of this decrease in turbulent stresses Fig. 9. The third time scale, of a few hours, is of the order of the thermal lag characteristic of the soil as a conducting medium, a drop in air tem-

TABLE III

*Summary of micro-meteorological observations of the effects of the eclipse at Raichur*

$t=0$	1st contact (1425hr)	Mean and fluctuating temperature at $z \sim 1.3\text{m}$ start falling
$+ \frac{1}{2}\text{hr}$		Velocity fluctuations start falling
$+ 1\text{hr}$		Small wisp of fair weather cumulus disintegrates, to reform less than 7 min. later
$+ 1\text{hr } 20\text{min.}$	2nd contact (1543hr 40s)	Mean temperature $T_1$ at $z=1.3\text{m}$ drops by $\sim 3-4^\circ\text{C}$ , reaches minimum, starts rising; distribution stable
$+ 1\frac{1}{2}\text{hr}$	3rd contact (1546hr 22s)	Mean velocity slightly higher than on next day, fluctuations lower
$+ 2\frac{1}{2}\text{hr}$	4th contact (1655hr)	$T_1$ back to normal, reaches a second maximum, starts falling
$+ 5\frac{1}{2}\text{hr}$	(2000hr)	$T_1$ lower than on next day by $\sim 3^\circ\text{C}$ Mean velocity at $10.25\text{m} \sim 0.2\text{ m/s}$ , (vs. $3\text{m/s}$ on non-eclipse days) Fluctuations rising
$+ 9\frac{1}{2}\text{hr}$	(2440hr)	Mean velocity at $10.25\text{m} \sim 5-6\text{ m/s}$ , as on other days

perature is accompanied by a very pronounced decrease in wind velocities.

On the whole, a total solar eclipse has significant and unusual micro-meteorological effects, and these may in part explain the atmosphere of mystery that has always surrounded this spectacular visual phenomenon in the popular mind.

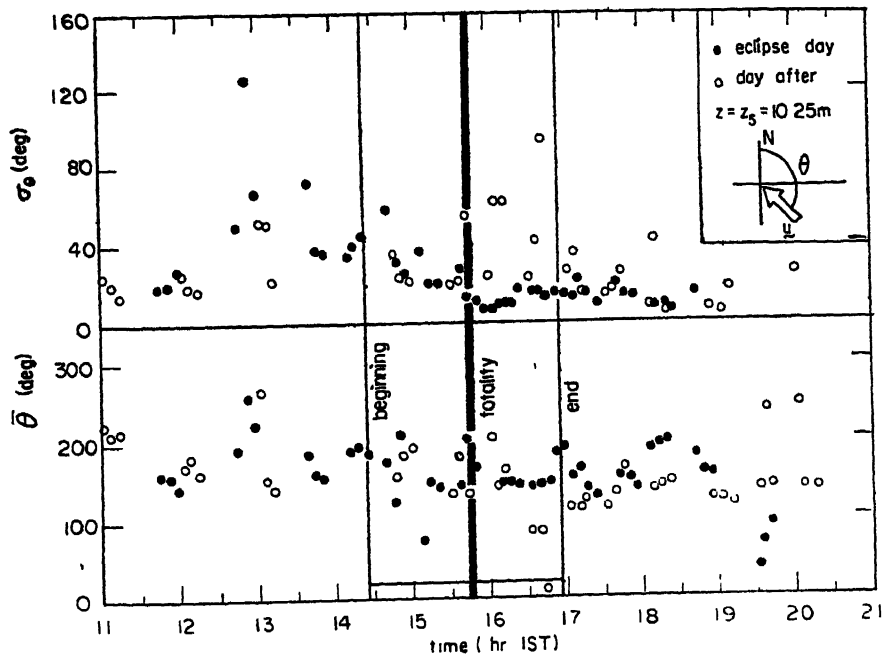


FIG 9 Mean and standard deviation of direction of horizontal wind vector. Note how the wind veers from generally south-easterly to easterly around 1950hr (IST)

The present discussion, of course, cannot provide final explanations, which would have to await more detailed observations at some future favourable eclipse, and more detailed calculations using available (or suitably modified) numerical models for the atmospheric boundary layer. It is hoped that such observations and calculations will be undertaken, if only to assure ourselves that the models in use are adequate to explain the puzzling behaviour observed during the eclipse

#### ACKNOWLEDGEMENTS

The Solar Eclipse Experiment reported in this paper was supported financially by the University Grants Commission and the Indian Space Research Organization, the Director of National Aeronautical Laboratory kindly loaned us the use of a van from his laboratory for the Experiment. We are indebted to Mr B. S. Adiga of NAL, Mr S. Ameenulla and Mr S. S. Padbidri for their technical assistance.

#### REFERENCES

- Adiga, B. S., Prabhu, A., and Syed Ameenulla (1981) The MOBLE Data Acquisition System *Rep 81 FM 4, Dept. Aero. Engg., IISc, Bangalore*
- Antonia, R. A., Chambers, A. J., Phong-Anant, D., Rajagopalan, S., and Sreenivasan, K. R. (1979) *J. geophys. Res.*, **84**, 1689-1692
- India Meteorological Department (1979) *Total Solar Eclipse of 16 February 1980* IMD, New Delhi.
- Lenschow, D. H., Stankov, B. B., Mahrt, L. (1979) The rapid morning boundary-layer transition *J. atm. Sci.*, **36**, 2108-2124.
- Neumann, J., and Mahrer, Y. (1974) A theoretical study of the sea and land breeze of circular islands. *J. atm. Sci.*, **31**, 2027-2039.
- Pearson, R. A. (1980) Local flows. In. *Atmospheric Planetary Boundary Layer Physics* (Ed A Longhetto). Elsevier.
- Prabhu, A., Narahan Rao, K., and Narasimha, R. (1980) The effect of a total solar eclipse on the atmospheric surface layer, A03 *Proc. First Asian Congress of Fluid Mechanics*, December, Bangalore.
- Prabhu, A., Narahan Rao, K., Adiga, B. S., Nagabhushana, S., and Syed Ameenulla (1981) An atmospheric surface layer instrumentation system *Rep 81 FM 2, Dept. Aero. Engg., IISc, Bangalore*.
- Prasad, C. R. (1981) A sensor for measuring solar radiation *Rep. Mech. Engg. Dept., IISc, Bangalore*.
- Rao, K. N., and Venkataraman, P. S. (1981) Software for analysis of atmospheric boundary layer data *Rep. 81 FM 5, Dept. Aero. Engg., IISc, Bangalore*
- Wyngaard, J. C. (1973) On surface-layer turbulence. In *Workshop on Micro-Meteorology* (Ed. D. A. Haugen), 101-149. Am. Met. Soc., Boston, Mass.

Printed in India

**Atmospheric Boundary Layer**

**DYNAMICS OF THE ATMOSPHERIC BOUNDARY LAYER DURING  
THE 1980 TOTAL SOLAR ECLIPSE**

**S. SETHU RAMAN**

*Atmospheric Sciences Division, Brookhaven National Laboratory, Upton,  
New York 11973, U.S.A.*

*(Received 19 September 1981)*

An atmospheric boundary layer experiment was conducted at Raichur, India to study the variations in the surface shear stress, heat flux and the meteorological processes that take place during a total solar eclipse. Interesting results were observed regarding the evolution of the planetary boundary layer. Changes in atmospheric stability from unstable to stable to unstable were observed during different phases of the eclipse. Downward propagation of negative heat flux associated with decreasing scales of convective eddies was also observed during the eclipse.

**Keywords:** Atmospheric Boundary Layer; Scales of Turbulence; Solar Eclipse; Air pollution

**INTRODUCTION**

DURING daytime conditions, temperature of the air near the earth's surface is warmer than the air above it. This causes vertical accelerations and displacement of air parcels resulting in thermally induced atmospheric turbulence. As the sun sets, temperature of the ground decreases rapidly below that of the adjoining air. Layers of air close to ground get cooler and become denser. Maintenance of turbulence implies that air is being moved continuously in the vertical plane. If the fall of density with height is large, lifting denser air against gravity at the expense of energy from mean motion is rather difficult. Turbulent motion thus becomes small. Again at the next sunrise, incoming radiation raises the temperature of the ground and that of the lowest air layers resulting in less dense air below. This causes the tendency for vertical motion to be enhanced increasing turbulence. Diurnal evolution of the atmospheric boundary layer thus depends on the variations in the incoming and outgoing radiation. An ideal experiment to study the dynamics and the evolution of the atmospheric boundary layer would be to study the variations in the boundary layer characteristics by decreasing and then increasing the solar radiation abruptly. A total solar eclipse provides the right setting for such an experiment due to near-instantaneous cut-off of the solar radiation. A patch of clouds will not satisfy the required conditions due to complex reflection and scattering of light. Constantly changing angles of the sun to the earth surface makes it difficult to interpret the results that may be obtained from an evening or an early morning experiment. A survey of the literature indicates no study of the atmospheric boundary layer during a total solar

eclipse. A partial solar eclipse (80 per cent) was studied by Antonia *et al.* (1979) in Australia. The final stages of the eclipse coincided with the normal sunset thus making it difficult to isolate the effect of the eclipse from the diurnal changes.

The atmospheric boundary layer experiment described in this paper was conducted during a total solar eclipse that occurred on 16 February 1980 over the southern part of India. Width of the shadow was about 125 km. The experiment was conducted at Raichur, India ( $16^{\circ}22'N$ ,  $77^{\circ}21'E$ ). The first contact or partial solar eclipse at Raichur began at 1425 IST (Indian Standard Time), total eclipse (second contact) occurred at 1543 IST and lasted 2 minutes and 42 seconds; the eclipse ended (fourth contact) as a partial one at 1655 IST. Normal sunset was at 1820 IST on the day of the eclipse. Thus a well-developed convective atmospheric boundary layer was present before the first contact and there was sufficient time to warm the surface of the earth after the third contact (around 1545 IST).

One of the atmospheric variables that can influence the boundary layer characteristics significantly is the synoptic condition which is a largescale feature that

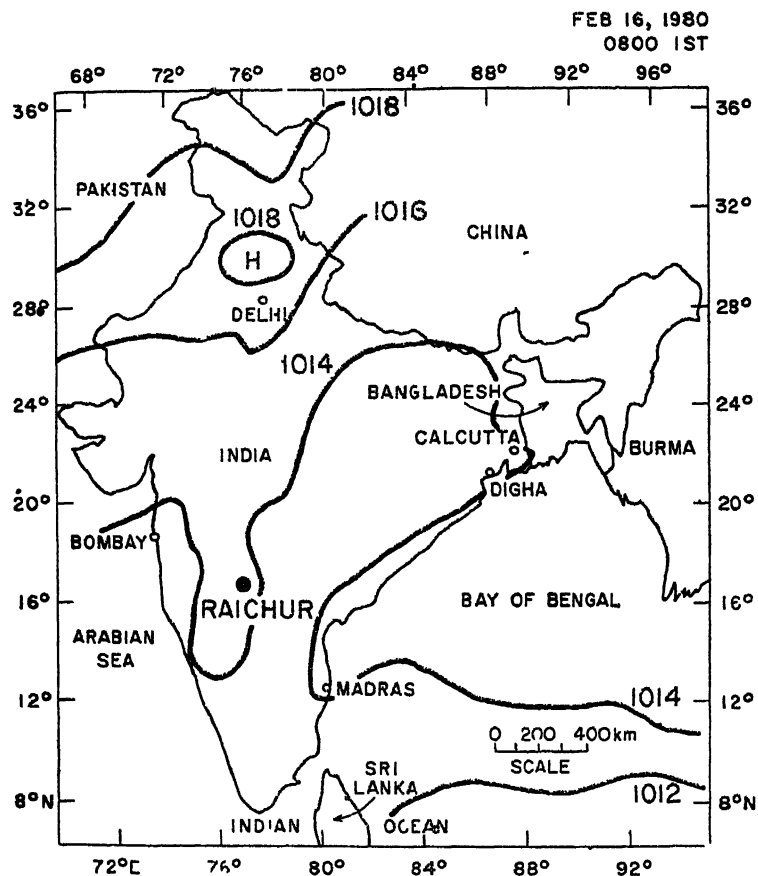


FIG 1 Surface weather chart at 0800 IST on 16 February 1980 indicating weak pressure gradients. This is typical of the synoptic conditions that existed over the southern part of India during the week of the eclipse



modifies the day-to-day flows. The conditions experienced at Raichur were ideal for a boundary layer experiment of this type due to near-constant fair weather conditions that prevailed. This was expected over most of the interior southern part of India due to the month of February being in a non-monsoon period of the year. Synoptic surface weather map for 16 February 1980 shown in Fig 1 indicates weak pressure gradients over southern India. Surface maps for 15, 17, and 18 February also indicated the same feature. Thus significant free convection was present, providing an opportunity to study the evolution of the boundary layer during the eclipse.

### MEASUREMENTS

The boundary layer experiment described in this paper was conducted in collaboration with the Indian Institute of Science (I. I. Sc), Bangalore. Our objective was to study the dynamics of the boundary layer through the observations of the variations in the surface fluxes of momentum and heat and the thermal structure. The measurement system had the following components: (a) a 12m micro-meteorological tower (Fig 2) with instruments to measure longitudinal, lateral, and vertical velocity and temperature fluctuations at four levels, mean winds at five levels and mean temperatures at two levels; (b) a mini-radiosonde system to measure mean temperature profiles to a height of 2 to 3km—it used slowly rising balloons with battery-operated instrument packages that measured and telemetered pressure and temperature information to a microprocessor-controlled ground station, (c) pilot balloon sounding system to measure wind speed and direction in the planetary boundary layer, and (d) a pyranometer to measure direct solar radiation.

The surface layer fluxes discussed in this paper were measured at a height of 6.8m above the surface. The measurements at this height consisted of longitudinal velocity fluctuations with a small three-cup anemometer (developed by the I. I. Sc), vertical velocity fluctuations by a propeller-type anemometer (of R. M. Young Inc) and the temperature fluctuations with a resistance element thermometer (of A. I. R. Inc). The distance constants of the cup anemometer, propeller anemometer, and the temperature sensor are estimated to be about 0.5m, 0.8m and 0.1m, respectively. The analog data were recorded with a magnetic recorder, digitized at the rate of eight per second and analyzed with a digital computer. The fluxes were computed with the eddy-correlation technique by correlating the longitudinal and vertical velocity fluctuations for momentum and the vertical velocity and the temperature fluctuations for sensible heat. The observations were made for two days prior to and one day after the day of the eclipse to determine the characteristics of the atmospheric boundary layer that may be site-dependent.

### DISCUSSION OF RESULTS

#### *Dynamics of the Surface Layer*

Variation of the thermal stability of the atmospheric boundary layer during the eclipse due to changes in the solar radiation is of major interest. Changes in the stability in turn affect the turbulence characteristics of the boundary layer. Mean potential temperatures measured at 2m and 12m successively by the same sensor

eclipse. A partial solar eclipse (80 per cent) was studied by Antonia *et al.* (1979) in Australia. The final stages of the eclipse coincided with the normal sunset thus making it difficult to isolate the effect of the eclipse from the diurnal changes.

The atmospheric boundary layer experiment described in this paper was conducted during a total solar eclipse that occurred on 16 February 1980 over the southern part of India. Width of the shadow was about 125 km. The experiment was conducted at Raichur, India ( $16^{\circ}22'N$ ,  $77^{\circ}21'E$ ). The first contact or partial solar eclipse at Raichur began at 1425 IST (Indian Standard Time), total eclipse (second contact) occurred at 1543 IST and lasted 2 minutes and 42 seconds; the eclipse ended (fourth contact) as a partial one at 1655 IST. Normal sunset was at 1820 IST on the day of the eclipse. Thus a well-developed convective atmospheric boundary layer was present before the first contact and there was sufficient time to warm the surface of the earth after the third contact (around 1545 IST).

One of the atmospheric variables that can influence the boundary layer characteristics significantly is the synoptic condition which is a largescale feature that

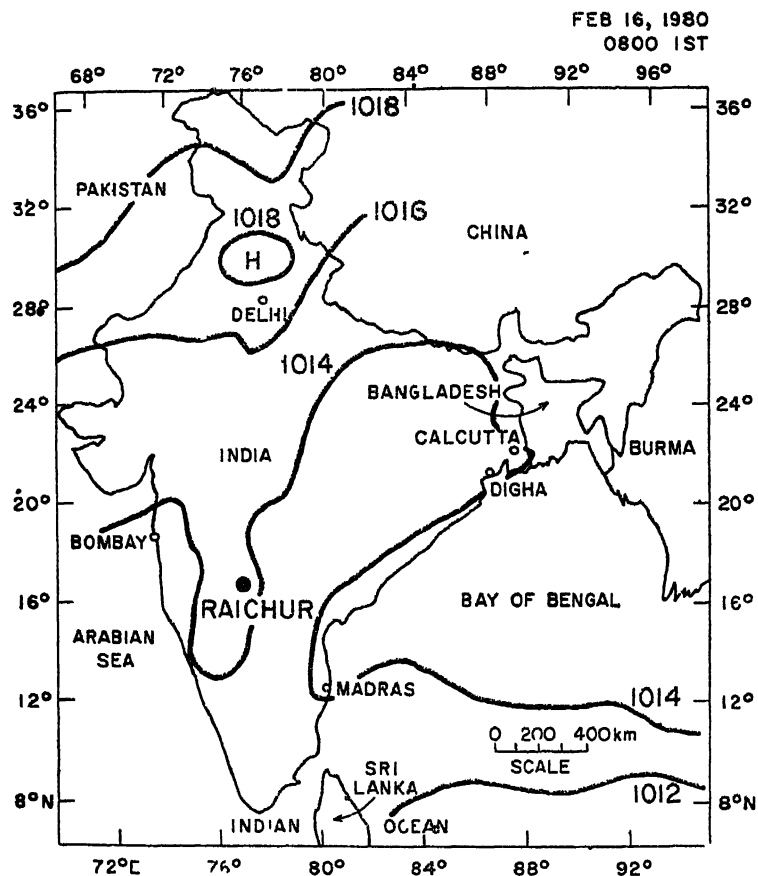


FIG 1 Surface weather chart at 0800 IST on 16 February 1980 indicating weak pressure gradients. This is typical of the synoptic conditions that existed over the southern part of India during the week of the eclipse

TABLE I  
Temperature lapse rates in the surface layer

Time (IST)	Potential Temperature (C)		Phase of the eclipse
	2m	12m	
1055	29.4	28.4	First contact
1430	32.7	32.1	
1503	33.7	32.8	
1551	31.5	31.6	3 minutes after 3rd contact
1606	32.0	31.9	10 minutes before 4th contact
1635	33.5	33.4	
1900	28.9	30.8	

where  $\rho$  is the density of air,  $C_p$  is the specific heat of air at constant pressure, and  $\overline{W'T'}$  is the cross-covariance between the vertical velocity and temperature fluctuations. A positive  $H$  indicates upward heat flux found in a convective boundary layer and a negative  $H$  represents downward heat flux usually present during clear nights over land surface with stable atmospheric conditions. Fifteen minute average values of  $H$  estimated from the measurements of the fluctuations of vertical velocity and temperature during different phases of the eclipse on 16 February are shown in Fig. 3. The dotted line shows the variation observed at the site on 17 February, a non-eclipse day. Observations of heat flux indicate a sharp decrease immediately after the first contact, a gradual decrease for the next hour, a sharp decrease just before totality with a change in sign and a gradual increase to the normal non-

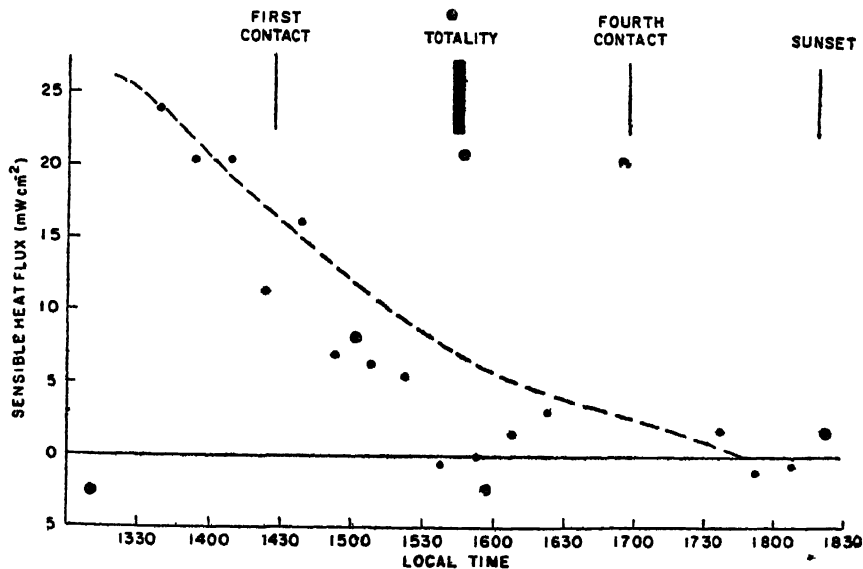


FIG 3 Variation of the sensible heat flux during different phases of the eclipse. Dotted line indicates the variation at the site a day after.

eclipse day values after the third contact. It is interesting to note that the negative sensible heat flux occurs even before the second contact. This is somewhat similar to the conditions that exist just before sunset with reduced radiation due to a low angle to the sun.

In order to be able to use the results obtained from this experiment to other sites and other heights in the surface layer, Monin-Obukhov length  $L$ , a similarity parameter and an index of stability was computed. This length is defined as

$$L = \frac{-u_*^3}{kgH/\rho C_p \theta} \quad \dots 2$$

where  $u_*$  is the friction velocity,  $k$  is Von Karman constant ( $\sim 0.4$ ), and  $\theta$  is the mean absolute potential temperature. On any given occasion  $L$  is constant, and all height-dependent quantities such as gradients, and transfer coefficients are expected to be, when suitably normalized, universal functions of  $z/L$ , where  $z$  is the height of measurement. In unstable conditions,  $L$  is negative, in stable conditions positive. With strong thermal effects as is usually found with large heat flux and weak wind,  $L$  is small. For near-neutral conditions,  $L$  becomes very large. Variation of  $z/L$  during different phases of the eclipse is shown in Fig. 4. Values of  $L$  varied from about  $-22\text{m}$  to  $+100\text{m}$ . Dotted line indicates the normal variation of  $z/L$  on a non-eclipse day. The similarity parameter varied in essentially the same way as the heat flux. Change in sign corresponding to stable condition occurred a few minutes before totality.

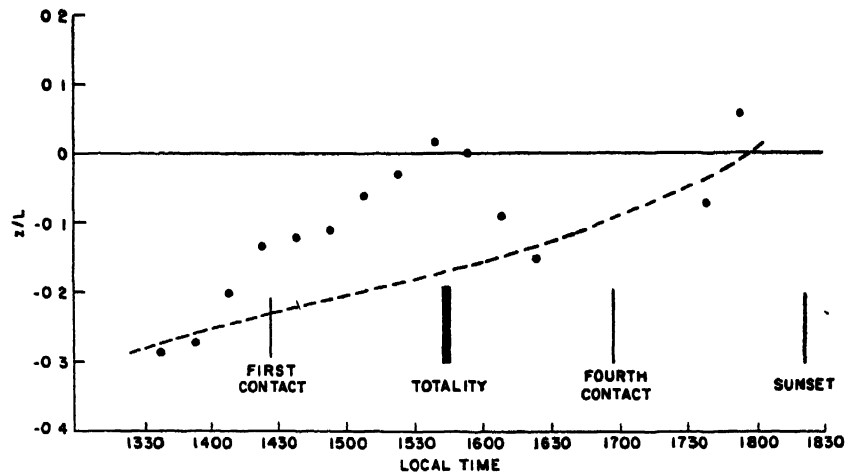


FIG. 4 Variation of the Monin-Obukhov similarity parameter,  $z/L$ , for different phases of the eclipse. Dotted line indicates the variation at the site a day after.

Variations of the friction velocity,  $u_*$ , and the standard deviation of the vertical velocity fluctuations,  $\sigma_w$ , on 16 February are given in Table II. The measurements were made at a height of 6.8m. The values of  $u_*$  and  $\sigma_w$  decreased by a factor of about four just before totality and increased again after the third contact. The response of the surface layer to solar radiation seems to be of the order of a few ( $< 10$ ) minutes.

TABLE II  
Variation of  $u_w$  and  $\sigma_w$  at 6.8m above the surface

Time (IST)	$\bar{u}$ (cm sec <sup>-1</sup> )	$\sigma_u$ (cm sec <sup>-1</sup> )	$\bar{u}$ (cm sec <sup>-1</sup> )	$\sigma_w$ (cm sec <sup>-1</sup> )	Phase of the eclipse
1330-1345	107	47	35	65	
1345-1400	129	43	35	70	
1400-1415	118	52	39	74	
1415-1430	115	51	41	71	First contact 1425 IST
1430-1445	105	49	43	57	
1445-1500	83	58	34	64	
1500-1515	76	61	41	43	
1515-1530	98	49	35	51	
1530-1545	122	9	10	14	Second contact 1543 IST
1545-1600	137	17	20	20	Thrd contact 1546 IST
1600-1615	130	19	22	28	
1615-1630	126	25	23	29	Fourth contact 1655 IST
1730-1745	85	28	25	34	
1745-1800	83	32	28	28	

### Dynamics of the Boundary Layer

Mean temperature profiles from the surface to a height of about 4km were measured at about 30-minute intervals in the afternoon on the day of the eclipse

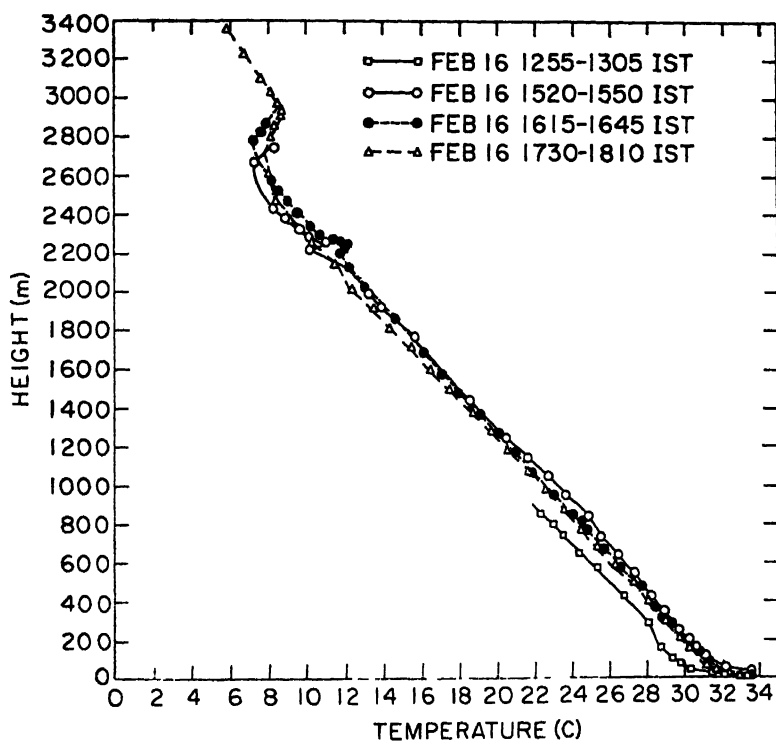


FIG. 5. Typical mean temperature profiles on a non-eclipse day. Note the super-adiabatic lapse rate near the surface and an elevated inversion at about 2500m.

(16 February), a day before and the day after (17 February). From the rate of rise of the balloon and from the response time of the temperature sensor, depth of resolution of the temperature measurements was estimated to be 10m. Mean temperature profiles measured on 17 February, a day after the eclipse, are shown in Fig 5. A well developed convective boundary layer or mixed layer appears to be present to a height of about 2500m capped with an inversion. Although the height of this mixed layer might vary from day to day within a few hundred meters, it is reasonable to expect that the basic structure would remain the same. The thermal structure during typical daytime conditions normally consists of a superadiabatic lapse rate near the surface ( $\sim$ tens of meters), dry adiabatic lapse rate for the remaining portion of the convective boundary layer ( $\sim$ hundreds of meters) and a stable layer on the top.

Mean temperature profiles to heights of about 3km measured with mmirradiosondes during the day of the eclipse are shown in Fig 6. Inversioncapped height of the convective mixed layer was observed to be about 2800m on 15, 16 and 17 February. On the day of the eclipse (16 February) temperature profiles showed a second inversion at about 2100m for two ascents, one immediately prior to totality and the other towards the end of the eclipse. Referring to Table I, the first period (1520–1550 IST) is approximately the same as the one during which stable atmospheric conditions existed in the surface layer. The inversion aloft (at about 2100m) persisted

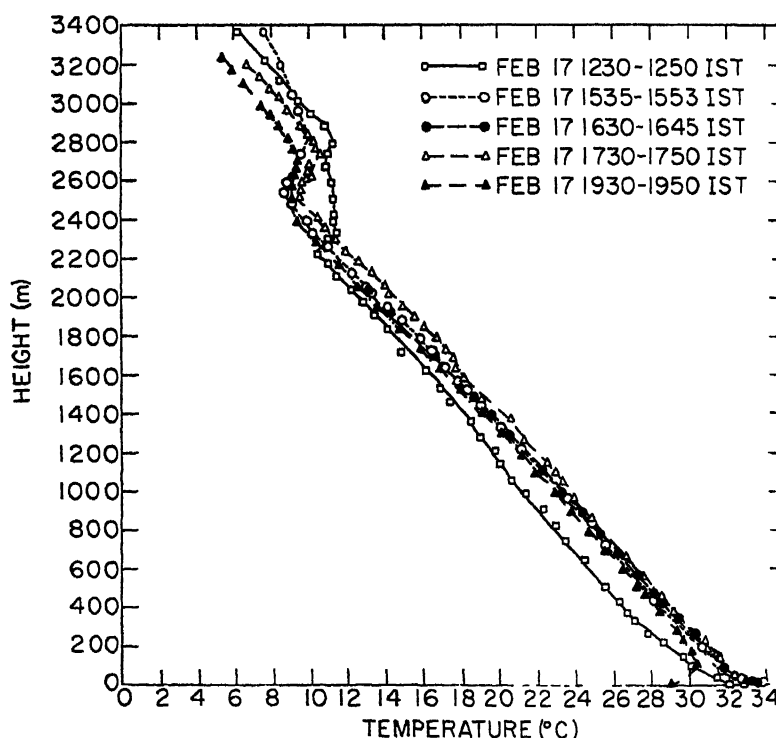


FIG 6 Mean temperature profiles on 16 February during different phases of the eclipse. Note the onset of a second inversion at 2200m (negative heat flux) and its disappearance after the fourth contact.

longer than the one near the surface. Caughey and Kaimal (1977) found that around sunset the transition to negative heat flux occurs first in the upper regions of the boundary layer propagating downward to the surface. Temperature profile taken after the fourth contact does not show the second inversion indicating build-up of the convective boundary layer once again. The second inversion appeared at about  $0.75h$  where  $h$  is the mixing height ( $\sim 2800\text{m}$ ). The downward propagation of negative heat flux is believed to be related to the reduction in the size of the convective eddies as the solar radiation is diminished.

### CONCLUSIONS

The boundary layer experiment conducted during the 1980 total solar eclipse revealed the changes in the atmospheric stability occurring during different phases of the eclipse. Boundary layer became stable just before totality. Convective processes were observed immediately after totality which suggests that the response of the boundary layer is of the order of a few ( $\sim 1-10$ ) minutes. The negative heat flux seems to propagate downwards when the solar radiation was diminished. This is probably related to the variations in the scales of the convective eddies due to changes in the solar radiation received by the earth surface. This feature is closely related to the evolution of the atmospheric boundary layer. Solar eclipse provides a unique opportunity to study the dynamics of this process and understand the physical processes involved in the diurnal evolution of the earth's planetary boundary layer.

### ACKNOWLEDGMENTS

Catherine Henderson helped in the data analysis. The author would like to thank Professor Narasimha and his colleagues of the Indian Institute of Science for their assistance in conducting this experiment. This research was supported by the Astronomy Centers Section of the U.S. National Science Foundation and the U.S. Department of Energy under contract DE-ACO2-76CH0016.

### REFERENCES

- Antonia, R. A., Chambers, A. J., Phong-Anant, D., Rajagopalan, S., and Sreenivasan, K. R. (1979) Response of atmospheric surface layer turbulence to a partial solar eclipse. *J. geophys. Res.*, **84**, 1689-1692.
- Caughey, S. J., and Kaimal, J. C. (1977) Vertical heat flux in the convective boundary layer. *Q. J. R. met. Soc.*, **103**, 811-815.

Printed in India.

Atmospheric Boundary Layer

## TOTAL SOLAR ECLIPSE OF 16 FEBRUARY 1980 AND THE VERTICAL PROFILES OF ATMOSPHERIC PARAMETERS IN THE LOWEST 200M

V. RAMESH BABU and J. S. SASTRY

*National Institute of Oceanography, Dona Paula-403004, Goa, India*

*(Received 21 September 1981)*

Vertical profiles of air temperature, wind and humidity at Raichur ( $16^{\circ}12'N$  &  $77^{\circ}21'E$ ) in the lowest 200m of the atmosphere are presented for the period 15-18 February 1980. The effect of the total solar eclipse, on 16 February 1980 is seen in the lowering of air temperature in the entire air column which persisted for a few hours.

**Keywords:** Atmospheric Boundary Layer; Vertical Profiles; Air Temperature; Tethersonde

### INTRODUCTION

In the present note, the authors present vertical profiles of air temperature, wind and humidity upto a height of 200m at Raichur ( $16^{\circ}12'N$  &  $77^{\circ}21'E$ ) during the period 15-18 February 1980. The shadow of the moon passed across the Indian peninsula and Raichur was selected as one of the places for carrying out several experiments. At this place, the eclipse began at 14h 25m IST on 16 February and ended at 16h 54.6m IST with second and third contacts observed at 15h 43.7m and 15h 46.4m IST respectively.

### METHODS OF OBSERVATION

The data presented in this report were obtained by means of a tethersonde system, (*Make:* A. I. R. Inc. U.S.A.) which consists of a blimp-shaped balloon, an airborne telemetry package housing dry and wet bulb thermistors, pressure, wind speed and direction sensors, a ground station and an electric winch (Fig. 1). The accuracies of sensors in tethersonde (*Model.* TS-1A-I) are  $\pm 0.5^{\circ}C$  for air temperatures,  $\pm 1mb$  for pressure,  $\pm 0.25m/s$  for wind speed and  $\pm 5^{\circ}$  for wind direction as per manufacturer's specifications. The ground station (*Model.* AS-2AR) resolves the signals from the airborne telemetry package into two channels—a time-multiplex one which contains information from all sensors and the other one which gives continuous information from one selected sensor only. Further, the ground station processes the data with the help of a built-in microcomputer and then sends to several output devices such as an internal strip-chart recorder, a visual display unit and a printer to print the displayed data.



Before taking each ascent, ground tests were carried out to check the dry bulb temperature and wet bulb depression, wind speed and direction and the differences were found to be within the accuracy limits of the system. The pressure sensor is adjusted to a convenient value which indicates ground pressure and as the instrument package moves upward, it gives the differential pressure which can be related to the height of the balloon. The visual display unit displays data frames which consist of data from all sensors at a rate of the one frame in 24secs.

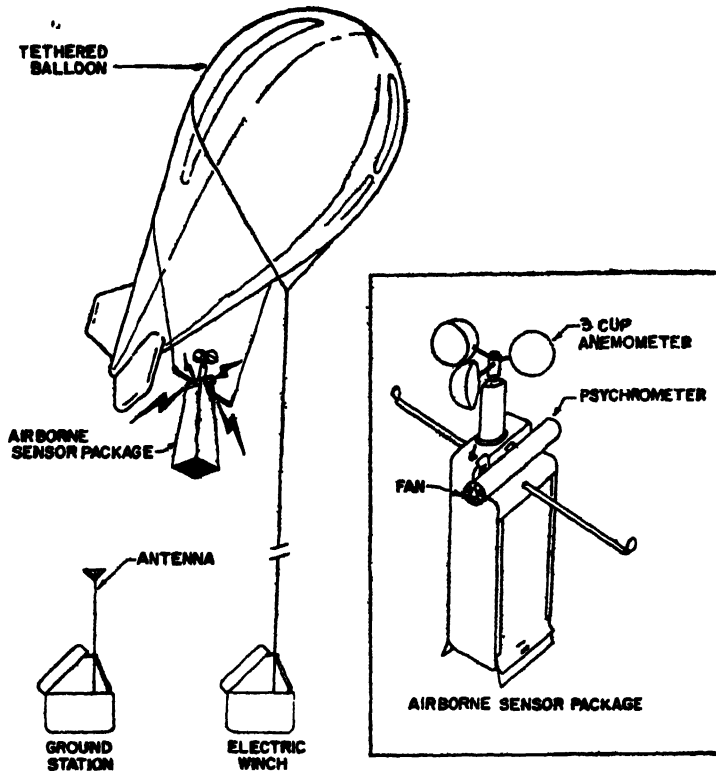


FIG 1 Tethersonde system.

## RESULTS

Figs. 2 to 4 show vertical profiles of dry bulb temperature, wind speed and direction and relative humidity upto a height of 200m. These observations were collected twice daily between 0700 and 0800hr in morning and between 1945 and 2115hr in night. Due to the operational problems it was not possible to take an ascent during the eclipse time. One of the important features observed in the vertical profiles is the lowering of air temperature, throughout the air column by about  $1.5^{\circ}\text{C}$  on 16 February 1980, a few hours after the eclipse (Fig. 2). This figure clearly reveals that above

50m, day-to-day temperature variations are relatively small in the morning on all days and also on 15th and 17th in the early night hours. However, a drop in temperature on the eclipse day appears to be clearly due to the effect of the solar eclipse. Soon after the totality the air temperature near the ground level showed a lowering of about 3 °C. As seen from Fig 2, the 17th morning profile shows no such deviation in the general pattern suggesting that a perturbation appears in the air temperature

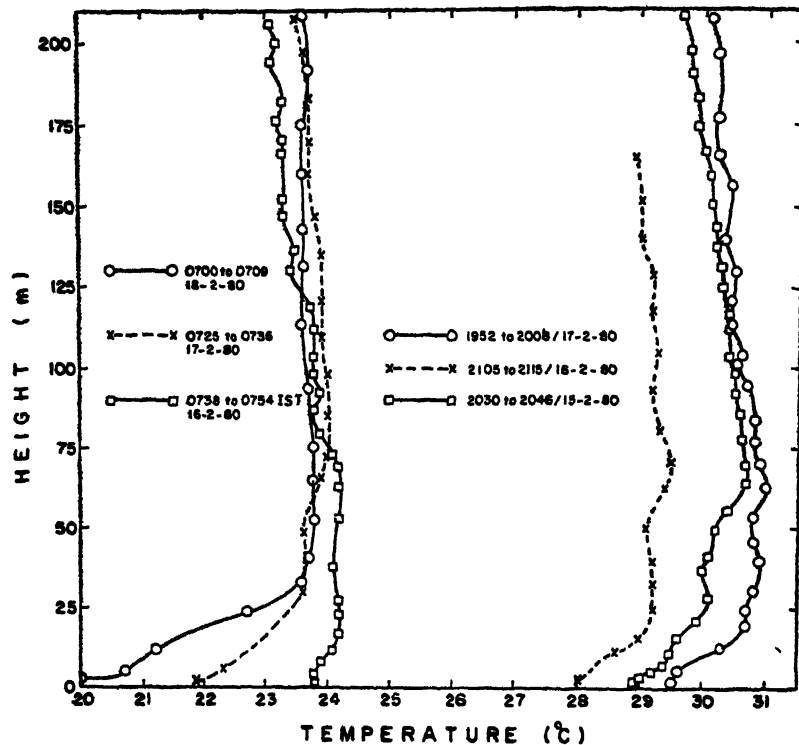


FIG. 2. Vertical air temperature profiles.

associated with the solar eclipse and its effect persists for a few hours only. In all, the profiles of the relative humidities in the air column are higher in the morning compared to those in the night (Fig 3). Fig. 3 shows a slight increase by about 5 per cent in relative humidity on the night of 16 February which may be partly due to the lowering of air temperature and partly due to the advection of moisture into the region. The 16th morning and evening ascents show relatively higher winds above 100m which are predominantly south-southeasterly whereas the winds observed on the other days are weak (Fig 4). Winds in the early hours of day are found to vary in both speed and direction from day-to-day compared to the winds in the early hours

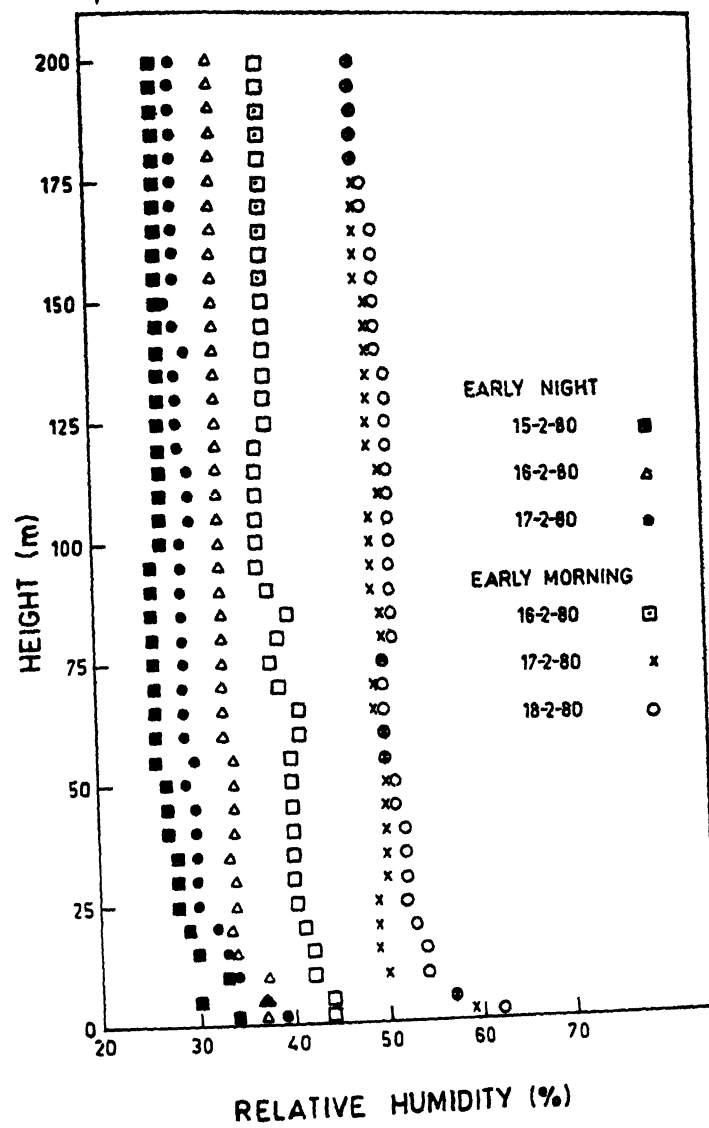


FIG 3 Relative humidity profiles.

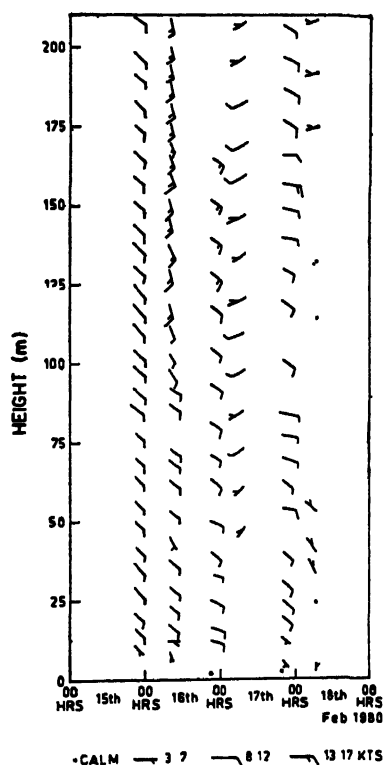


FIG. 4. Wind profiles.

of night. Fig 5 shows the variations in surface air temperature, the heights of ground level inversions and the average temperature gradients in the inversion layers. The morning temperature inversions are relatively strong and these are associated with weak winds. One may expect moisture convergence under stable conditions. This along with general cooling of the atmosphere in the early hours of the day account for higher relative humidity during morning ascents.

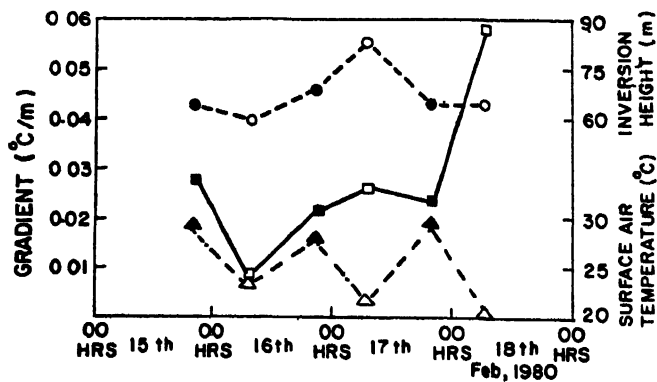


FIG. 5. Characteristics of ground level inversions (O---O height, □—□ gradient, Δ---Δ surface air temperature)

## ACKNOWLEDGEMENTS

The authors wish to express their thanks to Dr S. Z. Qasim, Director and Dr V. V. R. Varadachari, Deputy Director, National Institute of Oceanography, Goa for their interest. The authors further acknowledge the support of Dr (Miss) A. Mani, Raman Research Institute, Bangalore and the authorities of the Agricultural Engineering Institute, Raichur. This experiment was carried out with the cooperation of scientists from the India Meteorological Department and their help is appreciated.

## REFERENCES

- India Meteorological Department (1956) *Indian J. Met. Geophys.*, 7, 215.  
Jagannathan, P, Chacko, O, and Venkateswaran, S. P. (1957) *Indian J. Met. Geophys.*, 8, 93.

Printed in India.

**Meteorology**

**METEOROLOGICAL PARAMETERS NEAR THE EARTH'S SURFACE  
ALONG THE PATH OF TOTALITY DURING THE TOTAL  
SOLAR ECLIPSE OF 16 FEBRUARY 1980**

**S. K. DAS\*, S. M. KULSHRESTHA\*, KALIPADA CHATTERJEE\* and  
C. K. CHANDERASEKHARAN**

*Instruments Divisions, India Meteorological Department, New Delhi & Pune, India*

*(Received 18 July 1981)*

The instruments divisions at New Delhi and Pune of the India Meteorological Department planned an exhaustive programme to take frequent dry bulb and wet bulb temperature measurements at 14 observatories, including experimental stations at Gadag and Raichur, along the path of totality on 15, 16 and 17 February, 1980. The frequency of observations was stepped up between 1530 & 1630 IST when readings were taken at 2 minutes interval. These measurements taken at the 14 observatories have been analysed and presented in the paper. Soil surface temperatures recorded at Gadag on 15, 16 and 17 February 1980 have also been plotted, analysed and presented. Sunshine duration record of 16 February 1980 of Gadag has also been discussed in the paper.

**Keywords:** Dry bulb, Wet Bulb and Soil Surface Temperature; Path of Totality

**INTRODUCTION**

THE occurrence of total solar eclipse on 16 February 1980, provided a unique opportunity to the India Meteorological Department to set up suitable experiments for special observations and collection of meteorological data from soil surface to the upper atmosphere upto 30km. Earlier in the century, 2 solar eclipses had occurred over the Indian territory, one in 1914 and the other in 1954. But both these eclipses were observationally unimportant in India because the shadow of the moon hardly touched the Indian territory. The path of totality of the total solar eclipse of 16 February 1980 swept over the Indian peninsula from Karwar on the west coast to Puri on the East Coast. Fig 1 shows the path of totality and the locations of observatories and the special expedition sites which the Meteorological Department had organised for this total solar eclipse. The present paper deals with the variation of dry bulb, wet bulb and soil surface temperatures on 15, 16 and 17 February 1980 and the effect of the total solar eclipse on the air temperatures (D B. and W B). The sunshine duration record of 16 February 1980 over Gadag has also been presented in the paper.

**EXPERIMENTAL SET-UP**

In order to study the nature of variations and to clearly identify those effects that can be attributed to the total solar eclipse, it was considered necessary to take meteorological

---

\*IMD, New Delhi.

logical observations a day prior and a day after the eclipse, that is on 15 and 17 February 1980 in addition to the observations on 16 February 1980.

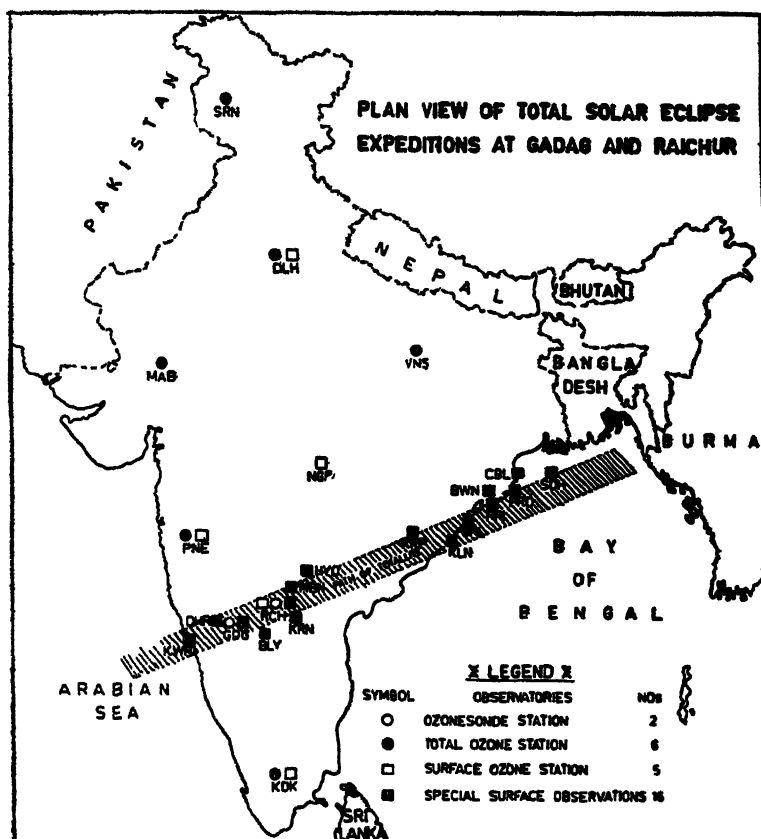


FIG 1.

The following two experimental stations were established in the belt of totality of the eclipse

1. Gadag (Lat  $15^{\circ}25'8''N$  Long  $75^{\circ}38.3'E$ )
2. Raichur (Lat  $16^{\circ}12'2''N$  Long  $77^{\circ}21'4'E$ )

These two sites had been chosen keeping in view the relatively high altitude of the sun at the time of eclipse, longer duration of totality, likelihood of clear sky during the month, absence of sea breeze, easy accessibility for transportation of instruments and necessary support facilities from New Delhi and Pune.

Dry bulb and wet bulb thermometers alongwith thermograph and hygrograph were housed in two Stevenson Screens in a special observatory enclosure in an open field of the J T College at Gadag. The Soil Surface thermometer was placed on ground surface of this special observatory enclosure. The sunshine recorder was however installed on the flat open terrace of the college building for un-obstructed sunshine

## DATA

*Dry Bulb and Wet Bulb Temperature Measurements*

Visual observations of dry bulb (D.B.) and wet bulb (W.B.) temperatures were taken at the expedition sites at Gadag (J.T. College) and Raichur, and at the following observatories of the India Meteorological Department along the path of totality during 15–17 February 1980. Karwar, Bellary, Mahbubnagar, Kurnool, Hyderabad, Kalngapatnam, Gopalpur, Puri, Bhubaneshwar, Paradip and Chandbali. On all the three days between 1530hr and 1630 IST, frequency of observations was stepped up, and observations were taken at 2 minutes interval to study any rapid variation of D.B. and W.B. temperatures. These data have been plotted in Figs 2a and 2b.

*Soil Surface Temperature Measurements (SST)*

SST observations were taken at the expedition site at Gadag by placing soil surface thermometer just on the surface of the soil of the special observatory and SST thermometer readings were taken on 15, 16 and 17 February 1980. During all these days, the frequency of observation was stepped up to 2 minutes interval between 1540 and 1630 IST to study any rapid variation of SST. These data along with eye readings of D.B. temperatures taken at the expedition site at Gadag (J.T. College) on 15, 16 and 17 February 1980 have been plotted in Fig. 2c.

*Duration of Sunshine*

Duration of sunshine was recorded by sunshine recorder on 15, 16 and 17 February 1980 at the expedition site at Gadag and the photocopy of the sunshine duration record on 16 February 1980 is given in Fig. 3.

## DISCUSSION

On an analysis of the D.B. and W.B. temperatures in Figs. 2a, b and 2c the following salient features are brought out

- (i) On 15 and 17 February 1980 variations of both D.B. and W.B. temperatures follow the normal expected trends modified at times by local weather conditions like cloudiness, etc
- (ii) Both the D.B. and W.B. temperatures taken on the day of totality at most of the stations and the expedition sites at Gadag and Raichur (Figs. 2a–b) showed a gradual fall and reached their minimum values at about 10 to 15 minutes after the totality over the respective stations.
- (iii) The D.B. temperature drop from Karwar to Chandbali was of the order of 1.5 °C to 3.0 °C which can be attributed to the effect of total solar eclipse
- (iv) Later, most of the stations showed the normal tendency of increase in D.B. and W.B. temperatures
- (v) Bhubaneshwar and Chandbali did not however exhibit similar type of variations in temperatures and this may be due to the fact that both the stations reported appreciable cloudiness over the stations during the eclipse and thereafter



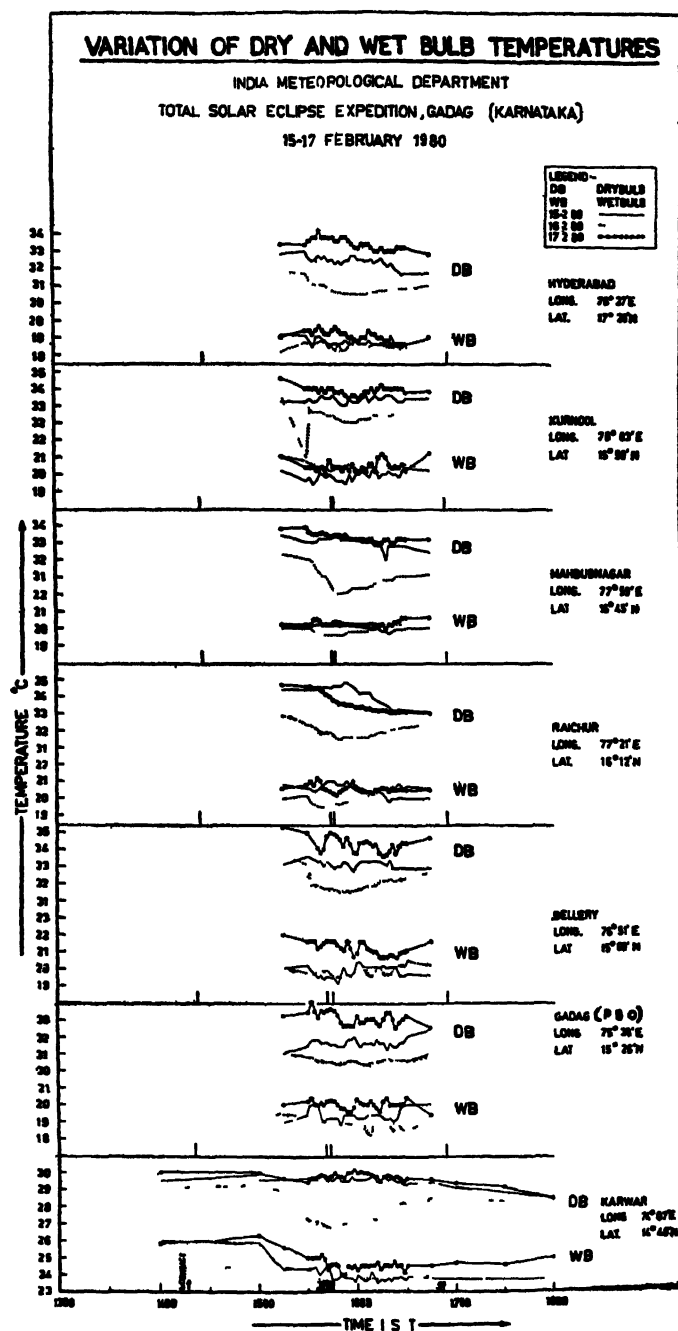


FIG 2a.

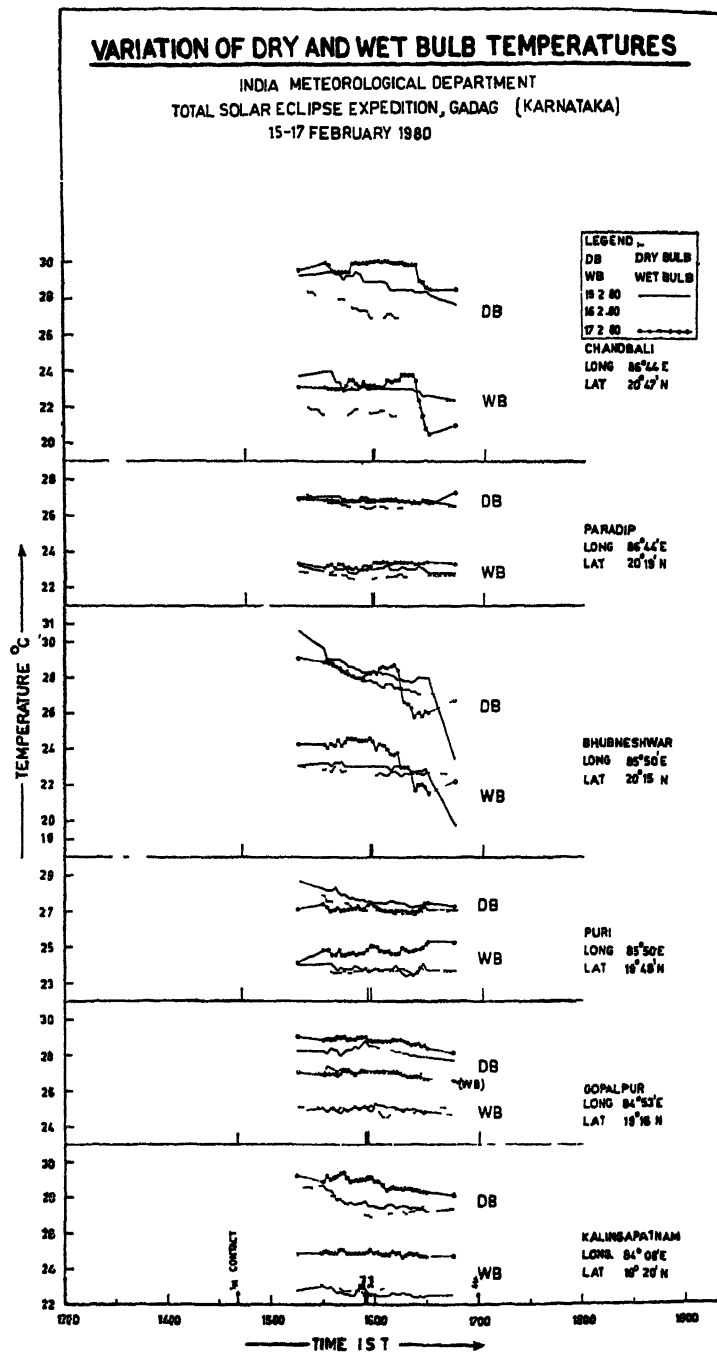


FIG. 2b

INDIA METEOROLOGICAL DEPARTMENT  
TOTAL SOLAR ECLIPSE EXPEDITION, GADAG (KARNATAKA)

16-FEB 1980 (TOTAL SOLAR ECLIPSE)  
VARIATION OF SOIL SURFACE TEMPERATURE AND AIR TEMPERATURE

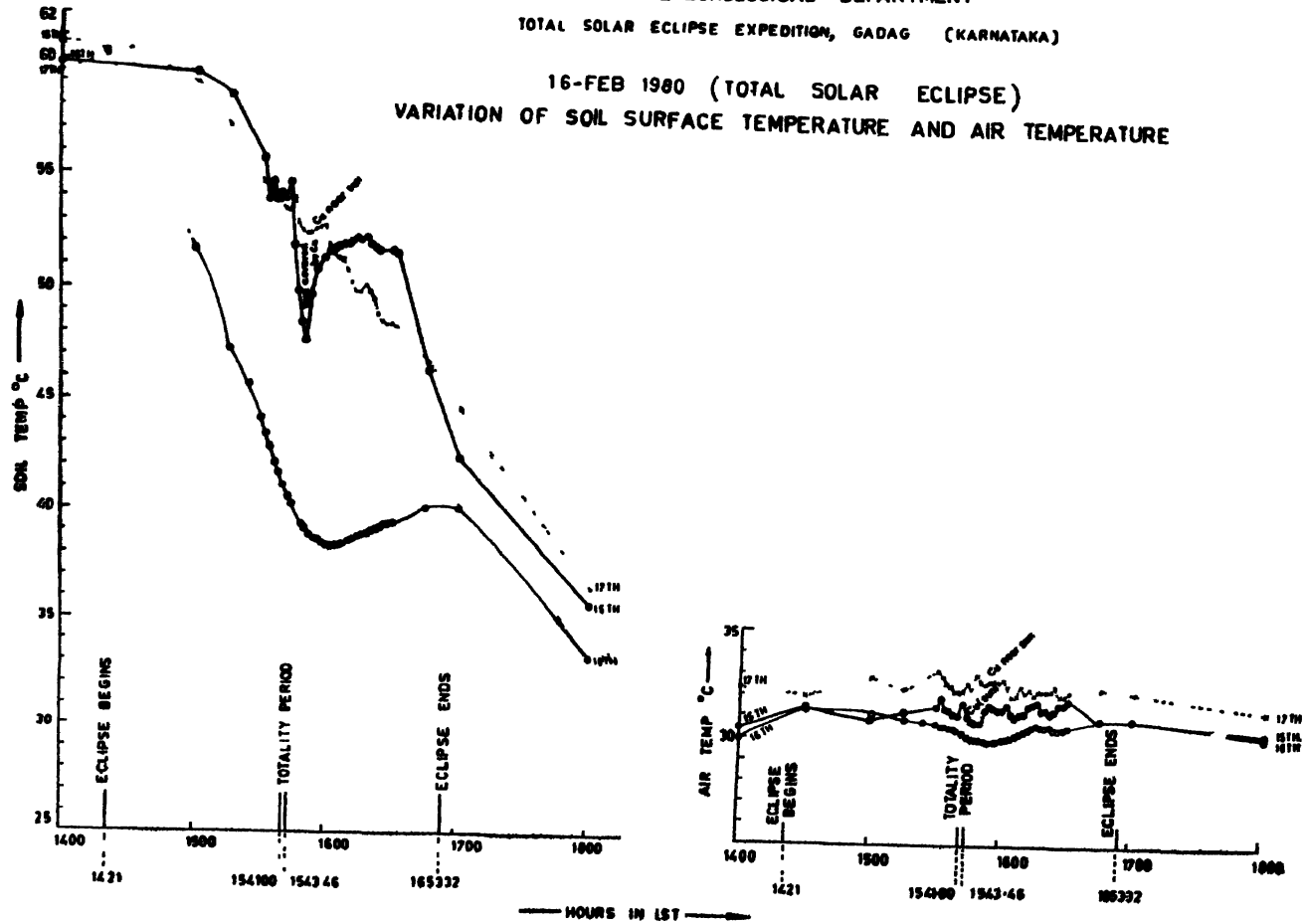


FIG. 2c.

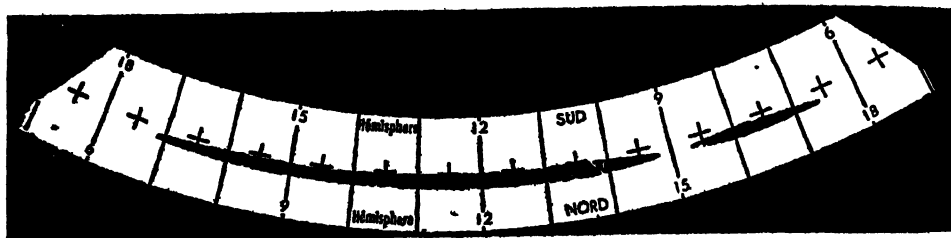


FIG. 3 Duration of sunshine on 16 February 1980.

#### *Soil Surface Temperature (SST)*

On an analysis of variations of soil surface temperature on the 15, 16 and 17 February, 1980 at the expedition site at Gadag (Fig 2c), the following salient features are brought out:

- (i) At 1400hr IST on the 15 and 17 February, 1980 the SSTs at Gadag were 59.7 °C and 59.4 °C respectively. On 16 February 1980 at the same hour, the SST was 60.7 °C. The solar eclipse started over Gadag at 1421 IST and the totality lasted between 15h41m to 15h43m 46s and the eclipse ended over Gadag at 16h53m. On an inspection of the variations of the SST, it is seen that the temperature at the surface of the soil dropped from 60.7 °C at 1400 IST to 38.4 °C at 1600 IST on the day of the eclipse, whereas on 15 and 17 February 1980, the SSTs at the expedition site were 51.7 °C and 51.9 °C respectively at 1600 IST.
- (ii) The rapid fall of soil surface temperature by 22.3 °C during the eclipse of 16 February 1980 at Gadag is considered to be a very significant feature of the effect of total solar eclipse on the temperature structure near the ground surface. This resulted in a very steep gradient of temperature near the ground surface and appeared to be responsible for the appearance of haze over the horizon. This also resulted in the development of inversion layer near the ground surface and damping of all convective processes in the earth's surface boundary layer.

#### *Duration of Sunshine*

Record of duration of sunshine as recorded by Sunshine Recorder on 15, 16 and 17 February 1980 at the expedition site at Gadag has been analysed. The duration of sunshine on 15 and 17 February 1980 showed the normal trend. The duration of sunshine record of 16 February 1980 (Fig. 3) shows that charring of sunshine chart due to sunshine through the spherical convex lens stopped at 1534 IST, that is about 7 minutes before the commencement of totality, and did not record any significant sunshine upto 1553 IST, that is about 9 minutes after the totality ended. During this 19 minute interval, the solar radiation was cut off or diminished to zero.

#### ACKNOWLEDGEMENT

The authors express their grateful thanks to Dr P. K. Das, F.N.A., Director-General Observatories for providing necessary facilities for conducting the experiments and for permission to communicate this paper.

Printed in India.

Meteorology

## SOLAR ECLIPSE OF 16 FEBRUARY, 1980—ITS EFFECT ON METEOROLOGICAL PARAMETERS

K. MOHANAKUMAR and S. DEVANARAYANAN

*Department of Physics, University of Kerala, Kariavattom, Trivandrum-695 581, India*

*(Received 7 March 1982)*

A study of the meteorological parameters across the penumbral and umbral regions during the 16 February 1980 Indian total solar eclipse has been made. Surface pressure, air temperature, soil surface temperature and relative humidity measurements have been made at Trivandrum, which had 80 per cent obscuration, Hyderabad which was almost in the totality path, Calcutta which had 96 per cent obscuration and New Delhi 65 per cent eclipse, are discussed. It was found that the surface pressure was not much affected by the eclipse. Air temperature measured at a height of 12m above the ground showed a decrease of 2.8 °C at Trivandrum, 3.1 °C in Calcutta and 2.7 °C at Hyderabad. Soil Surface temperature had fallen by 16.3 °C at Trivandrum on the eclipse day. An increase in relative humidity was found as the eclipse advanced, reaching the highest value just after the final contact.

**Keywords:** Meteorological Parameters; Surface Pressure; Soil Surface Temperature; Relative Humidity

### INTRODUCTION

THE conditions in the earth's atmosphere may be altered during a solar eclipse as a result of the transitory variation in the thermal equilibrium within the region of the moon's shadow. Chimonas and Hines (1970) proposed that the cooling of ozone in the upper atmosphere would trigger internal gravity waves which in turn interfere to produce a bow wave that could cause barometric pressure changes at ground level. Total solar eclipse observations of Anderson *et al.* (1972) on pressures showed that the pressure amplitudes were of two to three orders in excess to the ones predicted by Chimonas and Hines. Chimonas (1973), later suggested that the large pressure amplitudes could be due to the triggering of Lamb waves as a result of the cooling in the tropospheric water vapour. Depending on the water vapour beneath the penumbra, the Lamb wave could be of the order of magnitude enough to cause microbarometric pressure changes at the ground level regions of even 80 per cent eclipse. However, microbarometric pressure observations over Africa during the total solar eclipse in 1973 by Schödel *et al.* (1973) and Beckman and Celucas (1973) did not prove this. Similarly, Jones and Bogart (1975) showed that the variation seen in the microbarograph records from the region of totality were only due to the ongoing

pressure fluctuations. The existence of an eclipse generated gravity wave has not yet been verified.

Regarding the effect of eclipse on temperature, it is well established by Gringorten and Kantor (1965) that although the earth's surface temperature may fall by about  $6^{\circ}\text{C}$ , the air temperature response at one or two metres above this surface, is of the order of  $1$  to  $2^{\circ}\text{C}$  only. According to Chimonas (1973) any reasonable extrapolation of the near-surface temperature response into the lowest few hundred metres of the atmosphere shows that the associated change in atmospheric heat budget is a very small percentage of the solar energy screened by the earth's surface.

With this information in background we have undertaken a study of the effect of the solar eclipse of 16 February 1980 on meteorological parameters across the totality path in order to verify the earlier observations connected with solar eclipse.

### OBSERVATIONS

Special observations of surface pressure, air temperature, soil surface temperature and relative humidity during both the eclipse time and the previous day at the same time were taken every 10 minutes in Trivandrum ( $8^{\circ}\text{N}$ ,  $77^{\circ}\text{E}$ ), using a Fortin's barometer. To compare the results of Trivandrum, observations were also taken from Hyderabad ( $17^{\circ}\text{N}$ ,  $78^{\circ}\text{E}$ ), Calcutta ( $22^{\circ}\text{N}$ ,  $88^{\circ}\text{E}$ ) and New Delhi ( $28^{\circ}\text{N}$ ,  $77^{\circ}\text{E}$ ), using barographs, which were frequently corrected to the standard. Trivandrum experienced 80 per cent eclipse on the southern side of the totality path whereas Hyderabad fell very close to the totality path (i.e., 99 per cent obscuration), Calcutta which had 96 per cent obscuration and New Delhi 65 per cent eclipse lay on the northern part of the totality path. The eclipse began to manifest itself at Trivandrum in the afternoon, exactly at 1420hr (all times in IST, Indian Standard Time) reached the maximum at 1540hr and receded at 1650hr. During the eclipse time, the sky was clear above most of the stations, except New Delhi where the sky was overcast due to the presence of active westerly disturbance.

### RESULTS AND DISCUSSION

#### *a. Surface Pressure*

Fig 1 is a plot of the surface pressure recorded at the time of eclipse at Trivandrum, Hyderabad, Calcutta and New Delhi. The times of first contact, maximum phase and the fourth contact have been shown by letters A, B and C respectively for each place. At Trivandrum sharp decrease in the pressure began 20 minutes before the first contact and reached the lowest value of 1009.3 millibar, 40 minutes after the first contact. The surface pressure remained constant at this value for about an hour, the interval including the maximum phase. During the eclipse time the surface pressure was lower by about 0.3 millibar than that on the previous day (No observations of surface pressure were taken on 17 February, the next day). Soon after the fourth contact the surface pressure was found to be increasing.

On the other hand, for Hyderabad, Calcutta and New Delhi surface pressures during the eclipse time were not at all affected. In New Delhi, the pressure on the eclipse day and the next day have the same feature. Routine observations (not presen-

ted here) from Bangalore (92 per cent obscuration) and Cochin (82 per cent obscuration) did not indicate any pressure fluctuations. The surface pressure observations at these stations were taken only hourly, so it is difficult to detect any pressure waves generated due to the eclipse.

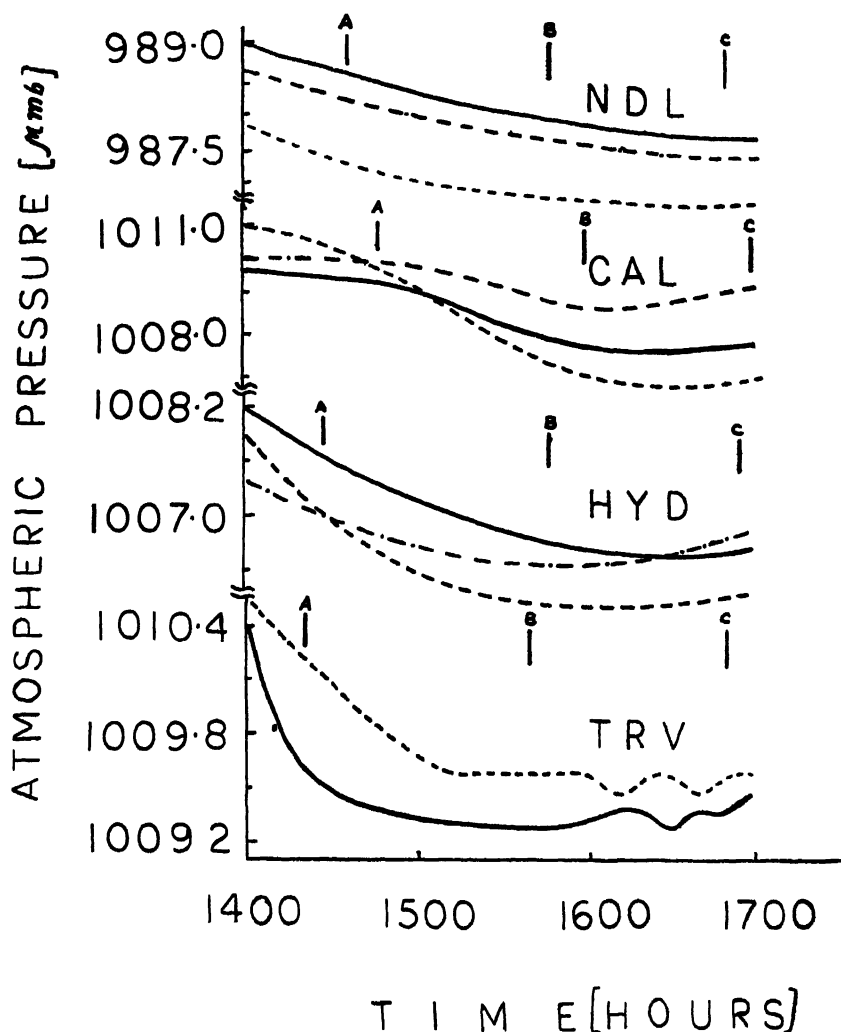


FIG 1 Variation of surface pressure during the eclipse at Trivandrum (TRV), Hyderabad (HYD), Calcutta (CAL) and New Delhi (NDL).  
(.. 15 February, — 16 February, ..... 17 February 1980)

The measurements of Anderson *et al* (1972) in the umbral region of the 1970 solar eclipse at Florida did show fluctuations which were attributed to eclipse-associated waves. On the other hand, Jones and Bogart (1975) who studied the African total solar eclipse of 1973, reported that the microbarograph records reflected only the ongoing pressure fluctuations. They commended on the similarity between their

observations and those of Anderson *et al.* (1972), and concluded that the pressure fluctuations seen in the 1970 event was probably not eclipse induced. Beckman and Clucas (1973) also observed null results. Schödel *et al.* (1973) reported that the naturally occurring wave-like fluctuations on ground based microbarographs were rare events that seemed to be associated with tropospheric events. In the present study we did not find any pressure fluctuations, and, therefore, conclude that the significant features seen at Trivandrum could not be due to the eclipse.

*b. Temperature*

The air temperature measurements made at a height of 1.2 metre above the ground at Trivandrum have been plotted in Fig. 2. The diurnal maximum of air

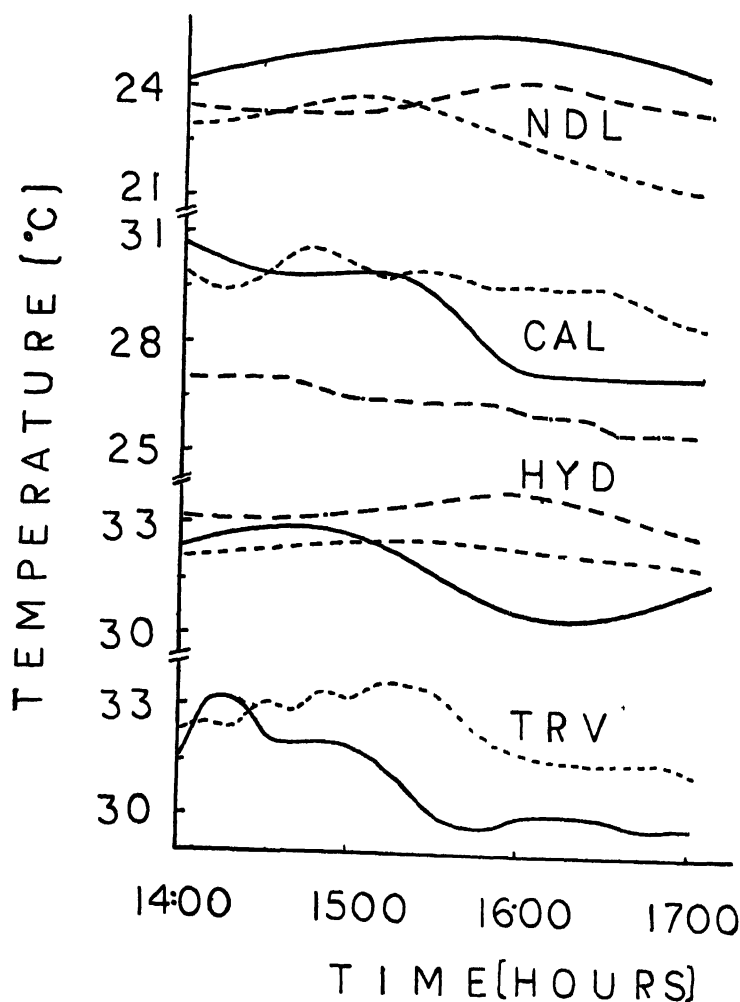


FIG. 2. Effect of the eclipse on air temperature at Trivandrum (TRV), Hyderabad (HYD), Calcutta (CAL) and New Delhi (NDL)

( . . 15 February, ——— 16 February, . . . 17 February 1980)



temperature usually is reached at about 1500hr. But on the eclipse day, the maximum temperature observed was at 1420hr, the time of first contact, after which the temperature was found to be ever decreasing. The lowest day temperature of  $29.8^{\circ}\text{C}$  was found during the time of maximum phase. This means a decrease of  $2.8^{\circ}\text{C}$  due to the eclipse from the day temperature on the previous day at the same time. At Hyderabad, the air temperature during the eclipse time showed a decrease of  $2.4^{\circ}\text{C}$  compared to the previous day and  $3.3^{\circ}\text{C}$  the next day (Fig. 2). The observations at Calcutta showed a decrease of  $3.1^{\circ}\text{C}$  compared to normal days. But the air temperature observations of New Delhi were not much affected by the eclipse, because of the presence of active western disturbances on these days.

Special observations of the soil surface temperature were taken only at two stations, viz, Trivandrum and Hyderabad, and these have been plotted in Fig. 3.

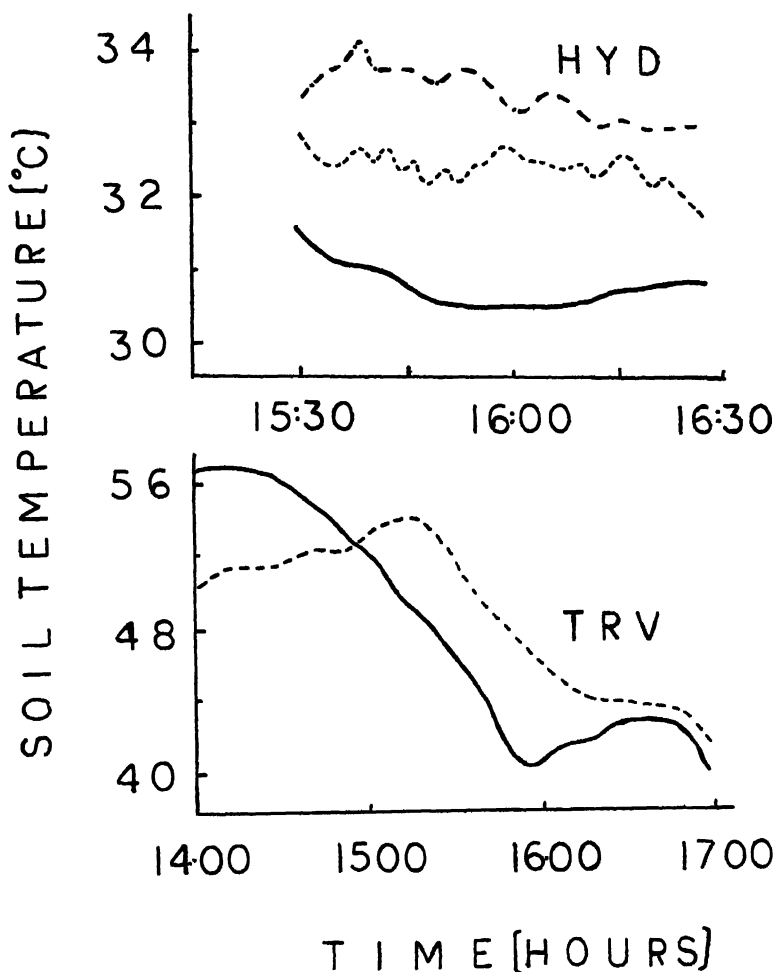


FIG 3. Soil surface temperature changes due to the eclipse at Trivandrum (TRV) and Hyderabad (HYD)  
 ( . . . 15 February, — 16 February, ... 17 February 1980)

At Trivandrum, the soil surface temperature data were taken every 10 minutes, whereas in Hyderabad, these were taken every 2 minutes. At Trivandrum, the diurnal maximum of surface temperature usually occurs around 1520hr (as seen in the diagram). But on the eclipse day the day-maximum was 56.9 °C since 1340hr whereas on the previous day it was only 51.2 °C at the same time, which means on the eclipse day the soil surface temperature was 5.7 °C warmer than the previous day. The day-maximum was constant for 40 minutes till the first contact. It reached the lower temperature of 40.6 °C at 1555hr i.e., 15 minutes after the maximum phase. The effect of the eclipse was thus to reduce the day-maximum to the minimum rapidly by 16.3 °C within 95 minutes. This difference of 16.3 °C on the eclipse day is definitely note-worthy compared to the corresponding 10.2 °C difference on the previous day. At Hyderabad which was very close to the totality path, there was also a considerable fall in the soil surface temperature due to the eclipse. The day-minimum reached soon after totality and it remained constant for about 15 minutes, having the same trend as in Trivandrum. Thereafter, the surface temperature was found to be increasing slowly.

The present study clearly shows that both air temperature and the soil surface temperature were lowered due to the eclipse; the effect on the latter was more pronounced. Data from other stations (not given here) also showed a decrease in air temperature of the order of 2 to 3.5 °C during the eclipse time. The air temperature within the lower atmosphere is related to the surface temperature. According to Gringorten and Kantor (1965) the decrease of soil surface temperature is about 4 to 5 times that of the air temperature. The maximum variation in temperature occurs near the earth's surface, because there is influence of ground temperature on air temperature. This explains the resultant cooling during the eclipse maximum when the insolation is cut off. During this time, the earth's surface cools rapidly than the overlying air, and hence the larger variation found closest to the earth's surface as reported here. These results are in agreement with those reported earlier (see, for example, Anderson *et al.*, 1972 for March 1970 solar eclipse and Anderson and Keefer, 1975 for 1973 solar eclipse).

#### c. *Relative Humidity*

The variation of relative humidity with time due to the eclipse at Trivandrum is given in Fig. 4. It is seen that the relative humidity was quite higher during the time of eclipse. Soon after the first contact till about 20 minutes, the relative humidity remained constant at 55 per cent, it abruptly changed to 65 per cent for the next 20 minutes. After the maximum phase, the relative humidity showed further increase, reaching the maximum of 67 per cent at the final contact. The data from Hyderabad, Calcutta and New Delhi also showed higher values during the eclipse time than on normal days (Fig. 4).

#### CONCLUSIONS

The surface pressure was not at all affected by the total solar eclipse of 16 February 1980, in most of the stations. The air temperature may register a drop of 2–3.5 °C, on account of the total solar eclipse. But the eclipse did certainly influence the soil

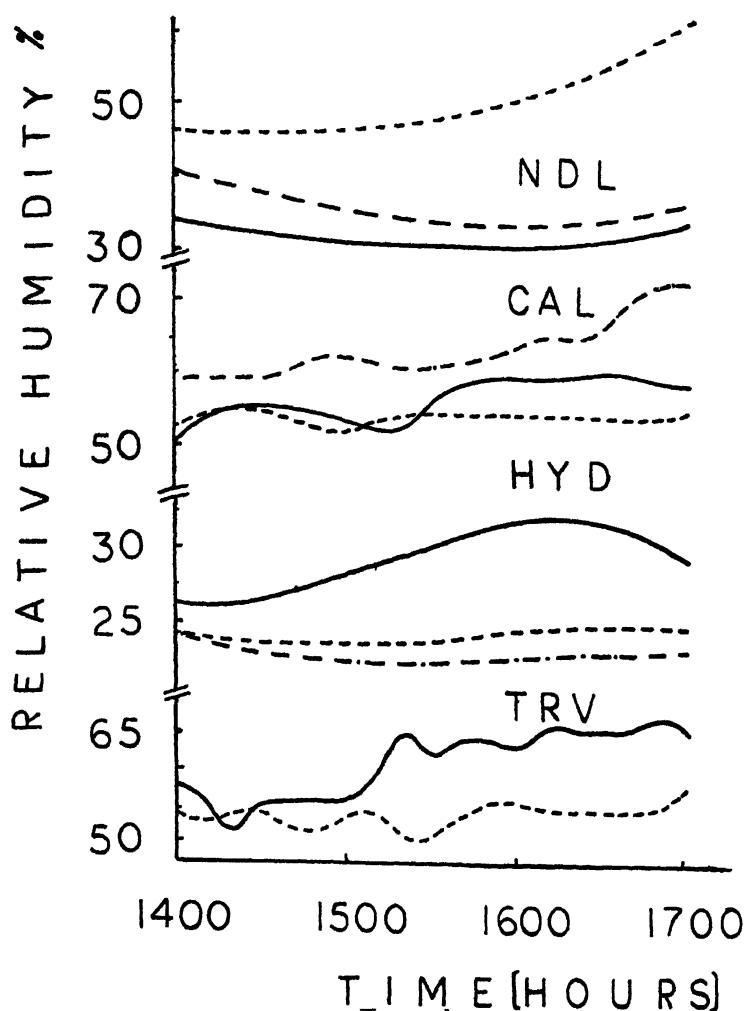


FIG 4 Changes of relative humidity during the eclipse at Trivandrum (TRV), Hyderabad (HYD), Calcutta (CAL) and New Delhi (NDL).  
( . . . 51 February, ——— 16 February) . 17 February 1980)

surface temperature to a great extent, since, for example, at Trivandrum a decrease of about  $16^{\circ}\text{C}$  was found from the day-maximum. The lowest day temperature observed on the eclipse day was just after totality. The relative humidity during the eclipse time showed higher values, and it is evidently due to the decrease of temperature at this time, since they are reciprocally related.

#### ACKNOWLEDGEMENTS

The authors wish to thank much Dr V. Narayanan and his colleagues at the Meteorology Division, TERLS, Trivandrum for their help. We also express our sincere thanks

to the DDGM, India Meteorological Department, New Delhi for the kind supply of data.

#### REFERENCES

- Anderson, R. C., and Keefe, D. R. (1975) Observation of the temperature and pressure changes during the 30 June 1973 solar eclipse *J. atm. Sci.*, **32**, 228–231.
- Anderson, R. C., Keefe, D. R., and Myers, O. E. (1972) Atmospheric pressure and temperature changes during the 7 March 1970 solar eclipse *J. atm. Sci.*, **29**, 583–587.
- Beckman, J. E., and Clucas, J. I. (1973) Search for atmospheric gravity waves induced by the eclipse of June 30, 1973. *Nature*, **246**, 412.
- Chimonas, G. (1973) Lamb waves generated by the 1970 solar eclipse *Planet Space Sci.*, **21**, 1843–1854.
- Chimonas, G., and Hines, C. O. (1970) Atmospheric gravity waves induced by a solar eclipse *J. geophys. Res.*, **75**, 875.
- Gringorten, I. I., and Kantor, A. J. (1965) Atmospheric temperature, density, pressure and moisture *Handbk. Geophys. Space Environ.*, AFCRL—USAF, 3–17.
- Jones, B. W., and Bogart, R. S. (1975) Eclipse induced atmospheric gravity waves *J. atm. terr. Phys.*, **37**, 1223–1226.
- Schodel, J. P., Klostermeyer, J., and Rotteger, J. (1973) Atmospheric gravity wave observations after the solar eclipse of June 30, 1973 *Nature*, **245**, 87.

Printed in India.

**Atmospheric Boundary Layer (Meteorology)**

**MEASUREMENTS OF METEOROLOGICAL PARAMETERS AT THE LOWEST LAYERS OF THE ATMOSPHERE DURING TOTAL SOLAR ECLIPSE OF 1980**

R K KANKANE, B K HAZRA and A B SARKAR

*Meteorological Office, Pune, India*

*(Received 21 July 1981)*

Observations of various meteorological parameters viz, wind speed, wind direction at two levels 3.0 and 13.5m, air temperature at four levels 0.3, 3.0, 6.5 and 13.5m. soil surface temperature and atmospheric pressure were made at Raichur (77°21'E 16°12'N) during the total solar eclipse of 16 February 1980. Sensitive photo-electric anemometers and potentiometric windvanes were used for measuring wind speed and direction, sensitive linear bead thermistors were used for measuring temperature, a differential capacitor transducer was used for the measurement of atmospheric pressure. The above parameters were continuously and automatically recorded on strip chart recorders. The results of the observations made are presented in this paper.

**Keywords.** Wind—Speed & Direction; Temperature & Pressure—Air, Surface; Photoelectric Anemometers; Potentiometric Windvanes; Differential Capacitor Transducer

INTRODUCTION

THE spectacle of the sun, which provides about 99.97 per cent of the heat energy required for the physical processes taking place in the earth-atmosphere system, being blotted out of the day sky is so unusual that it has always created a sense of wonder and awe in the minds of its viewers. During a solar eclipse when solar radiation is blocked from reaching the earth's atmosphere, it can reasonably be expected that the conditions are altered in the atmosphere because of the transitory change in the heat balance within the moon's shadow. Accordingly, the measurement of atmospheric parameters has been considered important by both meteorologists and amateur observers, since the 19th century. The total solar eclipse of 16 February 1980 provided for the first time a unique opportunity to the scientific community in India to repeat the common experiments.

SITE CONDITIONS

The experiment described here was conducted at the Agricultural Research Institute, Raichur, 16°21'N, 77°21'E very near the central line of the totality path of the solar eclipse on 16 February 1980. A site in an open field free from obstructions such as buildings and trees was chosen to minimize any disturbances caused by wind gusts.

On the morning of the eclipse the sky was partly cloudy with a light breeze from southeast. The temperature was around 22 °C. Southeasterly to Southerly winds continued at about 3–4 knots but the sky became absolutely clear just before the first contact at slightly after 1425hr IST and remained clear throughout the duration of the eclipse which ended at about 1655hr IST.

#### INSTRUMENTAL SET-UP

##### *Pressure*

The atmospheric pressure measurement was made using a differential capacitor electrical transducer (Plate I) developed in the Instruments Division of the India Meteorological Department at Pune. An evacuated and sealed aneroid bellows is used as the basic sensor in the transducer. The expansion or contraction of this bellow due to variation in the atmospheric pressure is converted to corresponding variations in the capacitance value of a pair of parallel plate capacitors. These capacitors are connected in a differential mode with the common plate controlled by the aneroid bellows. The differential capacitance value is converted by a suitable circuit to an analog DC voltage linearly varying with the atmospheric pressure and recorded continuously on a strip chart recorder.

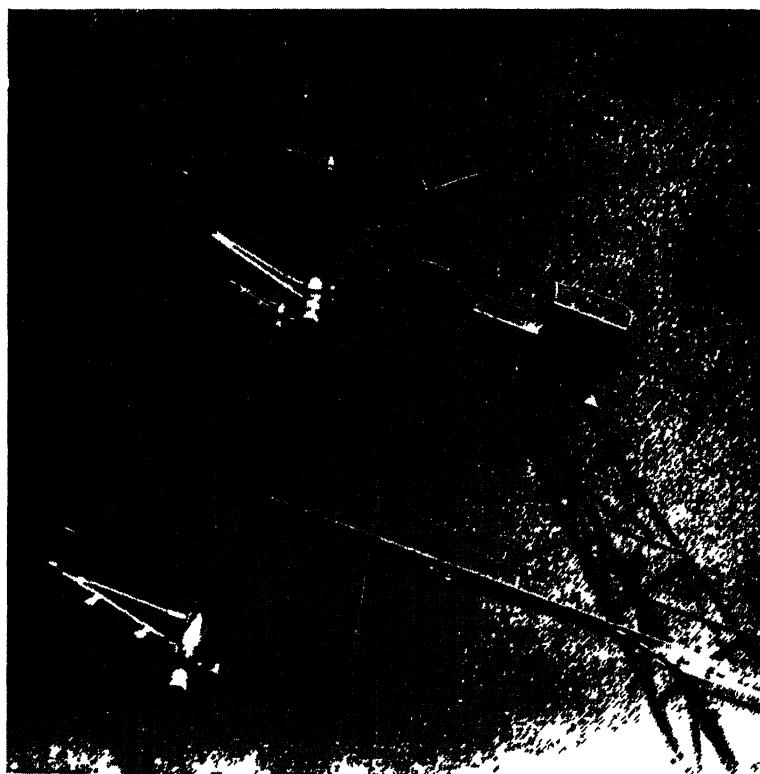


PLATE I. Tower instrumental set-up at Raichur during total solar eclipse of 1980

### Temperature

The soil surface temperature and air temperature at 4 levels upto 13.5m above the ground were measured during the eclipse using linear bead thermistor composite thermometers. The thermistors used for measuring the air temperature were provided with polished anodised aluminium louvred radiation shield and mounted on bracket arms at the appropriate heights on a 13.5m mast. The thermistor sensor was connected as a feed back resistor in the operational amplifier circuit and the output was fed to the strip chart recorders.

### Wind

Sensitive, light weight 3 cup photoelectric anemometers developed by the Pune Instruments Division were used for measuring wind speed. When the cups rotate, a disc with 32 holes attached to the anemometer spindle cuts the light emitted by LED, thus giving the electrical pulses proportional to the wind speed. These pulses are converted to a D. C. voltage and recorded on strip chart recorders calibrated in terms of knots.

Potentiometric windvanes with strip chart recorders were used for the measurement and recording of wind direction

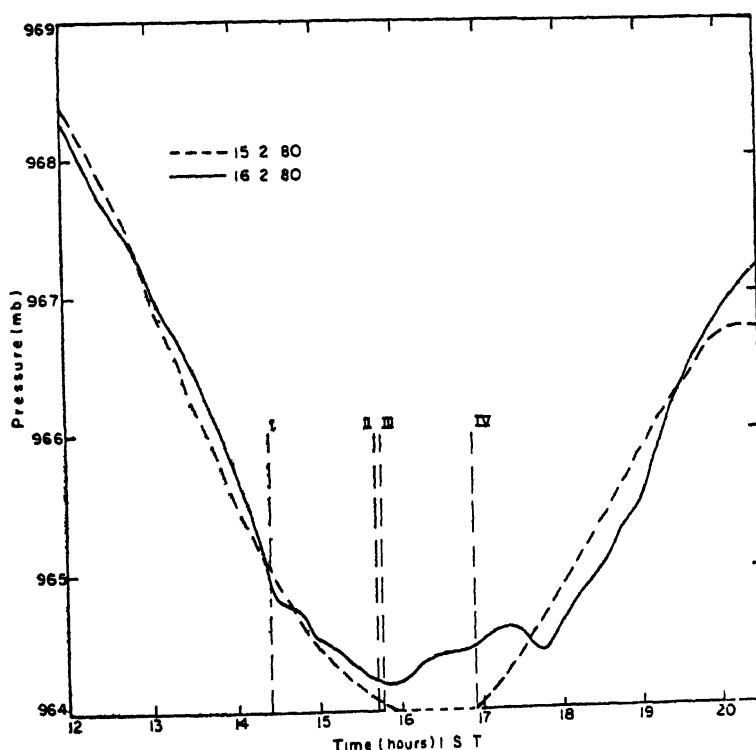


FIG 1. Pressure changes on 15 and 16 February 1980 at Raichur.

## RESULTS

Chimonas and Hines (1970) predicted that cooling in the upper atmosphere would trigger internal gravity waves, with pressure amplitudes large enough to be detected at the surface of the earth. Anderson *et al* (1972) summarised previous pressure measurements during solar eclipses and observed that the atmospheric pressure record showed oscillations and in addition, all but one of the authors reported two maxima and two minima beginning with a minimum after first contact, the average of the pressure amplitude being  $244\mu\text{b}$

The atmospheric pressure measurements recorded during 1200hr IST through 2030hr on 16 February 1980 at Raichur are shown in Fig. 1. The pressure changes on a typical day 15 February 1980, are also shown for comparison. The roman numerals I through IV indicate the time of first, second, third and fourth contacts respectively of the eclipse on 16 February 1980. One oscillation having amplitude of about  $200\mu\text{b}$  in pressure with a weak second minimum is seen in the pressure profile of 16th. The first minimum occurred just after totality and the maximum and the second minimum occurred after the eclipse ended. It was seen that there was no

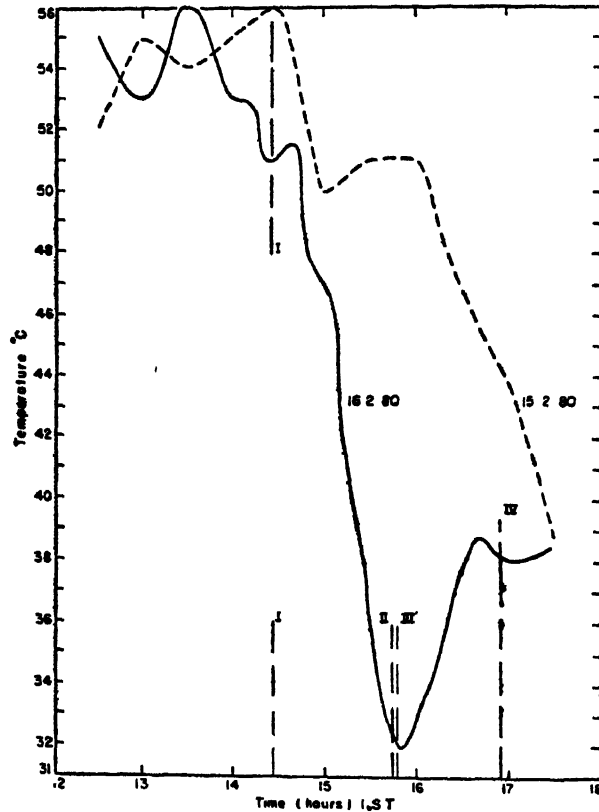


FIG. 2 Soil surface temperature changes at Raichur recorded during the 16 February 1980 solar eclipse.



appreciable variation in pressure value between 1600hr and 1700hr on 15 February, thus giving a flat profile.

The results of soil surface temperature and atmospheric temperature measurements described in the earlier section are shown in Figs 2 & 3. A maximum change of 19.5 °C in soil temperature and 4 °C in air temperature at the height of 0.3m were observed just after totality. The drop in temperature at 3.0, 6.5 and 13.5m levels was 2.4 °C, 1.8 °C and 1.4 °C respectively. It may be noted that the atmospheric conditions were quite favourable for measuring the eclipse induced temperature change, in that, the sky was absolutely clear and the ambient temperature returned to within 0.5–1 °C of its normal value after the eclipse.

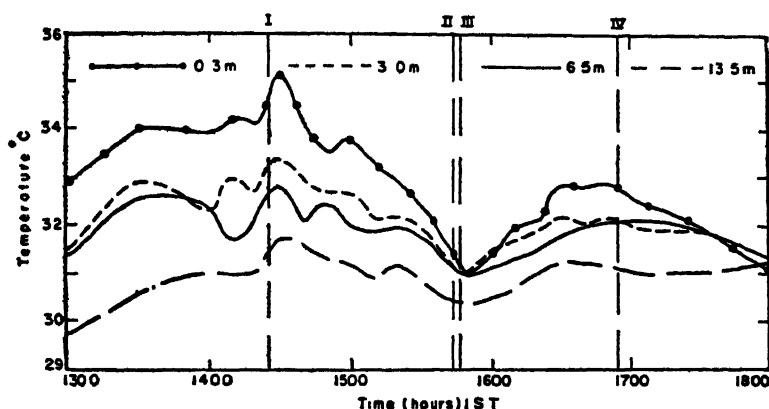


FIG 3 Temperature changes at altitudes 0.3, 3.0, 6.5 and 13.5m, recorded at Raichur, India, during the solar eclipse on 16 February 1980

Figs 4, 5 and 6 show the variation of wind speed and direction from 1300hr to 1800hr IST at two different levels, 3.0m and 13.5m at Raichur for 15, 16 and 17 February 1980 respectively. The wind speed at 3.0m at about 1545hr on 16 February 1980 shows a minimum value of 1 knot while on 15th and 17th the wind speed was about 2.5 and 3 knots respectively. This sudden dip in the wind speed on 16th could be presumably due to the effect of eclipse during totality though apparently there seems to be no physical reason as to why the wind should die down to very low values during totality. Earlier workers, Anderson *et al* (1972) have also reported that the wind dies down to a dead calm especially during totality. It is however, seen at Raichur that the wind speed did come down to very low values during totality though it did not die down to a dead calm. The low wind speed at 1330hr on 16 February 1980 could be due to some other causes. The wind speed profile at the higher level of 13.5m generally follows the low level profile on all the three days though the values are higher at 13.5m.

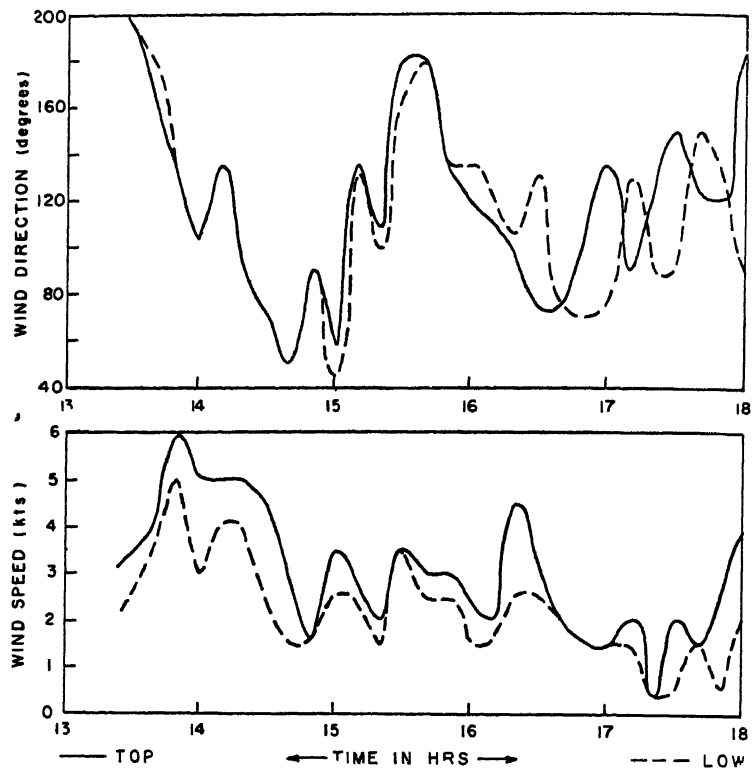


FIG 4 Wind speed and wind direction recorded at Raichur, India on 15 February 1980

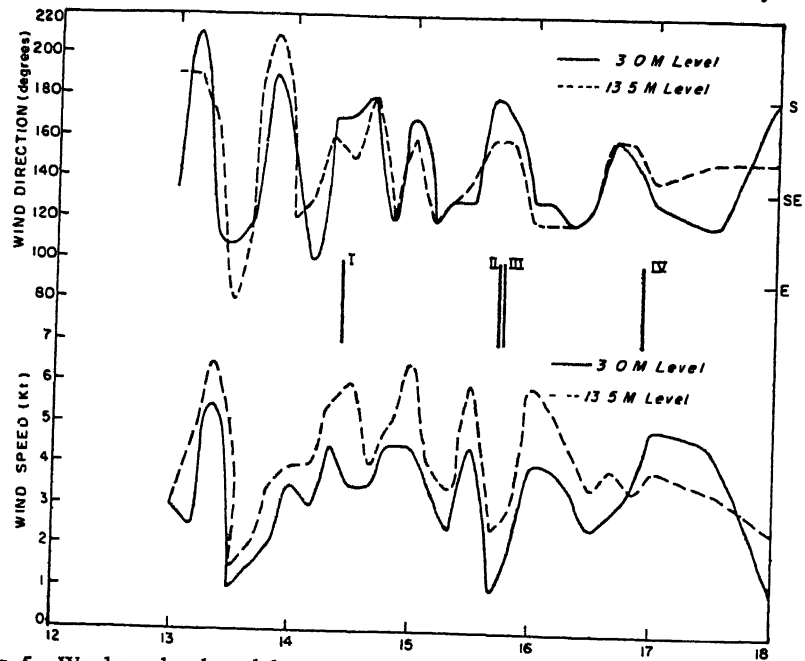


FIG 5 Wind speed and wind direction recorded at Raichur, India, on 16 February 1980

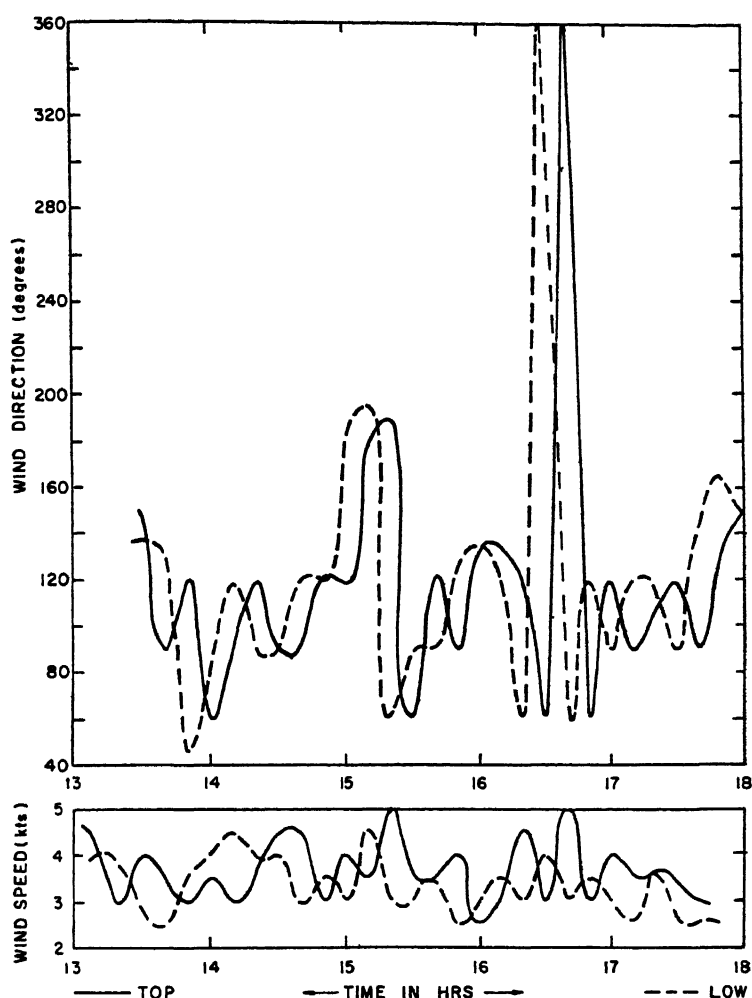


FIG 6. Wind speed and wind direction recorded at Raichur, India, on 17 February 1980.

#### ACKNOWLEDGEMENT

We gratefully acknowledge the hospitality of the Agricultural Research Institute, Raichur during our stay at Raichur

#### REFERENCES

- Chimonas, G , Hines, C O (1970) International gravity wave motions induced in the earths' atmosphere by a solar eclipse *J. geophys Res* , 75, 5545-5551  
 Anderson, R. C., Keefer, D R , and Myers, O. E , (1972) Atmospheric pressure and temperature changes during 7 March 1970 solar eclipse *J atm. Sci* , 29, 583-587

Printed in India.

Atmospheric Boundary Layer

## A STUDY OF CHANGE IN THE ATMOSPHERIC PROPERTIES DURING SOLAR ECLIPSE OF 16 FEBRUARY 1980

RAMESH K. KAPOOR *and* B B ADIGA

*Health Physics Division  
Bhabha Atomic Research Centre, Bombay 400 085, India*

*and*

S P SINGAL, S K. AGGARWAL *and* B. S GERA

*National Physical Laboratory, New Delhi-110 012, India*

*(Received 23 March 1982)*

In this paper, the observations made by monostatic sodar and a number of meteorological sensors to study the variations in the atmospheric boundary layer at Delhi ( $28^{\circ}6'N$ ,  $77^{\circ}2'E$ ) and Tarapur ( $19^{\circ}50'N$ ,  $72^{\circ}41'E$ ) during the solar eclipse of 16 February 1980 are reported. The atmospheric instability (atmospheric mixing and turbulence) and solar UV component were found to have been reduced below normal values during the solar eclipse period. The atmosphere at no time showed to have become stable and the sodar echograms did not show the presence of wave motion (undulations) before, during and after the solar eclipse at either of the two places.

**Keywords:** Atmospheric Boundary Layer; Monostatic Sodar; Sodar Echograms; Mixing Height; Thermal Structure Parameter; Global & UV Solar Radiation; Radon

### INTRODUCTION

THE total solar eclipse of 16 February 1980 offered a good opportunity to study the changes in the atmospheric properties during the eclipse period. It also offered a chance to show the potential of the sodar technique to study the stability of the lower atmosphere in the first few hundred metres of the boundary layer, a region of great importance in hazardous situations of air pollution, aviation and microwave communication.

In Delhi ( $28^{\circ}6'N$ ,  $77^{\circ}2'E$ ) and at Tarapur ( $19^{\circ}50'N$ ,  $72^{\circ}41'E$ ) where the monostatic sodar and a number of tower mounted meteorological sensors were set in operation for the above studies, the maximum observation of the sun's disc during the eclipse was 65 per cent and 84 per cent respectively. The times of various phases of eclipse at the two places were 1419-1652hr at Tarapur and 1436-1651hr at Delhi with times of greatest phase being 1540hr at Tarapur and 1547hr at Delhi.

## EXPERIMENTAL SET-UP

The various instruments used are shown in Fig 1. The monostatic sodar (Singhal *et al*, 1978) capable of studying the thermal structure of the lower atmosphere to a height range of 700m was used at both the places. Tarapur additionally had the facility of an instrumented tower (BARC, 1974) 120m high with arrangements for measurements of air temperature, wind speed and direction and solar radiation, both global and UV component, at a number of levels. Surface measurements of air temperature using Stevenson screen were also available at both the places. Besides, radiosonde data from Delhi and Bombay observatories of India Meteorological Department were also available twice daily at 00GMT and 1200GMT. The types of the various sensors used at the two places alongwith their resolution, parameter measured, level range etc. are shown in Table I.

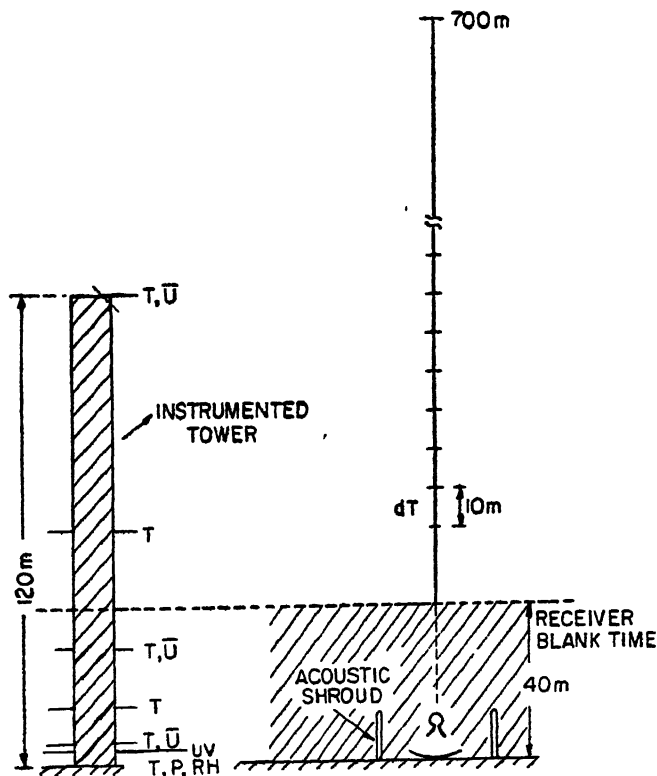


FIG 1 Diagrammatic representation of the range and resolution of the various meteorological sensors used.

## STUDIES OF THE ATMOSPHERIC BOUNDARY LAYER

A visual picture of the atmospheric boundary layer during the eclipse period compared to a normal day of solar heating can be seen in Figs 2 and 3. A general decrease

TABLE I

*Level, range, resolution etc. of the various sensors used to measure the atmospheric parameters*

S No	Variable	Sensor	Resolution	Continuous Recording	Levels/Range (m)	Place(s)
1	Thermal Structure	SODAR	10m	Yes	700m	Tarapur/NPL
2.	Air Temperature					
	(a) On Tower	Semiconductor Diode	$\pm 0.1$ °C	Yes	30 & 120m	Tarapur
	(b) On a Stevenson Screen	Bimetallic Thermograph	$\pm 0.5$ °C	Yes	1 2m	Tarapur/NPL
3	Wind					
	(a) Speed	Cup Anemometer	$\pm 0.2$ m/s	Yes	6, 60 and 120m	Tarapur
	(b) Direction	Potentiometric Wind Vane and Bivane	4 5 °C	Yes	6, 30 and 120m	Tarapur
4	Solar radiation					
	(a) Global	Kipp & Zonen Solarimeter	—	Yes	4m	Tarapur
	(b) UV Component	Epply UV Radiometer	290–385 micrometer	Yes	4m	Tarapur/NPL

in the height of the thermal plumes can be seen in the echograms both at Delhi and Tarapur during the eclipse period. However, the echogram at Tarapur is more representative of the varying phase of the solar eclipse since the day at Tarapur was clear while the sky over Delhi was partially covered with clouds.

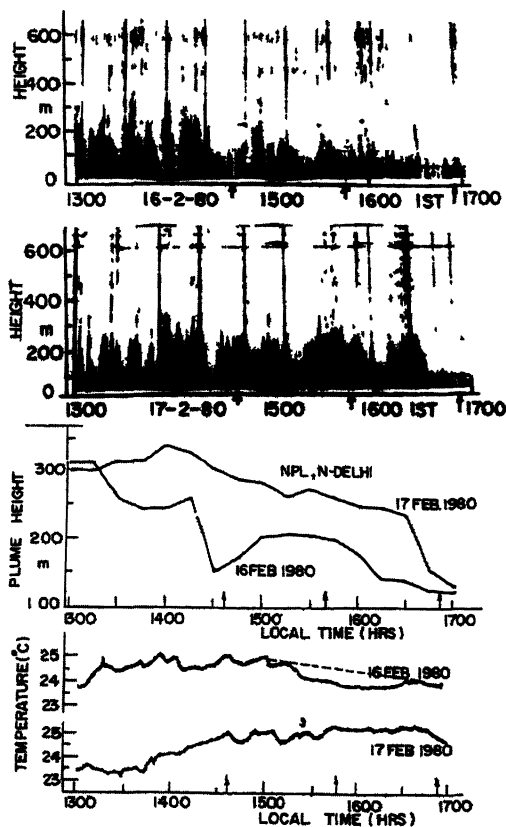


FIG 2. Solar echograms and surface temperature record for 16-17 February 1980 in Delhi

The echogram at Tarapur clearly shows that the height of the thermal plumes was 250m a little before the onset of the eclipse (this is a height of the same order as on the previous day), a fall in the height of the thermal plumes started around the time of the onset of eclipse, the falling trend remained till 1530hr, a time close to the maximum phase of the eclipse, when a rise in the height of the thermal plumes started, this rising trend remained till 1630hr a time a little earlier to the end time of the eclipse, whereafter it levelled off more or less. The minimum height of the thermal plumes at Tarapur during the eclipse was seen to be 170m while the post eclipse height of the thermal plumes was observed to be around 200m. Compared to this the height of the thermal plumes on a day prior to the eclipse during the same

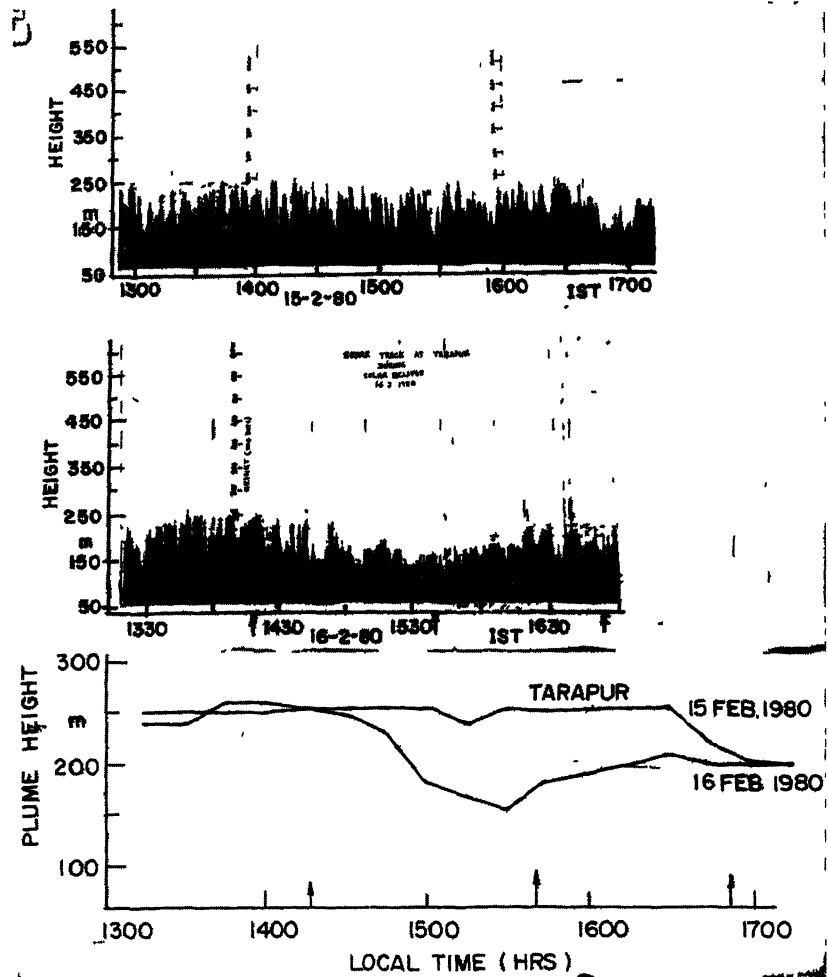


FIG 3. Sodar echograms for 15-16 February 1980 at Tarapur

period had been more or less uniform (around 250m), a characteristic of the marine boundary layer at Tarapur

The measurements of the air temperature and wind velocity at a number of levels on the Tarapur instrumented tower (Fig 4) seem to conform to the observations made by the sodar. From the diagram it is clearly seen that the air temperature shows a fall during the increasing phase period of the eclipse and an increase during the recovery phase period at all the three levels of measurement. The air temperature becomes normal soon after the full recovery of the eclipse. It is also seen that the variations in temperature decrease as we go up in the atmosphere.

This behaviour of the variations in air temperature at the various levels of measurement, however, can be better studied through a plot of temperature gradient which is also shown in Fig 4. It is clearly seen that the changes in the temperature



gradient are larger in the lower layers of the atmosphere and with height not only the gradient decreases but even the variations in the gradient become low, a behaviour responsible for the formation of the thermal plumes during the day on the sodar echograms only up to a certain height (conforming to the sensitivity of the system) showing decreasing intensity with increasing height of the plumes. The flatness of the temperature gradient curve in the 30–120m layer of the atmosphere over a large period around the maximum phase of the solar eclipse and its levelling off before the end time of the eclipse are also in conformity with the sodar behaviour.

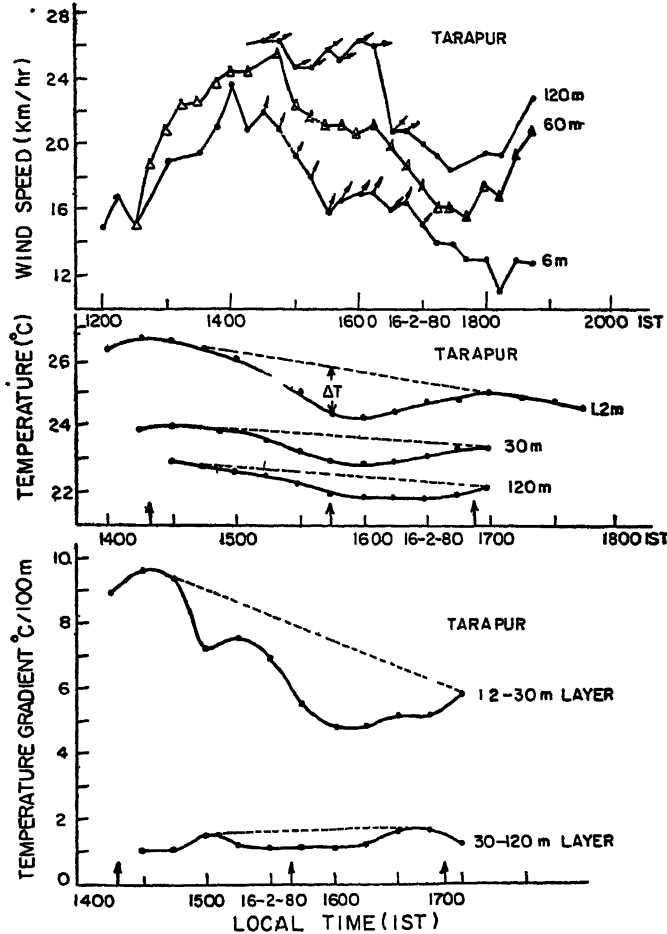


FIG 4 Variations of air temperature and wind velocity on 15-16 February 1980 at the various levels on the Tarapur instrumented tower

The temperature lapse rates due to eclipse at the greatest phase time of the eclipse in the layer range 12–30m and 30–120m are seen to be respectively  $4.8^{\circ}\text{C}/100\text{m}$  and  $1.1^{\circ}\text{C}/100\text{m}$  while the anticipated lapse rates without the solar eclipse as shown by the dashed line should have been  $7.4^{\circ}\text{C}/100\text{m}$  and  $1.5^{\circ}\text{C}/100\text{m}$  respectively

These lapse rates indicate a large drop in the instability of the atmosphere during the solar eclipse. The decrease in the instability of the boundary layer is further shown by the wind velocity measurements at the various levels of the tower. Fig. 4 clearly shows that the variations in wind velocity during the eclipse period at the various levels of measurement are very small. Further, it was seen that even the fluctuations in the horizontal and vertical wind directions at the various levels were very small during the eclipse period.

The decrease in the instability of the boundary layer during the solar eclipse was also evidenced by the surface temperature plot (Fig. 2) in Delhi. However, at no time during the solar eclipse, the atmosphere was observed to have become stable at either of the two places, Tarapur and Delhi. The formation of thermal plumes and the absence of wave motion on the sodar echograms at both the places show that the boundary layer continued to remain unstable at both the places throughout the solar eclipse.

To show the above result more explicitly, data of the mixing height and thermal structure parameter  $C_T^2$  have been computed for a few days before and after the day of eclipse for the duration of the eclipse period. The mixing height has been obtained by using the empirical relationship (Singhal *et al.*, 1980):

$$y = 4.24x + 95$$

where  $x$  and  $y$  denote the observed height of the plumes and the extrapolated height of the mixing boundary layer respectively, measured in metres. The thermal structure parameter at Tarapur has been estimated directly from the tower data while at Delhi it has been estimated from the intensity of the received power on the sodar echograms by using the following relations applicable for a monostatic sodar (Little, 1969)

$$\sigma(180^\circ) = 0.0039k^{1/3} \frac{C_T^2}{T^2} \text{ MKS Units}$$

$$\text{and } P = P_r \frac{C \tau \sigma(180^\circ) ALB}{2R^2}$$

where  $\sigma(180^\circ)$  is the backscattered acoustic power per unit incident power per unit solid angle,  $k$  is the wave number of the acoustic wave,  $C_T^2$  is the temperature structure parameter,  $T$  is the mean absolute temperature within the scattering volume,  $P_r$  is the received acoustic power,  $P_t$  is the transmitted acoustic power,  $\tau$  is the pulse length,  $C$  is the velocity of sound waves,  $R$  is the range height,  $A$  is the collecting area of the acoustic antenna,  $L$  is the round trip attenuation of the acoustic wave and  $B$  is the beam shape compensation factor which includes the efficiency of the acoustic transducer and the directivity pattern of the antenna.

The computed values of the various parameters are given in Table II. A look at the table shows that the mixing height during the eclipse period at Delhi decreases on all days irrespective of the occurrence of eclipse on 16 February 1980. However, the values are slightly lower on the eclipse day with the end time height of the mixing layer being about the same on all the days. The lower values of the mixing height at the greatest phase time seem to be due to the solar eclipse only while the lower value of the mixing height at the onset time can be due to the presence of a cloud patch at that time over the sounder. Compared to this, the mixing height of the boundary layer at Tarapur shows the distinct effect of the solar eclipse on 16 February 1980.

TABLE II

*Data of mixing height and temperature structure parameter on and around the solar eclipse day at NPL, New Delhi and M M L, Tanapur*

Date	Time of the Day or Eclipse Stage	N P L				TARAPUR			
		Visibility condition	Plume Height (SODAR) m	Mixing Height m	$C_T^2$ at 100m (SODAR) $K^2 m^{-2/3}$	Visibility Condition	Plume Height (SODAR)	Mixing Height m	$C_T^2$ at 60m (Tower) $K^2 m^{-2/3}$
15 2.80	Around 1430hr	Intermittent Clouds	210	980	$4.7 \times 10^{-3}$	Clear Day	250	1150	—
	Around 1545hr	„	200	940	$3.6 \times 10^{-3}$	„	250	1150	—
	Around 1650hr	„	110	560	—	„	200	940	—
16 2.80	Onset Time	Clouds patches	160	780	$5.7 \times 10^{-3}$	Clear Day	250	1150	$8.6 \times 10^{-3}$
	Greatest Phase Time	„	150	710	$2.1 \times 10^{-3}$	„	170	810	$6.5 \times 10^{-3}$
	End Time	„	120	610	$4.2 \times 10^{-3}$	„	200	940	$1.3 \times 10^{-1}$
17 2 80	Around 1430hr	Clear Day	300	1360	$9.8 \times 10^{-3}$	Clear Day			$7.8 \times 10^{-3}$
	Around 1545hr	„	260	1200	$7.0 \times 10^{-3}$	„			$9.3 \times 10^{-3}$
	Around 1650hr	„	120	610	$3.8 \times 10^{-3}$	„			$7.8 \times 10^{-3}$

A clear recovery of the mixing height during the recovery phase is seen compared to a normal day where only the effect of advancing time of the day is seen.

A decrease in the instability of the boundary layer during the solar eclipse has been more clearly shown by the computed values of the thermal structure parameter  $C_T^2$  which is an indicator of turbulence in the atmosphere. From Table II, it is clearly seen that  $C_T^2$  has the lowest value at the time of greatest phase of the solar eclipse at both the places compared to the values at the onset and end time of the solar eclipse

#### GLOBAL AND UV SOLAR RADIATION

As indicated in Table I, global solar radiation and the ultraviolet component (290–385m) of the solar radiation were also studied at Tarapur during the solar eclipse of 16 February 1980. It was seen that these radiations were affected considerably, as expected, by the solar eclipse. The behaviour of the observed UV component of the solar radiation and the obscuration percentage is shown in Fig. 5. It is seen that as the eclipse progressed, the radiation progressively showed a decrease, became steady during the period of the greatest phase and rose to normal value again after the solar eclipse. Further, it is seen that the fall in the UV radiation during the first contact and the second contact of the eclipse was steeper compared to the recovery phase, the fall in the UV radiation due to obscurity compared to a normal day value (shown dotted) has been 81 per cent at the peak and 33 and 27 per cent respectively at the mid point of the first and second contact and in the recovery phase. Taking into account the observational errors in the UV measurements, it is considered that

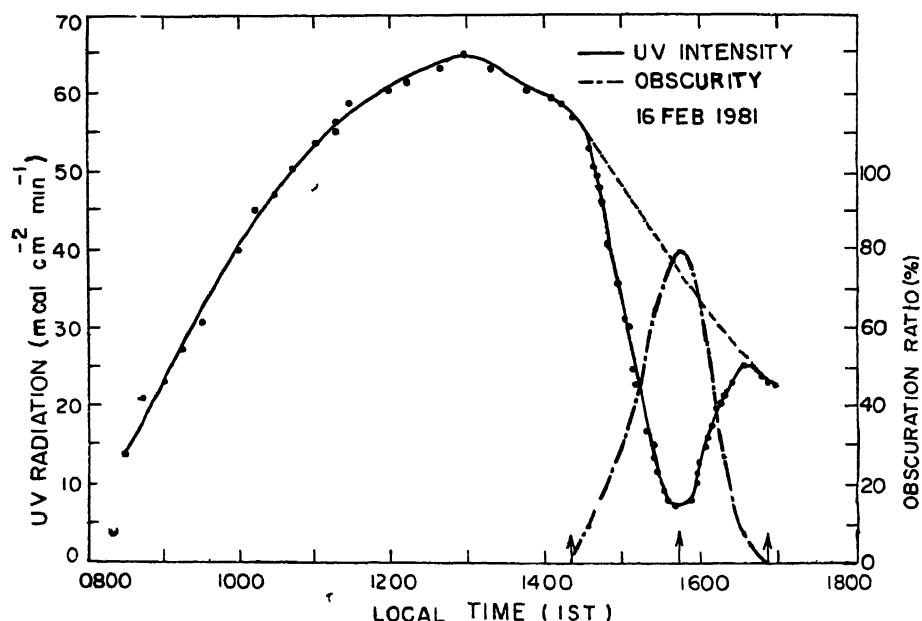


FIG 5 Variations of the ultraviolet radiation intensity and obscuration percentage during the solar eclipse at Tarapur.

the change in the observed UV radiation is purely due to the covering of the disc, however, the pattern of the fall during the first and second contact and the recovery phases of the eclipse seem to indicate that radiation may not be uniform over the whole of the solar disc

Though both these radiations reduced during the eclipse period, their difference in behaviour was studied by looking at the ratio of UV to total solar radiation. However, this ratio could be studied only at the peak eclipse time and at the pre-eclipse time. It could not be calculated accurately at other times of the eclipse since the global solar radiation measuring system developed some trouble and the chart speed of the record of the total solar radiation was small and even a mistake of 3 minutes would have given an error of 10 per cent in the ratio. On the other hand, at the peak of the solar radiation, both the radiations could be read accurately because of the exact identification of point on the chart as also due to the flatness of variation in the radiation at this point. The ratio was found to be the same ( $5 \times 10^{-2}$ ) at both the peak eclipse time and at the pre-eclipse time.

### CONCLUSIONS

The observations made by sodar and other tower mounted meteorological instruments on the event of the solar eclipse of 16 February 1980 clearly show that the atmospheric instability during the solar eclipse has fallen below its normal value. These observations have also shown that sodar can be used as an effective tool to study the stability of the atmosphere. The fall in atmospheric instability during the solar eclipse has resulted in a fall in the atmospheric mixing height, a parameter of great value in hazardous situations of air pollution.

The decrease in instability during the eclipse period at Bombay ( $19^{\circ}1'N$ ,  $72^{\circ}55'E$ ) has also been inferred by Kotrappa *et al* (1981) from measurements of radon. Radon originates from earth's crust and diffuses in the atmosphere. The concentration of radon increases with the decrease in the atmospheric instability. During eclipse radon concentration seemed to have increased from the pre-eclipse and post eclipse value of  $56 \text{ pci/m}^3$  to  $86 \text{ pci/m}^3$ , indicating a fall in the instability of the atmosphere.

The sodar echograms at none of the two places have shown the formation of stable atmosphere. Wave motion has been seen on the sodar echograms which may have indicated the presence of stable atmosphere in the boundary layer.

### REFERENCES

- BARC (1974) *Climatological Summary for Tarapur Atomic Power Station Site for 1971* Rep No BARC/1-300, Meteorology Group, Environmental Studies Section, Health Physics Division, BARC, Bombay
- Kotrappa, P., Maya, Y S, Dua, S K, and Gupta, P C (1981) Increase in ground level concentration of radon during solar eclipse *Health Phys*, 1981
- Little, C G (1969) *Proc IEEE*, 57, 571
- Singal, S P, Aggarwal, S K, and Gera, B S (1980) *J scient ind Res*, 39, 73
- Singal, S P, Dutta, H N, Gera, B S, Aggarwal, S K, and Saxena, M. (1978) Acoustic sounder (SODAR) *Centrop Rep No 28*, NPL, New Delhi.

A clear recovery of the mixing height during the recovery phase is seen compared to a normal day where only the effect of advancing time of the day is seen.

A decrease in the instability of the boundary layer during the solar eclipse has been more clearly shown by the computed values of the thermal structure parameter  $C_T^2$  which is an indicator of turbulence in the atmosphere. From Table II, it is clearly seen that  $C_T^2$  has the lowest value at the time of greatest phase of the solar eclipse at both the places compared to the values at the onset and end time of the solar eclipse

#### GLOBAL AND UV SOLAR RADIATION

As indicated in Table I, global solar radiation and the ultraviolet component (290–385m) of the solar radiation were also studied at Tarapur during the solar eclipse of 16 February 1980. It was seen that these radiations were affected considerably, as expected, by the solar eclipse. The behaviour of the observed UV component of the solar radiation and the obscuration percentage is shown in Fig. 5. It is seen that as the eclipse progressed, the radiation progressively showed a decrease, became steady during the period of the greatest phase and rose to normal value again after the solar eclipse. Further, it is seen that the fall in the UV radiation during the first contact and the second contact of the eclipse was steeper compared to the recovery phase, the fall in the UV radiation due to obscurity compared to a normal day value (shown dotted) has been 81 per cent at the peak and 33 and 27 per cent respectively at the mid point of the first and second contact and in the recovery phase. Taking into account the observational errors in the UV measurements, it is considered that

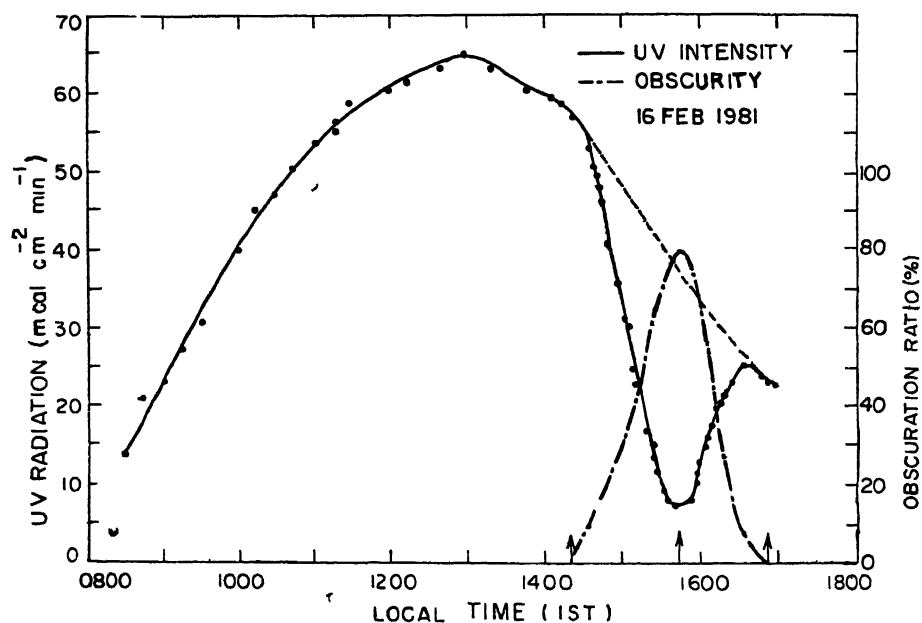


FIG 5 Variations of the ultraviolet radiation intensity and obscuration percentage during the solar eclipse at Tarapur.

the sun is measured as an increase or decrease of the relative power as the case may be over the sun level. The magnitude of the sun level is calibrated by means of an argon discharge noise source, where a known amount of power corresponding to the difference in the sky and the sun level is introduced by adjusting the calibrated attenuator. This then gives the power at the sun level. The radiometer at 22.235 GHz is working in the emission mode and looking at the zenith (Uppal *et al.*, 1979). Any change in the water level is measured as an enhancement of the antenna temperature over the sky level. It is also calibrated by means of an argon discharge noise source.

Both the systems are basically Dicke-type where radiations directed into the antenna are compared to the radiations from an internal load maintained at a constant temperature. The comparison is made at the modulation frequencies of 45 Hz and 90 Hz respectively. The radiometer output is recorded on the chart recorder. The sensitivity of the systems are 5 °K and 3 °K respectively. The radiometers were continuously in operation 48 hours before and after the event.

### RESULTS AND DISCUSSION

Fig. 1 shows the variation of the microwave radiations from the sun at 11 GHz during the period of the eclipse. This is the original record and as seen, we find that as the eclipse progressed, the microwave radiations showed a variation between 1 to 2 dB from the sun level. However around 15h 47m (maximum phase) there was a sharp dip of 6 dB for a duration of 20 seconds after which the variation in the radiations continued to vary between 1 to 2 dB. This sudden change could be due to the difference in geometry between the leading occulting edge of the moon and the trailing uncovering edge, so that source would be covered in a relatively short period of time producing a sudden change on the record but would be uncovered much more gradually, producing a much smaller but more prolonged distortion in the record (Croom & Powell, 1967).

Fig. 2 shows the variation of water vapour during the period of the eclipse. As seen there is a variation of around 10 to 15 °K. This corresponds to the enhancement of around 0.6 to 0.8 dB. In terms of water vapour content this amounted to the variation between  $0.84 \times 10^4 \text{ gm/m}^2$  to  $0.86 \times 10^4 \text{ gm/m}^2$ . This was calculated by using an inversion technique (Vandana, 1979) and the equation

$$T_a = 1.34 \times 10^{-3} W + 3.5$$

where  $T_a$  is the observed antenna temperature from the radiometer in °K and  $W$  is the integrated water vapour content in  $\text{gm/m}^2$ .

The enhancement over the sky level and subsequent increase in the water vapour content could be due to the formation of water vapour clusters. This possibility is being further studied and detailed work is underway.

### ACKNOWLEDGEMENT

The authors wish to thank Dr A. P. Mitra, Head, Radio Science Division for valuable suggestions and constant encouragement.

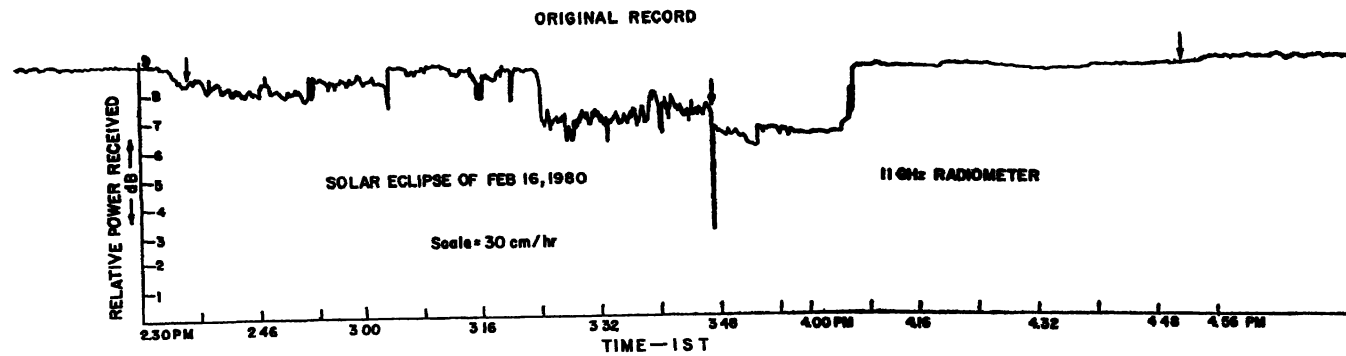


FIG 1 Variations of the microwave radiations from the sun at 11GHz during the period of eclipse

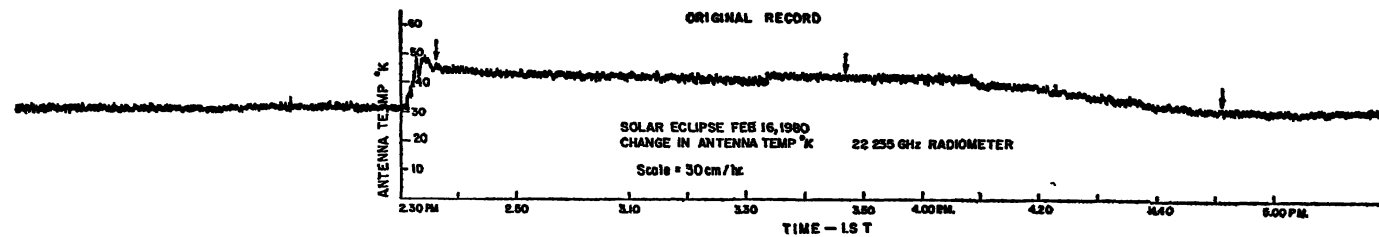


FIG 2 Variation of water vapour at 22.235GHz during the period of eclipse.



## REFERENCES

- Croom, D L , and Powell, R. J (1967) Solar radiation at 19.0Gc/s during the eclipse of May 20, 1966. *Nature*, **215**, 260-261.
- Raina, M K (1978) Rain attenuation over Delhi with microwave radiometers at 10 and 11GHz. *Ph D thesis*, Delhi University, Delhi.
- Uppal, G S., Raina, M K , Chadha, R. and Vandana Dubey (1979) Design, development and initial measurements of microwave radiometers at X and K-bands. *J. Inst. Electron. Telecom. Engrs* , **25**, No 11, pp 450-452.
- Vandana Dubey (1979) Microwave radiometric studies of atmospheric water vapour and attenuation measurements at 22.235GHz. *Ph.D. thesis*, Delhi University, Delhi.

Printed in India

Atmospheric Pressure Variations

## ATMOSPHERIC PRESSURE PERTURBATIONS DURING TOTAL SOLAR ECLIPSE ON 16 FEBRUARY 1980

P K. KUNHIKRISHNAN and B V KRISHNA MURTHY

*Space Physics Division, Vikram Sarabhai Space Centre, Trivandrum-695 022, India*

*(Received 18 July 1981)*

Pressure variations recorded at three stations situated in the penumbral region during the total solar eclipse on 16 February 1980, have been analysed to study eclipse induced effects, if any. By statistical analysis, it has been established that the eclipse has produced pressure perturbations observable at the ground level.

**Keywords:** Atmospheric Pressure Variations; Solar Eclipse; Bow Wave; Penumbral Eclipse Zone; Air-flow Meter; Pressure Sensor

### INTRODUCTION

CHIMONAS and Hines (1970) and Chimonas (1970) proposed that the supersonic movement of a cold region in the atmosphere due to the passage of the lunar shadow during a solar eclipse produces a 'bow wave', comprising of internal atmospheric gravity waves. They examined, in particular, the effects of cooling of ozonosphere and predicted that internal atmospheric gravity waves can be observed as pressure perturbations at ground level and as Travelling Ionospheric Disturbances (TIDs) at ionospheric levels. At an observation site located at a great distance from the extended source region, waves with shorter wavelengths will be attenuated while at locations close to the source, these dominate. The predicted fractional pressure perturbation level is nearly  $10^{-5}$  at ground and  $10^{-1}$  at 200km altitude at locations about 10000km perpendicular distance away from the eclipse totality path. There are reasonably good observational evidences of detection of eclipse induced wave-like disturbances at ionospheric levels (Davies & da Rosa, 1970, Vaidyanathan *et al*, 1978, and Butcher *et al*, 1978).

Observations at ground level have not been conclusive in this respect, despite many attempts by various workers. Anderson *et al* (1972) reported ground level atmospheric pressure perturbations at a station situated in the path of totality of 7 March 1970 solar eclipse. The reported amplitude is quite large ( $\sim 500\mu b$ ) compared to the predicted one (Chimonas, 1970). To explain this departure, Chimonas (1973) considered the generation of Lamb waves due to the cooling of tropospheric water vapour during a solar eclipse. Later reports by Anderson and Keefer (1975) and Jones and Bogart (1975) for the 30 June 1973 eclipse indicated a null result.

Many of the earlier observations were single station observations. It is difficult to bring out unambiguously, the eclipse effects from observations at a single location.

especially when the expected amplitude of the eclipse induced variations are much smaller than the normal variations. However, if observations are made at 2 or more number of widely separated locations, the criteria that any eclipse induced effect should be similar in nature at all the locations can be applied to extract the eclipse effects from the data.

With this in view, an array of three pressure sensors has been set up in the penumbral zone of the total solar eclipse of 16 February 1980 in India. Statistical methods have been applied to extract the presence of any similar variations in the data at the three stations. The results of this investigation are presented in the following sections.

### PRESSURE SENSORS

The pressure sensor used is essentially an air-flow meter which measures the atmospheric pressure variations with respect to the pressure of a reference volume maintained at a constant temperature. The sensing element consists of a network of sensitive thermistors. The instrument is similar to the one analysed by Fehr and Gazley Jr (1967). The sensors have been calibrated for sinusoidal pressure variations for periods of 1min and 10min. For longer periods, the calibration is obtained by extrapolation using these values along with the theoretical frequency response curve of the sensors.

The sensors were deployed at Trivandrum (TVM,  $8^{\circ}36'N$ ,  $76^{\circ}57'E$ ), Gauribidanur (GBN,  $13^{\circ}36'N$ ,  $77^{\circ}26'E$ ) and SHAR ( $13^{\circ}36'N$ ,  $80^{\circ}18'E$ ) the locations of which are shown in Fig. 1. It may be noted that SHAR and Trivandrum are due east and south (very nearly) of GBN respectively. The percentage obscuration of the solar disc by diameter is indicated in the figure in terms of percentage ranges (80–89 & 90–99 per cent).

### ANALYSIS AND RESULTS

The data, recorded on pen recorders, are scaled at 10min intervals. The scaled values are plotted as shown in Fig. 2 for 16 February 1980 (day of eclipse) and 18 February 1980 (for comparison), for Trivandrum and Gauribidanur. The three arrows in the figure indicate the times of first contact, maximum phase and last contact of the eclipse.

The data in the figure do not show prominently the expected semidiurnal pressure oscillation with the maxima at 1000hr and 2200hr for an equatorial station. This is because the response of the sensors is very weak for such long period variations which is also affected by the diurnal temperature changes. It has been found experimentally as well as from estimates of thermal time constants of the system, that the pressure sensors are insensitive to temperature variations with periods less than about 5 hours. Any variations in the data with periods less than 5 hours represent only the pressure variations.

As can be seen from Fig. 2 there is general similarity between the variations on 16 and 18 February 1980 at each of the stations prior to the commencement of the eclipse. During the eclipse and a little later, there are very significant departures in

Printed in India

Atmospheric Pressure Variations

## ATMOSPHERIC PRESSURE PERTURBATIONS DURING TOTAL SOLAR ECLIPSE ON 16 FEBRUARY 1980

P K. KUNHIKRISHNAN and B V KRISHNA MURTHY

*Space Physics Division, Vikram Sarabhai Space Centre, Trivandrum-695 022, India*

*(Received 18 July 1981)*

Pressure variations recorded at three stations situated in the penumbral region during the total solar eclipse on 16 February 1980, have been analysed to study eclipse induced effects, if any. By statistical analysis, it has been established that the eclipse has produced pressure perturbations observable at the ground level.

**Keywords:** Atmospheric Pressure Variations; Solar Eclipse; Bow Wave; Penumbral Eclipse Zone; Air-flow Meter; Pressure Sensor

### INTRODUCTION

CHIMONAS and Hines (1970) and Chimonas (1970) proposed that the supersonic movement of a cold region in the atmosphere due to the passage of the lunar shadow during a solar eclipse produces a 'bow wave', comprising of internal atmospheric gravity waves. They examined, in particular, the effects of cooling of ozonosphere and predicted that internal atmospheric gravity waves can be observed as pressure perturbations at ground level and as Travelling Ionospheric Disturbances (TIDs) at ionospheric levels. At an observation site located at a great distance from the extended source region, waves with shorter wavelengths will be attenuated while at locations close to the source, these dominate. The predicted fractional pressure perturbation level is nearly  $10^{-5}$  at ground and  $10^{-1}$  at 200km altitude at locations about 10000km perpendicular distance away from the eclipse totality path. There are reasonably good observational evidences of detection of eclipse induced wave-like disturbances at ionospheric levels (Davies & da Rosa, 1970, Vaidyanathan *et al*, 1978, and Butcher *et al*, 1978).

Observations at ground level have not been conclusive in this respect, despite many attempts by various workers. Anderson *et al* (1972) reported ground level atmospheric pressure perturbations at a station situated in the path of totality of 7 March 1970 solar eclipse. The reported amplitude is quite large ( $\sim 500\mu b$ ) compared to the predicted one (Chimonas, 1970). To explain this departure, Chimonas (1973) considered the generation of Lamb waves due to the cooling of tropospheric water vapour during a solar eclipse. Later reports by Anderson and Keefer (1975) and Jones and Bogart (1975) for the 30 June 1973 eclipse indicated a null result.

Many of the earlier observations were single station observations. It is difficult to bring out unambiguously, the eclipse effects from observations at a single location.

the variations on the eclipse day from those on February 18. This type of departures is also observed in SHAR data (not shown in the figure).

As the eclipse induced disturbances may contain components with periods less than about 4 hours, it is necessary first to remove longer period components from the data which could be much larger in amplitude than the shorter ones. In order to remove the long period components, namely 24 hours, 12 hours, 8 hours and 6 hours without affecting the shorter period components, the data are subjected to harmonic analysis for each of the days separately after subtracting any linear trend in the data. The amplitudes of the steady ( $P_0$ ), 24hr ( $P_1$ ), 12hr ( $P_2$ ), 8hr ( $P_3$ ) and 6hr ( $P_4$ ) components along with the phases of the harmonic components are thus determined. These components can be summed up as,

$$P_h(t) = P_0 + \sum_u P_n \sin(n\omega t + \Phi_n).$$

where  $\omega = \frac{2\pi}{1440}$  (rad/min), and  $n = 1, 2, 3, 4$

Using  $P_h(t)$ , two series of residuals are obtained which can be expressed as

$$\Delta P_2 = (P(t) - P_h(t)) \text{ (upto } n = 2)$$

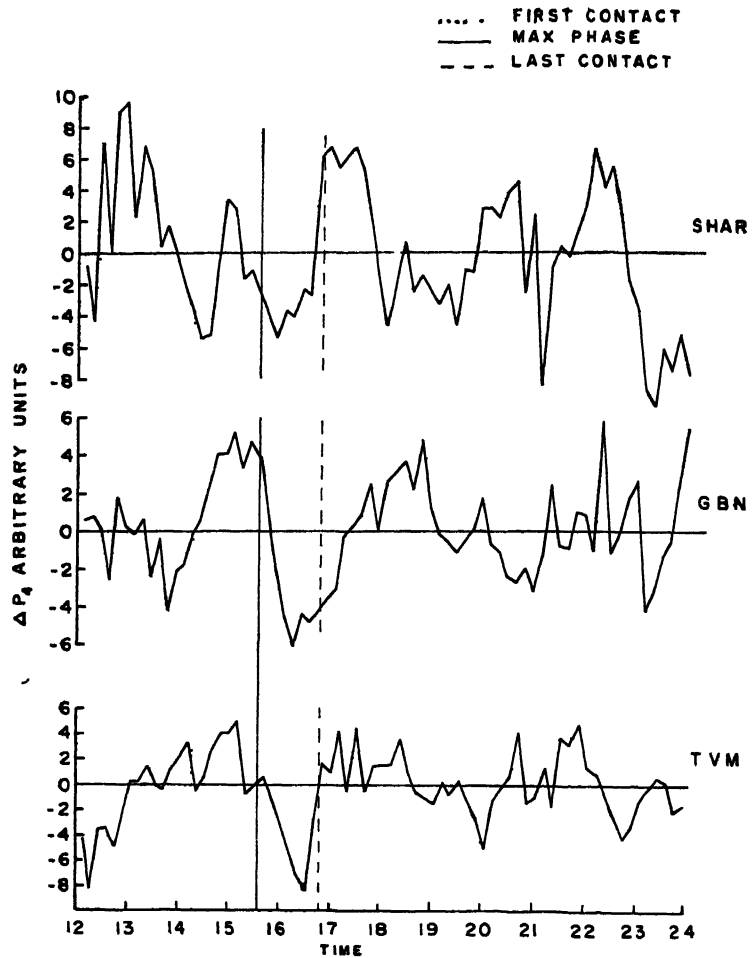
$$\text{and } \Delta P_4 = (P(t) - P_h(t)) \text{ (upto } n = 4)$$

where  $P(t)$  is the original data.

In harmonic analysis, it is implicit that the harmonic components are present throughout the length of the data maintaining their respective phases. While this could be the case for diurnal and semidiurnal components it might not be so for 8hr and 6hr components especially because of the contamination of the data due to temperature effects. If the components are not present throughout the length of the data or present only in some segments of the data, then the data reconstructed [ $P_h(t)$  in the present notation] by using the harmonic coefficients would be in error. We considered both  $\Delta P_2$  and  $\Delta P_4$  in the following statistical analyses with a view to see the effect of contamination by spurious components, if any, in the residuals due to harmonic analysis of the data.

The residuals  $\Delta P_4$  thus obtained are presented in Fig. 3 for the eclipse day from 1200hr to 2400hr IST. The times of first contact, maximum phase and last contact of the eclipse are marked by dotted, continuous and dashed lines respectively drawn parallel to the ordinate. A comparison of the variations in  $\Delta P_4$  at the three stations reveals their similarity during the eclipse period. The most conspicuous similar feature is the trough in  $\Delta P_4$  which occurred a little later than the eclipse maximum phase. Soon after the first contact a positive excursion occurred in  $\Delta P_4$ . This one and the positive excursion which occurred after the trough are not exactly similar at the three stations. This probably is due to the contamination by some local variations. At other times than the eclipse period, there are no striking similarities between  $\Delta P_4$  variations at the three stations.

We show in Fig. 4,  $\Delta P_4$  on another day (17 February) for the same duration (i.e., 1200hr to 2400hr). It is evident from Fig 4, that no such similarities in  $\Delta P_4$  variations at the three stations as on 16 February during the eclipse period, occurred during the same or any other period. So Figs. 3 and 4 clearly indicate the presence of a pressure disturbance similar in nature at the three stations attributable

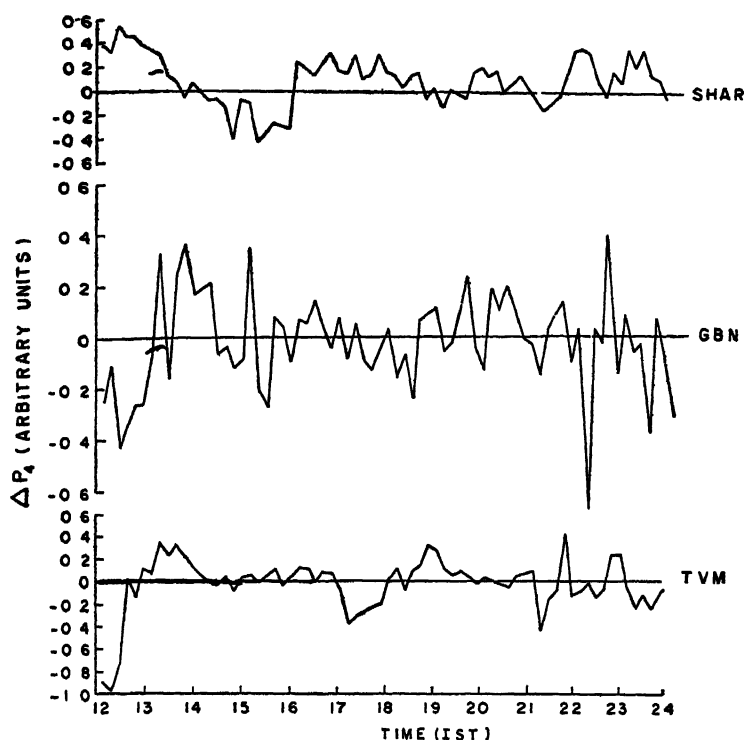
FIG 3  $\Delta P_4$  on 16 February 1980

to the eclipse effect. The residual  $\Delta P_2$  showed similar features as  $\Delta P_4$  on eclipse day and the normal day.

In order to establish on a quantitative basis the presence of pressure disturbance attributable to solar eclipse effect and to extract the common components present in the residual data at the three stations, statistical methods are applied. If such a disturbance is present, then the data should satisfy the following requirements on a quantitative basis:

- (1) Any disturbance due to the eclipse should be similar at all the three stations.
- (2) At each station, such a disturbance should not be present at any other time on the eclipse day and also on a reference day at the eclipse time.

In order to increase the number of data samples, the raw data are scaled at intervals of one minute for the period 1000hr to 2200hr on the eclipse day and for 1400hr to 1900hr on 17 and 18 February 1980 which serve as reference days. Using the harmonic coefficients determined for the respective days,  $\Delta P_4$  are obtained at

FIG 4  $\Delta P_4$  on 17 February 1980

one minute intervals for each of the days for the periods mentioned above. The  $\Delta P_4$  values thus obtained for the period 1000–2200hr on the eclipse day are divided into overlapping four hour segments with each successive segment shifted by one hour, like 1000–1400hr, 1100–1500hr, 1700–2100hr and 1800–2200hr. Cross correlograms for all the three station pairs (i.e.) TVM-GBN, GBN-SHAR and TVM-SHAR have been obtained for a total of +140 and –140 lags (1 lag = 1 min) for each of the segments. These are shown in Figs 5a and b for TVM-GBN, Figs 6a and b for GBN-SHAR, and Figs 7a and b for TVM-SHAR. For a station pair viz., TVM-GBN, positive lags mean TVM leading GBN and negative lags mean the other way. The total number of data samples in the cross correlograms is in the range of 240 to 100 corresponding to 0 to  $\pm 140$  lags.

The cross correlogram for 1000–1400hr (corresponding to a period prior to the eclipse) of TVM-GBN shows a trough-like structure with minimum around zero time lag while that of TVM-SHAR shows a linear trend starting from a positive correlation for negative lags to a negative correlation for positive lags. GBN-SHAR correlogram for the same period also shows a linear trend but with opposite slope to that of TVM-SHAR. As the time segment is shifted towards the 1400–1800hr segment which covers the eclipse period, not only the correlation builds up but also the correlogram patterns of the three pairs of stations become more and more similar. For the later time segments, the correlograms become gradually dissimilar to each other.

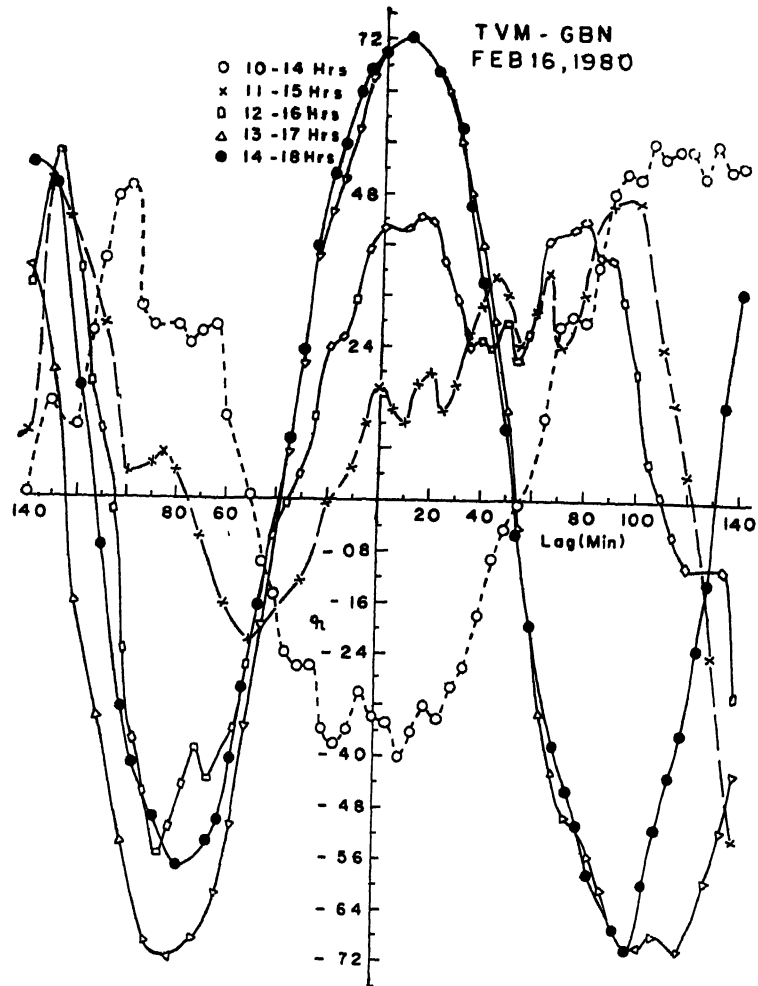


FIG 5a Cross correlograms for TVM-GBN for the first five segments

The correlograms in Figs. 5 to 7 clearly show that the correlations build up and exhibit similar patterns for all the three pairs of stations for the time segment 1400–1800hr (covering the eclipse period) compared to any other four hour segment (from 1000 to 2200hr). We show in Fig 8, cross correlograms on 17 February for the three station pairs for the segment 1400 to 1800hr. In striking contrast to the correlograms on the eclipse day for the segment 1400–1800hr, these show dissimilar patterns and also lower correlations. The correlations for the other reference day of 18 February 1980 for the period 1400–1800hr, also are dissimilar (not shown in the Figure) to each other.

The results of the correlation analysis described above are summarized in Table I for the time segment 1400–1800hr. In this we show the maximum correlation coefficients along with the corresponding time lags (delay) for both the residual series  $\Delta P_2$  and  $\Delta P_4$ .



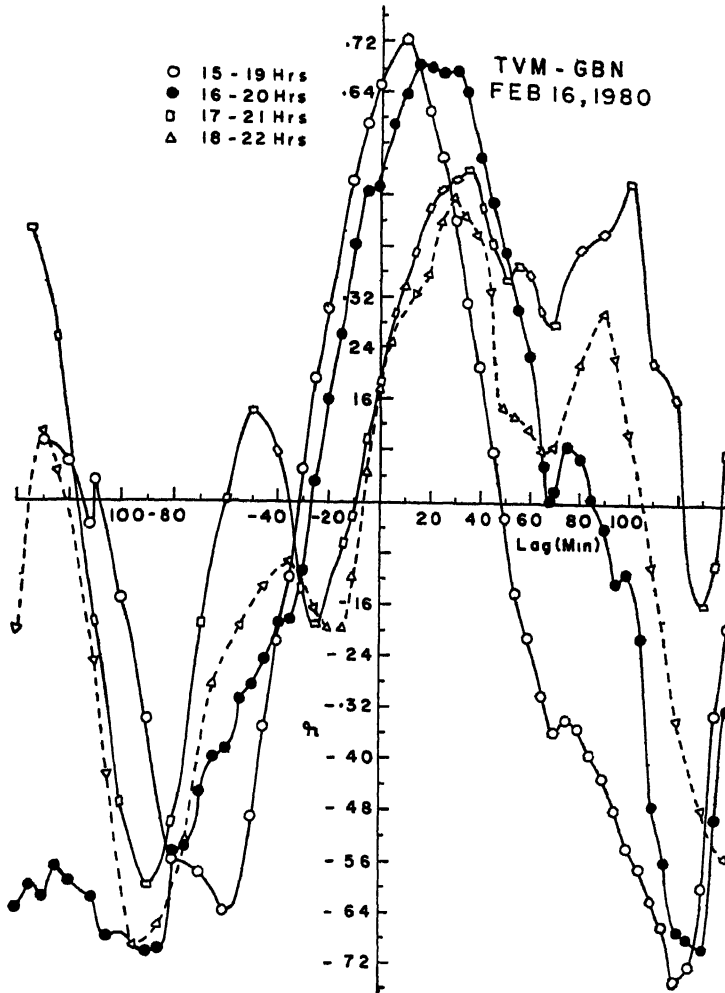


FIG 5b Cross correlograms for TVM-GBN for the last four segments.

Table I shows that the correlation coefficients are greater on 16 February for all the three station pairs for both  $\Delta P_2$  and  $\Delta P_4$  as compared to the corresponding coefficients on the other two days. There is very much less variability between the correlation coefficients obtained with  $\Delta P_2$  and  $\Delta P_4$  on 16 February, than on the other two days. Time delays obtained with  $\Delta P_2$  and  $\Delta P_4$  are in good agreement with each other on 16 February. In marked contrast, the delays obtained with  $\Delta P_2$  and  $\Delta P_4$  are very much different from each other on 17 and 18 February. It has also been found that the correlogram patterns for  $\Delta P_2$  and  $\Delta P_4$  are similar for a station pair on 16 February whereas they are quite different on the other two days.

Table I shows as described above that the correlations are quite consistent whether  $\Delta P_2$  or  $\Delta P_4$  is considered, on 16 February. The correlograms with  $\Delta P_2$  showed similar results as with  $\Delta P_4$ . This indicates that the strong correlations and

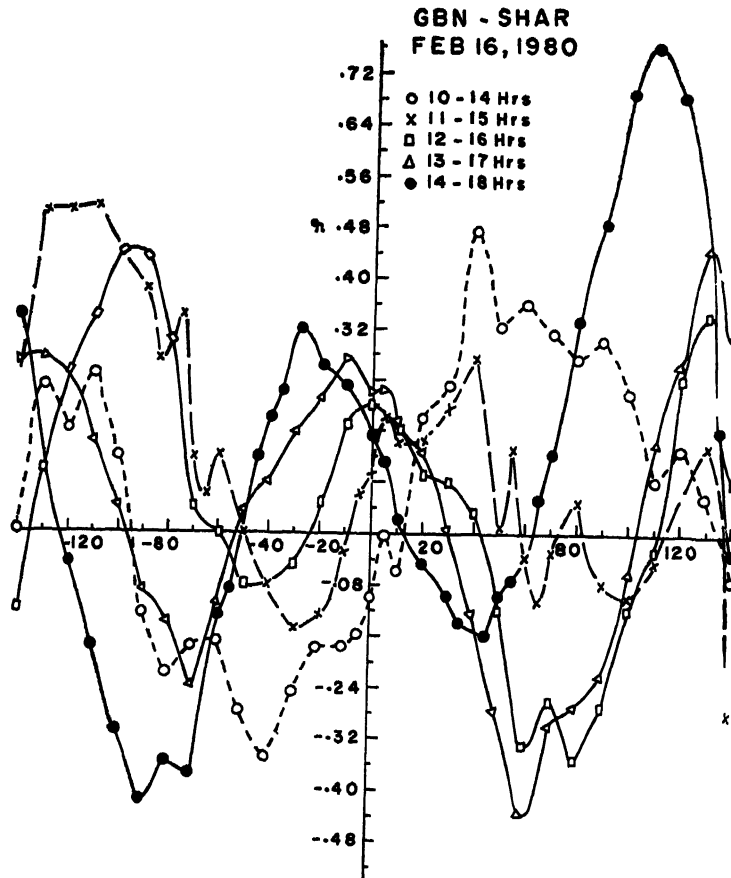


FIG 6a Cross correlograms for GBN-SHAR for the first five segments

TABLE I

Date	Stations Pair	Correlation coefficient ( $\Delta P_2$ )	Delay (Min) ( $\Delta P_2$ )	Correlation coefficient ( $\Delta P_4$ )	Delay (Min) ( $\Delta P_4$ )
16-2-80	TVM-GBN	0.87	+24	0.71	+11
	TVM-SHAR	0.75	+150	0.50	+116
	GBN-SHAR	0.71	+129	0.82	+113
17-2-80	TVM-GBN	0.38	+137	0.45	-8
	TVM-SHAR	0.80	+195	0.50	+134
	GBN-SHAR	0.42	+180	0.50	-8
18-2-80	TVM-GBN	0.52	-117	0.63	-77
	TVM-SHAR	0.59	+49	0.42	+45
	GBN-SHAR	0.37	-189	0.62	+112

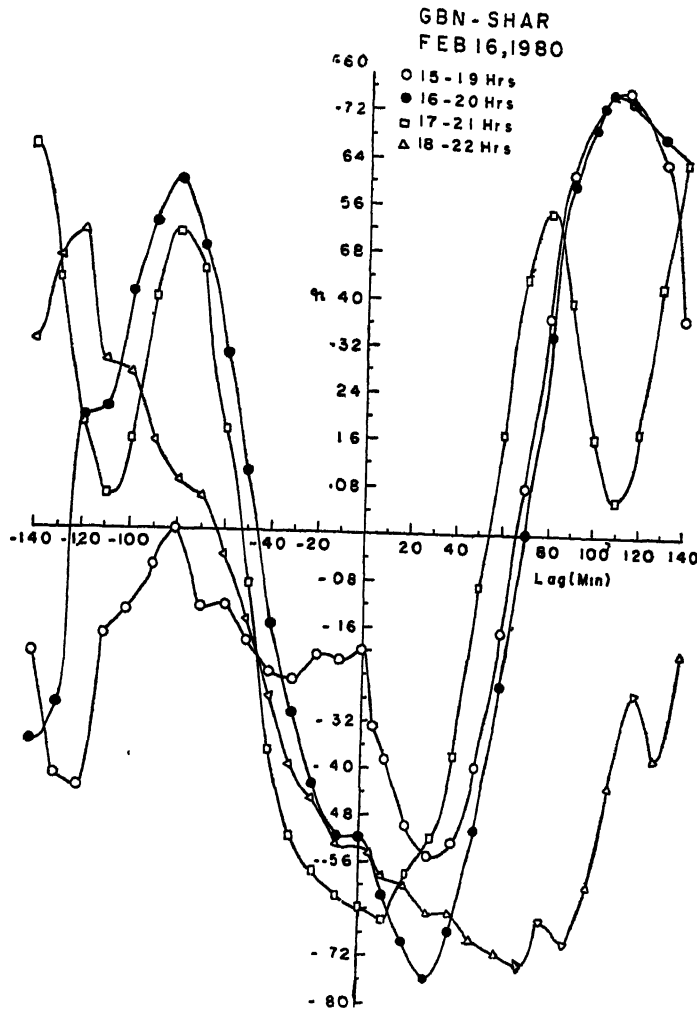


FIG 6b Cross correlograms for GBN-SHAR for the last four segments

the similar patterns of correlograms are due to a real effect present in the data but not due to any spurious variations introduced in  $\Delta P_2$  or  $\Delta P_4$  because of any possible discontinuities or, absence for a short period, of the harmonic components determined by the harmonic analysis

All the statistical analyses described above, establish beyond any reasonable doubt that a pressure disturbance which is similar in pattern at all the three stations is indeed presented during the period covering the eclipse on 16 February 1980. We subjected the residual data  $\Delta P_4$  for the period 1400–1815hr (making the number of samples as 256) to FFT analysis in order to obtain the spectral composition of the disturbance. Here again, we divided the data covering the eclipse period into overlapping segments of 128 minutes (having 128 data samples) with each segment shifted by 30 minutes starting from 1400hr and the last segment ending at 1807hr

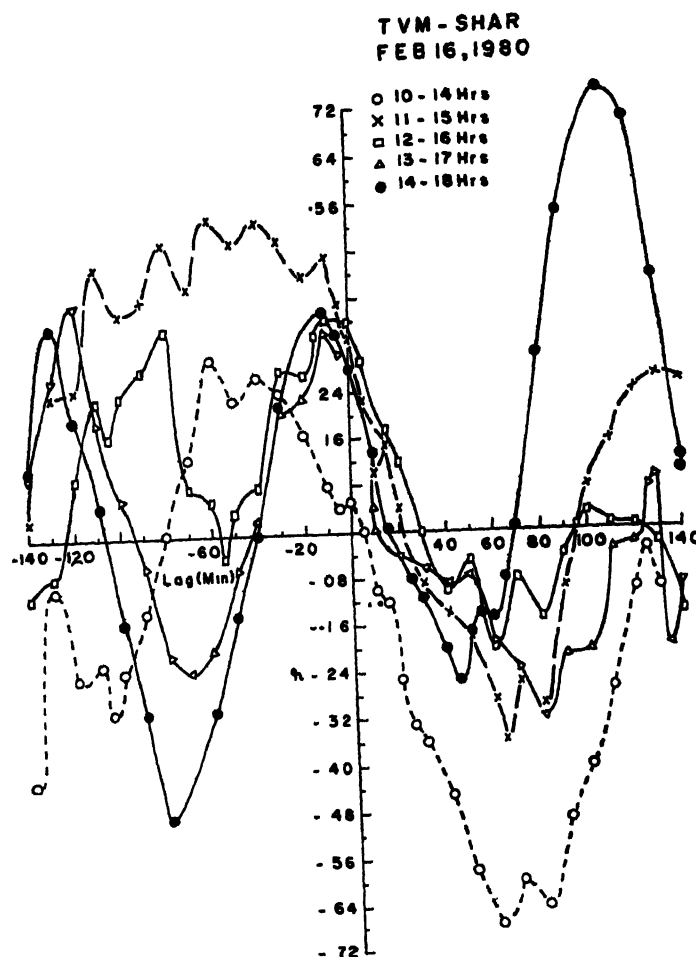


FIG 7a Cross correlograms for TVM-SHAR for the first five segments.

The reason for this again is that the individual wave components may not be present throughout the length of the data (in fact, the disturbance starts only after the first contact of the eclipse). Though, we lose information on longer periods than 128min by this segmenting, the information on the shorter period waves would be quite reliable. Before subjecting to FFT, the data have been detrended by linear regression method.

The amplitudes of the spectral components are converted to powers. The power spectra thus obtained, of the 5 data segments are averaged. The average power spectra for the three stations, TVM, GBN and SHAR are shown in Fig. 9 and the power spectra for the entire data segment from 1400-1816hr IST are shown in Fig. 10. Because of the smaller data length, the average spectra (Fig 9) have less resolution than the one for entire data length (Fig 10).

In both the power spectra (Figs. 9 & 10) for all the three stations, the 128min component stands out very prominently over other components. This clearly indi-

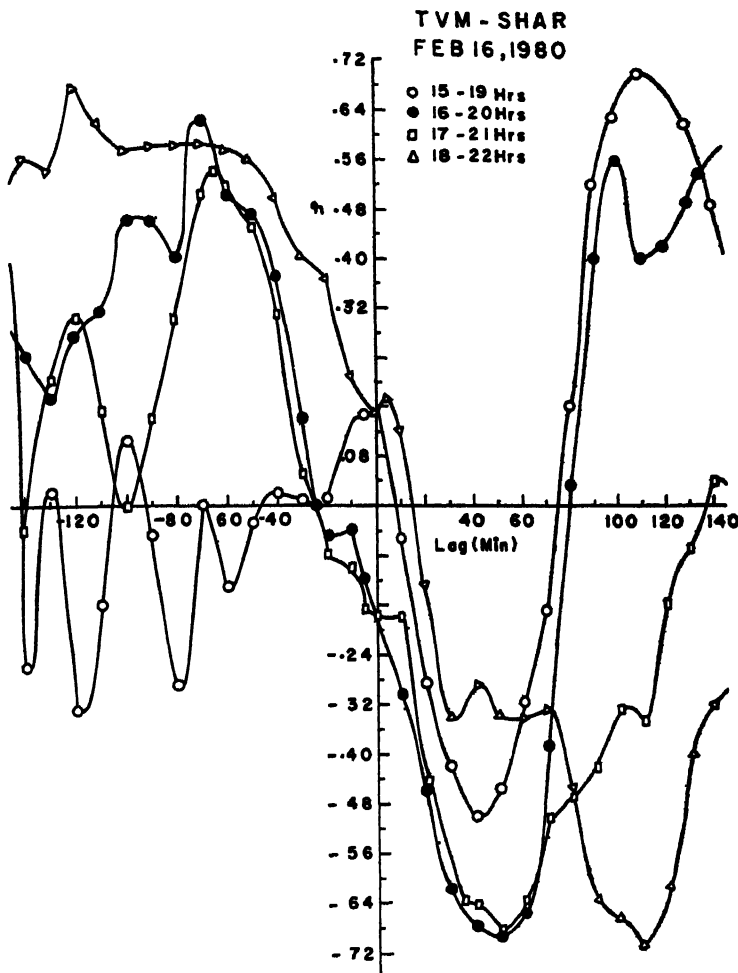


FIG 7b Cross correlograms for TVM-SHAR for the last four segments

cates the reality of this component. A peak around 16min is shown in Fig. 10 for all the three stations. In Fig. 9 also this peak is shown but with a little shift for GBN. The 32min component which is indicated in Fig. 9, is present only for TVM and GBN in Fig. 10. Except these, no other significant component appeared at all the three or at least two stations either in the averaged (Fig. 9) or the total data (Fig. 10) spectra. This means that the eclipse induced pressure disturbance mainly consists of 128min, 32min and 16min components.

#### DISCUSSION

The foregoing results establish unambiguously the presence of eclipse induced pressure disturbances on 16 February 1980. Spectral analysis revealed the presence of a strong 128min component and weaker 32 and 16min components. From the sensor

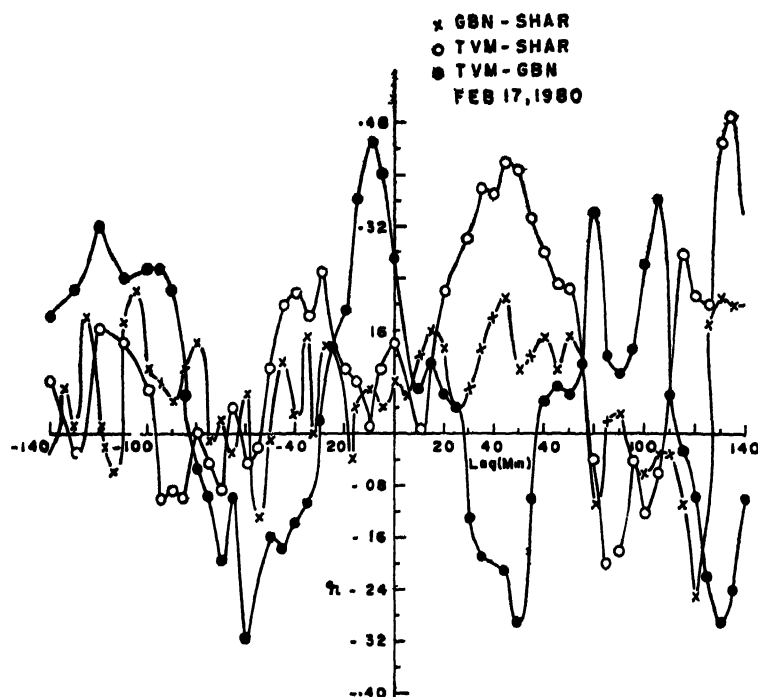


FIG 8 Cross correlograms for TVM-GBN, GBN SHAR and SHAR-TVM for the period 1400-1800hr on 17 February 1980.

calibration, the amplitude of the pressure disturbance as shown in Fig. 3 (average of positive and negative peaks) is estimated as  $500\mu\text{b}$  (approx) for TVM and GBN and  $400\mu\text{b}$  (approx) for SHAR, taking that the disturbance is mainly composed of 128min component

Anderson *et al* (1972) reported ground pressure changes during the 7 March 1970 solar eclipse. The peak to peak amplitude of the main perturbation was about  $750\mu\text{b}$ . Spectral analysis showed a dominant 89min component with  $250\mu\text{b}$  amplitude followed by shorter periods upto 12.3 min with amplitudes less than one fourth of the 89 min component. Anderson *et al* presented a summary of earlier observations which, in general, indicate the occurrence of pressure perturbations with amplitudes ranging from 100 to  $450\mu\text{b}$ , associated with solar eclipses. Later, observations by Jones and Bogart (1975) in northern Kenya and Anderson and Keefer (1975) in Chinguetti, Mauritania, during the 30 June 1973 solar eclipse, produced null results. Both these observing sites are situated near the path of totality. Anderson and Keefer attributed the null result to local weather conditions. Observations by Jones (1976) at two sites situated at a range of about 2500km from the centre of the eclipse path, during the 86 per cent solar eclipse of 11 May 1975 indicated the occurrence of pressure perturbations.

So far, all the observed pressure perturbations (including the results of the present investigation) point to a large amplitude of a few hundreds of microbars ( $100\text{--}500\mu\text{b}$ ) and periods in the range of about 1-2 hours. The amplitude is much

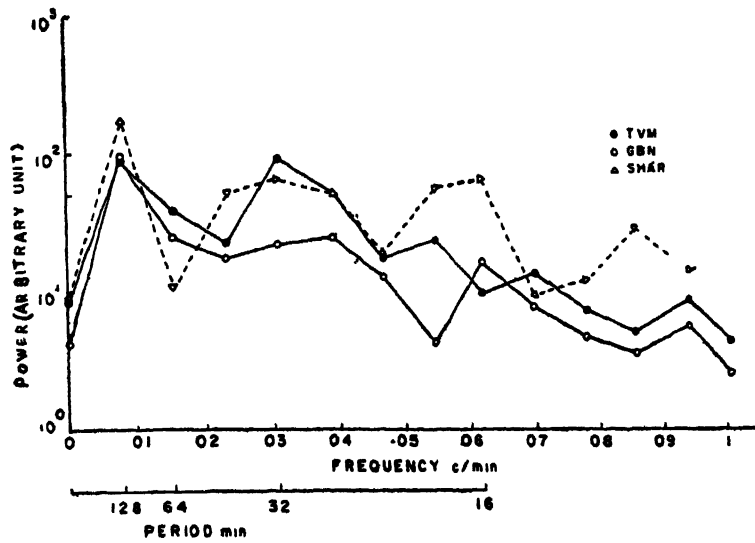


FIG. 9 Average power spectrum.

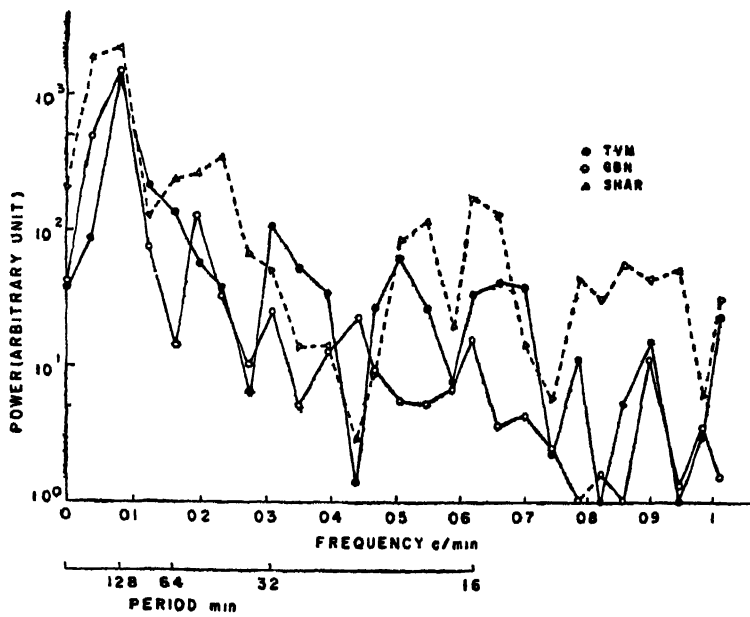


FIG. 10 Power spectrum for the period 1400-1815hr

above the predicted one due to the ozonosphere source Chimonas (1973) invoked tropospheric water vapour source to explain the large amplitude of the pressure perturbations due to solar eclipse. He showed that Lamb waves generated by the cooling of tropospheric water vapour and the supersonic movement of the cooled region, would be generating perturbation amplitudes of about  $300\mu\text{b}$ . He considered the contribution due to internal gravity waves from tropospheric water vapour source to be insignificant because of the constraints on the source volume. He also showed that significant internal gravity waves would not be generated due to the tropospheric source unless the modulus of their vertical wave number is greater than

$$(1 - \gamma/2)g/c^2$$

where  $\gamma$  is the ratio of specific heats,  $g$  is the acceleration due to gravity and  $c$  is the sound speed.

The present observations as well as the earlier ones reported by others lend support to the Lamb wave hypothesis of Chimonas (1973) as far as the observed amplitudes are concerned. Final confirmation of this and establishment of inadequacy of internal gravity wave source to explain the observed features can come through observations on propagation characteristics of the perturbations.

The three observation sites in the present investigation are located in the penumbral region of the eclipse. The obscuration areas at TVM, GBN and SHAR are 80, 93 and 91 per cent respectively, of the area of the solar disc. It is quite reasonable to consider that the tropospheric source region extends upto about 0.5 obscuration, in which case all the three stations are in the source region. (It may be noted that TVM has generally high humidity levels, compensating for the smaller area of obscuration). Because of this, the disturbance patterns would not be fully developed. In the case of stations situated in the far field zone of the source region one would observe fully developed patterns. Thus, time delays between similar wave components at the three stations (which can be obtained from the phase information in FFT analysis) or the time delays in the cross correlograms cannot be interpreted as propagation time delays for estimating the speed and wavelength of the wave components or the disturbance. For this, the stations need to be situated in the far field zone. But, in this case there is a risk of attenuation and/or modification of the wave components by orographic features during the propagation over long distances. In fact, some of the earlier observations at locations far away from the source, which produced null results, might have suffered from this drawback apart from the distinct possibility of lack of sufficient tropospheric water vapour over the eclipse path.

#### REFERENCES

- Anderson, R. C., and Keefer, D. R. (1975) Observations of the temperature and pressure changes during the 30 June 1973 solar eclipse. *J. atm. Sci.*, **32**, 228–231.
- Anderson, R. C., Keefer, D. R., and Myers, O. E. (1972) Atmospheric pressure and temperature changes during the 7 March 1970 solar eclipse. *J. atm. Sci.*, **29**, 583–587.
- Butcher, E. C., Downing, A. M., and Cole, K. D. (1978) Wave-like variations in the F-region in the path of totality of the eclipse of October 23, 1976. *J. atm. terr. Phys.*, **41**, 439–444.
- Chimonas, G. (1970) Internal gravity-wave motions induced in the earth's atmosphere by a solar eclipse. *J. geophys. Res.*, **75**, 5545–5551.
- (1973) Lamb waves generated by the 1970 solar eclipse. *Planet. Space Sci.*, **21**, 1843–1854.



- Chimonas, G , and Hines, C O (1970) Atmospheric gravity waves induced by a solar eclipse. *J. geophys Res* , 75,
- Davies, M J., and da Rosa, A V (1970) Possible detection of atmospheric gravity waves generated by the solar eclipse *Nature*, 226, 1123.
- Fehr, V., and Gazley, Jr. C (1967) Theoretical evaluation of an oscillating mass flow in the modified Moore variometer configuration. *Rev scient Instrum* , 38, 1502-1507.
- Jones, B. W. (1976) A search for Lamb waves generated by the solar eclipse of 11 May 1975. *J. atm. terr Phys.*, 33, 1820-1823
- Jones, B W., and Bogart, R. S. (1975) Eclipse induced atmospheric gravity waves. *J. atm terr. Phys* , 37, 1223-1226.
- Vaidyanathan, S , Raghava Reddi, C , and Krishna Murthy, B. V (1978) Quasi-periodic fluctuations in electron content during a partial solar eclipse. *Nature*, 271, 41.

Printed in India

Atmospheric Boundary Layer

## BOUNDARY LAYER STUDIES CONDUCTED AT GADAG DURING THE TOTAL SOLAR ECLIPSE OF 16 FEBRUARY 1980

KALIPADA CHATTERJEE, C. K. CHANDRASEKHARAN\* and V P VERMA

*Instruments Division, India Meteorological Department, New Delhi, India*

*(Received 21 July 1982)*

Special meteorological observations during the period covering total solar eclipse of 16 February 1980 were arranged at Gadag (Lat 15°24'N, Long 75°38'E) which lay in the path of totality of the eclipse to study the changes occurring in the lower boundary layer. Wind speed, wind direction, temperature and humidity instruments were installed on a micro meteorological tower at four levels 1.2m, 3.3m, 6.5m and 13.5m meter above ground and the observations were continuously recorded on strip chart recorders. The results of these observations are presented in this paper.

**Keywords:** Atmospheric Boundary Layer; Meteorological Parameters; Micro-meteorological Tower; Temperature & Wind Sensors; Wind-vane

### INTRODUCTION

DURING the total solar eclipse of 16 February 1980 India Meteorological Department arranged for special observations at all the existing observatories in or near the path of totality. Two expedition teams also organised and established special observation stations at Gadag and Raichur, where a comprehensive observations programme was mounted to study the effect of the total solar eclipse on the meteorological parameters, especially those in the earth's immediate boundary layer. The present paper deals with the micro-meteorological observations conducted at Gadag on 15, 16 and 17 February 1980 near the earth's planetary boundary layer.

### INSTRUMENTATION

A micro-meteorological tower was set up in an open field free from obstructions in the J T College campus, Gadag, where the India Meteorological Department had set up various experiments during the total solar eclipse expedition (Fig 1).

Temperature sensors (D.B. & W.B.) were installed at four levels, viz 1.2m, 3.3m, 6.5m and 13.5 metres above ground on the micro-meteorological tower. The sensors used were YSI thermistor composite which produces a linear resistance ( $R_T$ ) change with temperature and have the following specifications

$$R_T = (-32.402) T \pm 4593.39, T \text{ in } ^\circ\text{C}$$

$$\text{Thermistor absolute accuracy and interchangeability} = \pm 0.15 ^\circ\text{C}$$

---

\*IMD, Pune

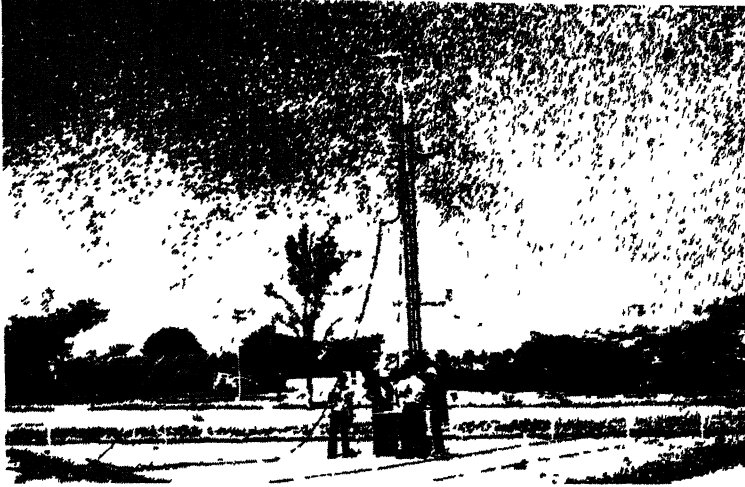
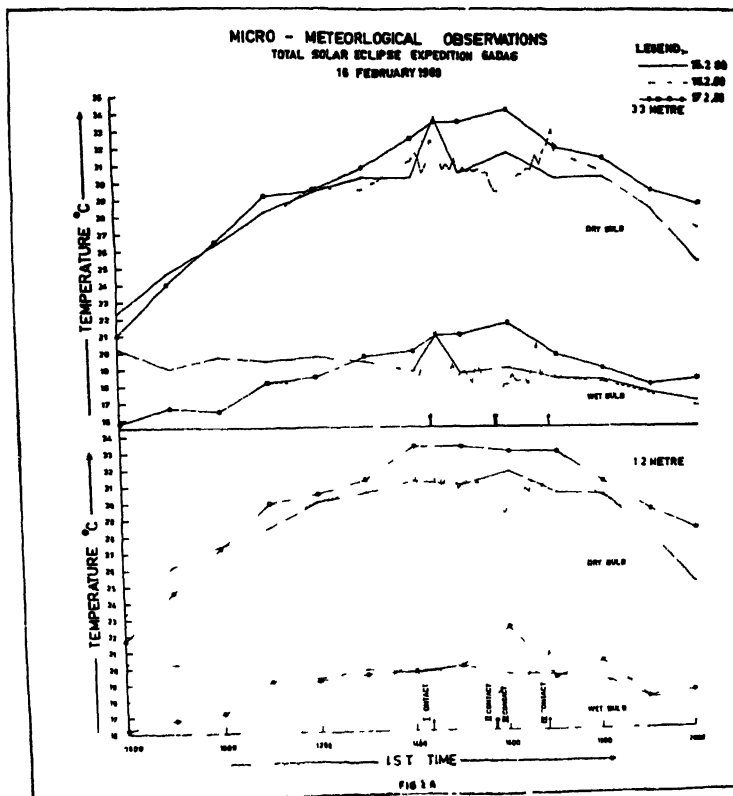


FIG. 1.



FIG, 2A

Linearity deviation  $= \pm 2.11$  ohms  
 Sensitivity  $= 32\,402$  ohms/°C

Time constant The time required for the thermistor to indicate 63 per cent of a new impressed temperature, in free air, 10sec.

In order that the thermistor thermometers would measure the true air temperature, the sensors were housed in louvred radiation shields made out of polished, anodised aluminium and mounted on bracket arms at the appropriate heights. The output of the thermistors after amplification were recorded continuously on separate strip chart galvanometric recorders 0–1mÅ full scale deflection with internal impedance of 1.5K ohms. The chart speed was 60mm/hr. On the temperature scale, each division of 2mm width corresponded to 0.5 °C and it was possible to read the temperature values correct to 0.2 °C.

Wind sensors were also installed on the same micrometeorological tower at 1.2m and 13.5m above the ground. The wind sensors consisted of specially designed

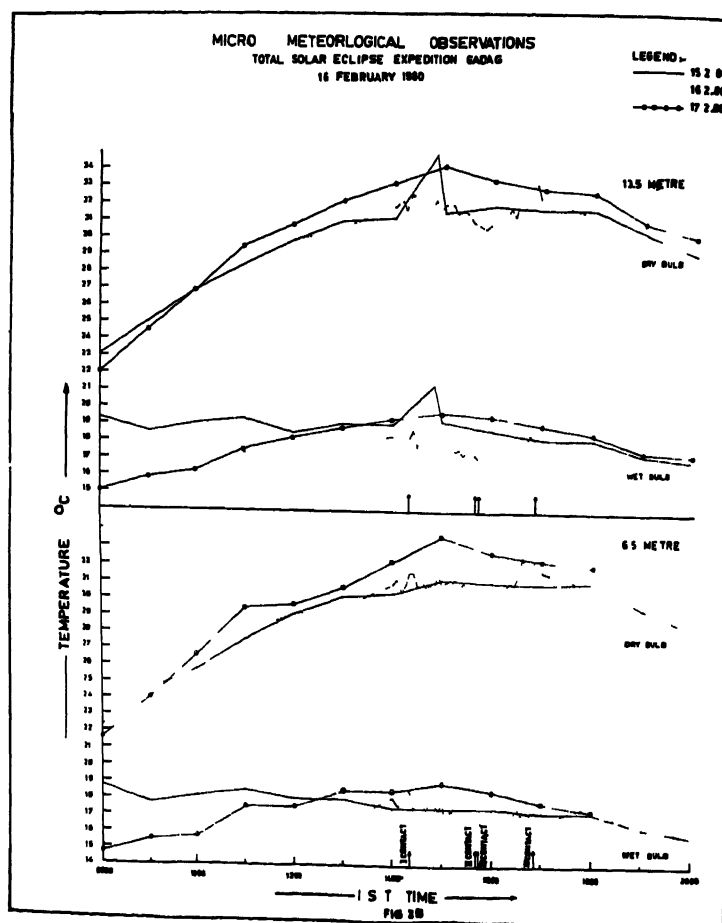


FIG. 2B

and laboratory tested photo-electric anemometers and potentiometric wind vanes. The anemometers were provided with very light weight cups mounted on a frictionless shaft and the threshold speed was found to be 0.3 kt. The speed sensing was made using infrared L.E.D. with infrared solid state copper detector, thus reducing the magnetic drag normally present in a cup-generator type anemometer. The anemometer output was suitably amplified by a solid state amplifier and recorded on a strip chart galvanometric recorder.

The potentiometric wind-vane consisted of a very low torque (3 gm cm) continuously variable potentiometer coupled to a geared output of 1:2. The wind direction record was also obtained continuously on the strip chart recorder.

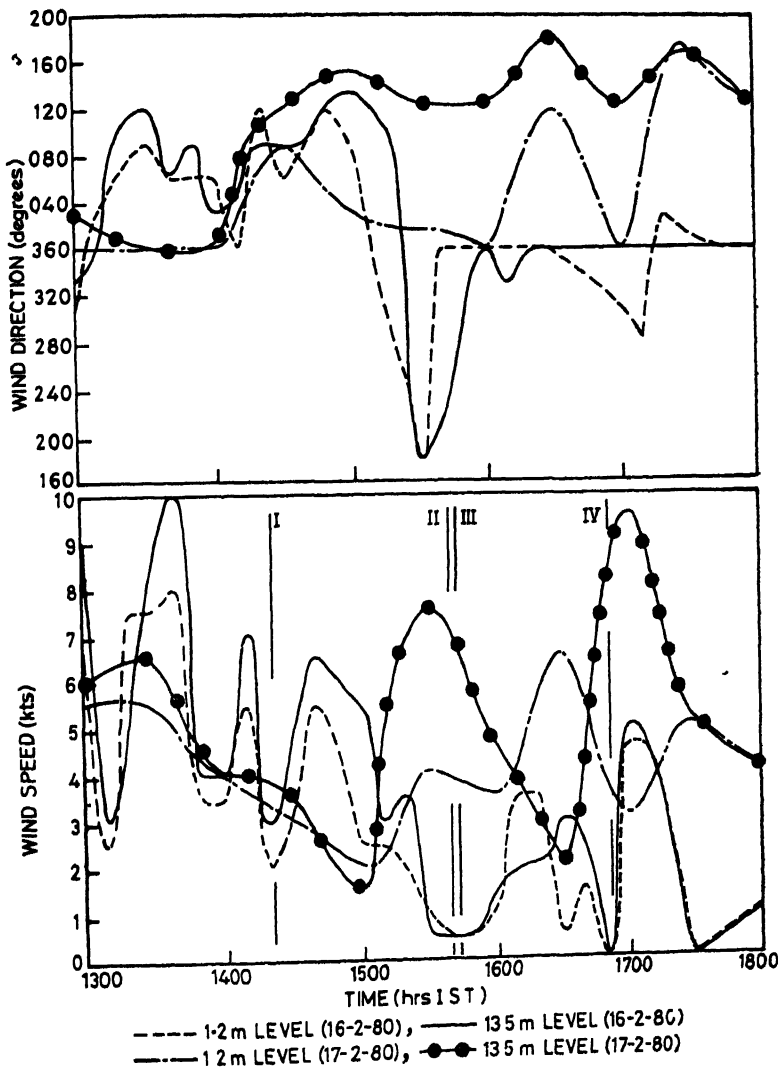


FIG 3.

## DATA

Dry bulb and wet bulb temperature as recorded at levels 1.2m, 3.3m, 6.5m and 13.5 meters of the micro-meteorological tower have been plotted in Fig 2A, 2B, 3 & 4 for 15, 16 and 17 February 1980. Wind data of 16 and 17 February 1980 from 1.2m and 13.5m levels have been plotted in Fig 3.

VERTICAL PROFILES OF TEMPERATURE  
FROM MICROMET TOWER, (GADAG)  
16 FEBRUARY 1980

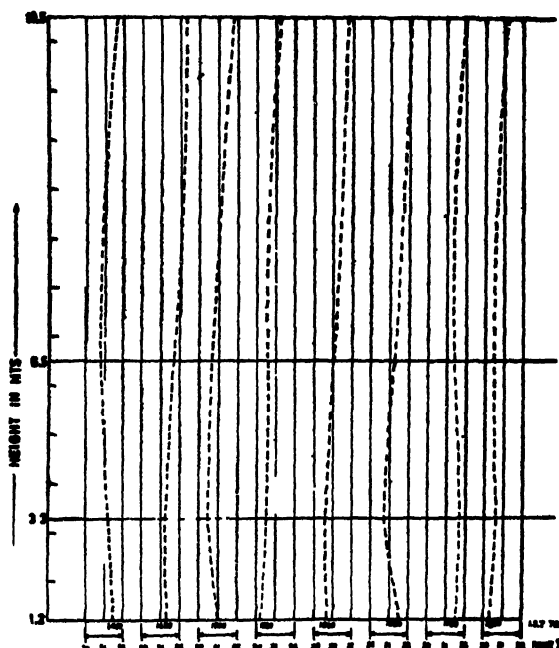


FIG 4

Vertical profile of temperatures as observed from Micro-Meteorological tower at Gadag for 16 February 1980 have been plotted in Fig 4 to enable a detailed study of temperature variation in the vertical, during the eclipse

## DISCUSSION

Analysis of micromet data in Figs. 2A and 2B reveals the following salient features

- (i) At all levels both the Dry bulb and Wet bulb temperatures were lower on the 16 February 1980 during the entire duration of eclipse than on the 15 and 17 February 1980 during the same time over Gadag
- (ii) The maximum fall of both the Dry bulb and Wet bulb temperatures have been recorded at all levels of the tower on 16 February 1980 few minutes after the 3rd contact over Gadag

Fig. 4 gives the vertical profile of air temperature at 30 minutes interval between 1400hr and 1800hr on the 16 February as recorded by the micrometeorological tower at Gadag. It is interesting to note that during the period of eclipse temperature inversion was noticed upto 1800hr IST as tabulated below (Table I):

TABLE I

Time in IST	Height of base inversion layer (in meter)	Thickness		$(t_2 - t_1)$ = $\Delta t$
		From ( $h_1$ ) (metre)	To ( $h_2$ ) (metre)	
1400	6.5	6.5	13.5	$(31.7 - 30.7) = 1.0^\circ\text{C}$
1430	3.3	3.3	13.5	$(32.3 - 31.2) = 1.1^\circ\text{C}$
1500	3.3	3.3	13.5	$(31.8 - 30.4) = 1.3^\circ\text{C}$
1530	1.2	1.2	13.5	$(31.2 - 30.2) = 1.0^\circ\text{C}$
1600	3.3	3.3	13.5	$(30.8 - 29.6) = 1.2^\circ\text{C}$
1630	3.3	3.3	13.5	$(32.1 - 30.7) = 1.4^\circ\text{C}$
1700 (i)	1.2	1.2	3.3	$(31.7 - 31.5) = 0.2^\circ\text{C}$
(u)	6.5	6.5	13.5	$(32.0 - 31.4) = 0.6^\circ\text{C}$
1800 (i)	1.2	1.2	3.3	$(30.6 - 30.3) = 0.3^\circ\text{C}$
(u)	6.5	6.5	13.5	$(31.2 - 30.5) = 0.7^\circ\text{C}$

\*  $t_1$  = temperature corresponds to  $h_1$

$t_2$  = temperature corresponds to  $h_2$

The maximum temperature inversion of  $1.4^\circ\text{C}$  occurred at 16.30hr. The height of the base of the inversion was at 3.3 meters above the ground.

From the above table it is also noticed that the height of the base of inversions was gradually lowered from 6.5 to practically near the surface 1700hr and at 1800hr it showed double inversions between 1.2m and 13.5m levels.

Another special feature that is prominent in the micro-meteorological observations is that with the progress of the eclipse, the winds became lighter and died down to almost a dead calm at the time of totality. The wind speed and direction at 1.2m and 13.5m on 16 February 1980 are shown in Fig. 3. The wind data on a typical day 17 February 1980 are also shown for comparison. The stillness resulted in damping of all mixing processes in the earth's planetary boundary layer.

#### ACKNOWLEDGEMENTS

The authors express their grateful thanks to Dr P. K. Das, F.N.A., Director-General of Meteorology, for providing the facilities and for communicating the paper.

The authors are also thankful to Shri S. K. Das, Additional Director-General of Meteorology (Instruments) for his guidance and valuable suggestions during the preparation of this paper.

Printed in India

**Shadow Bands**

**PHOTOELECTRIC OBSERVATIONS OF SHADOW BANDS DURING  
16 FEBRUARY 1980 TOTAL SOLAR ECLIPSE FROM  
JAPAL-RANGAPUR OBSERVATORY**

A. BHATNAGAR, D B JADHAV, R M. JAIN\*, R N SHELKE and S P PUROHIT

*Vedhshala Udaipur Solar Observatory, Udaipur, India*

*and*

R V BHONSLE and R. PRATAP

*Physical Research Laboratory, Ahmedabad, India*

*(Received 27 September 1981)*

Intensity fluctuations of shadow bands observed photoelectrically during total solar eclipse of 16 February 1980 are reported. Power spectrum analysis indicates that significant power appears at frequencies 0.32 and 0.58 Hz, thus corresponds to periods of 3 and 1.7 seconds.

**Keywords** Shadow Bands; Photoelectrics; Power Spectrum Analysis

**INTRODUCTION**

DURING the total solar eclipse of 16 February 1980, an experiment was conducted to determine the period and intensity fluctuations due to the shadow bands, from Japal-Rangapur Observatory campus.

Just before the totality, conspicuous bright and dark bands have been observed moving on the ground, these are called the shadow-bands and are known to travel randomly at high speed. Several attempts have been made in the past to photograph these shadow bands, but due to high speed and low light level, it has not been possible to photograph them, except for one photographic record on the wings of an aircraft. Our attempt was to measure the light fluctuations using photo cells and recording at high speed.

**EXPERIMENTAL AND RESULTS**

Three photocells were placed on the ground to form an equilateral triangle, each separated by about 18-inch apart and were connected to a four channel fast-strip chart recorder, with a high gain built-in amplifier. The sensitivity of the built-in amplifier was kept at 100 millivolts/cm and the response frequency of the recorder

---

\* Presented by R. M. Jain



was 50Hz. A chart speed of 50mm per second was used to record the shadow band intensity fluctuations. Out of the three channels one performed very well, while the other two did not work. A record of the light intensity variation is shown in Fig. 1. From the photoelectric tracing it appears that the intensity fluctuations due to bands started at 15 45 47 IST and ended nearly 2 seconds before the beginning of the totality. Each peak in this record corresponds to bright ribbon of shadow bands.

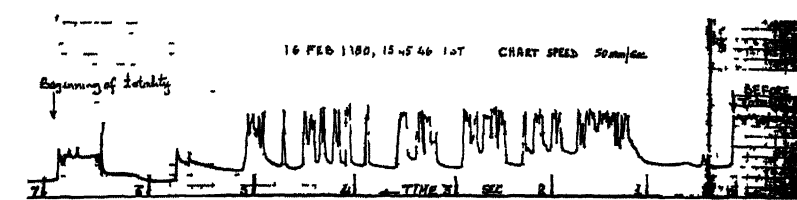


FIG 1 Photoelectric tracing of intensity fluctuations of shadow bands

Fig 2 shows power spectrum of the intensity variations using the Maximum Entropy Method (MEM). This analysis indicates that significant power appears at frequencies 0.32 and 0.58Hz, thus giving the period of intensity fluctuations of shadow bands as 3 and 1.7 seconds. The peaks other than frequencies at 0.32 and 0.58Hz are neglected because of their extremely low power. MEM analysis also indicates that the power spectrum is non-Gaussian.

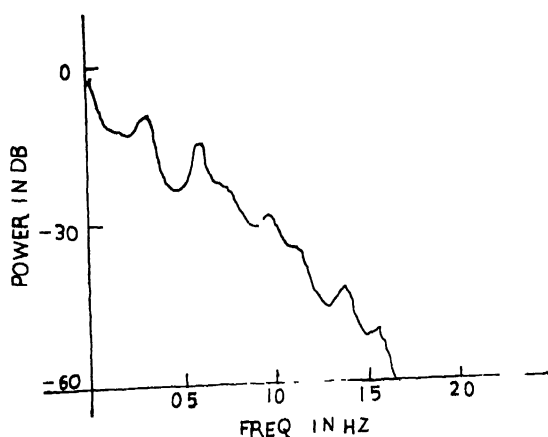


FIG 2 Power spectrum of the intensity variations of shadow bands

Visual observations by several observers at Rangapur indicate that the shadow bands were wavy in appearance and travelled extremely fast from north-west direction and were separated approximately by about 8 to 12 inches. The bands were quite conspicuously visible on dull brownish gravel ground and also on white surfaces.

## ACKNOWLEDGEMENTS

The financial support for this total solar eclipse experiment was given by the Department of Space, under the RESPOND programme. Our thanks are also to Professor K D Abhyankar for generously providing all facilities at the Japal-Rangapur Observatory and to M/s Digital Electronics Limited, Bombay for providing a fast strip chart recorder for the eclipse experiment

Printed in India

Atmospheric Electricity

## VARIATIONS IN ATMOSPHERIC ELECTRICAL PARAMETERS DURING SOLAR ECLIPSE\*

S. NIZAMUDDIN, R. RAMANADHAM and A. M. RAO

*Department of Meteorology and Oceanography, Andhra University, Waltair, India*

M. K. KHERA, B. A. MAKHDOUNI, A. R. RAFIQUI, B. N. RAINA and  
VENKATANARAYANA REDDY MUKKU

*Post-Graduate Department of Physics, Kashmir University, Srinagar, India*

and

R. K. GOEL, P. P. PATHAK, J. RAI and N. C. VARSHNEYA

*Physics Department, University of Roorkee, Roorkee-247 672, India*

(Received 18 July 1981)

Results of solar eclipse observations conducted at Nagarampalam near Vishakhapattanam ( $\lambda=77^{\circ}23'N$ ,  $\psi=148^{\circ}65'E$  Geomagnetic) are presented. Observed variations in atmospheric conductivities, potential gradient and air earth current are explained by correlating them with the variations in solar wind flux on earth (as a result of eclipse by moon) and the resulting change in atmospheric ionization. Observations by previous workers, of a different pattern of variation in conductivity during solar eclipse of high latitudes, have also been explained on the same theoretical basis. While there are marked solar eclipse changes in the atmospheric electrical parameters, no definite effects on meteorological parameters have been observed.

**Keywords:** Atmospheric Electricity; Sun-Weather Relationship; Solar Activity; Cosmic Rays; Thunderstorm Activity

### INTRODUCTION

ATMOSPHERIC electrical parameters were continuously recorded during the total solar eclipse of 16 February 1980. The aim was to obtain a definite view concerning the effect of the eclipse on these parameters. Both the polar conductivities of atmosphere, potential gradient and the air-earth current alongwith the meteorological parameters were recorded continuously for three days i.e., on 15, 16 and 17 February 1980. Here we describe the main features of experimental set-up, the site of observations and a theoretical explanation for the observed variations in these parameters.

---

\* Presented by J. Rai

## EXPERIMENTAL SITE AND INSTRUMENTS

For these observations an open space, free from trees etc, was chosen to avoid any type of interference. The nearest trees were at a distance of more than 500m from the sensors and antennas. The site was chosen near the Radio Physics Observatory of Andhra University, Waltair, situated at Nagarampalam, about 15km from the University campus. All the effects of sea breeze and land breeze could also be observed as the site was not far from the sea coast.

The negative and positive conductivities were measured by two Gerdian Chambers (see Fig 1) of critical mobility  $3 \times 10^{-4} \text{ m}^2 \text{ v}^{-1} \text{ s}^{-1}$  (i.e., all the ions below this mobility could be caught by the central cylinder to contribute to current). The air was sucked at the rate of  $1 \text{ ms}^{-1}$ . Current signal, amplified by electrometer, was recorded on a chart recorder. The air-earth current was collected by  $1 \text{ m}^2$  circular

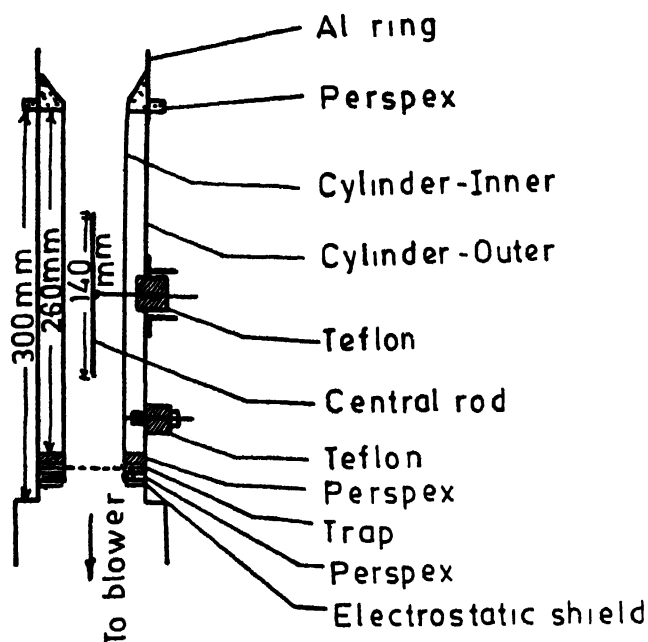


FIG 1 Vertical Section through Gerdian apparatus tube

aluminium plate with a capacitor shunted across the high resistance of electrometer which gave a time constant of about 9min, as suggested by Kasemir (1955), to remove the displacement currents. The potential gradient was measured by the passive antenna (Figs 2 and 3) as described by Crezier (1963).

Alongwith these electrical parameters, the meteorological elements, like wind speed and its direction, temperature and humidity were also recorded with appropriate recorders.

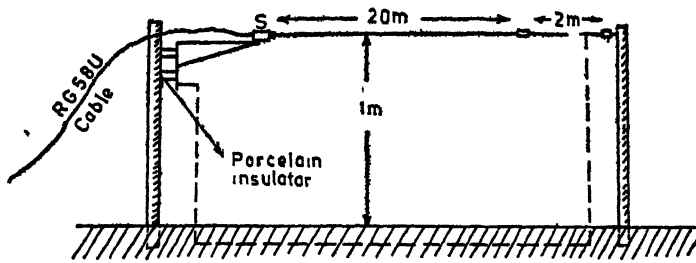


FIG. 2 Field installation of passive antenna.

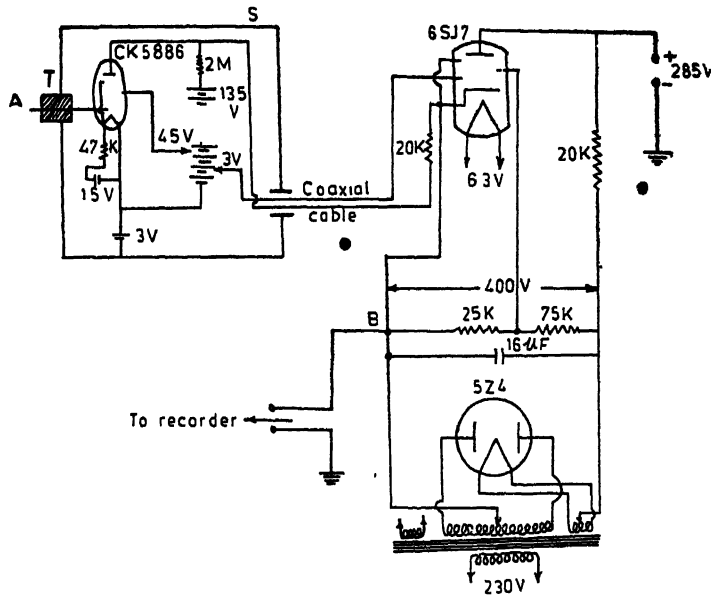


FIG. 3 Circuit diagram of sensing unit for potential gradient by passive antenna.

### OBSERVATIONS AND INTERPRETATIONS

The observed variations in the electrical parameters are shown in Figs 4-7. Figs. 4 and 5 show the increase in polar conductivities which become maximum at the time of maximum phase of the eclipse (0 95). This increase can be attributed to the solar wind particles. During the eclipse, the moon obstructs the passage of solar wind particles coming towards the earth. The decrease in the flux of these particles (this flux modifies the earth's magnetic field) results in an increase of cosmic ray intensity at low latitudes and hence in the increase of ionisation at these latitudes. This enhancement of ionisation becomes wholly responsible for increase in polar conductivities. Naturally, the increase should record itself with the first contact of the eclipse and should peak at the maximum phase, with a time lag corresponding to the atmospheric relaxation time. At the high latitudes on the other hand, the atmospheric ionization has a

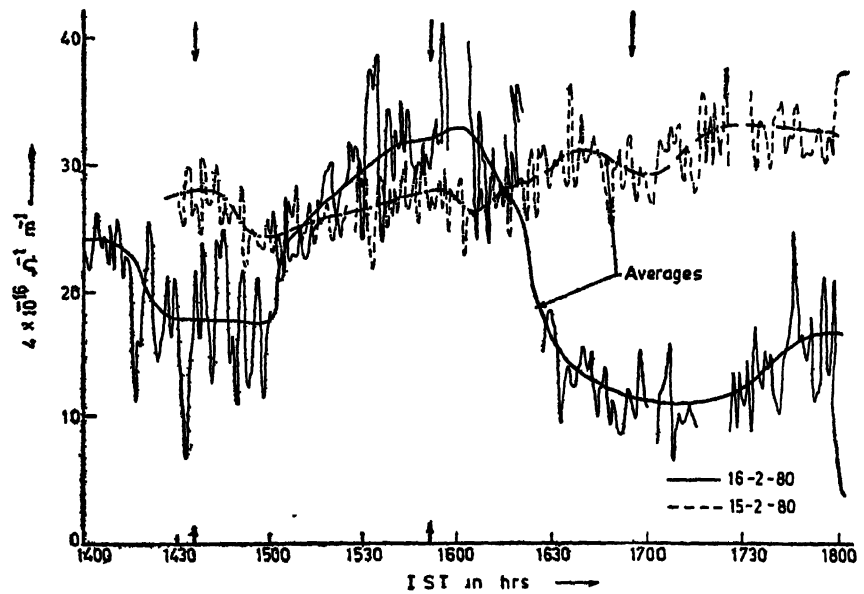


Fig 4 Variation of positive conductivity during eclipse and on previous day for comparison.

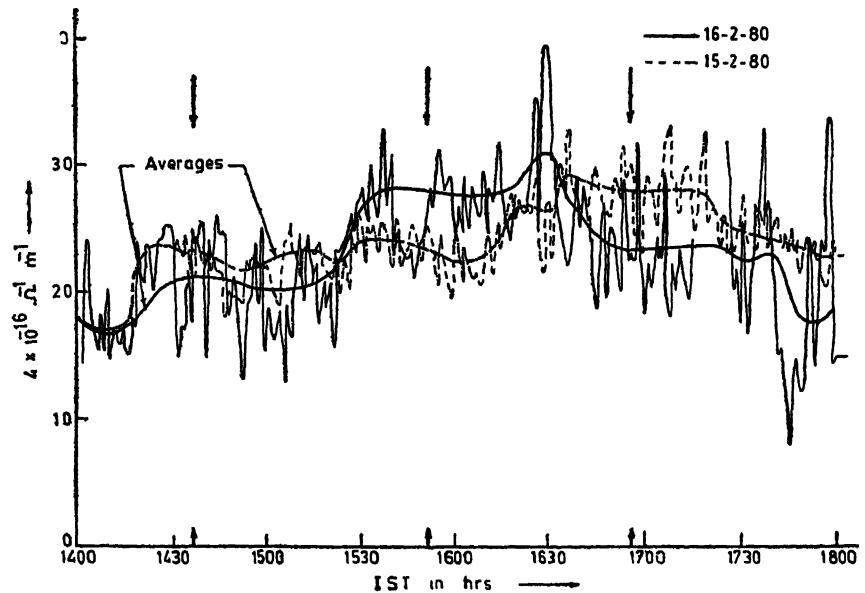


FIG 5 Variation in negative conductivity during solar eclipse and on previous day

significant contribution from the solar wind particles, which, being of low energy can reach these latitudes along the magnetic lines of force. A decrease in solar wind particles due to eclipse results at these high latitudes in a significant decrease of conductivity.

According to this approach the variation in conductivities at low and at high latitudes should vary in the opposite manner. At high latitudes, at the time of solar eclipse, the conductivity should decrease, whereas at low latitudes it should increase. This type of variation in conductivities at geomagnetic latitudes ( $\lambda = 50.206^\circ\text{N}$ ,  $\phi = 9.805^\circ\text{E}$ ) has actually been observed by Anderson and Dolezalek (1972). They attributed this to turbulence. If this were the effect of turbulence it should have the same variation everywhere independent of latitudes, and hence the effect of solar eclipse on ionization should be the same at all latitudes which, obviously it is not. Our explanation of this observation therefore seems more plausible.

Fig. 6 shows the variation in potential gradient which starts decreasing after about an hour of the first contact, and becomes minimum in about two-and-a-half hours. Thereafter, it again starts increasing to attain its normal value, soon after last contact of the eclipse. The time lag between the rise in conductivity and the fall in potential gradient is in keeping with the relaxation time of the atmosphere.

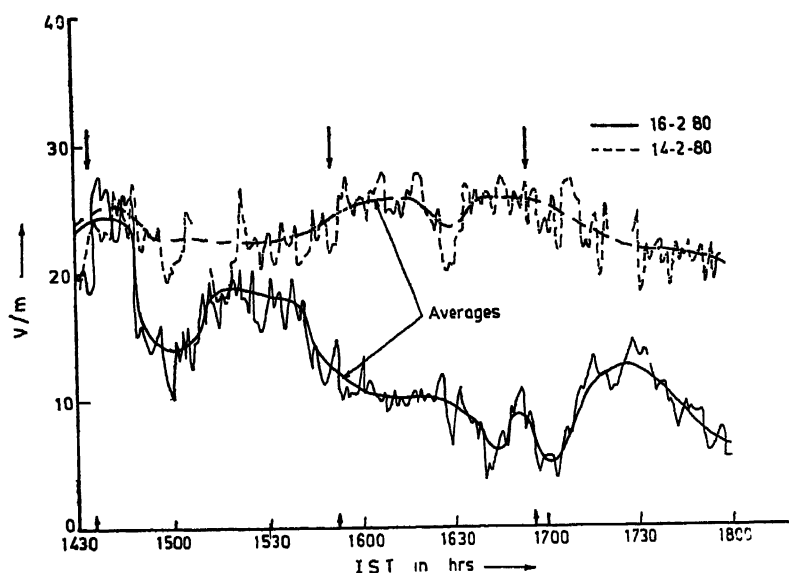


FIG 6 Variation in potential gradient during the solar eclipse and on previous day

Fig. 7 shows the variation in air-earth current which follows similar qualitative trend as the potential gradient. One should have expected a large increase in the current density  $J$ , since the  $\lambda$ 's have increased, and the potential gradient remains practically unchanged. In the beginning this, however, has not happened. The explanation may be as follows—there are two sources of electrical energy input to the atmosphere: one is in the form of solar heating, a part of which contributes to electrical energy density,  $J \cdot E$ .

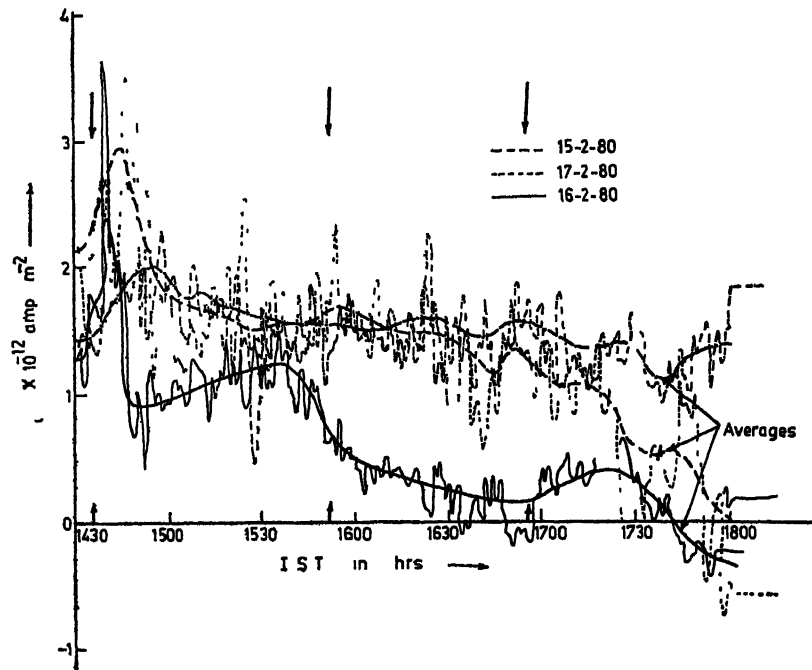


FIG. 7 Variation in air-earth current during solar eclipse and on preceding and succeeding days

This part is decreasing during solar eclipse, and the other input which is through cosmic ray ionisation, most of which is in the form of electrical power, is increasing during solar eclipse at lower latitudes. Hence the net contribution to electrical energy density, J.E., remains compensated for some time in the beginning until the solar heating input reduces considerably. When this happens to the extent that its contribution to J.E. through lightning activity is highly reduced, the net current density also reduces. Reversal occurs when the eclipse passes beyond the maximum phase. In both the processes there is a time lag corresponding to the relaxation time of atmosphere.

One observation, which is characteristic of experimental site, is the unequal variation in negative and positive conductivities. Figs 2 and 3 show that the increase in  $\lambda_+$  is more pronounced than that in  $\lambda_-$ . The reason for this difference is clear. Earlier, when the wind was coming from the land, both  $\lambda_+$  and  $\lambda_-$  were almost of the same magnitude. Due to eclipse, when land cooled down and the wind direction changed to make it a sea-breeze (Fig 8),  $\lambda_+$  increased much faster than  $\lambda_-$ . This extra increase in  $\lambda_+$  may be due to positive space charge, which is produced over sea surface (possibly by surfing and electrochemical effect of ventilation) and is brought about by the sea-breeze.

Fig 8 gives the variation of a few meteorological parameters, viz., wind direction, temperature, relative humidity and luminosity. The wind direction change from land breeze to sea breeze can be noted. There is no regular change in humidity. The luminosity during the near total eclipse was about 1/4000 of the original.



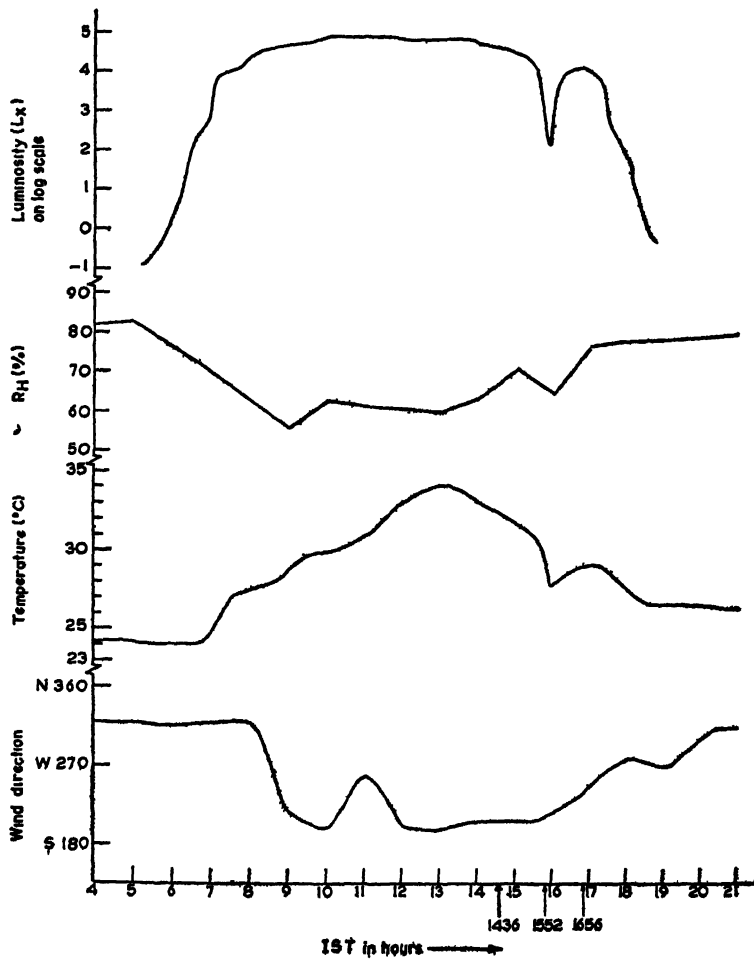


FIG 8 Variation in few meteorological parameters

## CONCLUSIONS

These observations show that the atmospheric electric parameters are affected during solar eclipse. The changes are well attributable to change in flux of solar wind protons, which get obscured by moon during eclipse, and consequent change in cosmic ray flux reaching earth atmosphere at low latitudes. These changes cause an increase in ionisation at low latitudes, and decrease at high latitudes. The electrical parameters are accordingly changed, at these respective latitudes, in different ways.

## REFERENCES

- Anderson, R. V., and Dolezalek, H. (1972) Atmospheric electricity measurements at Waldorf Maryland during the 7 March 1970 solar eclipse *J atm terr Phys*, **34**, 561-566

- Crezier, W. D. (1963) Measuring atmospheric potentials with passive antennas *J. geophys. Res.*, **68**, 5173–5179
- Kasemir, H. W. (1955) Measurement of the air-earth current density *Proc. Conf. Atm. Elect.*, [Eds. R. E. Helzer and W. E. Smith], p. 91, Geophys. Res. Paper No. 42, Air Force Cambridge Research Centre, US Department of Commerce, Washington, D. C.
- Wahlin, L. (1973) A possible origin of atmospheric electricity *Found. Phys.*, **3**, 459–472

Printed in India

**Atmospheric Electricity**

**MEASUREMENTS OF ATMOSPHERIC ELECTRICITY PARAMETERS  
DURING THE TOTAL SOLAR ECLIPSE OF 16 FEBRUARY 1980**

G. P. SRIVASTAVA, V. SRINIVASAN and A. K. DE

*Instruments Division, Meteorological Office, Pune, India*

*(Received 18 July 1981)*

Continuous recordings of atmospheric potential gradient, polar conductivities and positive and negative ion densities were made close to the ground during the total solar eclipse of 16 February 1980 at Raichur, India (77°21'E 16°12'N). Measurements of positive and negative electrical conductivities were also made on a 15m high tower simultaneously. A few low level potential gradient soundings were made close to the eclipse time to study the vertical distribution of potential gradient at lower troposphere. The results are compared with the measurements taken two days before and two days after the eclipse together with the description of the instruments used for the above measurements.

**Keywords:** Atmospheric Electricity; Potential Gradient; Polar Conductivity; Ion Density; Eddy Turbulence; Polonium 210 Probe; Gerdien Cylinder

**INTRODUCTION**

THE effect of solar eclipse on atmospheric electricity parameters has been studied previously by many workers. Reports on the effect of an eclipse on these parameters as measured on the ground showed contradictory results. Israel (1955) summarized all such reports upto 1954. His tabulation indicates that in 20 out of 27 cases the potential gradient diminished, in 3 cases it increased and in 4 cases there was no change. Koenigsfeld (1953) studied the effect of solar eclipse of 1952 (in Belgian Congo) on atmospheric potential gradient both at ground and above the earth's surface. He showed that the potential gradient at the ground changed from positive value passing through zero and reversing its sign. In the upper air potential gradient, during the middle of the eclipse he found that the fair weather potential gradient value became nearly zero between 5km and 15km. Another case of ground level potential gradient reversal during a partial eclipse was reported by Kamra and Varshneya (1967). Anderson and Dolezalek (1972) studied the effect of solar eclipse of March 1970 on atmospheric electricity parameters. They presented a model to account for the observed phenomena. It is shown that the diminution and subsequent restoration of eddy turbulence near the ground can produce effects of the type observed if adequate consideration is given to the existing electrical state of the atmosphere during the fully developed turbulence prior to the eclipse. Eclipse conditions provide a unique opportunity to investigate phenomena which are strongly

influenced by atmospheric turbulence. Eclipse condition produces observable phenomena which exhibit behaviours not seen during normal sunrise-sunset sequence. In the normal sunrise, there has been a span of many hours of darkness in which the settling of large ions and the stratification of the lowest layers of the atmosphere can proceed. Whereas, the time scale inherent in an eclipse does not permit any extensive settling to occur and limits the amount of stratification which may take place. During the total solar eclipse of February 1980, the authors made measurements of (1) Potential gradient at ground and above the earth's surface using balloon borne sondes (2) Atmospheric polar conductivities near ground and (3) Number density of both types of small ions.

#### INSTRUMENTATION

Surface potential gradient measurement was made using a compact mobile equipment which housed (1) sensor (2) insulator (3) power supply and (4) solid state electrometer amplifier. Polonium 210 probe was used as potential equaliser. The atmospheric potential sensed by the probe was divided by a divider circuit using special high megohm resistors (of values  $10^{12}$  and  $10^9$ ) mounted on a specially designed teflon insulator and fed to high input ( $10^{14}$ ) ultra low drift electrometer amplifier. The unit was placed in the open field. Mains power and output lines were connected by means of two weather-proof connectors. The output was fed to a 0-1mA strip chart galvanometric recorder.

Upper air measurement of potential gradient was made using balloon-borne special sondes. In these two polonium 210 collectors spaced 50cm apart in the vertical were used as the sensors whose output was given to an inverted triode electrometer. The output voltage of the electrometer was converted to frequency (0-200Hz, for a range of 135 to 0 volts of potential difference between the sensors) to modulate a 401MHz transmitter. A solid state switch was used to monitor the zero of the electrometer every two minutes. The sondes were released to the atmosphere with the help of hydrogen filled balloons with a rate of ascent of about 18km/hr. Heights attained by the sondes were monitored by incorporating precalibrated baroswitches in the circuit. Arrangement was made to switch off the transmitter in flight before releasing the next sonde to avoid interference from the previous sonde. The signals from the sonde were received and recorded on a 401MHz ground receiver system.

Measurements of polar conductivities and small ion densities were made using aspirated Gerdien condensers. The aspiration rate was kept constant at 4m/sec. All the four Gerdien cylinders were mounted in a common aspiration chamber and each was insulated from the other. Appropriate charging voltages were provided to each cylinder by dry batteries. A four channel high input, ultra low drift electrometer amplifier provided the necessary conversion of ionic currents to output currents of recordable levels (0-1mA). The aspirated cylinders, DC power supplies and electrometers were all mounted on a compact mobile unit. The system was kept at a height of 1.15 metres from the ground on open field. Mains power and outputs were connected by cables. The outputs were fed to four 0-1mA strip chart galvanometric recorders having 1.5K input impedance. The recorders were housed in the laboratory.

## RESULTS

Fig. 1 shows the surface potential gradient recorded at Raichur during the period 13-2-80 to 18-2-80. Curve 1 shows the hourly mean values of potential gradient (without applying any correction for exposure factor) for the period 13-2-80 to 18-2-80 excluding the data for 16-2-80. Curve 2 shows the actual data for 16-2-80 and Curve 3 shows the hourly mean for 16-2-80. Study of these curves shows that values of surface potential gradient markedly decreased during 1st and 3rd contacts. After the 3rd contact the value started increasing till about 1730hr after the 4th contact. Thereafter, the value dropped down considerably, attaining negative values with a minimum around 1900hr. Afterwards the value built up and merged with the normal mean value.

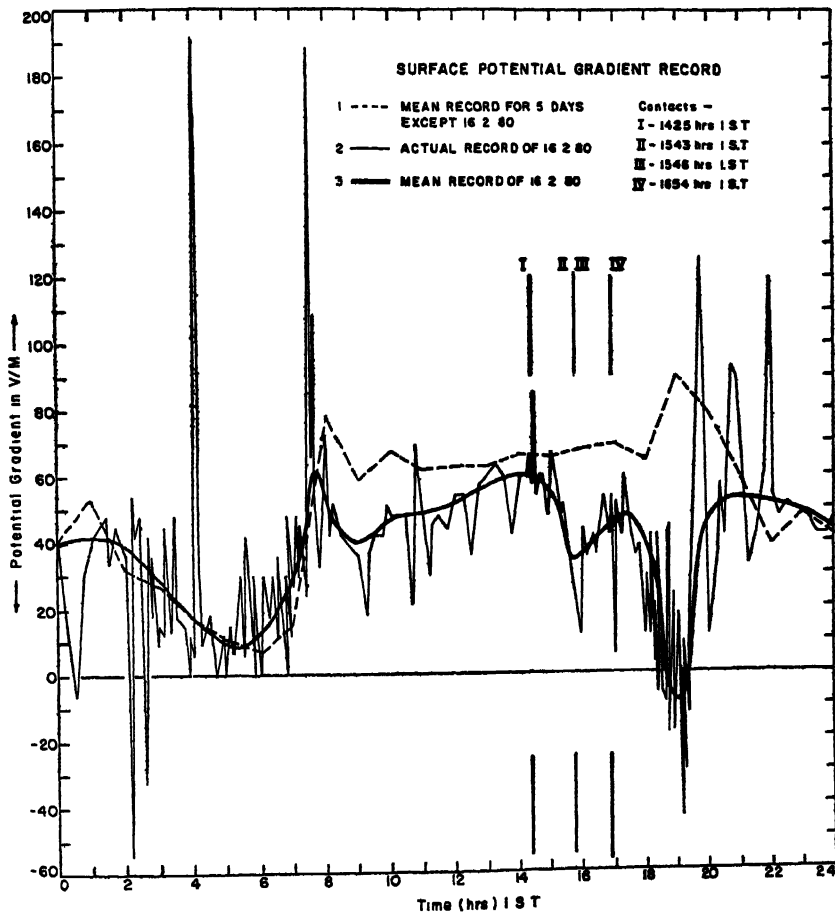


FIG. 1

Figs 2 and 3 show the variation of polar conductivities over surface. Curves 1 show the hourly mean value for the period 13-2-80 to 18-2-80 excluding the data for 16-2-80. Curves 2 show the actual value for 16-2-80. Curves 3 show the hourly mean

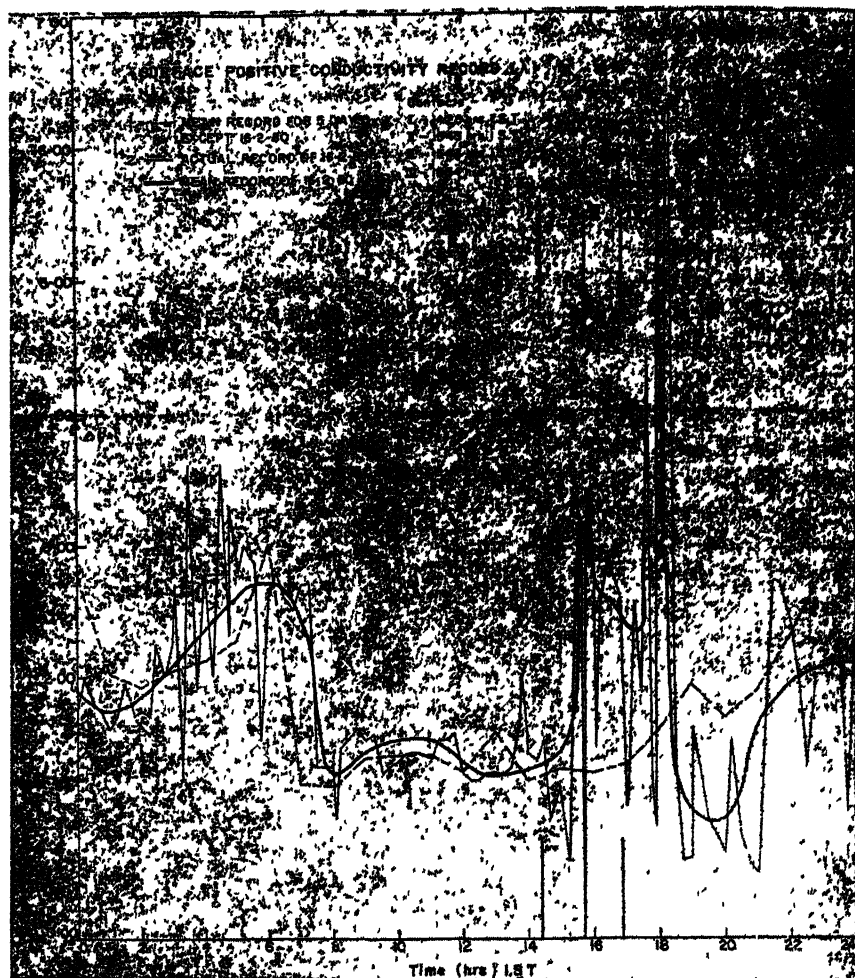


FIG 2

value for 16-2-80. These curves show both conductivity values increasing during 1st and 3rd contacts. Values decreased from 3rd contact till about 1730hr after the 4th contact. Thereafter, the value attained a maximum around 1800hr and then decreased to a minimum value around 1930 hrs and then increased towards the normal mean value. Figs 4 and 5 show the variation of small ion densities. These are similar to those of polar conductivity curves shown at Figs 2 and 3. Fig 6 shows the variation of potential gradient with height as measured by potential gradient sondes. Soundings at 1438hr on 15-2-80, at 2150hr on 16-2-80 and at 1443hr on 17-2-80 show the normal pattern at Raichur. Sounding at 1424hr (very close to the 1st contact time) on 16-2-80 shows peak around 950mbs. Ascent on the same day at 1505hr (between 1st and 2nd contacts time) shows very high value near the surface and also a peak around 700mbs.

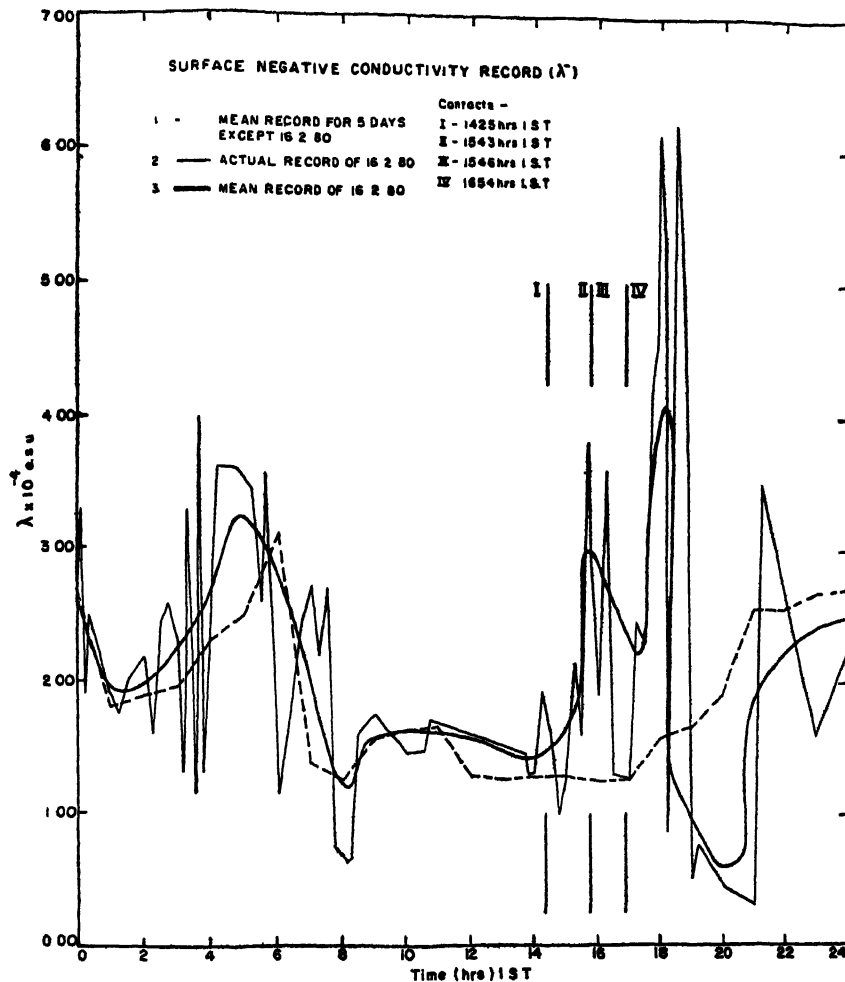


FIG 3

## DISCUSSION

Comparing the different atmospheric electricity parameters recorded at Raichur from those at Pune or any urban location it can be seen that at Raichur values of surface potential gradient, are much lower whereas the values of polar conductivities are much higher (3 times compared to Pune values) This shows that the atmospheric electrical structure is different at Raichur from any urban location. Studying the diurnal variation of potential gradient and conductivity we can assume that the eddy turbulence plays an important role. In the absence of any turbulence near the surface, the atmosphere comprises of more small ions than large ions as a consequence of some ionising agent. Thus during night time, values of conductivity are higher compared to day time value. The reverse is the case with potential gradient. During day time when lower atmosphere is turbulent, destruction of small ions takes place

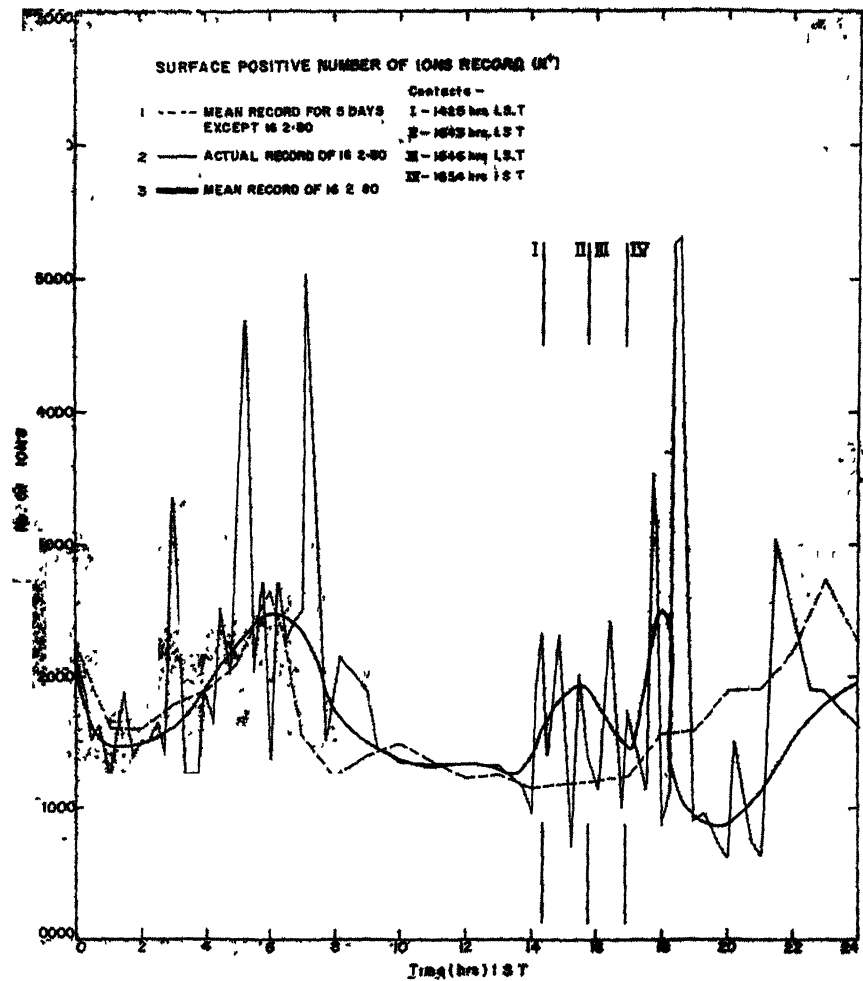


FIG 4

by the presence of large ions/pollutants brought by eddies from overlying layer. This is a daily feature at Raichur. The low value of polar conductivity (of the order of urban value) measured at 15 metres high tower at Raichur also support the assumption.

Studies of hourly mean value curves i.e., curve 3 of potential gradient, conductivity and small ion density for 16-2-80 (eclipse day) in Figs 1 to 5 show that the potential gradient value decreased, conductivity value and small ion density value increased between 1st and 3rd contacts as a consequence of gradual lowering of turbulence. These decrease and increase in values attained their maximum at the 3rd contact. Between 3rd contact and 1730hr the above trends were reversed as a consequence of resumption of solar heating and eddy convection. After the eclipse was over at 1654hr, the curves should have followed the normal sunset trend, attaining values towards normal mean. But in all the curves for 16-2-80 some departure from the normal mean is observed after the eclipse was over. These departures may be attributed to some perturbation in



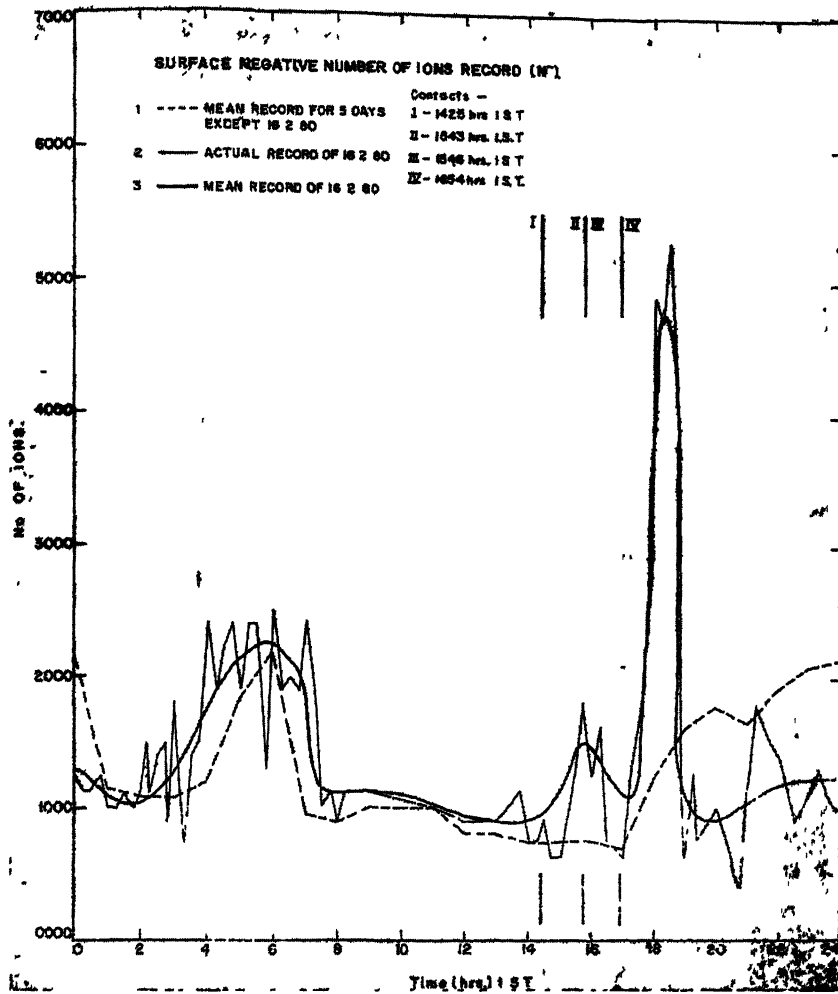


FIG 5

the electrical state of the atmosphere produced partly by the pseudo sunset-and-sunrise effect due to eclipse and partly due to changed human activities as governed by local prevailing customs on the eclipse day. Of these, mention may be made of the increase in the number density of small negative ions in relation to that of positive ions around 1800hr. The negative value in potential gradient around that time is due to this increase in space charge. All the curves for 16-2-80 show a decreased human activity from a time much earlier to the occurrence of eclipse.

In conclusion though all the major features seen on the experimental records can be accounted for even with the present limitation of the instrumentation and some need to invoke particular local conditions for the explanation, it must be acknowledged that any understanding based on one series of observations must further be tested.

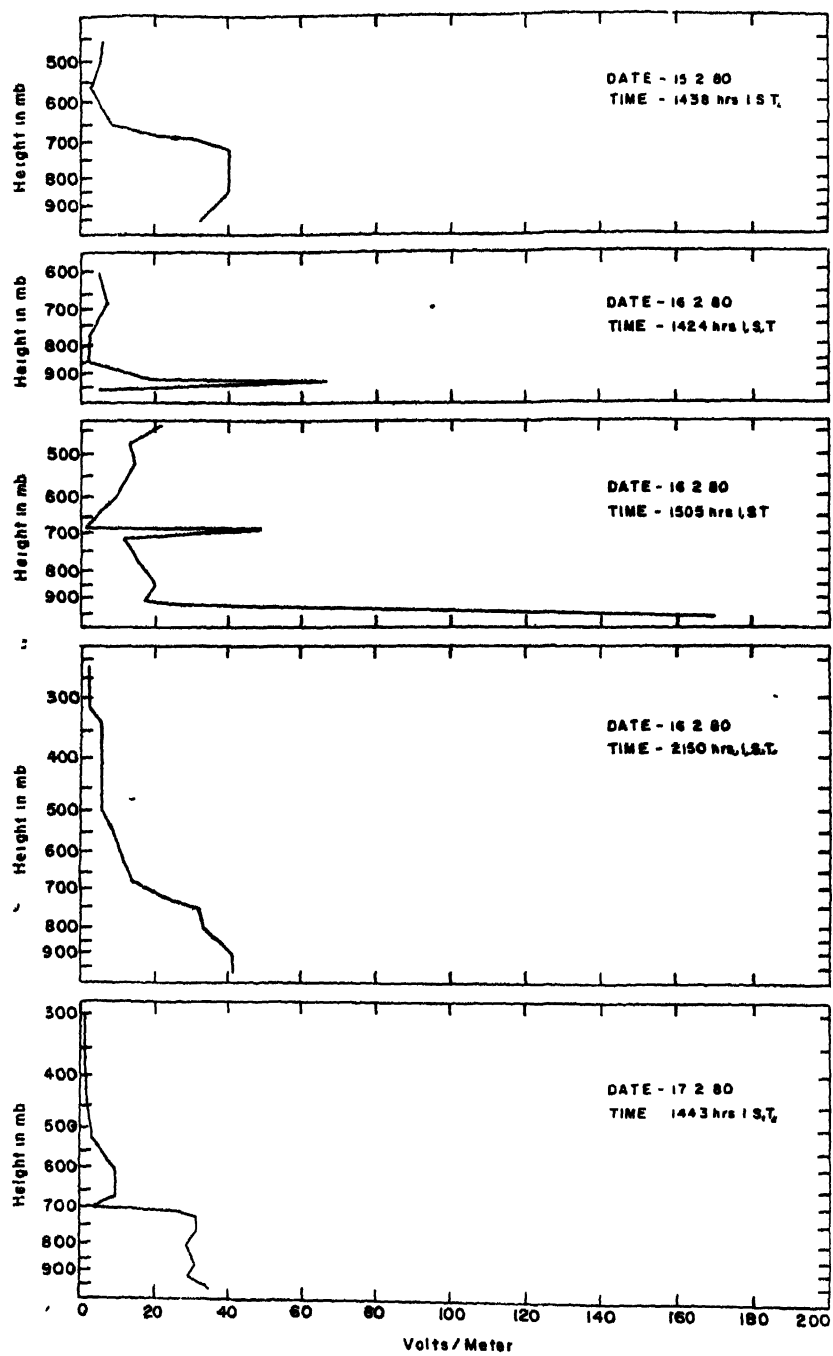


FIG 6

## REFERENCES

- Anderson, R V , and Dolezalek, H. (1977) *J. atm. terr. Phys.*, 34, 561-566  
Israel, H. (1955) *Z. Geophys* , 20, 137.  
Kamra, A. K , and Varshneya, N. S. (1967) *J. atm. terr Phys.*, 29, 527.  
Koenigsfield, L. (1953) *Thunderstorm Electricity* (Ed : H. R. Byers), p 24. Univ. Chicago Press, Chicago.

Printed in India

**Solar Energy Variation**

**VARIATION IN SOLAR ENERGY INTENSITY DURING TOTAL  
SOLAR ECLIPSE OF 16 FEBRUARY 1980**

U. K. CHATURVEDI, S. K. AGRAWAL, N. RAJAN, R. BHANJA and A. K. NIGAM  
*Department of Physics, Banaras Hindu University  
Varanasi-221 005, India*

*(Received 18 July 1981)*

All the solar energy trapping systems become inactive in a belt of hundreds of kilometers for hours together during a Total Solar Eclipse. This inspired us to measure the changes in the intensity of the sunlight during the total solar eclipse of 16 February 1980 at Puri (India). Puri is situated at  $19^{\circ}55'N$ ,  $85^{\circ}40'E$ . It was only 10 km north to the middle line of the totality path of the said eclipse. The intensity of the sunlight during the eclipse, was measured by a CEL Suryamapi. The intensity of the sunlight at Puri sea beach decreased from  $76 \text{ mW cm}^{-2}$  to  $0.01 \text{ mW cm}^{-2}$  at the peak of totality. The temperature of the environment at the site was also measured by a sensitive alcohol thermometer. The temperature variation from  $29^{\circ}\text{C}$  to  $24^{\circ}\text{C}$ , was observed during the same period. The sea became more violent and the velocity of wind increased significantly during the total solar eclipse.

**Keywords:** Solar Energy Intensity; Solar Eclipse; Diamond Ring

**INTRODUCTION**

We carried out intensity and temperature variation measurements at Puri during the total solar eclipse on 16 February 1980. Due to various limitations we performed the integrated intensity measurement in the visible region only.

**EXPERIMENTAL SITE**

There were more than one reason for selection of Puri as the experimental site. Puri is situated at  $19^{\circ}55'N$  and  $85^{\circ}40'E$  and was only  $\approx 10 \text{ km}$  north to the middle line of the totality path (IMD, 1980). The added advantage of Puri was its sea beach, from where a close watch at the sea could be kept during the eclipse. In spite of the fact that the previous 10 years' weather record of the places falling under the totality path predicted a possibility of a fair weather, we were familiar with the weather uncertainty of Puri. However, as it was the only good seacoast on the totality line, we chose it as the site for our measurements during the eclipse.

**MEASUREMENTS AND PSYCHOLOGICAL EFFECTS**

On 15 February 1980 it was quite a sunny day till the afternoon when it suddenly started raining. But fortunately on the 16th morning it was a sunny and cloudless sky. The atmosphere was quite windy and waves were at full swing in the sea.

Before the start of the solar eclipse, the experimental set-up was properly arranged for the measurements. A sensitive alcohol thermometer was employed for the temperature measurement. It was shielded from direct sun rays and from the wind by keeping it behind a boat which was lying on the beach. The solar intensity was measured by a CEL Suryamapi whose light sensing area was facing the sun throughout the experiment. Just before the eclipse (i.e., at 14 30 IST) the intensity was recorded to be  $76 \text{ mW/cm}^2$  and the temperature was  $29^\circ \text{C}$ .

The intensity and temperature measurements were continued upto 15 15 IST without any interruption, when suddenly a small patch of dark cloud passed through the region of the sun. This was recorded in the intensity measurement as a small kink in the falling solar intensity curve. This patch of cloud soon went away but just before the 2nd contact the sun was covered with dense patch of clouds for sometime. However clouds dissipated soon and immediately after that the second contact occurred. At the time of second contact, we could see the diamond ring but not the shadow bands. The measurements were continued.

Soon the sky was clear and the totally eclipsed sun with its corona in full glory appeared in the sky. The solar intensity and temperature measurements were made very carefully at regular intervals. The whole sea beach was covered with yellowish brownish pale light. The sea became very violent, the wind was found to be a bit chilly with greater velocity. Duration of totality was passed within "no time" and suddenly at the moment of third contact a bright "Diamond Ring" again appeared (shown in Fig 1) in the cloudy sky. Then, slowly the reverse process started and the

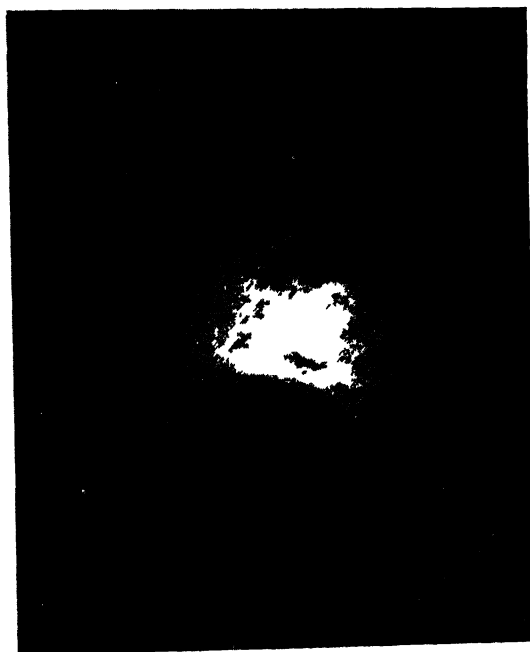


FIG 1 Diamond ring photographed at Puri just before the 3rd contact (16 February 1980)

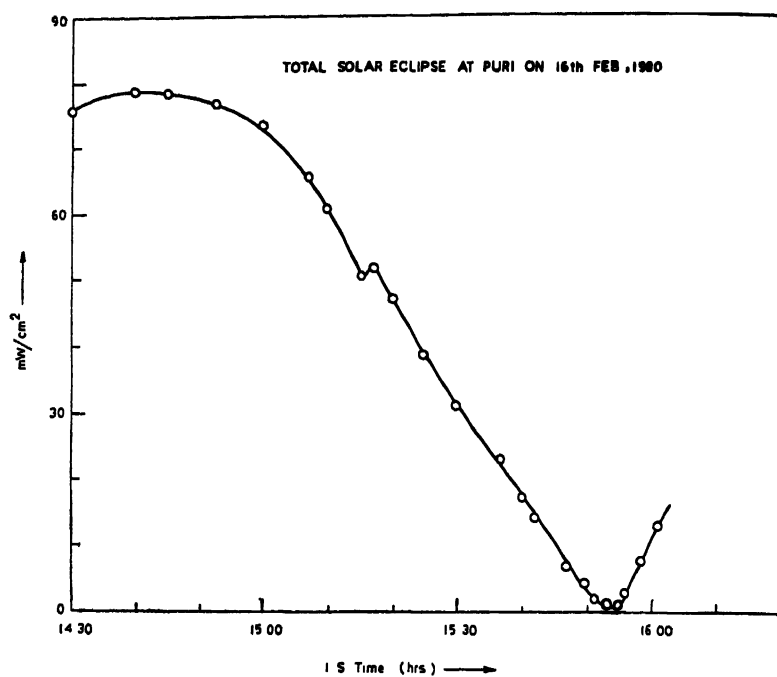


FIG 2. Variation in the solar intensity during the total solar eclipse of 16 February 1980 at Puri (India).

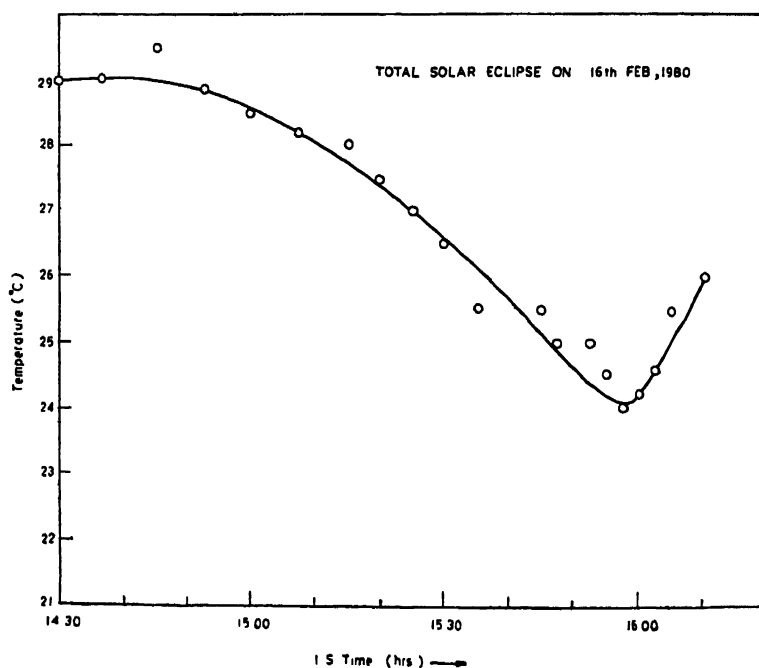


FIG 3 Variation in the temperature at Puri sea beach during the total solar eclipse of 16 February 1980

solar disc began to be more and more visible. The observations were continued to be recorded for some more time. At this time also, authors were unable to observe the much expected "shadow bands". The results of solar intensity and temperature variation are shown in Figs. 2 and 3.

#### SOLAR ENERGY LOSS DUE TO SOLAR ECLIPSE

A total solar eclipse causes a tremendous loss of energy. In the eclipse of 16 February 1980, which affected the solar intensity for some time or more in the whole country (India), spread in an area of three million square kilometers, there has been considerable average energy loss experienced. The analysis will be reported elsewhere.

#### ACKNOWLEDGEMENTS

The authors are grateful to many unknown persons who helped us in taking our observations during the time of eclipse at the Puri sea beach.

#### REFERENCE

IMD (1980) *Total Solar Eclipse of 16 February 1980 Circumstances Relating to India*

Printed in India.

**Mesospheric Emissions**

### Session C : IONOSPHERIC PHYSICS

## DETERMINATION OF OZONE FROM ECLIPSE OBSERVATIONS OF $O_2(^1\Delta_g)$ DAYGLOW

V. V. AGASHE and S. M. RATHI

*Department of Physics, University of Poona, Pune-411 007, India*

*(Received 3 February 1982)*

Observations of 1270nm dayglow radiance of molecular oxygen during the total solar eclipse of 16 February 1980 have been described. Rate equations for production and loss of  $O_2(^1\Delta_g)$  have been used together with observed data to examine the changes in the concentration of ozone during the eclipse. It is found that ozone concentration increased during the eclipse. At 66km altitude, ozone concentration increased by more than a factor of two at the mid-eclipse time over its prevailing value at the first contact.

**Keywords:** Mesospheric Ozone; Solar Eclipse Measurements of  $O_2(^1\Delta_g)$ ; Changes in Ozone during Eclipse;  $O_2(^1\Delta_g)$  Dayglow during Eclipse

### INTRODUCTION

$O_2(^1\Delta_g)$  plays a significant role in the photochemistry of the mesosphere. Numerous studies have been carried out, both in the laboratory and in the earth's environment, with a view to determine production and loss processes of singlet molecular oxygen in the mesosphere [Llewellyn & Evans (1971), Evans & Llewellyn (1972); Gattinger (1971), Jones (1973), and Wayne (1971)]. In the earth's atmosphere singlet molecular oxygen is monitored by observing its optical emissions at 1270nm and 1580nm in the near infrared region. These optical emissions (Fig. 1) is a major component of the day and night airglows.

Singlet molecular oxygen is believed to be produced during the day in the primary step of ozone photolysis, chiefly in the Hartley continuum, between 200nm to 310nm,



(Thomas & Bowman, 1972, and Shimazaki & Laird, 1972)

Other sources producing this species must exist to account for the observed presence of its optical emissions in the nightglow. The observed rate of decay of the radiance after sunset is a useful test of the production theory, however, normal twilight observations serve only a limited purpose. A solar eclipse provides a much better opportunity for testing the theory. Eclipse observations have been reported by Noxon



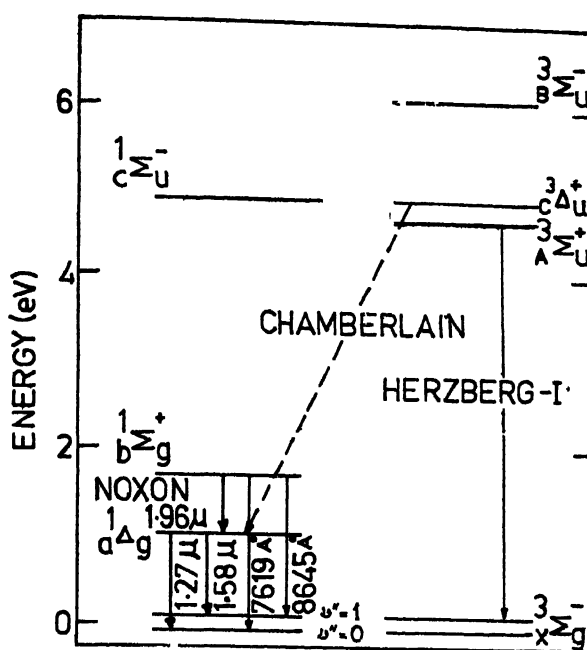


FIG. 1. Energy level diagram of molecular oxygen

(1967, 1968) and Wraight and Gadsden (1975) During the total solar eclipse of 16 February 1980 the authors studied the dayglow radiance at 1270nm. Results of these measurements are presented in this paper.

### EXPERIMENTAL

A two channel atmospheric photometer was constructed for making these observations. The photometer consists of a baffle system and a condensing lens which collects light from a patch of bright sky within a field of view of  $5^\circ$  half angle. The collected light beam is chopped by a motor driven disc chopper in the focal plane of the condensing lens. A cooled lead sulphide detector receives the chopped beam and produces a signal voltage which is given to the phase sensitive electronics detection system. A small low brightness lamp, carefully shielded and suitably placed above the chopper disc, produces reference signal required in the phase sensitive detection. Block diagram of the electronic detection system is shown in Fig 2. Photometer is calibrated in the laboratory using a precalibrated photometric standard lamp.

For the eclipse experiment, the photometer was operated from the terrace of J T College at Gadag (lat  $15^\circ 25' 8''$ N, long  $75^\circ 38' 3''$ E) within the totality belt. Meteorological reports indicated greater possibility of clear sky conditions for the month of February during which eclipse was taking place. Observation station was set up two days prior to the day of eclipse and trial observations of zenith sky brightness of dayglow radiation at 1270nm were resumed. On both days, prior to eclipse day, slightly cloudy conditions prevailed, particularly, just above horizon. The eclipse day was, however, remarkably clear. Eclipse day has been reported to be magnetically disturbed,

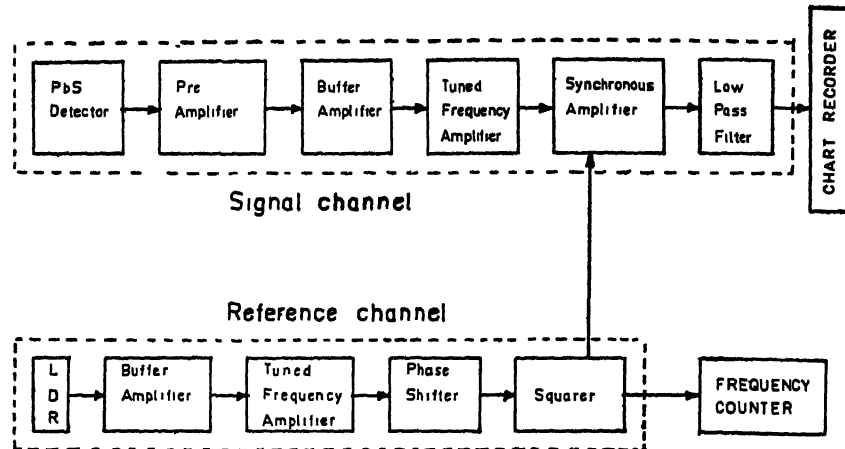


FIG 2 Block diagram of electronic detection system.

the sun being near the phase of maximum activity.

Eclipse timings are given in Table I. At the time of mid eclipse sun was at an elevation of  $37.2^\circ$  in the west. Geometry of the eclipse showed that the region of atmos-

TABLE I

*Eclipse parameters for Gadag*  
(Lat  $15^\circ 25' 8''$ N Long  $75^\circ 38' 3''$ E)

Phase of the Eclipse	Time IST HRS	Solar elevation angle Degrees
Beginning of the Eclipse	14-21-03	52.7
Centre of the Eclipse	15-42-23	37.2
End of the Eclipse	16-53-31	21.7
Duration of Totality	2m 46s	

phere extending beyond 100km would be in the zone of totality in the zenith direction which was the direction of observation of dayglow radiation. All the equipment performed satisfactorily during the experiment and good data were obtained. Observations were obtained using optical interference filters. Typical traces showing chart records of emission and background channel are shown in Fig 3. Fig. 3a refers to observations before the start of eclipse and Fig. 3b shows the chart record during the eclipse. Difference in signal levels of two channels is due to the different pass band widths of corresponding optical filters. Correction for background contamination was made by following two colour photometric method. Calibration factors for the

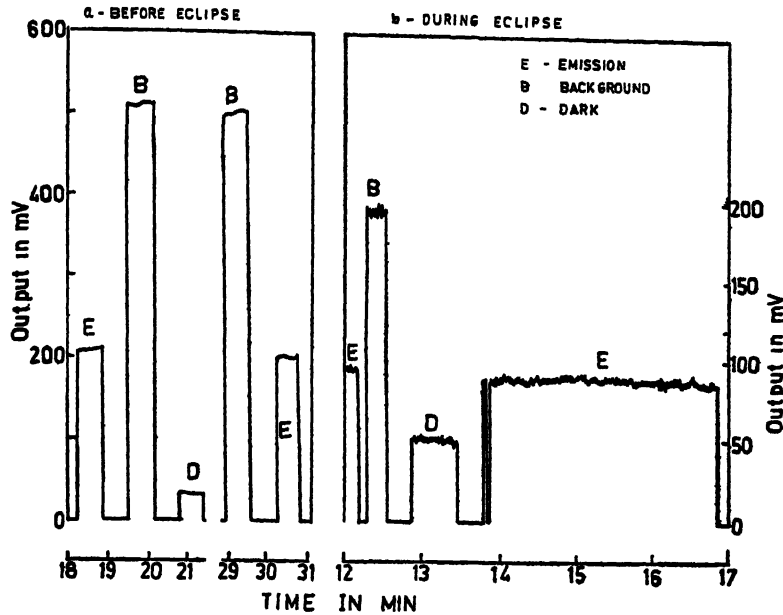


FIG. 3. Typical chart records.

two channels take into account differences in the filter pass bands, these factors were checked by comparing intensities recorded by the two channels during pre-sunrise period when dayglow radiation is absent. Correction of emission channel data for background contamination during the eclipse period needs a certain amount of circumspection. During the eclipse, intensity of scattered sunlight decreases rapidly; the rate of decrease of background channel signal is found to be faster than that of emission channel (Fig. 4).

Dayglow radiation at 1270nm is heavily absorbed by oxygen molecules in the lower atmosphere and only about 6 per cent of the emission reaches the ground level [Evans *et al.* (1970b); and Gadsden & Wraight (1975)] It is rather difficult to correct properly for atmospheric absorption during the eclipse period. As the sunlight is progressively cut off, concentration of excited oxygen molecules is depleted more rapidly in the lower boundary of the emission layer, this is because, at lower altitudes quenching of excited molecular oxygen dominates over the radiation loss. This increases the effective height of emission layer. Since atmospheric absorption depends on emission altitude, knowledge of the rate constant for quenching of excited oxygen molecules is required for proper estimation of percentage absorption. With certain reservations, one can make correction for atmospheric absorption and describe the observed behaviour during the eclipse approximately. The observed intensity of dayglow at 1270nm during the eclipse of 16 February 1980 is plotted against time in Fig. 5. Intensity at the second contact reached a value of 288KR which was just above the threshold of sensitivity of the photometer. For comparison, data recorded on the previous day of the eclipse are plotted in the same figure. However, data on previous day are available only during the period of good observing conditions.

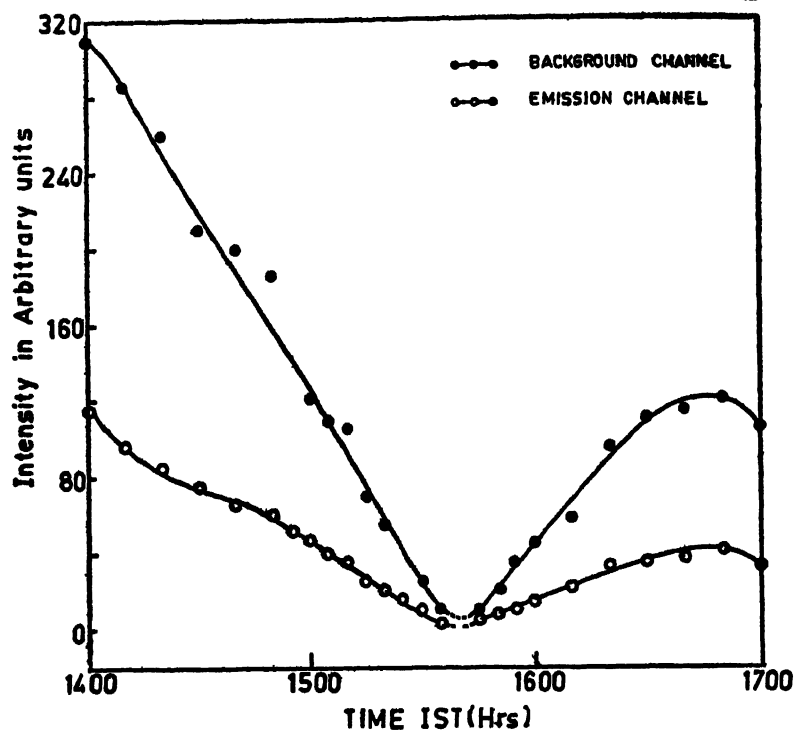


FIG. 4. Observed signals during eclipse.

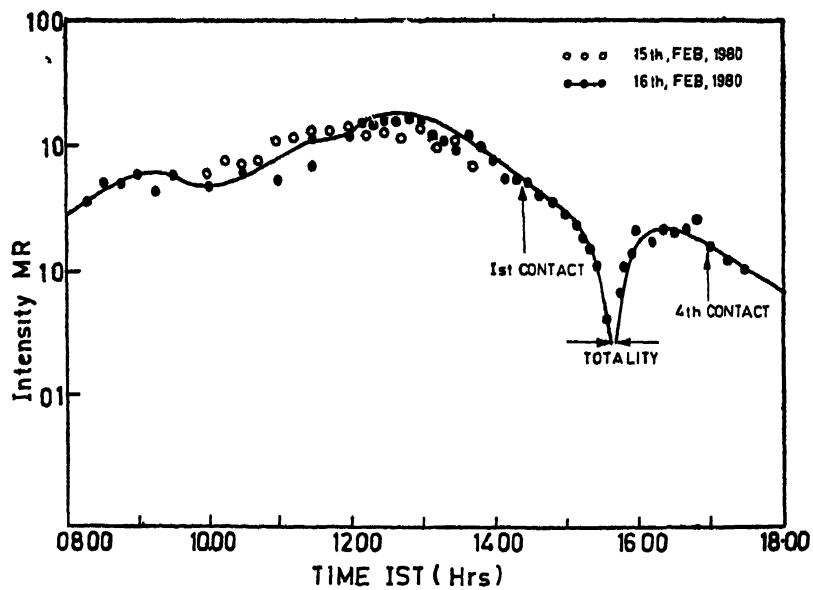


FIG. 5. Observed intensity of 1270nm dayglow during eclipse.

## ANALYSIS OF ECLIPSE DATA

Since the eclipse occurred during the afternoon period, intensity variation of Fig. 5, before and after totality, is not symmetrical. It is also found that the dayglow intensities recorded on the eclipse day (and the one preceding) are smaller by a factor of two than those routinely observed from Poona (lat. 18.5°N). Since no other observations were made from Gadag except around the eclipse days, it is not known whether data of Fig. 5 represent normal dayglow intensity level at Gadag or whether intensities happened to be abnormally low around eclipse day. Both days of observations at Gadag were magnetically disturbed days but it is not known whether magnetic disturbance affects the mesospheric dayglow intensity of singlet molecular oxygen. Table II shows the dayglow intensities observed at different epochs during the eclipse.

TABLE II

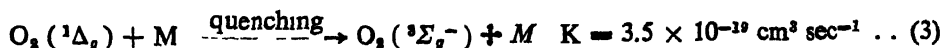
*Zenith radiance of 127.0nm dayglow during eclipse*

Epoch of the Eclipse	TIME IST HRS.	Observed intensity of $O_2(^1\Delta_g)$ (O-O) band in the zenith (in Mega Rayleigh)
First contact	14-21-03	5.800
Second contact	15-41-00	0.288
Third contact	15-43-46	0.300
Fourth contact	16-53-31	1.900

The loss processes for excited oxygen molecules are



(Badger *et al.*, 1965)



(Evans & Llewellyn, 1970)

$M$  stands for air molecules in the mesosphere. Since the loss processes are not affected during an eclipse, changes in the concentration of  $O_2(^1\Delta_g)$  are the result of combined effect of changes in photolysis rate of ozone and simultaneous loss processes.

In the analysis of our data, we have assumed that the excited oxygen molecules are produced through photolysis of ozone at a rate  $J$ , which depends on height  $h$ . It is further assumed that at all heights, the production rate of excited oxygen molecules is proportional to the amount of solar illumination. The excited molecules either

radiate spontaneously (reaction 2) or are quenched by collision (reaction 3). At a given altitude in the emitting region we can then write:

$$\frac{d[O_3^*]}{dt} = J[O_3] + (A + K[M]) \times [O_3^*] \quad \dots (4)$$

where quantities in square brackets represent the concentration of respective species at respective times. On integration with respect to time we get,

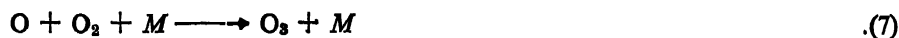
$$[O_3^*]_t = [O_3^*]_{t=0} \exp(-\beta t) + \exp(-\beta t) \int_0^t J(t') [O_3] \exp(\beta t') dt' \quad \dots (5)$$

$$\text{where } \beta = (A + K[M]). \quad \dots (6)$$

Thus one can obtain the concentration of excited species at any time 't' during the eclipse. With the help of above equations and the observed dayglow radiance during an eclipse one can estimate quenching rate *K* for an assumed ozone concentration. Conversely, one can use a plausible value for the quenching rate and determine the ozone concentration for the latitude of observing station, with the help of equations (4) and (5), together with eclipse observations of dayglow radiance. We have adopted the second approach in our analysis of eclipse data. Preliminary calculations using CIRA 1965 model for [*M*] show that ozone concentration increased during the eclipse. It is found that at the altitude of 66km, ozone concentration starts increasing at 1501 IST i.e., forty minutes after the first contact. At mid-eclipse, increase in the ozone concentration is about 2.4 times its value at the first contact. Ozone concentration after totality shows a steeper fall after 1655 IST i.e., approx. twelve minutes after totality.

#### DISCUSSION

The primary mechanism for the production of ozone at all heights in the mesosphere is the three-body recombination:



During the first part of the eclipse the production of  $O_3$  by reaction (7) and the simultaneous reduced loss by photodissociation reaction (1) leads to increased concentration at the height considered. The other loss process for  $O_3$



becomes important during totality at altitudes above 70km, since it depends on concentration.

Possible changes in the concentration of ozone during solar eclipses have been studied before. From measurements made during the eclipse of 12 November 1966, Randhawa (1968) reported an increase in the ozone concentration at 57km by more than a factor of two. From eclipse measurements of 7 March 1970, Smith (1972) reported an increase by a factor of two in the ozone concentration around 60 to 68km. Changes in the atmospheric composition at mesospheric heights during eclipse have

been studied theoretically for model atmospheres containing oxygen and hydrogen as constituents. Increase in ozone concentration and decrease in  $O(3p)$  concentration has been predicted through theoretical calculations (Thomas & Bowman, 1974; and Hunt, 1965).

### CONCLUSIONS

Eclipse observations of 1270nm band provide a sensitive method of determining ozone concentration in the mesosphere. The ground based measurements made during the eclipse of 16 February 1980 show that at 66km ozone concentration increased by more than a factor of two. This conclusion is based on preliminary reductions at only one altitude.

### ACKNOWLEDGEMENTS

This research was supported by ISRO Grants under the RESPOND programme in the University of Poona. Special thanks are due to Professor B. C. Hoskeri, Principal, J. T. College, Gadag for providing required facilities for making observations, to Professor A. S. Nigavekar, Head of the Physics Department, University of Poona, and others for help in organizing solar eclipse expedition and to Professor P. V. Kulkarni for use of facilities at P. R. L., Ahmedabad.

### REFERENCES

- Badger, R. M., Wright, A. C., and Whitlock, R. F. (1965) Absolute intensities of the discrete and continuous absorption bands of oxygen gas at 1.26 and 1.065  $\mu$  and the radiative lifetime of the  $^1\Delta_g$  state of oxygen. *J. chem. Phys.*, **43**, 4345.
- Evans, W. F. J., and Llewellyn, E. J. (1970) Molecular oxygen emissions in the airglow. *Ann. Geophys.*, **26**, 167.
- Evans, W. F. J., Wood, H. C., and Llewellyn, E. J. (1970) Transmission of oxygen infrared emission at 1.27  $\mu$  in atmosphere. *Can. J. Phys.*, **48**, 747.
- (1972) Measurements of mesospheric ozone from observations of the 1.27  $\mu$  band. *Radio Sci.*, **7**, 45.
- Gadsden, M., and Wraight, P. C. (1975) Atmospheric transmission of the 1.27 micron band of oxygen. *J. atm. terr. Phys.*, **37**, 287.
- Gattinger, R. L. (1971) Interpretation of airglow in terms of excitation mechanisms. In *The Radiating Atmosphere* (Ed. B. M. McCormac) D. Reidel, Dordrecht, Holland, P. 51.
- Hunt, B. G. (1965) A theoretical study of the changes occurring in the ozonosphere during a total eclipse of the sun. *Tellus*, **17**, 516.
- Jones, A. V. (1973) The infrared spectrum of the airglow. *Space Sci. Rev.*, **15**, 355.
- Llewellyn, E. J., and Evans, W. F. J. (1971) The dayglow. In *The Radiating Atmosphere* (Ed. B. M. McCormac) D. Reidel, Dordrecht, Holland, P. 17.
- Noxon, J. F. (1967) Oxygen spectra in dayglow, twilight and during an eclipse. *Nature*, **213**, 350.
- (1968) Day airglow. *Space Sci. Rev.*, **8**, 92.
- Randhawa, J. S. (1968) Mesospheric ozone measurements during a solar eclipse. *J. geophys. Res.*, **73**, 493.
- Shimazaki, T., and Laird, A. R. (1972) Seasonal effects on distributions of minor neutral constituents in the mesosphere and lower thermosphere. *Radio Sci.*, **7**, 23.
- Smith, L. G. (1972) Rocket observations of solar UV radiation during the eclipse of 7 March 1970. *J. atm. terr. Phys.*, **34**, 601.

- Thomas L., and Bowman, M. R. (1972) The diurnal variations of hydrogen and oxygen constituents in the mesosphere and lower thermosphere *J atm terr Phys*, **34**, 1843
- (1974) Changes in concentration of oxygen and hydrogen constituents in the mesosphere during an eclipse. *J atm terr Phys.*, **36**, 1421
- Wayne, R. P (1971) The photochemistry of ozone and singlet molecular oxygen in the atmosphere In *Mesospheric Models and Related Experiments* (Ed G Fiocco) D Reidel, Dodrecht, Holland, p 240.
- Wraight, P. C., and Gadsden, M (1975) Dayglow of the infrared atmospheric band system of O<sub>2</sub> during a total eclipse of the sun *J atm terr Phys*, **37**, 717.



Printed in India

**Ionization & Wave Motion**

## VLF/LF DETECTION OF IONIZATION CHANGES AND WAVE MOTIONS IN THE MIDDLE ATMOSPHERE ASSOCIATED WITH THE FEBRUARY 1980 TOTAL SOLAR ECLIPSE

Y. V. RAMANAMURTY, S. C. GARG, M. V. S. N. PRASAD *and* A. HAMID

*National Physical Laboratory, Hillside Road, New Delhi-110 012, India*

*(Received 24 February 1982)*

Based on VLF/LF radio observations, the first evidence of wave motions in the middle atmosphere associated with the total solar eclipse of 16 February 1980 is presented. The ionospheric effect on 16kHz monitored at New Delhi (path mid point 47°N, 29°E) manifested itself as a precursor corresponding to a decrease followed by the main increase in height of reflection because of loss of electrons due to recombination in the partially eclipsed lower D-region. Succeeding this main effect, there was a phase overshoot due to the rather complex aeronomical processes. Soon after the appearance of the precursor, small periodic fluctuations in the phase are observed. The VLF paths (12.8kHz, La Reunion-New Delhi; 12.3kHz, Tsushima Island-New Delhi) crossing the path of totality showed larger phase retardations compared to the 16kHz Rugby-New Delhi path which is far away from the path of totality.

**Keywords:** Gravity Waves; VLF; LF; Solar Eclipse; Ionization Changes

### INTRODUCTION

ESSENTIALLY one looks for two types of physical aspects when dealing with the VLF or LF radio techniques as a tool for investigating the ionospheric D-region during solar eclipses. One aspect is the time variation of electron density at a particular height. If one measures simultaneously the ionizing radiations, chiefly the solar Lyman- $\alpha$  radiation and X-rays, then it becomes possible for a better understanding of the rather complex aeronomical changes during the eclipse time. Another aspect would be to know something about the dynamics of the middle atmosphere and the possible generation of gravity waves (Chimonas & Hines, 1970, and Chimonas, 1970) because of the passage of the moon's shadow at supersonic speed. If the gravity waves are at all generated, their possible detection in the atmosphere at various levels also comes into question. The present paper deals with VLF/LF detection of ionization changes and gravity waves in the middle atmosphere associated with the Indian total solar eclipse of 16 February 1980.

### METHODOLOGY OF VLF/LF DETECTION

The short path (<500km) measurements offer advantages atleast in two respects.

(i) Localized effects (for example, eclipse associated ionization changes at a particular

place) can be detected and studied more unambiguously and (ii) relatively easy interpretation of data in relation to D-region profiles. The long path measurements offer the following advantages: (i) one can select the desired frequencies and propagation paths by making use of the existing VLF/LF transmitters in the world, (ii) one can monitor ionization changes with better sensitivity and look for dynamical effects over large geographical areas. For maximising the VLF/LF detectability of ionization changes, propagation paths for which the path mid-point falls within the fully eclipsed region would be preferable. For maximising the VLF/LF detectability of buoyancy type of wave motions or the so-called gravity waves, one has to look for propagation paths such that the path mid-point lies close to the regions where the gravity waves are expected to come to a focus. Focussing of these waves can occur due to the curvature of the eclipse path and due to the fluctuations in the speed of the moon's shadow. These focussing regions can be predicted in advance and would be typically several thousand kilometers northwards or southwards of the path of totality (Ball, 1979).

#### SOLAR AND GEOMAGNETIC ACTIVITIES ON THE ECLIPSE DAY

For unambiguous detection and quantitative interpretation of VLF/LF effects due to a solar eclipse, it is desirable that quiet solar and geomagnetic conditions prevail on the eclipse day. A magnetic storm of SC type was reported on 15 January (U.S. Dept. Comm., 1980*b*) and it continued through the eclipse day. The  $H_\alpha$  flares of minor importance, one with start time at 0835 and ending at 0844 with maximum at 0838 IST and the other with start time at 1600 and ending at 1628 with maximum at 1608 IST were reported (U.S. Dept. Comm., 1980*b*) on the eclipse day. Near 1319 IST, there was X-ray flux enhancement in 0.5 to 4 Å range by a factor of about 15 and in 1–8 Å solar X-ray flux, the enhancement was by a factor of 7. These X-ray enhancements started near 1246 IST and ended near 1403 IST with its peak near 1319 IST. Multifrequency microwave solar radio flux measurements during eclipse time by Bhonsle *et al.* (1981) showed characteristic time variations with sudden changes of slope at certain times. Prior to 1900 IST (sunlit VLF/LF paths, receiver at New Delhi) the meter wavelength solar radio emission with the largest duration (415 minutes) peaked near 1320 IST and more intense bursts of 1 to 3 minutes duration occurred near 1444 and 1520 IST (U.S. Dept. Comm., 1980*c*).

#### VLF/LF OBSERVATIONS

The (relative) phase of 16 kHz transmissions (Rugby-New Delhi, path mid-point 47°4'N, 29°6'E) observed by us on 16 February 1980 during the afternoon period is shown in Fig. 1 as the dotted line (scaled every 1.25 minutes). The phase variations on the control days (14 and 15 February 1980) are also shown for comparison. Some interesting features of the phase variation on 16th in relation to those on the control days are marked by arrows. The small phase retardation observed at about 1228 IST could well be the onset of the eclipse associated effect. A large phase advance amounting to about 4.6 μs began at about 1240 IST, the phase minimum reaching at about 1259 IST. The decrease in ionization due to the main phase eclipse effect showed

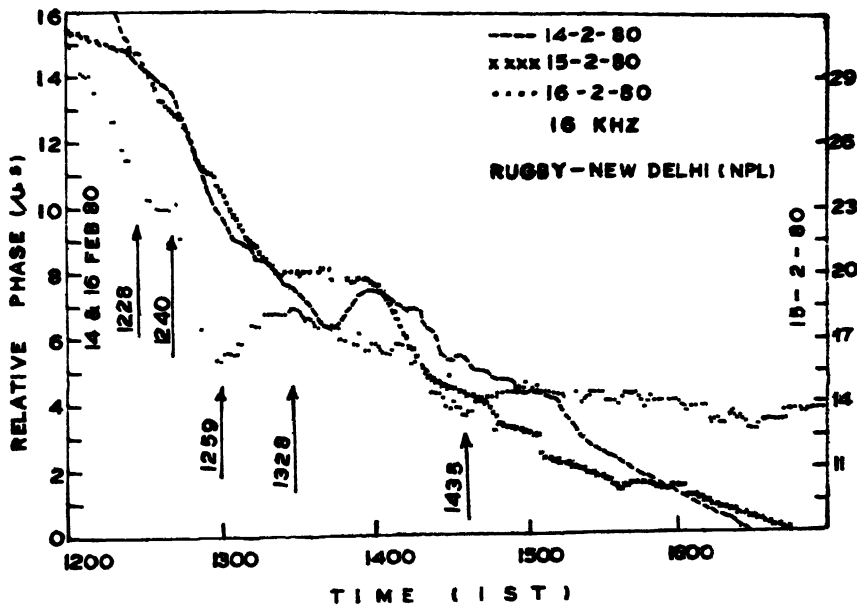


FIG 1 Phase variation of 16kHz transmissions received at NPL, New Delhi.

as phase retardation amounting to about  $1.6\mu\text{s}$  reaching at about 1328 IST. While the VLF phase effect appears to have ended at 1435 IST, there was phase overshoot to values considerably higher than expected as per diurnal trend observed on control days beyond this time.

The published information on VLF phase monitored by U S Naval Observatory, USNO (1980) (corresponding to nearly full daylight VLF paths) on paths which are away (eastwards/westwards) from the path of totality showed propagation phase disturbances of 1 to  $2\mu\text{s}$  near 2030 IST. The difference between the USNO master clock and the arriving phase of the carrier frequency from Rugby at 16kHz (as affected by the daylight phase delay and the USNO master clock and the time reference pulses of the Loran C, D stations and TV transmissions) continuously decreased from  $519\mu\text{s}$  on 14,  $518\mu\text{s}$  on 15,  $515\mu\text{s}$  on 16,  $514\mu\text{s}$  on 17 and  $510\mu\text{s}$  on 18 February 1980. Similarly, the 18.6kHz NLK transmissions monitored by the USNO master clock also showed a steady decrease in phase value from  $325\mu\text{s}$  on 15,  $324\mu\text{s}$  on 16,  $321\mu\text{s}$  on 17 and 18 February 1980. The omega transmissions on 11.8, 13.1 and 13.6 kHz are far more stable and showed a decrease of  $1\mu\text{s}$  only on the eclipse day.

A photograph of the LF signal strength observations on 164kHz (Tashkent-Delhi, path mid-point  $35^{\circ}4'N$ ,  $73^{\circ}24'E$ ) are shown in Fig 2. The top photograph (Fig 2a) shows the record obtained using System I (chart speed 3 inches per hour) and the bottom record (Fig 2b) shows the one obtained using System II (chart speed 25cm per hour). The field strength observed by System I responds to the reflection coefficient  $\|R\|$  of the ionosphere and has to be viewed as a vector sum of ground and skywaves if there is significant ground wave. The field strength observed by System II is proportional to the conversion coefficient  $\|R\|$ . The dominant features observed

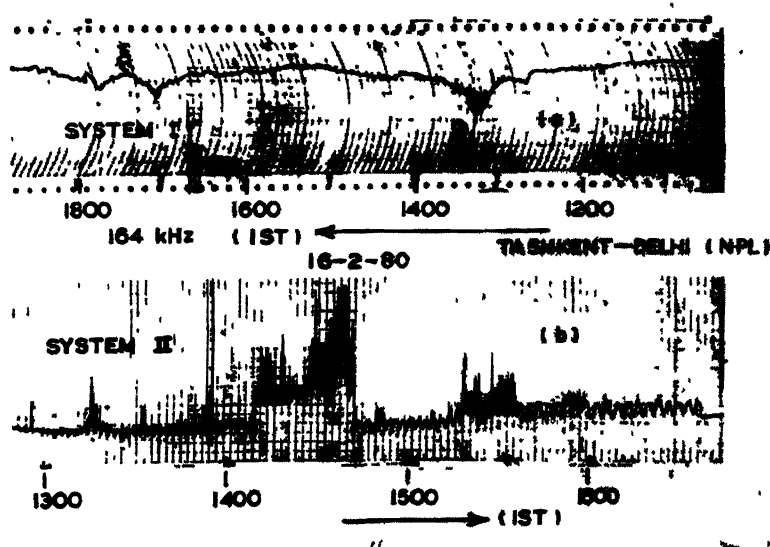


FIG 2. Field strength (relative) variation of 164 kHz transmissions received at NPL, New Delhi (a) on System I and (b) on System II

on the total field record (Fig 2a) was a deep minimum in field strength near 1329 IST and a small minimum near 1550 IST. This small minimum is about 6 minutes after the time of the greatest phase at Srinagar (Total Solar Eclipse, 1979) which is close to the path mid-point.

The dominant characteristic observed by System II was the periodic variation which started to appear on the record at about 1248 IST. We tried to see whether these periodic variations were due to system malfunctioning by rotating the antenna between 1351 and 1422 IST. Near 1409 IST, the gain of the D C amplifier associated with the chart recorder was increased by a factor of two. At 1422 IST the recorder gain was put back to its normal value. The receiver itself was left untouched in any of these operator interventions. From 1422 IST onwards, the receiving system together with the chart recorder was left untouched.

The periodic features were observed continuously throughout the progress of the central eclipse and ended rather abruptly at about 1636 IST. The record shows finer details in the peak to peak amplitude and periodicities throughout the duration of the periodic variations which lasted for nearly 3 hours and 48 minutes. The striking feature is the observation of a well-defined large period large amplitude oscillation of field strength due to the abnormal component of the skywave starting from about 1535 IST onwards corresponding to the partially eclipsed ionosphere conditions at the path mid-point.

Besides our VLF/LF observations, there were reports of 22.3 kHz phase observations by Subrahmanyam (1981) and 16 kHz and omega observations by Sen Gupta *et al* (1981). The Indian Space Research Organization (ISRO) also monitored the phase of 16 kHz at Kavalur (Dixit *et al*, 1981). There are quite a few reports of LF

observations by others as well (Mitra, 1981; Mangal Sain, 1981; and Sen *et al*, 1981).

### DISCUSSION

To assess the implications of these VLF/LF observations, an attempt is made to intercompare the observations reported by several investigators in so far as access to data was possible. Some salient features of intercomparison are shown in Table I. The column numbers are indicated in parenthesis at the top of Table I. The monitoring group is indicated in the first column. Column 2 gives the monitored frequency in the VLF/LF bands. Column 3 gives the geographic co-ordinates of the transmitter and receiver. Column 4 gives the details of occurrence of ionospheric effect preceding eclipse associated main effect corresponding to increase in height of reflection. The magnitude of the eclipse-associated main ionospheric effect is given in Column 6.

Several interesting features can be observed from the results tabulated in Table I and from Figs. 1 and 2. The large phase retardations of  $17.4\mu\text{s}$  on 12.8kHz, La Reunion-New Delhi path and  $12.7\mu\text{s}$  on 12.3kHz, Tsushima Island-New Delhi path are typical of the VLF effects on paths crossing the path of totality of the solar eclipse. The small phase retardation of 1.6 or  $1.8\mu\text{s}$  (corresponding to a change in reflection height of about 0.8km, Wait, 1959) on 16kHz Rugby-New Delhi path which is far away from the path of totality is also typical of the eclipse associated ionospheric effect. The total field observations on 164kHz in New Delhi (System I) showed a 6dB decrease in fieldstrength. This can be understood as due to an increase in the phase height of reflection rather than a decrease expected in the case of X-ray flare effects (Ramanamurty, 1970). Field strength increases by as large as 20dB and 18dB were reported by Mitra (1981) and Sen *et al* (1981) at 164kHz (Tashkent-Roorkee path) and 280kHz (Jessore-Calcutta path) respectively (Table I).

#### *Precursor Effect*

The observation of a precursor effect before the main ionospheric effect, the periodic phase variations throughout the duration of the eclipse and the phase overshoot after the main effect are the most interesting features observed at 16kHz (Fig. 1). Prior to the main ionospheric effect which manifests itself as a phase retardation (corresponding to increase in height of reflection) a significant phase advance amounting to  $4.6\mu\text{s}$  began at about 1240 IST (Table I). A similar precursor effect on 16kHz monitored at Kavalur which is close to the path of totality was also observed by Dixit *et al* (1981). Sen *et al* (1981) observed precursor effects at MF (870kHz) and HF as well. On three of the four VLF paths monitored at a high latitude station (College, Alaska,  $65^\circ\text{N}$ ), Albee and Bates (1965) detected a similar phase advance prior to the main eclipse associated phase retardation associated with the 20 July 1963 total solar eclipse. A phase overshoot after the main effect was also noticed by Albee and Bates.

On 16 February 1980 only one minor SID (IMP 1) was reported by US Dept Comm (1980b) by only one observatory with starting time at 1247 and ending at 1323 with maximum at 1303 IST. If this SID as well as the phase advance on 16kHz starting at 1240 IST were due to a solar flare, we expect correlation with the solar X-ray enhancements immediately preceding the times. As discussed in a previous section,

TABLE I  
*VLF/LF ionospheric effects associated with the total solar eclipse on 16-2-1980*  
 (Times are in IST = UT + 0530, 5h 30m is written as 0530 and so on)

Monitoring Group	Frequency (kHz)	Geographic Co-ordinates of		Precursor/SI D Times			Eclipse associated Times			Magnitude of Effect
		Transmitter	Receiver	Begin	Max	End	Begin	Max.	End	
Sen Gupta <i>et al</i> (1981)	12.3	20°58'S, 55°17'E	28°37'N, 77°13'E	1224	1248		1348	1512	1636	12.7 μs
	12.8	34°37'N, 129°27'E	-do-	1248	1248	1400	1500	1612	1636	10.2 μs
	16.0	52°22'N, 1°11'W	-do-	1240	1254	1512				17.2 μs 1.8 μs
Authors	16.0	-do-	-do-	1240	1259		1259	1328	1435	1.6 μs
Dixit <i>et al</i> (1981)	16.0	-do-	12°34'N, 78°49'E	1424	1437	1451		1545	1655	
N P L { System I	164.0	41°25'N, 69°12'E	28°37'N, 77°13'E	1245	1329	1352	1547	1550		6 dB decrease
	164.0	-do-	-do-				1248		1636	
Dixit <i>et al</i> (1981)	164.0	-do-	23°1'N, 72°36'E	1230	1400	1500	1400	1600		
Mitra (1981)	164.0	-do-	29°51'N, 77°54'E							
	182.0	43.7°N, 76°58'E	29°51'N, 77°54'E					1545		20 dB increase
Sen <i>et al</i> (1981)	280.0	23°10'N, 89°10'E	22°34'N, 88°24'E				1524	1531	1536	18 dB increase

ted wave motions in the middle atmosphere associated with the 16 February 1980 total solar eclipse at places far away from the path of totality and separated by about 12 degrees in latitude. The periodic variations at VLF are similar to those reported elsewhere. The first dominant periodicity of about 12.8 minutes observed at 164 kHz agrees well with the value of 10 minutes observed by Lauter (1974) on the same frequency for the spring season. Lauter as well as Gossard and Paulson reasoned that the periodic variations such as those observed by them at LF and VLF match the known characteristics of gravity waves. To that extent, our observations lend support to the view that the observed wave motions could be due to propagating gravity waves generated from the cooling regions as a result of the moon's shadow sweeping the earth and its atmosphere at supersonic speeds. It appears that ours is the first comprehensive evidence of this kind for the detection of eclipse associated gravity waves. The observed periodicities are about an order of magnitude less than those observed on ground level pressure oscillations (Reddy, 1981) near the path of totality.

#### ACKNOWLEDGEMENT

One of us (YVR) wishes to acknowledge the discussions with Dr A. P. Mitra and Dr R. V. Bhonsle. We are thankful to Mr S. P. Suri for his keen interest on the hardware part of radio receiving System II.

#### REFERENCES

- Albee, P. R., and Bates, H. F. (1965) VLF observations at College, Alaska of various D-region disturbance phenomena. *Planet Space Sci.*, **13**, 175–206.
- Ball, S. M. (1979) Atmospheric gravity wave production from the Australian total solar eclipse of 23 October, 1976. *Aust. J. Phys.*, **32**, 287–288.
- Beynon, W. J. G. (1981) Comments during the presentation of this paper.
- Bhonsle, R. V., *et al.* (1981) Solar radio flux measurements during the total solar eclipse of 16 February 1980. In *Observations of Total Solar Eclipse of 16 February 1980 (Preliminary Results)* INSA, New Delhi, 77–79.
- Brigham, E. O. (1974) *The Fast Fourier Transform*. Prentice-Hall, N. J., Englewood Cliffs, p. 163.
- Chimonas, G. (1970) Internal gravity wave motions induced in the earth's atmosphere by a solar eclipse. *J. geophys. Res.*, **75**, 5545–5551.
- Chimonas, G., and Hines, C. O. (1970) Atmospheric gravity waves induced by a solar eclipse. *J. geophys. Res.*, **75**, 875.
- Dixit, P. S. *et al.* (1981) Phase and field measurements in VLF, LF and HF regions during the solar eclipse of 16 February 1980—preliminary results. In *Observations of Total Solar Eclipse of 16 February 1980 (Preliminary Results)* INSA, New Delhi, 67–70.
- Lauter, E. A. (1974) Evidence and characteristics of internal and planetary waves within the D-region plasma. In *Methods of Measurements and Results of Lower Ionosphere Structure* (Ed. K. Rawer) Akademie-Verlag, Berlin, 377–382.
- Mangal Sain (1981) Experiment No. 20 listed under Ionospheric Physics. In *Summary of the Experiments conducted in India during Total Solar Eclipse of February 16, 1980* INSA, New Delhi.
- Mitra, A. P. (1974) *Ionospheric Effects of Solar Flares*. Reidel, Dordrecht, p. 21.
- Mitra, S. N. (1964) A radio method of detecting solar flares. *J. atm. terr. phys.*, **5**, 375–398.
- (1981) Effect of solar eclipse of February 16, 1980 on lower ionosphere. Abstr. C-4. In *Abstracts, International Symposium on Solar Eclipse* INSA, New Delhi.
- Ramanamurty, Y. V. (1970) Flare effects on LF radio waves propagated over a distance of about

- 1600km *Indian J pure appl Phys*, 8, 569-572.
- Reddy, C. A. (1981) Presented papers C-26 and C-27 In: *Abstracts, International Symposium on Solar Eclipse*, 27-31, Jan 1981. INSA, New Delhi
- Sen A K. *et al* (1981) Radiowave propagation during the total solar eclipse of 16 February 1980 In: *Observations of Total Solar Eclipse of 16 February 1980 (Preliminary Results)*. INSA, New Delhi, 77-79.
- Sen Gupta *et al* (1981) Effect of the 16 February 1980 solar eclipse on VLF propagation *J. atm terr Phys*, (In press).
- U.S Dept Comm (1980a) *Solar Geophysical Data*, 431, Part I, p 10 p 152, July 1980, (1980b) 427, Part I, p 18, March 1980; (1980c) 432 Part II, p. 23, August 1980; (1980d) 432 Part II, p. 32, August 1980, U.S.
- Subrahmanyam, C. V (1981) Experiment No. 14 listed under Ionospheric Physics In *Summary of the Experiments Conducted in India during Total Solar Eclipse of February 16, 1980*, dated 27-1-81 INSA, New Delhi, p. 6.
- India Meteorological Department, (1979) Total Solar Cclipse of 16 February 1980, Circumstances relating to India.
- U.S Naval Observatory (1980) Daily time differences and relative phase values, Series 4, No. 681, 21 Feb. 1980, published by U.S. Naval Observatory, Washington, D C 20390, USA
- Wait, J R (1959) Diurnal change of ionospheric heights deduced from phase velocity measurements at VLF. *Proc. IRE*, 47, 998
- U.S. Dept. Comm (1980b) *Solar Geophysical Data*, 427, Part I, p. 18. U.S. Dept. Comm, Boulder, Colorado.



Printed in India.

**Radio Propagation**

**CHANGES IN THE FIELD INTENSITY OF RADIO SIGNALS AND NOISE  
DURING THE TOTAL SOLAR ECLIPSE OF 16 FEBRUARY 1980 IN  
RELATION TO IONOSPHERIC RADIO WAVE PROPAGATION**

A K SEN, B SAHA, S. K. TREHAN, S SEKSHAR DEY, S K SAHA, R. N DUTTA,  
S K. CHATTERJEE, J. S. SEHRA and M K DAS GUPTA

*Centre of Advanced Study in Radio Physics & Electronics  
92 Acharya Prafulla Chandra Road, Calcutta-700 009, India*

*(Received 15 February 1982)*

Various scientific observations for the studies on the ionospheric propagation of radio signals and noise in the VLF to HF bands were made at different Indian locations in umbral and penumbral regions of the solar eclipse on 16 February 1980. Analysis of the results indicate that, in general, there is an improvement of radio propagation during the eclipse. Some evidence of travelling ionospheric disturbances apparently related to the eclipse is indicated. Besides, a peculiar absorption of signal starting even before the first contact has been observed. The results obtained are compared with other eclipse results and critically examined in the light of the current knowledge about the mechanisms of the ionospheric changes involved, including the gravity wave perturbations.

**Keywords:** Field Intensity; Ionospheric Radio Wave Propagation; Solar Eclipse; VLF, MF & HF Bands; Gravity Wave

**INTRODUCTION**

STUDIES on the changes of the ionosphere during a Solar Eclipse have been made extensively by many workers (Beynon & Brown, 1956, Smith, Jr, 1962; Mavretic, 1968; Narcisi *et al*, 1969, Brace *et al*, 1972; Chakraborty & Chakraborty, 1974; and Jain & Subrahmanyam, 1979). The main objective of these studies was to investigate how the cut-off of the solar ionizing radiations during the eclipse directly affects the different regions of the ionosphere. After the pioneering work of Hines (1960) on the nature and origin of atmospheric gravity waves, other workers (Chimonas, 1970; Chimonas & Hines, 1970; and Datta, 1972, 1973) have studied the effect on the ionosphere during an eclipse by invoking in the phenomena of the gravity wave perturbations. Besides these, reports have been made of some peculiar absorption events occurring before and after the eclipse period apparently related to the eclipse phenomenon (Hennessey & Torres, 1956). During the total solar eclipse of 16 February 1980 which was visible from Indian sub-continent a series of experiments were programmed and conducted by various groups of investigations in different parts of India covering the umbral and penumbral regions of the eclipse. We also participated in some of these programmes (Sen *et al*, 1980, 1981). Our experiments were mainly aimed at obtaining information about the changes of the ionospheric propagation.

characteristics during the eclipse. We observed, apart from a general improvement of the ionospheric propagation due to the decrease of electron density in the lower ionosphere, a peculiar pulse type field change of radio signals before the peak phase of the eclipse. Also some evidence of a pre-eclipse field changes was obtained. Some of these interesting results are presented in the paper.

### EXPERIMENTS

The receiving stations were set up at Puri ( $19^{\circ}50'N$ ,  $85^{\circ}50'E$ ), Varanasi ( $25^{\circ}6'N$ ,  $82^{\circ}42'E$ ) and Calcutta ( $22^{\circ}34'N$ ,  $88^{\circ}24'E$ ). The location of the transmitting and receiving stations is shown in Fig. 1. HF radio broadcast signals from Radio Ceylon

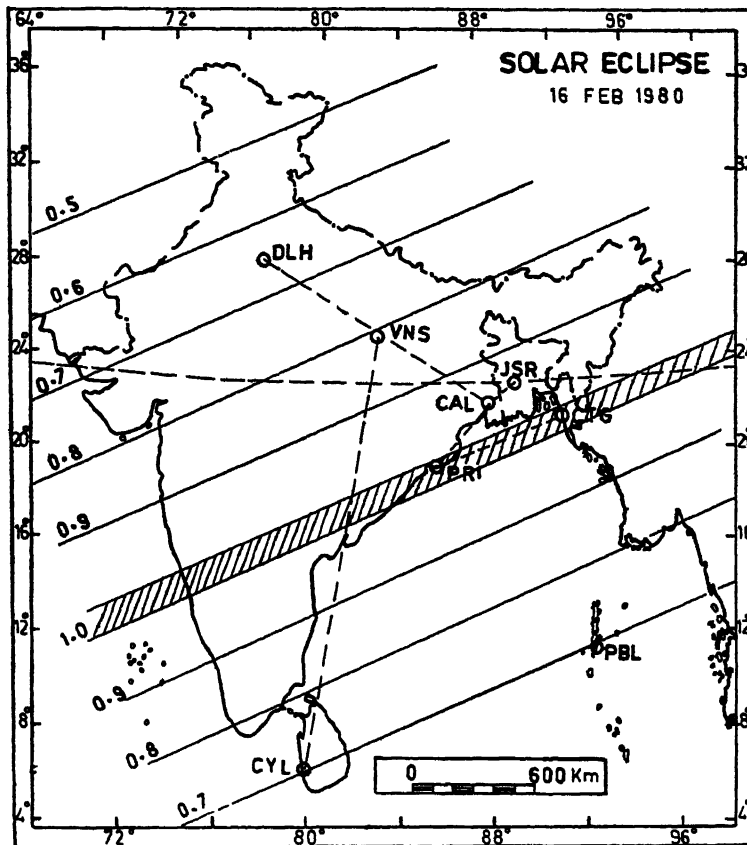


FIG 1 Location of different observational sites for the study of solar eclipse effects

( $6^{\circ}52'N$ ,  $79^{\circ}50'E$ ) on 11.8 MHz was recorded at Varanasi, while MF radio broadcast signal from Chittagong ( $22^{\circ}27'N$ ,  $91^{\circ}48'E$ ) in Bangladesh on 870 kHz was recorded at Puri. From Calcutta the radio signals recorded include the HF standard frequency transmission on 10 MHz, ATA, from New Delhi ( $28^{\circ}33'36'N$ ,  $77^{\circ}18'48'E$ ). LF radio navigational signal on 280 kHz from Jessore ( $23^{\circ}10'N$ ,  $89^{\circ}10'E$ ) in Bangladesh

Also the radio noise due to the atmospherics in the VLF band on 30kHz was recorded in Calcutta.

### OBSERVATION

The records obtained at different stations are reproduced on a common time scale in Fig 2. The times of start, peak phase and end of the eclipse are indicated by arrows. In all these records, we notice a general trend of increase of the field strength during the peak phase of the eclipse. The increase is most marked in the HF band. Besides this general trend, a remarkable pulse type field change having a duration of about 20 minutes has been observed in each of the records. The field change is in the form

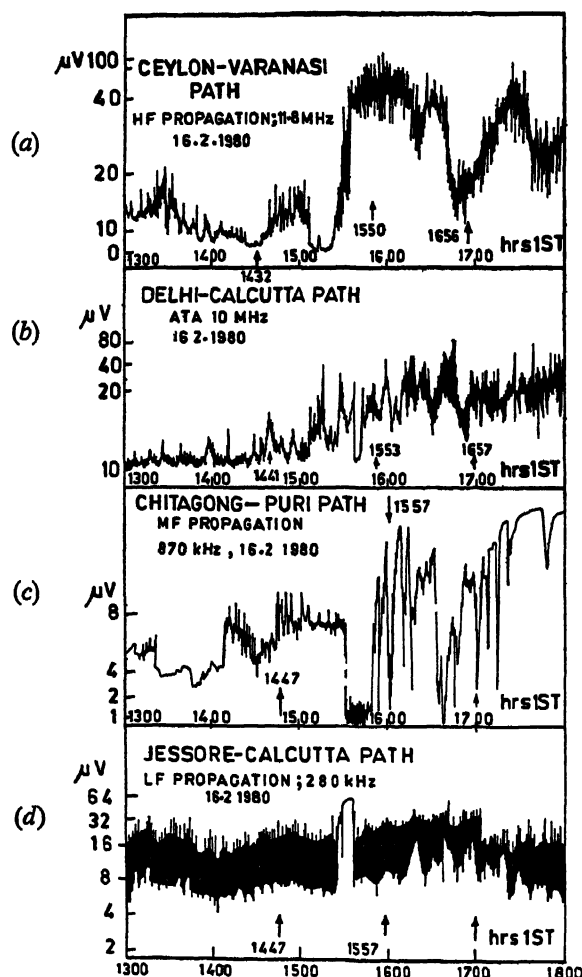


FIG 2 Records showing effects of the total solar eclipse in the reception of (a) HF broadcast at Varanasi, (b) HF standard broadcast at Calcutta, (c) MF broadcast at Puri and (d) LF navigational signal at Calcutta.

of an absorption in the HF and MF band while it appears as an enhancement in the LF band. The duration and time of start of the field changes are shown in Table I.

TABLE I

Radio Propagation path	Time of 1st contact at mid path point IST	Time of peak phase of eclipse at path mid point IST	Time of onset of field change IST	Delay of onset effect relative to 1st contact	Delay of onset effect relative to the effect at Varanasi	Duration of pulse type field change	Nature of pulse type field change
Ceylon-Varanasi	1432	1550	1508	36min	0min	21min	Absorption HF
Delhi-Calcutta	1441	1553	1537	56 "	29 "	9 "	" HF
Chittagong-Puri	1447	1557	1530	43 "	22 "	19 "	" MF
Jessore-Calcutta	1448	1557	1522	34 "	14 "	14 "	Increase LF

which also indicates the times of start of the first contact and the peak phase of the eclipse.

#### DISCUSSION

The decrease in the D-region ionization during the eclipse with no significant effect in the  $F_2$ -region is borne out by the effects observed on the HF propagation for the Ceylon-Varanasi path. The distance between the stations being 2150km, the HF propagation at 11.8MHz is supported by the E-layer, with the D-region acting as the absorber. The electron density in the D-region decreases causing the signal to go up during the eclipse. In fact, the downward passage of the E-layer reflected signal through the D-region occurs in the path of totality. With the progress of the eclipse the ionization in the E-region drops to a value which no longer permits reflection from the layer. At such times efficient reflection from  $F_2$ -region which is little affected, starts in the absence of a sizeable absorption in D- and F-regions. All these factors together cause the signal strength to increase by about 20dB from the pre-eclipse value.

In contrast to the HF result of the Ceylon-Varanasi path where the path mid-point is near the path of totality, other HF signal strength result due to the Delhi-Calcutta path on 10MHz exhibits a much less marked effect with the increase of signal being more gradual. This may be due to the fact, that the path mid-point lies over Varanasi where the obscuration of the Sun was 81 per cent compared to 100 per cent for the Ceylon-Varanasi path.

In the MF band the general level is found to increase by about 8dB during the peak phase of the eclipse although the increase is accompanied by marked fading effect.

In the LF band the increase in the general level is smaller about 6dB, whereas the atmosphere radio noise in the VLF band observed on 30kHz showed a slight increase during the event (Fig. 3).

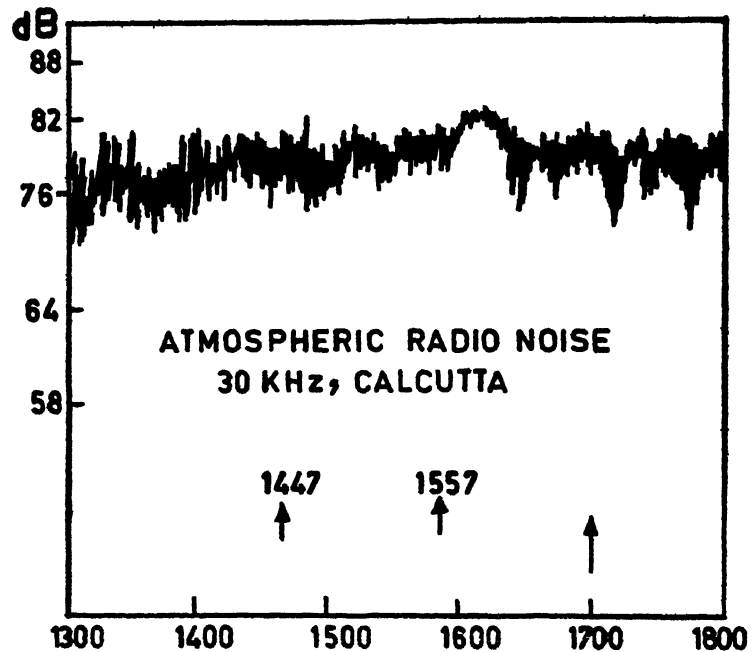


Fig. 3. Record showing eclipse effect on atmospheric noise at 30kHz, received at Calcutta.

From the table we also notice an interesting sequence of start of the pulse type absorption with the effect starting earliest for the Ceylon-Varanasi path, for which the path mid-point is near the path of totality. The gravity wave perturbations at 80–90 km level may be caused in two different ways, one is by direct cooling at that level while the other is through cooling at lower atmosphere and subsequent transportation of the generated gravity waves to lower ionospheric heights. It appears from the table that the delay of the effect after the first contact is more than that of the expected travel time of any gravity wave perturbations. Actually, the bow waves associated with the first contact are inclined to the direction of travel of the cooling spot, so that at a point remote from the path of totality the effect would be observed later.

If we consider the pulse type depression in each of the records, we notice that they do not occur simultaneously as would be expected during a solar flare, but there exists a sizeable time shift between the depressions observed for different propagation paths. The timeshift is indicative of the role of a travelling ionospheric disturbance associated with the eclipse phenomena. The effect seems to be a probable cause of such small scale TID's generated at such times. It is believed that the passage of the cool-shadow-region through the atmosphere at supersonic speeds of the order of 6000–8000 km per hour causes gravity wave perturbations in the troposphere. The gravity waves from this source region propagate upwards to lower ionospheric heights producing a sudden increase of ionization at 80–90 km through a redistribution of existing ionization (Datta, 1973, Chimonas, 1970, and Chimonas & Hines, 1970). It may be mentioned here that enhanced ionization at the 80–90 km level may indeed, result in the absorption of HF signals while at the same time causing an in-

crease of reflection of LF signal. This may explain the pulse type enhancement in the LF band. The characteristics of the pulse type absorption also suggest that it cannot be the effect of any ionization mechanism at the heights involved. For no ionization or recombination mechanism can have such high time constants. Also, the formation of gravity wave perturbations requires the presence of appreciable water vapours in the atmosphere, which do in fact exist in the tropical regions like India. In places where the water vapour content is small, such gravity wave perturbations may be insignificant.

#### REFERENCES

- Beynon, W. J G, and Brown, G M (1956) *Solar Eclipse and the Ionosphere*. Pergamon Press, London.
- Brace, L H, Mayer, H G, Pharo, III M W., Scot, L. R., and Spencer, N. W (1972) *J. atm terr. Phys*, 34, 673
- Chimonas, G (1970) *J. geophys Res*, 75, 5545.
- Chimonas, G, and Hines, C O (1970) *J. geophys. Res*, 75, 875
- Chakraborty, Purabi and Chakraborty, D K (1974) *Indian J Radio & Space Phys.*, 3, 319.
- Datta, R. N (1972) *J geophys Res.*, 77, 260
- (1973) *J. geophys Res*, 78, 320.
- Hines, C. O (1960) *Can J. Phys*, 38, 1441
- Hennessey, J J, and Torres, J S. (1956) *Sp Suppl J A.T.P., Solar Eclipse and the Ionosphere*, 16, 65
- Jain, S L, and Subrahmanyam, C V. (1979) *Indian J Radio & Space Phys*, 8, 348.
- Mavretic, Aution (1968) D-region parameters from continuous waves, low frequency, rocket propagation, Experiments during the Solar Eclipse of November 12, 1966 *Ionospheric Research Scientific Report No 323*. (Final report Part A) Sept Pennsylvania State University Contract, DAADO5-67-C-0005
- Narcisi, R. S, Bailey, A D, and Della Laca, L (1969) *Aeronomy Rep No. 32* University of Illinois, Illinois, 450
- Sen, A K, Trehan, S K, Dey, S, Sekhar and Saha, S K (1980) Enhanced sweeper activity during the total solar eclipse of Feb 16, 1980 in relation to transionospheric propagation. Presented at the Symposium on 'Communication' sponsored by IETE being held at Calcutta on May 23-24
- Sen, A K, Saha, B, Trehan, S K, Dey, S, Sekhar, Saha, S K, Datta, R N, Chatterjee, S K, Sehra, J S, Das Gupta, M K, and Sen, S K (1981) Radio wave propagation during the total solar eclipse of February 16, 1980. *Proc Indian natn Sci Acad*, 47, A, 77
- Smith (Jr), E K (1962) *Monograph on Ionospheric Radio* (Ed W. J G Beynon) Elsevier Publishing Co Inc, New York, 53

Printed in India.

Radio Propagation

## MULTI-STATION MONITORING OF SHORT AND MEDIUM WAVE BROADCAST CIRCUITS DURING SOLAR ECLIPSE OF 16 FEBRUARY 1980

D. R. LAKSHMI *and* B. M. REDDY

*National Physical Laboratory, New Delhi-110 012, India*

*and*

R. CHAKRAVARTHY *and* MANGAL SAIN

*Research Department, All India Radio, New Delhi-110 001, India*

*(Received 15 February 1982)*

During the 16 February 1980 total solar eclipse, several short wave and medium wave broadcasts of All India Radio were monitored at several locations on either side of the path of totality, the disposition of the stations so chosen as to locate the control points of the circuits in the totality path. Special mention may be made of the short wave transmissions at 15.25 MHz from Delhi and 9.55 MHz from Bombay which were monitored at Madras and Trivandrum. In addition, a few medium wave transmissions also were monitored so that information can be derived on the change in the pattern of field intensity recording with change in the altitude of the control points. Ionosondes were specially pressed into operation for this event at two stations located in the totality. It was observed that the increase in the signal intensities during the totality is higher than the total ionospheric absorption given by the CCIR formula. This indicates that the CCIR formula underestimates the ionospheric absorption by as much as 12 dB in certain cases.

**Keywords:** Radio Communication; Field Strength; Ionospheric Absorption; Solar Eclipse

### INTRODUCTION

THE rapid change in the lower absorbing region as eclipse onsets and recedes gives valuable information which will help in estimating the absorption for varying solar conditions. For example, none of the existing methods for field strength calculations in the HF bands including the latest CCIR method agree with the observations because of several uncertainties in ionospheric reflected propagation. The estimation of non-deviative absorption in the D-region is a critical parameter in designing HF links and the total solar eclipse is uniquely suited for this purpose because of the rapid collapse of the D-region during the eclipse with marginal changes in the F-region, which is the reflecting region, for several HF circuits chosen in this study.

## FIELD STRENGTH MEASUREMENTS OF SHORT AND MEDIUM WAVE BROADCASTS

During the 16 February 1980 event, several short wave and medium wave broadcasts of All India Radio were monitored at several locations on either side of the path of totality (Table I), the disposition of the stations so chosen as to locate the

TABLE I

*Details of various short and medium wave broadcast circuits monitored during 16 February 1980 solar eclipse*

Transmitter Location	Receiver Location	Power KW	Frequency kHz	Great circle distance km	Reflection point (1 hop) Latitude Longitude	Maximum percentage obscuration at reflection point
Ceylon	Delhi	100	11800	2420	17°52'N 78°34'E	97
Visakhapatnam	Delhi	100	927	1370	23°10'N 80°16'E	85
Nagpur	Delhi	100	585	840	24°52'N 78°07'E	75
Delhi	Madras	50	15250	1762	20°54'N 78°45'E	90
Bombay	Madras	10	9550	1035	16°03'N 76°34'E	Total
Nagpur	Madras	100	585	900	17°05'N 79°39'E	Total
Bombay	Madras	20	1188	1035	16°03'N 76°34'E	Total
Ceylon	Calcutta	100	11800	1924	14°48'N 84°15'E	Close to totality
Visakhapatnam	Calcutta	100	927	770	20°10'N 85°15'E	Total
Delhi	Trivandrum	50	15250	2240	18°36'N 77°03'E	Total
Jafna (Sri Lanka)	Kozhikode	20	990	510	10°30'N 78°03'E	95

control points of the circuit in the totality path. An ionosonde was also specially pressed into operation at Cuttack, which was in near totality zone to derive information on variations in ionospheric communication parameters viz.,  $f_oF_2$ ,  $h_mF_2$  and  $f_oE$  during the eclipse.

The field strength measurements were started about four days prior to the eclipse day and continued for another four days after. The measurements were restricted only to the period 1330–1700hr (IST). Sufficient care was exercised to ensure that the terminal parameters of the transmitting and receiving equipments such as effective radiated power, antenna gain and receiver sensitivities were maintained constant during the entire period of operation.



Fig. 1 shows the field strength measurements of the short wave broadcasts at 15.25MHz from Delhi and 9.55MHz from Bombay. The Delhi transmission at 15.25MHz was monitored both at Madras and Trivandrum, whereas the 9.55MHz transmission from Bombay was monitored only at Madras. Field strength variation for the eclipse day as well as for control days are plotted in the figure. The control day curve is derived from the median values of field strength during a seven day period preceding and following the eclipse day.

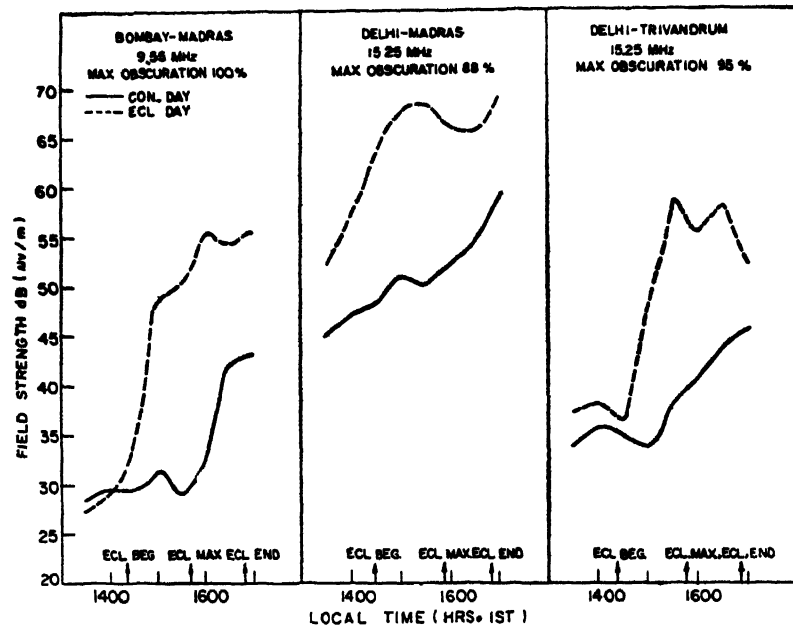


Fig 1 Measured field strength values for three shortwave broadcast circuits during control days and eclipse day. The steep increase in field strength during the solar eclipse period can be seen in all the cases.

The reflection points for one-hop propagation mode for Bombay-Madras and Delhi-Trivandrum were under 100 per cent obscuration level at the maximum phase of the eclipse, whereas the reflection point was at 88 per cent obscuration level for Delhi-Madras path for the same mode of propagation. The field strength values increased very rapidly during the eclipse, the increase being as much as 23dB in case of 9.55MHz transmission from Bombay recorded in Madras during the maximum phase of the eclipse. It has also been observed that maximum increase in field strength occurred earlier to the eclipse maximum. It has to be also noted here that field strength values at Madras for 15.25MHz transmissions from Delhi showed an increasing trend earlier to the onset of eclipse. In other cases shown in Fig 1 the increasing trend almost coincided with the beginning of the eclipse.

Medium wave transmissions from several AIR stations were monitored for more than a week, from 12-19 February 1980, at several locations in India and in addition Radio Ceylon medium wave transmissions from Jafna were monitored at

Kozhikode during the same period. Fig. 2 shows the observed values of field strength for both eclipse day and control day for AIR transmission on 585kHz from Nagpur recorded at Madras and for 927kHz transmission from Visakhapatnam recorded at Delhi. The figure also shows the values for Jafna transmission on 990kHz

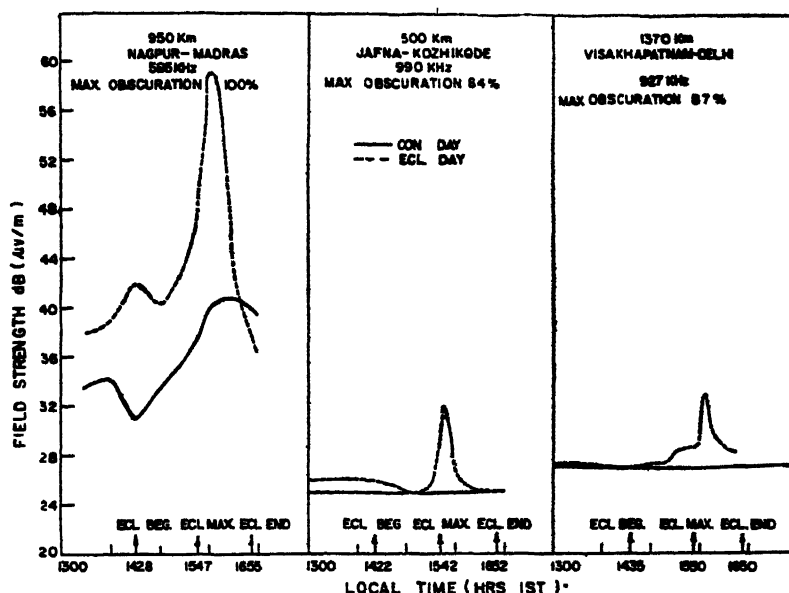


FIG 2. Measured field strength values for three medium wave broadcast circuits during control days and eclipse day. The remarkable increase in field strength following the maximum phase of solar eclipse can be seen for Nagpur-Madras circuit at 585kHz

recorded at Kozhikode. In all the cases, it has been observed that contribution to field strength has been only from ground wave between 1330 and 1700hr and the sky wave contribution can be seen only during the maximum phase of the eclipse. The most significant result is the spectacular increase in field strength for 585kHz transmission from Nagpur recorded in Madras and the reflection point for one-hop propagation mode for this circuit was under 100 per cent obscuration level during the maximum phase of the eclipse. The increase in field strength was as much as 30 dB from its control day value. It has been found that the increased field strength value during the eclipse maximum corresponds to estimated value of field strength based on CCIR procedures for medium wave field strength calculations, for midnight conditions (CCIR, 1976a, 1980a).

The increase in field strength for Visakhapatnam-Delhi and Jafna-Kozhikode circuits are not very spectacular and the reflection points for one-hop propagation mode for these circuits are in 87 per cent and 84 per cent obscuration levels respectively at the maximum of the eclipse. The CCIR estimates have indicated that the increased values correspond only to sunset conditions for Visakhapatnam-Delhi and Jafna-Kozhikode circuits.

## DISCUSSION

There have been several attempts in the past to measure field strengths of HF transmission during solar eclipses (Kanaya & Ueno, 1958, and Rastogi *et al*, 1956). These studies have yielded valuable information on variations in HF propagation modes during eclipses consequent to changes in ionospheric layers. In the present study, the eclipse time HF field strength measurements along with ionosonde measurements have been used for the first time to evaluate quantitative estimates of ionospheric absorption based on CCIR field strength calculation procedures (CCIR, 1976b; and CCIR 1978).

There is overwhelming evidence to show that D-region ionization decreases markedly during an eclipse and reaches negligible levels during the totality of the eclipse (Chakravathy & Mitra, 1974). This decreased ionization in D-region also results in decrease levels of non-deviative absorption for a radiowave as it travels through this region and consequent sharp increases in the field strength values. There is also experimental evidence to believe that the ionospheric changes at higher heights are marginal when compared to changes in D-region.

An estimation of ionospheric absorption using CCIR-recommended procedures is made for various HF circuits listed in Table I. The ionospheric absorption was calculated for the most dominant modes of propagation depending upon the great circle distance between the transmitter and receiver locations. For example, the two most dominant modes of propagation considered for Delhi-Madras and Bombay-Madras circuits are 1F and 1E modes. For Delhi-Trivandrum circuit both one-hop and two-hop F-region modes (1F and 2F) are considered while contributions to field strength by E-region propagation is found to be not significant.

Figs. 3, 4 and 5 show the measured field strength values for control days (curve 1) and eclipse day (curve 2) for the above mentioned circuits. The field strength values are also plotted for different modes of propagation for each of the circuits. The curves marked '3' in Figs. 3, 4 and 5 show the field strength values for 1F mode of propagation whereas curves marked '4' in Figs. 3 and 4 show the values for 1E mode. The curve marked '4' in Fig. 5 represents the values for 2F mode. However, these values represent the situation where the ionospheric absorption is totally absent. The values have been obtained for various modes by enhancing the control days values by an amount equal to the loss in the field strength due to ionospheric absorption as estimated by CCIR procedures.

It is expected that the observed field strength value during the total solar eclipse should be approximately equal to the field strength value on normal days plus the estimated ionospheric absorption loss for different modes. However, the results show that the observed field strengths on the eclipse day are much higher than expected on the basis of the observed field strength on control days plus the CCIR-estimated absorption loss. Thus the present study clearly demonstrates that the increase in the field strength during totality is not compatible with the CCIR estimate of ionospheric absorption. In fact, the results indicate that the CCIR formula underestimates the ionospheric absorption by as much as 12 decibels. It should also be mentioned that enough care was taken in choosing the data, so that the effect of other factors such as change in propagation modes, change in deviative absorption, eclipse-

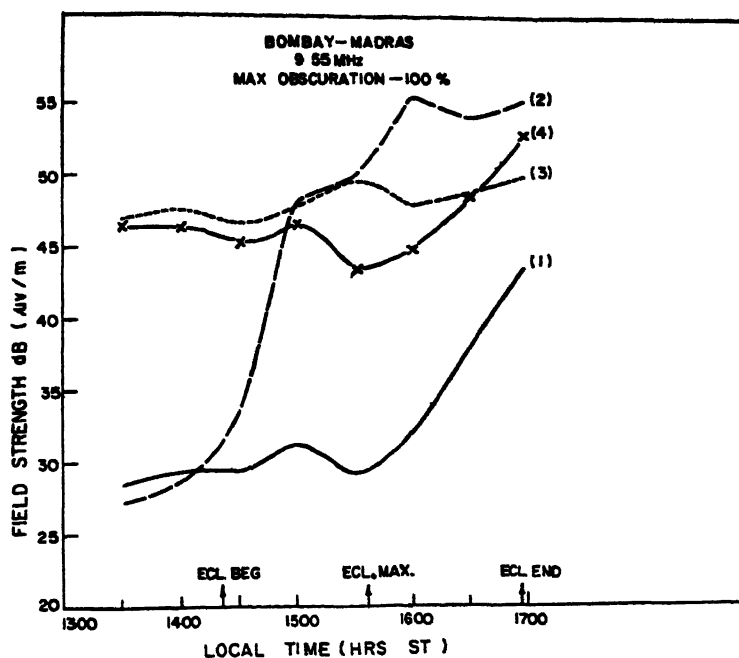


FIG. 3. The curves marked 1 and 2 show the field strength values of 9.55MHz transmissions from Bombay monitored at Madras on control days and eclipse day respectively. The curves marked 3 and 4 show the computed field strength values for 1F and 1E modes of propagation for Bombay-Madras circuit in absence of ionospheric absorption.

time tilts in the ionosphere, etc. are minimised. The ionosonde measurements also indicate only marginal changes in the F-region critical frequency and peak heights on eclipse day as compared to the control days, which only confirm that the propagation modes have not altered on the eclipse day.

### CONCLUSION

It has been realised for quite sometime now that the CCIR formula for estimating the ionospheric absorption in HF communication is inaccurate by varying degrees at different latitude zones (CCIR, 1980b). Under normal conditions it is difficult to exclusively estimate the ionospheric absorption from the observed field strengths of HF transmissions due to uncertainties in effective radiated power, antenna gain, focusing and defocusing effects, polarisation coupling loss, etc. However, a total solar eclipse, which essentially eliminates the non-deviative absorption term without significantly affecting all other existing propagation conditions, provides a unique opportunity of verifying the CCIR formula. Perhaps, the only inaccurate presumption is that the non-deviative absorption has disappeared completely where actually there will be some remnant contribution. Thus the departure from the CCIR formula estimate observed here should be viewed as the minimum error in the CCIR estimate. This argument should be valid as long as the operating frequencies are well below

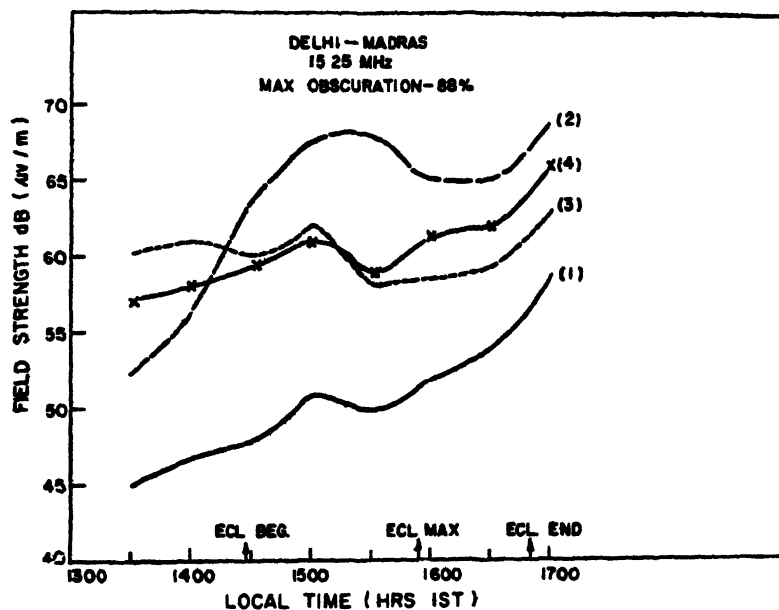


FIG 4. The curves marked 1 and 2 show the measured field strength values for Delhi-Madras circuit at 15.25MHz on control days and eclipse day. The curves marked 3 and 4 show the computed field strength values for 1F and 1E modes of propagation for the same circuit in absence of ionospheric absorption.

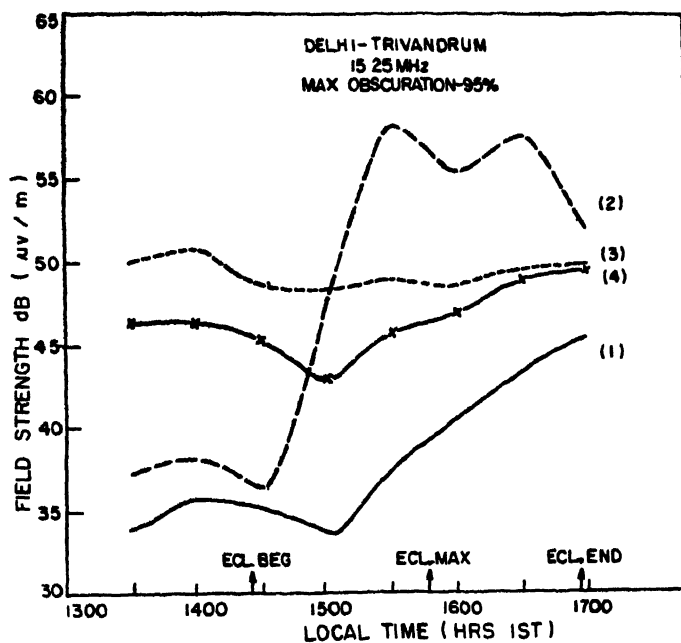


FIG 5. The curves marked 1 and 2 show the measured field strength values for Delhi-Trivandrum circuit at 15.25MHz on control days and eclipse day. The curves marked 3 and 4 show the computed field strength values for 1F and 2F modes of propagation for the same circuit in absence of ionospheric absorption.

the maximum usable frequency for that particular circuit to keep deviative absorption at a negligible level and in all the cases reported here this condition was satisfied.

#### REFERENCES

- CCIR (1976a) Methods for predicting sky-wave field strengths at frequencies between 150kHz and 1600kHz; Rep. 575 (Rev 76), Documents of Interim Meeting of Study Group 6 (Ionospheric Propagation), International Telecommunication Union, Geneva
- (1976b) Second CCIR computer based interim method for estimating sky-wave field strength and transmission loss at frequencies between 2 and 30MHz; Rep 252-2 (Rev. 76), Documents of Interim Meeting of Study Group 6 (Ionospheric propagation), International Telecommunication Union, Geneva
- (1978) Developments in the estimation of sky-wave field strengths and transmission loss at frequencies above 1.6MHz Draft new report, Documents of Final Meeting of Study Group 6 (Ionospheric Propagation), International Telecommunication Union, Geneva.
- (1980a) Prediction of sky-wave field strength between 150 and 1600kHz, Recommendation 435-3, Documents of Interim Meeting of Study Group 6 (Ionospheric propagation), International Telecommunication Union, Geneva.
- (1980b) Comparisons between observed and predicted sky-wave signal intensities at frequencies between 2 and 30MHz, Report 571-1 Documents of Interim Meeting of Study Group 6 (Ionospheric propagation), International Telecommunication Union, Geneva
- Chakravarthy, D. K., and Mitra, A. P. (1974) D-region during solar eclipse. In: *Methods of Measurements and Results of Lower Ionosphere Structure* (Ed. K. Rawer). Akademik-Verlag, Berlin, 183-194.
- Kanaya, S., and Ueno, K. (1958) Propagation mechanism of high frequency waves related to the annular eclipse of 19th April, 1958 *Rep Ionosphere Res. Japan*, XII, 188-195.
- Rastogi, R. G., Sheriff, R. M., and Nanda, N. G. (1956) Some measurements of the signal strengths of radio waves reflected from the ionosphere during the solar eclipses of 30 June 1954 and 20 June 1955 In *Solar Eclipses and Ionosphere* (Eds W. J. G. Beynon and G. M. Brown) Pergamon Press, London, New York, 137-142.

Printed in India.

Radio Propagation

## IONOSPHERIC RADIO EFFECTS OF THE SOLAR ECLIPSE ON 16 FEBRUARY 1980

K. G. JANI, G. DATTA, D. B. PATEL and K. M. KOTADIA

*Physics Department, Gujarat University, Ahmedabad 380 009, India*

*(Received 26 March 1982)*

The solar eclipse at Karwar (14°N, 74°E) was total for about 2½ minutes around 1540hr IST and this place happens to be the midpoint of one-hop Colombo-Ahmedabad ionospheric radio propagation path. The field strength of radio signals on 11.8 MHz transmitted from Radio Sri Lanka and received at Ahmedabad showed an increase of about 23dB above the normal value and the maximum of increase occurred during the totality of the solar eclipse. This effect was clearly noticed in spite of the fact that the eclipse day was magnetically disturbed.

At Ahmedabad (23°N, 72°E) where the solar eclipse was about 75 per cent at its maximum phase around 1541hr IST, vertical incidence A1-ionospheric radio pulse absorption on 2.2 and 1.8 MHz reduced to half of its normal value (22-25dB) with a time-delay of about 18 minutes following the maximum phase. The above results are discussed in relation to the changes in the ionisation in the lower ionosphere and the modes of oblique path radio propagation associated with the obscuration of solar radiation during the eclipse.

**Keywords:** Ionosphere; Solar Radiation; Radio Propagation

### INTRODUCTION

DURING the total solar eclipse that occurred on 16 February 1980, we were interested in seeing the changes that took place in the ionosphere which greatly affects the radio communication in the medium and short wave bands. While many observations have been made in the past on eclipse-associated ionospheric phenomena and reported in literature there are still some outstanding problems for further investigations such as distribution of active areas on the solar disc emitting radiations in different wavelength regions, effective eclipse-function for coronal X-rays, response of the ionospheric layers contributing deviative and nondeviative absorption of radio waves, gravity waves and so on.

### METHODS OF MEASUREMENT AND ANALYSIS

Short-wave radio signals on 11.8 MHz frequency transmitted from Radio Sri Lanka were received and continuously recorded at Ahmedabad employing a half-wave dipole antenna, a communication receiver and a D C amplifier-cum-pen recorder. The pen-recorder scale was calibrated in terms of millivolts input to the receiver.

using a standard signal generator. The strengths of the radio signals thus received along an oblique path after reflection at a certain height from the ionosphere during the eclipse were compared with their control days' mean value at corresponding hours. At Ahmedabad, absorption of vertically incident radio pulses of width  $100\ \mu\text{s}$  and repetition rate  $30\text{Hz}$  was measured at 15-minute intervals on the eclipse day and half-hourly on  $\pm 3$  control days.

## RESULTS

### a) Short-Wave Radio Signal on 11.8MHz From Colombo

The surface distance between Colombo and Ahmedabad is about 2000km. One-hop E-layer propagation over this distance is not possible, but the signal can travel to Ahmedabad either by two-hop E-layer reflection or one-hop  $F_1/F_2$ -layer reflection. For 11.8MHz operating frequency at oblique incidence, the corresponding equivalent vertical incidence frequency is 2.32MHz for E-layer reflection, about 3.0MHz for reflection at 250km height, 3.5MHz for reflection at 300km height in the  $F_2$ -layer, and 2.35MHz for reflection at 200km height in the  $F_1$ -layer.

Fig. 1 gives reproduction of the actual pen-chart record of the received signal

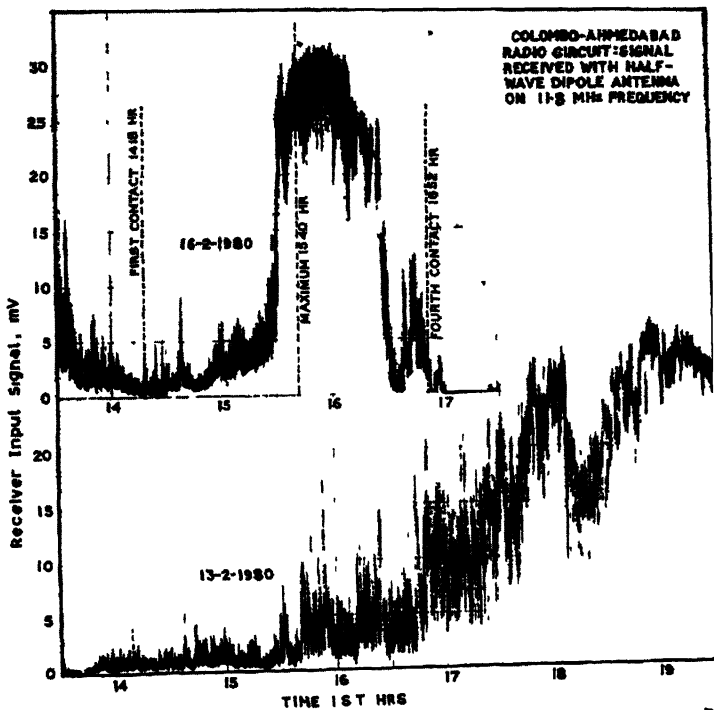


FIG 1 Pen-chart records of short wave signal strength received at Ahmedabad from Colombo on 11.8MHz. The eclipse-day (16-2-1980) record is compared with that on one of the control days (13-2-1980).



at the input of the receiver terminals on the solar eclipse day and it is compared with that on a control day, 13 February 1980 (Planetary magnetic activity index sum  $\Sigma K_p = 4_+$ ). Incidentally, a geomagnetic storm was in progress on the eclipse day ( $\Sigma K_p = 34_+$ ) whereas the shown control day was a relatively quiet day.

It may be noted that the received signal under normal day during 1200–1500hr is about 1.5mV, but it has already begun to increase after the time of first contact of the eclipse (1418hr) and rose to a maximum value of 27mV during the period of totality around 1540hr IST at the midpoint of the propagation path by one-hop. It is interesting to note that the recorded signal during the maximum phase of the eclipse was nearly of the same magnitude as that recorded just near the sunset time when usually the D-, E- and F<sub>1</sub>-layers practically disappear, or the electron concentration in them is below the value needed for reflecting or largely absorbing the HF radio waves traversing through them. Moreover, the record shows violent fluctuations, this being a general characteristic feature of the F<sub>2</sub>-layer propagation condition near sunset time and also during a magnetically disturbed day. In spite of this disturbance, the eclipse-effect on the short-wave radio reception was distinct and it may be attributed to the decrease in absorption of its power in the underlying D- and E-layers and it seemed as if sunset condition was created during the totality of the eclipse. The recovery of the signal to the normal value after the last contact (1652hr IST) was followed by oscillatory changes and even the general level of the signal on the eclipse (disturbed) day was below normal.

In Fig. 2 are shown the variations in decibels (dB) of the received signal level on the eclipse day relative to the mean of the signal values recorded on control days 13–19 February, excluding 15 February which day was magnetically disturbed. It could be seen that during the eclipse the signal rose to 23dB about 10 minutes before the time of totality and it sustained at high level falling gradually to 18dB until a few minutes before the last contact of the eclipse after which it fell fast to the normal level. The progress and regress of the eclipse are also shown in the figure in terms of the fraction of the solar disc occulted by the moon's shadow moving eastwards. Although the radio signal was much absorbed in the lower regions of the ionosphere along the oblique path during the eclipse, the instantaneous changes and the rates of increase and decrease in the signal do not match with those of optically eclipsed solar disc, which in fact indicates that the observed effects of radio communication cannot be due to the obscuration of the incident ionizing radiation alone, but they are rather complexly involved in context with the structural dynamics of the ionosphere. Rastogi *et al* (1956) reported a maximum increase of about 8dB in the Colombo—Ahmedabad transmission on 7.19MHz for the condition of 77 per cent maximum eclipse at the point of reflection on 20 June 1955 at 0812hr IST. This maximum increase occurred 8 minutes before the maximum phase of the eclipse.

#### *b) Vertical-Incidence Radio Pulse Absorption*

Transmission vertically upwards of radio pulse of 100μs duration and 30Hz pulse repetition rate on 1.8 and 2.2MHz were done and the amplitudes of the echoes received downwards after reflection from the E-layer were recorded on a strip-chart over an interval of 5 minutes. This transmission and reception were repeated quarter-hourly on the eclipse-day and half-hourly on control days. Fig. 3 shows the variation

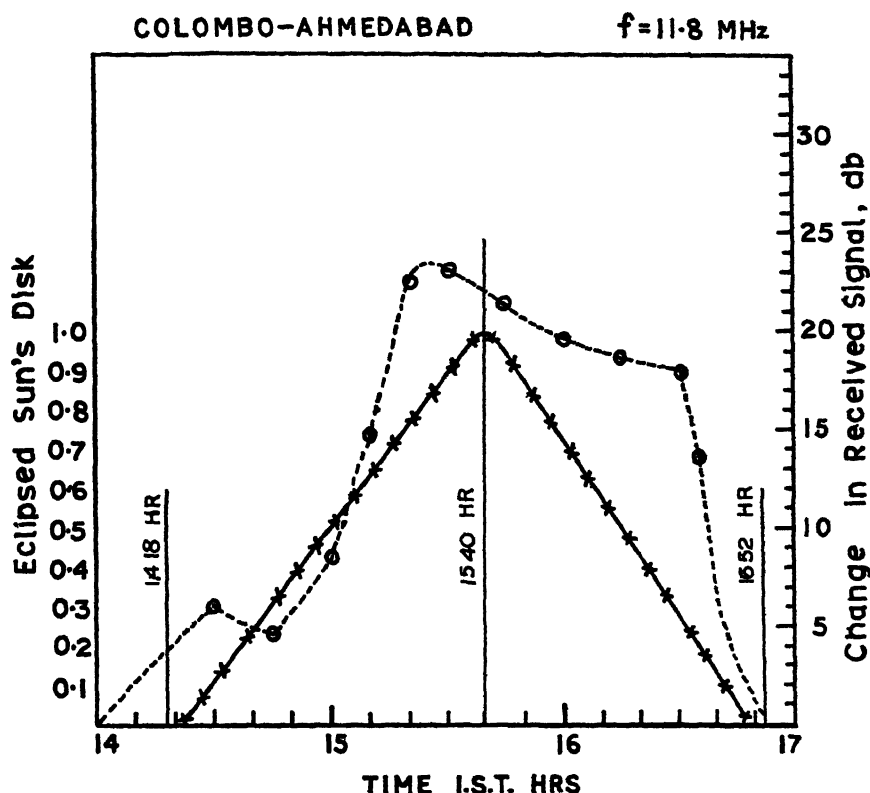


FIG 2 Effect of the solar eclipse on the signal in the Colombo-Ahmedabad radio circuit shown in terms of decibels relative to the mean value of signal strengths on the control days at corresponding hours. The fraction of the solar disc eclipsed is also shown from first to last contact.

of absorption (1dB) of the radio pulses on the eclipse-day compared with its mean for the control days for 1.8 and 2.2 MHz. Also shown in it are the variation of  $\cos \chi$  ( $\chi$  is solar zenith angle abbreviated as SZA) with time for the middle of the month and the eclipse-associated SZA, viz.,  $(1-f)\cos \chi$  is also shown along with. Here,  $f$  is the fraction of the sun's disc eclipsed and hence  $(1-f)$  is the fraction of the sun's disc open, i.e., not eclipsed. It may be seen that the absorption under normal conditions in February 1980 varied from 33dB to 16dB on 2.2 MHz in the time interval of the eclipse and 23dB opposite the lowest value of the absorption on the eclipse-day, about 18 minutes after the time of maximum phase of the eclipse at Ahmedabad (1541hr IST). The eclipse-affected absorption had the lowest value of 12dB which normally is observed about an hour or so before sunset time  $(1-f)\cos \chi$  at maximum eclipse also fell to the value of  $\cos \chi$  at this pre-sunset hour. Similarly on 1.8 MHz, the normal absorption varied from 37dB to 25dB, with a value of about 32dB at the time of its maximum decrease on the eclipse day. The lowest value of absorption observed on the eclipse-day was about 18dB after the maximum phase of the eclipse. This value also corresponds to that normally observed at the pre-sunset

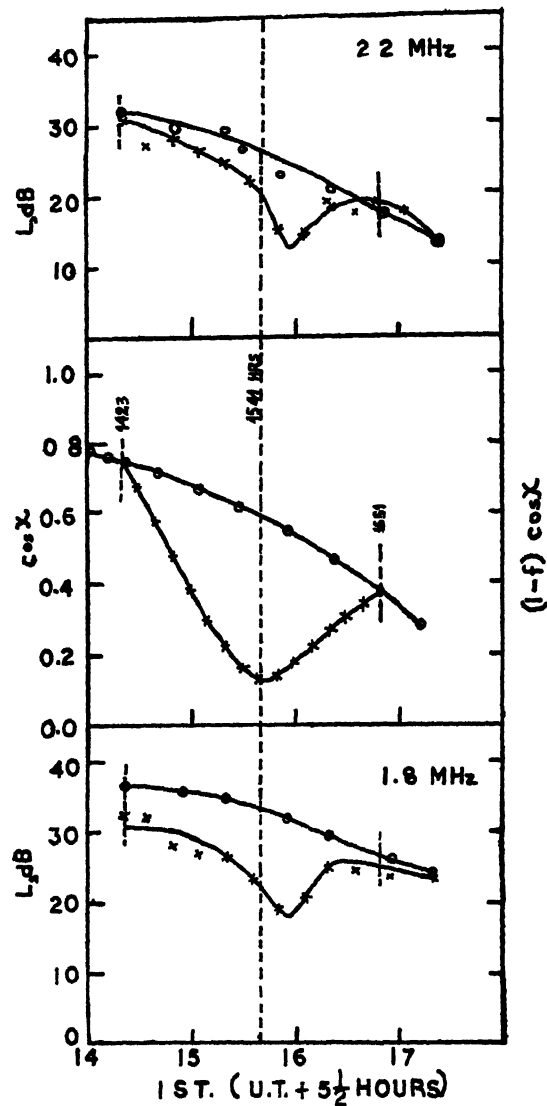


FIG 3 Vertical-incidence A1 radio pulse absorption on 1.8 and 2.2 MHz during the solar eclipse compared with its control days' mean value. Diurnal variation of  $\cos \chi$  on the middle of the month and eclipse-associated  $(1-f) \cos \chi$  are also shown for clarity of the effect on absorption at different times.

time. It is clear that the absorption on 1.8 MHz is 4–6 dB higher than that on 2.2 MHz on the control days as well as on the eclipse-day depending on the time. Although the initial value at the start of the eclipse was lower than the control days' mean value, it began to fall at a faster rate after the eclipse commenced than its rate of fall in the normal diurnal variation. The initial low value on the eclipse day is only a day-to-day variation and has nothing to do with the eclipse or the magnetic storm.

The plots of actual values of absorption shown in Fig. 3 are shown in another way in Fig. 4 to show the net effect of the eclipse as to how much reduction was observed in absorption during the course of the solar eclipse. To facilitate the com-

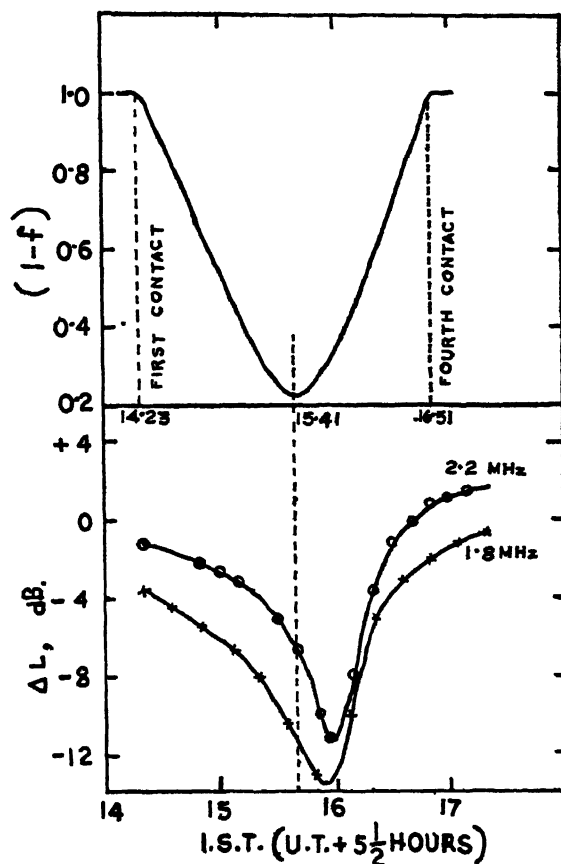


FIG. 4. Deviation of radio pulse A1 absorption observed on the eclipse day from that of the control days' mean value. The fraction of the solar disc un eclipsed is also shown giving times of different contacts of the eclipse. Note the differences in the shapes of fall and recovery of absorption in context to those of the eclipse and the time-lag of minimum in absorption behind the time of maximum phase of the eclipse.

parison between absorption and the eclipse conveniently, the eclipse of the Sun is shown by plotting the fraction of the solar visible disc left un eclipsed or open. In the case of Colombo-Ahmedabad radio signal strength, such facility required the plot of the fraction of the solar disc that was eclipsed, because the signal strength increases as the eclipse grows and vice versa.

It would be seen that the absorption on 1.8 MHz fell down to the lowest value by about 13.5 dB and that on 2.2 MHz by about 11 dB following the maximum phase of the eclipse with a time delay of 18 minutes. As already stated before, the absorption before the start of the eclipse was slightly lower than the control days' mean value,

however, it began to fall further below after the first contact, slowly in the beginning and then rapidly after the sun's disc was less than 40 per cent open, but it recovered quite rapidly to the normal value after the minimum was reached. Thus the decrease and recovery rates of absorption are not similar, nor do they follow exactly the shape of changes in the uneclipsed part of the sun's disc. At the maximum phase, the solar disc was 25 per cent open and the absorption fell down to nearly half of its normal value (not exactly half but 2 or 3dB above half of the normal) at the two frequencies a little after the maximum phase.

#### DISCUSSION

The reception of radio signals at Ahmedabad from Colombo could be possible either by way of reflection from the E-layer in two hops or from the  $F_1$ - or  $F_2$ - layer in one-hop. In either case, the main contribution to the absorption of the signal intensity comes from the D- and E-layers of the ionosphere and normally the signal is only 1.5mV from 1200hr to 1500hr. With the eclipsing of the sun and obscuration of the ionizing radiation, absorption of radio signal in the lower regions decreases depending on how much radiation flux is obscured. It is significant that the maximum signal strength recorded near the totality of the solar eclipse was almost the same and similar in character as that normally observed around the sunset time when the D-, E- and  $F_1$ - layers do not cause any significant absorption of the radio signal. Moreover, since the eclipse-day was magnetically disturbed and the  $F_2$ -layer is much affected by such disturbances both as regards its height and electron density, we should expect fluctuations in the received signal which are in fact observed and therefore, from the above two observations of near-sunset condition temporarily created around the totality of the eclipse and fluctuations of the signal, it is concluded that the propagation path of Colombo-Ahmedabad radio circuit was of one-hop mode via the  $F_2$ -layer. Under such circumstances, one cannot expect that the rate of increase and decrease in the field-strength would follow in a manner similar to the rate of progress and regress of the eclipse. Besides, what are the individual contributions to absorption by the different underlying layers and their time-variations and how the  $F_2$ -layer undergoes the dynamical changes make it difficult to predict and estimate the course of the effective variations in the received signal. Observations on different frequencies of oblique-incident signals (Rastogi *et al.*, 1956) suggest that higher the transmission frequency, earlier is the time of maximum of the signal strength slightly before (4-10 minutes) the maximum phase of the eclipse. Although the midpoint of propagation path in the present experiment was under totality for about  $2\frac{1}{2}$  minutes, the signal travelled obliquely through the ionosphere under influence of varying eclipse magnitudes (say 80 per cent to 100 per cent at the time of maximum phase). So this variability also adds to complexity in the strength of the received signal and one need not wonder why the signal remained steadily high until a few minutes before the last contact of the eclipse.

Coming to the vertical incidence radio pulse absorption measurements during the solar eclipse at Ahmedabad, the reduction in total absorption to nearly half of the normal value would apparently seem to be the most attractive result because only one-fourth of the solar disc was open at the maximum phase of the eclipse. One

would be tempted to jump to the conclusion that the ultraviolet radiation responsible for ionizing the main absorbing D-layer was obscured to one-fourth and hence the electron density all along the path of the radio pulse was reduced to half of its normal profile as  $N \propto \sqrt{q}$  and hence  $\sqrt{I}$ , where  $N$  is electron density,  $q$  rate of electron-ion production and  $I$  intensity of radiation. But this is true only on the assumption that the ultraviolet ionizing radiation is uniformly distributed over the whole solar disc which in reality may not be so. Kane (1970) found a reduction by an order of magnitude in the D-region ionization near totality of eclipse on 20 May 1966 but not so much in the E-region. Again, the coronal X-radiations responsible for the ionization in the D and E regions are not eclipsed in a manner as the visible disc. It is known that 10–15 per cent of this X-radiation is unobscured even when the sun's visible disc is totally eclipsed (Elwert, 1958; and Taubenheim & Serafinov, 1969). This may explain to some extent why the absorption was 2–3dB higher than half of the total normal absorption following the maximum phase of the eclipse which occurred in the year of high solar activity. The radiation is not the only factor for the effect on total absorption, because the measured radio pulse absorption consists of the deviative absorption in the E-layer and nondeviative absorption in the D-layer at the operating frequencies. The ionosonde at Ahmedabad recorded 3.5 MHz as normal-day critical frequency of the E-layer and this fell down to 2.7 MHz on the day of eclipse near its maximum phase. This means a reduction of about 46 per cent in  $N_{\max}$  of the E-layer. Particularly, the deviative absorption on 2.2 MHz increased during the eclipse while the nondeviative absorption in the D-layer decreased on both 1.8 and 2.2 MHz frequencies. These two features may be seen in Fig. 4. It is, therefore, difficult to say definitely about the relative contributions of the ultraviolet and the coronal X-radiation to the total absorption. The shape of the fall and recovery of the radio pulse absorption during the course of the eclipse cannot hence be expected to follow that of the optical eclipse. However, observed similarities in the shapes of the fall and recovery rates of E- and  $F_1$ -layer ionization and the total absorption of radio wave during the eclipse of 25 February 1952 at an equatorial place, Ibadan have been reported elsewhere. Papers presented by Gupta (1981) and Subbaraya *et al* (1981) in the present symposium on the results of their rocket experiments to measure electron density ( $N-h$ ) profiles and Lyman-alpha radiation intensity in the D- and E-layers of the ionosphere indicated reduced values of electron density (though not in a uniform way) in the  $N-h$  profile and in the Lyman-alpha radiation flux during one of the flights when the eclipse was about 70 per cent above Thumba (magnetic equator). A detailed calculation of total absorption  $L \propto \int N \nu dh$  in the height range 60 km upto the height of reflection of the radio pulse taking into account the above stated rocket data and other model profiles would help in ascertaining the results of pulse absorption presented here and estimating the relative contributions to it of the D- and E- regions. This work is being taken up and the outcome of the process will be reported elsewhere.  $\nu$  in the above expression is electron collision frequency which varies with height in direct proportion to the atmospheric pressure in the regions of interest.

As regards the delay of about 18 minutes in the minimum of absorption after the maximum phase of the eclipse and sluggishness in the change of absorption, it is a well-known fact that the recombination coefficient plays an important role. This

value of time-delay indicates that most of the changes in electron density due to the eclipse might have been produced in the height range 80–95 km. The observed time-delay is just half of what is normally observed in the minimum of diurnal variation of absorption in the month of February (Gupta & Kotadia, 1976) and this result agrees with that based on theoretical considerations (Rydbeck, 1956). The time-delay reported was also of the same value. Bischoff and Taubenheim (1964), however, observed minimum absorption coinciding with the maximum phase of the eclipse on 15 February 1961 at midlatitudes at about 0854 hr (perhaps as seen in winter anomaly months). Further, the absorption in the lower ionosphere at Ahmedabad is free from any effect of the geomagnetic storm (Kotadia & Jani, 1980) and the results presented here for A1-absorption testify no correspondence with the results on the short-wave Colombo-Ahmedabad radio circuit through the  $F_2$ -layer which is very sensitive to magnetic activity and travelling disturbances.

#### ACKNOWLEDGEMENTS

The authors are grateful to their colleagues Mr R. M. Kotak, Mr M. S. Bhatt and Miss R. M. Phanse for their help in successfully carrying out the eclipse observational programme. We also gratefully acknowledge the financial support given by the Council of Scientific and Industrial Research and the University Grants Commission.

#### REFERENCES

- Bischoff, K., and Taubenheim, J. (1964) Die ionospherische absorption von Kurzwellen während der sonnenfinsternis am 15 February 1961 *Gerlands beitr. geophys.*, **73**, 93–101.
- Elwert, G. (1958) The distribution of X-rays emitted by solar corona and the residual intensity during solar eclipses *J. atm. terr. Phys.*, **12**, 187–199.
- Gupta, A., and Kotadia, K. M. (1976) Ionospheric absorption on 2.5 MHz at Ahmedabad *Indian J. Rad. Space Phys.*, **5**, 110–113.
- Gupta, S. P. (1981) Measurement of plasma parameters in the equatorial D- and E- regions during the solar eclipse of 16 February 1980 *Int. Symp. Solar Eclipse, Paper C-37* Indian Natn. Sci. Acad., New Delhi.
- Kane, J. A. (1970) D-region electron density measurements during the solar eclipse of May 20, 1966, in *Solar Eclipses and the Ionosphere* (Ed. M. Anastassiades) Plenum Press, New York, 199–210.
- Kotadia, K. M., and Jani, K. G. (1980) Geomagnetic storms and associated ionospheric effects *Indian J. Rad. Space Phys.*, **9**, 15–19.
- Rastogi, R. G., Sheriff, R. M., and Nanda, N. G. (1956) Some measurements of the signal strengths of radio waves reflected from the ionosphere during the solar eclipses of 30 June 1954 and 20 June 1955, in *Solar Eclipses and the Ionosphere* (Eds. W. J. G. Beynon and G. M. Brown) Pergamon Press London, 137–142.
- Rydbeck, O. E. H. (1956) A theoretical study of E-layer behaviour during a solar eclipse, in *Solar Eclipses and the Ionosphere* (Eds. W. J. G. Beynon and G. M. Brown) Pergamon Press, London, 14–21.
- Subbaraya, B. H., Shyam Lal and Jayaraman, A. (1981) Rocket measurement of solar UV and MUV radiations, mesospheric molecular oxygen densities and ozone concentrations at stratospheric and mesospheric altitudes over Thumba during the 16 February 1980 solar eclipse *Int. Symp. Solar Eclipse, Paper B-1* Indian Natn. Sci. Acad., New Delhi.
- Taubenheim, J., and Serafinov, K. (1969) Brightness distribution of soft X-rays on the sun inferred from ionospheric E-layer variation during an eclipse *J. atm. terr. Phys.*, **31**, 307–312.

Printed in India

Radio Propagation

## EFFECTS OF SOLAR ECLIPSE ON SHORTWAVE TRANSMISSIONS

E. P. RADHAKRISHNAN\*, N. BALAN\*, A. A. SRIDHAR<sup>+</sup> and K. USHA DEVI<sup>+</sup>

*\*Department of Physics, University of Kerala, Kariavattom, Trivandrum 695 581, India*

*<sup>+</sup>Research and Development Section, KELTRON, Trivandrum 695 001, India*

*(Received 15 February 1982)*

The effects of solar eclipse on long distance communications have been studied by monitoring the Delhi shortwave transmissions on 15.25 MHz at Trivandrum during the total solar eclipse of 16 February 1980. Signal strength shows a maximum enhancement of 30 dB 15 minutes before the maximum phase of the eclipse at the path mid-point. During the beginning of the eclipse the signal strength remains steady around the control day value for 20 minutes after the first contact while at the end of the eclipse it falls sharply to the control day value. Signal fading rate is very high at the beginning and at the end of the eclipse while it is very low during the maximum phase of the eclipse. Probability distribution of the signal strength exhibits a double hump during the eclipse period. The results are interpreted in terms of the possible changes in the lower ionosphere and at the reflection level by means of model computations for Delhi-Trivandrum propagation path.

**Keywords:** Solar Eclipse; Shortwave Transmission; Signal Strength

### INTRODUCTION

DURING solar eclipse, ionization is nearly stopped at all heights while the loss processes continue. This sudden arrival of the night time conditions would lead to the disappearance of the D-layer where the relaxation time is very small. Experiments conducted during the past solar eclipses (Anastassiades, 1970; Kane, 1970; Tsagakis, 1970; and Belrose & Ross, 1972) showed decreases in D-region electron densities by factors of more than 10. E-region is similarly affected but to a lesser extent (Thomas & Rycroft, 1970). F-region relaxation time is of the order of eclipse duration or even more and this region exhibits complex dynamics. So the behaviour of this region during solar eclipse is highly unpredictable. Previous eclipse measurements indicated increase (Evans, 1965), decrease (Denisse, 1944), and even steady values (Minnis, 1956) of F-region electron densities. However, total electron content would show a significant reduction as observed by Marriott *et al*, during the eclipse of 7 March 1970 (Marriott *et al*, 1972). Above the F<sub>1</sub>-layer, there is a possibility for the formation of an additional layer called F<sub>11</sub>-layer during a solar eclipse in the equatorial region. Such a layer was observed at Tokyo during the solar eclipse of 14 February 1953 (Nakata & Yonezawa, 1956).



Disappearance of the D-layer results in an appreciable reduction in the non-deviative absorption of the radio waves reflected from the overlying layers, which would lead to an enhancement in the strength of the received signal. Over five-fold signal strength enhancements were observed during the past solar eclipses (Rastogi *et al.*, 1956; and Sethuraman *et al.*, 1980). In addition to the enhancement in the gross signal level, some changes may be expected also in the fading characteristics of the received signal in view of the possible effects that an eclipse may have on the irregular structure of the ionosphere.

The total solar eclipse of 16 February 1980 has presented yet another opportunity to study its effects upon long distance communications. Using a simple receiving system, the shortwave transmissions from Delhi ( $28^{\circ} 35'N$ ,  $77^{\circ} 13'E$ ) on 15.25MHz were monitored at Trivandrum ( $8^{\circ} 33'N$ ,  $76^{\circ} 52'E$ ) on the eclipse day and a few control days around it. The following sections present an account of the experiment conducted, data analysis performed, and the results obtained.

#### EXPERIMENTAL SET-UP AND DATA COLLECTION

The monitoring system consists of a vertical monopole antenna, a Racal receiver, and a twin channel strip chart recorder. The vertical monopole is resonant at 15 MHz and was erected at a height of 8 meters above ground. Eight radials having lengths equal to the height of the antenna were provided to make an almost perfect ground. The signal received by the antenna was brought to the racal receiver tuned at 15.25MHz by a 10 meter length 50 ohm coaxial cable. The line output of the receiver was fed to the twin channel strip chart recorder which was run at a constant speed of 6cm/sec. Signals were recorded from morning to evening on five continuous days from 15 to 20 February 1980 with a break on 19th. During the course of recording, suitable attenuation levels were used whenever the signal strength tended to attain saturation. Calibration curves were drawn for the signals recorded on all the five days to convert the signal strength to dBm. 0dBm denotes a power dissipation of 1mw in a resistive load of 50 ohms.

The path of totality, transmitting station, receiving station, and the reflection points are shown in Fig. 1. Maximum obscuration of the sun was 65 per cent at the transmitting station and 80 per cent at the receiving station. At the receiving station, the eclipse started at 1419hr, reached maximum at 1539hr, and ended at 1649hr (all times are in IST). Delhi-Trivandrum distance is 2270km. For this long distance, shortwave communication will be either by I-hop or II-hop reflections or by both from F-layer. The I-hop reflection point is marked as "O" where maximum obscuration was 95 per cent at 1549hr. The II-hop reflection points are marked as "X" where maximum obscurations were 80 per cent and 95 per cent at 1547hr and 1644hr respectively.

#### DATA ANALYSIS

The solar eclipse occurred at a time of high solar activity and when a magnetic storm was in progress. The sunspot number on the eclipse day was 165. Magnetograms recorded at Trivandrum indicate the occurrence of a magnetic storm on 15 February 1980. The storm recovered to normal level by 17 February 1980. 18th and 20th were

magnetically quiet and are taken as the normal days. Main phase of the storm reached its maximum value of  $\Delta H$  equal to  $-195$  gamma at 1200hr, on the eclipse day. The eclipse period, indicated by the arrows, falls on the recovery phase of the storm. During the eclipse period  $\Delta H$  varies from  $-90$  gamma to  $-35$  gamma with  $-50$  gamma at the time of maximum phase of the eclipse. This value of  $\Delta H$  is of the same order of magnitude as the day to day variability in the magnetic field. Thus the eclipse time observations might not have been affected very much by the magnetic activity conditions prevailing at that time.

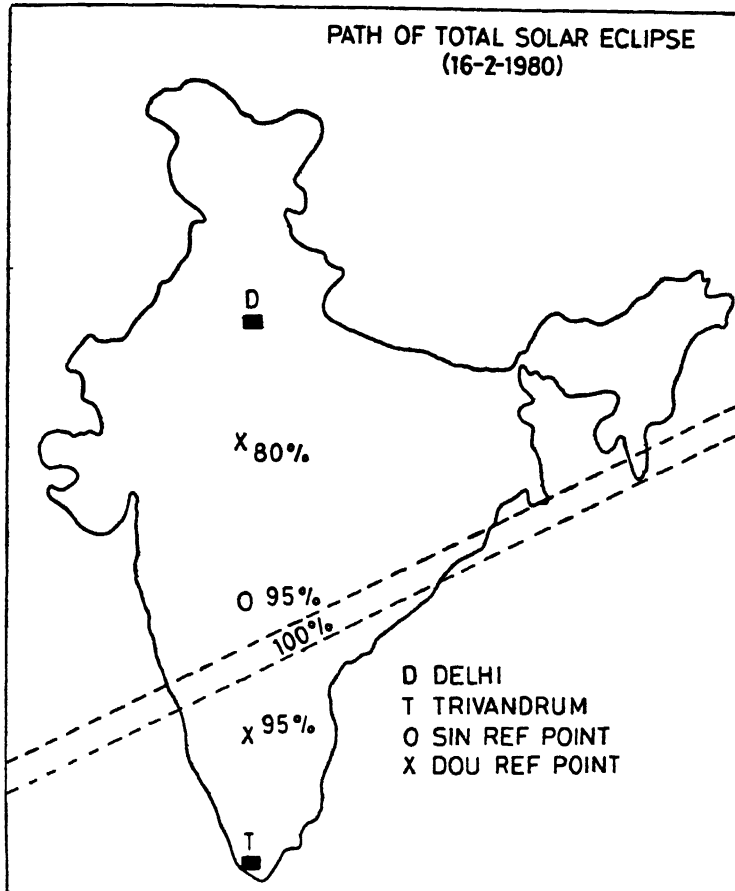


FIG 1 Path of the total solar eclipse.

The records on the two control days and on the eclipse day were sampled at every 15 seconds. To smooth out the random variations in the signal strength, running averages were obtained using a five minute window. The values were then converted to signal strength in dBm by using the calibration curves. The fading rates of the received signal were obtained by counting the number of peaks in each five minute interval as a function of time. The peaks that are recognized for counting

are only those which exceed the mean signal level by at least 25 per cent of the maximum signal excursion in the five minute interval. The data samples scaled at 15 second intervals have been divided into one hour segments and hourly probability distributions have been computed for the received signal power

### RESULTS AND DISCUSSION

Signal strength variations with time on two control days and on the eclipse day are shown in Fig. 2. On both the control days starting from morning until 1500hr, the signal strength is weak and almost a constant with a mean value of  $-96\text{dBm}$ . After 1500hr the signal strength gradually increases till it reaches  $-65\text{dBm}$  at 1730hr. Minimum and maximum deviations of signal strength on the two control days are 0 and  $10\text{dBm}$  so that  $5\text{dBm}$  can be taken as an average day-to-day deviation. On normal days, the transmitted signal is strongly absorbed by the lower layers of the ionosphere during its propagation from Delhi to Trivandrum and hence the received signal is rather weak.

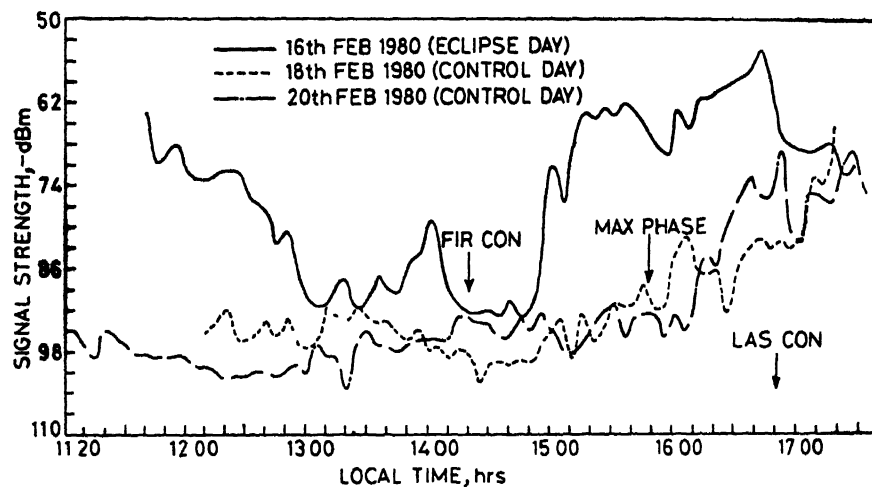


Fig 2 Signal strength variations with time on the control days (dashed and dot-dashed) and on the eclipse day (continuous)

On the eclipse day, during the morning even before the onset of eclipse, the signal strength has assumed  $-65\text{dBm}$  which is quite high compared to a corresponding value on a control day. The high signal strength on the morning of the eclipse day seems to be associated with the magnetically disturbed conditions prevailing at that time. As the magnetic storm recovered, the signal strength also has recovered and reached almost to the normal control day level by about 1300hr. From 1300hr to 1445hr the signal strength remains steady near the control day level except for a sharp rise just before the onset of the eclipse. The anomalous rise in the signal strength seems to be associated with some sort of a transient at the beginning of the eclipse although its exact source could not be identified.

Different phases of the eclipse period are as indicated in the figure. Signal strength remains steady for about 20 minutes after the first contact. This time delay is clearly due to the relaxation time of the lower layers of the ionosphere. From 1445hr the signal strength starts rising sharply and reaches a value of  $-62\text{dBm}$  with in half an hour time. From 1515hr to 1640hr, the signal strength rises with the same slope as the normal evening rise and reaches to a maximum value of  $-53\text{dBm}$  at 1640hr, five minutes before the end of the eclipse. Then the signal level falls sharply to normal control day value at the end of the eclipse. Maximum deviation of signal strength from mean control day value is  $30\text{dB}$  and occurs 15 minutes before the maximum phase of the eclipse at the path mid point.

Percentage deviation,  $S(\%) = \frac{S_E - S_C}{S_C} \times 100$ , of the signal strength on the eclipse day from the average signal strength on the control days is plotted in Fig. 3. It may be noted that  $S_E$  and  $S_C$  in the above expression are measured in  $\text{dBm}$  and not in absolute power units. The quantity  $\Delta S$  is maximum at the time of maximum phase of the eclipse and is equal to 36 per cent. The delayed sharp rise of signal strength after the first contact and rapid fall of signal strength just before the end of the eclipse are very clear from this figure.

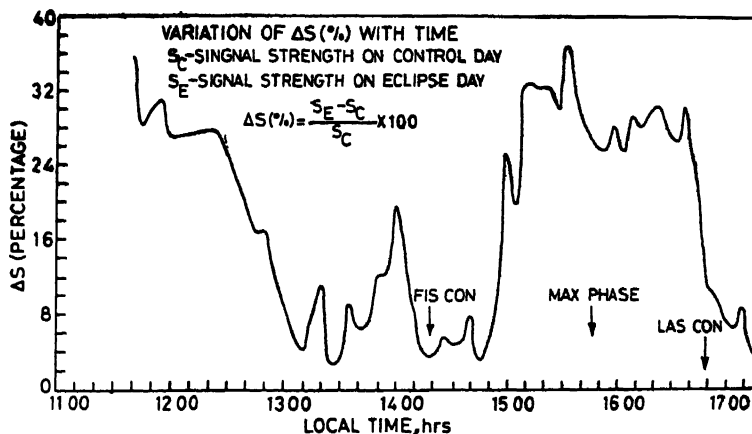


FIG 3 Percentage deviation of the signal strength on the eclipse day from the average signal strength on the control days

The observed enhancement of the signal strength during the solar eclipse may be interpreted in terms of the following three mechanisms: (1) Non-deviative absorption (2) Deviative absorption and (3) Focussing due to eclipse related deformation of the ionosphere. The non-deviative absorption occurs mainly in the D-region. During a solar eclipse, the D-region would essentially disappear and as a result the non-deviative absorption would become almost absent. It is not certain how the deviative absorption changes due to a solar eclipse. It depends on how the electron density distribution changes in the F-region and how it effects the mode of propagation relative to the control day propagation conditions. In regard to the focussing effect, there is now good reason to believe that it can contribute significantly to the

observed signal enhancement. It was observed that the electron density contours in the ionosphere rise appreciably in the eclipse region and form a large scale dome type structure centering on the path of the eclipse. If the obliquely propagating radio waves are reflected from the concave surface of the distorted contours, focusing can take place causing considerable enhancement in the strength of the received signal.

An estimate has been made of the non-deviative absorption for a control day ionospheric conditions for Delhi-Trivandrum propagation path. The propagation modes have been identified on the basis of the ionograms taken at the SHAR centre. This was considered adequate for the kind of approximate estimate aimed at in this computation. The SHAR ionograms suggest that on the control day of 18 February 1980, the propagation from Delhi to Trivandrum at 1545hr, corresponding to the eclipse time, is by the II-hop  $F_2$ -layer mode. On the eclipse day, however, the propagation at 1547hr seems to be predominantly by the I-hop  $F_2$ -layer mode. The control day II-hop mode has an angle of incidence  $\phi$  of  $55^\circ$  and was reflected from a virtual height of 395km. The equivalent vertical frequency  $f_o$  for this mode was 8.7MHz. The non-deviative absorption for a vertically reflected wave at the equivalent frequency  $f_o$  is given in dB as.

$$L_o = \frac{2.33 \times 10^6}{(f_o \pm f_L)^2} \int_{60}^{120} \frac{N \nu}{dh} dh$$

where  $f_L$  is the longitudinal component of the gyrofrequency,  $N$  is the electron density and  $\nu$  is the collision frequency. The electron density and the collision frequency profiles used in the calculation are shown in Fig. 4. The electron density profile was taken from a rocket experiment conducted at Thumba at 1212hr on 2 January

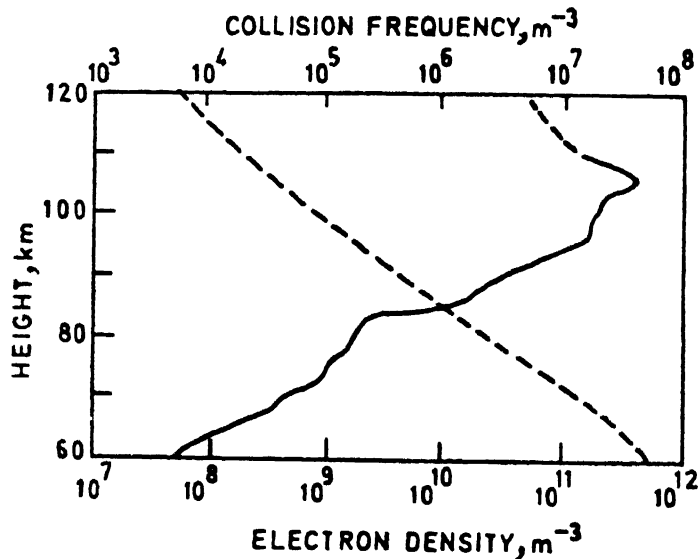


FIG. 4. Electron density profile (recorded at Thumba at 1212hr on 2 January 1970) and collision frequency model.

1970 The collision frequency was calculated using 1970 CIRA atmospheric model and the expression  $\nu = 5.4 \times 10^{-6} n T^{1/2}$ . The parameters  $n$  and  $T$  are the neutral particle density and neutral temperature respectively. From the vertical absorption  $L_o$ , the absorption for the oblique transmission can be calculated using the relation  $L_o = L_e \cos \phi$ . For the II-hop mode, which is of interest here, the absorption would be  $2L_o$ . On the basis of the above model, the non-deviative absorption for the control day II-hop mode was computed as 12dB. In addition there is the difference in the free space loss between the control day and the eclipse day because of the difference in the mode of propagation on the two days. The difference in the free space loss and the non-deviative absorption on the control day taken together will account for a gain of 7dB in the signal strength during the period of eclipse. This estimate falls short of the observed signal enhancement by 23dB.

There is thus 23dB enhancement in the signal strength left to be explained by processes other than non-deviative absorption. Since the II-hop mode penetrates deeper into the layer and traverses the ionosphere twice, it is expected to suffer more deviative absorption than the I-hop mode. There would be some signal gain since the propagation on the control day was by II-hop and on the eclipse day by I-hop. However, the deviative absorption itself being generally not high, its difference between the control day and the eclipse day is not considered adequate to account for the entire 23dB. It is, therefore, believed that the focussing effect resulting from the distortion of the contours of constant electron density during the period of eclipse plays an important role in contributing to the large enhancement observed in the received signal strength.

Fading of the signal on two control days and on the eclipse day is studied. Fading rate (cycles per minute, cpm) on two control days is almost similar and is shown separately in the lower portion of Fig. 5. During morning hours, the fading rate is high and is of the order of 12cpm. During noon time the fading is almost steady with a mean value of 9cpm. After 1500hr, the fading rate decreases gradually and reaches to a mean value of 4cpm at 1700hr.

Eclipse day fading rate along with the mean of the fading rates on the two control days is shown in the upper portion of Fig. 5. Starting from morning till 1300hr, the eclipse day fading is not much different from that on the control day. After 1300hr, there are three large excursions and one deep depression in the fading rate. The first excursion is around 1330hr about an hour before the start of the eclipse. Other two excursions are such that one is after the first contact and the other is before the last contact. Maximum fading occurs after the first contact and is 16cpm. Around the maximum phase of the eclipse, the fading rate has dropped down to the lowest value of 2cpm. Peak deviation in the signal fading rate during the eclipse period is  $\pm 5$ cpm. Superposed on this dominant fading there are rapid but small fluctuations present on both control and eclipse days except for a brief period around the maximum phase of the eclipse. The absence of the short period fluctuations during the eclipse suggests that the irregularities responsible for them have a dependence upon solar radiations in some way for their maintenances.

To study the characteristics of the fading pattern we found the probability distribution of the signal strength on one control day (18 February) and on the eclipse

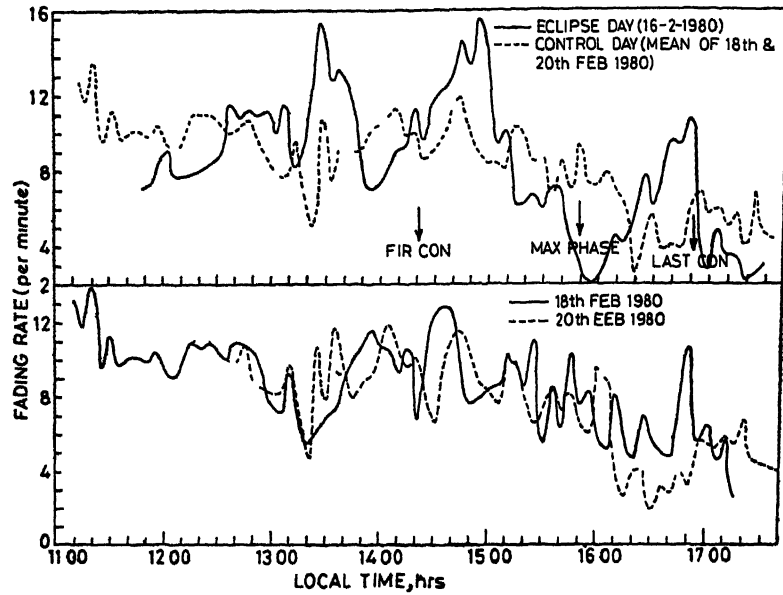


FIG 5 Signal fading rates on the control days (bottom) and on the eclipse day (top).

day at one hour intervals from 1139hr to 1739hr. Normalised probability distributions for selected intervals are shown separately for the control day and the eclipse day in Fig. 6. Distribution curves for the corresponding periods on both the days look almost similar except for two features (1) the width of the distribution curves during the eclipse period is more than that during the same period of the control day; (2) distribution curve for 1439–1539hr during the eclipse period shows double hump. The observed distributions seem to resemble closely to that described mathematically by Rice. The enhancement in the width of the distribution functions, there-

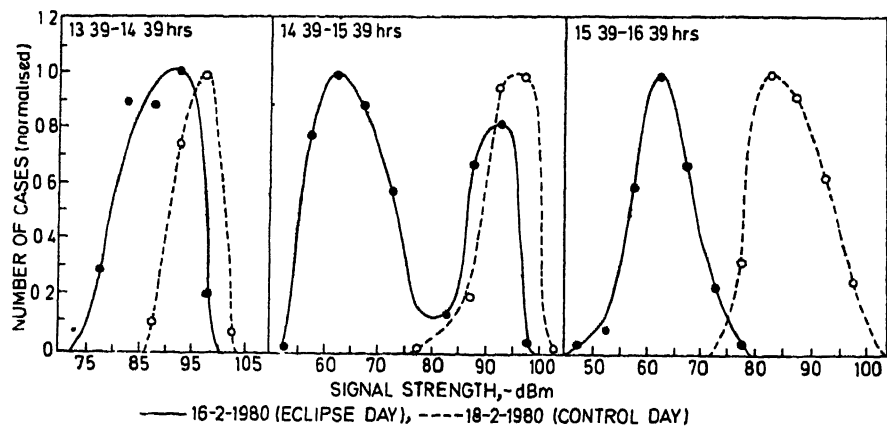


FIG 6 Probability distribution of signal strength on one control day (18 February 1980) and on the eclipse day.

fore, suggests that as a result of the solar eclipse there is a marked increase in the ratio of the steady to the random components of the received signals. The second feature showing a double hump in the distribution curve may be a manifestation of a wave motion excited by the solar eclipse. As the ionospheric wave disturbance propagates through the reflection point, the reflected signal undergoes focussing or defocussing depending on whether the reflections take place from a concave or convex surface of the wave motion. If the interval of the distribution functions contains one full cycle of the wave motion, then both focusing and defocusing would take place and a double hump distribution would result. The observed double hump as a result of a wave motion has been verified by taking smaller time intervals during which only focusing or defocusing will occur and as a result only one of the two peaks will occur in the distribution curve.

#### ACKNOWLEDGEMENTS

The authors are grateful to Professor P. B. Rao of the Department of Physics, University of Kerala for his directions in doing this work and also for the valuable discussions we had with him in preparing this manuscript. Thanks are also due to Dr B. V. Krishnamoorthy of V. S. S. C., Thumba for providing the eclipse day magnetogram.

#### REFERENCE

- Anastassiades, M. (1970) *Proc. Symp. Solar Eclipses and the Ionosphere*. NATO Advanced Studies Inst., Greece, p. 253.
- Belrose, J. S., and Ross, D. B. (1972) *J. atm. terr. Phys.*, **34**, 627.
- Denisse, J. F., Seligmann, P., and Gallet, R. (1944) *C. r.*, **225**, 1169.
- Evans, J. V. (1965) *J. geophys. Res.*, **70**, 733.
- Kane, J. A. (1970) *Proc. Symp. Solar Eclipses and the Ionosphere*. NATO Advanced Studies Inst., Greece, p. 199.
- Marriott, R. T., St. John, D. E., Thorne, R. M., and Venkateswaran, S. V. (1972) *J. atm. terr. Phys.*, **34**, 695.
- Minnis, C. M. (1956) *J. atm. terr. Phys.*, **6**, 81.
- Nakata, Y., and Yonezawa, T. (1956) *J. atm. terr. Phys.*, **6**, 33.
- Rastogi, R. G., Sheriff, R. M., and Nanda, N. G. (1956) *J. atm. terr. Phys.*, **6**, 137.
- Sethuraman, R., Jayaraman, R., Alamelu, V., and Ravichandran, C. (1980) *Indian J. Radio Space Phys.*, **9**, 198.
- Thomas, J. O., and Rycroft (1970) *Proc. Symp. Solar Eclipses and the Ionosphere*. NATO Advanced Studies Inst., Greece, p. 237.
- Tsagakis, E. (1970) *Proc. Symp. Solar Eclipses and the Ionosphere*. NATO Advanced Studies Inst., Greece, p. 211.



Printed in India.

**Radio Propagation**

**IONOSPHERIC ABSORPTION CHANGES IN 11.8MHz RADIO  
PROPAGATION DURING THE TOTAL SOLAR ECLIPSE OF  
16 FEBRUARY 1980**

GIRIJA RAJARAM, T. R. RAO\* and D. D. PATIL

*Indian Institute of Geomagnetism, Colaba, Bombay 400 005, India*

*(Received 7 September 1981)*

Variations in the 11.8MHz signal strength (Colombo-Bombay propagation path) during the total solar eclipse of 16 February 1980 are interpreted in terms of possible changes in the lower ionosphere. The main features observed are a sharp rise of almost 20dB following onset of the eclipse, followed by two distinct drops in signal strength which were separated by a brief interval of enhanced signal, a marked rise in the received signal was also noticed about an hour before first contact. The eclipse night was characterised by regular, periodic fading which is not a normal night-time feature for this propagation path. These eclipse-induced changes are discussed in the light of astronomical and ionospheric observations of this same eclipse reported by other workers.

**Keywords:** Ionospheric Absorption; Radio Propagation

**INTRODUCTION**

THIS paper refers to the changes seen in the signal strength and fading pattern of the 11.8MHz radio transmission from Colombo, recorded at Bombay during the recent solar eclipse of 16 February 1980. From the layout of the transmitter and the receiver, it was recognised that for a one-hop propagation path, the ionospheric reflection point would experience around 95 per cent obscuration, and hence substantial changes were likely to occur in the recorded signal strength.

**EXPERIMENTAL SET-UP AND PROPAGATION GEOMETRY**

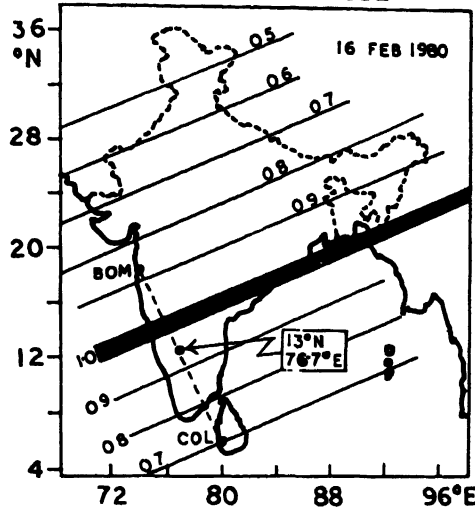
A conventional straight wire antenna was used; the band-width of the receiver was kept at 4kHz and the RF-gain of the system for an input of 2mV was 54dB. On the day of the eclipse, and on the following control days, the record-chart was run at a speed of 12cm/hr thereby ensuring clear resolution of the recorded signal.

The geometry of the 11.8MHz Colombo-Bombay propagation path, and the magnitude of the eclipse at Bombay, Colombo, and the reflection point can be seen from Fig. 1. The distance between Colombo and Bombay is approximately 1600km, for a single hop reflection, the coordinates of the reflection point are 13°N, 76°E, with maximum eclipse magnitude of approximately 95 per cent. For this reflection

---

\*Now at Space Physics Division, Gujarat University, Navrangpura, Ahmedabad 380 009

# REFLECTION POINT (COLOMBO-BOMBAY) ECLIPSE MAGNITUDE



# GEOMETRY OF 11.8 MHz PROPAGATION (COLOMBO-BOMBAY)

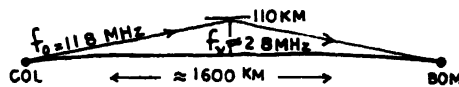


FIG 1. Geometry of the 11.8 MHz Colombo-Bombay propagation path, and the magnitude of the eclipse at the one-hop reflection point

point, the first contact of the eclipse was at 14 21 IST, the second contact at 15.43 IST, and the fourth contact at 16 53 IST. From the secant law for a curved earth and a curved ionosphere, the equivalent vertical frequency for 11.8 MHz oblique propagation with this geometry works out to be about 2.8 MHz (Rastogi, 1960). This suggested reflection of the radio signal to be mainly from the E-region, this was confirmed from the ionograms for 14 05 IST and 14 10 IST of 16 February 1980 from SHAR (Sriharikottah, with coordinates roughly 13°N, 80°E, due east of the reflection point), which were kindly supplied to us through the courtesy of the Space Physics Division of VSSC (Vikram Sarabhai Space Science Centre).  $f_oE$  at these times preceding the eclipse was around 3.4 MHz.

## OBSERVATIONS OF 11.8 MHz SIGNAL ON ECLIPSE AND CONTROL DAYS

The recordings of the 11.8 MHz signal on the eclipse day (16 February 1980) and on the following control day (17 February 1980) are compared in Fig 2 for 12–17 IST in the upper half of the figure, and for 17–22 IST in the lower half of the figure. The times of beginning, maximum, and end of the eclipse are indicated by arrows in

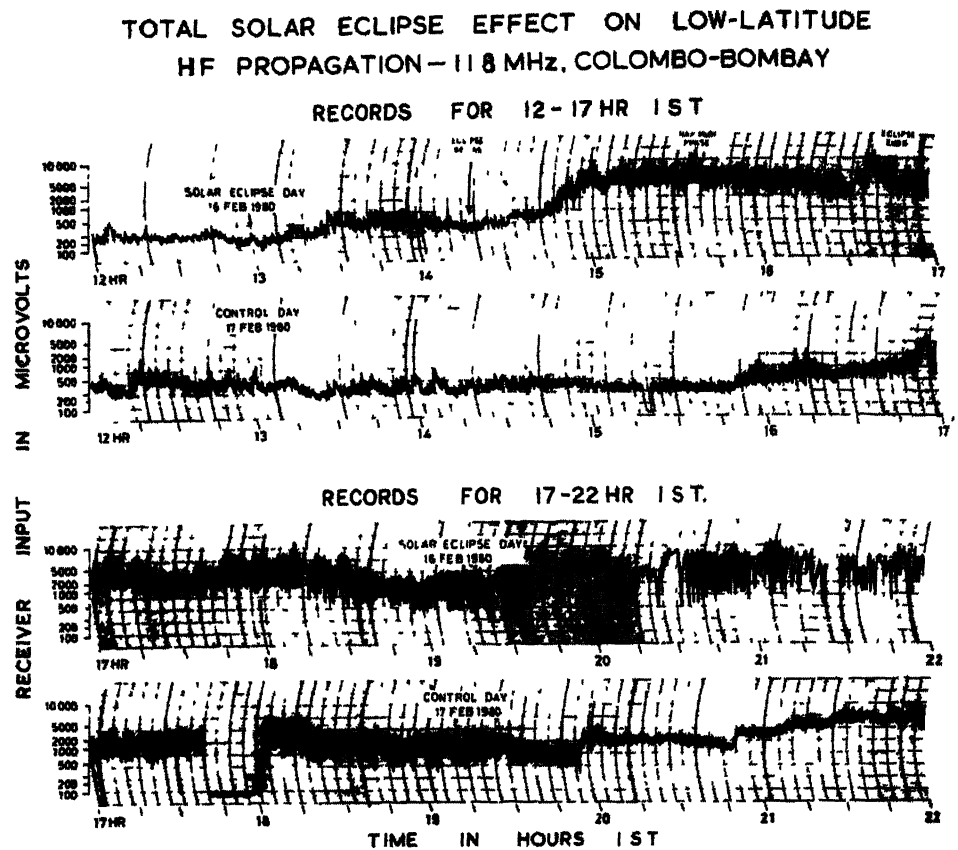


Fig 2 Records of 11.8 MHz field strength on eclipse day (16 February 1980) and control day (17 February 1980) for 12–17 IST and 17–22 IST. The beginning, maximum, and end of eclipse at the reflection point are indicated. Note the regular, periodic fading of the signal on the eclipse night, an unusual feature for this propagation path.

the topmost record. The pronounced rise in signal strength within 20 minutes after first contact is clear in the figure, and there is another small rise seen about 20 minutes before the end of the eclipse. In contrast, the signal strength on the control day is almost unchanged till after 16 IST, and thereafter shows a gentle, gradual rise. Another characteristic of the eclipse night is the clear, periodic fading of the radio signal, starting at about 18 40 IST and persisting right till 22 40 IST when Colombo switched off transmission. This is very different from the rapid irregular fading seen for the corresponding hours on the control day, 17 February 1980, which is the generally occurring pattern on most nights.

The signal strength shown in Fig 3 is averaged at successive 5-minute intervals and these values are shown in Fig 3 for the post-noon hours of the eclipse (16 February shown by thick full line) and the two control days; 17 February is shown by a dashed

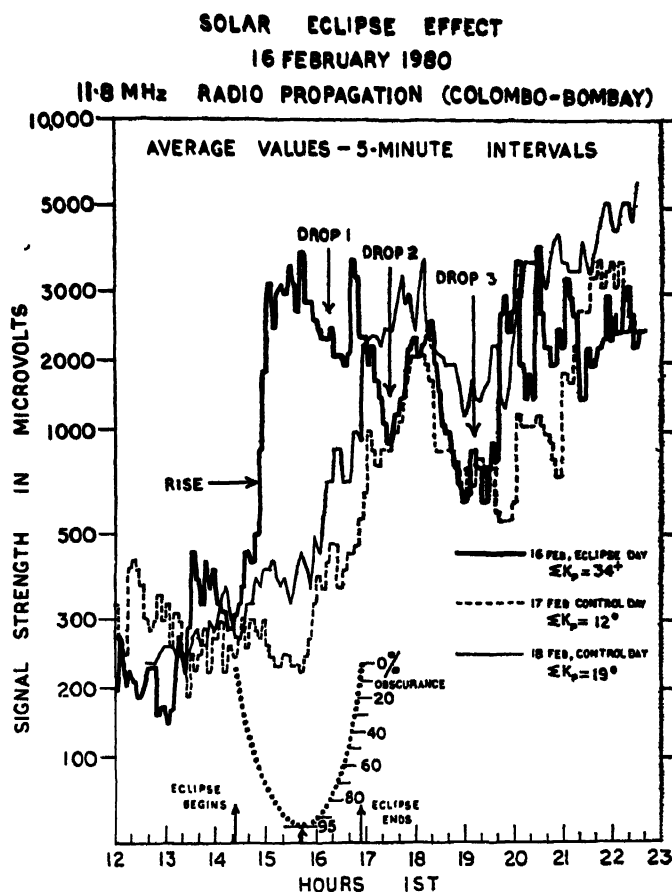


FIG 3 Average values over 15-minute intervals, of 11.8 MHz signal strength on eclipse day (thick full line) and on control days (dashed line and thin full line) the solar obscuration curve at the reflection point is also shown. Note the eclipse-associated features on 16 February depicted as Rise, Drop 1 and Drop 2.

line, and 18 February by a thin full line. The dotted curve in the lower part of Fig. 3 depicts the obscuration curve for the eclipse at the reflection point. It is worth noting that the full-line curve for the eclipse period between 14:20 IST and 16:50 IST is not symmetric with respect to the solar obscuration curve. Also there is a marked rise in the full-line curve almost one hour prior to the onset of the eclipse.

The full-line curve for the eclipse day shows three clear depressions shown as Drop 1, Drop 2 and Drop 3 which we attempt to interpret in terms of ionospheric effects. Almost instantaneously with the onset of the eclipse, the signal strength starts rising sharply, indicating reduced radio wave absorption and hence a rapid loss of electrons within the ionospheric propagation path. The first electrons to be affected would be the D-region electrons considering the small recombination time of a few seconds for this region. The signal strength touches almost peak values (minimum absorption) a few minutes before maximum obscuration. Soon after peak obscuration

the signal starts falling (indicated as DROP 1); this could be due to strong deviative absorption in the E-region when  $f_oE$  drops to values below the equivalent vertical frequency of 2.8 MHz. The sharp short-lived rise in signal strength following Drop 1 could indicate reflection of the 11.8 MHz signal from the  $F_1$ -region. Drop 2 follows the unmasking of the solar disc, and it could again be deviative absorption in the E-region as  $f_oE$  recovers to values exceeding 2.8 MHz, with the restoration of solar radiation. Drop 2 is clearly an eclipse-associated feature as it is not seen on the signal strength curves for the control days, 17th and 18th. DROP 3 occurring soon after 18 IST seems to be a daily feature, as it is seen at the same time on the signal strength curves for the above control days. This drop again seems to be connected with deviative absorption in the E-region as  $f_oE$  following sunset gradually drops to values near the equivalent vertical frequency 2.8 MHz. After sunset, the D- and E-region ionisation is gradually destroyed, and absorption is greatly reduced; the signal strength picks up as the signal starts getting reflected from the F-region. On 16 February, the level of the signal at night is comparable to the noon-time eclipse level; on the control days, the night levels exceed the noon signal levels.

It may be mentioned that the eclipse day was magnetically disturbed with a sum  $K_p$  figure of 34+, but the control days were quiet with sum  $K_p$  values of 12° and 19° respectively. Perhaps it was because of magnetic disturbance that the signal strength on the eclipse day was rather low between 12–13 IST, as compared to the other days. This lowered signal strength was noticed during the forenoon hours of 16 February too, though these hours are not shown in Fig. 3 which concentrates on the eclipse effect. The lowered signal strength in the forenoon hours of 16 February indicates reduced absorption; hence larger ionisation densities in the lower ionosphere, and there could be a storm-associated effect.

#### DISCUSSION

An attempt is now made to understand the observed changes in terms of the known physics of eclipses, and to compare them with observations of other workers during this same eclipse. During the eclipse of 16 February 1980 several groups in India have used LF, MF or HF to monitor ionospheric changes (Sethuraman, 1980; and Mitra, 1981). It merits attention that the signal strength variations seen in Fig. 3 of this paper, are very similar to those observed by Sen *et al.* (1981) for the same Colombo transmission of 11.8 MHz received at Varanasi, but there is a large time-shift in every feature which is not quite understandable. The mid-point of the Colombo-Bombay path (13°N, 76.7°E) experienced 95 per cent totality, while that of the Colombo-Varanasi path (13°N, 80°E) experienced 97 per cent totality, the latter point saw the entire eclipse event with a delay of about 5–7 minutes with respect to the former.

Since the equivalent vertical frequency for the 11.8 MHz oblique propagation was 2.8 MHz for the Colombo-Bombay path, we are mainly concerned with changes in the lower ionospheric regions D and E. During the eclipse, radio wave absorption is reduced because the production function ' $q$ ' is decreased with the masking of the solar disc. ' $q$ ' however, cannot be taken as proportional to the uneclipsed fraction of the solar disc, because the ionising sources themselves are not distributed uni-

formly across the solar disc (Piddington, 1951; and Minnis, 1955). Friedman (1960) showed that X-rays originating in limb plagues or from coronal condensations can contribute to upper atmospheric ionisation even for total eclipse of the solar disc. The SOLRAD 8 satellite observations of the solar eclipse of 20 May 1966 show that UV radiation at 1225–1350Å decreases uniformly with obscuration, but not so the X-ray bands (Landini *et al.*, 1966). The X-ray band 44–60Å showed a residual intensity of 10–13 per cent at eclipse totality (Friedman, 1962).

These points are particularly relevant to the solar eclipse of 16 February 1980, because minimum absorption was reached almost 20 minutes before maximum obscuration and remained in the vicinity of that value for almost 35 minutes. There were two prominent groups of sunspots visible on the solar disc that day, it is quite possible that one or both these sunspot groups were localised regions of strong X-ray and UV radiation, and their masking resulted in a sharp fall in the production function 'q'. Bhonsle *et al.* (1981) from their radiometer observations report a residual flux of 23 per cent at 2.8GHz with a minimum occurring a few minutes before totality. The Ooty radio telescope operating at 327MHz (Rao & Bagri, 1981) reported an active region on the sun of angular size 4 arc-minute and a coronal streamer extending 10 arc-minutes above the south-west limb. Saito *et al.* (1981) report three active regions near the solar west limb, and one near the east limb, with coronal loops clearly seen over these regions. It was noted in connection with Fig. 3 that a marked rise in signal strength occurred almost an hour before first contact of the eclipse, a rise before first contact is also reported by Lakshmi *et al.* (1981). Perhaps this effect is connected with eclipse of some coronal emission region on the solar west limb as has been discussed by Sen Gupta and Mitra (1954).

The sharp narrow rise following Drop 1 in Fig. 3 was attributed to a brief period of reflection from the F1-region. It is established that reflections from F1 and intermediate stratifications F1/2 become prominent during eclipses. This is attributed to the layer shape parameter  $G = \frac{\beta^2}{\alpha_e}$  undergoing drastic changes because of eclipse-induced changes in the effective recombination coefficient  $\alpha$  and the production function  $q$  (Rishbeth & Garriott, 1969). The SHAR ionograms for 14 05 IST and 14 10 IST show some F1 stratification before eclipse onset; there is every possibility that during the eclipse, SHAR ionograms would be showing intense F1 and F1.5 stratifications as were reported by Chandra *et al.* (1981) for Ahmedabad. Girish Kumar and Ramana (1981) from ionospheric absorption measurements on 2.4MHz at Waltair (99 per cent totality) report that from 15 minutes before totality to 15 minutes after totality the E-region was transparent to 2.4MHz and the echoes were from the F1-region.

The fading pattern observed on the night of the eclipse (Fig. 2) seems to be connected with the absence of Spread F. During the entire fortnight centered around the eclipse day, the night of the eclipse was the only one which showed no Spread F. (Tuhī Ram Tyagi *et al.*, 1981, Deshpande *et al.*, 1981, and Ernest Raj *et al.*, 1981). The absence of Spread F was possibly due to the magnetically disturbed conditions prevalent that day. The regular periodic fading observed could happen by combination of one-hop and two-hop propagation modes, of the 11.8MHz signal over the Colombo-Bombay path; due to reduced absorption the latter mode would be quite effective at

night. The other possibility is to explain the eclipse night fading as due to vertical oscillations in the reflecting layer set up in the wake of the eclipse. These oscillations could be a manifestation of gravity waves triggered off by reduction in neutral temperature and turbulence (Chimonas & Hines, 1970). Venkatanarayana and Somayaji (1981) for the present eclipse estimate a drop of  $74^{\circ}\text{K}$  at an altitude of 127.5km. The time-period in minutes of this signal fading rate from 5-minute sampling of the fades is shown in Fig. 4. The time period maintains large values of 10

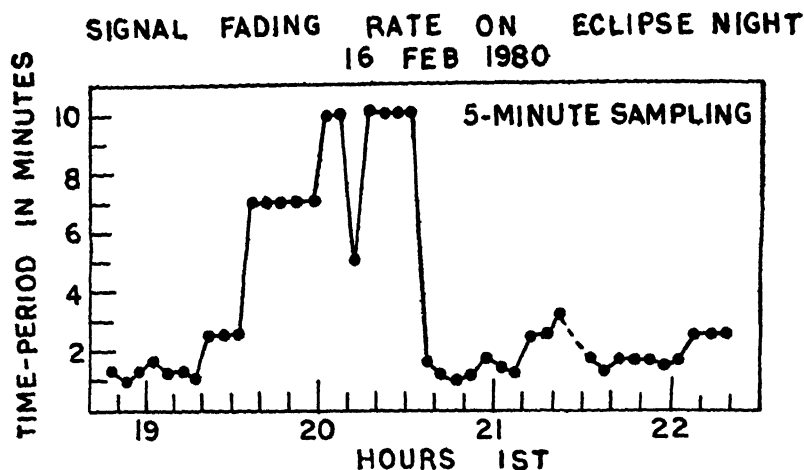


FIG. 4. Signal fading rate from 5-minute samplings on the night of the eclipse. Note that the time-period of fades has a maximum value of 10 minutes centred around 20 20 IST.

minutes for about 40 minutes after 20 IST, and drops to around 1–3 minutes on either side; the implications of these periodicities are not clear.

#### ACKNOWLEDGEMENTS

The authors express their deep gratitude to Professor R. G. Rastogi for his interest in this work and helpful discussions on the interpretation of these observations.

#### REFERENCES

- Bhonsle, R. V., Alurkar, S. K., Degaonkar, S. S., Calla, O. P. N., Raju, G., Rana, S. S., Lokanadham, B., and Vijay Gopal, B. (1981) Solar flux measurements during the total solar eclipse on 16 February 1980. In: *Observations of Total Solar Eclipse of 16 February 1980 (Preliminary Results)*, 80–83 INSA, New Delhi.
- Chandra, H., Sethia, G., Vyas, G. D., Deshpande, M. R., and Vats, H. O. (1981) Ionospheric effects of the total solar eclipse of 16 February 1980. In: *Observation of Total Solar eclipse of 16 February 1980 (Preliminary Results)*, 57–60 INSA, New Delhi.
- Chimonas, G., and Hines, C. O. (1970) Atmospheric gravity waves induced by a solar eclipse. *J. geophys. Res.*, 75, p. 875.
- Deshpande, M. R., Vats, H. O., Sethia, G., Chandra, H., Iyer, K. N., and Janve, A. V. (1981) Detection of ionosphere polarisation scintillations. In: *Observations of Total Solar Eclipse of 16 February 1980 (Preliminary Results)*, 65–66 INSA, New Delhi.

- Dixit, P. S., Rao, P. K., Bhonsle, R. V., Sethia, G., Deshpande, M. R. and Chandra, H (1981) Phase and field measurements in VLF, LF and HF regions during the solar eclipse of 16 February 1980—preliminary results. In: *Observations of Total Solar Eclipse of 16 February 1980 (Preliminary Results)*, 67–70. INSA, New Delhi.
- Ernest Raj, P., Srirama Rao, M., Jogulu, C., and Madhusudhana Rao, B (1981) Unusual phase path and group path variations during the solar eclipse of 16 February 1980. In: *Int. Symp. Solar Eclipse (Abstr)* INSA, New Delhi
- Friedman, H. (1960) The Sun's ionising radiations. In: *"Physics of the upper atmosphere"*, 133–218 (Ed J. A. Ratcliffe), Acad. Press, N.Y., and London
- (1962) Solar observations obtained from vertical soundings *Rep Progr. Phys.*, **25**, 163–217.
- Girish Kumar, U V., and Ramana, K. V. V. (1981) A-1 absorption measurements during the total solar eclipse of 16 February 1980. In: *Int. Symp. Solar Eclipse (Abstr.)* INSA, New Delhi.
- Lakshmi, D R., Chakravarthy, R., Mangal Sain and Reddy, B M (1981) Multi-station monitoring of HF broadcast circuits during the solar eclipse of 16 February 1980. In: *Int. Sym. on Solar Eclipse (Abstr)*, p 46 INSA, New Delhi
- Landini, M., Russo, D., and Tagliaferri, G L (1966) The solar eclipse of May 20, 1966 observed by the SOLRAD 8 satellite in the X-ray and UV bands *Nature*, **211**, 393–394.
- Minnis, C M (1955) Ionospheric behaviour at Khartoum during the eclipse of 25 February 1952. *J atm terr Phys.*, **6**, 91–112.
- Mitra, S. N (1981) Effect of solar eclipse of February 16, 1980 on lower ionosphere. In: *Int Symp. Solar Eclipse (Abstr)* INSA, New Delhi.
- Piddington, J. H (1951) The modes of formation of the ionospheric layers. *Geophys. Res.*, **56**, 409–429
- Rao, P A., and Bagri, D S (1981) Radio observations of the solar eclipse of 16 February 1980 at Ootacamund. In: *Int Symp Solar Eclipse (Abstr.)*, p 11. INSA, New Delhi.
- Rastogi, R G (1960) Propagation of radio waves reflected from the ionosphere during a solar eclipse *Geophys Pure Appl—Milano*, **45**, 123–152.
- Rishbeth, H., and Garriott, O K (1969) Chemistry of the E and F1-regions. In: *Introduction to Ionospheric Physics*, p 115 Acad. Press, N.Y., and London.
- Saito, S., Kurokawa, H., and Ogimachi, Y. (1981) Heterogeneous structures of the lower corona. In: *Observations of Total Solar Eclipse of 16 February 1980 (Preliminary Results)*, 31–33 INSA, New Delhi
- Sen, A K., Saha, B., Trehan, S K., Sekhar De, S., Saha, S K., Datta, R N., Chatterjee, S K., Saha, J S., Das Gupta, M. K., and Sen, S K. (1981) Radio wave propagation during the total solar eclipse of 16 February 1980. In: *Observations of Total Solar Eclipse of 16 February 1980—Preliminary results*, 77–79 INSA, New Delhi
- Sen Gupta, P K., and Mitra, S N. (1954) Corpuscular eclipse in the F2-layer and its association with solar-flares and M regions *Nature*, **173**, 814–819
- Sethuraman, R (1980) Electromagnetic field strength measurements during solar eclipse of 16 February 1980 *Indian J Rad Space Phys*, **9**, 198–200.
- Tuhi Ram Tyagi *et al* (1981) A multi-station satellite radio beacon study of ionospheric variations during the total solar eclipse of 16 February 1980. In: *Int Symp Solar Eclipse (Abstr)* INSA, New Delhi
- Venkatanarayana, R., and Somayaji, T S N (1981) Lower ionospheric effects of the solar eclipse of 16 February 1980 p 50 In: *Int Symp Solar Eclipses (Abstr)* INSA, New Delhi



Printed in India.

Invited Review (Gravity Waves)

## ATMOSPHERIC GRAVITY WAVES PRODUCED BY SOLAR ECLIPSES—A REVIEW

KENNETH DAVIES

*National Science Foundation, Washington DC 20550, USA*

*(Received 31 July 1981)*

The paper reviews the theoretical and experimental bases for gravity wave production resulting from cooling produced by the moon's shadow. Theoretically, it is reasonable to expect waves from the low shock after propagation in a dispersive and anisotropic atmosphere and that focusing should be expected from the eclipse geometry. Experimental evidence from the eclipses of 7 March 1970 in North America, 30 June 1973 in Africa and 23 October 1976 in Australia leave doubts as to whether such waves have been observed.

**Keywords:** Gravity Waves; Solar Eclipse; Propagation in Dispersive & Anisotropic Atmosphere; Chimonas' Model; Brunt-Väisälä Frequency

### INTRODUCTION

DURING a solar eclipse, the moon's shadow moving at supersonic speed, cuts off solar heating radiation. This results in cooling of the atmosphere, particularly in the troposphere and the ozonosphere, accompanied by a condensation of air in the cooled regions. It was suggested by Chimonas and Hines (1970) that this cooling would generate atmospheric waves. Since the generator is moving at supersonic speed it produces a bow wave somewhat similar to that produced by a ship travelling through water. Chimonas (1970) used a model in which the main source of gravity waves was centered around 45km although he recognized that cooling around 90km and in the troposphere could be sources also.

Following their generation, the gravity waves propagate outward and upward to the ionosphere. Because atmospheric density decreases exponentially with height, the amplitude of the wave may increase with height (*see* Hines, 1960) and thus may be detected in the ionosphere by radio soundings. Chimonas (1970) calculations were made for the eclipse over North America of 7 March 1970.

Starting with this eclipse, numerous attempts have been made to detect such waves both in the ionosphere and on the ground. In this paper, we discuss the experimental evidence for and against the existence of gravity waves produced by solar eclipses.

### GENERATION MECHANISM

Chimonas (1970) considered the case of a localized heat source (or sink) moving through a gravitationally stratified atmosphere. In the case of a solar eclipse the

moon's shadow travels with a speed,  $V$ , of about 2500km/hr ( $\approx 700\text{m/s}$ ) whereas an individual disturbance generated by the cooling will expand outward at approximately the speed of sound,  $C$ , ( $\approx 300\text{m/s}$ ). This results in a bow wave, as sketched in Fig. 1, in which the bow front makes an angle  $\theta$  with the eclipse path where  $\sin \theta \approx C/V$ .

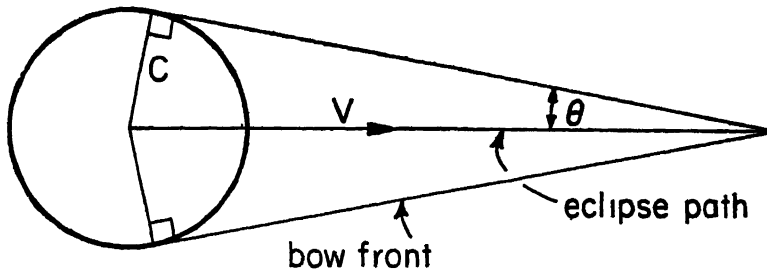


FIG. 1. Bow wave.

Complete shielding of the atmosphere from solar radiation occurs only during a total eclipse and even then the width of the umbra never exceeds 280km. The radius of the penumbra is around 3480km and causes significant shielding over about half the umbral diameter. In Chimonas' model the Gaussian source with half-width of 15km was located in the ozonosphere (at 45km) with a temperature rate of change of  $9^\circ\text{K}$  per day resulting from the cut-off of solar ultraviolet radiation. He calculated the steady state wave system about a cooling spot moving with constant speed through a flat gravitationally stratified isothermal atmosphere to obtain a reasonable order-of-magnitude description of a wave system with frequencies less than the isothermal Brunt-Väisälä frequency  $\omega_b$ . Because of the very long wavelengths there will be considerable coherence across the source region resulting in strong wave generation.

The mathematics of the model is given in Chimonas (1970) and references contained therein to which the reader is directed. The characteristic frequency of the source is of the order of  $2\pi$  times the shadow speed divided by the shadow length ( $\omega \approx 6 \times 10^{-4} \text{ sec}^{-1}$ ) which is much less than the Brunt-Väisälä frequency ( $\omega_b \approx 10^{-2} \text{ sec}^{-1}$  at 45km). The fractional pressure perturbation at 200km altitude and 10,000km from the eclipse path as a function of distance along the eclipse path,  $y$ , is shown in Fig. 2. From this figure we see that the maximum pressure perturbation is of the order of 10 per cent and the wavelength in the  $y$  direction is of the order of 10000km. The horizontal wavelength perpendicular to the bow front is  $10,000 \sin \theta \approx 5000\text{km}$ . Assuming a horizontal speed of 700m/s in the ozonosphere, we obtain a wave period of the order of four hours.

#### IONOSPHERIC OBSERVATIONS

##### 7 March 1970

The Chimonas and Hines (1970) calculations were made with the total eclipse of 7 March 1970 in mind. The path of this eclipse along the east coast of North America is shown in Fig 3. These authors pointed out that the geometry of the eclipse path would tend to focus the wave energy into an area centered more or less on Cali-

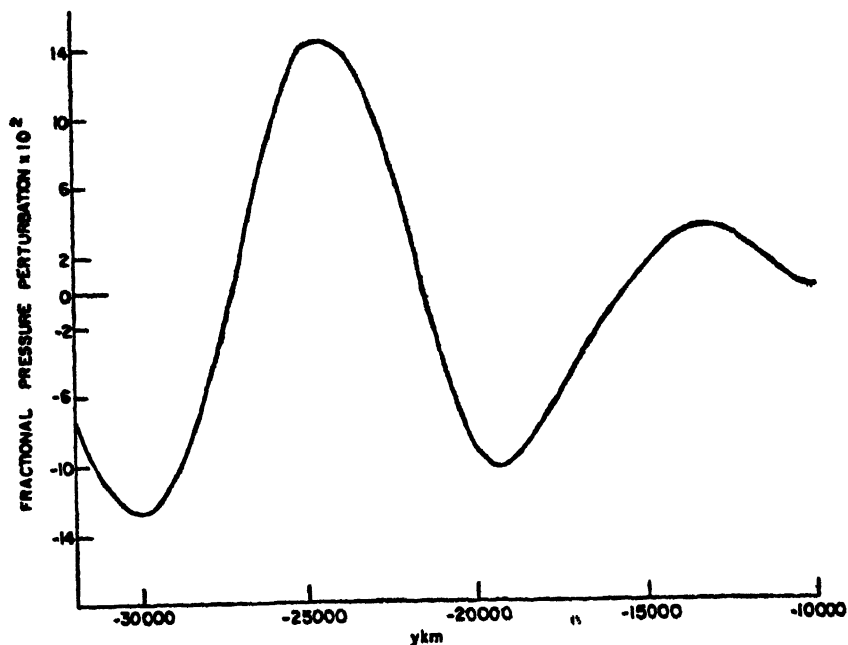


FIG. 2. The fractional pressure perturbation 200km above the earth's surface, at a point 10,000km from the eclipse shadow, as a function of distance parallel to the path (after Chimonas, 1970).

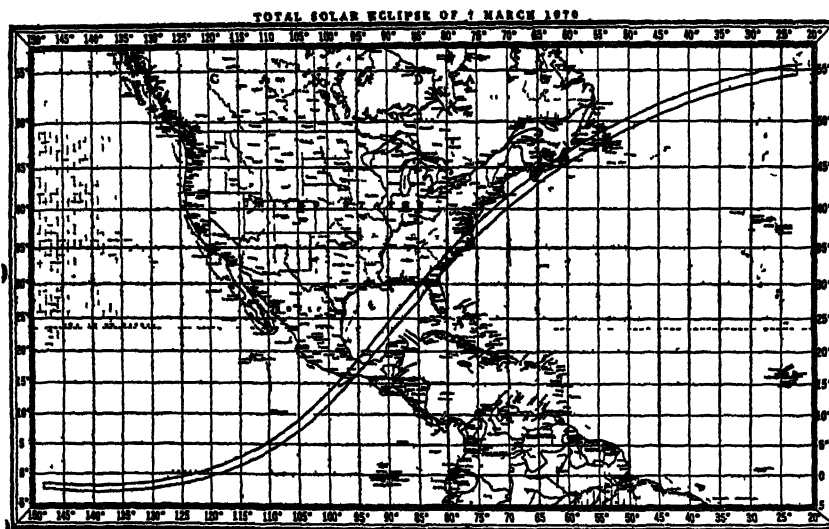


FIG 3 Path of the 7 March 1970 eclipse—from *Solar Eclipse Bulletin* (1970)

forma which would lead to interference effects, and particularly to an enhanced amplitude in that region. Maximum signal would be expected in California at around 1900 UT.

Following the publication of the model predictions, a number of ionospheric radio measurements were made during the eclipse. The most notable of these were made in the west and south west of the USA. In particular, Davis and da Rosa (1970) reported on the *possible* detection of atmospheric gravity waves generated by this eclipse. They measured the changes in the Faraday rotation of very high frequency ( $\approx 137\text{MHz}$ ) radio signals from the geostationary satellites ATS-1 and ATS-3 at several sites. They observed the passage of travelling ionospheric disturbances at Stanford, California, Clark Lake, California and Fort Collins, Colorado and from the geographical separations and time displacements deduced that a disturbance moved approximately from east to west. Their record is shown in Fig. 4. It indicates

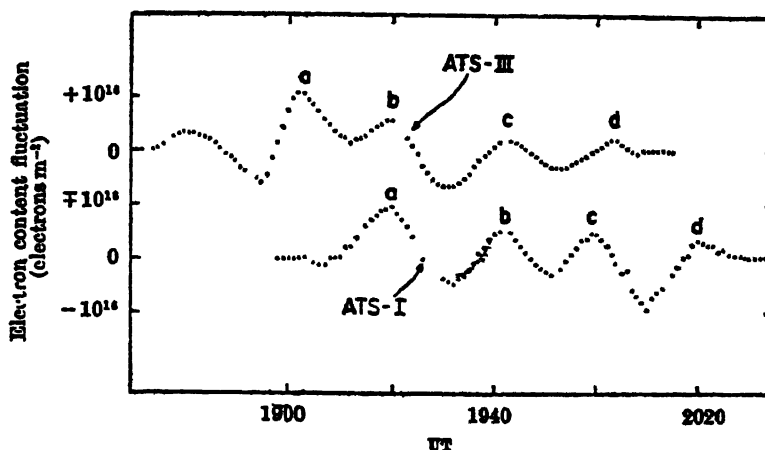


FIG 4 Travelling ionospheric disturbances observed by Davis and da Rosa on March 1970 (after Davis & da Rosa, 1970)

a wave period of about 20min and a velocity of  $620 \pm 120 \text{ms}^{-1}$  at  $279 \pm 2^\circ \text{S}$  east of north. The peak-to-peak fluctuation in Faraday rotation was around 1.5 per cent. Lerbald *et al* (1972a, b) using radio pulse soundings of the ionosphere, with vertical and oblique propagation, saw evidence of an east-west travelling ionospheric disturbance between 1930 and 2030 UT, i.e., at about the expected time.

Using a very sensitive high-frequency doppler technique Sears (1972) made observations at Palo Alto, California of the frequency stability of ionospheric echoes from WWV-5, -10 and -15MHz at Fort Collins, Colorado. His records were not well defined but there was some evidence for a TID with period near 25min between 1800 and 1900 UT. Sears points out that Yeh reported a disturbance in Faraday rotation at Urbana, Illinois moving from west-to-east, i.e., in the opposite direction to that expected of an eclipse generated disturbance. Evidence in favour of eclipse generated waves with periods near 18min have been advanced by Arendt (1971, 1972) from Faraday rotation measurements at Fort Monmouth, New Jersey and ionosonde soundings at Wallops Island, Virginia. He observed undulations in Faraday rotation and true height of the ionosphere during the early stages of the eclipse, and estimated their speed as about 300m/s. It should be noted that although it was magnetically quiet at the time of the eclipse, the latter was sandwiched between two

magnetic disturbances. Anastassiades and Moraites (1970) observed TIDs on 8 March 1970 at Athens, Greece, but they felt it was premature to ascribe them to the eclipse.

Possible evidence for a gravity wave in the phase height of reflection of radio echoes from the F-region at Huntsville, Alabama between 1700 and 1800 UT were reported by Butcher (1973) with a wave period near 18 min and with a peak-to-peak change of 0.5 to 1 km. However, the oscillation is evident before the start of the eclipse.

Evidence for eclipse generated waves in incoherent scatter data at Arecibo have been presented by Carlson *et al.* (1970). Contour plots of constant backscatter power versus time reveal *weak* wave-like disturbances between 1725 and 1800 AST in the height range 175 to 225 km, with wave period near 15 min and speed of around 200 m/s during magnetically disturbed conditions. On the other hand Baron and Watt (1970) found that downward propagating disturbances observed with the incoherent scatter technique at Stanford on 7 March 1970 were not significantly different from those on control days. Some of the evidence for and against the detection of gravity waves coming from eclipses is summarized in Table I. Negative results have been reported by several investigators as for example MacDougall (1970) and Oetzel and Chang (1970).

### 30 June 1973

This provided another opportunity to test whether waves, produced by a solar eclipse, could be detected in the atmosphere. The path of totality over North Africa is shown in Fig. 5 which shows several areas in which wave focusing should occur. Of particular interest is the region in Southwest Africa where strong focusing was predicted by Beer and May (1972) so that the gravity wave signature should be an order of magnitude larger than that predicted for California on 7 March 1970 (see Frost & Clark, 1973).

Ionospheric observations of Faraday rotation, ionosonde, HF pulse back-scatter and microbarograph were made in Southwest Africa by Schodel *et al.* (1973a, b) with negative results. Travelling ionospheric disturbances were observed but these were attributed to a prevailing geomagnetic storm ( $K_p \leq 6+$ ). Likewise, there was no evidence for pressure (microbarograph) waves at ground level. Similar negative results were reported by Hunter (1973) and Hunter *et al.* (1975) who used the Faraday rotation technique at Nairobi, Dar-es-Salaam, Blantyre and Grahamstown but found that any fluctuation was less than 1 per cent although conditions were favourable.

A much more positive interpretation of data from this eclipse is provided by Broche and Crochet (1975) and by Broche *et al.* (1976) from measurements made close to the path of totality. Using the HF doppler technique in Chad, Broche and Crochet (1975) found evidence of 1) an overall eclipse effect  $S_1$  resulting from the cut-off of ionizing radiation, 2) a periodic variation  $S_2$  with  $\Delta f = \pm 0.5$  Hz and with wave period near 10 min; and 3) a fluctuation  $S_3$  with period near 30 min and  $\Delta f \approx \pm 1$  Hz. They conclude that the  $S_2$  disturbance originated in the eclipse shadow and the ionospheric perturbation was about 5 per cent. Evidence of a weak wave disturbance has been found by Bertin *et al.* (1977) travelling with a speed of  $275 \pm 25$  m/s. Broche and Crochet (1975) attributed the fact that the wave period was shorter than expected to interference effects in the near field of the source.

TABLE I

*Evidence for gravity waves generated by solar eclipse*

Authors	Date	Positive (P) or negative (N) or uncertain (U)	Close(C) or Far (F)	Period (min)	Horizontal Speed m/s	Technique	Ionosphere (I) Troposphere (T)	Location
Anastassiades & Moraites	7 March 1980	U	F	—	—	Ionosonde	I	Greece
Arendt	"	P	C	18	300	Faraday	I	New Jersey
Anderson, Keefer & Myers	"	P	C	90	—	Pressure	T	Florida
Butcher	"	U	C	18	—	Phase height	I	Alabama
Carlson <i>et al.</i>	"	P	C	15	200	IS	I	Puerto Rico
Davis and da Rosa	"	U	F	20	620	Faraday	I	California
Lerfald <i>et al.</i>	"	U	F	—	—	HF pulse	I	SW — USA
Sears	"	U	F	25	—	HF doppler	I	California
Bertin, Hughes & Kersley	30 June 1973	P	F	18	275	Faraday	I	Europe
Broche & Crochet	"	P	C	10	—	HF doppler	I	Chad
Broche, Crochet & Maistre	"	P	C	—	—	Ionosonde	I	Chad
Hunter <i>et al.</i>	"	N	C&F	—	—	Faraday	I	Africa
Jones & Bogard	"	N	C	—	—	Pressure	T	Africa
Schodel <i>et al.</i>	"	N	F	—	—	Ionosonde Pressure Faraday	I	Southern Africa
Baulch & Butcher	23 October 1976	P	C	—	—	HF, angle	I/E	Victoria, A
Butcher, Downing & Cole	"	P	C	30–35	210	Ionosonde	I	Victoria, A
Hajkowicz	"	P	—	—	556	Satellite ratio fading	I	Brisbane
Lilley & Woods	"	U	C	—	—	Magnetic	—	Australia
Morton & Essex	"	N	C	—	—	Faraday	—	Victoria, A
Scheepers	"	U	F	—	—	Magnetic	—	South Africa
Ichinose & Ogawa	19 April 1958	P	—	22	—	HF doppler	I	Tokyo
Vaidyanathan <i>et al.</i>	29 April 1976	P	—	11	—	Faraday & phase	I	Trivandrum

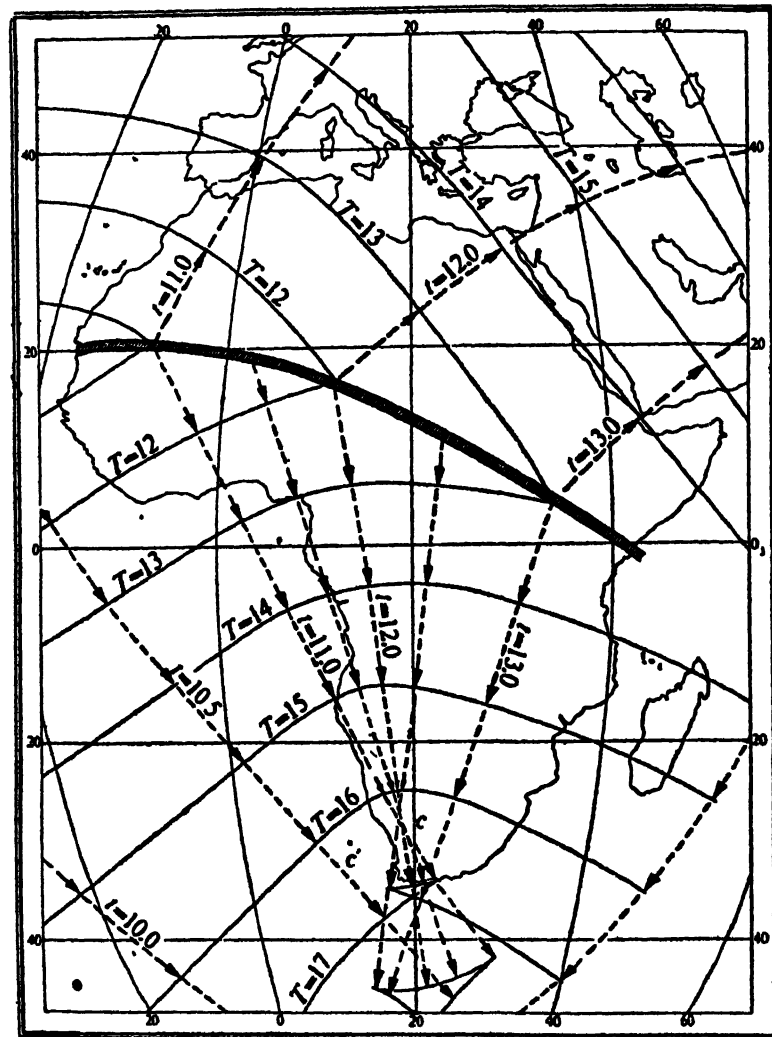


FIG 5 Path of the solar eclipse of 30 June 1973 with the expected areas of gravity wave focusing (after Beer & May, 1972)

### 23 October 1976

The path of totality of this eclipse passed over the state of Victoria in Southeast Australia. Several papers have reported identification of waves from this eclipse. Baulch and Butcher (1977), Butcher *et al* (1979), Hajkowicz (1977), with a dissenting opinion from Morton and Essex (1978) from their array of Faraday polarimeters. In particular, Butcher *et al* (1979) used a digital ionosonde to obtain accurate measurements of group height on several frequencies reflected from the F-region in the path of totality. Their results are shown in Fig 6 the most striking feature of which is the appearance of an oscillation with period near 35min. Spectral analyses in the time interval 1700 to 2000 LT showed periods near 35 and 15min. The longer period is

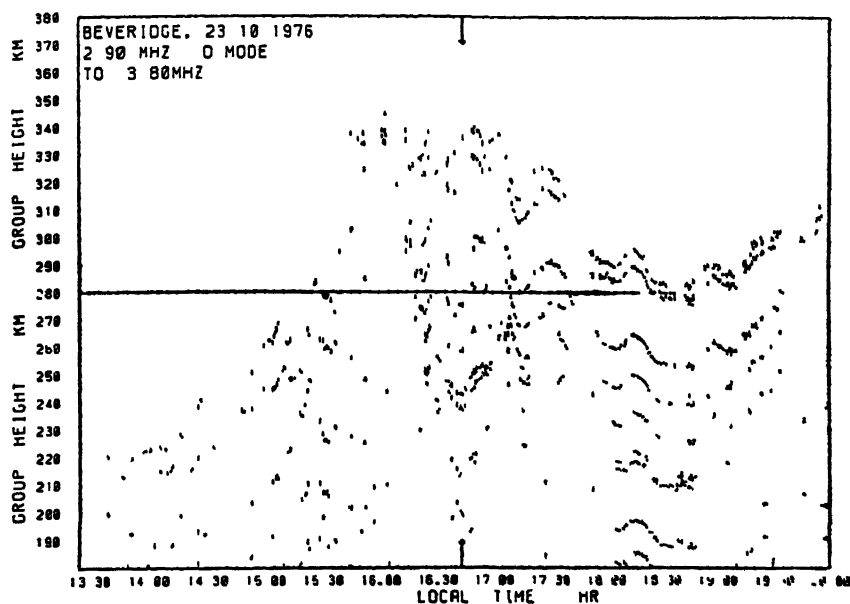


FIG. 6 Group height measurements on 23 October 1976 at Beveridge for frequencies 2.9 to 3.8 MHz. The plots are displaced for clarity descending in order of frequency (after Butcher *et al.*, 1979)

excited near 1700 and the shorter period appears after 1830 local time. The longer period wave has a vertical wavelength of  $200 \pm 20$  km, a horizontal wavelength of about  $190 \pm 20$  km. The vertical and horizontal phase speeds are  $210 \pm 20$  m/s and  $120 \pm 15$  m/s respectively. During this eclipse the geomagnetic field was extremely quiet ( $K_{sum} = 15$ ). Lilley and Woods (1977) point out that the solar eclipse can cause geomagnetic variations by perturbing electric currents in the ionosphere. From an analysis of magnetic declination data from ten locations in Australia, Lilley and Woods (1977) concluded that *possible* eclipse effects were present although this conclusion has been challenged by Scheepers (1978) who deduced, from a study of the magnetic declination in South Africa, that the waves reported by Lilley and Woods is a manifestation of a minor magnetic disturbance.

#### Other Evidence

Evidence of waves from eclipses have been presented for two other eclipses. Ichinose and Ogawa (1976) report waves in HF doppler records in Japan during the 19 April 1958 solar eclipse, with period near 22 min. During the partial eclipse of 29 April 1976, Vaidyanathan *et al.* (1978) detected quasi-periodic fluctuations in the Faraday rotation,  $\Omega$ , and modulation phase,  $\Phi$ , of the radio signals from the geostationary satellite ATS 6 (see Davies, 1980) received in Trivandrum, India. Their results are shown in Fig. 7. Spectrum analyses of their data yield the periods shown in Table II. It is difficult to accept the authors' explanation of the differences in the periods of the two types of measurement.



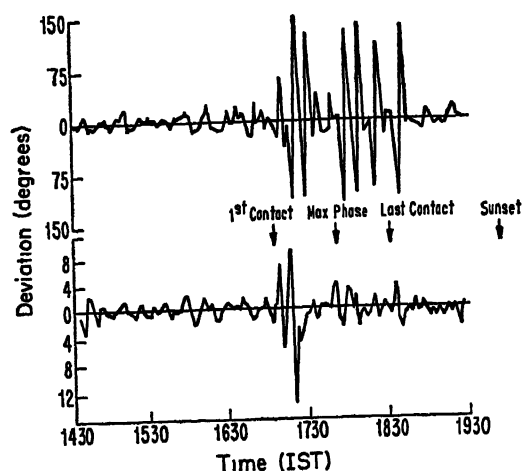


FIG. 7. Faraday and phase fluctuations, ATS-6 to Trivandrum during the partial eclipse of 29 April 1976 (after Vaidyanathan *et al.*, 1978).

TABLE II

*Periods of waves in Faraday rotation  $\Omega$  and modulation phase  $\phi$  observed during the solar eclipse of 29 April 1976 at Trivandrum*

(after Vaidyanathan *et al.*, 1978)

Period (min)					
$\phi$	—	12.8	9.8	8.0	6.1
$\Omega$	42.7	16.0	10.7	8.5	6.5

#### GROUND PRESSURE OBSERVATIONS

A gravity wave generated by an eclipse cooling should be detected by sensitive microbarographs at the earth's surface. The source of such waves is expected to lie in the troposphere and be caused by cooling resulting from cut-off of infrared absorbed by water and water vapour. Variations in atmospheric pressure in Florida during the eclipse of March 1970 have been reported by Anderson *et al.* (1972) and are shown in Fig. 8. They cite eclipse observations from 1887 to 1952, as well as their own, that show two maxima and two minima, beginning with a minimum after first contact. The period near 90 min is quite different from those reported for the ionosphere.

During 30 June 1973 eclipse over Africa, Anderson and Keefer (1973) were unable to detect eclipse associated pressure changes if they were present. Small changes that did occur after first contact could not be attributed to the eclipse since similar waves were observed prior to first contact. Gierasch (1973) found no strong wave phenomena in Kenya and neither did Jones and Bogart (1975) nor Schodel *et al.* (1973a, b).

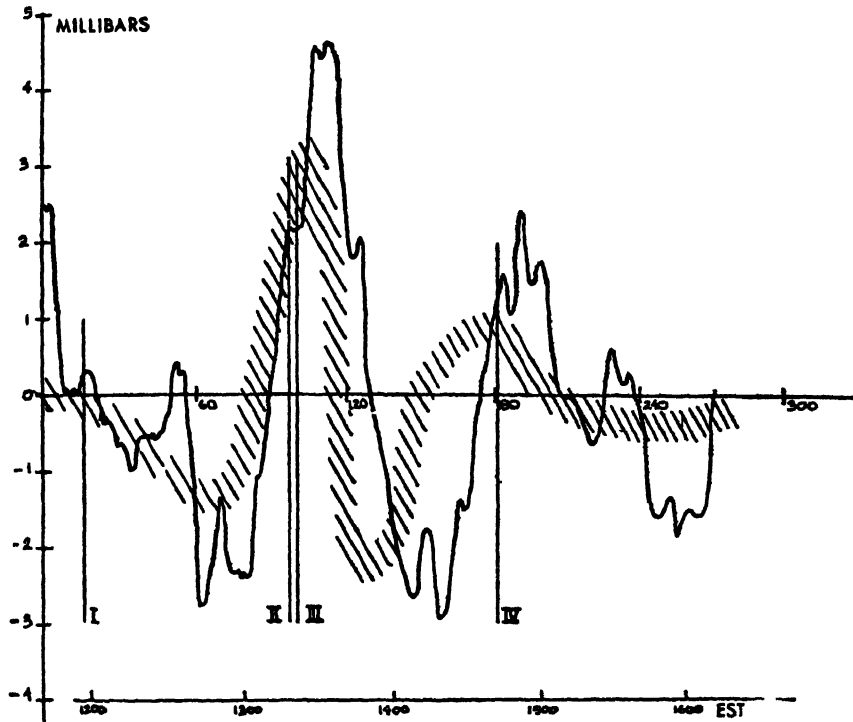


FIG. 8 Corrected barometric pressure variations on 7 March 1970 at Lee, Florida (after Anderson *et al.*, 1972)

#### DISCUSSION

##### *Experimental Evidence*

The positive evidence for gravity waves in the ionosphere from a solar eclipse source is still weak. Most observers of the 1970 eclipse were cautious of claiming that their data provided definite proof of waves from the eclipse bow wave. The wave periods they observed (20 to 30 min) are common on days without eclipses. As pointed out by Frost and Clark (1973) "*the lack of unique or identifiable characteristics makes any correlation between observations, to establish or confirm acoustic wave parameters, conjectural.*" Furthermore, the eclipses of 7 March 1970 and 30 June 1973 were accompanied by magnetic disturbance and, during such disturbances, gravity waves are often generated in the auroral zones and travel equatorward. Even on magnetically quiet days waves are present in the F-region with periods ranging from about 5 min up to several hours. Some wave-like disturbances seen during an eclipse were apparent before first contact so these can hardly be attributed to the eclipse. There are some difficulties with equipment sensitivity. For example, in the 7 March 1970 eclipse Davis and da Rosa identified waves with the relatively insensitive Faraday rotation technique whereas Sears (1972) was quite uncertain although he used the highly sensitive HF doppler technique. If the waves were sufficiently large to be detected in California from the eclipse it might be expected that they would be seen at Boulder, Colorado

which lies between the eclipse path and California HF doppler observations at Boulder by the present author failed to reveal such waves and I never published this negative result. It could not be argued that this is due to sharp focusing over California since the measurements of Davis and da Rosa covered a large geographical area. Indeed Frost and Clark (1973) place the focus east of California. Further, they point out that whereas the ATS 1 event of Davis and da Rosa agrees with their estimate of the arrival time the ATS 3 event is somewhat early. Thus there is some basis for skepticism. There is also some question about the speed of the waves ( $620 \pm 120 \text{ m/s}$ ) observed by Davis and da Rosa. This speed is considerably larger than the speeds of gravity waves with periods near 20 min ( $\sim 200 \text{ m/s}$ ) which led Sears (1972) to suggest that they were surface waves.

In the case of 30 June 1970 eclipse all indications were that Southwest Africa would be ideal to observe wave effects because of focusing. But again the results were negative. More positive results seem to obtain close to the path of totality in the three main eclipses of 1970, 1973 and 1976. Thus although we might expect some type of disturbance in the atmosphere to be created by the rapidly moving noon shadow, the experimental evidence should be viewed with caution.

### Theory

Comparison of theory and experiment revealed several discrepancies. The initial model of Chimonas (1970) predicted wave periods of several ( $\approx$  four) hours and attention was confined to an ozonospheric source and detection in the ionosphere. To account for the differences in predicted and observed periods, Chimonas and Hines (1971) pointed out that the difference was apparent rather than real because the bow shock in the penumbra is dominated by short wavelengths generated at the foremost part of the penumbra. Their essential point is that the observations of Davis and da Rosa were made much closer to the path of totality than was assumed for the published theoretical wave forms. There is bias towards shorter periods because long-period gravity wave components cannot ascend steeply from the source (Hines, 1967). Chimonas and Hines (1971) repeated the earlier calculations for a near field point and their results, shown in Fig. 9, give a period near 20 min and the overall growth and decay pattern is similar to that observed by Davis and da Rosa (1970).

One important detail emerged from these new calculations that concerns the validity of the "fully developed" bow wave theory. When the computation was continued to greater times, after those shown in Fig. 9, a second wave system of longer period but much smaller amplitude was found starting about 3 hours after the first received signal. This latter wave could not be predicted by the steady state solution. Chimonas and Hines (1971) insist that "*Regardless of the uncertainties in the precise manner of its excitation, and the limitations of any model calculation applied to the real atmosphere, the present calculations appear to confirm beyond reasonable doubt that Davis and da Rosa in fact did observe the predicted bow wave.*"

To account for the pressure fluctuations observed by Anderson *et al.* (1972), Chimonas (1973) used a tropospheric source of gravity waves and proposed that, rather than internal waves, the observed waves are surface or Lamb waves in which the energy is trapped in the lower troposphere and propagates horizontally from almost the entire shadow region to any observation point.

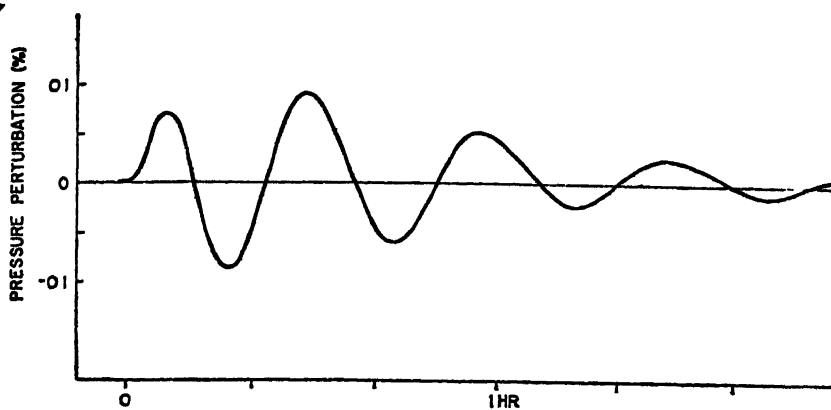


FIG. 9. Pressure perturbation bow wave for a point 5000km off the axis of totality (after Chimonas & Hines, 1971)

Butcher *et al* (1979) noted that their observed wave periods differed from those predicted and those observed under similar eclipse conditions by Bertin *et al.* (1977) and proposed a model that reconciled the differences. The model depends on the recovery of the wake of the umbral region by inward collapse of the atmosphere horizontally and that the observed wave periods are doppler shifted by motion of the source. They calculated the expected wave periods for four modes of source excitation, i.e., the number of wavelengths of sound across the horizontal dimension of the umbral region across the path of the eclipse. In this way, they account for a wide range of periods although they pointed out that some of their model periods have not been observed.

#### CONCLUSIONS

There is little doubt that some form of atmospheric disturbance should be expected to emanate from a solar eclipse. Furthermore, one would expect dispersion of such a disturbance in propagation through the atmosphere so that the period and wave shape would be a function of the distance from the moon shadow to the point of observation.

In spite of the remarks of Chimonas quoted above one can hardly be satisfied with the experimental evidence. It is interesting to note a trend in the literature with time in connection with the much quoted paper by Davis and da Rosa (1970). These authors stressed the uncertainties in their observations, which is very appropriate, but their caveats have sometimes been lost sight of in subsequent literature. The main difficulty is the fact that waves with the observed periods are present on most days and particularly on days of solar-terrestrial disturbance. In almost every case in which positive evidence has been advanced there are disquieting aspects. We have already referred to the question of equipment sensitivity in the case of 7 March 1970 eclipse. Even more disquieting are the negative results from South-west Africa which should have given the most conspicuous signatures. In the Australian eclipse of 23 October 1976 some observations are positive and some are

negative. Finally, the observations of Vaidyanathan *et al.* (1978) give rise to some doubt because the wave periods, obtained from two sets of measurement of the same radio signals, differ.

Thus, in conclusion, I want to point out that the experimental evidence for gravity waves generated by solar eclipses is unsatisfactory.

#### REFERENCES

- Anderson, R. C. *et al.* (1972) Atmospheric pressure and temperature changes during the 7 March 1970 solar eclipse. *J atm Sci*, **29**, 583–587
- Anderson, R. C., and Keefer, D. R. (1973) Temperature and pressure changes during the solar eclipse. In: *Solar Eclipse 1973 Bull 5 Nat Sci. Found.*, 99–102
- Anastassiades, M., and Moraitis, G. (1970) Travelling ionospheric disturbances in Athens during the March 7 solar eclipse. *Nature*, **226**, 1125–1126.
- Arendt, P. R. (1971) Ionosphere-gravity wave interactions during the March 7, 1970 solar eclipse. *J. geophys. Res.*, **76**, 4695–4697.
- (1972) Ionospheric undulations during the solar eclipse of 7 March 1970. *J. atm. terr Phys.*, **34**, 719–725.
- Baron, M., and Watt, T. M. (1970) Incoherent scatter observations. *Solar Eclipse 1970 Bull. F Nat. Sci. Found.*, 246–247
- Baulch, R. N. E., and Butcher, E. C. (1977) Atmospheric waves in the ionosphere due to total solar eclipse *Nature*, **269**, 497
- Beer, T., and May, A. N. (1972) Atmospheric gravity waves to be expected from the solar eclipse of June 30, 1973 *Nature*, **240**, 30–32.
- Bertin, F. *et al.* (1977) Atmospheric-waves induced by the solar eclipse of 30 June 1973 *J atm terr. Phys.*, **39**, 457–461
- Broche, P., and Crochet, M. (1975) Generation of atmospheric gravity waves by the 30 June 1973 solar eclipse in Africa. *J atm terr. Phys.*, **37**, 1371–1374.
- Broche, P. *et al.* (1976) Gravity waves generated by the 30 June 1973 solar eclipse in Africa *J atm terr. Phys.*, **38**, 1361–1364
- Butcher, E. C. (1973) Possible detection of a gravity wave in the phase height of the F-region due to the eclipse of March 7, 1970 *J geophys. Res.*, **78**, 7563–7566.
- Butcher, E. C. *et al.* (1979) Wavelike variations in the F-region in the path of totality of the eclipse of 23 October 1976 *J. atm terr. Phys.*, **41**, 439–444
- Carlson, H. C. *et al.* (1970) Eclipse observations at Arecibo, Puerto Rico on March 7, 1970 *Nature*, **226**, 1124–1125.
- Chimonas, G. (1970) Internal gravity-wave motions induced in the earth's atmosphere by a solar eclipse *J geophys. Res.*, **75**, 5545–5551.
- Chimonas, G. (1973) Lamb waves generated by the 1970 solar eclipse, *Planet Space Sci.*, **21**, 1843–1854
- Chimonas, G., and Hines, C. O. (1970) Atmospheric gravity waves induced by a solar eclipse *J geophys Res.*, **75**, 875.
- (1971) Atmospheric gravity waves induced by a solar eclipse, 2 *J geophys Res.*, **76**, 7003–7005
- Davies, K. (1980) Recent progress in satellite radio beacon studies with particular emphasis on the ATS-6 radio beacon experiment *Space Sci Rev.*, **25**, 357–430
- Davis, M. J., and da Rosa, A. V. (1970) Possible detection of atmospheric gravity waves generated by the solar eclipse. *Nature*, **226**, 1123.
- Frost, A. D., and Clark, R. R. (1973) Predicted acoustic gravity wave enhancement during the solar eclipse of June 30, 1973 *J geophys Res.*, **78**, 3995–3997.
- Gierasch, P. J. (1973) Atmospheric pressure fluctuations during the solar eclipse In *Solar Eclipse 1973 Bull 5 Nat. Sci. Found.*, 103
- Hajkowicz, L. A. (1977) Periodic fadings in VHF radio-satellite transmission during the solar eclipse on 23 October 1976 *Nature*, **266**, 5598, 147–148.

- Hines, C. O (1960) Internal gravity waves at ionospheric heights *Can. J. Phys.*, **38**, 1441-1481.
- (1967) On the nature of travelling ionospheric disturbances launched by low-altitude nuclear explosions *J. geophys. Res.*, **72**, 1877-1882.
- Hunter, A. N (1973) Atmospheric gravity waves generated by the eclipse In: *Solar Eclipse 1973 Bull Nat Sci. Found.*, **5**, 85-86.
- Hunter, A. N. *et al.* (1975) Faraday rotation studies in Africa during the solar eclipse of June 30, 1973 *Nature*, **250**, 205.
- Ichinose, T, and Ogawa, T. (1976) Internal gravity waves deduced from the HF doppler data during the April 19, 1958 solar eclipse. *J. geophys Res.*, **81**, 2401-2404.
- Jones, B. W., and Bogart, R. S (1975) Eclipse induced atmospheric gravity waves. *J. atm. terr. Phys.*, **37**, 1223-1226.
- Lerfeld, G. M. *et al* (1972a) Travelling ionospheric disturbances observed near the time of the solar eclipse of 7 March 1970. *J. atm. terr. Phys.*, **34**, 733-741.
- (1972b) Propagation of submicrosecond HF pulses through travelling ionospheric disturbances. *Proc. AGARD Conf.*, No. 115, *Effects of Atmospheric Acoustic Gravity Waves on Electromagnetic Wave Propagation*, 34-1-34-19
- Lilley, F. E M, and Woods, D V. (1977) Magnetic observations of the solar eclipse of 23 October 1976 in Australia *Nature*, **226**, 823-824.
- MacDougall, J (1970) Detection of ionospheric gravity waves. *Solar Eclipse Bull. F Nat. Sci. Found.*, **221**.
- Morton, F. W., and Essex, E. A. (1978) Total electron content observations during the 23 October 1976 solar eclipse over south-eastern Australia *J. atm terr. Phys.*, **40**, 111-114.
- Oetzel, G N, and Chang, N J. F (1970) TID investigation at Stanford, Calif, during the 1970 solar eclipse *Solar Eclipse Bull. Nat. Sci. Found.*, **230**.
- Scheepers, G L. M. (1978) Possible solar eclipse effect 23 October 1976. *Nature*, **271**, 5640, 91-92.
- Schodel, J P. *et al.* (1973a) Atmospheric gravity wave observations after the solar eclipse of June 30, 1973 *Nature*, **245**, 5419, 87-88.
- (1973b) Atmospheric gravity wave observations after the solar eclipse. In: *Solar Eclipse 1973 Bull. 5 Nat Sci Found.*, 92-93.
- Sears, R. A. (1972) Ionospheric HF doppler dispersion during the eclipse of 7 March 1970 and TID analysis *J atm terr Phys.*, **34**, 727-732.
- Vaidyanathan, S, Raghava Reddy, C, and Krishna Murthy, B. V (1978) Quasi-periodic fluctuations in electron content during a partial solar eclipse *Nature*, **271**, 40-41.

Printed in India.

Review (Gravity Waves)

## ATMOSPHERIC PRESSURE WAVES GENERATED BY SOLAR ECLIPSES

C. A. REDDY

*Space Physics Division, Vikram Sarabhai Space Centre, Trivandrum 695 022, India*

(Received 31 July 1981)

A review of the present state of knowledge about the solar eclipse-induced pressure perturbations in the atmosphere is presented. The results of experimental measurements on the ground-level pressure perturbations during solar eclipses are critically reviewed and compared with theoretical predictions. The Lamb wave hypothesis of Chimonas (1973) is shown to provide a satisfactory explanation for the ground-level pressure perturbations; but more theoretical modelling work is needed to find out the reasons for the low amplitudes or the non-existence of eclipse-induced pressure perturbations during several observations. It is also pointed out that the ionospheric observations on solar eclipse-induced perturbations in the upper atmosphere are inconclusive in relation to the hypothesis that the gravity waves generated in the stratosphere in the wake of the moon's shadow can generate ionospheric perturbations. It is concluded that further theoretical work and well-planned measurements from a network of observing stations are needed for further elucidation of the relevant questions.

**Keywords:** Atmospheric Pressure Waves; Electron Density & Content

THE most spectacular and visually appealing phenomena which take place during a solar eclipse are those involving the sun. However, the earth's atmosphere, which is directly and indirectly influenced by solar radiations in so many ways, responds readily to the rapid reduction of the solar radiation during an eclipse. Some of the resulting atmospheric changes are straightforward and easy to understand like the decrease in air temperature at ground level and above, and the general decrease of the wind and turbulence in the atmospheric boundary layer. On the other hand, some other changes in the atmospheric state have their origin in more complex processes caused by the solar eclipse. One such phenomenon is the quasiperiodic fluctuation of the ground level atmospheric pressure during the solar eclipse. This phenomenon has received considerable attention of atmospheric scientists in the last ten years primarily because of the theoretical models proposed by Chimonas and Hines (1970) and Chimonas (1970, 1973) delineating the physical processes which could generate such wave-like perturbations in the atmospheric pressure. This is one atmospheric phenomenon which is simple in nature but complex in its origin.

Chimonas and Hines (1970) proposed the idea of atmospheric gravity waves being generated in the wake of the moon's shadow which sweeps across the stratosphere with supersonic speed and cools the region around 45km altitude. Normally, the heating rate is high in this region because of the solar UV absorption by ozone.

The gravity waves thus generated can propagate upward into the upper atmosphere and give rise to observable ionospheric perturbations. Propagating downward, the gravity waves can generate small but still measurable fluctuations of the atmospheric pressure at ground level. The attempts to measure the predicted gravity wave perturbations at ionospheric heights have produced both positive evidences and negative results to-date. The measurements of ground-level pressure perturbations have shown that a surface wave (Lamb wave) type perturbation, originating in the troposphere rather than in the stratosphere, is the likely cause of the observed pressure fluctuations during the eclipses

In this review paper, an overview of the theory and experimental observations of the ground-level pressure perturbations during solar eclipses is presented. Only a brief mention is made about the other aspect of atmospheric gravity waves in the upper atmosphere during the solar eclipses

#### EARLY OBSERVATIONS

On simple physical considerations, one would expect changes in the ground-level atmospheric pressure during a solar eclipse. At the time of eclipse, the heating of the ground and the overlaying air mass is reduced. As a consequence of this reduced heating and the spatial gradients of the temperature, one would expect a change in the ground level atmospheric pressure. At any given location, the pressure change need not necessarily have a simple relationship, in phase or amplitude, with the temperature change at that location. Realising the importance of measurements on the solar eclipse-induced pressure changes, observations were carried out even during the 19th century. A summary of the early observations on pressure changes is given in Table I, while some typical records of the early observations are shown in Fig 1. Both are taken from Anderson *et al.* (1972)

TABLE I

*Early measurements of ground level pressure changes during solar eclipses*  
[after Anderson *et al.* (1972)]

	Date of Eclipse	Approximate pressure change ( $\mu$ b)	Number of		Location
			Maxima	Minima	
1	19 August 1887	260	0	1	Russia
2	"	N A	1	0	"
3	"	230	2	2	"
4	1 January 1889	280	2	2	California (U S A)
5	4 April 1893	150	2	2	Chile
6	28 May 1900	100	0	1	Georgia (U S A)
7	18 June 1918	200	—	—	U.S A
8	8 April 1921	280	2	2	Sweden
9	25 February 1952	450	2	3	Israel

Excepting 1, 2, 7, all other cases are single station observations.



Two features in Fig. 1 are worth noting: (a) the presence of irregular pressure fluctuations of much shorter duration than that of the longer period smoothly varying components which are attributed to the solar eclipse effect; the shorter period fluctuations can have large amplitudes on some occasions, and obscure the solar eclipse-induced perturbations; (b) the presentation of a 'mean' curve after averaging the perturbations during many eclipses (or for many stations in some cases). Such 'mean' curve may not always be very meaningful, if the characteristics of the eclipse-related perturbations are not repetitive from eclipse to eclipse (or from station to station), particularly with regard to their phase in relation to the eclipse time.

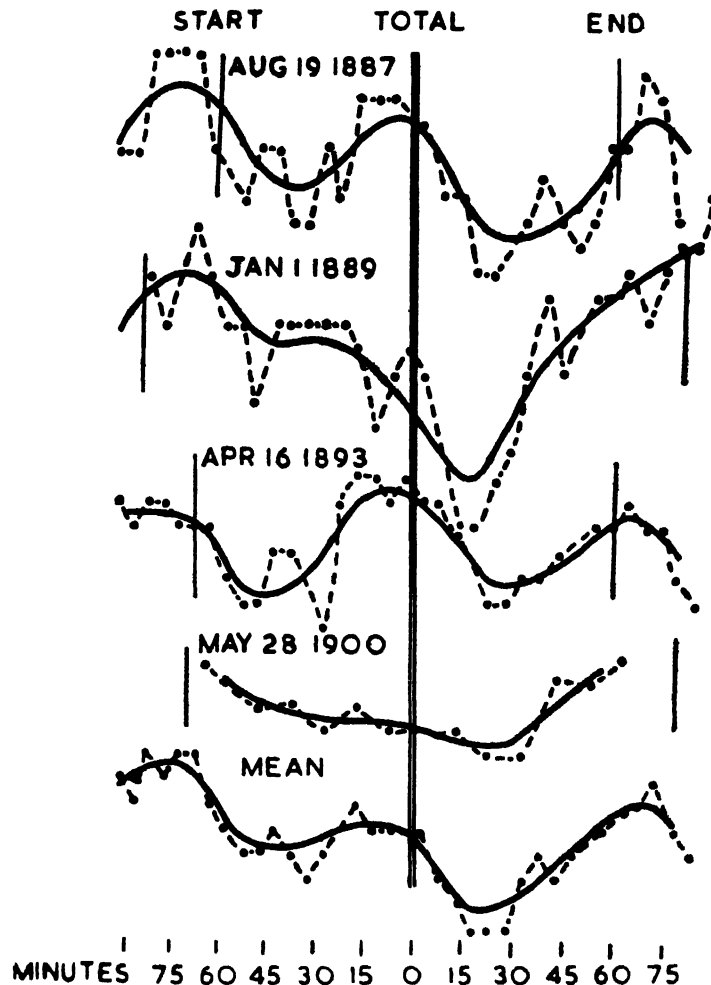


FIG 1 Some early observations on atmospheric pressure fluctuations during solar eclipses. Time is centred around the maximum phase of eclipse denoted by double vertical bars. The length of the short vertical lines at the 'start' and 'end' of the eclipse corresponds to 150 microbars approximately in case of 1893 event [after Anderson *et al* (1972)]

The early observations indicate, on the whole, the presence of significant pressure perturbations during solar eclipses, with typical amplitudes of about 200–300 microbars and quasiperiods corresponding to the semi-duration of the eclipse. It is not entirely clear, however, that how successfully the eclipse-induced perturbations have been isolated from the atmospheric pressure perturbations of other origins. Moreover, the scientific effort in making such measurements has remained rather sparse until 1970, mainly due to lack of theoretical models.

#### THEORETICAL MODEL OF GRAVITY WAVE GENERATION DURING A SOLAR ECLIPSE

The theoretical work of Chimonas and Hines (1970) gave a strong impetus to a new scientific interest in measuring the atmospheric pressure changes during solar eclipses. They proposed a theoretical model of a physical mechanism which can give rise to pressure perturbations in the upper atmosphere as well as at ground level. They argued that the atmospheric region around 45km, in which the daily heating rate due to the solar UV radiation absorption by ozone was a maximum, could get cooled significantly during the solar eclipse in the absence of the UV radiation. Since the moon's shadow in the stratosphere travels with supersonic speed along the line of totality, the progressive cooling of the stratospheric air mass with such supersonic speed would generate acoustic gravity waves in the wake of the high speed shadow, and a bow wave would result. Based on the estimates of Murgatroyd and Goody (1958) for stratospheric heating rates, Chimonas (1970) computed theoretically the pressure perturbations that would result in the upper atmosphere (i.e., at F-region heights) and at the ground level, at distances of several thousand kilometres away from the source region. While the fractional pressure change caused by the acoustic gravity waves (generated in the wake of moon's shadow in the stratosphere) is about 5 per cent of the ambient in the 200–250km altitude region, the estimated change is only 0.002 per cent or a few microbars at the ground level. Chimonas and Hines (1970) and Chimonas (1970) pointed out that the comparatively large pressure changes in the upper atmosphere would be easily detectable through radio methods of measuring the ionospheric perturbations caused by the gravity waves. The detection of the small pressure changes at the ground level would be a much more difficult task, though the modern microbarographs have the required sensitivity levels

#### *Ionospheric Observations*

Subsequent to the theoretical prediction by Chimonas and Hines (1970) and Chimonas (1970), several observations were made on the ionospheric changes during the solar eclipses of 7 March 1970, 30 June 1973, 11 May 1975, 29 April 1976 and 23 October 1976 in an attempt to detect and delineate the nature of the predicted acoustic gravity wave-generated disturbances [Anastassiadis & Moraites, 1970, Carlson *et al.*, 1970, Davis & da Rosa, 1970, Arendt, 1971, 1972, Lurfald *et al.*, 1972, Sears, 1972, Butcher, 1973, Baulch & Butcher, 1977, and Vaidyanathan *et al.*, 1978] Among all the observations, the observations of Davis and da Rosa (1970) show most clearly the wave-like nature of the ionospheric perturbation in the total electron content. From two station records, they could also deduce the direction of the disturbance motion which was as theoretically predicted. There

are a number of other observations which indicate the occurrence of quasi-periodic variations during the solar eclipses, but their detailed characteristics do not fully match the theoretically predicted characteristics like the wave periods, the propagation delays expected, the horizontal/vertical speeds and wavelengths [Broche & Crochet, 1975; Bertin *et al.*, 1977; Lilley & Woods, 1977; and Scheepers, 1978] Schödel *et al.* (1973) and Hunter *et al.* (1974) reported a negative result from their observations of the F-region maximum electron density and the total electron content (TEC) respectively. The presence of geomagnetic storm and substorm effects during the solar eclipses might have obscured sometimes the real eclipse-related gravity wave perturbations, if any; and the substorms might have produced perturbations which were in some cases attributed wrongly to the gravity waves generated in the stratosphere due to the eclipse effect

On the whole, the experimental evidence in support of the hypothesis of Chimonas and Hines (1970) about the generation of acoustic gravity waves in the stratosphere in the wake of moon's shadow remains inconclusive at present. In addition to the natural limitations imposed by the circumstance of magnetic storm effects getting mixed up with the solar-eclipse induced effects, the other limitations in a quantitative comparison of theory and observations are: (a) theoretical predictions are made for the far-field effects i.e., the bow wave perturbation characteristics at distances of several thousand kilometres away from the source region are described, whereas many of the observations are made inside or near the source region; (b) the atmospheric effects of refraction, reflection, ducting and dissipation, which are not considered in the theoretical model of Chimonas (1970), can significantly modify the wave characteristics; and (c) other source regions in the upper mesosphere and lower thermosphere, though energetically weaker, may make a significant contribution to the observed perturbations at F-region levels. Further detailed consideration of the above factors is beyond the scope of this paper. A more detailed review of the eclipse-generated gravity waves in the upper atmosphere is presented in Dr Kenneth Davies' article in this volume. The article by Butcher *et al.* (1979) as quoted by Kenneth Davies contains a good discussion of the various observations *vis-a-vis* the theoretical predictions

#### GROUND LEVEL PRESSURE CHANGES DURING SOLAR ECLIPSES

Interestingly, the observations reported in the literature on the ground level atmospheric pressure disturbances during solar eclipses are much fewer than those on corresponding ionospheric disturbances. Anderson *et al.* (1972) reviewed briefly the earlier measurements reported in the literature and concluded that the pressure changes were consistently oscillatory with a quasiperiod approximately equal to the semi-duration of the eclipse and with an amplitude of 200–250 microbars, with very few exceptions. Their own observations during 7 March 1970 solar eclipse showed oscillatory pressure changes at eclipse time, consisting of one dominant period around 90 minutes with an amplitude of 250 microbars and other smaller periods with one-fourth or less of the above amplitude. The observed dominant period ( $89 \pm 4$  minutes) was nearly equal to the semi-duration of the eclipse (81 minutes), while the amplitude was also the same as that in the earlier observations. The residual pressure fluctua-

tions, which were extracted from a background of larger pressure changes caused diurnal thermal tide and a linear trend, are shown in Fig. 2 along with the pressure fluctuations observed by Klein and Robinson (1952) during 25 February 1952 eclipse. The similarity of the fluctuations on the two occasions is to be noted, particularly the occurrence of two cycles of perturbation. Lindholm and Bergstein (1923) also reported similar features from their observations during 8 April 1921 eclipse.

From the above, Anderson *et al* (1972) concluded that their observations on the centre line of the eclipse path could successfully detect the eclipse-induced pressure fluctuations at ground level

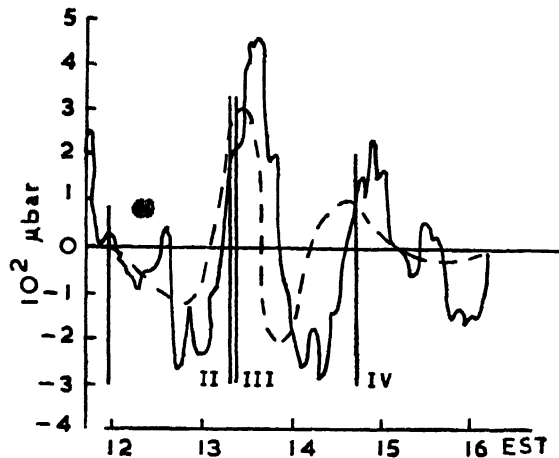


FIG. 2 Residual fluctuations of the ground-level atmospheric pressure (after removing linear trends are the daily tides) during 7 March 1970 solar eclipse as observed by Anderson *et al* (1972). The broken curve shows the corresponding fluctuations during 25 February 1952 eclipse.

However, many other recordings by other scientists during the same eclipse did not show the presence of eclipse-induced pressure fluctuations. Anderson *et al* (1972) attributed this negative result to the instrumental limitation of other experimenters who used cut-off filters which suppressed fluctuation periods longer than about 17 min. The result of Anderson *et al* (1972) also shows a major discrepancy between the observed amplitude ( $\sim 250\mu\text{b}$ ) vs the predicted amplitude ( $\sim 2\mu\text{b}$ ). They pointed out that the larger observed amplitude was probably the result of the solar insolation absorption by water vapour in the lower troposphere being a much stronger source compared to the UV absorption by stratospheric ozone. In their theoretical treatment of the problem, Chimonas and Hines (1970) did not include the contribution of the troposphere water vapour, though they recognized its potential importance.

#### Theoretical Model

In an attempt to explain the observations of Anderson *et al* (1972), Chimonas (1973) worked out a theoretical model in which the eclipse-time reduction of solar insolation absorption by lower tropospheric water vapour was considered as the source for the generation of atmospheric waves. The accurate modelling of the tropospheric water vapour is indeed a very difficult task, considering the scarce observational

data and the high spatial and temporal variability of the water vapour content. In spite of this major difficulty, Chimonas' (1973) theoretical work brought out many interesting points about the characteristics of the atmospheric waves that are generated in the troposphere. Firstly, propagating acoustic gravity waves generated in the troposphere were shown to be very weak because of the nearness of the reflecting ground surface and the consequent destructive interference. The effect is particularly severe for waves with vertical wavelengths greater than about a density scale height. He showed further that the source region beams towards the ground free internal waves within a very narrow cone with its axis inclined at  $3.7^\circ$  to the horizontal and with its semi-angle being only  $1.5^\circ$ . Concluding that the strength of propagating internal waves or acoustic gravity waves generated in the lower troposphere was negligible, he worked out a simplified theoretical model for the generation of Lamb waves or surface waves which have their energy trapped in the lower troposphere and thus propagate horizontally along the surface away from the shadow region to large distances with comparatively small losses. Through his model numerical calculations, Chimonas (1973) showed that given the presence of a sufficient water content in the troposphere—as during the presence of clouds for example—a Lamb wave could be generated efficiently during a solar eclipse and that the surface pressure wave thus generated has an intensity, a period and a wave shape which were very similar to those observed by Anderson *et al.* (1972). Chimonas (1973) pointed out that during the 7 March 1970 eclipse there was a dense cloud cover at the Florida site of observations by Anderson *et al.* (1972), whereas clear sky conditions prevailed at another Florida site where the atmospheric pressure fluctuations could not be detected (Frostman & Dabberdt, 1970). Chimonas argued that the cloud cover at one site provided a tropospheric water content which was above normal, while the water content at the cloudless site was perhaps inadequate to generate Lamb waves of detectable intensity. The correctness or otherwise of this argument is not easy to verify in the present state of poor monitoring of the water content in the atmosphere. Apart from this argument—which explains in a single breath the occurrence as well as the non-occurrence of eclipse-generated ground level pressure waves—the theoretical work of Chimonas (1973) provides a plausible explanation of the somewhat definitive observation of Anderson *et al.* (1972).

The satisfactory match of observation and theory, as outlined above, did not get strengthened further through later observational results. During 30 June 1973 solar eclipse, the path of totality spanned across the African continent, and ground level pressure changes were measured at different locations in the path of totality. At Chinguetti ( $20^\circ 27'N$ ,  $12^\circ 22'W$ ) in Mauritania, Anderson and Keefer (1975) recorded the atmospheric pressure, temperature and wind. They used an improved version of their earlier pressure sensor (Model 210 MKS Baratron), but the experiment led to a null result because of a large pressure depression arising from local weather conditions being superposed on the eclipse-induced changes, if any. Fig 3 shows the records. Two features are to be noted in this figure (a) the presence of similar pressure fluctuations before and after the first contact, and (b) the onset of a large pressure depression, obviously due to some local weather disturbance, soon after the maximum phase. The above two features together make it impossible to identify the eclipse-induced pressure changes, even if they were present.

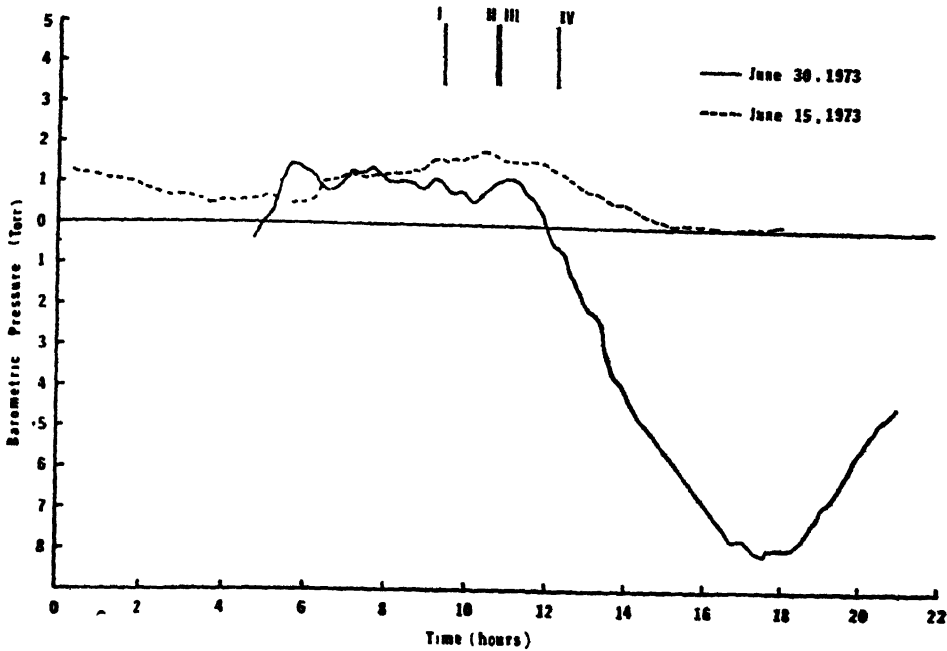


FIG 3 The ground-level pressure changes recorded by Anderson and Keefer (1975) during 30 June 1973 eclipse.

Jones and Bogart (1975) also reported a null result for the 30 June 1973 eclipse from their microbarometer recordings at a location ( $2^{\circ}45'N$ ,  $36^{\circ}43'E$ ) in northern Kenya. Under the conditions of very light winds, excellent records of pressure changes were obtained. The mean pressure and the diurnal and semi-diurnal pressure cycles were removed by curve-fitting procedures to arrive at the residual pressure variations due to other processes including the solar eclipse effect. The residuals are shown in Fig. 4 for the eclipse day and for a non-eclipse day with light winds and little cloud cover. Similar pressure fluctuations are observed before, during and after the eclipse time, making it impossible to draw any definite conclusion about the presence of eclipse-induced pressure fluctuations. The observation of comparable fluctuations in the same local time sector on the non-eclipse day strengthens the doubt about the presence of eclipse-related fluctuations. Apart from the region of totality, two other experimental observations in locations well away from the path of totality also produced null results (Schodel *et al*, 1973, and Beckman & Clucas, 1973).

Jones and Bogart (1975) reported that the cloud cover was 15 per cent cumulus with a slight haze, while Anderson and Keefer (1975) did not comment on the cloud conditions. Assuming that the presence of any significant cloud cover would have led to a comment in their paper to that effect by Anderson and Keefer, and assuming further that the 15 per cent cloud cover reported by Jones and Bogart was not large enough to increase the tropospheric water content significantly above the normal value, the observed null results in both cases can be interpreted to mean (in the light of Chimonas' (1973) Lamb wave hypothesis) that the source strength was not adequate to

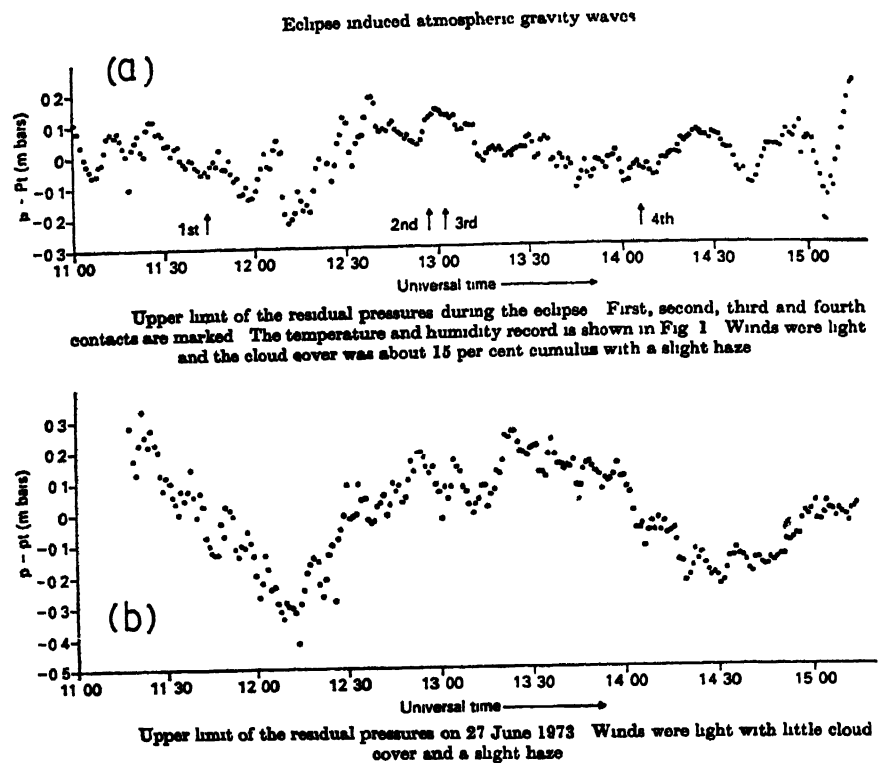


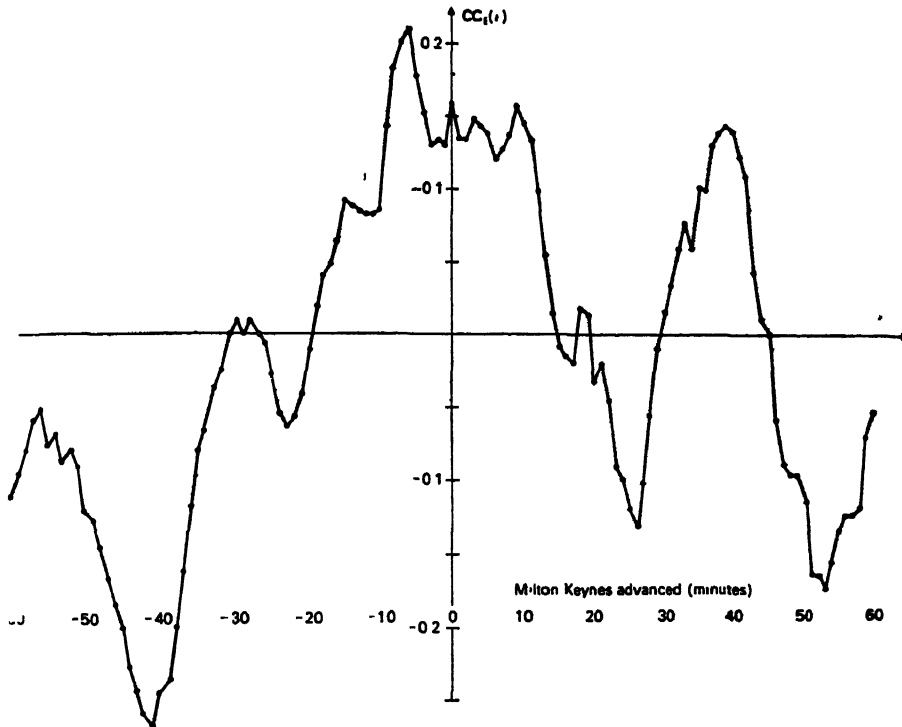
FIG. 4a. The ground-level residual pressure fluctuations observed by Jones and Bogart (1975) during 30 June 1973 eclipse. The mean pressure, the diurnal tide and the semi-diurnal tide are removed by curve-fitting procedures to arrive at the residual pressure fluctuations.

b. Residual pressure fluctuations on a non-eclipse day (27 June 1973).

generate Lamb waves of large enough magnitude above the background 'noise' level of the pressure fluctuations caused by other natural weather processes. In spite of such a reconciliation of theory and observation in qualitative terms, the null result leaves behind a feeling of scientific uncertainty. More importantly, the observational results of Anderson and Keefer (1975), and Jones and Bogart (1975) focus attention on the fundamental limitation of single location recordings. Only through multiple point observations it is possible to isolate the solar eclipse-related pressure changes from the background of other pressure changes due to local weather conditions. At two locations which are sufficiently away from each other (say a 100km or more), the local weather-related pressure fluctuations can be expected to be largely uncorrelated, while solar eclipse induced fluctuations would be well-correlated, with or without a time lag.

Realising the importance of multiple point observations, Jones (1976) used ground level pressure sensors at two sites, Oxford and Milton Keynes, in U.K. during the partial (86 per cent) solar eclipse of 11 May 1975. The two places were separated by 51km. The distance from the above two places to the centre of the penumbral shadow region varied with time from 3500km to 1500km and to greater than 3500km

as the shadow moved from northern Africa through the Atlantic to northern Canada. Thus, the observations of Jones can be considered as far-field observations in contrast to the centre-line observations discussed earlier. Good recordings of pressure fluctuations were obtained at the two locations under favourable weather conditions and the data were subjected to careful analysis. The cross-correlation of the detrended residuals at the two stations did exhibit important maxima for certain values of time lag, as shown in Fig. 5. However, quantitative statistical tests of significance led to an uncertain result which was well summarized in Jones' statement "... *therefore, the hypothesis cannot be refuted that all the structure in Fig 1 (Fig. 5 of this paper) arises from two first-order autoregressive processes and consequently, exhibits*



The cross-correlation function of the residual pressure records at the two sites for the interval 0800 to 1200 GMT

FIG 5 The computed cross-correlation function of the residual pressure fluctuations at Oxford and Milton Keynes (separated by 51km) in UK during 11 May 1975 eclipse (after Jones, 1976)

*no eclipse-induced waves*" It appears that the chosen separation of only 51km for the two observing stations was too low to avoid correlated weather disturbances in ground level pressure at the two stations. From the cross-correlation analysis, Jones (1976) also estimated an approximate upper limit of  $170\mu\text{bars}$  for the wave-like perturbation observed at the two UK sites. Since the theory of Chimonas (1973) gives an estimate only for the points on the path of totality but not for the far away points from totality, it was not possible to make a comparison between the estimated



upper limit of the observed perturbation and the theoretically expected value. Thus, this experimental attempt to match the observation with theory has again led to an inconclusive result.

### THREE-STATION EXPERIMENT IN INDIA DURING 16 FEBRUARY 1980 ECLIPSE

With a view to achieve a more decisive result than what was achieved previously on the possible generation of atmospheric pressure waves during solar eclipses, a three-station experiment was conducted in India during the total solar eclipse of 16 February 1980. Atmospheric pressure changes were recorded with suitable microbarographs at the three locations of Gauribidanur (93 per cent obscuration), Sriharikota (91 per cent obscuration) and Trivandrum (80 per cent obscuration). The separation distances for the three stations are 277km, 667km and 575km. With such large separations, the local weather-generated pressure disturbances can be expected to have negligible correlation except perhaps through a rare coincidence of similarity in their temporal variations. On the other hand, the solar eclipse-induced pressure fluctuations can be expected to have a high degree of correlation. A cross-correlation analysis of the pressure variations at the three stations has brought out the reality of an eclipse-related pressure disturbance at all the three stations. The disturbance amplitude is about  $400\mu\text{bar}$ ; and it consists of a dominant component of 128min period and two weaker components of 32min and 16min periods. Full details of the results are available in the paper by Kunhikrishnan and Krishna Murthy (1981) in this volume.

It is to be noted that at all the three stations cloudless conditions prevailed at the time of observations. Considering the large amplitude of the observed perturbation, it appears that a large increase in the tropospheric water content in terms of clouds is not an essential condition for the generation of Lamb waves. A large amount of water vapour in the tropical atmosphere, especially at coastal locations like Sriharikota and Trivandrum, may be adequate for the generation of Lamb waves of large enough amplitude.

### DISCUSSION AND CONCLUSIONS

From the review of the experimental results on the ground level atmospheric pressure perturbations during the solar eclipses two important features emerge. (a) whenever the solar eclipse-related pressure perturbations could be isolated from other perturbations simultaneously present, the perturbation amplitudes turn out to be large, with typical values in the  $200\text{--}200\mu\text{bar}$  range, and the largest values approach  $500\mu\text{bar}$  level; and (b) the solar eclipse-related pressure fluctuations are quite often obscured by the pressure fluctuations caused by local weather disturbances, indicating thereby that the eclipse-related perturbations are either too weak or absent on such occasions. Thus, a large variability in the amplitude of the solar eclipse-induced pressure changes is indicated.

The hypothesis of Lamb wave generation due to the eclipse-time reduction of solar insolation absorption by the tropospheric water vapour (Chimonas, 1973) explains successfully the main characteristics of the observed perturbations, like the amplitudes, the periods and the shapes of the wave-like perturbations. The absence

or the uncertain presence of the expected perturbation in many cases is not satisfactorily explained as yet. Fig. 6 shows the theoretically computed perturbation in ground pressure, and also the locations of the two observational sites A and B used by Anderson *et al.* (1972) and Frostman and Dabberdt (1970), respectively. The pressure of a cloud cover at A and its absence at B are to be noted. However, large areas surrounding B are having cloud cover; and it is difficult to imagine how a strong Lamb wave generated in the nearby region of cloud cover would not propagate

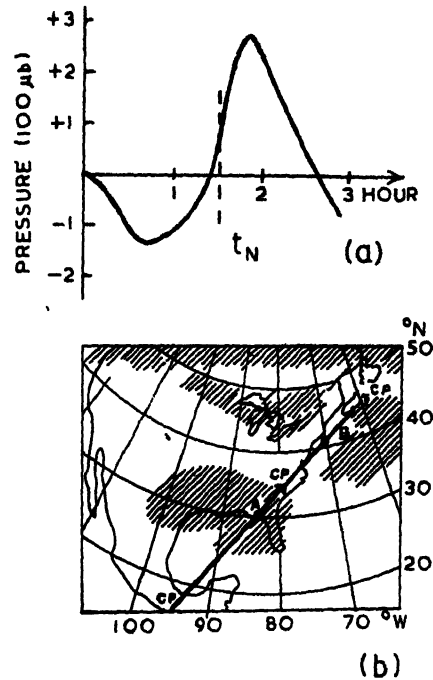


FIG. 6a. Theoretically computed pressure disturbance at ground-level at site A in Fig. 6b due to the Lamb wave Frain induced by the action of the eclipse of 7 March 1970 on the cloud bank over site A

b The central path (CP) of 7 March 1970 eclipse in North America and the cloud areas (hatched) as revealed by satellite photographs. Observations by Anderson *et al.* (1972) were at site A, and those by Frostman and Dabberdt (1970) were at site B (after Chimonas, 1973).

to B and register a pressure perturbation there. Thus, the idea of the large water content in an overhead cloud cluster being responsible for the generation of large amplitude Lamb waves detected at a given location is qualitative at best and it is not entirely satisfactory. This idea is not supported by recent observations in India (Kunhikrishnan & Krishna Murthy, 1981). A generalized model computation with different levels of water vapour content in the troposphere will be very valuable for understanding the relationship between the amplitude of the Lamb waves generated, and the tropospheric water content and its spatial distribution. Such a model study may provide a satisfactory explanation of why the solar eclipse-induced atmospheric waves are strong on some occasions at some places, and they are comparatively weak

or non-existent at other times or places. A second aspect which needs a theoretical modelling study is the propagation of the Lamb waves from the source region. The attenuation and other characteristics of the waves in regions far away from the source region are to be investigated, taking into account the orographic effects.

The future experimental observations should emphasise simultaneous measurements of the related parameters at a number of selected locations. The ground-level pressure changes, the altitude profiles of water vapour in the lower troposphere, the cloud structures and heights and the tropospheric winds and temperatures are to be measured at a large number of suitably chosen sites which are spread along and across the path of totality and cover the source region as well as the far-field region. Only such well-planned observations from a network of stations are likely to lead to decisive advances in our observational knowledge of the physical processes involved in the generation of atmospheric waves by the solar eclipse-associated cooling in the atmosphere.

#### REFERENCES

- Anastassiadis, M., and Moraitis, G (1970) Travelling ionospheric disturbances in Athens during the March 7 solar eclipse. *Nature*, **226**, 1125–1126.
- Anderson, R. C., Keefer, D. R., and Myers, O. E. (1972) Atmospheric pressure and temperature changes during the 7 March 1970 solar eclipse. *J. atm Sci*, **29**, 583
- Anderson, R. C., and Keefer, D. R. (1975) Observation of the temperature and pressure changes during the 30 June 1973 solar eclipse. *J. atm. Sci*, **32**, 228.
- Arendt, P. R. (1971) Ionosphere-gravity wave interactions during the March 7, 1970 solar eclipse. *J. geophys. Res*, **76**, 4695–4697
- (1972) Ionospheric undulations during the solar eclipse of 7 March 1970. *J. atm terr Phys*, **34**, 719–725
- Baulch, R. N. E., and Butcher, E. C (1977) Atmospheric waves in the ionosphere due to total solar eclipse. *Nature*, **269**, 497
- Beckman, J. E., and Clucas, J. I (1973) Search for atmospheric gravity waves induced by the eclipse of June 30, 1973. *Nature*, **246**, 412
- Bertin, F., Hughes, K. A., and Kersley, L (1977) Atmospheric waves induced by the solar eclipse of 30 June 1973. *J. atm terr Phys.*, **39**, 457.
- Broche, P., and Crochet, M (1975) Generation of atmospheric gravity waves by the 30 June 1973 solar eclipse in Africa. *J. atm terr Phys*, **37**, 1371
- Butcher, E. C (1973) Possible detection of a gravity wave in the phase height of the F-region due to the eclipse of March 7, 1970. *J. geophys. Res*, **78**, 7563
- Carlson, H. C., Harper, R., Wickwar, V., Showen, R. L., Behnke, R., Trost, T. F., Cogger, L. R., and Nelson, C. J (1970) Eclipse observations at Arecibo, Puerto Rico, on March 7, 1970. *Nature*, **226**, 1124–1125.
- Chimonas, G (1970) Internal gravity-wave motions induced in the earth's atmosphere by a solar eclipse. *J. geophys. Res*, **75**, 5545
- (1973) Lamb waves generated by the 1970 solar eclipse. *Planet Space Sci*, **21**, 1843
- Chimonas, G., and Hines, C. O (1970) Atmospheric gravity waves induced by a solar eclipse. *J. geophys. Res*, **75**, 875
- Davis, M. J., and da Rosa, A. V (1970) Possible detection of atmospheric gravity waves generated by the solar eclipse. *Nature*, **226**, 1123
- Frostman, T. O., and Dabberdt, W. F (1970) Solar radiation and surface temperature measurements during the solar eclipse of 7 March 1970, Nantucket Island. *Bull. Am. met. Soc.*, **51**, 868
- Hunter, A. N., Holman, B. K., and Feldgate, D. G (1974) Faraday rotation studies in Africa during the solar eclipse of June 30, 1970. *Nature (London)*, **250**, 205

- Jones, B. W. (1976) A search for Lamb waves generated by the solar eclipse of 11 May 1975. *J. atm Sci.*, **33**, 1820.
- Jones, B. W., and Bogart, R. S. (1975) Eclipse induced atmospheric gravity waves. *J. atm. terr. Phys.*, **37**, 1223
- Klein, M., and Robinson, N. (1952) Solar eclipse of 25 February, 1952 and its influence on the insolation and on various meteorological elements *Israel met. Ser. Meteorology Notes*, No. 11.
- Lerfald, G. M., Jurgens, R. B., Vesecky, J. F., and Washburn, T. W. (1972) Travelling ionospheric disturbances observed near the time of the solar eclipse of 7 March 1970. *J. atm. terr. Phys.*, **34**, 733-741.
- Lilley, F. E. M., and Woods, D. V. (1977) Magnetic observations of the solar eclipse of 23 October 1976 in Australia. *Nature (London)*, **266**, 823.
- Lindholm, F., and Bergstein, F. (1923) Influence des eclipses de soleil sur la circulation atmospherique. *Geogr. Ann.*, **5**, 309-321.
- Murgatroyd, R. J., and Goody, R. M. (1958) Sources and sinks of radiative energy from 30 to 90km. *Q. J. R. met. Soc.*, **84**, 225
- Scheepers, G. L. M. (1978) Possible solar eclipse effect 23 October 1976. *Nature (London)*, **271**, 91.
- Schodel, J. P., Klostermeyer, J., and Rottger, J. (1973) Atmospheric gravity wave observations after the solar eclipse of June 30, 1973 *Nature*, **245**, 87.
- Sears, R. D. (1972) Ionospheric HF Doppler dispersion during the eclipse of 7 March 1970 and TID analysis. *J. atm. terr. Phys.*, **34**, 727-732.
- Vaidyanathan, S., Raghava Reddi, C., and Krishna Murthy, B. V. (1978) Quasi-periodic fluctuations in electron content during a partial solar eclipse *Nature*, **271**, 41.

Printed in India.

Gravity Waves

## EVIDENCE OF ATMOSPHERIC GRAVITY WAVES IN THE WAKE OF THE ECLIPSE SHADOW

R. VENKATACHARI, A. K. SAHA and C. V. SUBRAHMANYAM

*Radio Science Division  
National Physical Laboratory  
New Delhi-110 012, India*

and

S. K. CHATTERJEE  
*Institute of Radio Physics & Electronics,  
Calcutta-700 009, India*

(Received 15 February 1982)

In this paper, an attempt at obtaining evidences of atmospheric gravity waves at ground level and at ionospheric heights during the total solar eclipse of 16 February 1980 is described. The observations were made with two microbarographs located at Hyderabad (maximum obscuration 99 per cent) and at Delhi (65 per cent), a Dopplometer at 10MHz located at Calcutta receiving ATA, Delhi and an ionosonde at Delhi. Wavelike disturbances could be distinguished in the Hyderabad microbarograph and in the Dopplometer records that would tend to suggest as originating from the region of totality. No clear evidence of wave motion could be detected at Delhi either on microbarograph or in the ionograms.

**Keywords:** Gravity Waves; Microbarograph; Dopplometer; Ionogram; Infrasounds; Ionosonde

### INTRODUCTION

In previous eclipses, many experiments were concerned for detecting atmospheric gravity waves (as predicted by Chimonas & Hines, 1970) caused by the cooling action of the moon's shadow when it crosses the atmosphere with supersonic speed (Davies & da Rosa, 1970; and Anastassiades & Moraitis, 1970). Considerable success was claimed regarding gravity waves in the higher regions of the ionosphere (Chimonas, 1973). Experiments conducted to detect such wave motions at ground level by monitoring the ground level pressure variations (Anastassiades & Moraitis, 1970; and Anderson *et al*, 1972) could not provide results that were conclusive.

The total solar eclipse of 16 February 1980 offered an opportunity for the study of its effect, especially generation of atmospheric gravity waves, in the ionosphere, lower atmosphere and at ground level. It was all the more interesting because the eclipse occurred during afternoon and a totality path was available in India and the duration of totality was for about 2 minutes.

Two microbarograph units of identical type (for details, see Venkatachari & Bhartendu, 1979) were operated, one at Hyderabad (maximum obscuration 99 per cent)

and the other one in Delhi (65 per cent) to monitor any eclipse effect superposed on the normal infrasonic pressure variations. The effect was also studied by monitoring frequency deviation with a Dopplometer (10MHz) operated at Haringhata, Calcutta which monitors ATA signals from Delhi. An ionosonde was also operating at Delhi.

The primary objective of the study was to look for evidence of atmospheric gravity wave motions caused by the supersonic movement of the moon's shadow during the total eclipse of 16 February 1980.

### OBSERVATION AND INTERPRETATION

#### (a) *Infrasonic Observations*

Over Delhi, eclipse began at 1436hr and ended at 1651hr with maximum obscuration at 1547hr IST. A study of the infrasonic pressure variation at Delhi (Fig. 1) shows that the amplitude of the pressure changes are comparatively less than on

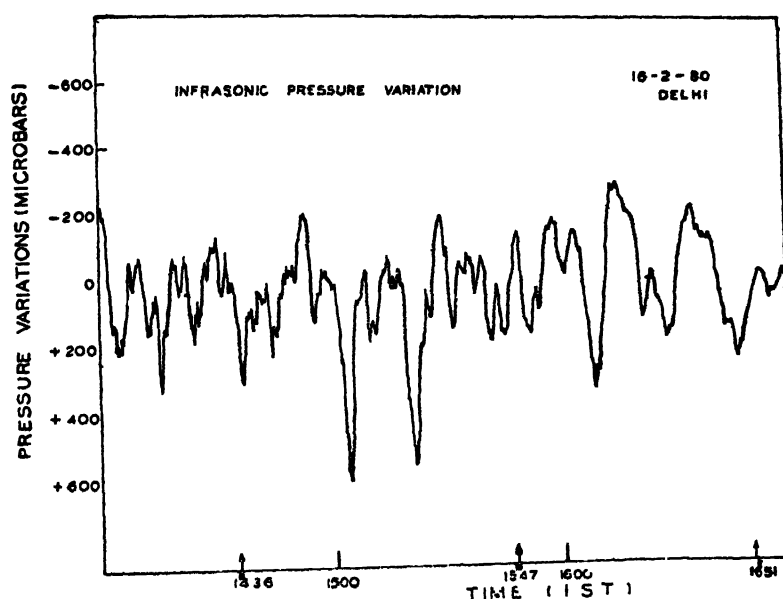


FIG. 1 Infrasonic pressure variations at Delhi on the eclipse day (16-2-1980) B-beginning; M-Maximum phase, E-end of eclipse

other days for the duration of the eclipse. This is due to decrease of temperature during the eclipse. But there are no indications of any gravity wave type motions on the records.

At Hyderabad, eclipse started at 1428hr and ended at 1656hr with maximum obscuration at 1547hr IST. A study of the infrasonic pressure variations at Hyderabad (Fig. 2) reveals that the amplitude is less from the start of the eclipse indicating a temperature effect. There was no perceptible wavelike motion, either before the start of the eclipse or till the maximum phase is reached. But from this time, a definite wave motion is seen for 1 to 2 hours, superposed on the random variations. The

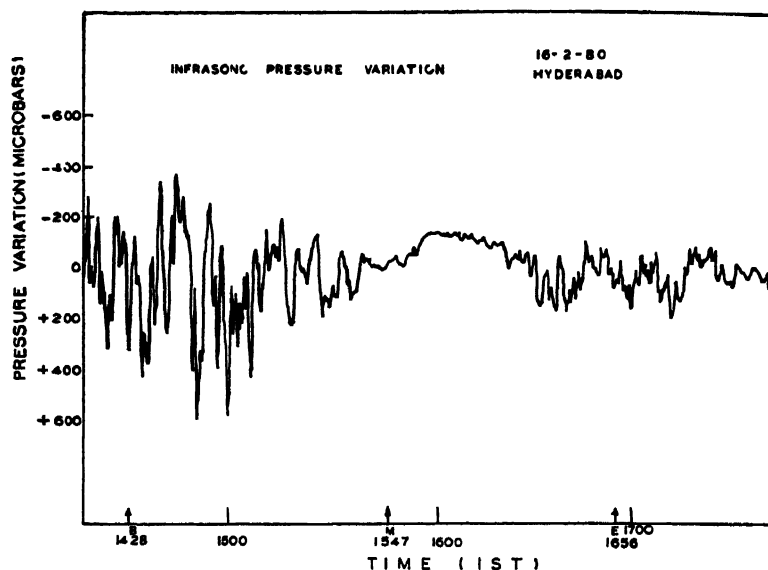


FIG. 2. Infrasonic pressure variations at Hyderabad on the eclipse day (16-2-1980) B—Beginning; M—Maximum phase, E—end of the eclipse

initial period was 55 minutes, and it decreased gradually

A magnetic storm was in progress on the eclipse day. Infrasonic pressure records are generally more agitated on the storm days compared to magnetically quiet days (Srivastava *et al.*, 1981). The decrease in amplitudes of the infrasonic variations of thermal origin, noted during the eclipse, would eliminate any storm time variations and the amplitude fluctuations with larger periods could be ascribed to the eclipse effect.

Power spectra analysis (Blackman & Tukey, 1958) for Hyderabad for the eclipse duration showed that it was maximum around a period of 33 minutes whereas on control day (for the same time block) it was maximum around 17 minutes. This may mean that the longer period waves were present on the eclipse day. Similar analysis for Delhi did not give any significant variations. The maximum was around 17 minutes on both days.

#### (b) Dopplometer Observations

The ATA signals (10MHz) would normally be propagated *via* F-layer at a height of about 160km with an equivalent vertical incidence frequency of about 4.2MHz and reflected over an area roughly above Banaras (Maximum obscuration 81 per cent). The Dopplometer records (Fig. 3) of Delhi-Calcutta path definitely showed a wave-like pattern on the eclipse day, in striking contrast to the control day. Wave motions with shorter periods were found even before the start of the eclipse. Near the maximum phase, the period of oscillations is roughly one hour, the subsequent oscillations being of gradually decreasing periods. This is similar to that observed at Hyderabad with the microbarograph. The delay in the onset of the wave disturbance between Hyderabad and Banaras is of the order of 5 minutes.

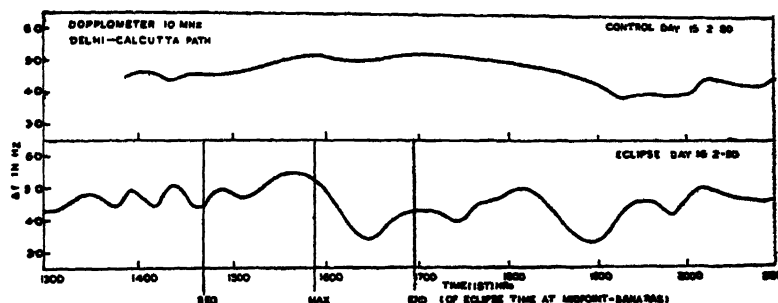


FIG. 3. Dopplometer 10MHz records (Delhi-Calcutta path) on the eclipse day (16-2-1980) and on control day (15-2-1980) Beg—beginning, Max—maximum phase and End—end of the eclipse

### (c) Ionosonde Observation

A J-5 ionosonde (1–20MHz) operating at Delhi did not show any significant change in  $f_oF_2$ . This may be due to the fact that a magnetic storm was in progress on the eclipse day and any eclipse effect was masked by it. F1- and E-layer critical frequencies decreased following expected patterns of insolation during the eclipse. No attempt was made to obtain electron density true height ( $N-h$ ) profiles as they would be doubtful without any information regarding the valley between E and F1 and also because some travelling wavelike disturbances with kinks in the F1 trace were observed. This may be an evidence of wave motion in the F1-layer caused by the eclipse. However, no significance is attached to this because such patterns are quite commonly observed in F1 traces at that time on other days as well.

## DISCUSSIONS

Chimonas and Hines (1970) predicted generation of atmospheric waves by the supersonic motion of the moon's shadow during solar eclipses. Studies on previous solar eclipses have revealed the presence of atmospheric waves in some cases but in some cases the wave motions were not found. It was assumed that the principal source of generation of these waves was ozone heating region around 45km (Chimonas & Hines, 1971). So it was concluded that the contradictory result was due to differing ozone concentrations during the epoch of the eclipse (Tom Beer, 1974). But there are other sources like molecular oxygen heating around 90km and low altitude tropospheric heat absorbers like  $H_2O$  and  $CO_2$  where the wave motions can be generated. It was also thought that if the generation is at ground level or tropospheric origin, the effect would be picked up by sensors at ground. If the generation is at higher level, it is difficult to monitor the effect at ground level (Tom Beer, 1974).

In the present study, the wave motions were revealed by infrasonic pressure variations at Hyderabad, but not at Delhi. As the lunar shadow moves along the path of the eclipse, it produces effective cooling spots that act as source of gravity waves. Hyderabad, being very close to the totality path, recorded the effect. The reason, for not observing wave motions at Delhi, may be the distance factor (about 1500km from the totality path). No reinforcement of the waves due to focusing would be



expected as the curvature of the eclipse path was not favourable for Delhi. Apparently, they were attenuated to below the level of detection

Observation of the wave motions in the F1-layer around Banaras with the Dopplometer would indicate that waves in that height region were much less attenuated than at the ground level. The wave motions noted prior to the start of the eclipse are difficult to understand unless there are some movements associated with the magnetic storm in progress (Davies & da Rosa, 1970)

In conclusion, it can be stated that the wave motions were possibly generated by the supersonic travel of the totality shadow and spread outwards. The tropospheric waves perhaps, were attenuated to a larger extent, but the disturbance could travel with much less impedance at F1-layer heights.

#### ACKNOWLEDGEMENTS

We are thankful to Mr B. J. Srivastava of National Geophysical Research Institute, Hyderabad for help in running the microbarograph at their magnetic observatory. We are also thankful to Professor P. Bandyopadhyay and to Mr N. K. Chakrabarty, of Institute of Radio Physics and Electronics, Calcutta University for help in running the Dopplometer equipment. Thanks are also due to Mr C. B. Nair and Mr A. R. S. Vasisht of NPL for maintenance work on the microbarograph and Dopplometer respectively.

#### REFERENCES

- Anastassiades, M., and Moraitis, G. (1970) Travelling ionospheric disturbances in Athens during the March 7 solar eclipse *Nature*, **226**, 1125
- Anderson, R. C., Keefer, D. R., and Myers, O. E. (1972) Atmospheric pressure and temperature changes during 7 March 1970 solar eclipse. *J. atm Sci.*, **29**, 583.
- Blackman, R. B., and Tukey, J. W. (1958) *The Measurement of Power Spectra* Dover, New York
- Chimonas, G. (1973) Lamb waves generated by the 1970 solar eclipse *Planet Space Sci.*, **21**, 1843
- Chimonas, G., and Hines, C. O. (1970) Atmospheric gravity waves induced by a solar eclipse. *J. Geophys. Res.*, **70**, 875
- (1971) Atmospheric gravity waves induced by a solar eclipse-II *J. geophys. Res.*, **76**, 7003
- Davies, M. J., and da Rosa, A. V. (1970) Possible detection of atmospheric gravity waves generated by the solar eclipse *Nature*, **226**, 1123.
- Srivastava, B. J., Venkatachari, R., and Saha, A. K. (1981) Low latitude infrasonics associated with geomagnetic activity (*Under publication*)
- Tom Beer (1974) *Atmospheric Waves* Adam Hilger, London, 273
- Venkatachari, R., and Bhartendu (1979) Infrasonic pressure variations and some atmospheric phenomena *Indian J. Rad Space Phys.*, **8**, 273

Printed in India

Gravity Waves

## SOLAR ECLIPSE EFFECTS ON THE LOWER IONOSPHERE

R. VENKATANARAYANA\* and T. S. N. SOMAYAJI

*Space Research Laboratories, Department of Physics, Andhra University,  
Waltair-530 003, India*

*(Received 15 February 1982)*

Short term fluctuations in ionospheric first order echo amplitude at Waltair are investigated for eclipse effects. Power spectrum analysis of short term fluctuations during the period 1500-1630 hours on 16 February 1980 when a near total solar eclipse (99 per cent) occurred, showed periods with a lower cut-off period equal to 6.75 minutes significantly higher than the cut-off period of 5.25 minutes for the corresponding period on 15 February 1980 taken as the control day. The group height was found to increase from 110km just before the eclipse to an average of 127.5km around the middle of the eclipse period. The larger cut-off period on the eclipse day is attributed to the increase in the level of altitude region where most of the ionospheric absorption is caused. Neglecting the effect of neutral winds and assuming the absence of significant ionization at the D-region heights during a near total eclipse, we infer that the temperature at an altitude of about 127.5km is significantly lowered during the eclipse.

**Keywords:** Solar Eclipse; Gravity Wave; Ionospheric Cooling

### INTRODUCTION

THE amplitude records obtained at Waltair ( $17^{\circ} 43'N$ ,  $83^{\circ} 18' E$ ) for measuring ionospheric absorption by the A1 technique always exhibit quasi-periodic oscillations, which can be attributed to short term variations in the electron concentration at altitudes where significant absorption is caused. There is some evidence to show that internal gravity waves might cause the often observed short term variations in the electron concentrations at D-region heights (Manson & Meek, 1977). The power spectra of these short term fluctuations of ionospheric absorption or ionospheric echo amplitude generally show a high frequency cut-off. The period corresponding to this cut-off frequency is hereafter referred to as the 'cut-off period'.

In the absence of neutral winds, the lower cut-off period of internal gravity wave induced perturbations equals the Brunt period. Titheridge (1971) has used the power spectrum analysis of total electron content variations to determine the scale height or temperature of the F-region using the cut-off period of the power spectrum as an indicator of the Brunt period. If the short period fluctuations observed in our present investigation can all be ascribed to internal gravity waves, then neglecting the effect of neutral winds one can identify the observed cut-off period with the Brunt period.

---

\* Now at LRDE, Bangalore

corresponding to the height below which no significant absorption is caused. Therefore, by investigating the power spectra of short term fluctuations in ionospheric echo amplitude, one can in principle, study the variations in the Brunt period and hence the temperature of the regions where significant absorption is caused.

During a total or near total solar eclipse, the ionization at lower altitudes decreases rapidly (Bowling *et al.*, 1967) leading to increase in the height of reflection. Also, for a properly chosen probing frequency, during such periods most of the ionospheric absorption will be caused near the level of reflection and therefore, the cut-off period of the power spectrum will indicate the Brunt period and hence the temperature at an altitude close to the level of reflection. By knowing the apparent height of reflection one can infer the changes in temperature that take place at that height because of the eclipse.

Continuous records of amplitudes of vertically reflected first order ionospheric echo signals of 2.4MHz pulsed radio waves are taken at Waltair on 15, 16 and 17 February 1980 to investigate the changes in short term variability of the lower ionosphere because of the eclipse. The results of the investigation are presented in the following sections.

#### OBSERVATIONS AND METHOD OF ANALYSIS

The Solar Eclipse of 16 February 1980 as observed at Waltair had the following features:

a) Beginning of eclipse	1437hr IST
b) Middle of eclipse	1549 "
c) End of eclipse	1658 "
d) Percentage of sun's disc obscured	99

The amplitude of 2.4MHz pulsed radio transmissions received vertically was recorded continuously from 1430hr to 1730hr on 15, 16 and 17 February 1980. The data in the time block 1500–1630hr was chosen for analysis to cover most part of the eclipse period.

The desired echo was integrated with a time constant of forty seconds. Data sampled at one minute intervals were then filtered using a numerical filter given by

$$A'(t) = A(t) - \frac{1}{T} + \int_{-T/2}^{+T/2} A(t) dt,$$

where  $T$  is a particular time period chosen. This has the effect of a high pass filter with a lower cut off frequency equal to  $\frac{2}{T}$ . The cut-off period  $T$  was chosen as 24 minutes for the present investigation to eliminate the effect of slowly varying trends.

The filtered data, were analysed to obtain power spectra of the amplitude variations, following the method suggested by Blackman and Tukey (1958). Power spectral estimates were obtained at twenty equal intervals in the frequency range 0 to 0.5  $\text{min}^{-1}$ . The spectral estimates were normalised to have a total power of hundred

units. Assuming the noise to be white, the estimated noise level was fixed. The spectra were then examined for studying the effect of the eclipse on the short term variability of the lower ionosphere.

In a separate study we found that the enhancements of 1–8 Å X-ray flux during solar flares, in general, do lower the cut-off period, whereas the cut-off period is not dependent on magnetic activity. On 17 February 1980, a strong solar flare occurred at 1530hr and lasted for 15 minutes. The echo amplitude was found to show unusual changes between 1500–1630hr on 17th, perhaps because of the flare. Therefore, the results of 17th were not considered for comparison and 15 February 1980 was taken as the control day. Although there was a magnetic storm during the same period on 15th, magnetic activity has little effect on the short term variations in ionospheric absorption.

### RESULTS AND DISCUSSION

The power spectra of short term fluctuations in the ionospheric first order echo amplitude of 2.4 MHz pulsed radiowaves vertically reflected for 15 and 16 February 1980 during the time block 1500–1630hr are shown in Fig. 1. Two inferences can readily be made viz ,

1. There were no unusual periodicities observed on the eclipse day. This observation leads to the conclusion that there was no extra gravity wave activity inducted by the solar eclipse.
2. The cut-off period for the eclipse day is 6.75 minutes as compared to 5.25 minutes for the control day i.e., 15 February 1980.

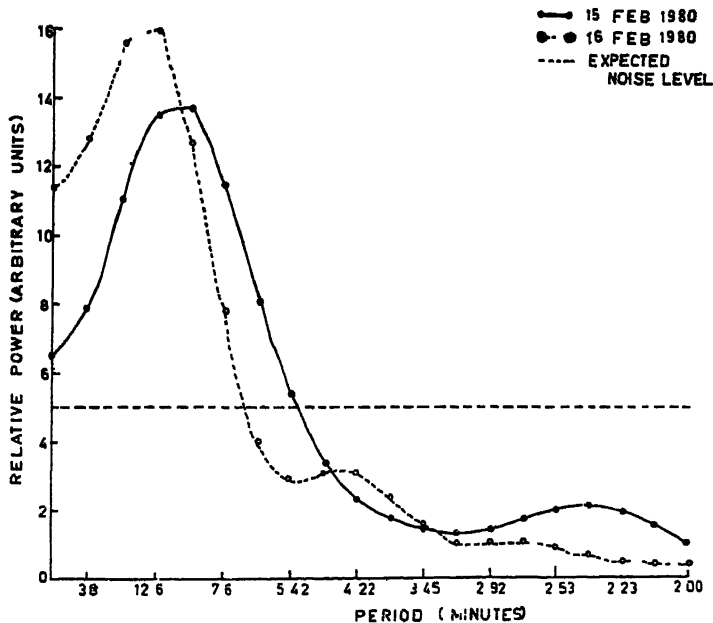


FIG 1 Power spectrum of amplitude fluctuations between 1500–1630hr.

During the period 1500–1630hr, the apparent height of reflection was found to change from 110km to 127.5km on the eclipse day. The temperature corresponding to a Brunt period of 6.75 minutes is 415 °K. Assuming most of the absorption during the eclipse is caused at a level close to the level of reflection and neglecting the effect of neutral winds, one can infer that the temperature at an altitude nearly equally to 127.5km is 415 °K during the eclipse period. The average temperature profile gives a temperature of 489 °K at an altitude of 127.5km on a normal day (CIRA, 1972). Therefore, it appears that at this station at 127.5km altitude the temperature of the atmospheric gas is lowered by about 74 °K because of the eclipse.

The present result is in agreement with earlier rocket borne measurements made by Horvath and Theon (1972) at Wallops islands. They have reported a decrease of molecular gas temperature from nearly 415 °K to 345 °K at an altitude of 120km during the solar eclipse of 7 March 1970. The result of our present investigation, however, is to be taken with caution, and only qualitatively, because of several uncertainties. Mainly, the effect of neutral winds on the observed cut-off period is neglected and the identification of the cut-off period is somewhat subjective.

#### *Effect on Wave Type Perturbations*

The present investigation clearly shows no detectable gravity wave activity induced by the eclipse, as the forms of the power spectra for the eclipse day and the control day were highly similar. However, the cut-off period was larger on the eclipse day which can be attributed to the changes in the reflection height and the disappearance of the D-region ledge during the eclipse. This result is in agreement with the earlier investigation by Cornelius and Essex (1978) who did not observe any eclipse induced gravity wave activity in the records of Doppler shift of HF transmissions on 2.5MHz during the eclipse of 23 October 1976.

In a separate study, we observed that enhancements in solar X-ray flux in the spectral range 1–8Å during a solar flare in general cause a lowering of the cut-off period. If one can assume the internal gravity wave spectrum to be a white noise spectrum at lower levels, say the lower boundary of the ionosphere, the propagational characteristics of the upward flux of the gravity wave energy show that the lower periods of higher frequencies are progressively filtered, as the altitude increases. Therefore, the power spectrum of fluctuations induced by internal gravity waves will have progressively increasing values of cut-off periods at higher altitudes. Our earlier observation of the effect of solar flares on the cut-off period can easily be explained on the basis of this model. During a solar flare with enhancement in 1–8Å X-ray flux, the contribution of the lower regions of the ionosphere to the measured total absorption increases and the cut-off period of the short term fluctuations in the ionospheric echo amplitude decreases. Thus the effect of the solar flares on the cut-off period can be attributed to changes in the altitude levels where most of the observed absorption is caused. The result of the present investigation shows that during the eclipse the cut-off period has a higher value. This is in conformity with our earlier observation of the effect of the solar flare on the cut-off period because the solar eclipse will have an effect opposite to that of a flare. During an eclipse the altitudes where most of the absorption is caused will be higher and therefore, the

observed cut-off periods must be larger. This in fact, is what has been observed in our present study.

With regard to our observation in the present investigation that no eclipse induced gravity wave activity could be detected, we have to state that this could perhaps be due to the limitations inherent in the experiment. Our observations are made at a single station and therefore any eclipse induced gravity wave activity with periodicities in the usually present range cannot be distinguished from the usually present gravity waves. Multi-station observations to separate out phase coherent perturbations during the eclipse are needed to detect eclipse induced gravity wave activity. Also, the path of the present eclipse is almost linear and hence, one cannot expect the focusing of radio waves at a shorter distance location, where the eclipse is nearly 99 per cent.

### CONCLUSIONS

1. No eclipse induced gravity wave activity in the lower ionosphere is detected at this station
2. The higher value of the cut-off period observed during the eclipse is attributed to an increase in the altitude where most of the ionospheric absorption is caused.
3. The upper atmospheric temperature is roughly estimated to be lowered by about 74 °K at an altitude of about 127.5km during the eclipse.

### ACKNOWLEDGEMENT

One of the authors (RVN) wishes to thank the University Grants Commission for financial assistance.

### REFERENCES

- Blackman, R B, and Tukey, J M (1958) *Measurement of Power Spectra*. Dover publ Inc, New York.
- Bowling, T S, Norman, K, and Williamore, A P (1967) D-region measurements during a solar eclipse *Planet Space Sci*, **15**, 1035-1047.
- CIRA (1972) *COSPAR International Reference Atmosphere* Akademie Verlag, Berlin
- Cornelius, D W, and Essex, E. A (1978) HF doppler observations of 23 October 1976, total solar eclipse over southeastern Australia *J atm terr Phys*, **40**, 497-502.
- Hines, C O (1960) Internal atmospheric gravity waves at ionospheric heights *Can J Phys*, **38**, 1441-1481
- Horvath, J J, and Theon, J S (1972) Response of neutral particle upper atmosphere to the solar eclipse of 7 March 1970 *J atm terr Phys*, **34**, 593-599
- Manson, A H, and Meek, C E (1977) Gravity waves in the lower thermosphere at 35°S (South Australia) *J atm terr Phys*, **39**, 1411-1416
- Titheridge, J K. (1971) The spectrum of electron content fluctuations in the ionosphere *Planet Space Sci*, **19**, 1593-1608

Printed in India

**Ionospheric Absorption**

## A1 ABSORPTION MEASUREMENTS DURING THE TOTAL SOLAR ECLIPSE OF 16 FEBRUARY 1980

U. V. GIRISH KUMAR *and* K. V. V. RAMANA

*Ionosphere and Space Research Laboratories, Andhra University,  
Waltair-530 003, India*

*(Received 15 February 1982)*

A1 absorption measurements taken during the total solar eclipse of 16 February 1980 at a frequency of 2.4 MHz are used to obtain the temporal variation of  $N_mE$  at 105 km and  $R_mD$  at 75 km. The contributions from E- and D-regions to the total absorption are also computed and it is found that during the time of near totality, the contributions are approximately equal. The decrease in the total absorption from the time of beginning of the eclipse to the time of minimum absorption is about 25 dB with a time lag of 9 minutes. A 30 per cent decrease in  $N_mE$  and a 70 per cent decrease in  $N_mD$  with time lags of 9 minutes and 19 minutes, respectively, are noted in the temporal variations of  $N_mE$  and  $N_mD$  during the time of eclipse. The contributions from the uniform solar disc, solar corona and active regions distributed over the solar disc to the total absorption are 45 per cent, 25 per cent and 20 per cent respectively.

**Keywords:** A1 Absorption; Uniform Solar Disc; Solar Corona

### INTRODUCTION

As the ionospheric absorption suffered by a radio wave depends on the electron density in the path of the wave, the changes in electron density reflect in the value of absorption. The results of the analysis of A1 absorption measurements taken during the total solar eclipse of 16 February 1980 are presented in this communication.

At Waltair (Lat 17° 7' N, Long 83° 3' E), the eclipse of the sun began at 1437 hr IST and ended at 1658 hr IST. Waltair was just off the lower edge of the totality path and the magnitude of the eclipse was 98.8 per cent, occurred at 1554 hr IST.

### DATA AND ANALYSIS

Continuous measurements of ionospheric absorption at a frequency of 2.4 MHz were undertaken during February 15 and 17 (control days) and 16 (the eclipse day) by the vertical incidence pulse reflection method. Absorption was calculated for every 15 minutes interval on all the three days with a 10 minutes sampling.

As the  $f_oE$  data at Waltair were not available, Ahmedabad ionosonde data for  $f_oE$  have been used with proper latitudinal correction. These  $f_oE$  values have been used to obtain the peak electron density at 105 km at the time of the first contact. The  $N_mE$  value, thus obtained at the first contact, has been used to compute the value

of  $\alpha_{eff}$ , the effective recombination coefficient of the E-region following the method of Rydbeck (1956). In this calculation, the time lag between the time of maximum obscuration and the time of minimum absorption has been used for the time delay of  $N_m E$  response. The electron density at the time of minimum absorption has been obtained by using the values of  $\alpha_{eff}$ ,  $N_m E$  at the time of first contact, and the time lag mentioned above. The rate of change of electron density at the time of first contact has been computed. This value is taken as negative before maximum obscuration positive after the time of totality. The  $N_m E$  value at the first contact and the rate of change together give the temporal variation of  $N_m E$  at the assumed E-region peak height of 105km. This profile of temporal variation in  $N_m E$  is then used to calculate the contribution of the E-region to the total absorption,  $L_E$ , assuming the E-layer to be parabolic. The D-region contribution of absorption,  $L_D$ , is obtained after subtracting the value of  $L_E$  from  $L_T$ , the total absorption. Assuming the D-region also to be parabolic between 60–90km, the temporal variation of  $N_m D$  at 75km has been calculated using the temporal variation of  $L_D$ .

### RESULTS

The results of the diurnal variation in absorption at 2.4MHz on the eclipse and control days are presented in Fig. 1. The dashed curve gives the value of  $L$  on the day of the eclipse and the continuous curve gives the mean value over the control

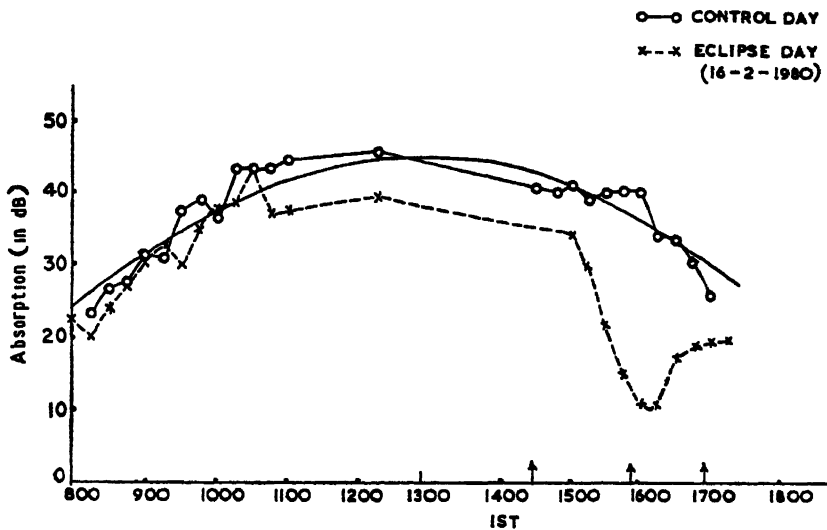


FIG 1 Diurnal variation of absorption,  $L$ , in dB during control and eclipse day.

days. The smooth continuous curve is a parabolic fit for the control day absorption variation. Generally, absorption maximum occurs around local noon decreasing towards the morning and evening hours. The absorption, on the eclipse day, started decreasing from the time of first contact to a minimum of 10dB occurring with a time lag of 9 minutes from the time of maximum obscuration. A decrease of 25dB in



absorption during the period of eclipse can be seen from the figure. Shirmammedov and Boltayev (1978) obtained a maximum absorption decrease of about 18dB during the 29 April 1976 annular solar eclipse at 2.6MHz. Around the time of maximum phase, for about 15 minutes, the reflection appeared to come from the F2-layer (about 300km). The reflection height reached 120km a few minutes after the maximum phase. A similar change in reflection height was reported by Shirmammedov and Boltayev (1978) at a frequency of 2.6MHz for the 29 April 1976 annular solar eclipse.

In the present investigation, it is assumed that the time of maximum visual obscuration of the solar disc and the time of minimum ionizing radiation fluxes from the sun are equal. Fig. 2 shows the temporal variation of  $N_m E$  at 105km. It can be seen from this figure that the maximum electron density in the E-region decreases by about

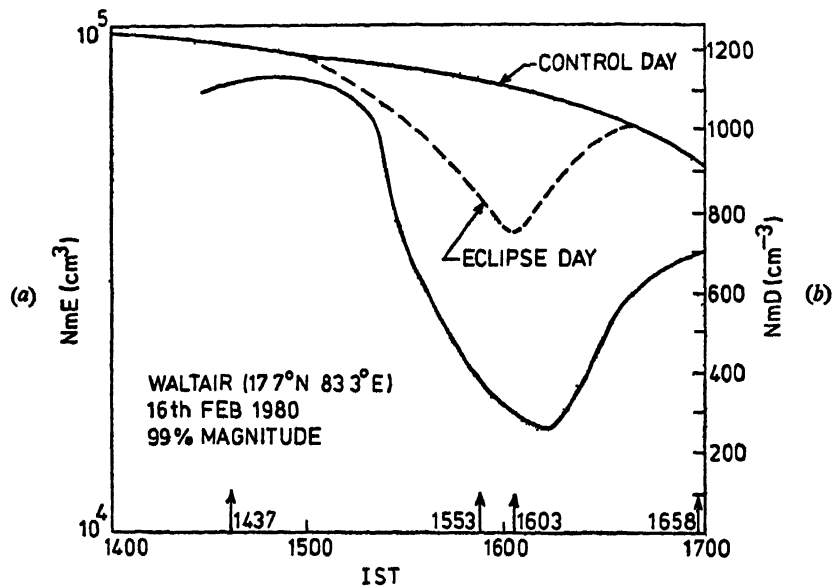


FIG 2.(a) Temporal variation of  $N_m E$  at 105km during the period of eclipse  
(b) Temporal variation of  $N_m D$  at 75km during the period of eclipse

30 per cent when minimum absorption is recorded. The value of  $\alpha_{\text{eff}}$  is obtained as  $1.2 \times 10^{-8} \text{ cm}^3 \text{ sec}^{-1}$ . On the control day,  $\alpha_{\text{eff}}$  has been obtained as  $1.33 \times 10^{-9} \text{ cm}^3 \text{ sec}^{-1}$ . The increase in  $\alpha_{\text{eff}}$  during the time of eclipse is in good agreement with the previous observations.

The temporal variation curves of  $L_E$  and  $L_D$ , E- and D-region contributions to the total absorption, respectively, along with temporal variation curves of total absorption on control day and eclipse day are shown in Fig. 3. From this figure, it can be noted that the E and D-region contributions to the total absorption are nearly equal around the time of totality. The time lag between the time of maximum phase and the time of minimum absorption in the E-region contribution of absorption is the same as that in the temporal variation of total absorption, on the eclipse day, which is 9 minutes. But, the time lag in the case of D-region contribution of absorption is 19 minutes. Tsagakis (1970) obtained a time lag of 23 minutes from the temporal

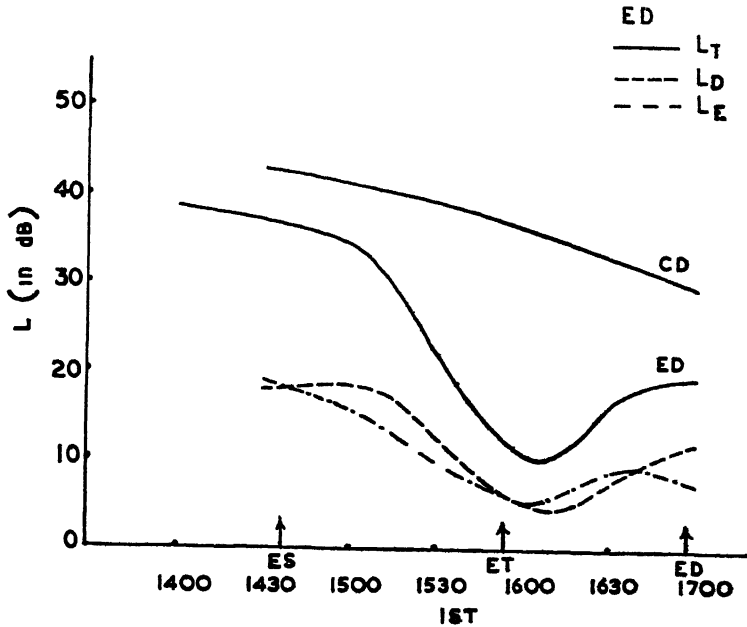


FIG. 3 Temporal variation plots of  $L_E$ ,  $L_D$  and total absorption during control and eclipse day.

variation of electron density at 74km from the partial reflection technique, while, Bischoff and Taubenheim (1967) found that the contributions of the E- and D-layers to the total absorption were nearly equal from A1 absorption measurements on 3.86MHz during 20 May 1966 solar eclipse

The temporal variation of the D-region contribution of absorption has been used to compute the temporal variation of the electron density at 75km assuming the D-region to be parabolic between 60km and 90km with peak ionization at 75km and this is shown in Fig. 2. A decrease of about 70 per cent in the D-region electron density can be seen around the maximum phase of the eclipse. The time lag of 19 minimum electron density noted, gives an effective recombination coefficient of  $1.7 \times 10^{-6} \text{ cm}^3 \text{ sec}^{-1}$  at this altitude

#### PERCENTAGE CONTRIBUTION FROM UNIFORM SOLAR DISC, SOLAR CORONA AND ACTIVE REGIONS DISTRIBUTED OVER SOLAR DISC

Fig. 4 shows the distribution of the active regions on the solar disc and the 10.7cm flux distribution across the solar disc on 16 February '80. The path of the eclipse at Waltair is also shown. The ratio,  $\eta$ , of the moon's apparent diameter to the sun's apparent diameter is taken as 1.02. This parameter has been used in drawing geometrically the progression of the eclipse from the time of first contact to the time of maximum phase and regression of the eclipse from the time of maximum phase of the eclipse to the time of last contact. The results are shown in Fig. 5. These figures help in knowing the fraction of the disc covered or uncovered at any particular time. As 16 February 1980 was a highly active day with  $R_s$  equal to 163 and with a

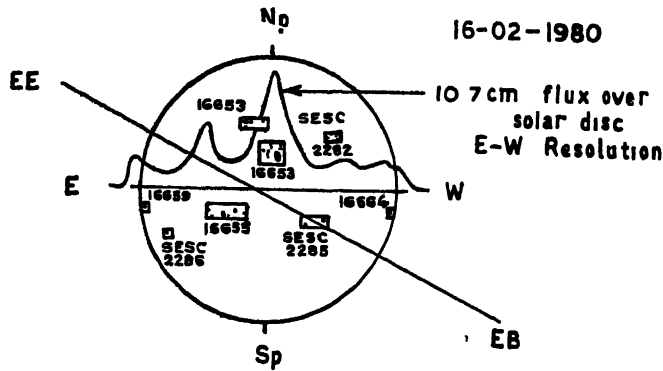


FIG. 4. Distribution of the active regions on the solar disc and the 10.7cm flux distribution across the disc and the eclipse path

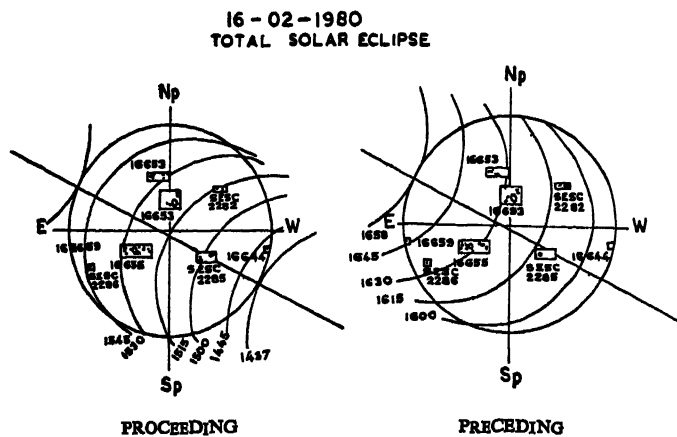


FIG. 5. Moon's shadow fronts at various times during progression and regression of the solar eclipse, on solar disc

10.7cm solar flux of 205.1 flux units, a number of active regions are distributed over the solar disc, with a greater density in the central region of the disc. It can be seen that the 10.7cm solar flux curve shows peaks corresponding to the active regions. Just before the time of maximum phase of the eclipse, all active sources are being covered excepting those that might exist outside the NE limb of the sun. The coronal green line contour from the Sacramento Peak Observatory was not, unfortunately, available for the eclipse day. At this point, it has been assumed that the radiations are coming from the uniform disc only. As the magnitude of the eclipse at this station was only 98.8 per cent, the active region at the western limb of the disc was uncovered at the time of totality and this gives the possible explanation for the observed high electron density in the D-region height (at 75km).

If the absorption were caused by the solar radiation coming from the uniform solar disc, the  $dL/dt$  must correspond to  $dS/dt$  (where  $S$  is the visible fraction of solar disc) with the appropriate time lag between these terms being taken into account. Larger  $dL/dt$  magnitude compared to that of  $dS/dt$  should indicate the contribution

due to the radiations from the active sources of the solar disc. The rate of change of absorption as a function of time between the first and last contacts of the eclipse has been calculated using Fig. 3 and the dependence of  $dL/dt$  on the solar zenith angle has been removed by taking into account the  $dL/dt$  values on control day. Fig. 6 gives the final  $dL/dt$  as a function of time on the eclipse day. The area enclosed by the  $dL/dt$  curve before it changes to positive values gives the amount of absorption decrease from the time of first contact to the time of minimum value of absorption. The area enclosed by the rest of the curve gives the absorption increase from the time of minimum absorption to the time of last contact. Fig. 6 also shows that  $dS/dt$  multiplied by a factor 13.6 such that  $dL/dt$  and  $dS/dt$  coincide shortly before the maximum phase of the eclipse where no active sources are present on the solar disc. Also, the

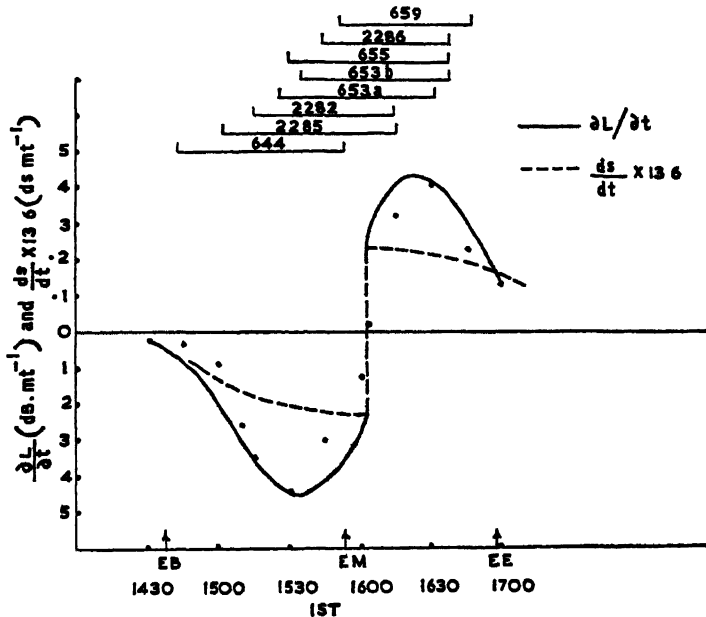


FIG. 6. Variation of  $dL/dt$  and  $dS/dt$  with time

$dS/dt$  curve is shifted by 9 minutes to take into account the time delay between these two curves. It may be seen that  $dL/dt$  is always greater than  $dS/dt$  (from uniform disc), thus, showing that the contribution to the absorption from active regions is significant. This figure also shows the times of the obscuration of various active regions on the solar disc. The starting point gives the time when the active region with the number given begins to be completely obscured and the last point gives the time when the same active region begins to be completely uncovered. The contribution from each individual active region is calculated first and later summed to give the total contribution from various active regions distributed over the solar disc. The contribution from the uniform disc can be calculated from the area covered by the corrected  $dS/dt$ . A greater part of the minimum absorption recorded is attributed to solar corona. This is done because the minimum absorption recorded at the maximum phase has

components from the corona as well as the solar disc. If the eclipse were total and has a longer duration, then one is justified in attributing this completely to the corona. The percentage contribution to the total absorption from various regions are summed up and are given as

Uniform solar disc	.	45 per cent
Active regions	.	30 "
Solar corona	.	25 "

#### DISCUSSION

Elwert (1958) has computed residual radiations for different ratios of lunar to solar radii for solar eclipses.

If  $\eta=1.02$ , the residual radiation flux is 17–22 per cent and if  $\eta=1.06$ , it is 10–12 per cent

In the present investigation,  $\eta$  is taken as 1.02 from an examination of the eclipse configuration and thus the residual radiation obtained is in good agreement with Elwert's results, that the residual radiation is about 20 per cent. It may be pointed out at this stage that an assumption has been made that the total obscuration of the solar disc corresponds to the total obscuration of ionizing radiations, which is not strictly valid. But, still, it is hoped that the analysis gives some insight with regard to the contributions to the ionization from various sources in the sun and outside. Further, the assumption that the minimum part of the absorption corresponds to the coronal radiations is also not strictly valid because of relaxation effects and also because of the small duration of the eclipse. Still, the observed 25 per cent contribution to the ionizing radiation due to solar corona gives an upper limit to the contribution for the solar corona. In practice, this percentage might be in the range 15–20 per cent.

Taubenheim and Serafimov (1969), from the brightness distribution studies during 20 May 1966 eclipse, derived the contributions to ionizing radiations from the various sources as listed below

Uniform disc	70 per cent
Corona	.. 23 "
Active sources	7 "

The high percentage of contribution from uniform disc in this case may be due to the low solar activity when compared to the present situation. On 20 May 1966, the day of their observation,  $R_s = 57$  and 10.7 cm solar flux was 112.8 flux units.

#### ACKNOWLEDGMENTS

One of the authors (UVGK) acknowledges the financial support given by the Council of Scientific and Industrial Research, New Delhi.

#### REFERENCES

- Anastassiades, M. Ed (1970) The annular solar eclipse on May 20, 1966 and the ionosphere. In *Solar Eclipses and the Ionosphere* Plenum Press, New York, London, 253–272.

- Bischoff, K , and Taubenheim, J (1967) A study of ionospheric pulse absorption (A1) on 4Mc/s during the solar eclipse of May 20, 1966. *J. atm terr. Phys* , 29, 1063-1069.
- Elvert, G. (1958) Distribution of X-rays emitted by the solar corona and the residual intensity during solar eclipses. *J. atm terr. Phys* , 12, 187.
- Rydbeck, O E. H (1956) A theoretical study of E-layer behaviour during a solar eclipse. *Solar Eclipses and the Ionosphere* (special suppl, 6 to *J atm. terr. Phys.*) Pergamon Press, London, 14-20
- Shirmammedov, M , and Boltayev, D (1978) Ionospheric radio wave absorption during the annular solar eclipse of April 29, 1976. *Geomagnet. Aeron* , 18, 4, 501-502.
- Taubenheim, J , and Serafimov, K. (1969) Brightness distribution of soft X-rays on the sun, inferred from ionospheric E-layer variations during an eclipse. *J. atm. terr. Phys.*, 31, 307-312.
- Tsagakis, E. (1970) Partial reflection measurements on the D-region during the May 20, 1966 solar eclipse. In: *Solar Eclipses and the Ionosphere* (Ed.: Michael Anastassades). Plenum Press, New York, London, 211-224.

Printed in India.

### **Ionospheric Absorption**

## **MULTIFREQUENCY IONOSPHERIC ABSORPTION RESULTS DURING THE SOLAR ECLIPSE OF 16 FEBRUARY 1980 OVER UDAIPUR**

**B. L. ACHARYA, H. K. YAGNIK, T. C. BANSAL, S. K. VIJAYVERGIA and R. K. RAI**

*Department of Physics, University of Udaipur, Udaipur 313 001, Rajasthan, India*

*(Received 7 April 1982)*

The present communication embodies the results of multi-frequency ionospheric absorption during the solar eclipse of 16 February 1980 at Udaipur (Geogr latitude, 24°35'N and longitude 73°42'E). Round the clock measurements of ionospheric absorption have been made at wave frequencies 2.5, 2.8 and 5.0 MHz during 13-18 February 1980. The absorption started to fall after sometime with the first contact of the eclipse at all the frequencies and reached its minimum value after the occurrence of the maximum phase of the eclipse. The delay was of about 05-10 minutes. The absorption became normal after about 10 minutes of the fourth contact of the eclipse. Simultaneous measurements of relative variation of temperature (infrared radiations) at the junction of thermocouple have also been made during the eclipse period. The nature of the curve is similar to that observed absorption during the eclipse period. The time delay in the dip in the case of temperature is negligible. No significant change in night time absorption on eclipse night was observed. The electron density profile during the eclipse period has been generated using observed absorption data.

**Keywords:** Ionospheric Absorption; Solar Eclipse; Lowering of Temperature; Electron Density

### **INTRODUCTION**

THE solar eclipse at this latitude was 72 per cent (28 percent solar disc was visible during the maximum phase). The first maximum and fourth contacts of the eclipse at this latitude occurred at 1428, 1542 and 1649hr IST respectively. Measurements of ionospheric absorption on frequencies 2.5, 2.8 and 5.0 MHz were made during the solar eclipse of 16 February 1980 and on control days. The working frequencies were chosen to give reflections from E-region (2.5 and 2.8 MHz) and from F-region (5.0 MHz). The relative cut-off of infrared radiation was estimated by measuring the temperature difference at the junction of a thermocouple. On one of the junctions, solar rays were focused during the solar eclipse and control day. The electron density profile for D-region has been generated using the observed absorption data during the eclipse period. The principal aim of this investigation was to study the structure of the lower ionosphere during the eclipse time at this latitude.

### **VARIATION OF TOTAL AND D-REGION ABSORPTION**

Diurnal variation of total absorption during solar eclipse day (16 February 1980) and control days at 2.5, 2.8 and 5.0 MHz are shown in Fig. 1. From Fig. 1, it is

observed that the absorption starts to fall after sometime with the first contact of the eclipse at all the frequencies and reaches its minimum value after the time of the maximum phase of the solar eclipse. The dip in absorption occurred between 1547 and 1552hr, IST on all the frequencies. The minimum absorption is obtained after the maximum phase of the solar eclipse. The transmitter used for 2.8MHz failed at 1550hr IST. Therefore, observation at this frequency is available only upto 1550hr IST. However, the observation at this frequency covered the maximum phase of the solar eclipse. A comparison of eclipse day absorption with normal days shows that the absorption decrease is of the order of 14dB, 18dB and 12dB on 2.5, 2.8 and

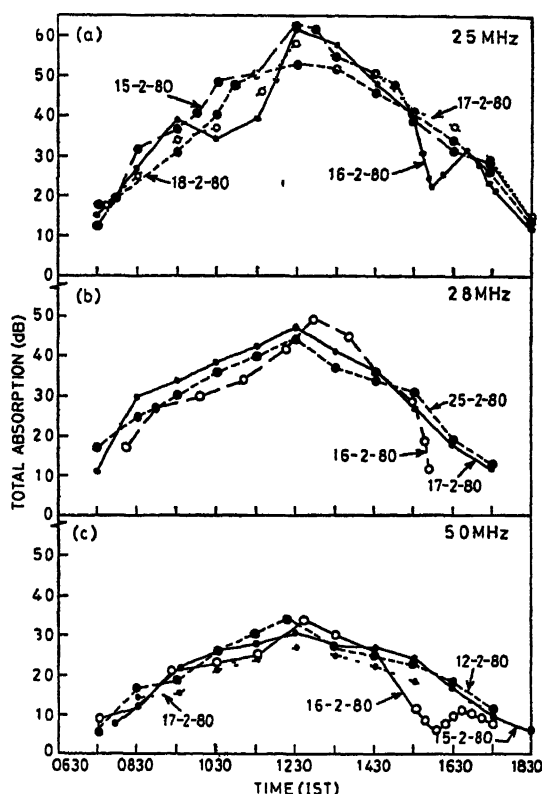


FIG. 1. Diurnal variation of total absorption on eclipse and control days at 2.5, 2.8 and 5.0MHz

5.0MHz respectively near 1550 IST. The values of  $f_oE$ , and  $f_oF2$  observed at Ahmedabad during the solar eclipse and control days (Private communication from Dr H Chandra) have been used in the present investigation. These are used for the purpose of separation of absorption in the E- and F-region on eclipse and control days. The modified Jaeger's formulae (Vijayvergia & Rai, 1979) have been used for the purpose of separation of absorption in the E- and F-regions. Other parameters in the formulae for separation of E- and F-region absorption have been assumed to be constant throughout the period of solar eclipse. The separation of E- and F-region



absorption from the total one gives the value of D-region absorption. Fig. 2 shows the plot of diurnal variation of D-region absorption on eclipse and control days (15 and 17 February 1980) at 2.5, 2.8 and 5.0 MHz respectively. From Fig. 2, it is observed that the nature of variation of D-region absorption at all the frequencies on eclipse and control days are the same as observed in Fig. 1. The value of D-region absorption is about 19.5 dB at 2.5 MHz (1547 IST), 9.5 dB at 2.8 MHz (1550 IST) and 5.0 dB at 5.0 MHz (1552 IST). The absorption on control days at the same time is about 33, 22 and 14 dB at 2.5, 2.8 and 5.0 MHz respectively.

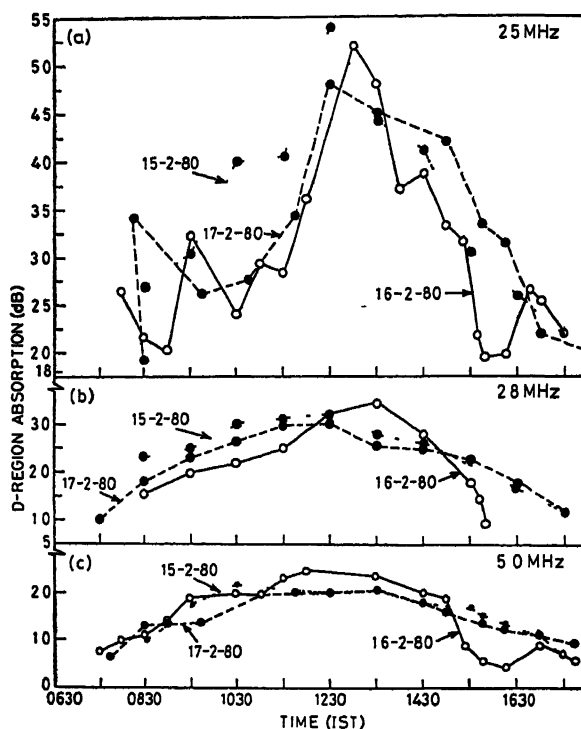


FIG 2. Variation of D-region absorption on eclipse and control days at 2.5, 2.8 and 5.0 MHz

The 10.7 cm solar flux on 15 and 16 February 1980 was 206 units, whereas on 17 February 1980, it was 183 units. A magnetic storm commenced on 15 February 1980 evening, the  $K_p$ -index values reached upto 7. The variation of absorption due to magnetic storm and day-to-day change in 10.7 cm solar flux during these days (15, 16 and 17 February 1980) is expected to be negligible.

The ratio of D and E-region absorption has been found to decrease during solar eclipse at 2.5 and 2.8 MHz (Fig. 3). It has been found that the E-region absorption is less affected by the eclipse than D-region absorption at 2.5 and 2.8 MHz. From Figs 1 & 2, it may be observed that the absorption becomes normal after about 10 minutes of the fourth contact of the solar eclipse. The minimum of the absorption was after the time of the maximum phase of the solar eclipse with 5–10 minutes delay.

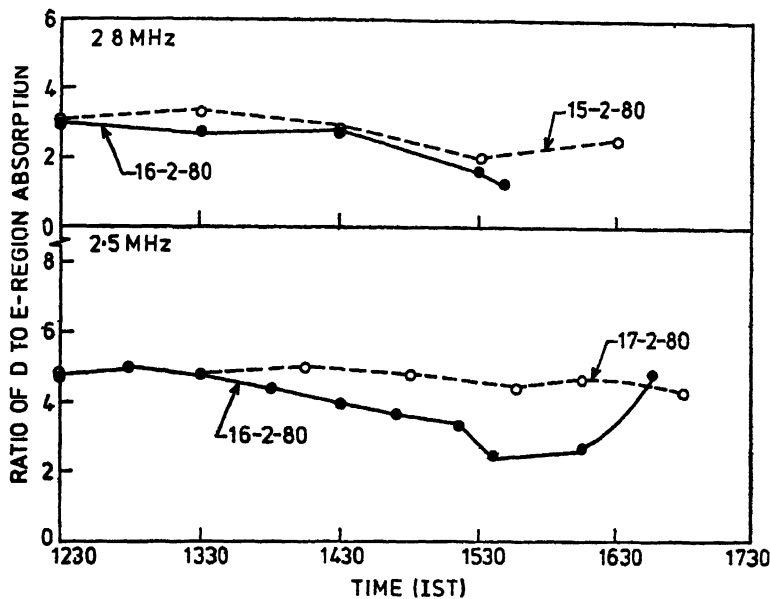


FIG. 3. Variation of the ratio of D- and E-region absorption at 2.5 and 2.8 MHz during eclipse period

#### FREQUENCY DEPENDENCE OF IONOSPHERIC ABSORPTION ON ECLIPSE DAY

The frequency dependence has been studied for D-region. Fig. 4 is the plot of time variation of the ratio of D-region absorption for the pairs of frequencies during the solar eclipse of 16 February 1980 and control days. The mean frequency exponent ( $m$ ) obtained for D-region for the period November 1977 to June 1980 is 1.5. A dotted horizontal line is plotted in Fig. 4, which is the inverse of  $(3.45/5.65)^{1.5}$  and  $(3.15/5.65)^{1.5}$  respectively. From Fig. 4, it is observed that the value of frequency exponent increases during the period of solar eclipse. The value of frequency exponent is maximum after the maximum phase of the solar eclipse and reached to its normal value after the fourth contact of the solar eclipse.

#### ABSORPTION IN THE NIGHT FOLLOWING THE ECLIPSE

Measurements of night time ionospheric absorption on eclipse night and other nights have been made at 2.5 MHz. Fig. 5 shows the nocturnal variation of absorption on eclipse night and other nights. The night time absorption at this latitude is influenced by geomagnetic activity (Acharya, 1981). The magnetic storm had commenced on 15 February 1980 evening, but the value of  $K_p$ -index reached its normal value on eclipse night ( $K_p \sim 3$ ). Therefore, the night time absorption on eclipse day is expected to be unaffected by the magnetic storm. A comparison of eclipse night absorption with other nights shows that the night time absorption is unaffected by the eclipse. It may be mentioned here that after the fourth contact of the eclipse, the absorption has been found to be of the same order as observed on control days.

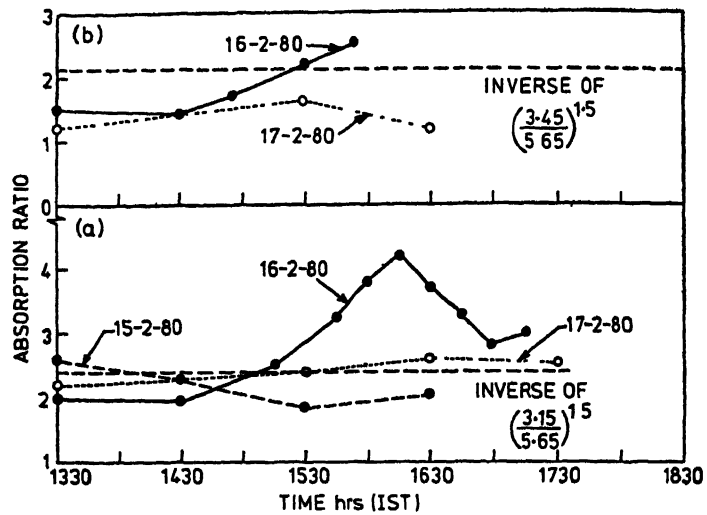


FIG. 4. Time variation of the ratio of D-region absorption for the pair of frequencies [(2.5 and 5.0 MHz) (a) and (2.8 and 5.0 MHz) (b)] during eclipse period.

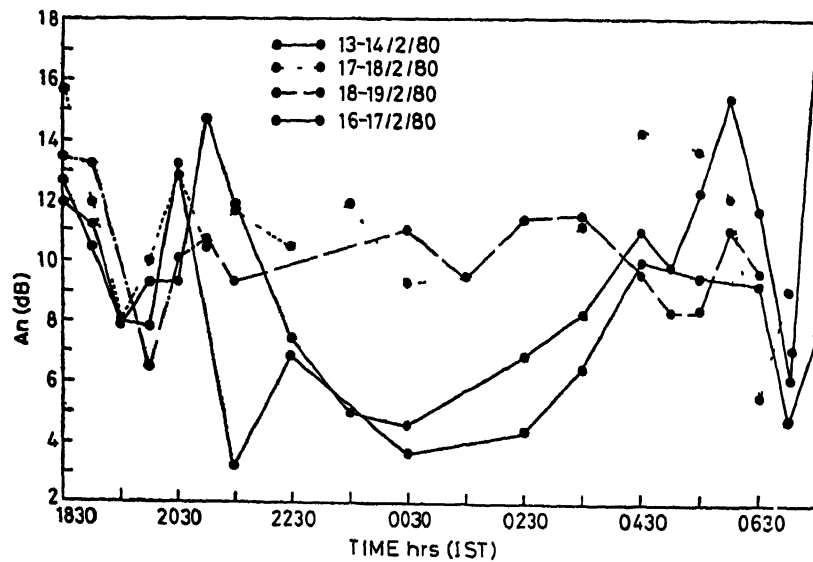


FIG. 5 Variation of absorption in the night following the eclipse

## RELATIVE CHANGE IN INFRARED RADIATIONS (LOWERING OF TEMPERATURE)

The schematic diagram for the measurement of relative change in temperature (infrared radiations) at the junction of a thermocouple is shown in Fig. 6. The rays from the sun fall on a convex lens. Then all the rays are focused at the cromel-alumel junction connected to a spot galvanometer. The spot galvanometer is calibrated in  $^{\circ}\text{C}$ . The apparatus is steerable and could be adjusted in such a way, that the sunrays

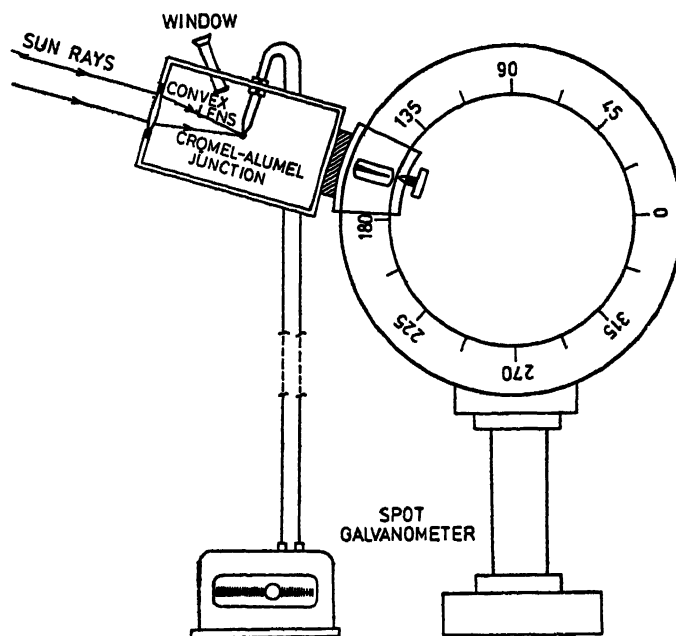


FIG 6. Schematic diagram for the measurement of relative change in temperature (infrared radiations) at the junction of a thermocouple

remain focused on the junction. The measurements of relative temperature at the junction on control and eclipse day for the period from 1400 to 1710hr IST have been made at one minute interval. The relative change in temperature at the junction of the thermocouple on control and eclipse day period is shown in Fig. 7. The relative temperature begins to fall with the first contact of the eclipse and reaches to its minimum value at the time of maximum phase of the solar eclipse. Again it starts increasing and reaches to its normal value at the time of the fourth contact of the solar eclipse. The minimum value of temperature difference at the junctions at the time of maximum phase of the solar eclipse was  $61^{\circ}\text{C}$ , whereas on a control day the temperature difference at the same time was  $79^{\circ}\text{C}$ . The nature of the curve (Fig. 7) is similar to that of observed absorption during eclipse period. The time delay in maximum phase of the eclipse and the minimum value of the relative temperature difference is almost negligible.

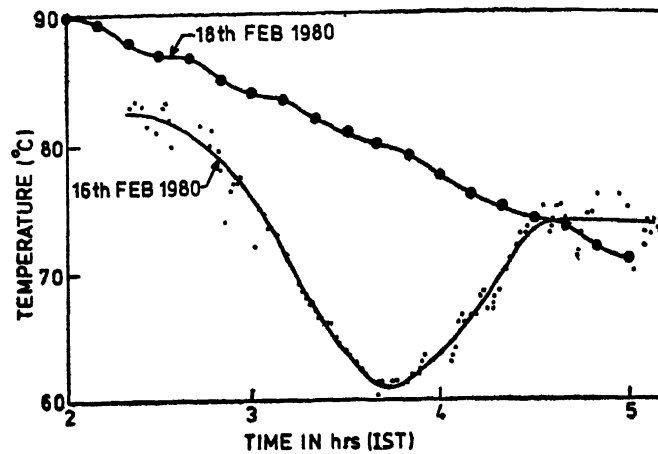


FIG. 7. Relative change in temperature during eclipse period.

#### ELECTRON DENSITY PROFILE IN THE LOWER IONOSPHERE

The electron density profile may be generated from the observed ionospheric absorption data by the method of polynomial or modifying any observed electron density profile. The modification of an electron density profile may be made by the method of trial and error in such a way that the theoretically computed absorption results agree with the observed one at the place of interest for the same solar activity and seasonal conditions. The polynomial method has been tried, but the results obtained were not satisfactory. Therefore, the method of modifying observed electron density by trial and error has been adopted in the present investigation. The electron density

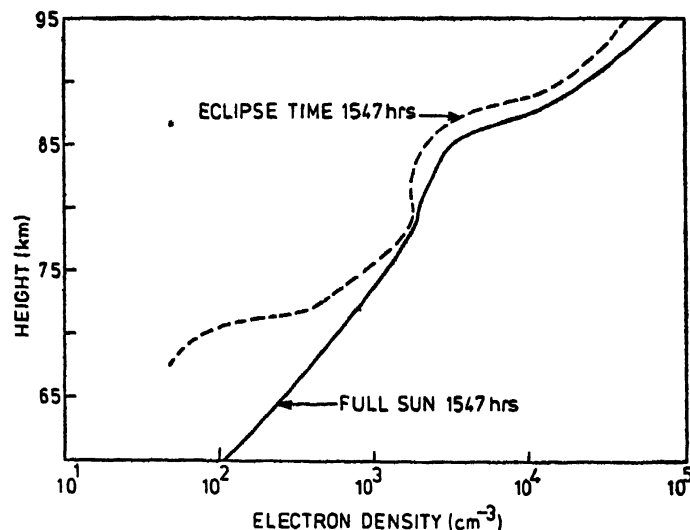


FIG. 8 Electron density profile at 1547hr IST on eclipse day.

and ion-composition measurements in the lower ionosphere have been made at Thumba/SHAR on the day of solar eclipse. We have used one of the electron density profiles measured for about 75 per cent solar eclipse by Mechtly and Seino (1969) during the November 1966 eclipse in Southern Brazil.

Using the above said electron density profile and collision frequency profile (Piggott & Thrane, 1966) suitable for this latitude, the theoretical computation of absorption at frequencies 2.5, 2.8 and 5.0 MHz have been made. For this purpose generalized theory of Sen and Wyller has been used (Sen & Wyller, 1960). The electron density has been modified in such a way that the computed absorption agree with the observed one at 1547IST on solar eclipse day. The modified electron density profile at 1547IST is shown in Fig. 8. Similar analysis have also been made for control day (15 February 1980) for the same time. The electron density at 1547IST on control day is also shown in the same figure. The computed and observed absorption on eclipse and control day at 1547IST is shown in Table I. A comparison of electron density profile on eclipse and control day shows that the electron density on eclipse day at 1547IST is lower than that on control day at the same time at all the heights.

TABLE I

*Computed and observed absorptions on eclipse and control day at 1547 hr IST*

Frequency MHz	Eclipse day		Control day	
	Observed absorption dB	Computed absorption dB	Observed absorption dB	Computed absorption dB
2.5	19.5	19.55	33.0	33.24
2.8	14.0	16.49	26.0	28.03
5.0	5.5	6.92	13.5	11.76

#### ACKNOWLEDGEMENTS

Authors are thankful to Dr Saiyed Nisar Ali for taking the observations of relative cut-off of infrared radiations during eclipse period. Authors are also very thankful to Dr A. P. Mitra, NPL, New Delhi for fruitful discussion on the results of solar eclipse.

#### REFERENCES

- Acharya, B. L. (1981) Study of the lower ionosphere using radio wave absorption phenomena. *Ph.D. Thesis*, University of Udaipur, Udaipur.
- Chandra, H. (1981) *Private Communication*.
- Mechtly, E. A., and Seino, K. (1969) *Radio Sci.*, **4**, 371.
- Piggott, W. R., and Thrane, E. V. (1966) *J. atm. terr. Phys.*, **28**, 467.
- Sen, H. K., and Wyller, A. A. (1960) *J. geophys. Res.*, **65**, 3931.
- Vijayvergia, S. K., and Rai, R. K. (1979) *Indian J. Radio Space Phys.*, **8**, 366.

Printed in India.

Radio Propagation

## PHASE HEIGHT AND ABSORPTION MEASUREMENTS DURING SOLAR ECLIPSE

N. N. PURKAIT *and* M. K. DAS GUPTA

*Centre of Advanced Study in Radiophysics & Electronics  
92, Acharya Prafulla Chandra Road, Calcutta-700 009, India*

(Received 7 September 1981)

The data on the measurement of absorption by A1 method and change in phase height, both at a frequency of 2.2 MHz and collected simultaneously on a control day and also on an eclipse day, have been represented. From an analysis of these data, a reduction in the values of absorption by about 10 dB and an elevation by nearly 2 km in phase height have been observed at the time of maximum obscuration. Attributing this elevation in phase height to the change in reflection height within the range 105–110 km, it has been estimated that the contribution of the E-layer to the observed change in absorption would be 5 dB and the remaining 5 dB change in absorption would occur in the underlying D-region.

**Keywords:** Phase Height; A1 Absorption Method; Pulse Transmitter; Diurnal Variation; Gravity Waves; Electron Density

### INTRODUCTION

THEORETICAL estimate by Schrader and Hower (1971) has indicated that the height distribution of the electron density in the D-region has little effect on the diurnal change in phase height at 2.155 MHz. Moreover, the observed day-time change in phase height at a frequency of 2.2 MHz is uniquely related to the change in reflection height in the E-region (Fraser & Vincent, 1970; and Bhar *et al.*, 1974). Thus, any unusual trend of variations in the diurnal curves on the change in phase height can be associated with some irregular change in the height distribution of the electron density at or near the reflection point in the E-region. On the other hand, any such fluctuation in the diurnal absorption curve is related to the change in electron density profile either of the D- and E-regions or both. Consequently, any change in electron distributions, in the D- and E-regions during a solar eclipse, can be investigated if data on the change in phase height and also on absorption at the same frequency are simultaneously collected. This motivation initiated simultaneous procurement of these data at a frequency of 2.2 MHz at Haringhata (22°58'N, 88°34'E) on the occasion of the solar eclipse of 16 February 1980. These observations are presented and discussed in this paper.

### EXPERIMENTAL ARRANGEMENT

The equipment used for the experiment consisted of a pulse transmitter delivering 13 kW peak power to a 600 ohm folded dipole antenna erected at a height of  $\lambda/4$ .

above ground. The signal, after being reflected vertically from the E-layer was received by two 600ohms horizontal aeriels. The output from one of the aeriels was used for measuring absorption by A-method and that from the other one was processed for the estimation of the change in phase height by a method described by Purkait (1977).

### RESULTS AND DISCUSSION

The results of the simultaneous measurements of change in phase height and absorption for a control day (the day following the eclipse day) and also for the eclipse day are shown in Figs. 1 and 2. Fig. 1 shows that on the control day the absorption at different hour exhibits the normal trend. That is, the absorption gradually increases from morning hours up to the local noon, passes through a broad maximum near the noon period and then gradually decreases towards the late afternoon hours. However, on the eclipse day, before the beginning of the eclipse, hourly values of absorption show reasonable agreement with the corresponding hourly values for the control day. But, with the progress of the eclipse, the absorption exhibits deviation from the hourly values for the control day until a maximum deviation of about 10dB ( $\approx 40$  per cent) occurs near the instant of maximum obscurity. Then the departure between the diurnal curves on absorption gradually decreases. Fig. 2 shows that except during the period of the eclipse, the diurnal curves on the change in phase height for both the control and eclipse days agree with each other. The diurnal curves retain their usual trend: from early morning up to the local noon the phase height

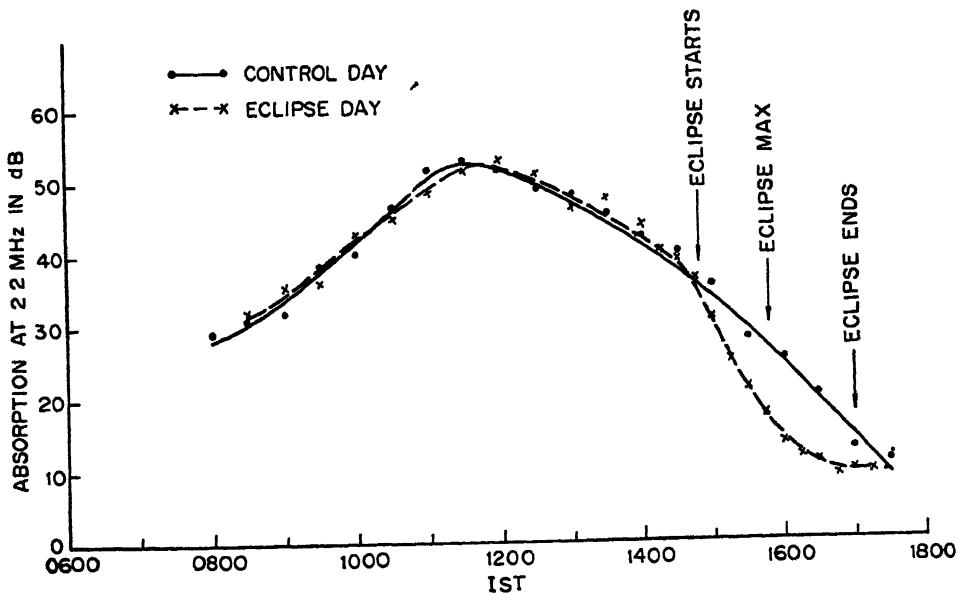


FIG. 1. Diurnal variation of absorption at 2.2 MHz for the control day and also for the eclipse day



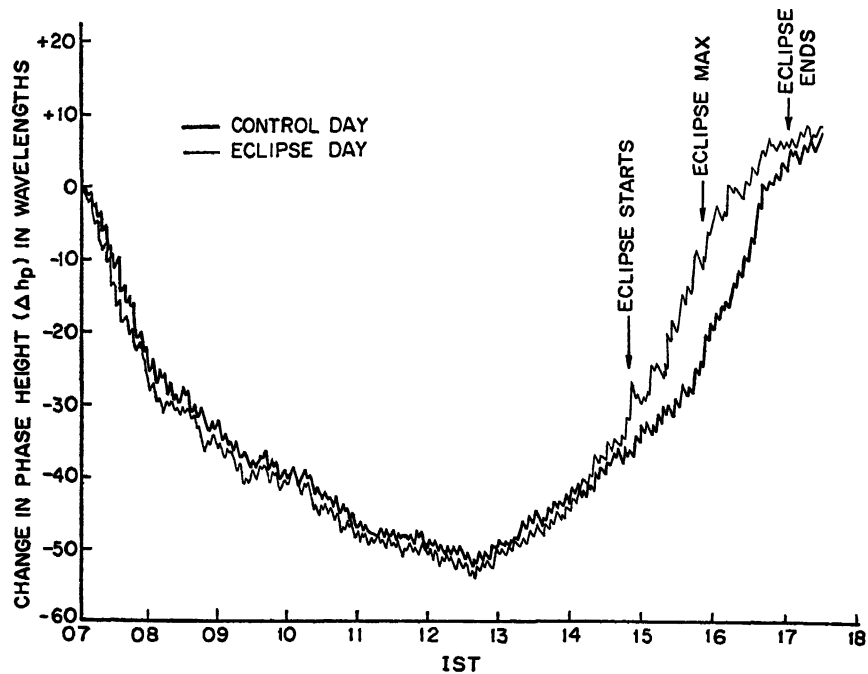


FIG. 2 Hourly variation of the change in phase height for the eclipse day and also for the control day.

decreases, attains its minimum at about an hour after the local noon, and increases rapidly in the afternoon hours. Superimposed on the regular diurnal variations for both the days are the short period fluctuations which are produced by the internal gravity waves (Vincent, 1969). With the start of the eclipse, the diurnal curve for the eclipse day indicates a faster rise in phase height. Near the time of maximum occultation it is elevated by about 2km with respect to that for the control day. Over Haringhata the eclipse became maximum at 1557hr and the corresponding value of the solar zenith angle was  $65^\circ$ . For this value of  $\chi$ , the contribution of the deviative component of the total absorption was nearly 60 per cent (Purkait, 1977). This result indicates that at 1557hr the observed uneclipsed value of 27dB for absorption contains a deviative component of 16dB and a non-deviative component of 11dB. The virtual heights of reflection on the control day and also on the eclipse day are found to be 108km and 112km respectively. It would, therefore, be reasonable to assume that the true heights of reflection for both the days are confined within the altitude range 105–110km. Within this altitude range a change in reflection height by 2km reduces the deviative component by 30 per cent on the average and at the time of eclipse maximum the deviative absorption in the E-layer will be reduced by 5dB. Since at this instant the measured reduction in the value of absorption is 10dB, the non-deviative component of the absorption will also be reduced by 5dB. Since the collision frequency profile does not alter from the control day to the eclipse day

(Jespersen & Pedersen, 1970), the observed change in deviative and non-deviative components arises mainly due to the reduction in the value of electron density in the D- and E-layers. It is thus concluded that at the time of eclipse maximum the electron distribution in both the D- and E-regions changes to such an extent that both the components of the total absorption at 2.2MHz reduce by the same magnitude. The details of the computed changes in electron density distributions in the D- and E-layers that will explain the observed variations of absorption and phase height, as discussed above, will be published in a separate article.

#### ACKNOWLEDGEMENTS

We the authors are indebted to Professor B. R. Nag for many helpful discussions. The services rendered by the Computer Centre, Calcutta University, are also thankfully acknowledged.

#### REFERENCES

- Bhar, J. N., Purkait, N. N., and Datta, S. K. (1974) Effect of sq. draft on the phase path of E-region reflections. *Indian J. Phys.*, **48**, 1117.
- Fraser, G. J., and Vincent, R. A. (1970) A study of D-region irregularities. *J. atm. terr. Phys.*, **32**, 1591.
- Haug, A., Thrane, E. V., Tsagakis, E., and Anastassiades, M. (1970) Ionospheric observations during the annular solar eclipse of May 1966-IV. *J. atm. terr. Phys.*, **32**, 1865.
- Jespersen, M., and Pedersen, B. M. (1970) Ionospheric observations during the annular solar eclipse of May 1966-III. *J. atm. terr. Phys.*, **32**, 1859.
- Purkait, N. N. (1977) Studies on D- and E-regions of the ionosphere. *Ph D. Thesis*, Univ. Calcutta, 84.
- Schrader, D. H., and Hower, G. L. (1971) Phase height measurements of the E-region. *J. atm. terr. Phys.*, **33**, 723.
- Vincent, R. A. (1969) Short period phase height oscillations in the E-layer. *J. atm. terr. Phys.*, **31**, 607.

Printed in India

Radio Propagation

## PHASE PATH AND GROUP PATH VARIATIONS DURING THE SOLAR ECLIPSE OF 16 FEBRUARY 1980

P. ERNEST RAJ, M. SRIRAMA RAO,\* C. JOGULU and B. MADHUSUDHANA RAO

*Ionosphere Research Laboratories, Andhra University, Visakhapatnam-530 003, India*

*(Received 7 September 1981)*

Results of phase and group path measurements of HF echo from the F-region of the ionosphere during the total solar eclipse of 16 February 1980, carried out at Waltair (Dip 20°) very near the path of totality (percentage of obscuration of sun's disc is 98.8), using pulsed vertical transmission are presented in this paper. Group path and phase path showed unusual variations. Around the time of maximum obscuration, electron density changes effect to a greater extent the phase path and group path lengths and at other times vertical layer movements seem to be predominant. Phase reversal occurred about 8 min after the time of maximum obscuration. Group path reversal occurred 30 min after the phase path reversal. The absence of post-sunset equatorial spread-F on solar eclipse day is discussed in relation to vertical drifts in the F-region during sunset times and the post-sunset vertical drift reversal.

**Keywords:** HF-Echo; Pulsed Vertical Transmission; Electron Density; Equatorial Spread-F

### INTRODUCTION

A change in the electron content of the ionosphere usually brings about a change in the phase path of the ionospherically reflected signals because of one or both of the following reasons:

- (i) a change of the height of reflection; or
- (ii) a change of the refractive index along the path below the level of reflection (Davies, 1965)

Changes in group height and phase height are equal in magnitude and sense when a change in the reflection height takes place, when significant electron density changes occur below the level of reflection, the refractive index of the medium through which the wave passes changes and this effect acts in opposite senses for the group and phase paths. A reduction in the refractive index increases the group path but decreases the phase path and vice versa.

Almeida and da Rosa (1970) mentioned that the rate of change of columnar electron content, especially during an eclipse time, can be determined with great

---

\* *Presently at* University of Sulaimaniyah, Sulaimaniyah, Iraq

accuracy from the phase path length experiment. Butcher (1973), Lørfald *et al.* (1970) and others have used phase path and group path measurements primarily to detect eclipse generated gravity waves.

The aim of the present study is to see how phase path and group path of vertically reflected HF radio waves vary during a total solar eclipse.

## RESULTS

Phase path and group path measurements of the HF-echo from the F-region of the ionosphere during the total solar eclipse of 16 February 1980 were carried out at Waltair (Dip  $20^\circ$ ) using 5.6 MHz fixed frequency pulsed vertical transmissions. The maximum obscuration of the solar disc at Waltair is 98.8 per cent. Changes in phase height recorded photographically, may be measured extremely accurately by the phase path technique, the details of which were discussed by Raghava Reddy (1969) and others.

### *Phase Path and Group Path Variations*

Group height (virtual height) measurements were made and the data for 15, 16 and 17 February 1980 is shown in Fig. 1. The regular feature at Waltair is that group height starts increasing slowly from around 1300 hr LT and the increase is rapid during

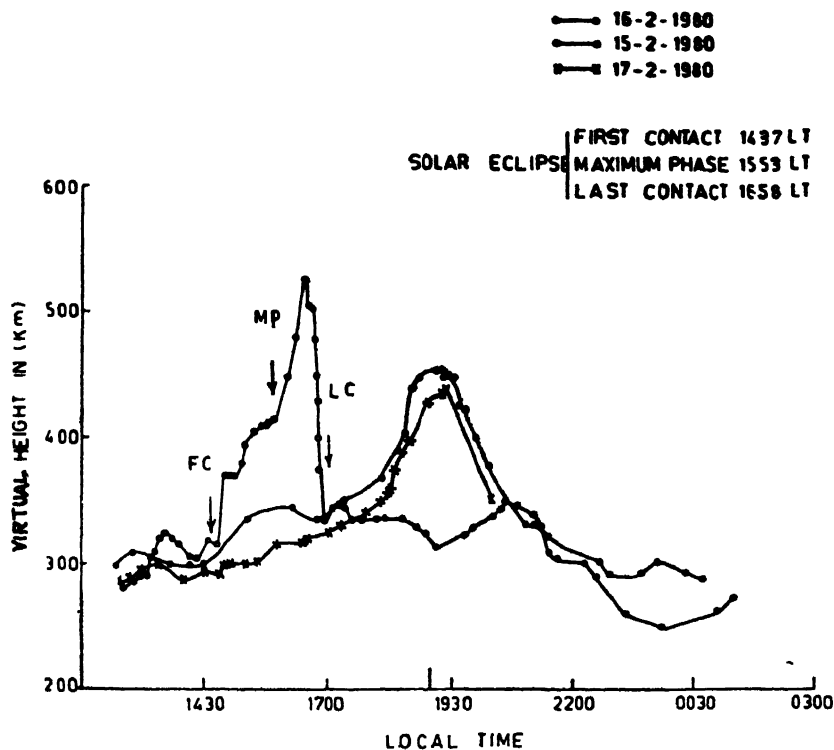


FIG 1. Variation of group height (virtual height) with local time, at Waltair ( $f = 5.6$  MHz)

sunset times. A post-sunset reversal from increase to decrease occurs around 1900hr LT. On the eclipse day group height increased more rapidly after first contact (1437hr LT) and even more rapidly after the time of maximum obscuration of the sun (1553hr LT). Group height reversal occurred about 38min after the time of maximum obscuration. The decrease in group height was very rapid and after the fourth contact (1658hr LT) it was more or less constant showing a slight decrease upto about 1930hr LT, the time at which the normal day group height reaches a maximum.

Phase path change of the ordinary ray for the period between 1300hr and 1800hr on 16 and 15 February 1980 is shown in Fig 2. On solar eclipse day phase path in-

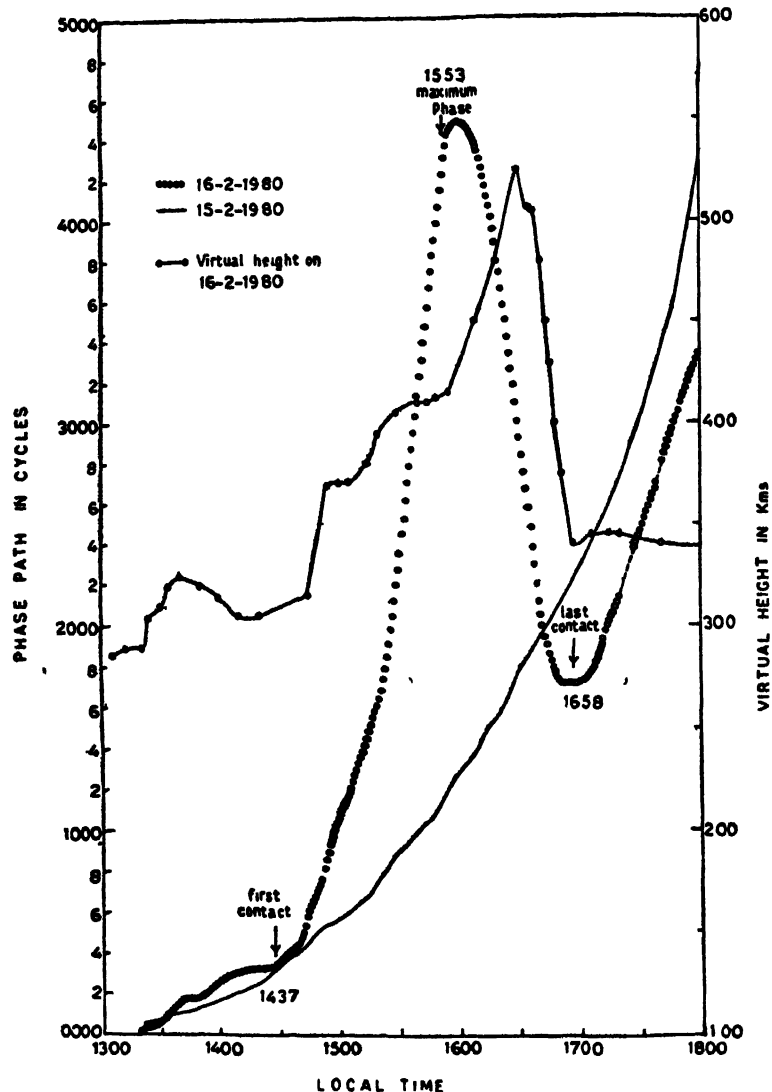


FIG 2 Variation of change of phase path (in cycles) with local time on 16.2.1980 (.....) and on 15.2.1980 (————) and variation of group height with local time (—•—•—)

creased first slowly and then rapidly after the first contact. Phase reversal on ordinary ray occurred 8min after the time of maximum obscuration. Phase path decreased rapidly till the last contact after which it started increasing again as on a normal day. Phase path plot from the beginning of the eclipse, right through the night for about ten hours, shows a long period, large amplitude damped oscillatory behaviour, the detailed discussion of which is to be given in a subsequent publication.

### DISCUSSION

The deviation of phase path length around maximum obscuration from normal day value was about 3000 cycles (rate of change of phase path being about 80m/sec) and such large deviations were reported earlier (Butcher, 1973). Such a large change could primarily be due to a large vertical motion of F-layers during eclipse conditions. It is felt (Thomas & Robbins, 1956; and Evans, 1965) that important changes of temperature, occur in the F2 layer during an eclipse which might cause movements and these movements during eclipse are seen to be noticeably larger than those present on normal days. Ionisation changes solely could not have brought about such a large variation in phase path length (Krishnamurthy *et al.*, 1976). After the maximum obscuration there is a 30min delay between the phase reversal and group height reversal. Electron densities in the D- and E-regions lowered due to sun's obscuration increase to their normal evening values, more or less, after the time of maximum obscuration. The refractive index of the medium below the reflection height consequently starts decreasing, thereby increasing the group path length and decreasing the phase path length of radio waves reflected from the F-region. This shows that the effect of electron density changes on phase path and group path variations is significant during this period of the eclipse when phase path starts decreasing and group path length continues to increase for about 30min. Curves of rate of change of phase path ( $dp/dt$ ) and rate of change of group path ( $dh/dt$ ) during eclipse condition show that the rates were in opposite senses more or less and after the last contact they have the same sense of variation (Fig. 3).

#### *Occurrence of Equatorial Spread-F in relation to Post-Sunset F-Region Fertilical Drifts*

The occurrence of post-sunset equatorial spread-F at Waltair during the months of February-March is common. Spread-F occurred on all the days from 11 to 20 February 1980 except on 16th, the solar eclipse day. Vertical drifts from phase path data were computed on all these days in the evening time. Data for 15, 16 and 17 February 1980 are shown in Fig. 4. Vertical drifts on 15 and 17 can be seen to be very large before the onset of spread-F (onset shown by an arrow), in agreement with our earlier reports on such a study (Srirama Rao *et al.*, 1978, and Ernest Raj *et al.*, 1980). But on 16 February vertical drifts during the same period of observation were noticed to be very low. An interesting point of note is that on 16 February, the post-sunset vertical drift reversal from upward to downward occurred much earlier than that observed on the control days. In fact, this reversal seems to be occurring earlier than what would be observed even on a no-spread-F day. An unfortunate circumstance was that the eclipse occurred on a magnetically disturbed day and it is known that magnetic activity and occurrence of spread-F are negatively correlated at low lati-

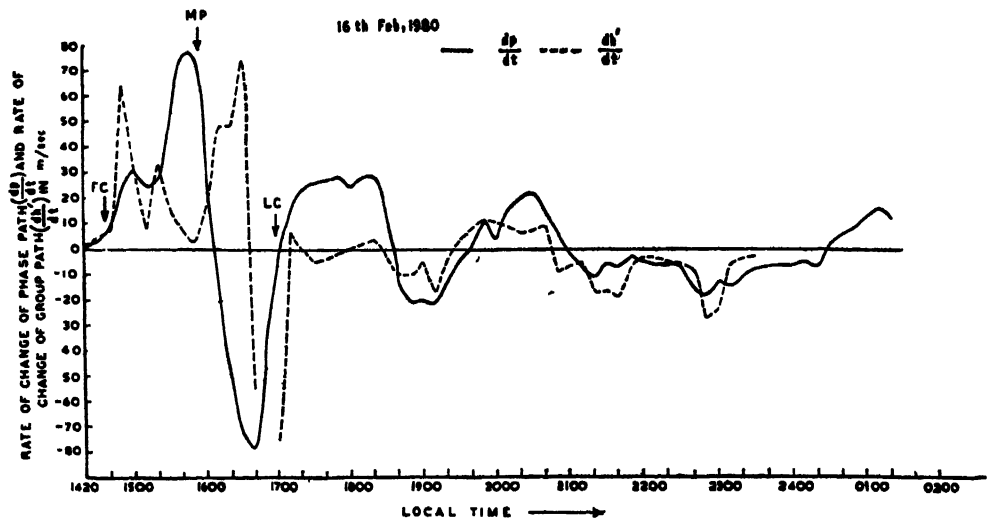


FIG. 3. Rate of change of group path (-----) and rate of change phase path (————) on 16 February 1980, total solar eclipse day

tudes (Shimazaki, 1959; Lyon *et al.*, 1961; and Rao & Rao, 1961). However, recent experimental observations reported by Subrahmanyam (1980) show that equatorial spread-F does occur during different phases of a magnetic storm. The magnetic storm on 14, 15 and 16 February might have inhibited vertical motions in the F-region on 16th and hence, low values were possibly observed on that day. However, this only points out that F-region vertical drifts in the sunset times play an important role in the occurrence and sustenance of post-sunset equatorial spread-F.

#### ACKNOWLEDGEMENT

One of the authors (PER) thanks the University Grants Commission, New Delhi for the award of a Junior Research Fellowship.

#### REFERENCES

- Almeida, O. G., and da Rosa, A. V. (1970) Observations of ionospheric electron content during the March 7, 1970 solar eclipse. *Nature*, **226**, 1115.
- Butcher, E. C. (1973) Possible detection of gravity waves in the phase height of the F-region due to the eclipse of March 7, 1970. *J. geophys. Res.*, **78**, 7563.
- Davies, K. (1965) *Ionospheric Radio Propagation* National Bureau of Standards Monograph, 80.
- Ernest Raj P, Srirama Rao, M, Jogulu, C., Madhusudhana Rao, B (1980) Study of night time vertical drifts in F-region over Waltair using phase path technique. *Indian J. Rad. Space Phys.*, **9**, 147.
- Evans J V (1965) An F-region eclipse. *J. geophys. Res.*, **70**, 131.
- Krishnamurthy, B. V, Raghava Reddi, C., and Subba Rao, K. S V. (1976) Some new observations on equatorial spread-F using phase path technique. *J. geophys. Res.*, **81**, 705.
- Lerfeld G M, John Vesecky and Kanelloukos, D. P. (1970) FDS. *Trans. Am. geophys. Union*, **51**, 784.

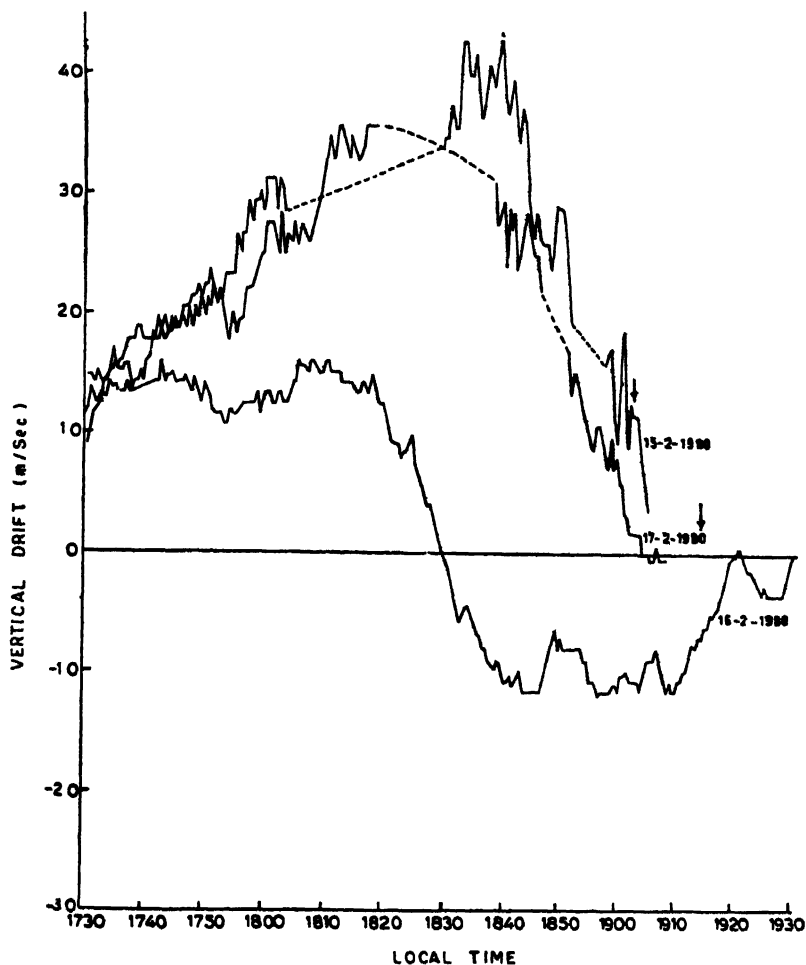


FIG 4 Vertical drift in the post-sunset period on 15, 16 and 17 February 1980—onset of Spread-F.

- Lyon, A J, Skinner, N. J. and Wright, R W H (1961) Equatorial spread-F and Ibadan, Nigeria. *J. atm terr Phys*, 21, 110
- Raghava Reddy, C (1969) Studies on ionospheric movements at Waltair, using phase path technique. *Ph D Thesis*, Andhra University
- Rao, M S V G, and Rao, B R (1961) Equatorial spread-F in relation to post-sunset height changes and magnetic activity *J geophys Res*, 66, 2113
- Shimazaki, T (1959) A statistical study of world-wide occurrence probability of spread-F *J Rad. Res Lab, Japan*, 6, 669
- Srirama Rao, M, Ernest Raj, P, and Madhusudhana Rao, B (1979) Phase path studies of spread-F over Waltair during Sept.-Oct, 1970 *Indian J. Rad Space Phys*, 8, 400
- Subrahmanyam, V (1980) Studies on some aspects of equatorial spread-F *Ph D Thesis*, Andhra University
- Thomas, J O, and Robbins, A R (1956) Movements in the F2-layer of the ionosphere during some solar eclipses In *Solar Eclipses and the Ionosphere* (Eds W J G Beynon & G M Brown), Pergamon Press, London, 94



Printed in India.

Gravity Waves

## IONOSPHERIC DISTURBANCES DURING THE TOTAL SOLAR ECLIPSE ON 16 FEBRUARY 1980

N. BALAN,<sup>1</sup> B V. KRISHNA MURTHY,<sup>2</sup> C. RAGHAVA REDDI,<sup>2</sup> P. B. RAO<sup>1</sup>  
*and*  
K. S. V. SUBBARAO<sup>2</sup>

<sup>1</sup>*Physics Department, University of Kerala, Kariavattom, Trivandrum-695 581, India*

<sup>2</sup>*Space Physics Division, Vikram Sarabhai Space Centre, Trivandrum-495 022, India*

(Received 7 September 1981)

A HF doppler sounder and a C4 ionosonde were operated simultaneously at Trivandrum (8°33'N, 76°57'E) during the total solar eclipse of 16 February 1980 and on a control day to study ionospheric disturbances generated by the eclipse. The gross electron density changes seen in the form of a rapid rise and fall of contours of constant electron density at various heights show how the ionosphere responds to the eclipse. The height dependence of the response time is shown clearly by plotting the time variation of a thickness parameter for adjacent electron density contours at four different height levels. The doppler observations reveal a complex ionospheric disturbance reflecting the effects due to both large scale electron density decay and build-up, and short scale wave perturbations. The disturbance was observed on four closely spaced antennas and the correlations among them were found to be excellent. A spectral analysis of the disturbance shows, besides the long period component associated with the gross electron density changes, short period components of 21 and 32 minutes which are most likely a manifestation of the atmospheric gravity waves excited by the eclipse.

**Keywords:** HF Doppler Sounder; Ionosonde; Electron Density; Gravity Waves

### INTRODUCTION

THERE are two basic aspects to the ionospheric changes produced during a solar eclipse. First, there will be gross changes in electron densities and consequent redistribution throughout the ionosphere due to sudden switching off of ionizing radiation in the eclipsed region. The second aspect is concerned with the dynamical effects connected with the atmospheric wave motions that are likely to be excited by the localized cooling action associated with solar eclipse (Chimonas & Hines, 1970). The observed ionospheric disturbances during an eclipse represent the composite phenomenon of the above two effects.

There has been a considerable amount of data collected during the earlier eclipses to speak on the large scale electron density changes in the ionosphere. The electron densities in the D- and E-regions of the ionosphere have been found to decrease rapidly with the onset of the eclipse (e.g., Kane, 1966, and Belrose & Ross, 1972). This was to be expected in view of the fast recombination process in the lower ionosphere coupled nearly with the extinction of photoionization. The changes that occur in the F-region, however, are not as consistent or predictable as in the lower ionosphere since

There have been relatively fewer observations on the wave perturbation aspect of the eclipse generated ionospheric disturbance. Except for very few cases such as have been reported by Davis and DaRosa (1970) and Vaidyanathan *et al.* (1978), the observations collected to date have been largely inconclusive on the question of atmospheric wave generation by a solar eclipse.

The total solar eclipse of 16 February 1980 offered yet another opportunity to observe the eclipse generated ionospheric disturbance from the standpoint of both electron density distribution changes and atmospheric wave excitation. To observe on both aspects of the disturbance, a C4 type ionosonde and a HF doppler sounder were operated simultaneously at Trivandrum (8°33'N, 76°57'E) on the eclipse day and a control day following the event. A brief account of the experiments conducted and the results obtained is given in the following sections.

The experimental set-up consists of two ionospheric sounders, a C4 ionosonde and a HF doppler system. Ionograms were recorded using the ionosonde, on the eclipse day at 5min intervals up to 1642hr I.S.T. and also on 21 February 1980 at 15min intervals to serve as control day data. The ionograms were reduced to electron density-true height profiles using the Budden matrix method.

**PULSE TRANSMITTER**

**PRE AMP.**

**COHERENT RECEIVER**

**50 MHz.**

**55 MHz.**

**KEYER PULSE**

**ATTN.**

**BAL MIXER**

**IF AMP.**

**500 kHz.**

**PHASE DET.**

**BAL / UNBAL AMP.**

**ACTIVE LPF**

**VOLT. FOLLO.**

**S/H**

**VOLT FOLLO.**

**A cos φ**

**A sin φ**

**500 kHz.  $\angle 0^\circ$**

**500 kHz.  $\angle 90^\circ$**

**DIVIDE BY 4**

**2 MHz**

**FREQUENCY SYNTHESIZER**

**GATE PULSE**

**DELAY 10 - 9999  $\mu$ Sec**

**FIG 1** Block diagram of the HF doppler system.

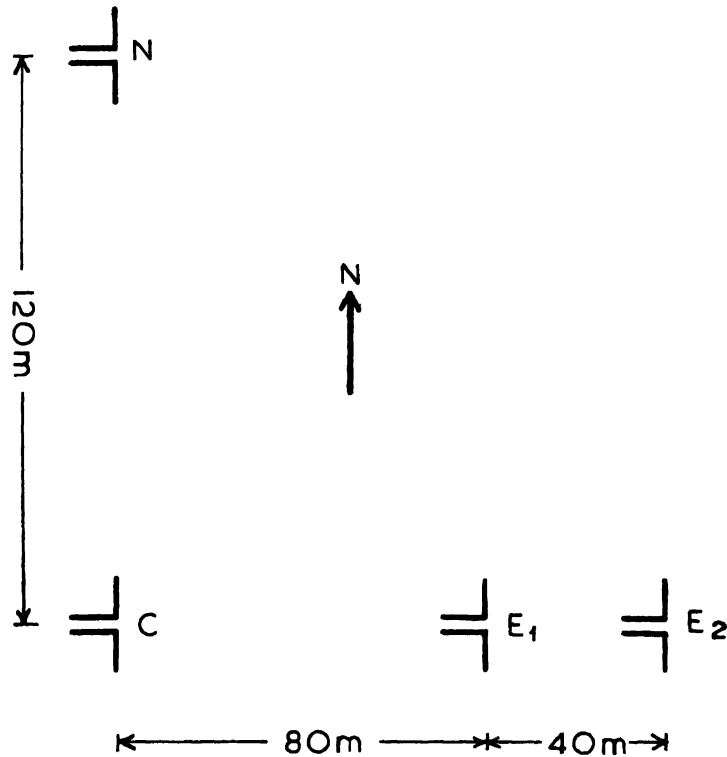
comprises of a wideband pulse transmitter, a phase coherent receiver and a frequency synthesizer. The pulsed HF, the Keyer pulse to the transmitter and the local oscillator frequencies for the receiver were all generated synchronously in the frequency synthesizer. In addition, the synthesizer supplied to the sample and hold circuit in the receiver a gate pulse of  $10\mu\text{s}$  of adjustable delay with respect to the transmitter pulse in steps of  $10\mu\text{s}$ . The frequency synthesizer consisted of a 10MHz crystal oscillator as master clock, having a stability better than one part in  $10^6$ . The various local oscillator frequencies and the timing pulses required for the system were derived from this master clock through digital division and analog mixing.

The transmitter is a conventional master oscillator power amplifier system with associated power supplies. The input to the transmitter is a HF pulse of 5V peak to peak,  $100\mu\text{s}$  width and 50Hz PRF. The pulsed HF is amplified successively by a pre-amplifier, a low power amplifier, and a final high power push-pull amplifier feeding its output to the transmitting antenna. All amplifiers are keyed to the transmitter pulse, and operate only during the pulse duration. The transmitting antenna was a three element folded dipole at a height of  $\lambda/4$  from the ground. The balanced RF output of the transmitter is fed to the antenna by an open parallel wire feeder of  $600\Omega$  impedance.

The signal reflected from the ionosphere is received by a half-wave dipole. A 1:1 balun converts the balanced output of the antenna to unbalanced input to the pre-amplifier of 25dB gain. The signal from the preamplifier is fed to the phase coherent receiver shown in the dotted section of the block diagram. First, it is converted down to 500kHz in a balanced mixer and then amplified in an IF amplifier having a bandwidth of 20kHz. The IF signal is phase compared against two 500kHz phase quadrature signals from a frequency divider in two separate phase detectors. The outputs of the two phase detectors are separately amplified and band limited before sampling and holding the echo amplitude. The two quadrature channel outputs X and Y can be identified as  $A \cos \phi$  and  $A \sin \phi$ ,  $A$  being the instantaneous amplitude and  $\phi$  the instantaneous carrier phase of the received signal. By recording the two receiver outputs,  $A$  and  $\phi$  can be computed as function of time.

The observations on the eclipse event reported here were collected using a spaced receiver set-up with antenna configuration as shown in Fig 2. The signals received by four identical phase coherent receivers of the type described above were recorded on four identical strip chart recorders running at a speed of 10cm per minute.

Doppler data were recorded at an operating frequency of 5.0MHz on the eclipse day and on 19 February 1980 from 1300hr to 1900hr IST. The quadrature channel outputs enable in principle the measurement of the carrier phase and its time variations to an accuracy of about  $5^\circ$ . The very fast quasi-sinusoidal oscillations (15 to 60 cycles per min) recorded on strip chart precluded the possibility of reading the data at close intervals. For the present purpose of measuring the doppler frequency shift, the number of cycles of carrier phase change per minute was considered to be adequate. For each of the quadrature channels the number of both positive and negative peaks of the quasisinusoidal variations were counted for each interval of 1 min and these four values have been averaged to obtain the doppler. The sense of the doppler was inferred from the relationship between the two quadrature channels and further confirmed by checking it against the measured group path variations.



RECEIVING ANTENNA ARRAY

FIG 2 Antenna configuration.

Fig. 3 shows sample records of the two quadrature channels for the eclipse day and a control day. The samples illustrate quite clearly the eclipse effects on the doppler of the received signal

As happened on some of the earlier eclipses, a magnetic storm which started a day earlier was passing through its main and recovery phases on the eclipse day. By the time of the eclipse, however, the magnetic field was found to recover to almost the quiet day level. In view of this recovery, it is believed that the magnetic storm has not affected the ionospheric disturbance observed during the eclipse period to any significant extent

## RESULTS AND DISCUSSION

### *Electron Density Variations*

Ionograms recorded at Trivandrum on the day of the eclipse have been reduced to electron density—true height ( $N-h$ ) profiles. Fig. 4 shows the constant electron density—height contours obtained from the  $N-h$  profiles. The times of first contact, maximum phase and last contact are indicated in the figure by arrow marks. Starting

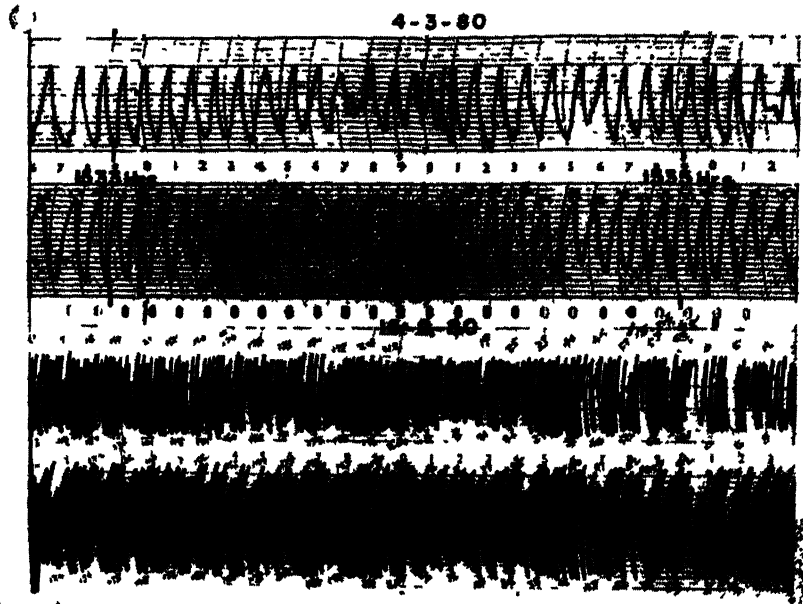


FIG 3 Sample records of the quadrature channels

from the time of first contact, the electron density contours show an increase in height, the increase being very rapid at lower levels of electron density. This can be mainly attributed to the role of production-recombination processes. The contours corresponding to electron densities up to  $2.0 \times 10^{11}$  el/m<sup>3</sup> reach peak altitudes at times close to the time of maximum phase, while the contours from  $3.1 \times 10^{11}$  el/m<sup>3</sup> to  $6.0 \times 10^{11}$  el/m<sup>3</sup> reach the peak with a very significant delay. The contours of still higher electron densities continue to increase in height even well after the time of maximum phase ( $t_m$ ). The delay in the occurrence of the peak with respect to  $t_m$  depends mainly on the chemical loss rate. This rate being slow at higher altitudes, the delay is more. This, of course, is a very simple picture because transport effects have to be taken into account at the heights under consideration. An important feature evident in Fig 4 is the changing width between any two contours with time, especially for the ones of lower electron density values. This aspect is more clear in Fig 2 where the thickness ( $T$ ) of the region between two fixed levels of electron density is plotted against time. In Fig 5, the thickness is shown for electron density levels corresponding to  $2.0$  to  $3.1 \times 10^{11}$  m<sup>-3</sup> ( $T_1$ ),  $3.1$  to  $4.4 \times 10^{11}$  m<sup>-3</sup> ( $T_2$ ),  $4.4$  to  $6.0 \times 10^{11}$  m<sup>-3</sup> ( $T_3$ ) and  $6.0$  to  $8.0 \times 10^{11}$  m<sup>-3</sup> ( $T_4$ ).

The thickness parameter ( $T$ ) decreases till about the time of maximum phase as expected from faster response of the ionosphere at lower heights to the declining production rate. Around the time of maximum phase,  $T_1$  starts rapidly increasing, attaining peak value at 1610hr following by rapid decrease. The rapid increase in  $T_2$  started 10 minutes later with respect to that in  $T_1$ , with a similar delay also in the occurrence of peak. The start of the increase in  $T_3$  and  $T_4$  occurred much later, with

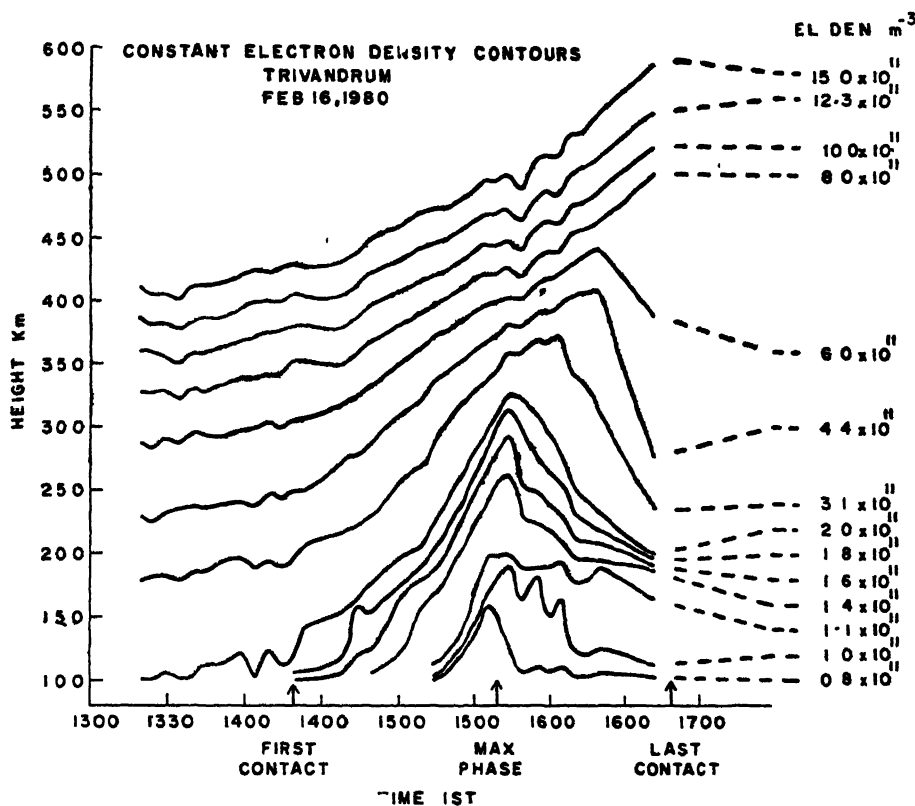


FIG 4 Electron density contours.

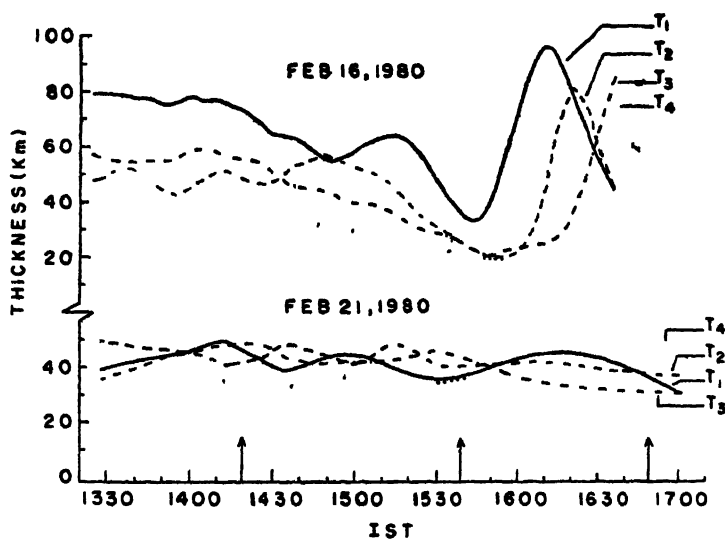


FIG 5. Thickness parameters  $T_1$ ,  $T_2$ ,  $T_3$  and  $T_4$ .

a delay of about 30 minutes with respect to that in  $T_1$ .

From the above it is clear that the increase in the thickness parameter following the maximum phase is due to a faster build-up of ionization at lower levels. The subsequent decrease in the thickness parameter noted for  $T_1$  and  $T_2$  cannot be explained on the basis of any single dominant process and must be the result of all the three processes namely, production, recombination and transport. In contrast to its behaviour during the eclipse, the thickness parameters  $T_1$  to  $T_4$  stay more or less the same on the control day during the same interval as shown in Fig. 5.

### *Doppler Variations*

The Doppler frequency data processed as described under 'Experimental Details' is shown in Fig. 6 for the central aerial. The doppler frequency starts decreasing in about

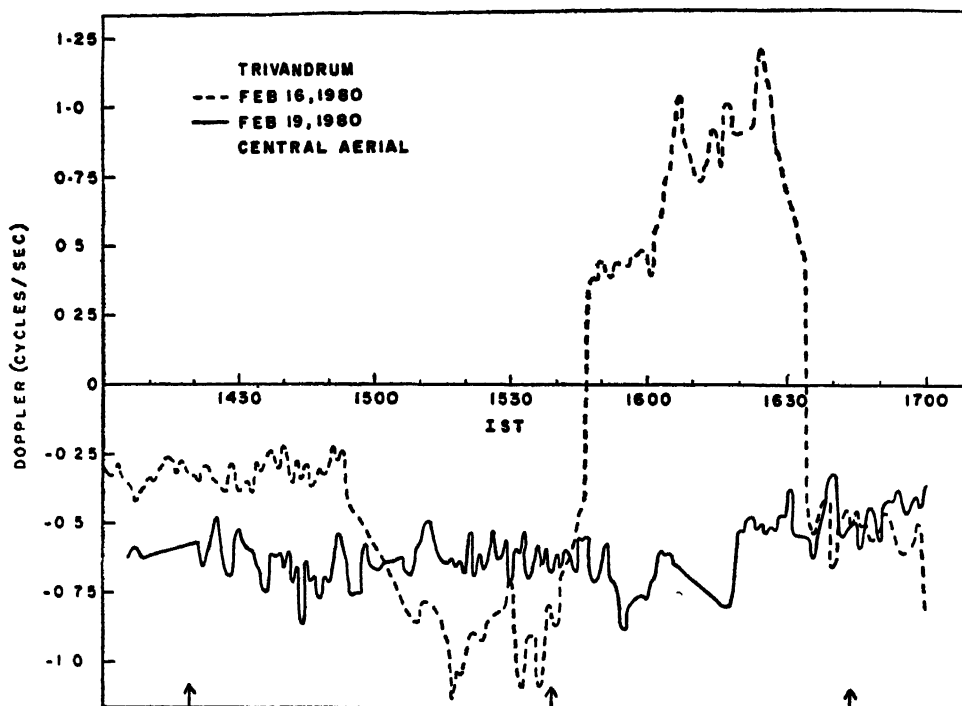


FIG 6 Doppler data for the central aerial

30min from the time of first contact and reaches a negative peak about 20min before the time of maximum phase, remaining at the same level till  $t_m$ . This is due to an upward movement of the ionospheric layer itself and/or a decay of ionization below the reflection level. Just after  $t_m$ , the doppler shows a rapid increase attaining a positive peak between 1610–1630hr. This means a downward movement of the ionospheric layer and/or a build-up of ionization below the reflection level. After 1630hr the doppler shows a rapid decrease again. These features are consistent with those shown by the constant electron density contours (Fig. 4) and the thickness parameter (Fig. 5).

This large amplitude oscillation of doppler with a duration of about 100min is the result of mainly production-recombination processes. The doppler on the control day (21 February 1980) remains more or less the same (Fig. 6) for the period corresponding to the eclipse duration, in striking contrast to its behaviour during the eclipse.

The doppler data at the other three aerials showed identical features to the central aerial as far as the large oscillation during the eclipse is concerned. This is further confirmed by obtaining correlograms for different aerial pairs. The correlogram, between central and  $E_2$  aerials is shown in Fig 7. The maximum positive correlation

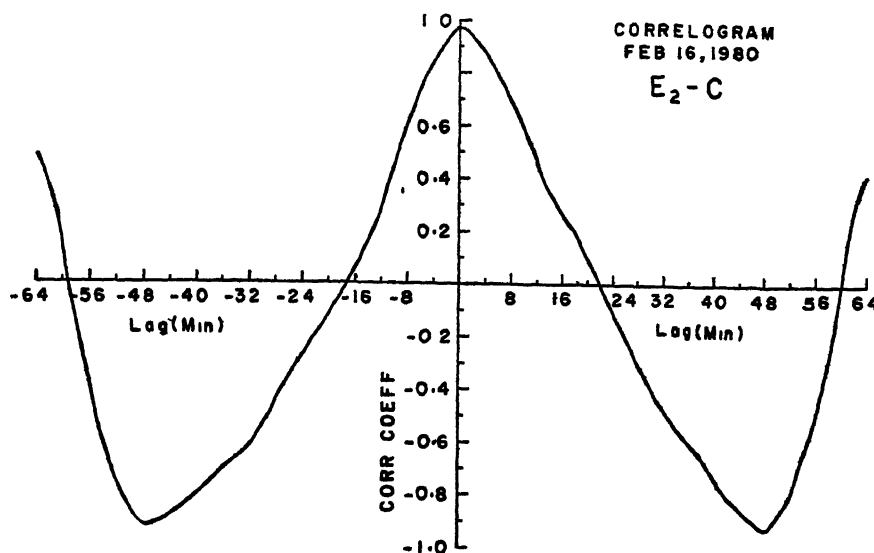


FIG 7 Correlogram for the aerial pair  $E_2$ -C.

coefficient is 0.97 occurring at zero time lag. The correlogram is dominated by the 100min oscillation. Correlograms corresponding to other aerial pairs showed similar features.

In the doppler data shown in Fig. 6 for the eclipse day, it can be seen that shorter period components are present superposed on the larger oscillation of 100min period. These short period components could be largely due to layer movements. In order to find out the spectra composition of these shorter period components, the doppler data from 1440–1647hr IST (giving 128 samples) is subjected to FFT analysis for both the eclipse and control days.

Fig 8 shows the amplitude spectrum for the aerials  $E_2$ , N and C for the eclipse and control days. The spectra on the eclipse day at the three aerials are quite similar to each other and are dominated by components with periods of 64min, 32min and 21.3min. The larger period component 64min is the result of the large oscillation seen prominently in the doppler data (Fig 6) and in the correlogram (Fig 7) which is attributed to the production-recombination processes. The difference in the period of this oscillation observed in the correlogram and in the spectra is due to lack of sufficient resolution at longer periods in the spectra. The other two components 32min



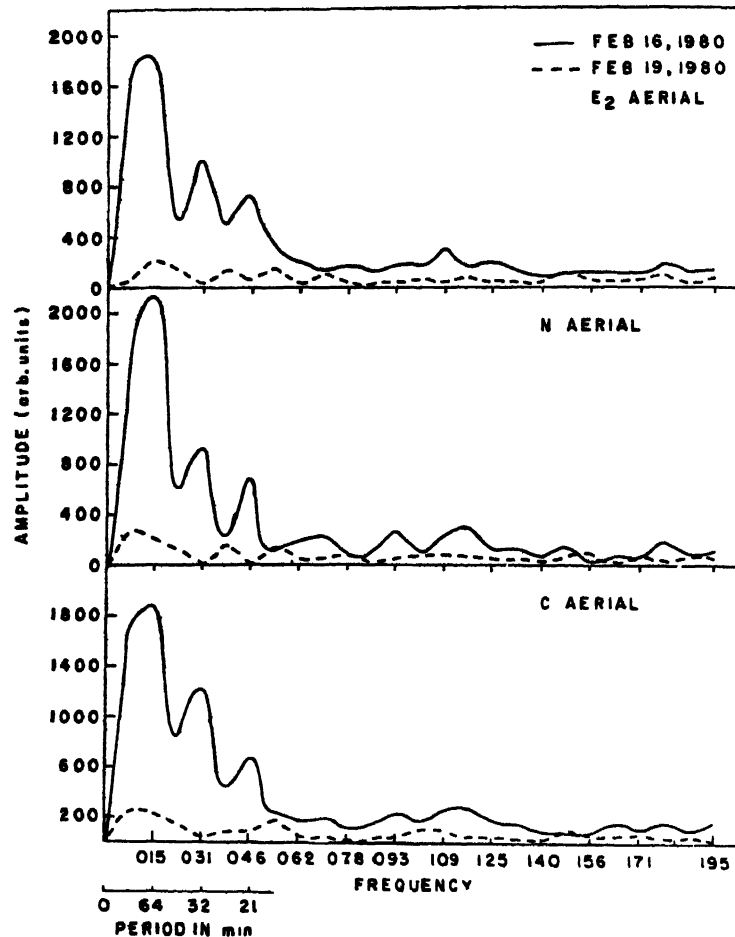


FIG 8 Amplitude spectrum for the eclipse and control days.

and 21.3 min are certainly due to eclipse induced dynamic effects. It may be noticed that control day spectra do not show such prominent components as on the eclipse day.

During the past few solar eclipse events, many groups have attempted to detect ionospheric wave motions associated with an eclipse. Some evidence has been presented for wave motions with periods ranging from 10 minutes to 30 minutes from observations conducted close to the path of eclipse (Davies & Da Rosa, 1970, Bertin *et al.*, 1977; Vaidyanathan *et al.*, 1978, and Butcher *et al.*, 1979). In many cases, the observed perturbations could not be identified with the eclipse with certainty because magnetically disturbed conditions prevailed at the time of the eclipse (Carlson *et al.*, 1970, and Lerfald *et al.*, 1972). From the observations of the total solar eclipse of 7 May 1970, Davis and Da Rosa, however, could identify a 20 minute period perturbation seen in the total electron content of ATS I and ATS III without any ambiguity with the eclipse event. This observation was shown to be in qualitative agreement with

the theory of Chimonas and Hines (1970) by computing the wave-form of pressure perturbation for the same field point as that corresponds to the observation. The diversity observed in the wave periods close to the source region has been explained recently by Butcher *et al.* (1978) by means of a simple empirical model in which the wake of the eclipse is supposed to be recovered by collapse of the atmosphere horizontally inwards from the sides. On the basis of simple model, they have computed wave periods for various modes of excitation. The wave periods of 21 and 32 minutes observed in this investigation agree quite well with the simple model of Butcher *et al.* (1978) for mode  $n = 2$ . Thus the wave perturbations observed in the doppler seem to support the view that a solar eclipse can excite wave motions in the atmosphere which manifest as detectable ionospheric wave perturbations.

#### REFERENCES

- Belrose, J. S., and Ross, D. B. (1972) Ionization changes in the lower ionosphere during the solar eclipse of 7 March 1970. *J. atm terr Phys*, **34**, 695.
- Bertin, F., Hughes, K. A., and Kersley, L. (1977) Atmospheric waves induced by the solar eclipse of 30 June 1973. *J. atm terr Phys.*, **39**, 457.
- Butcher, E. C., Downing, A. M., and Cole, K. D. (1979) Wavelike variations in the F-region in the path of totality of the eclipse of October 23, 1976. *J. atm terr. Phys*, **41**, 439.
- Carlson, H. C., Harper, R., Wickwar, V., Showen, R. L., Behnke, R., Trost, T. F., Cogger, L. R., and Nelson, C. J. (1970) Eclipse observations at Arecibo, Puerto Rico, on March 7, 1970. *Nature*, **226**, 1124–1125.
- Chimonas, G., and Hines, C. O. (1970) Atmospheric gravity waves induced by a solar eclipse. *J. geophys. Res.*, **75**, 875.
- Davis, M. J., and da Rosa, A. V. (1970) Possible detection of atmospheric gravity waves generated by the solar eclipse. *Nature*, **226**, 1123.
- Evans, J. V. (1965a) An F-region eclipse. *J. geophys. Res.*, **70**, 131.
- (1965b) On the behaviour of  $f_oF_2$  during solar eclipses. *J. geophys. Res.*, **70**, 733.
- Kane, J. A. (1966) D-region electron density measurements during the solar eclipse of May 20, 1966. In *Solar Eclipses and the Ionosphere* (Ed. M. Anastassiads), 199. Plenum Press, New York.
- Lerfeld, G. M., Jurgens, R. B., Vesecky, J. F., and Washburn, T. W. (1972) Travelling ionospheric disturbances observed near the time of the solar eclipse of 7 March 1970. *J. atm terr Phys*, **34**, 733.
- Ratcliffe, J. A., and Weeks, K. (1960) The ionosphere. In *The Physics of the Upper Atmosphere* (Ed. J. A. Ratcliffe), 434. Academic Press, London, 0960.
- Vaidyanathan, S., Raghava Reddi, C., and Krishna Murthy, B. V. (1978) Quasi-periodic fluctuations in electron content during a partial solar eclipse. *Nature*, **271**, 40.

Printed in India.

Electron Content

## IONOSPHERIC ELECTRON CONTENT VARIATION OBSERVED AT DELHI , DURING TOTAL SOLAR ECLIPSE OF 16 FEBRUARY 1980

LAKHA SINGH, T. R. TYAGI, P. N. VIJAYAKUMAR and Y. V. SOMAYAJULU  
*Radio Science Division, National Physical Laboratory, New Delhi-110 012, India*

(Received 17 August 1981)

This paper reports the variation of electron content of the ionosphere as observed over Delhi during the total solar eclipse of 16 February 1980, maximum decrease in electron content observed was 9 per cent. Apparently no TID's seem to have been generated by the eclipse. No scintillation activity was observed on the eclipse day as well as on the preceding and following days

**Keywords:** Ionospheric Electron Content; Eclipse; Travelling Ionospheric Disturbances

### INTRODUCTION

CHIMONAS (1970) and Chimonas and Hines (1970) have suggested that the localized cooling due to the supersonic motion of the moon's shadow across the earth's atmosphere may produce gravity waves in the ionosphere. Many attempts made in the past for the confirmation or otherwise of this theory have been inconclusive. Schodel *et al.* (1973) reported null results both in ionospheric and microbarographic observations. Bertin *et al.* (1977) observed a wave of 18 minute period but drew no conclusion regarding its source. Vaidyanathan *et al.* (1978) reported quasi-periodic fluctuations both in modulation phase delay and Faraday rotation angle recorded from ATS-6 observations at Trivandrum during the partial solar eclipse of 29 April 1976

The total solar eclipse of 16 February 1980 whose path of totality cut across the Southern Peninsula of the Indian sub-continent gave the opportunity to us to study the behaviour of the electron content during a solar eclipse. The electron content of the ionosphere is being monitored at Delhi on a continuous basis as a long term programme. This paper reports the variation of ionospheric electron content (IEC) as observed during the eclipse.

### DATA AND METHOD OF ANALYSIS

The 136MHz transmission from the geostationary satellite ETS-II were monitored using a Satellite Radio Receiving System (Garg *et al.*, 1977). The basic parameters monitored are (i) the amplitude and (ii) the Faraday rotation angle of the satellite radio signals. The amplitude is used to study the ionospheric scintillation and Faraday rotation angle can be converted to electron content (Garg *et al.*, 1977, and Tyagi *et al.*, 1977).

ETS-II satellite was stationed at  $130^{\circ}\text{E}$  longitude. The sub-ionospheric point corresponding to a height of 420km for Delhi comes out to be ( $26.06^{\circ}\text{N}$ ,  $84.47^{\circ}\text{E}$ ). This was at a horizontal distance of 750km from the path of totality (Fig. 1). The

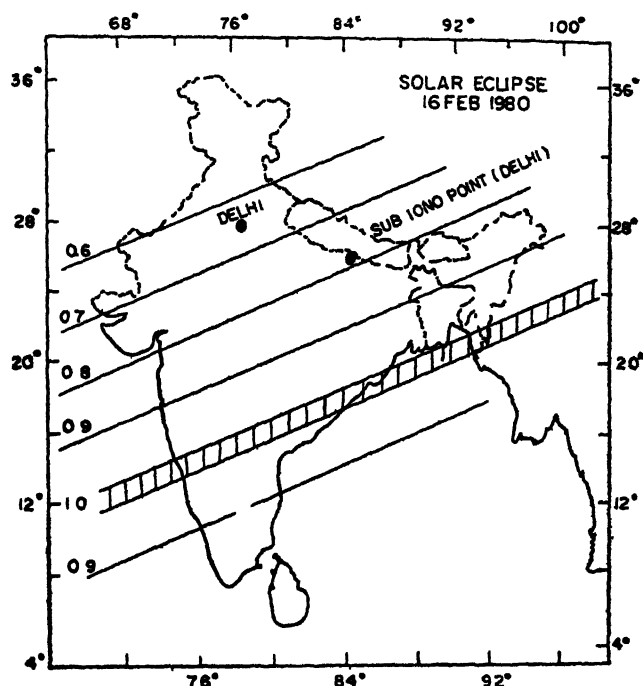


FIG. 1. Geographical location of the sub-ionospheric point for Delhi and the path of totality.

maximum obscuration at the sub-ionospheric point was 78 per cent. Other relevant details concerning the eclipse are given in Table I.

TABLE I

*Local circumstances of the total solar eclipse of 16 February 1980 at the sub-ionospheric point*

Time (IST) of 1st contact	Maximum phase	Last contact	Magnitude of Max phase
1442hr	1555hr	1657hr	78%

Fig 2 shows the variation of electron content, as observed over Delhi for the period 1400hr to 1800hr. It may be seen that following the first contact, the electron content starts decreasing and maximum decrease in electron content occurs about 11 minutes after the maximum obscuration at the sub-ionospheric point. The electron content then starts to recover and, in fact, attains a higher value than that at the start of the eclipse. This is because of the secondary evening maxima which are

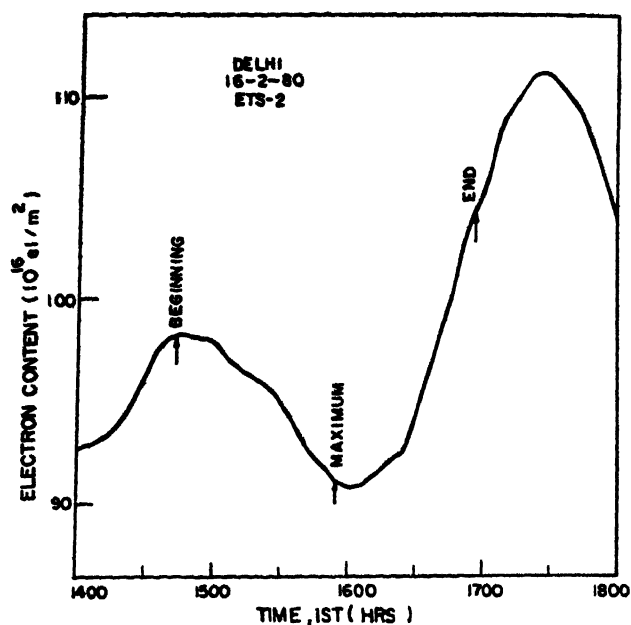


Fig. 2. Electron content variation during the solar eclipse of 16 February 1980.

usual during this part of the season. It may be noted that maximum change in IEC observed over Delhi is 9 per cent.

In an attempt to see if any eclipse generated travelling ionospheric disturbances (TID) could be identified, the data were detrended from diurnal variation using a digital filter. Apparently, no TID's seem to have been generated. Any firm conclusion can be drawn only when we analyse data from a number of stations. Such an analysis is in progress.

There was no scintillation on the eclipse day as well as on the preceding and following days.

#### ACKNOWLEDGEMENTS

The authors wish to thank Mr J. K. Gupta, Mrs P. Chopra for their help in scaling the data. They also thank Mr S. R. Bakshi and Mr N. N. Kaul for technical help.

#### REFERENCES

- Bertin, F., Hughes, K. A., and Kersley, L. (1977) Atmospheric waves induced by the solar eclipse of 30 June 1973 *J. atm. terr. Phys.*, **39**, 457.
- Chimonas, G. (1970) Internal gravity-wave motions induced in the earth's atmosphere by a solar eclipse *J. geophys. Res.*, **75**, 5545.
- Chimonas, G., and Hines, C. O. (1970) Atmospheric gravity waves induced by a solar eclipse. *J. geophys. Res.*, **75**, 875.
- Garg, S. C., Vijayakumar, P. N., Lakha Singh, Tyagi, T. R., and Somayajulu, Y. V. (1977) Early results of ATS-6 radio beacon experiment at New Delhi *Indian J. Radio Space Phys.*, **6**, 241.

- Schodel, J. P., Klostermeyer, J., and Rottger, J. (1973) Atmospheric gravity-wave observations after the solar eclipse of June 30, 1973. *Nature*, **245**, 87.
- Tyagi, T. R., Lakha Singh, Devi, M., and Barbara, A. K. (1977) Total electron content measurements at Gauhati using 140MHz ATS-6 transmissions.
- Vaidyanathan, S., Raghava Reddi, C., and Krishna Murthy, B. V. (1978) Quasi-periodic fluctuations in electron content during a partial solar eclipse. *Nature*, **271**, 40.

Printed in India.

Electron Content

## TOTAL ELECTRON CONTENT STUDIES DURING 16 FEBRUARY 1980 SOLAR ECLIPSE BY DIFFERENTIAL DOPPLER METHOD

M. R. DESHPANDE, H. CHANDRA, BANSHIDHAR, H. O. VATS, G. SETHIA *and*  
N. M. VADHER

*Physical Research Laboratory, Ahmedabad-380 009, India*

*and*

C. L. JAIN, M. R. SIVARAMAN, S. K. KOTHARI *and* SHEELA S. GOYAL

*Space Applications Centre, Ahmedabad-380 053, India*

*(Received 17 August 1981)*

Latitudinal profiles of the total electron content (TEC) were obtained during the total solar eclipse event of 16 February 1980, through the Differential Doppler method using US-NNS satellites. The experiment was conducted at the Nizamia Observatory, Rangapur, near Hyderabad (17°4'N, 78.6°E) in the totality zone. The latitudinal profiles of TEC covered right through the dip equator to the peak of the Appleton anomaly region. Comparison of the profiles on eclipse day with the nearest profiles on a control day (17 February 1981) show a decrease in TEC following the onset of the eclipse. Unique fluctuations were seen in records at times of scintillations and the extent of the belt of irregularities could also be estimated. On the eclipse night no irregularity patch could be observed.

**Keywords:** Total Electron Content; Differential Doppler Method; Appleton Anomaly

### INTRODUCTION

THERE are several methods for studying the total electron content (integrated columnar electron content per unit cross section) using satellite radio beacons. These are through the measurements of (1) Faraday rotation, (2) Group delay and (3) Differential Doppler. In the present study, TEC measurements have been made using Differential Doppler method during and after the total solar eclipse of 16 February 1980. A Georeceiver, commonly used for geodetic applications was employed for these measurements in a collaborative study between the Space Applications Centre, Ahmedabad and the Physical Research Laboratory, Ahmedabad. The experiment was conducted at the Nizamia Observatory, Rangapur, near Hyderabad, in the totality zone.

### EXPERIMENTAL DETAILS

The experimental details have been described in a separate report (Deshpande *et al*, 1980). The system essentially consists of two phase lock receivers at 400 MHz and

150MHz, a digital section and a digital cassette recorder. Simple vertical dipole antenna are used with preamplifiers to receive signals. The signals at 149.988MHz and 399.968MHz transmitted by US Navy Navigational satellites are received and suitably combined to give beat frequency which is known as differential doppler and is recorded on a paper chart. In addition, accurate time signal from the satellites once every two minutes is recorded on chart. The data are further analysed to obtain TEC values as described in the theory section. Digital information broadcast by the satellites are also recorded on cassette tapes which are later used to compute the sub-satellite points.

### THEORY

The transit time of a signal of frequency  $f$  Hz from a satellite to a ground observer is:

$$t = \frac{1}{c} \int_0^s n_g ds + \frac{40.3}{V_g f^2} \int_0^s N ds \quad \dots (1)$$

where  $V_g$  is the group velocity,  $c$  is the speed of light,  $n_g$  is the group refractive index and  $s$  is the slant range to the satellite and  $ds$  is an element of distance along the signal's path. The first term in equation (1) represents the transit time in free space whereas the second term represents the excess time delay due to the intervening ionization

If  $\chi_m$  is the zenith angle at  $h_{max} F_2$  then the second term can be expressed as:

$$P = \frac{40.3}{f^2} \sec \chi_m \cdot I \quad (2)$$

where  $I = \int N dh$ .

Differentiating equation (2) with respect to time and dividing by the free space wavelength ( $\lambda$ ) we have:

$$\frac{\Delta P}{\lambda} = \frac{40.3}{f^2} \left[ \sec \chi_m \dot{I} + I \frac{d}{dt} (\sec \chi_m) \right] \quad (3)$$

which is the ionospheric refraction frequency  $f_r$  and is experimentally known value Eq (7) can be written in the form

$$\dot{I} + f_1(t) I = f_2(t) \quad \dots (4)$$



$$\text{where } f_1(t) = \frac{d}{dt} (\text{Sec } \chi_m)$$

$$f_2(t) = \frac{f^2}{40.3} \frac{f_r(t)}{\text{Sec } \chi_m}$$

Thus the problem of determining TEC is reduced to solving the first order linear differential equation (4) for  $I(t)$  where the functions  $f_1(t)$  and  $f_2(t)$  are known functions of time. For this we need one boundary, namely the value of  $I$  at any time  $t$  which is also unknown.

We have used TEC values derived from Faraday rotation measurements at 136MHz which were made during the period of observations to solve this boundary value problem. If  $\Delta P_0$  is the group path at a time  $t_0$  measured by the differential Doppler technique and  $I_0$  the TEC measured by the Faraday rotation technique then:

$$\Delta P_0 = \frac{40.3}{f^2} \text{Sec } \chi_m I_0 \quad \dots (5)$$

If  $\Delta P$  is the group path at any instant ( $t$ ), near to, then we have:

$$\begin{aligned} \Delta P &= \Delta P_0 + \lambda \int \left( \frac{\Delta \dot{P}}{\lambda} \right) dt \\ &= \Delta P_0 + \lambda \int f_r(t) dt \quad \dots (6) \end{aligned}$$

## RESULTS

### (a) *Latitudinal Profiles of Total Electron Content (TEC)*

Differential Doppler measurements were carried out at Rangapur during 15–18 February 1980 using radio beacons (150 and 400MHz) from US-NNS satellites. Using these measurements a number of latitudinal profiles of TEC were obtained and are shown in Fig 1. Only that portion of each pass is utilized where the elevation is more than 20°. The latitudinal coverage is about 11°N to 23°N which includes the Appleton anomaly region. Profiles designated by 1, 2, 4, 5, 6, 10 and 13 correspond to the post-midnight or early morning hours. These profiles show absence of latitudinal gradients and the TEC value varies from 20 to 60 TEC units (1 TEC unit— $10^{16}$  el/m<sup>2</sup> column).

Rest of the profiles shown in Fig. 1 correspond to daytime hours and show equatorial anomaly at differential local times. The daytime values of TEC range from 80 to 130 TEC units.

On total solar eclipse day (16 February 1980) we could obtain six good profiles (4 to 9), out of which profile 3 is prior to eclipse onset and profile 9 is during the recovery phase of the eclipse. Both these profiles have been compared with the profiles obtained on 17 February 1980, around the nearest possible hours. This comparison is shown in Fig 2.  $\Delta$ TECs prior to eclipse have been calculated from profiles 8 and 11, whereas  $\Delta$ TECs during eclipse have been calculated from profiles 9 and 12. The local time differences at sub-ionospheric points for the first set (8 and 11) is about one hour and  $\Delta$ TEC values vary between 1 and 22 TEC units. (Table I). For the second set (9 and 12) though the local time difference is only 20 minutes, the  $\Delta$ TEC values

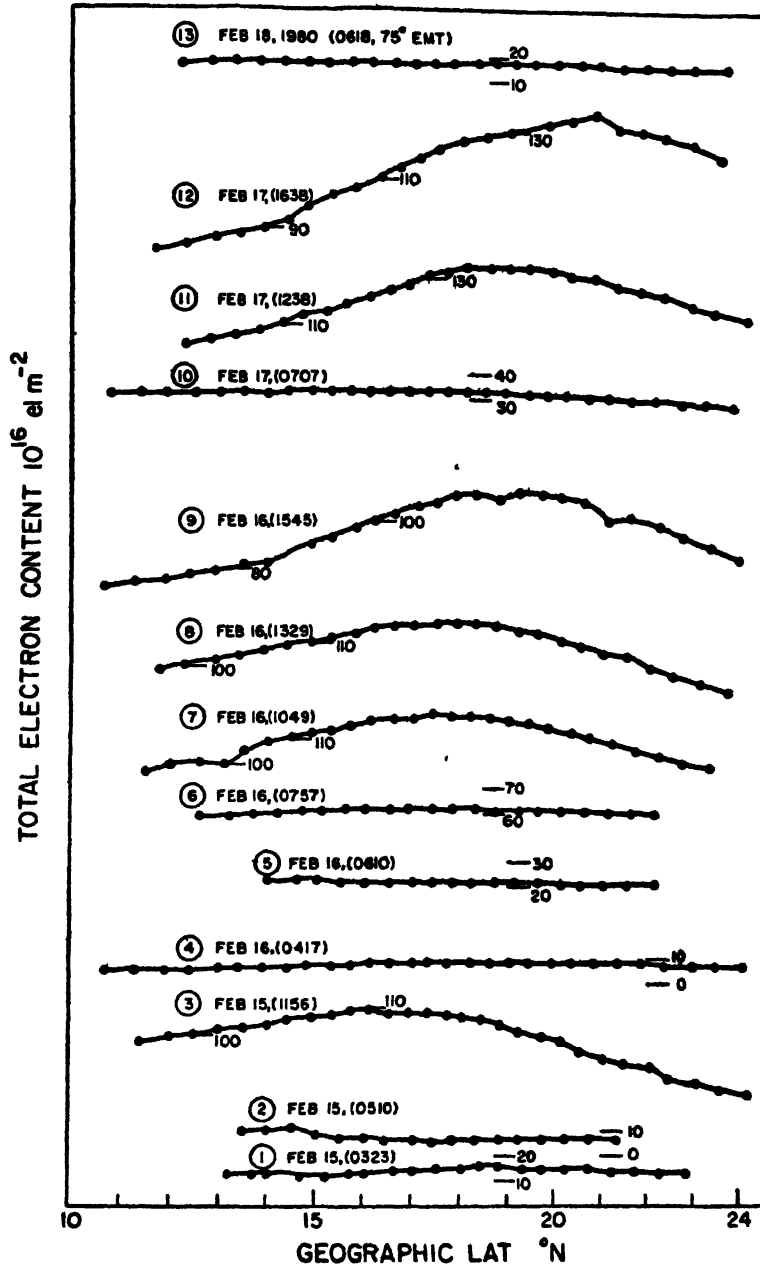


FIG 1. Latitudinal variation of TEC for satellite passes during the period 15-18 February 1980

are comparatively larger ranging between 5 and 32 TEC units. In both the cases  $\Delta\text{TEC}$  increases with latitude. The higher values of  $\Delta\text{TECs}$  from the second set (during eclipse) suggest a reduction in TEC due to solar eclipse. The development of the equatorial anomaly seems to be normal even on the eclipse day.

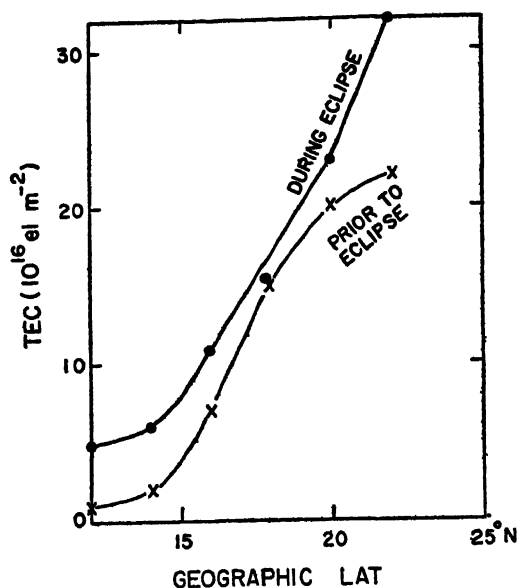


FIG 2 Latitudinal variation of  $\Delta\text{TEC}$  (difference between TEC 17 and 16 February 1980) from closest available passes (1) prior to the eclipse and (2) during the eclipse.

TABLE I  
TEC and  $\Delta\text{TEC}$  values ( $10^{16}$  el  $/\text{m}^2$  column)

Lat	Prior to Eclipse			During Eclipse		
	16 Feb.	17 Feb.	$\Delta\text{TEC}$	16 Feb.	17 Feb.	$\Delta\text{TEC}$
12	100	101	1	77	82	5
14	108	110	2	85	91	6
16	115	122	7	98	109	11
18	118	133	15	111	126	15
20	112	132	20	110	133	23
22	101	123	22	98	130	32

### (b) Irregularity Belts

During the differential doppler measurements, simultaneous amplitude measurements at 136MHz from ETS-2 were also carried out at the same location (Rangapur). Whenever amplitude of 136MHz showed violent fluctuation, the differential doppler too showed very unique fluctuations as shown in Fig 3.

These fluctuations are due to the presence of irregularities in the ionosphere. Since US-NNS satellites are orbiting, these measurements provide the extent of the belt of irregularities in the ionosphere. Thus the differential doppler technique could be used to estimate the presence and extent of ionization irregularities in the ionosphere. We examined the records of 15, 16 and 17 February 1980 for this purpose and noted that (a) on 15th there were two patches of irregularities, (b) on 17th there was one patch of irregularity; and (c) on eclipse night i.e., 16 there were no irregularities present. Although these results confirm the results reported by

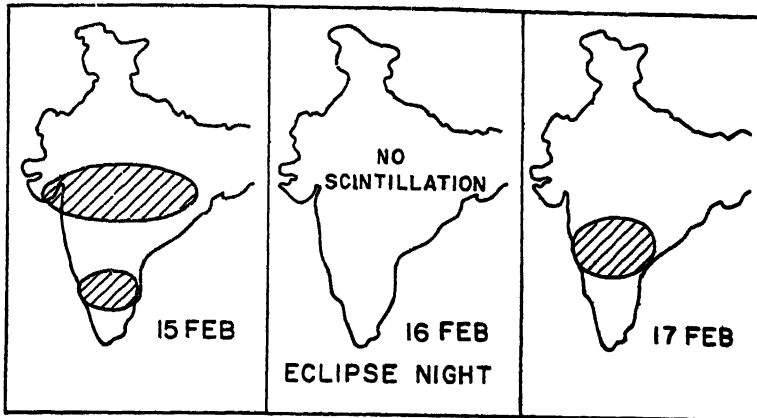


FIG. 3. Extent of ionospheric scintillation on 15, 16 and 17 1980.

Deshpande *et al.* (1980) for the same eclipse by another technique, namely the polarization scintillation, the present technique provides an excellent tool to estimate the latitudinal extent of the irregularities. Results further emphasize that the irregularities which could affect severely the propagation of VHF waves, confine themselves over the latitudes from equator to about  $25^{\circ}$  North and radio beacons from orbiting satellites could be used to study their extent.

#### DISCUSSIONS

Investigations of the eclipse effects on TEC at Ahmedabad, Rajkot, Poona and Rangapur during the total solar eclipse of 16 February 1980 were also made using the Faraday rotation measurements at 136 MHz using geostationary satellite ETS-2. Reduction of about (10 per cent) in TEC was noted at latitudes from Rangapur to Ahmedabad (Chandra *et al.*, 1980). The reduction inferred here comes out to be about 4 to 10 TEC units which again corresponds to about 3–8 per cent. Hence, these measurements are in close agreement with the TEC results using Geostationary satellites. However, the reduction of this magnitude is comparatively smaller than about 30 per cent reduction observed during the eclipse campaigns of 1969 and 1970 in United States (Marriott *et al.*, 1972). Probably the eclipse effects seem to be less marked at low latitudes.

#### ACKNOWLEDGEMENTS

The authors thank Dr T. A. Hariharan, Head, Geodesy Division and Professor P. D. Bhavsar, Chairman, Remote Sensing Area, Space Applications Centre, and Professor Yashpal, formerly Director, Space Applications Centre, Ahmedabad for their interest and encouragement for this work. Thanks are also due to Professor R. V. Bhonsle, Professor S. P. Pandya, and Professor D. Lal of Physical Research Laboratory, Ahmedabad for their encouragement and Professor K. D. Abhyankar and Dr B. Lokanadham of Nizamia Observatory, Hyderabad, for the facilities provided to

carry out the experiment successfully inside their campus, and to Shri K. C. Patel for computational assistance.

#### REFERENCES

- Chandra, H., Sethia, G., Vyas, G. D., Deshpande M. R., and Vats, H. O. (1981) *Indian J. Rad. Space Phys.* (In Press).
- Deshpande, M. R., Banshidhar, Vats, H. O., Sethia, G., Chandra, H., Baskaran, M., Jain, C. L., Sivaraman, M. R., Kothari, K. S., and Goyal Sheela, S (Mrs) (1980) Solar eclipse and its effects on total electron content over Indian sub-continent—differential doppler method. *Tech. Note*, PRL, Ahmedabad (1980)
- Marriott, R. T., St. John, D. E., Thorne, R. M., Venkateswaran, S. V., and Mahadevan, P. (1972) *J. atm. terr Phys*, **34**, 695.

Printed in India.

Electron Content

## EFFECTS OF THE TOTAL SOLAR ECLIPSE OF 16 FEBRUARY 1980 ON TEC AT LOW LATITUDES

M. R. DESHPANDE, H. CHANDRA, G. SETHIA, H. O. VATS *and* G. D. VYAS

*Physical Research Laboratory, Ahmedabad-380 009, India*

*and*

K. N. IYER *and* A. V. JANVE

*Department of Physics, Saurashtra University, Rajkot-360 005, India*

*(Received 14 February 1982)*

Polarimeters were set up at a few locations in India to record Faraday rotation of 136MHz radio beacon transmitted from the Geostationary satellite ETS-II, specifically to study the solar eclipse effects on the total electron content (TEC). The stations were situated at Rangapur in the totality zone and at Ahmedabad and Rajkot away from the totality. Decreases in TEC of about 8 per cent at Ahmedabad and Rajkot and about 20 per cent at Rangapur were observed with a time delay of about 20 minutes after the maximum obscuration. There is an increase in the slab-thickness following the eclipse. A search for eclipse induced TIDs showed a negative result. Polarisation scintillations were absent during the eclipse night.

**Keywords:** Total Electron Content (TEC); Polarimeter; TID; Polarisation Scintillation; ETS II

### INTRODUCTION

A chain of polarimeters was set up to investigate the ionospheric effects of the solar eclipse of 16 February 1980, through Faraday rotation measurements at 136MHz using radio beacon transmitted from the geostationary satellite ETS-II. The aims of the experiment were (1) to investigate the eclipse effects on total electron content (TEC) and (2) to detect any eclipse induced gravity waves which would interact with ionization and produce fluctuations in TEC. The details of polarimeters have been described earlier (Banshidhar *et al.*, 1977) and were set up at Rangapur (17°6'N, 78°43'E) in the totality zone and at Ahmedabad (23°02'N, 72°36'E) and Rajkot (22°19'N, 79°44'E) which were outside the totality. The locations are marked in Fig 1 which shows the path of totality in India and the various locations where Physical Research Laboratory had conducted experiments during the eclipse campaign. Rangapur experienced total solar eclipse for a duration of two minutes and nine seconds while both Ahmedabad and Rajkot had a maximum obscuration of 75 per cent.

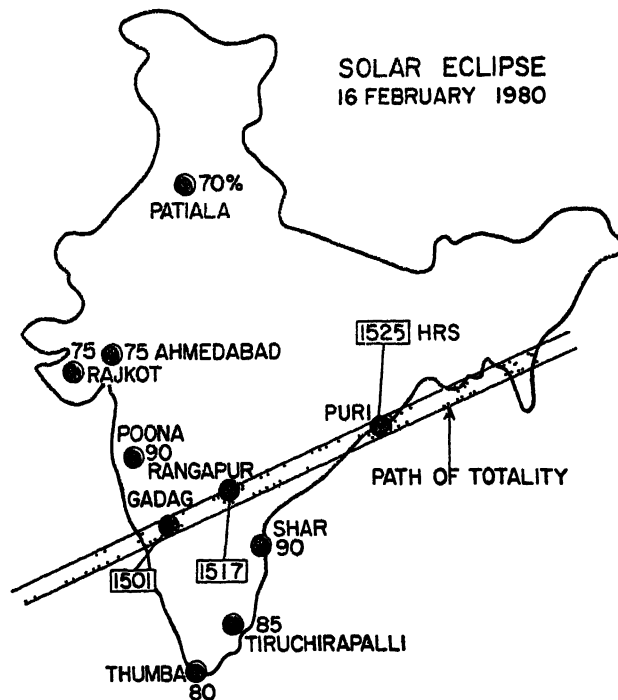


Fig. 1. Map of India showing the path of totality, locations of various experiments performed by PRL, alongwith percentage obscuration by the solar eclipse of 16 February 1980.

## RESULTS

### (a) *Changes in TEC*

TEC conversions were made assuming a mean field height of 400km. The daily variations of TEC on the eclipse day and on a control day (17 February 1980) at the three stations were derived from quarter hourly values. The decrease in TEC was very clear for Rangapur. For Ahmedabad and Rajkot the daily variation showed more than one peak because this eclipse was preceded by a magnetic storm and there was a tendency of two peaks one in morning and one around evening with a bite-out around noon on magnetically disturbed conditions at stations in the anomaly peak region. However, the second dip appears to be an eclipse effect. TEC at Ahmedabad and Rajkot was less on eclipse day than on a control day whereas for Rangapur opposite was the case. This again is due to the fact that 16 February was a disturbed day and in the anomaly crest region there would be a decrease in TEC while close to dip equator there would be an increase.

For calculations of the percentage change in TEC and the time delay involved TEC data were examined with sampling at every 3 minutes and a plot from 12hr to 17hr on eclipse day is shown in Fig. 2. The percentage change in TEC was about 17 per cent at Rangapur, 8 per cent at Rajkot and 7 per cent at Ahmedabad with time delays of 25 minutes, 15 minutes and 18 minutes respectively. These figures are also

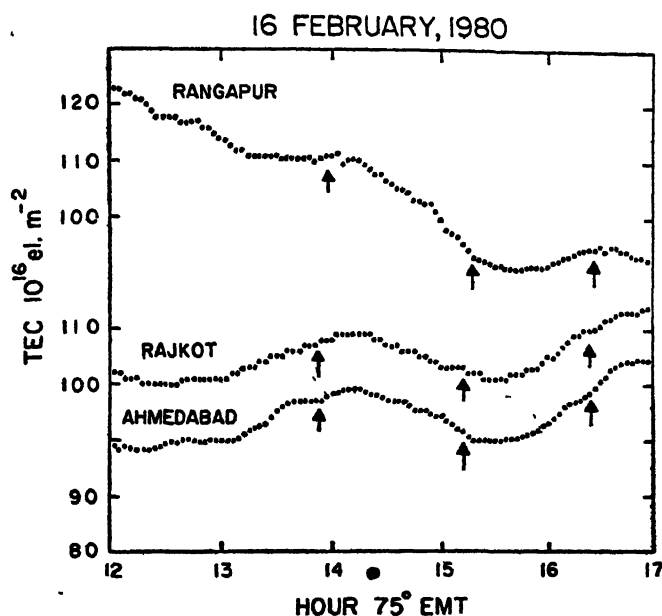


FIG. 2. Variation of TEC at Ahmedabad, Rajkot and Rangapur on 16 February 1980 during the period 12hr to 17hr based on data sampled every three minutes.

collected in Table I alongwith the maximum TEC on that day. The electron density profiles over Ahmedabad reduced from ionograms had shown time delay gradually increasing with altitude and reaching to about 40 minutes near F2-region peak (Chandra *et al.*, 1981) TEC being an integrated effect the observed delay is less than

TABLE I

*Location of stations and observed changes in TEC*

Station	Mean field height	Sub-ionospheric		$N_T$ (TEC) units	Per cent decrease ( $\Delta N_T$ )	Time delay in minutes
		latitude °E	Longitude °N			
Rangapur	400	81.9	14.3	125	17	25
Ahmedabad	400	80.2	21.0	115	7	18
Rajkot	400	78.9	20.4	115	8	15

near F2-peak. Eclipse campaigns in United States during 1969 and 1970 showed decreases of about 30 per cent with time delays varying between 20–50 minutes (Marriot *et al.*, 1972)

At Ahmedabad, ionosonde was in operation and it was possible to study the variations in the equivalent slab-thickness also. Daily variations of the TEC,  $N\tau$ , peak F2-region electron density  $N_m$  and the equivalent slab-thickness  $\tau$  ( $\tau = N\tau/N_m$ )



for Ahmedabad on 16 February 1980 are shown in Fig 3, which shows an increase in slab-thickness of nearly 100km due to the eclipse.

(b) *Eclipse Induced TIDs*

Generation of gravity waves by the shadow of moon as it moves supersonically across the earth's atmosphere had been predicted (Chimonas & Hines, 1970; and Chimonas 1970a, b). However, there has been a controversy about observing these

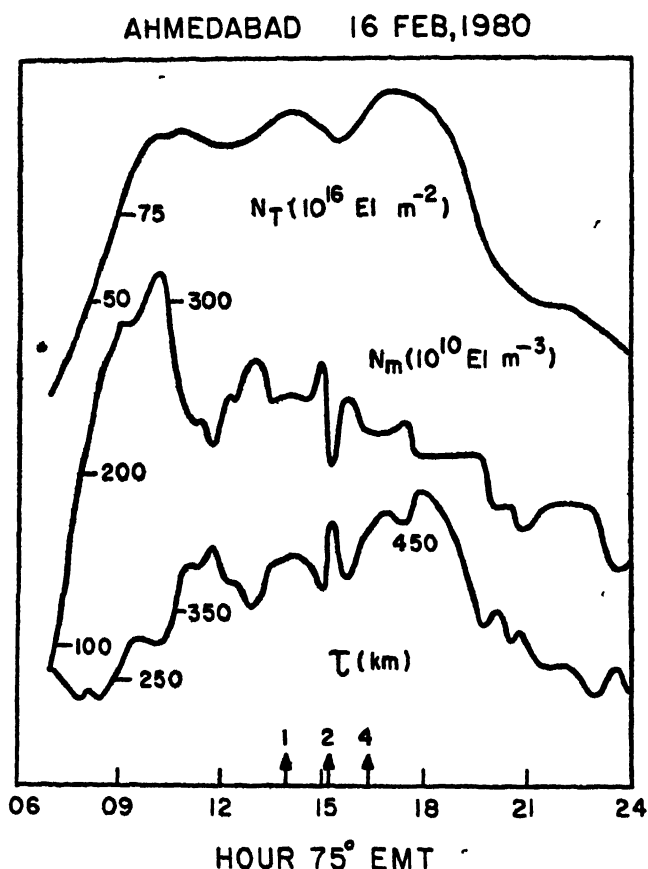


FIG 3. Daily variations of the TEC ( $N_T$ ), maximum E2-region electron density ( $N_m$ ) and equivalent slab-thickness ( $\tau$ ) at Ahmedabad for 16 February 1980

TIDs from TEC measurements (Sethia *et al*, 1980) and a conclusive evidence has yet to come. This chain of polarimeters was primarily set up to detect any TIDs associated with the eclipse.

To search for the eclipse induced fluctuations in TEC records for 16 February 1980 at the three stations have been sampled every 3 minute and computer plots shown in Fig. 4a. To remove the diurnal variation a running mean high pass filter with width of (9) minutes is used and the detrended fluctuations are also plotted in Fig. 4b.

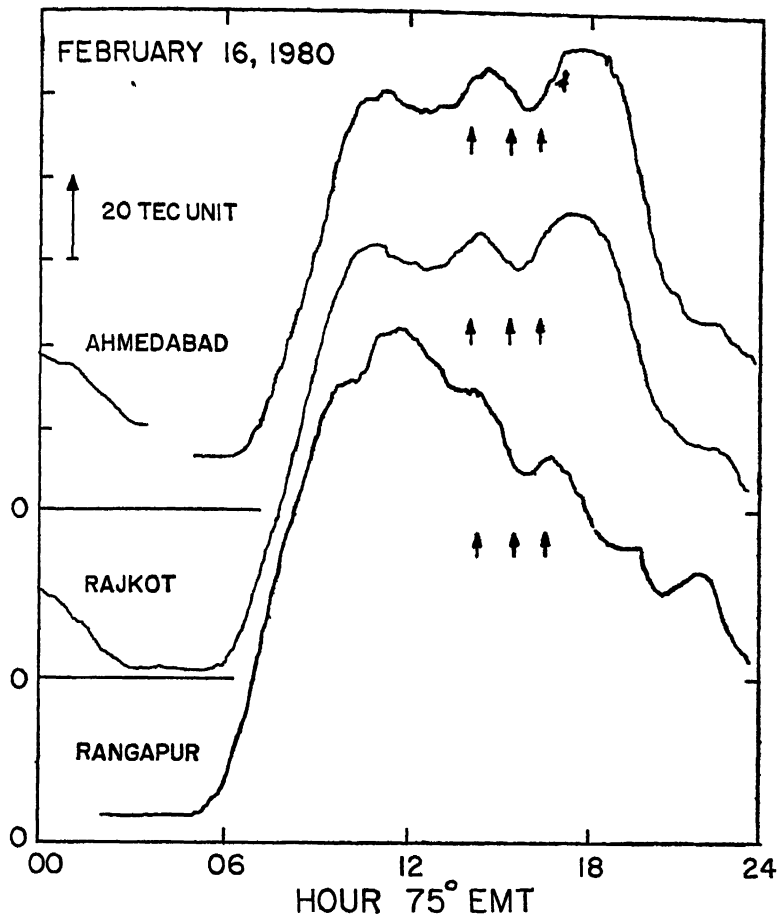


Fig 4a. Computer plots of the daily variations of TEC at Ahmedabad, Rajkot and Rangapur on 16 February 1980 based on data sampled every 3 minutes

There was no evidence of any eclipse induced fluctuation. Small fluctuations of the order of a fraction of a TEC unit were seen all throughout which are not significant considering the accuracy in scaling which is also of the same order. It must be added here that an earlier attempt to search for eclipse induced TEC fluctuations during the partial solar eclipse of April 1976 also showed negative results (Sethia *et al*, 1980). Taking into consideration the results of previous eclipse campaigns elsewhere it is now fairly certain that all these have failed to provide a conclusive evidence of eclipse induced fluctuations in TEC. Either gravity waves are not generated at all due to the eclipse or the TEC being an integrated effect is not sensitive enough to detect such fluctuations.

#### (c) *Polarisation Scintillations*

The Faraday rotation measurements at these stations showed polarisation scintillations on practically each night of the two weeks duration of measurements. How-

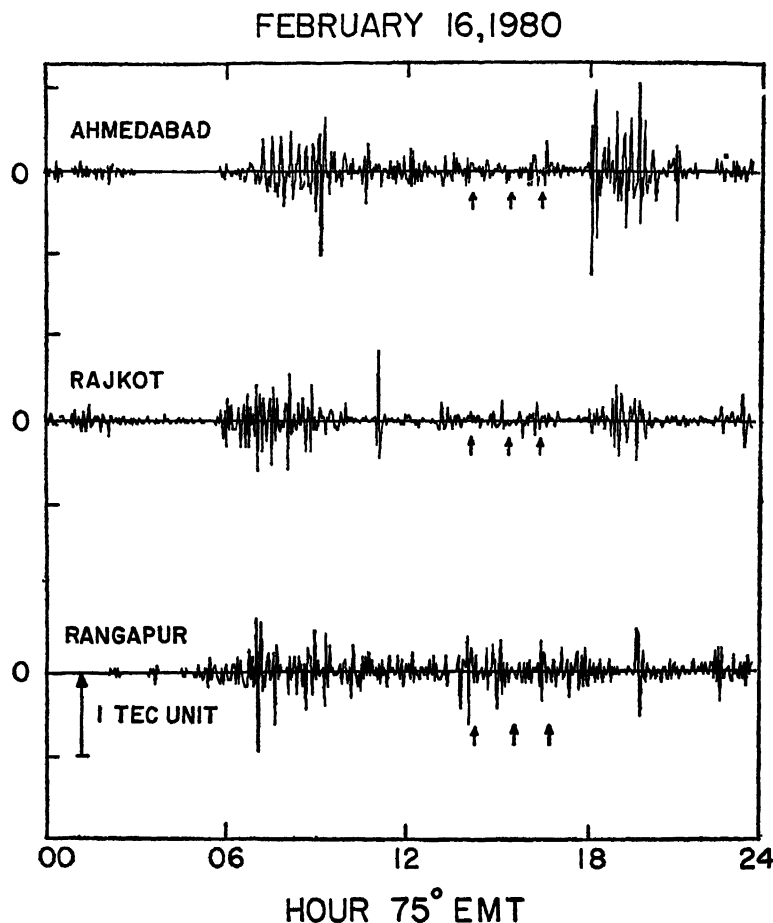


FIG. 4b. The detrended fluctuations in TEC using a high pass running mean filter of width 9 minutes are also shown in the same figure

ever, on eclipse night such scintillations were found to be absent. It must be noted here that the eclipse followed a magnetic storm and absence of scintillations is a storm effect rather than an eclipse effect. During high sunspot activity period magnetic activity is known to inhibit spread-F or scintillations at low latitudes (Chandra & Rastogi, 1972; Chandra & Vyas, 1978, and Chandra *et al.*, 1979)

#### ACKNOWLEDGEMENTS

The experiments were carried by Messrs Banshidhar, N M. Vadher, M B. Dadhania, H D. Parikh and V. D. Patel. We are grateful to Professor K. D Abhyankar, Director, Nizamia Observatory, Hyderabad and Dr B. Lokanadham for the facilities provided towards the experiment at their campus. Thanks are also due to Shri K. C. Patel for computational help

## REFERENCES

- Ball, S. M., Subbs, J. J., and Vincent, R.A. (1980) *J. atm. terr. Phys.*, **42**, 21.
- Banshudhar *et al.* (1977) *J. Inst. Telecom. Engrs.*, **23**, 708.
- Chandra, H., and Rastogi, R. G (1972) *Ann. de Geophys.*, **28**, 709
- Chandra, H., and Vyas, G. D. (1978) *Indian J. Rad. & Space Phys* , **7**, 263.
- Chandra, H , Vats, H. O , Sethia, G , Deshpande, M. R , Rastogi, R. G., and Hanumath Sastry, J. (1979) *Ann. de Geophys.*, **35**, 145.
- Chandra, H , Sethia, G., Vyas, G. D , Vats, H O., and Deshpande, M. R. (1981) *Indian J. Rad. Space Phys., (In Press)*
- Chimonas, G. (1970a) *Planet. Space Sci.*, **18**, 583.
- (1970b) *J. geophys Res.*, **75**, 5545.
- Chimonas, G., and Hines, C. O. (1970) *J. geophys. Res.*, **75**, 875.
- Marriot, R. J , St. John, D. E , Thorn, R. M., Venkateswaran, S. V., and Mahadevan, P. (1972) *J. atm. terr. Phys* , **34**, 695.
- Sethia, G., Chandra, H., and Deshpande, M. R. (1980) *Proc Indian Acad. Sci.*, **89**, 153.

Printed in India.

Electron Content

## TEC OBSERVATIONS AT WALTAIR DURING THE TOTAL SOLAR ECLIPSE OF 16 FEBRUARY 1980

P. V. S RAMA RAO, B. V. P. S. RAO, D. NRU and K. NIRANJAN

*Space Research Laboratories, Department of Physics, Andhra University,  
Waltair-530 003, India*

*(Received 17 August 1981)*

Faraday rotation measurements were made during total solar eclipse period of 16 February 1980 at Waltair (Lat 17.7°N, Long 83 3°E) using the VHF signal from the ETS-II (130°E long) geostationary satellite. The total electron content computed from the data has shown a 14 per cent depletion during the total obscuration (99 per cent) period. The minimum in the total electron content occurred 24 minutes after the maximum obscuration. The rate of decrease was found to increase by  $1.5 \times 10^{13}$  electron/m<sup>2</sup>/sec when the obscuration was reaching its maximum. The eclipse phenomenon did not seem to have produced any specific wavelike variations in TEC, since such variations are present on the days (15th and 17th) on either side of the eclipse day.

**Keywords:** TEC; Faraday Rotation; Gravity Waves

### INTRODUCTION

CONSIDERABLE work has been done using satellite data during solar eclipse periods. Beinstock *et al.* (1970) studied the TEC variations during solar eclipse of 7 March 1970 by recording the Faraday rotation angle of the VHF signals transmitted from ATS-1 and ATS-3 satellites at Miahualtan in Mexico. Klobucher and Malik also studied TEC variations during the same eclipse at Hamilton where the sun was 96 per cent obscured at the ground observing station, and found that the TEC was depleted by about 30 per cent and reached its minimum 20 minutes after the maximum obscuration. There were also other reports of similar nature of the same eclipse from different stations (Arendt, 1972, and Almeida & da Rosa, 1970).

Chimonas and Hines (1970) and Chimonas (1970) suggested that due to the movement of moon's shadow with supersonic speed, atmospheric gravity waves will be generated. This phenomenon was investigated by several workers. Davis and da Rosa (1970) and Chimonas and Hines (1971) observed gravity waves during solar eclipse whereas some workers such as Hunter *et al.* (1974), Schodel *et al.* (1973), Arendt *et al.* (1970) and Beckman and Clucas (1973) have reported the absence of gravity waves.

In the present paper we report the variations in the total electron content during the total solar eclipse period of 16 February 1980 obtained at Waltair (17 7°N, 83 3°E) by recording the Faraday rotation of the VHF signal from the ETS-II geostationary satellite (130°E longitude).

## DATA AND METHOD OF ANALYSIS

Records of the Faraday rotation angle obtained on a continuous basis are used to compute the total electron content. The mean magnetic field ( $M = 22.659$  MKS units), used, corresponds to a height of 420 km. The sub-ionospheric point of the observation is found to be at a latitude of  $16^{\circ}4'N$  and longitude of  $88^{\circ}3'E$ . The TEC data, thus obtained for the 15, 16 and 17 February 1980 are considered for the present study, where 15th and 17th are considered as control days. The diurnal variation of TEC calculated for each 15 minute interval for the three days of observation are utilized for studying the gross features observed in the eclipse data.

To study the variation of TEC during the eclipse, in greater detail, the Faraday rotation records are scaled at 2.5 minute intervals which are processed through a high-pass filter to remove the diurnal trend, using a computer programme. The detrended data are presented separately (Fig. 2) for examining wavelike variations in TEC.

## RESULTS AND DISCUSSION

At the present observing station the maximum obscuration was 99 per cent and it was about 40 km away from the edge of the totality path and the first contact is at 1437 hr, the maximum obscuration is at 1553 hr and the last contact is at 1658 hr local time.

In Fig. 1 is presented the diurnal variation of TEC for the 15, 16 and 17 February 1980. From this figure, it is clearly seen that there is a significant depletion in TEC during the eclipse period on 16th. The TEC started decreasing from 1445 hr i.e., 8 minutes after the first contact which continued upto 1617 hr i.e., 24 minutes after the maximum obscuration, from where the electron content started increasing upto 1658 hr i.e., the time of last contact and later it followed the regular diurnal trend of decrease in the late afternoon hours. The minimum value of TEC during the eclipse period is found to be  $63.8 \times 10^{16}$  electrons/m<sup>2</sup>, and the difference in electron content between the first maximum (the value at the time of the first contact) and this minimum is  $10.3 \times 10^{16}$  electrons/m<sup>2</sup> or a decrease of about 14 per cent. The difference in TEC values between the eclipse minimum and the second maximum (the value of TEC at the time of the last contact) is  $4.0 \times 10^{16}$  electrons/m<sup>2</sup> or an increase of 6.2 per cent.

The delay between the time of maximum obscuration and the time of the occurrence of minimum in TEC is also reported by many workers. Klobucher and Malik (1970) noticed a 20 minutes delay at Hamilton (95 per cent) during the solar eclipse of March 1970, Arendt *et al.* observed 23 minutes at Fort Monmouth. Flaherty *et al.* (1970) noticed 45 minutes delay while their theoretical computations showed a delay of 25 minutes. This delay in the occurrence of the minimum was attributed to the larger recombination times of electrons and ions in the F-region. Marriott *et al.* (1972) attributed the observed decreases in TEC values to the ionization transport, associated with the rapid cooling of the electron gas in the topside ionosphere.

*Loss and Recovery of Ionization during the Eclipse*

As most of the ionization is produced mainly by the solar ionizing radiations, it may be expected that there will be significant loss of ionization when the sun and its

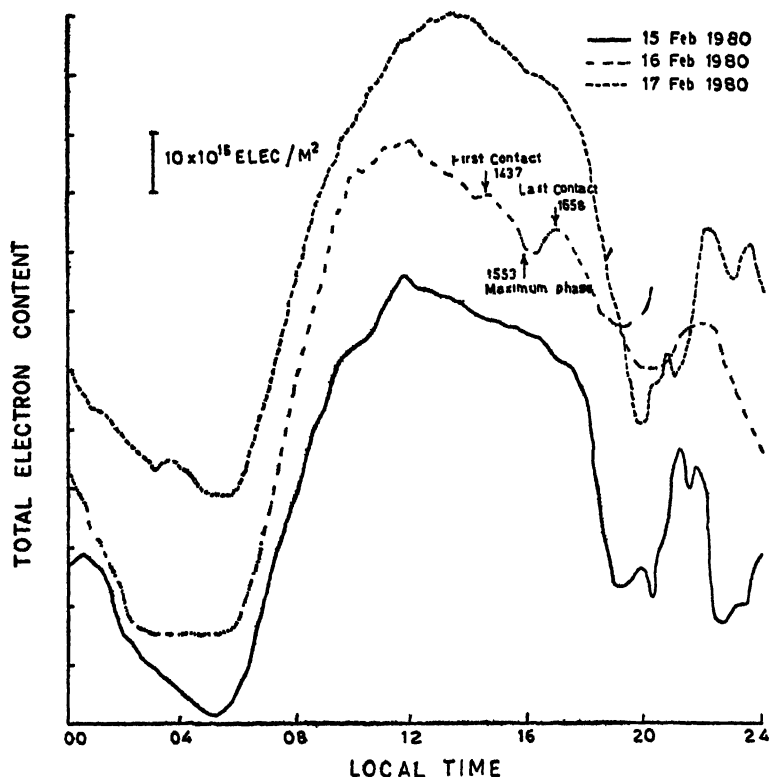


FIG. 1. Diurnal variation of total electron content for the 15, 16 and 17 February 1980 (Scales shifted to avoid overlapping)

radiations are obscured by the shadow of the moon during the solar eclipse period. In the case of the present eclipse, the starting and ending of the phenomenon has occurred during that portion of the diurnal variation of the total electron content where the ionization has already started decreasing at an average rate of about  $1.3 \times 10^{13}$  electrons  $\text{m}^2 \text{sec}^{-1}$ . After the onset of the eclipse, during the first one hour, i.e., from 1437 to about 1540hr the rate of decrease of ionization has increased to about  $1.7 \times 10^{13}$  electrons  $\text{m}^2 \text{sec}^{-1}$ . This increase in the loss rate may be mainly due to the decrease in the production owing to the decrease in the intensity of the solar ionizing radiations. From 1540 to 1617hr, i.e., upto 24 minutes after the maximum obscuration, the loss of ionization was found to increase much faster i.e., about  $2.8 \times 10^{13}$  electrons  $\text{m}^2 \text{sec}^{-1}$ . This increase in the loss rate may be due to the fast cooling of the atmosphere around the total obscuration period of the sun. The ionization recovered to its normal value, increasing at a rate of  $2.5 \times 10^{13}$  electrons  $\text{m}^2 \text{sec}^{-1}$  almost at the same rate at which it was lost just before total obscuration.

Another phenomena of interest is to study the gravity wave induced perturbations in TEC. In Fig 2 is shown the detrended TEC values for 15, 16 and 17 February 1980. From this figure it is clearly seen that there are quasiperiodic variations on all the three days of observation. Since wavelike variations in TEC are

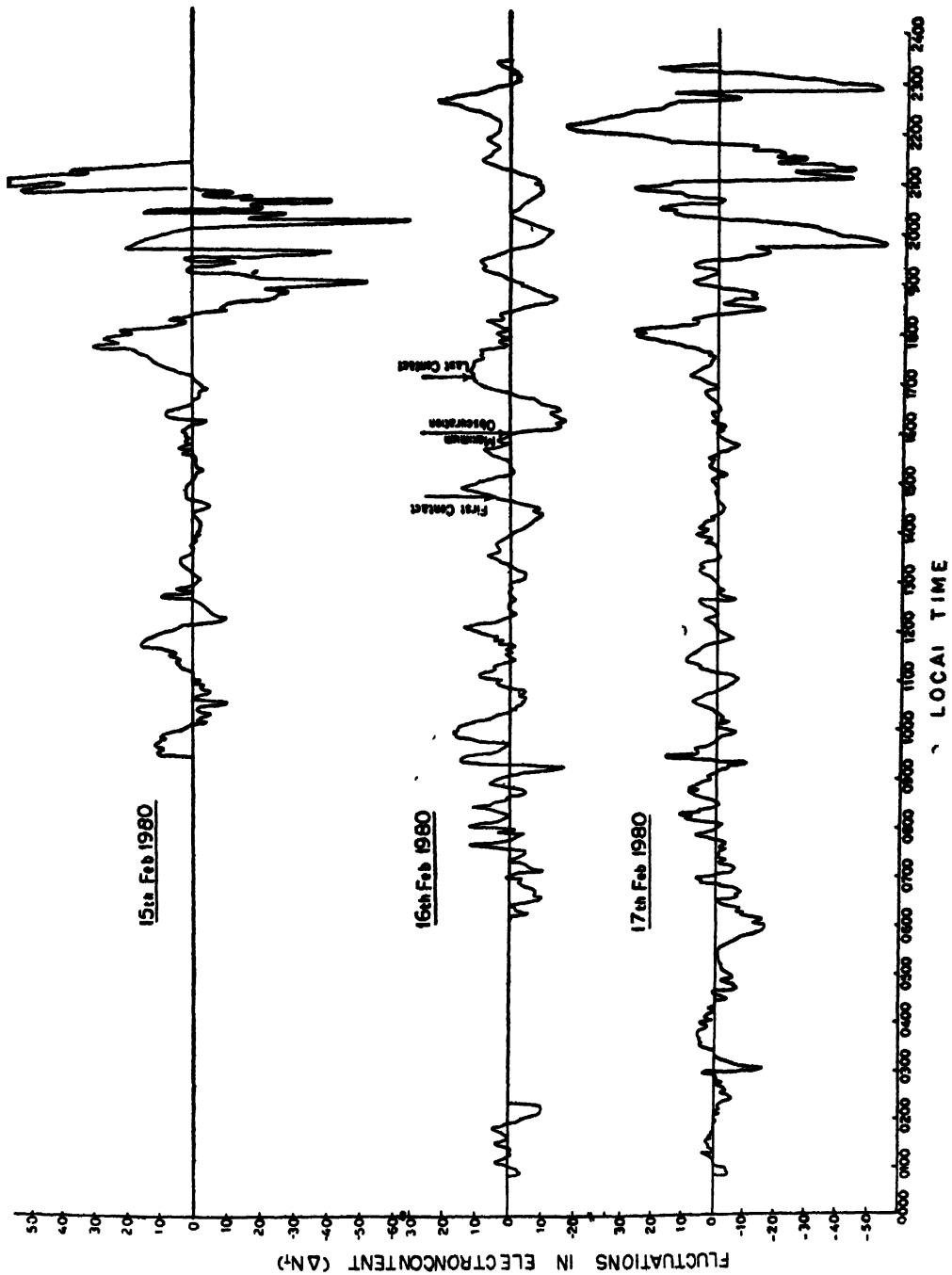


FIG 2 Plots of the detrended values of total electron content for 15, 16 and 17 February 1980.



present even before the starting of the eclipse, it is difficult to say that these wavelike variations are induced due to eclipse. Further, it is interesting to note that the amplitude of fluctuation of the observed variations in TEC during the night time period of the control days are much larger compared to those on the eclipse day. Strikingly enough, this is due to the absence of scintillations on the night of the eclipse day. Sethia *et al.* (1980) recorded Faraday rotation and differential doppler during partial solar eclipse of 29 April 1976 and reported that they did not notice the presence of gravity waves at Ootacamund, Patiala, Bombay, Ahmedabad and Udaipur, but they reported the presence of gravity waves at Trivandrum, an equatorial station.

Further, it is interesting to note that there are no scintillations on the eclipse day while severe scintillations are observed during the nights of both 15 and 17 February 1980. Spread-F observations made at 5.6 MHz at this station also show the absence of spread-F on the eclipse day while it is seen on the adjacent days.

#### ACKNOWLEDGEMENTS

The authors express their sincere thanks to the UGC and the CSIR for the financial assistance provided to carry out the experiment. They also wish to express their thanks to Mr B. V. Ramana Rao and Mr A. V. V. Satyanarayana Murthy for their assistance in the conduct of the experiment.

#### REFERENCES

- Almeida, O. G., and da Rosa, A. V. (1970) Observations of ionospheric electron content during the March 7, 1970 solar eclipse *Nature*, **226**, 1115.
- Arendt, P. R. (1972) Ionospheric undulations during the solar eclipse of 7 March 1970 *J. atm. terr. Phys.*, **34**, 719.
- Arendt, P. R., Gorman Jun, F., and Sonchar, H. (1970) Synoptic review of ionospheric data taken at Fort Monmouth, New Jersey during the eclipse, *Nature*, **226**, 1114.
- Beckman, J. E., and Clucas, J. I. (1973) Search for atmospheric gravity waves induced by the eclipse of June 30, 1973. *Nature*, **246**, 412.
- Beinstock, B. J., Marriott, R. T., St John, D. E., Thorne, R. M., and Venkateswaran, S. V. (1970) Changes in the electron content of the ionosphere *Nature*, **226**, 1111.
- Chimonas, G. (1970) Internal gravity wave motions induced in the earth's atmosphere by a solar eclipse. *J. geophys. Res.*, **75**, 5545.
- Chimonas, G., and Hines, C. O. (1970) Atmospheric gravity waves induced by a solar eclipse. *J. geophys. Res.*, **75**, 875.
- (1971) Atmospheric gravity waves induced by a solar eclipse *J. geophys. Res.*, **76**, 7003.
- Davis, M. J., and da Rosa, A. V. (1970) Possible detection of atmospheric gravity waves generated by the solar eclipse *Nature*, **226**, 1123.
- Flaherty, B. J., Cho, H. R., and Yeh, K. C. (1970) Response of the F-region ionosphere to a solar eclipse. *Nature*, **226**, 1121.
- Hunter, A. N., Holman, B. K., Feldgate, D. C., and Kelleher, R. (1974) Faraday rotation studies in Africa during the solar eclipse of June 30, 1973. *Nature*, **250**, 205.
- Klobuchar, J. A., and Malik, C. (1970) Comparison of changes in total electron content along three paths *Nature*, **226**, 1113.
- Marriott, R. T., St John, D. E., Thorne, R. M., Venkateswaran, S. V., and Mahadevan, P. (1972) Ionospheric effects of two recent solar eclipses *J. atm. terr. Phys.*, **34**, 695.
- Schodel, J. P., Klostermeyer, J., and Rottger, J. (1973) Atmospheric gravity wave observations after the solar eclipse of June 30, 1973 *Nature*, **245**, 87.
- Sethia, G., Chandra, H., and Deshpande, M. R. (1980) On the effect of the partial solar eclipse of 29 April 1976 on electron content *Proc. Indian Acad. Sci.*, **89**, 153.

Printed in India.

Electron Content

## IONOSPHERIC ELECTRON CONTENT CHANGES NEAR THE CREST OF THE EQUATORIAL ANOMALY DURING THE TOTAL SOLAR ECLIPSE OF 16 FEBRUARY 1980

A. MAITRA, S. K. DAS\*\*, A. DAS GUPTA\* and M. K. DAS GUPTA

*Institute of Radio Physics and Electronics, University of Calcutta,  
Calcutta-700 009, India*

*(Received 17 August 1981)*

The results of observations on the behaviour of ionospheric electron content during the total solar eclipse of 16 February 1980 obtained from the Faraday rotation measurements of a VHF satellite signal in Calcutta, which is situated below the northern crest of the equatorial anomaly, are presented. A small decrease of 5-6 per cent from the ambient level of the ionospheric total content around the time of totality and a prominent peak following the above have been obtained. The results are examined in the light of the phenomenon of the plasma transport connected with the Appleton anomaly.

**Keywords:** Ionospheric Electron Content (IEC); Appleton Anomaly; Faraday Rotation; VHF Satellite Signal.

THE measurement of the total electron content (TEC) by monitoring the Faraday rotation of a VHF satellite signal is one of the most popular and effective techniques for studying the F-region of eclipsed ionosphere. The investigations in respect of ionospheric effects have been carried out mainly on (1) eclipse induced gravity waves which might have a signature in the form of travelling ionospheric disturbances (TIDs) as suggested by Chimonas and Hines (1970) and (2) depletion in total ionization near the time of totality. The eclipse of 7 March 1970 in the North American Zone is the first widely studied eclipse using satellite beacons. The different groups, mostly from mid latitudinal stations, reported total ionization depletions associated with the eclipse in the range of 20-30 per cent for this eclipse (Klobuchar & Malik, 1970; Almeida & da Rosa, 1970, and Flaherty *et al*, 1970). For the solar eclipse of 30 June 1973, observations made by several groups were mainly in respect of eclipse induced gravity waves, while TEC depletion associated with the obscuration were not explicitly reported. However, Hunter *et al* (1974) apparently observed small depletions at low latitudes for the same eclipse. In the light of earlier eclipse observations, it is to be noted that although some information regarding eclipse induced ionization depletion is available for mid latitudes, the same for low latitudes is sparse.

---

\* *At present* NAS/NRC Senior Resident Research Associate, AFGL(PHP), Hanscom AFB, MA 01731, U.S.A. on leave from the University of Calcutta.

\*\*Also at Acharya P. C. College, New Barrackpore, W. Bengal.

During the total solar eclipse of 16 February 1980, the Institute of Radiophysics and Electronics of Calcutta University monitored the Faraday rotation of 136MHz signal from the geostationary satellite ETS-2 at a multistation network around Calcutta and near the path of the totality. The null result in search of the eclipse induced TIDs has recently been reported by Das Gupta *et al.* (1981) for the same eclipse observations. This paper presents some results on the behaviour of total ionization around the time of totality over Calcutta (Geographic lat: 23°N, long: 88 5°E, dip: 32°N), which is situated below the northern crest of the equatorial anomaly, and also to compare the same with some other eclipse observations. In the case of present eclipse the totality occurs in the subionospheric height range of 100–200km, whereas the mean ionospheric height of 400km used for the TEC computation lies close to the path of totality (98 per cent).

Fig. 1 shows the behaviour of TEC variation on the eclipse day in relation to the normalized mean curve for February 1980 obtained at Haringhata (Calcutta). It has been found that the eclipse day TEC variation exhibits a departure from the

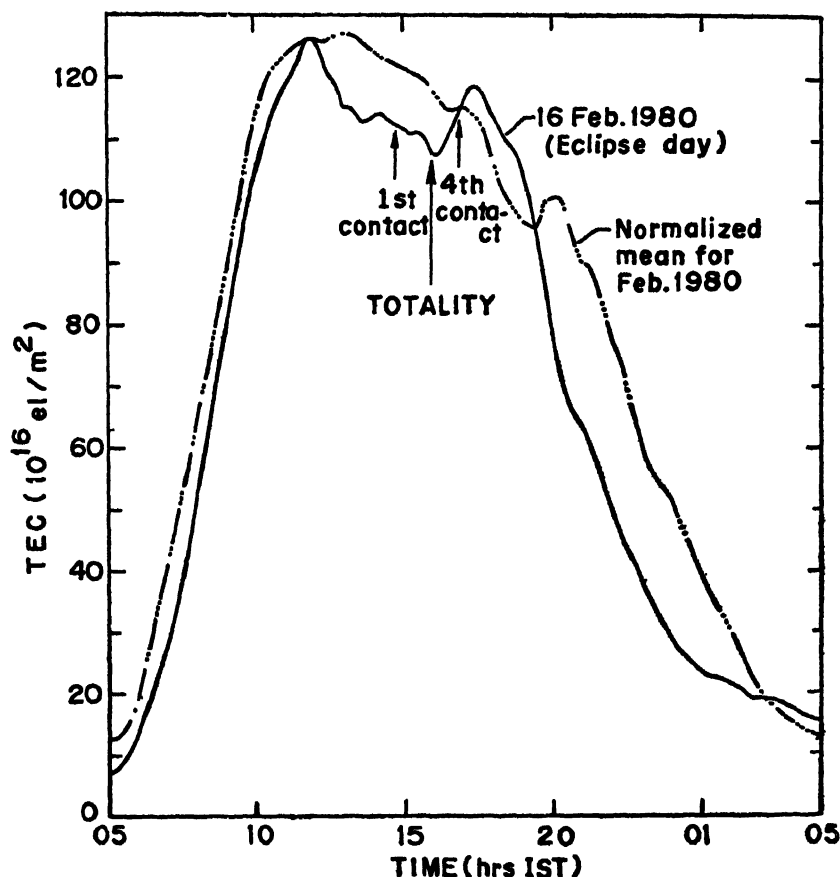


FIG. 1 Total electron content variation on the eclipse day in relation to the normalized mean variation for February 1980.

mean curve even before the start of the eclipse. A depletion around the time of totality and a prominent peak following it could also be noted therein. Some unusual fluctuations have been observed before the time of totality which may be attributed to the magnetic disturbances present on the eclipse day. These fluctuations as well as the prominent rise immediately after the totality have rendered the estimate of the eclipse induced TEC depletion somewhat uncertain and subjective. However a depletion of 5-6 per cent of the ambient level has been approximated around the time of totality in the present case. The percentage deviations during the time of obscuration as obtained from the high pass filter residues of TEC data are depicted in Fig. 2.

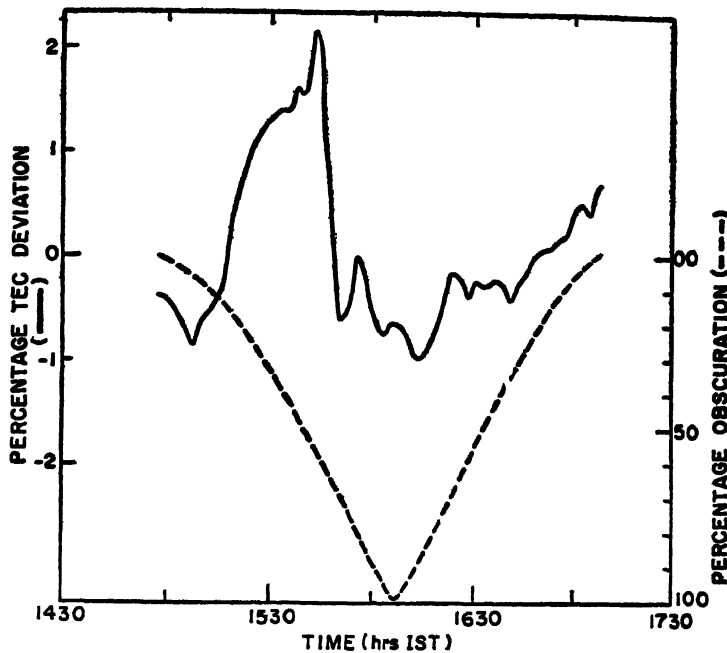


FIG 2 Percentage TEC deviations in relation to percentage obscurations.

Although some small amplitude TIDs have been observed before the totality, no TID of significant amplitude could be detected after the eclipse. The trough on TEC deviation curve around the time of maximum obscuration could be identified as the eclipse effect.

The TEC depletion obtained in the present case is much smaller compared to that reported for mid latitudinal stations during previous eclipses. An earlier ionosonde observation at the present location on a partial solar eclipse occurring in the morning hours also revealed a much higher depletion (26 per cent) in F2 ionization (Datta *et al*, 1959). But it is important to note here that the production of plasma is the dominating phenomenon in the morning hours, whereas the transport of plasma is dominating in the afternoon hours. Again plasma transport at a location depends on the local time and the geomagnetic field orientation. The present observing station being situated below the equatorial anomaly crest and the eclipse having taken place

in the afternoon hours, the processes connected with the afternoon phase of the equatorial anomaly have probably masked the eclipse induced perturbation. The prominent peak in TEC immediately following the totality is possibly due to the reappearance of the anomaly crest during its decaying phase in the afternoon hours.

For the present eclipse, Chandra *et al.* (1981) reported an eclipse induced TEC depletion of 15–20 per cent as obtained at Ahmedabad which has a geomagnetic location similar to Calcutta. It may be mentioned here that the subionospheric point for Calcutta is nearer to the totality belt compared to that for Ahmedabad. Moreover, maximum obscuration occurred about 30 minutes earlier at Ahmedabad. Bienstock *et al.* (1970), observing over two beacon paths, also obtained less depletion for a location nearer to the totality belt. It should be further noted that for the present eclipse, more of the bottomside ionosphere is obscured at Calcutta, whereas at Ahmedabad more of the topside is obscured. In view of the high value of  $h_m F_2$  during present high solar activity period, the effect of obscuration of the ionosphere on total electron content is expected to be greater at Ahmedabad than at Calcutta in the present case.

The amplitude of the afternoon peak, in terms of the percentage increase of TEC around 1730hr from the TEC value at 1600hr, has been found to be the highest on the eclipse day in the month of February 1980. This may be in conformity with that fact that the equatorial anomaly, as obtained from the multistation observations over the Indian subcontinent, was fairly well developed (Singh, Lakha, 1981, *private commun.*) The eclipse day being a magnetically disturbed one, the equatorial anomaly should have generally been inhibited (Basu & Das Gupta, 1968). However, the development of the Appleton anomaly depends mainly on the electrojet strength (Deshpande *et al.*, 1977), which may be weak or strong independent of the magnetic activity conditions (Kane, 1976). It may also be relevant to note here that Huang (1974) found evidences of large amount of plasma transport to the subtropical region after one hour from the start of the eclipse, as a result of the rapid change of  $h_m F_2$  over the equator during a high solar activity period.

#### ACKNOWLEDGEMENTS

The authors are indebted to J. A. Klobuchar and Air Force Geophysics Laboratory, Mass., U.S.A. for the help in providing the obscuration data for the eclipse.

#### REFERENCES

- Almeida, O. G., and da Rosa, A. V. (1970) Observations of ionospheric electron content during the March 7, 1970, solar eclipse *Nature*, **226**, 1115.
- Basu, S., and Das Gupta, A. (1968) Latitude variation of electron content in equatorial region under magnetically quiet and active conditions *J. geophys. Res.*, **73**, 5599.
- Bienstock, B. J., Marriott, R. T., St. John, D. E., Throne, R. M., and Venkateswaran, S. V. (1970) Changes in the electron content of the ionosphere *Nature*, **226**, 1111.
- Chandra, H., Sethia, G., Vyas, G. D., Deshpande, M. R., and Vats, H. O. (1981) Ionospheric effects of the total solar eclipse of 16 February 1980 *Proc. Indian natn. Sci. Acad.*, **47**, A, No 1, 57.
- Chimonas, G., and Hines, C. O. (1970) Atmospheric gravity waves induced by a solar eclipse *J. geophys. Res.*, **75**, 875.

- Das Gupta, A., Maitra, A., Das, S. K., and Sen, S. K. (1981) Ionospheric electron content observations during the total solar eclipse of February 16, 1980. *J. atm. terr. Phys.*, **43**, 135
- Datta, S., Bandyopadhyay, P., and Datta, R. N. (1959) Ionospheric observations on the F-region during the solar eclipse of 19 April 1958. *J. atm. terr. Phys.*, **16**, 182
- Deshpande, M. R., Rastogi, R. G., Vats, H. O., Klobuchar, J. A., Sethia, G., Jain, A. R., Subbarao, B. S., Patwari, V. M., Janve, A. V., Rai, R. K., Singh, Malkat, Gurm, H. S., and Murthy, B. S. (1977) Effect of electrojet on the total electron content of the ionosphere over the Indian subcontinent. *Nature*, **267**, 599
- Flaherty, B. J., Cho, H. R., and Yeh, K. C. (1970) Response of the F-region ionosphere to a solar eclipse. *Nature*, **226**, 1121
- Huang, C. M. (1974) The effect of upward plasma drift on the F2-layer during the solar eclipse. *J. atm. terr. Phys.*, **36**, 1701
- Hunter, A. N., Holman, B. K., Flegate, D. G., and Kelleher, R. (1974) Faraday rotation studies in Africa during the solar eclipse of June 30, 1973. *Nature*, **250**, 205.
- Kane, R. P. (1976) Geomagnetic field variations. *Space Sci. Rev.*, **18**, 413.
- Klobuchar, J. A., and Malik, C. (1970) Comparison of changes in total electron content along three paths. *Nature*, **226**, 1113

Printed in India.

Electron Content

## RESPONSE OF THE TOTAL ELECTRON CONTENT OF THE IONOSPHERE OVER NORTH AMERICA TO THE TOTAL SOLAR ECLIPSE OF 26 FEBRUARY 1979\*

E. A. ESSEX†, J. A. KLOBUCHAR and C. R. PHILBRICK

*Air Force Geophysics Laboratory, Hanscom AFB, MA 01731, U.S.A.*

and

R. LEO

*Electronics Research Laboratory, Montana State University  
Bozeman, Montana 59715, U.S.A.*

(Received 17 August 1981)

Ionospheric total electron content (TEC) observations were carried out from eight stations during 26 February 1979 total solar eclipse over North America. The TECs were determined from the Faraday rotation of the plane of polarization of the VHF signal from geostationary satellites. Local times of totality of the eclipse in the ionosphere observed from the various stations ranged from 0734hr to 1400hr. Depletion of the ionospheric total electron content from the non-eclipse average behaviour varied up to a maximum of 40 per cent for the ionosphere experiencing 100 per cent eclipse. Maximum TEC depletion occurred on average 33 minutes after maximum contact. Most of the stations showed a rapid rate of depletion of TEC about 30 minutes after first contact, the rate of depletion reaching a minimum value at or before maximum obscuration. Before fourth contact was reached, the rate of increase of TEC generally had overshoot the non-eclipse day average, gradually returning to that average after the fourth contact. Using ionosonde data, it was found that the peak density of the F-region and the TEC varied by approximately the same amount at those stations for which the E-region had formed before first contact of the eclipse. Slab thicknesses were not significantly changed during the eclipse.

**Keywords:** Total Electron Content; Faraday Rotation; Plane of Polarization; VHF Signal; Geostationary Satellite; Ionograms

### INTRODUCTION

EARLY research into ionospheric eclipse effects revolved around ground based techniques such as vertical incidence ionosondes and fixed frequency transmissions (Beynon & Brown, 1956). These techniques have now been supplemented by rocket and satellite studies as well as incoherent backscatter measurements (Rishbeth, 1968;

---

\*Invited Paper.

†Currently an NRC/NAS Senior Resident Research Associate on leave from La Trobe University, Bundoora, Vic 3083, Australia.

and *J. atm. terr. Phys.*, 34(4), 1972). The advent of geostationary satellites in conjunction with ionosonde measurements have enabled a more detailed study of the spatial and temporal variation of the eclipse effects to be performed (Klobuchar & Malik, 1970). Recently, interest has centered on the production of artificial holes in the ionosphere produced by rockets (Mendillo *et al.*, 1975, 1979) and the space shuttle (Mendillo *et al.*, 1978).

The total solar eclipse of 26 February 1979 provided an opportunity to study the response of the F-region of the ionosphere over North America during the production of a naturally occurring hole. Previous eclipses have produced both increases in the peak density of the F-regions (Evans, 1965) and decreases (Marriott *et al.*, 1972).

#### OBSERVATIONS

Ionospheric total electron content (TEC) observations were carried out from eight stations during 26 February 1979 total solar eclipse over North America. The TEC was determined from the Faraday rotation of the plane of polarization of the VHF signal from a suitably located geostationary satellite, using the method of Titheridge (1972). From one of the stations, Hamilton, observations were made using four satellites. Fig 1 shows the location of the stations together with the 420km sub-

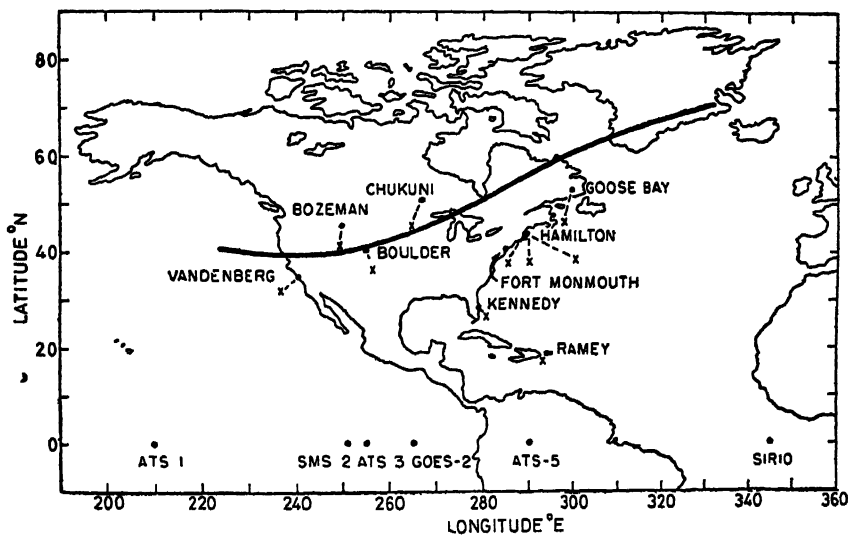


FIG 1. Map showing the centre line of path of totality at 420km for 26 February 1979 solar eclipse over North America. The TEC stations are shown together with the 420km sub-ionospheric points (crosses) along the ray paths to the geostationary satellites. The nominal sub-satellite positions of the various geostationary satellites are also shown.

ionospheric point along the ray path to the satellite. The sub-satellite locations of the satellites are also shown. The continuous line indicates the centerline path of totality of the eclipse at 420km. Table I lists the TEC stations, satellite beacons, and the 420km sub-ionospheric points and their invariant latitudes. As well, ionosonde stations and their locations are indicated.



TABLE I  
Total electron content observation sites and ionosonde locations

TEC Station	Satellite	Latitude °N	420km sub-ionospheric point	
			Longitude °W	$\Delta$ °N
Goose Bay	ATS-5	46.2	62.4	60
Chukuni	ATS-3	45.6	95.5	58
Bozeman	SMS-2	41.3	110.5	51
Hamilton	ATS-3	38.5	75.9	53
	SMS-2	38.5	76.7	53
	SIRJO	38.1	59.8	51
	ATS-5	37.9	70.7	53
	GOES-2	36.5	104.0	47
Boulder	ATS-1	31.8	123.8	39
Vandenberg	ATS-5	26.3	79.6	41
Ramey	ATS-5	17.1	67.4	36

Ionosonde Station	Latitude °N	Longitude °W	$\Delta$ °N
Fort Monmouth	40.2	74.1	53
Boulder	40.1	105.2	49
Vandenberg	34.8	120.5	40
Goose Bay	53.3	60.5	63

For the two stations located in the path of totality, Chukuni and Bozeman, the time sequences of the eclipse along the ray paths from 0 to 1000km are shown in Fig. 2(a) and 2(b). For Chukuni, totality extended almost to 900km, whereas for

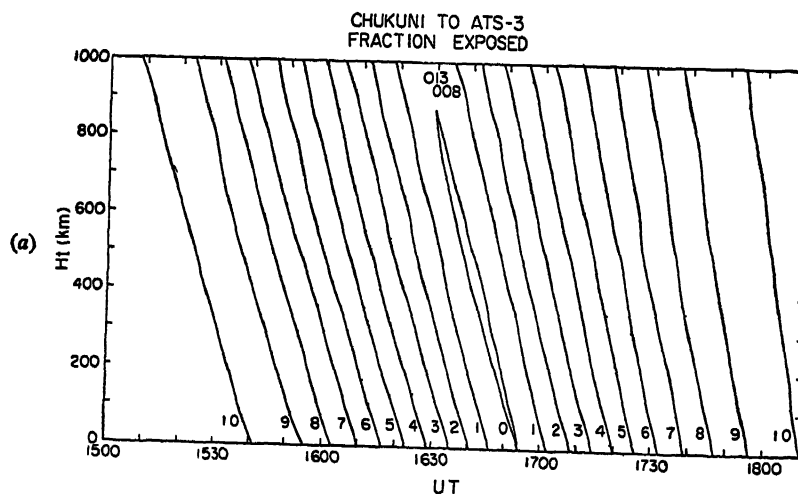


FIG. 2. Time sequences of the fraction exposed of the solar disc during the total solar eclipse of 26 February 1979 along the ray paths from 0 to 1000km for (a) Chukuni and (b) Bozeman.

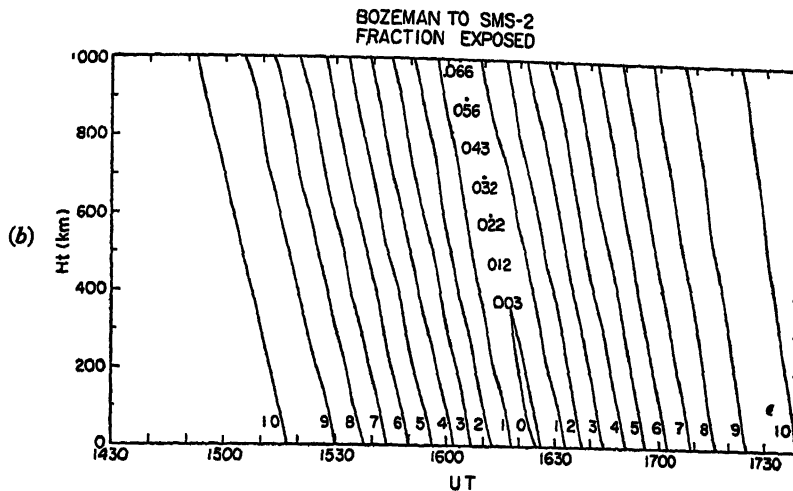


FIG. 2. (For caption see p. 446)

Bozeman, it reached almost 400km. For both stations, the contact times occurred at earlier times with increasing height.

Ionogram data from Fort Monmouth, Boulder, Vandenberg and Goose Bay were also used to investigate the bottomside changes during the eclipse.

## RESULTS

### (a) Total Electron Content

Figs. 3(a), (b) and (c) show the TEC results for the eight stations. Also shown in Figs. 3(a) are the Fredericksburg K indices for 26 February 1979. A magnetic storm had occurred on 22 February and the day of 26 February was still showing moderate activity. Numerous small substorms were reported from 0845 UT to 1900 UT. For the TEC results shown in Fig. 3, the continuous lines are the results for 26 February, the dashed lines are the average for several days around the eclipse day, and the crosses indicate TEC curves which have been obtained from the averages by normalization at a suitable time to the TEC curves for 26th. This procedure was adopted if the average curves differed markedly from the curves for the eclipse day. Arrows on each plot indicate the time of first contact, maximum obscurations, and last contact of the eclipse at a height of 300km. The eclipse day TEC values were taken at five minute intervals from 14 to 21 hours UT, all other data being taken at fifteen minute intervals. For each station, the average curve was derived from available data, this varied from two to six days around the eclipse day.

The time variation of the eclipse at 300km height for the ray path to the satellite for each observation from the stations together with the deviation of the TEC,  $\Delta N_t$ , from the average curve (dotted line) and the deviation from the normalized average curve (crosses) are shown in Figs. 4(a), (b) and (c). The rate of change of TEC,  $dN_t/dt$ , is also plotted in Fig. 4 together with that of the average curve. The vertical lines indicate the time of first and fourth contacts and the maximum obscuration at 300km. This height was chosen as an intermediate point between that of peak production and that of median height of the Faraday TEC.

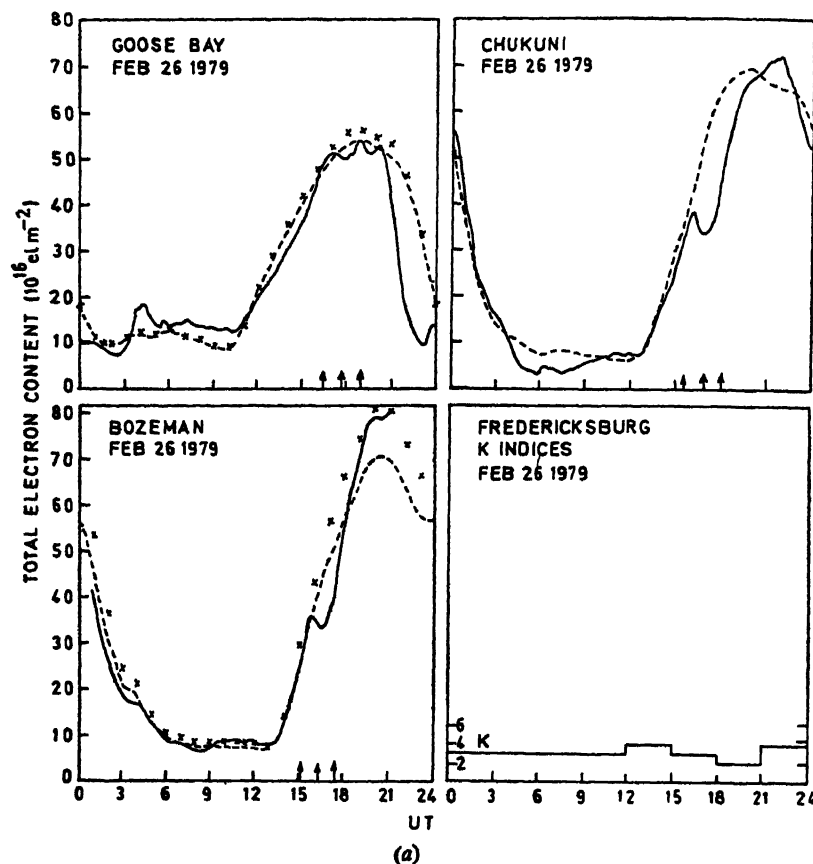


Fig. 3 (a), (b), (c) TEC results for the eclipse day (solid curve) together with the average variation (dashed curve) and normalized average values (crosses) (*see text*) from the various stations. Also shown are the K indices from Fredericksburg for the eclipse day.

For each of the TEC eclipse day results, the time delay of minimum TEC, and of maximum TEC depletion from the time of maximum eclipse were noted. Table II summarizes these results for each station and satellite observed together with the eclipse contact times, per cent maximum eclipse and the TEC per cent depletion. The TEC from all of the stations except Ramey and Goose Bay showed an effect which could be attributed to the eclipse. For the ray path from Ramey, the ionosphere was only 2 per cent eclipsed at 300 km at maximum contact and no effect which could be attributed to the eclipse was observed. Goose Bay TEC appeared to be under the influence of particle precipitation in the auroral regions as the effect of the photoionization cut-off was small. Scintillation activity occurred throughout most of the day. For the remaining nine TEC results, first contact commenced at local times ranging from 0632 hr at Vandenberg sub-ionospheric point to 1246 hr at the Hamilton to SIRIO satellite sub-ionospheric point. Hence, for Vandenberg, Bozeman, Boulder and Chukuni, the eclipse occurred during the morning increase in TEC and thus caused a delay in the morning increase. For the TEC results from Hamilton and Kennedy, the eclipse occurred near the peak of the TEC and hence caused a 'bite out'. However,

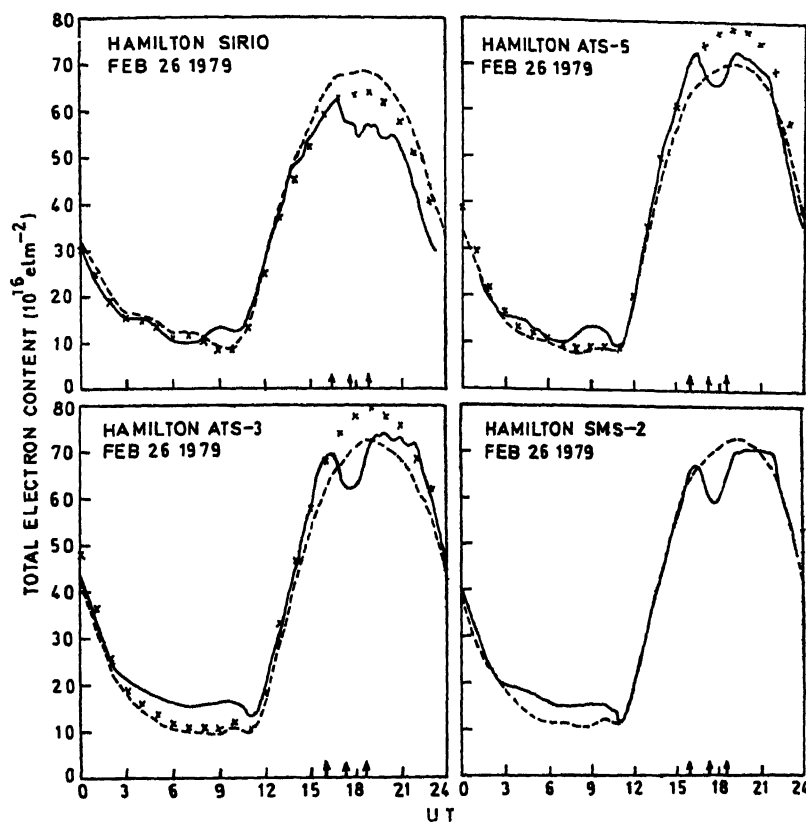


FIG 3(b) (For caption see p. 448)

TABLE II

Station	Satellite	300km					Time delay from maximum eclipse (minutes)	
		First Contact (U T)	Maximum (U T)	Fourth Contact (U T)	% Eclipse	TEC Depletion	Minimum TEC	Maximum TEC Depletion
Goose Bay	ATS-5	1626	1741	1854	71	11	14	14
Chukuni	ATS-5	1530	1645	1804	100	40	5	30
Bozeman	SMS-2	1510	1619	1734	100	38	16	36
Hamilton	ATS-3	1554	1714	1833	64	20	11	46
	SMS-2	1554	1714	1834	67	16	31	31
	SIRIO	1625	1739	1850	47	14	36	36
	ATS-5	1604	1723	1840	59	15	37	37
Boulder	GOES-2	1506	1618	1738	92	29	12	67
Vandenberg	ATS-1	1447	1549	1658	81	39	—	11
Kennedy	ATS-5	1534	1649	1807	39	7	—	26
Ramey	ATS-5	1633	1706	1740	2	0	—	—

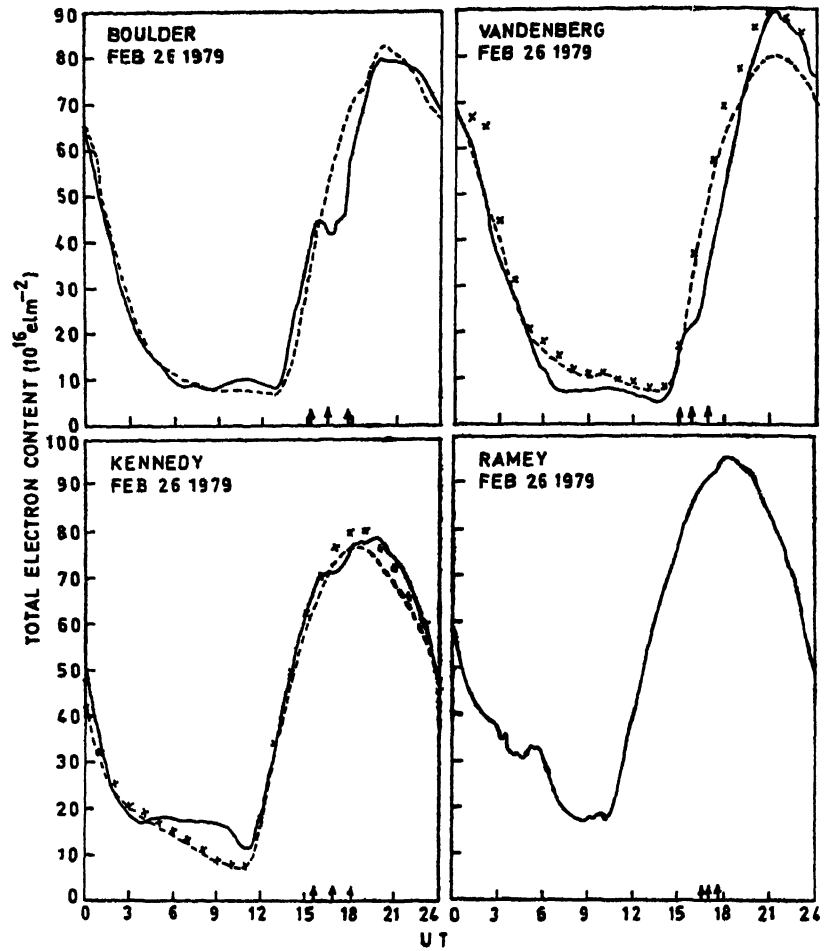
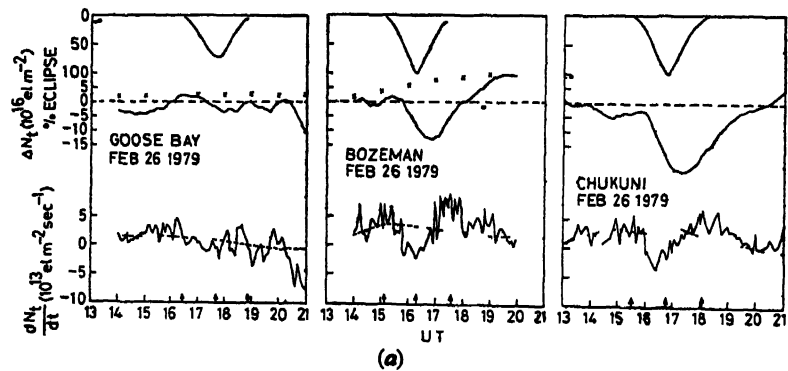


FIG 3(c) (For caption see p. 448.)



(a)

FIG. 4. (a), (b), (c) Time sequences of the percentage observation at 300km, the change in TEC and the rate of change of TEC for each station except Ramey for the eclipse day (solid lines), the average value (dashed lines) and normalized average values (crosses).

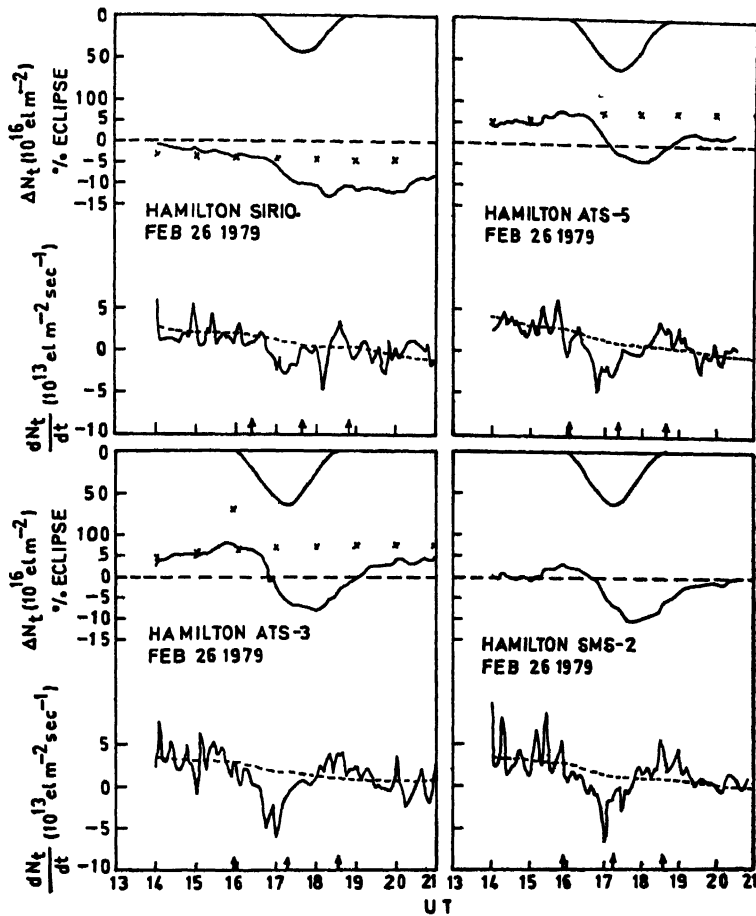


FIG. 4(b) (For caption see p. 450.)

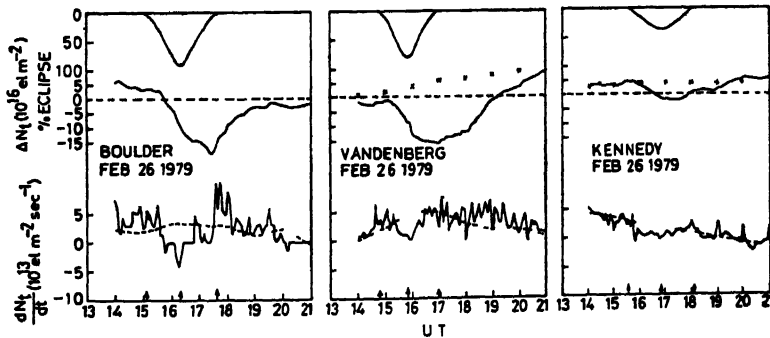


FIG. 4(c) (For caption see p. 450.)

for the Hamilton SIRIO satellite results, fourth contact occurred at the expected daily peak time of the TEC and hence, the TEC did not recover from the eclipse depletion before the afternoon decrease commenced (see Morton & Essex, 1978)

For the TEC results from Chukuni, the rate of depletion showed a rapid fall after about 30 minutes following first contact, reaching a minimum value before maximum contact. Before fourth contact was reached, the rate of increase of TEC had overshoot the non-eclipse average, gradually, returning to the non-eclipse average after the fourth contact. Maximum TEC depletion occurred at 30 minutes after maximum solar observation. This type of behavior was typical of most of the TEC results. Fig. 5 is a plot of the percentage depletion of the TEC results *versus* the percentage

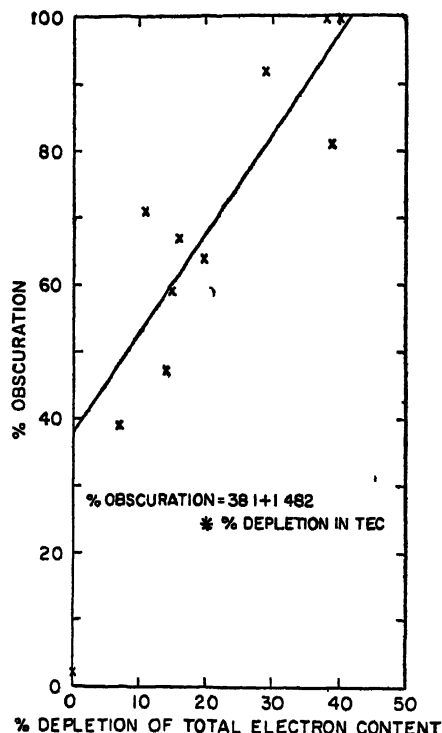


FIG 5 Graph of the percentage observation *versus* percentage depletion using data from the eleven TEC results. The line of best fit (excluding Ramey TEC data) is  $\% \text{ observation} = 38.1 + 1.482 + \% \text{ depletion in TEC}$

observation. As a first order approximation, the line of best fit for the points is:

$\% \text{ observation} = 38.1 + 1.482 + \% \text{ depletion in TEC}$  Hence, for this eclipse, no measurable effect occurred in the ionospheric total electron content until the percentage observation of the sun exceeded 38 per cent

#### (b) Ionograms

Ionosonde data from Fort Monmouth, Boulder, Vandenberg and Goose Bay for the eclipse period were analyzed to determine the bottomside response to the eclipse. The peak density of the ionosphere was determined from the  $f_oF_2$  values at five minute intervals obtained from the Fort Monmouth ionosonde for the eclipse period on 26 February 1979. The results are shown in Fig. 6(a) together with the

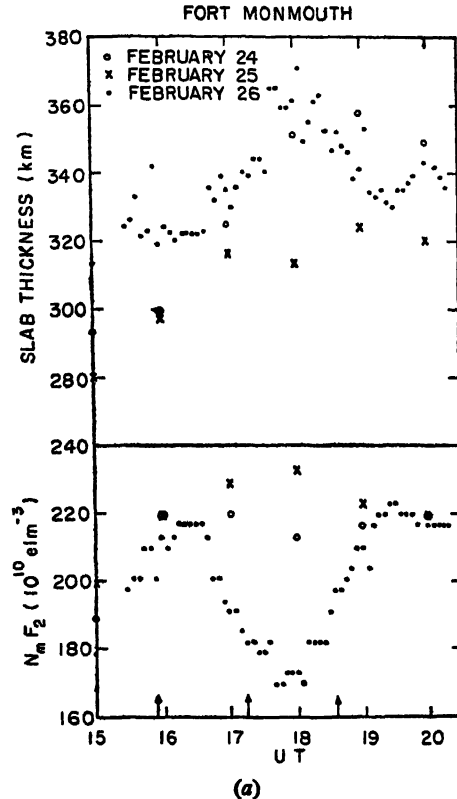


FIG 6. (a) Peak density and slab thickness variations at Fort Monmouth during the total solar eclipse of 26 February 1979 (dots at five minute intervals) and on February 24 (circles at hourly intervals) and February 25 (crosses at hourly intervals) (b) and (c) Topside and bottomside TEC, peak density, peak height and slab thickness variations at Boulder and Vandenberg during the total solar eclipse of 26 February 1979 (fifteen minute values) Also shown for Boulder are the peak density and slab thickness variations at hourly intervals (crosses) for 25 February 1979 (*see pp 454-55*). (d) Peak density variations at 10 minute intervals at Goose Bay during the total solar eclipse of 26 February 1979 Also shown are the hourly values for 24 (circles) & 25 (crosses) February 1979. The arrows indicate the first, maximum and fourth contact of the eclipse in the ionosphere at 300km (*see p 456*)

hourly values for 24 & 25 February 1979 The arrows indicate the eclipse contact times in the ionosphere at 300km. The Fort Monmouth peak density behaviour is very similar to the Hamilton TEC results In this case, the parts of the ionosphere being sampled are very close (*see Table I*) Slab thicknesses (the ratio of the TEC to the peak density) were calculated using the Hamilton ATS-3 satellite The slab thickness parameter is a first order measure of the shape of the ionosphere F-region profile Both the eclipse day and 24 February showed increases around the same UT times. Hence, the slab thickness increases on 26 February are not necessarily the result of the eclipse.

True height reduction of the ionosonde data were carried out for the eclipse period at fifteen minute intervals for Vandenberg and Boulder. From the calculations,



the bottomside TEC was obtained and thence the topside TEC by subtraction from the corresponding Faraday TEC recorded at that station. These results are plotted in Fig. 6(b) for Boulder, and Fig. 6(c) for Vandenberg together with the F-region peak density and height, and slab thicknesses. For Boulder, the peak density and slab

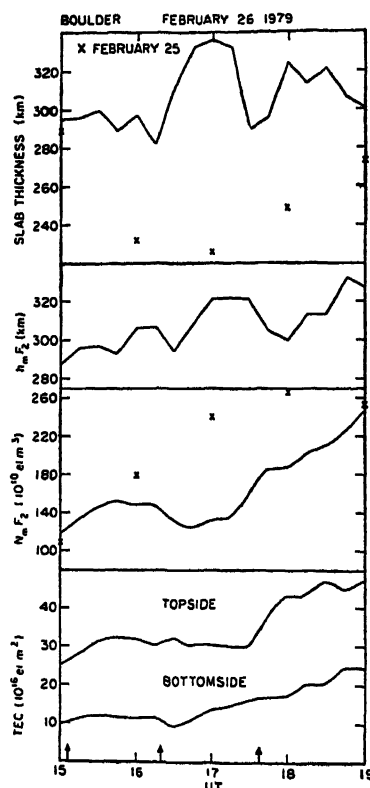


FIG 6(b). (For caption see p 453.)

thickness at hourly intervals on 25 February are also shown. The TEC and ionosonde data do not refer to exactly the same location, but within our limits of accuracy, the contact times of the eclipse are coincident. Comparison of the true height profiles (not shown), the bottomside, and topside TEC and  $h_m F1$  for Boulder indicates that a filling in of the bottomside ionosphere starts after maximum observation whereas the topside TEC does not start to increase for over an hour. This is partly caused by an increase in  $h_m F2$ , although the total TEC shows a similar behavior. The slab thickness parameters also shows an increase, indicative of a change in layer shape.

First contact of the eclipse at Vandenberg occurred before the E-layer had formed and hence bottomside observations are complicated by the normal morning formation of the E-layer and its depletion by the eclipse. Large variations in the height of the peak also modify the bottomside TEC results. The slab thickness parameter shows a continuous increase, indicating a change in layer shape. This is indicated on the bottomside by the changes in the true height profiles (not shown) as the E-layer forms.

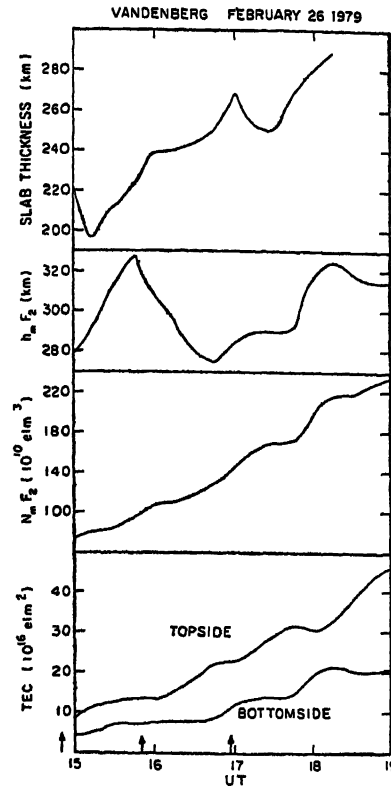


FIG. 6(c) (For caption see p. 453.)

Fig 6(d) is a plot of  $N_m F_2$  at Goose Bay on the eclipse day, 26 February, and on the two previous days, 24 and 25 February. The peak density for the eclipse day is considerably less than that for the two previous days. A decrease in the peak density commences around the time of maximum obscuration and recovery does not start until after the fourth contact. The peak density only recovers a small amount before the late afternoon decrease, which is generally rapid at Goose Bay, occurs. During the duration of the eclipse, the ionosonde data is complicated by the occurrence of a second F2-layer of higher density (see Fig 6(d)). This may be caused by other auroral activity or reflections from a higher density layer further to the south in a region of lower obscuration. The Goose Bay TEC (Fig 3(a)) shows only a small eclipse effect whereas the Goose Bay peak density which is observed further to the north and hence closer to the peak of totality (see Fig 1) shows a marked eclipse effect.

#### DISCUSSION

The TEC results presented here for the total solar eclipse of 26 February 1979 across North America show that the cut-off in solar ionizing radiation produced a significant depletion in the TEC along the path of the eclipse. At one of the stations, Goose Bay, the eclipse effect was probably partly masked by particle precipitation associated with substorm events. A first order approximation indicates that for this eclipse, for

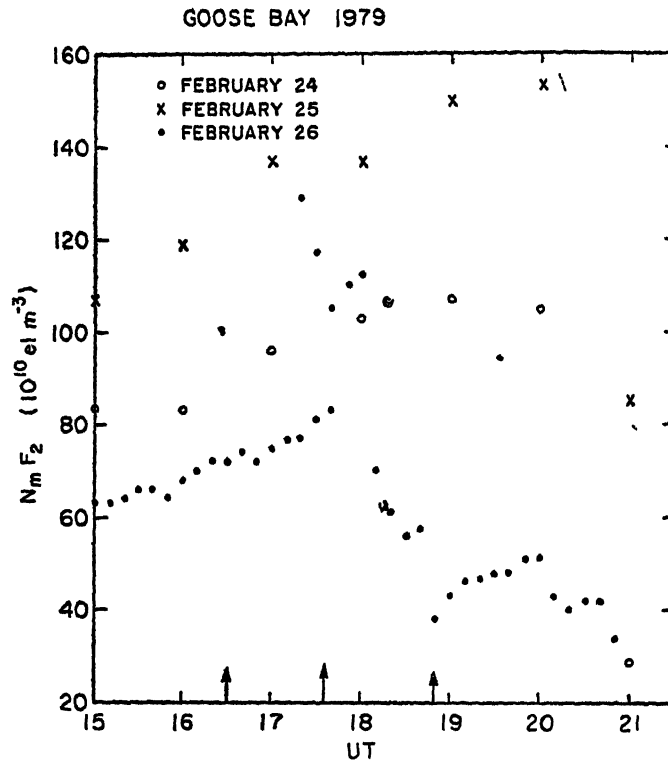


FIG. 6(d). (For caption see p. 453.)

observations greater than 38 per cent, a depletion in TEC occurred. This effect in TEC is larger than that reported by Almeida *et al.* (1972) and Marriott *et al.* (1972) for the 1970 total solar eclipse across North America. These differences may have been caused by oppositely directed vertical wind drifts during the two eclipses. For the 1979 eclipse the path of totality was northward for all the stations except for the two stations in the path of totality.

One of the interesting features of the TEC results from most of the stations for this eclipse was the recovery of the rate of change of the TEC to values greater than the average non-eclipse values before fourth contact and their slow return to the non-eclipse values after fourth contact. Possible explanations for this effect include the modification of neutral winds and electric fields during the eclipse. This effect requires further investigation.

Investigation of the peak density and bottomside ionosphere using ionosonde data showed that the peak density and TEC depletions were similar for two of the four stations for which data were available. For the third station, Vandenberg, the eclipse commenced early in the morning before the E-layer had formed and the peak density showed only small changes although the TEC results show a large depletion. This result is probably due to the combined effect of large changes in layer height ( $h_m F_2$ ) and shape (slab thickness) (see Fig. 6 (c)). Increases in slab thicknesses occurred at both Fort Monmouth and Boulder during the eclipse but these changes

cannot definitely be attributed to the eclipse as similar variations occurred on other days (see Fig. 6 (a)). Similar results have been reported by Klobuchar and Malik (1970) during the 1970 total solar eclipse. For the fourth station, Goose Bay, the proximity of the auroral oval and the spatial separation of the parts of the ionosphere being sampled by the ionosonde and the Faraday rotation measurements may have led to differences in the peak density and TEC.

#### ACKNOWLEDGEMENTS

The ionogram data and true height profiles from Boulder and Vandenberg were supplied by World Data Center A, Boulder CO. Special thanks go to Dr J. Buchau for the Goose Bay ionosonde data and to Dr H. Soicher for the Fort Monmouth ionosonde data.

#### REFERENCES

- Almeida, O. G., Waldman, H., and da Rosa, A. V. (1972) Neutral winds implied by electron content observations during 7 March 1970 solar eclipse. *J. atm. terr. Phys.*, **34**, 713–717.
- Beynon, W. J. G., and Brown, G. M. (1956) *Solar Eclipses and the Ionosphere*. Pergamon Press, London.
- Evans, J. V. (1965) An F-region eclipse. *J. geophys. Res.*, **70**, 131–142.
- Klobuchar, J. A., and Malik, C. (1970) Comparison of changes in total electron along three paths. *Nature*, **226**, 1113–1114.
- Marriott, R. T., St. John, D. E., Thorne, R. M., Venkateswaran, S. V., and Mahadevan, P. (1972) Ionospheric effects of two recent solar eclipses. *J. atm. terr. Phys.*, **34**, 695–712.
- Mendillo, M., Baumgardner, J., and Klobuchar, J. A. (1979) Opportunity to observe a large-scale hole in the ionosphere. *EOS Trans. AGU*, **60**, 512.
- Mendillo, M., da Rosa, A. V., and Bernhardt, P. A. (1978) Spacelab 2 plasma depletion experiments. *EOS Trans. AGU*, **59**, 334.
- Mendillo, M., Hawkins, G. S., and Klobuchar, J. A. (1975) A sudden vanishing of the ionospheric F-region due to the launch of Skylab. *J. geophys. Res.*, **80**, 2217.
- Morton, F. W., and Essex, E. A. (1978) Total electron content observations during 23 October 1976 solar eclipse over south-eastern Australia. *J. atm. terr. Phys.*, **40**, 111–114.
- Rishbeth, H. (1968) *Space Sci. Rev.*, **8**, 543.
- Titheridge, J. E. (1972) Determination of ionospheric electron content from the Faraday rotation of geostationary satellite signals. *Planet. Space Sci.*, **20**, 353–369.

Printed in India.

**Ionospheric Drifts**

## HORIZONTAL DRIFT MEASUREMENTS OVER UDAIPUR DURING THE SOLAR ECLIPSE OF 16 FEBRUARY 1980

D. V. SARDESAI, M. AGRAWAL, S. MATHUR and R. K. RAI

*Department of Physics, University of Udaipur, Udaipur-313 001, India*

*(Received 15 February 1982)*

The horizontal drift measurements have been made over Udaipur (Geogr lat 24° 6'N, Geogr long 73° 7'E) during the recent solar eclipse of 16 February 1980 using spaced receiver technique. Observations on 5.0 MHz during daytime and 2.5 MHz during night time for F-region drift have been made on 15, 16 & 17 February 1980 with half an hour interval round the clock except from 1330hr to 1630hr (75° EMT) when the unit was run nonstop. The observations have been analysed by similar fade analysis. A few samples have been subjected to correlation analysis. It has been found that the apparent drift speed increases about half an hour after the first contact, decreases in main phase and becomes normal after the fourth contact is over. Effect of solar eclipse on EW and NS components of apparent drift vector is also studied. All the timings are 75° EMT.

**Keywords:** Ionospheric Drift; Spaced Receiver Technique; Similar Fade; Correlation; EW&NS Components

### INTRODUCTION

For the last decade the horizontal drift measurements over Udaipur are going on with a set-up very much similar to Mitra's (1949) spaced receiver technique. The present paper communicates the results obtained from the observations taken at Udaipur during the recent solar eclipse. Maximum obscuration was 75 per cent at Udaipur. The first contact, maximum phase and fourth contact occurred at 1358, 1512 and 1615hr IST respectively.

### OBSERVATIONS AND ANALYSIS

The fading of amplitude at three spaced receiving aerials of the echoes of 5.0 MHz during daytime and 2.5 MHz during night time reflected from the F-region have been recorded. The receiving aerials are half wave dipoles located at the vertices of an isosceles right angled triangle with the sides 90m, 90m and 127m. Observations were recorded on NP55/35m negative film. On 15, 16 and 17 February 1980, observations were recorded nonstop from 1330hr to 1630hr (75° EMT). However, for other hours of these three days, the observations were taken for 5 to 7min after every half an hour. The speed of the recording camera was 5-6cm/s. Time markings at intervals of 12s are incorporated in the records using a synchronous motor.

TABLE I

$V'$			$V'_{EW}$						$V'_{EWNS}$								
16 02 1980			17 02 1980			16 02 1980			17 02 1980			16 02 1989			17.02.1980		
HRS	SFA	CA	HRS	SFA	CA	HRS	SFA	CA	HRS	SFA	CA	HRS	SFA	CA	HRS	SFA	CA
1410	56	78	1340	60	63	1410	—40	—44	1340	—34	—46	1410	—38	—64	1340	—28	—47
1415	57	64	1535	64	47	1415	—39	—46	1535	—30	—19	1415	—45	—44	1535	—57	—43
1450	111	119	1550	34	57	1450	18	22	1550	—28	—44	1450	—109	—117	1550	—6	37
1500	56	66	1620	37	42	1500	8	11	1620	—30	—37	1500	—50	—65	1620	20	19
1506	17	12	1705	17	16	1506	8	9	1705	16	14	1506	—14	—8	1705	—5	—7
1516	53	58	—	—	—	1516	26	27	—	—	—	1516	—45	—54	—	—	—
1550	38	38	—	—	—	1550	—8	—10	—	—	—	1550	25	37	—	—	—
1605	29	26	—	—	—	1605	—16	—14	—	—	—	1605	26	22	—	—	—
1620	26	37	—	—	—	1620	—17	—21	—	—	—	1620	—22	—30	—	—	—

HRS — 75°EMT

SFA — Results obtained by Similar Fade Analysis

CA — Results obtained by Correlation Analysis

The observations recorded from 1330hr to 1630hr on the said three days have been analysed by similar fade method of analysis for every five minute intervals. The rest of the observations taken at half an hour intervals on 15, 16 & 17 February 1980 are also analysed by similar fade method. A few fading records have been subjected to correlation analysis. For this, the fades were magnified (8cm=12sec) and traced on the graph paper. The amplitudes on all the three aeriels were then digitized with optimum time interval ( $\tau$ ) and fed to IBM-360 computer. The programming is based on the method given by Briggs *et al* (1950) and later on developed by Fooks (1965). Table I gives a comparative study of the results obtained from similar fade method and correlation method of analysis. Some of the typical samples of fading records obtained during eclipse and afterwards are shown in Fig. 1.

Since a geomagnetic storm was also observed on 15 and 16 February, and the

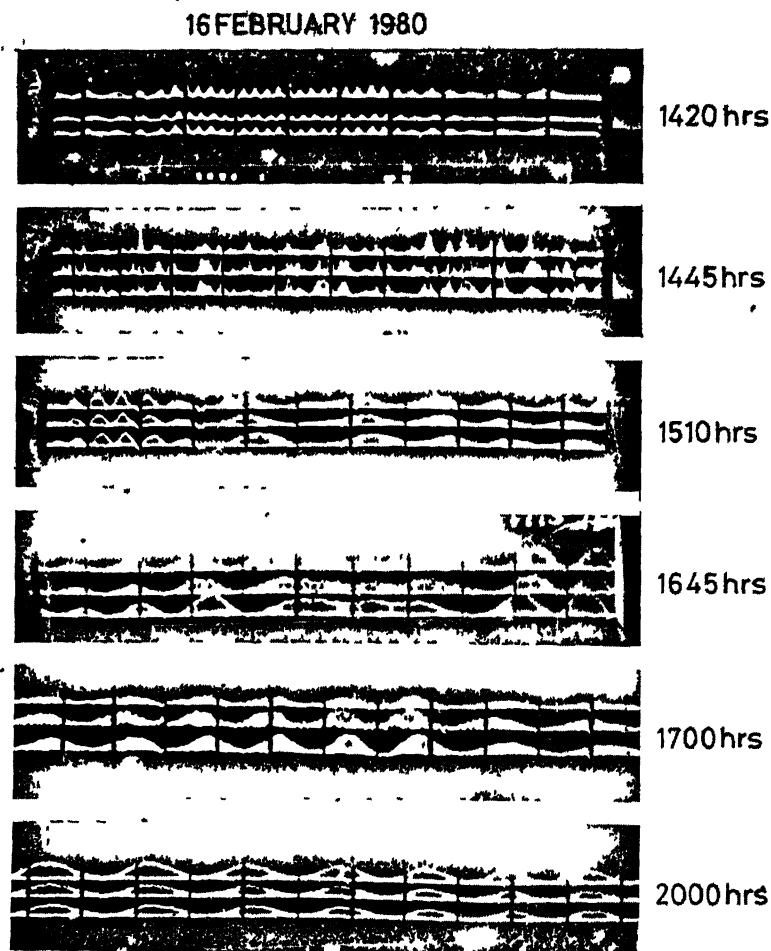


FIG 1 Some typical fades obtained on eclipse day (Time—75°EMT)

$\Sigma K_p$  for eclipse day was +40, a diurnal variation of apparent drift speed corresponding to a day in winter season with  $\Sigma K_p = +40$ , is also drawn for ready comparison (See Fig 2, curve D) Using the data for quiet days a mean profile is also drawn for winter season 1980 (Fig. 2, curve A) This agrees with the diurnal variation at this latitude (Kumar, 1975) The post eclipse day, 17 February was a quiet day ( $\Sigma K_p = +4$ ) Profile for this day is shown as curve C (Fig. 2). The observed diurnal variation of apparent drift speed on eclipse day is shown by curve B (Fig. 2).

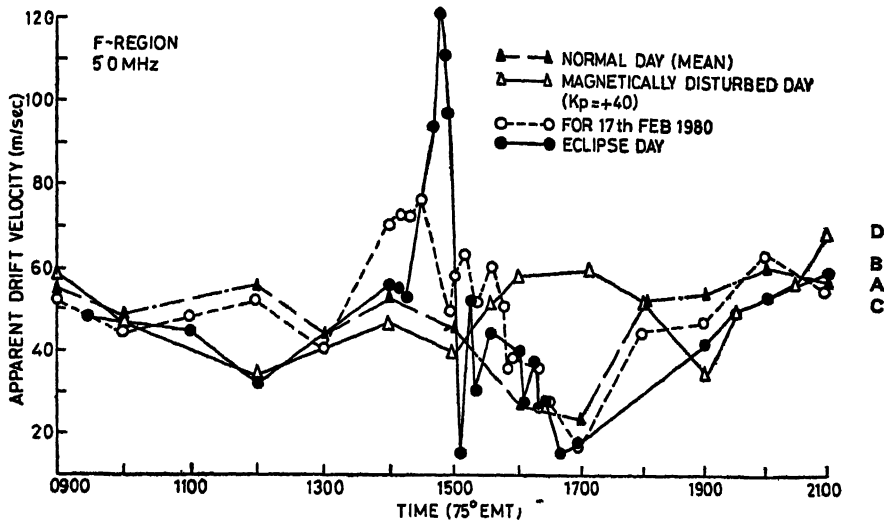


FIG. 2 Diurnal variation of apparent drift speed on normal days, magnetically disturbed day, 17 February 1981 and eclipse day (Curve A, DC & B respectively)

Figs 3 and 4 represent the EW and NS components of apparent drift vector on control days and eclipse day. In both the figures, curves A, B and C represent profiles for average of normal days, eclipse day and 17 February 1980.

### RESULTS AND DISCUSSION

Rao *et al* (1961) and Sastry and Rao (1971) have shown at Waltair that F-region drift decreases with increase in  $K_p$ . Rastogi *et al* (1971) have also reported negative correlation between apparent drift speed and  $K_p$ . Sardesai *et al* (1980) have shown a similar relationship between the two parameters at this latitude. The diurnal variation, curve D (Fig 2), for the day  $\Sigma K_p = +40$  has low values of apparent drift speed in comparison to quiet day results. This is in agreement with the above findings.

It may be observed that the value of apparent drift speed shows a sharp increase about 25 minutes after the first contact. The peak value is found at 1450hr (75° EMT). The value thereafter fluctuates and finally reaches the normal day value after the fourth contact is over. Davis & da Rosa (1970) in an observation on total electron content during eclipse of 7 March 1970 observed passage of TID during eclipse. Hajkowicz (1977) also confirmed presence of TID when monitored in the path away



from totality. Pradhan *et al.* (1972) have shown that during the passage of a TID, the observed fading rate was highly increased. Janve (1975) and other workers at this latitude have shown a positive correlation between the fading rate and the apparent drift speed. The increase in drift speed during the solar eclipse may, therefore, be explained on the basis of passage of TID over the receiving aerials thus increasing the fading rate as well. However, it is difficult to say whether such a sharp increase can be explained on the basis of TID presence. Another possible explanation could be the setting up of a temperature gradient due to uneven sudden cooling of the ionosphere.

The EW component of the apparent drift vector on normal days (curve A) remains for most part of the day westward (from 1100 to 1700hr). At the sunset hours, it changes its direction from westward to eastward. This is quoted also by earlier workers (Kumar, 1975). On the eclipse day, (Fig. 3, curve B) the component

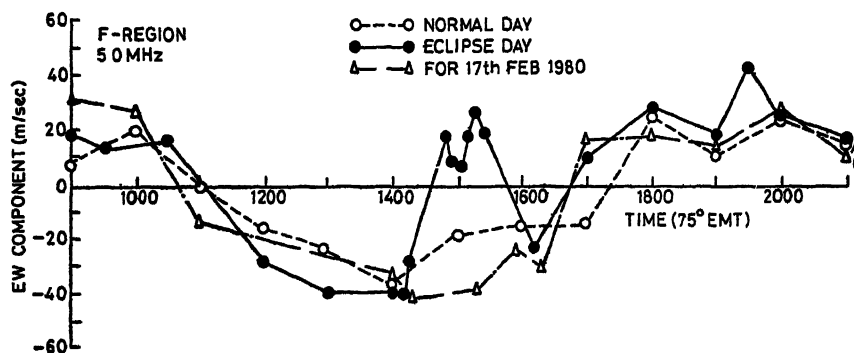


FIG. 3. Diurnal variation of EW component on normal days, eclipse day and 17 February 1980

became eastward at around 1450hr, remained eastward during the main phase of the eclipse from 1450 to 1600hr and finally turned westward. For the rest of the time it followed the normal day variation. On 17 February 1980 (curve C) the results are almost identical with control days.

This shows that sunset conditions were set-up at 1450hr and continued till the main phase was over.

The NS component of apparent drift vector in normal days, (Fig. 4, curve A) remains most part of the day southward. On the eclipse day (curve B), the NS component has shown the same tendency of remaining southward but a very large southward component is observed during the main phase of the eclipse. Udaipur was on the north of totality belt. Thus a temperature gradient from the region of totality towards Udaipur may be expected. This temperature gradient may cause the plasma flow and thus increase the southward component at this latitude. If this is one of the reasons for increase in southward component, the results at stations south of totality path should show an increase in northward component. Recently, some new stations have been established at Courtalam and Madras under the scheme "Indian Collaborative Work on Ionospheric Drifts," but unfortunately the equipment could not be run during the solar eclipse.

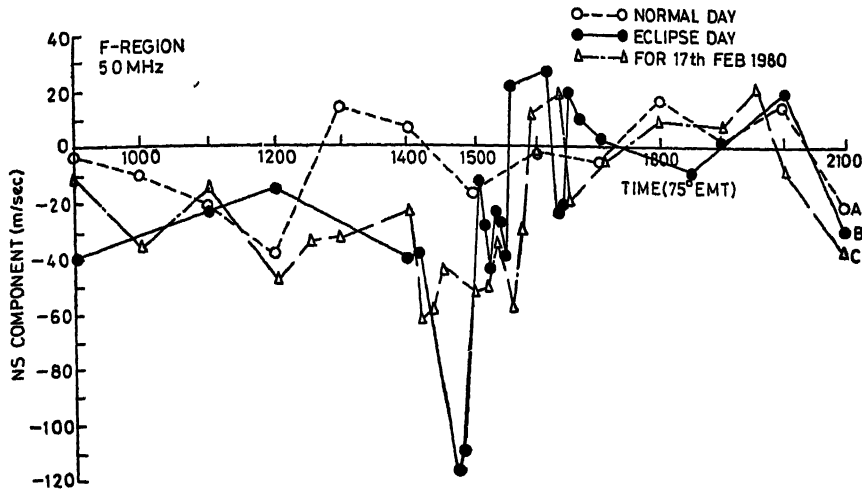


FIG. 4. Diurnal variation of NS component on normal days, eclipse day and 17 February 1980.

#### ACKNOWLEDGEMENTS

Authors are thankful to Professor R. G. Rastogi, IIG, Bombay and Dr H Chandra, PRL, Ahmedabad for helpful discussions. One of the authors (DVS) is thankful to UGC for financial assistance in the form of teacher research fellowship.

#### REFERENCES

- Briggs, B. H., Phillips, G. J., and Shinn, D. H. (1950) *Proc. phys Soc*, **B63**, 106.  
 Davis, M. J., and da Rosa, A. V. (1970) *Nature (London)*, **226**, 1123.  
 Fooks, G. F. (1965) *J atm terr. Phys.*, **27**, 979.  
 Hajkowicz, L. A. (1977) *Nature (London)*, **266**, 147.  
 Janve, A. V. (1975) *Ph D Thesis*, University of Udaipur, Udaipur.  
 Kumar, V. (1975) *Ph D. Thesis*, University of Udaipur, Udaipur.  
 Mitra, S. N. (1949) *Proc Inst Elec Engrs.*, **96**, 441.  
 Pradhan, S. M., Srivastava, S. K., Singh, B., and Tantry, B. A. P. (1972) *Indian J. Rad. Space Phys.*, **1**, 230.  
 Rao, B. R., Rao, E. B., and Murthy, Y. V. R. (1961) *Proc. I G Y Symp CSIR*, New Delhi, **205**.  
 Rastogi, R. G., Chandra, H., and Misra, R. K. (1971) *Nat phys Sci*, **233**, 36, 13-15.  
 Sardesai, D. V., Badala, P., and Rai, R. K. (1980) *J scient. Res B H. U Varanasi*. In Press.  
 Sastry, J. H., and Rao, B. R. (1971) *Ionosphere-Magnetosphere Interaction* New Delhi.

Printed in India.

Invited Review (Geomagnetism)

## SOLAR ECLIPSE EFFECTS ON GEOMAGNETISM

R. G. RASTOGI

*Indian Institute of Geomagnetism, Colaba, Bombay 400 005, India*

(Received 9 February 1982)

The paper re-examines the results of geomagnetic studies during solar eclipses conducted at different parts of the world. The solar eclipse effects are generally small and are often mixed up with other disturbance effects occurring simultaneously. Solar eclipses during geomagnetic quiet periods indicate significant effects more clearly at low, less at medium and least at tropical latitudes near the focus of Sq currents. One of the largest effects of solar eclipse on geomagnetic field was observed at Huancayo on 12 November 1966, amounting to a decrease of  $\Delta H$  by 48 nT. The largest per cent decrease of the ionospheric currents from the normally expected value amounting to 60 per cent was recorded in Ceylon on 20 June 1955.

**Keywords:** Solar Eclipse; Geomagnetism; Sq Currents

### INTRODUCTION

As early as 1900, Bauer expected that the effect of a solar eclipse on geomagnetism would be as though part of the night hours were suddenly imposed among the day hours. He organised the observations of geomagnetic field at a number of stations within as well as outside the track of totality of a solar eclipse. However, the occurrence of magnetic disturbance during the eclipse made it difficult to interpret the eclipse effect. Bremmelen (1905) examined the geomagnetic observations during several eclipses. Normand (1907) described the results of geomagnetic observations at a few stations within the region of totality and within the partial zone during the total solar eclipse of 30 August 1905. He showed perturbations in geomagnetic field occurring synchronously at widely separated stations which were of non-eclipse origin. He obtained difference curves for pairs of stations and concluded a definite eclipse effect on the declination, being about 8.8 nT. The maximum value of the declination effect coincided at all stations with the maximum phase of the eclipse itself. Chree (1913) discussed the results of geomagnetic observations at Kew Observatory in connection with the solar eclipse of 17 April 1912 and found the data insufficient to justify a conclusion either in favour of or against the eclipse effect. He (Chree, 1915) was more sceptical of the solar eclipse effect on geomagnetic field on the basis of observations at Kew Observatory during the solar eclipse on 21 August 1914. Gama (1948) studied the effect of solar eclipse of 20 May 1947 on geomagnetic field at Vassouras, Brazil (magnitude of eclipse 0.89). He used a special method to remove the influence of lunar effects and obtained a "normal" curve for the eclipse day on the basis of the data on the control days. He found that the horizontal intensity on the eclipse day started decreasing four hours before the commencement of the eclipse,

this decrease continued until the end of eclipse. A few minutes after the end of the eclipse the H field began to rise again and acquired its normal value two hours after the end of the eclipse. The declination began to change eastward from its normal position before the start of eclipse, reaching the maximum eastward deflection of  $3'.4$  towards the end of the eclipse. He estimated the eclipse effect to be approximately  $1'.4$ .

Kato (1951) observed the effect of solar eclipse on 12 September 1950 at a few Japanese stations where the maximum obscuration was from 0.27 to 0.58. A decrease of the declination was noticed beginning even before the start of the eclipse and continued till about an hour after the end of the eclipse. No distinct effects were seen in the horizontal field during the eclipse.

In India, regular routine observations of the magnetic field are available for a very long period starting from the Colaba Magnetic Observatory in 1841 and its transfer to Alibag Magnetic Observatory in 1905 and are continued till today. Malurkar (1954) examined the magnetograms of Colaba and Alibag observatories during the solar eclipses. However, he could not derive any conclusive evidence. Often magnetic disturbances intervene during the eclipse period. Even apart from the storm effects, fluctuations in the geomagnetic field vitiate the small eclipse effect being looked for. During his introductory speech at the Mixed Commission of the ionosphere at Brussels in July 1948, Chapman (1949) remarked that during an eclipse we get a reduction of conductivity at some part of the normal current sheet and a reorientation of the lines of current flow occurs on the original uniform current sheet. He doubted whether eclipse effects have ever been reliably established in magnetic records.

The total solar eclipse on 30 June 1954 provided an excellent opportunity for studying the effect on the geomagnetic field as the track of moon's shadow crossed over Scandinavian and East European countries where a dense network of permanent magnetic observatories were already in operation. Egedal and Ambolt (1955) collected and examined the magnetograms from eleven magnetic observatories in the region and isolated the eclipse effect on the declination at these observatories. The distance of the observatories from the ionospheric central line varied from  $0.1^\circ$  for Edh,  $0.4^\circ$  for Lerwick,  $1.7^\circ$  for Rube Skov to  $9.1^\circ$  for Abinger. For most of the observatories the totality occurred near noon hours when the ionospheric conductivities are at their daily maximum. The observations were normalised according to a method proposed by Ryd (1917). They isolated definite eclipse effect on the declination, the maximal deviation in declination occurred almost at the same time as the maximal obscuration at the solar disc at the station concerned. The maximum effect was found to be about 28 per cent of the daily range which was very close to the theoretical value suggested by Chapman in 1933. Mean of the deviation for each 10 min group averaged for all the stations is reproduced in Fig. 1 after Egedal (1956). It is seen that the maximum effect during the period of totality was only about  $1.5'$  in declination. The effect of the eclipse as a function of the distance from the centre of totality has been redrawn in Fig. 2 from the data given by Egedal (1956) in his paper. It is seen that at distance of 100 km the eclipse effect is reduced to about 35 per cent of what it is at the region of totality and at 500 km away the effect is reduced below 1/2 per cent of the effect at the centre. Thus the geomagnetic effect is reduced very rapidly as we move away

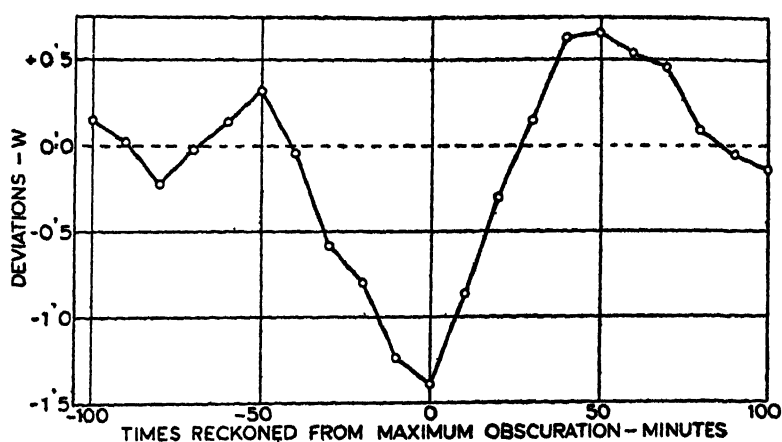


FIG. 1. Averaged deviation of the declination at European observatories during the total solar eclipse on 30 June 1954 after Egedal (1956).

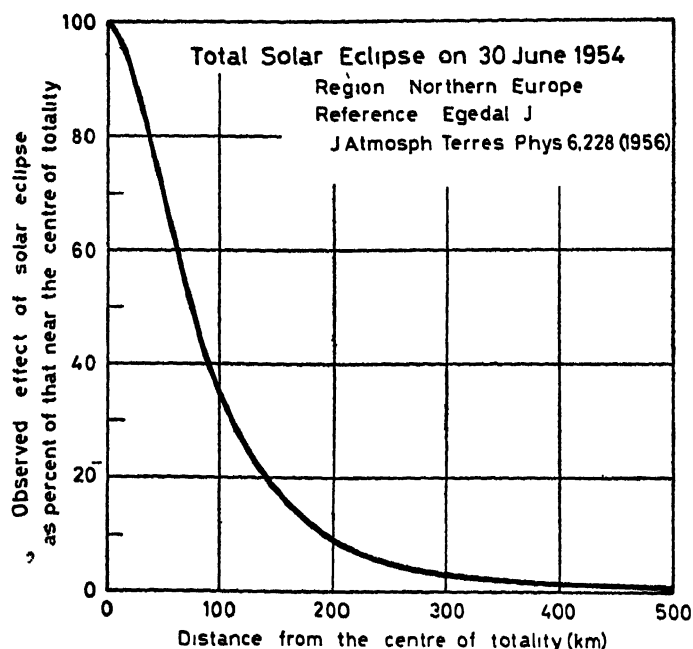


FIG. 2. Magnetic effect due to a total solar eclipse as a function of distance from the centre of totality after Egedal (1956)

from the region of totality. Ionospheric observations were also made during the same eclipse and abnormally large decrease in the ionization densities in the E-, F1- as well as F2-layers were noted. At Ekenas, Sweden, where the maximum obscuration of the sun was 100 per cent the E-region ionization was reduced to 25 per cent of the normal non-eclipse day (Stoffregen, 1956). Thus there was a decrease of 75 per cent

in the E-region ionization compared to only 28 per cent decrease in the magnetic field at ground level.

Another report of ionospheric as well as geomagnetic observations made simultaneously during a solar eclipse was by Bossolasco *et al.* (1961) for the total solar eclipse on 15 February 1961 at Genova, Italy. They found that the ionization of the E-region was reduced to 38 per cent of the normal quiet day value i.e., there was a reduction of 62 per cent. During the eclipse, the mean deviation of geomagnetic field from the unaffected variation interpolated with the aid of the two control days was about 5nT for  $H$  and 3nT for  $D$  as compared to normal sq amplitude of 9nT for the time of eclipse. They also noted that  $H$  variation at Tortosa (where the maximum obscuration at ground was 87 per cent showed a weaker depression than that recorded at Geneva, while at Wingst (83 per cent maximum obscuration) no appreciable depression was noted. This again stressed the narrowness of the region of geomagnetic effect of solar eclipse near the region of totality.

The moon's shadow during the solar eclipse on 20 June 1955 crossed over Ceylon, Southern Burma, and Phillipines. For studying the geomagnetic effect of the eclipse, Indian scientists had established a station at Hingurakgoda close to the central line (Sankar Narayan, 1956) and the Japanese team had their station at Kandy within the totality zone (Kato, 1956). During the same period intensive ionospheric/magnetic observations were undertaken at Kodaikanal Astrophysical Observatory in southern India, where the maximum obscuration of the sun was 91 per cent. In Fig. 3 after

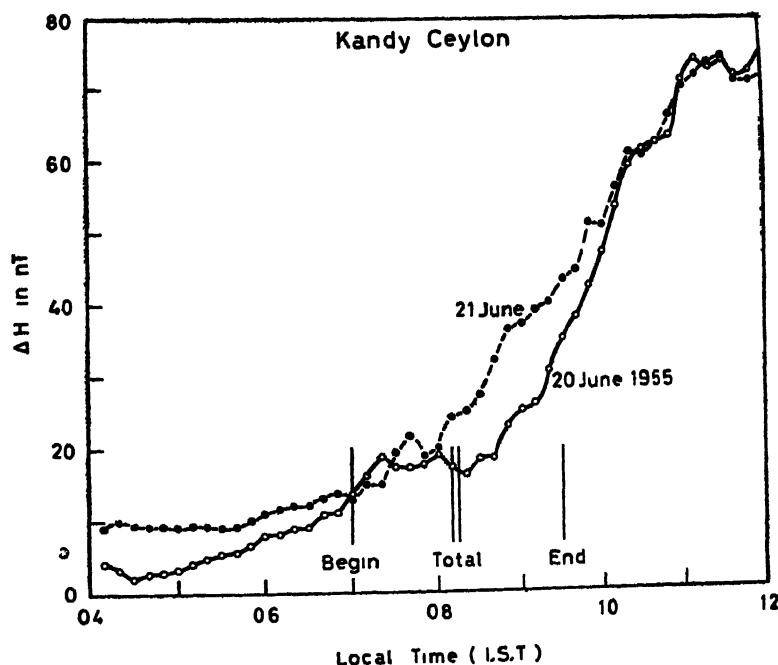


FIG 3 The variation of the horizontal geomagnetic field at Kandy, Ceylon during the solar eclipse (20 June 1955) and on the following day.

Kato (1956), are reproduced the  $\Delta H$  at Kandy on the eclipse day (20 June) and on the following day. The decrease of the horizontal field during the eclipse is very clearly shown. In Fig 4 are shown the variation of  $\Delta H$  at Hingurakgoda, Ceylon and of the critical frequency of the E-region ( $f_oE$ ) at Kodaikanal, India on 20 June 1955 around the eclipse period. It is interesting to note that with the start of the eclipse both  $f_oE$  as well as  $\Delta H$  started decreasing, reached the minimum value around the period of maximum phase of the eclipse after which both the parameters increased, rapidly towards the normal value. The minimum value of  $f_oE$  during the eclipse, was 1.85 MHz compared to the interpolated normal value of 2.95 MHz. During the maximum phase of the eclipse the E-region ionization was reduced to a value of  $(1.85/2.95)^2 = 0.4$  times that expected on a normal day. The decrease of the horizontal field near the eclipse maximum was about 24 nT lower than the interpolated normal day value. With reference to the minimum night time value, the minimum value of  $\Delta H$  at the time of totality was 16 nT, thereby giving the value of  $\Delta H_{\text{eclipse}}/\Delta H_{\text{normal}}$  to be  $16/40 = 0.4$ . This value is remarkably similar to the reduction of E-region ionization indicating that the reduction of the horizontal magnetic field during the eclipse was entirely proportional to the decrease of E-region ionization.

Another set of magnetic and ionospheric observations at low latitude regions

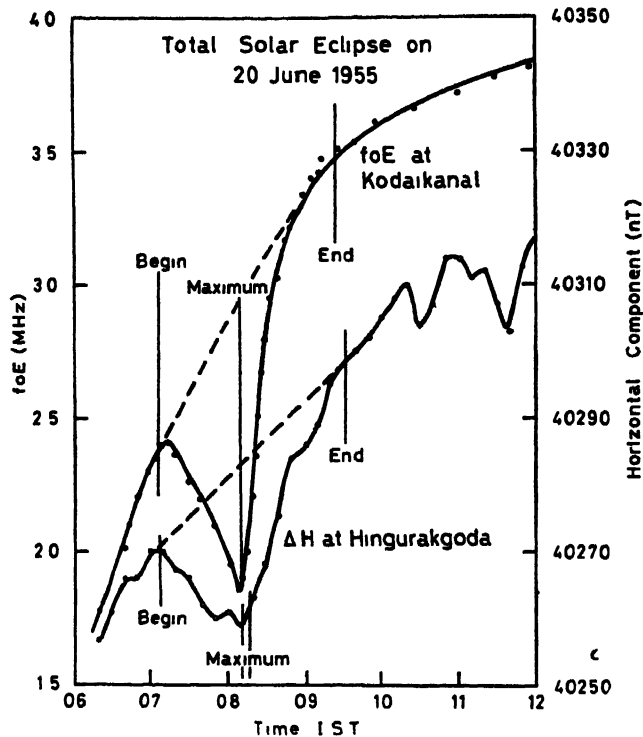


FIG 4 Temporal variations of  $\Delta H$  at Hingurakgoda, Ceylon and of  $f_oE$  at Kodaikanal, India around the solar eclipse on 20 June 1955

was available during the solar eclipse of 12 October 1958 Kato (1965) described the magnetic observations at Suvarrow Island ( $\phi = 13.25^\circ\text{S}$ ,  $\lambda = 163.1^\circ\text{W}$ , Dip  $25.4^\circ\text{S}$ ). A very definite depression of the horizontal field was noticed during the maximum phase of the eclipse, the magnitude of change being about 12 nT. Van Zandt (1960) described the results of ionospheric soundings at Danger Island ( $\phi = 10.8^\circ\text{S}$ ,  $\lambda = 166^\circ\text{W}$ , Dip  $= 22^\circ\text{S}$ ) also in the same region as the Suvarrow Island. A regular decrease in the ionization density at fixed heights was noticed; the value of  $N_m E$  near the period of maximum obscuration decreased to  $6.8 \times 10^5$  electrons/cc as compared to normally expected value of  $19.0 \times 10^5$  electrons/cc suggesting, during the eclipse, the E-region ionization had decreased to 38 per cent of the expected normal value. Correspondingly, the  $\Delta H$  with reference to the night value had decreased to only 75 per cent of the normally expected value during the eclipse. In this case ionospheric currents had decreased by 25 per cent as compared to ionization decrease by 62 per cent.

The most important study of the equatorial electrojet during a total solar eclipse was conducted in Peru during the solar eclipse on 12 November 1966. The track of moon's shadow crossed transversely the equatorial electrojet belt. The geomagnetic field was recorded at six stations within the electrojet region, the dip angle at the northernmost stations Ancon and Huancayo being  $2.1^\circ\text{N}$  while that at the southernmost station was  $4.6^\circ\text{S}$ . The results of the expedition have been described by Giesecke *et al.* (1968) and by Kato and Mori (1968). Regular ionospheric soundings were taken at Huancayo. In Fig 5 are shown the temporal variations of the horizontal geomagnetic field  $H$  and the E-region critical frequency  $f_o E$  at Huancayo during the solar eclipse on 12 November 1966. Distinct decreases of  $H$  and of  $f_o E$  during the eclipse period with the minimum at the maximum phase of the eclipse are clearly seen. The  $H$  field had decreased by about 48 nT and  $f_o E$  had decreased by 1.1 MHz. In other words  $\Delta H$  with reference to night time base value had decreased to 0.6 times the normal value but  $N_m E$  had decreased to 0.4 times the corresponding normal value, that is the currents decreased by 40 per cent while the E-region ionisation decreased by 60 per cent during the eclipse. In Fig 6 are shown the variations of normal  $Sq(H)$  as well as the maximum eclipse effect on  $H$  at different stations in Peru during the solar eclipse on 12 November 1966. It is interesting to see that the variations of both these parameters with the distance from the centre of the magnetic equator are very similar to each other. Furthermore,  $\Delta H$  due to eclipse had a linear relation with  $\Delta H$  due to  $Sq$  currents. This suggests that the normal electric field in the  $Sq$  band was left unaffected and the eclipse effect on geomagnetism at low latitudes was primarily due to the decrease of the E-region ionization. However, it is to be noted that the decrease of current ( $\Delta H$ ) in this eclipse was not of the same order as the decrease of E-region ionization as in the case of eclipse at Kodaikanal on 20 June 1955 (Sankar Narayan, 1956). The path of totality of eclipse on 20 June 1955 was almost parallel to the magnetic equator in the Indian ocean region and therefore a large portion of the equatorial electrojet region would be successively deprived of the normal solar emissions, thus causing a widespread decrease of the ionospheric currents and thereby  $\Delta H$ . The track of totality of the eclipse on 12 November 1966 crossed the magnetic equator in Peru almost transversely, hence, moon's shadow created large decrease of ionization in only a very localised region. There



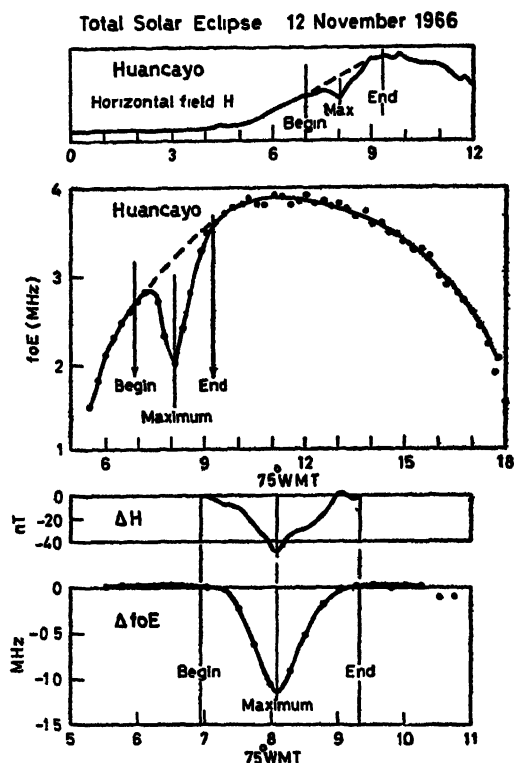


FIG. 5. Variations of the horizontal geomagnetic field,  $H$  and the critical frequency of the E-region,  $f_oE$  at Huancayo during the total solar eclipse on 12 November 1966.

occurred another solar eclipse in low latitude regions of South America during the morning hours on 24 December 1973. The maximum obscuration of the sun at Huancayo and Fuquene occurred at about 1400 UT or 0900 LT. The magnetograms did not indicate any depression in  $\Delta H$  associated with the solar eclipse. The track of totality passed close to Fuquene and still no effects were noted, suggesting that the horizontal geomagnetic field at stations close to the Sq focus, such as Fuquene is not affected by the solar eclipses.

### CONCLUSIONS

- (1) The effect of solar eclipse on geomagnetic  $H$ -field is definitely seen at equatorial electrojet stations specially when the track of totality is parallel to the magnetic equator.
- (2) Solar eclipse effects at mid latitude stations are smaller and are seen on  $D$  rather than on  $H$ -component.
- (3) Geomagnetic effects of solar eclipse decreases rapidly with the distance from

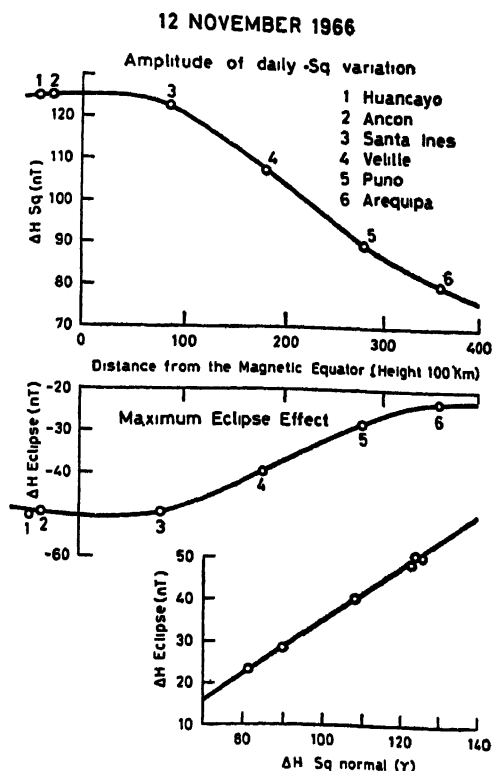


FIG 6. Latitudinal variation of normal  $Sq(H)$  and the maximum solar eclipse effect on the  $H$  field at Peruvian stations during the solar eclipse on 12 November 1966. Also, the linear relation between  $\Delta H$  due to eclipse and  $\Delta H$  due to normal  $Sq$  is shown.

totality and the effects are reduced to the level of noise at a distance of 500km from the regions of moon's shadow.

#### REFERENCES

- Bauer, L A (1900) *Terr magn atm Electr*, 5, 143  
 Bossolaco, A, Elena and Canena, A (1961) *Geofis pure appl (Milana)*, 48, 102.  
 Bremmelen, W von (1905) *Nat. Tijdschr Voor Ned Indie*, 64, afl, 3-4  
 Chapman, S (1949) *Proc. Mixed Commission on Ionosphere ICSU Brussels* (Jul 28-30), 65  
 ——— (1933) *Terr magn atm Electr*, 38, 175  
 Chree, C (1913) *J R met Soc*, 39, 231  
 ——— (1915) *Terr. magn atm Electr*, 20, 71  
 Egedal, J (1956) *J atm terr Phys*, 6, 228  
 Egedal, J, and Ambolt, N (1955) *J atm terr. Phys*, 7, 40  
 Gama, L (1948) *Terr magn atm Electr*, 53, 405  
 Giesecke, A. A, Casaverde, M, Kato, Y, Aoyama, I, and Takei, S. (1968) *Rep. Ionos Res Japan*, 22, 61  
 Kato, Y (1951) *Sci. Rep Tohoku Univ Ser*, 5, 3, 57  
 ——— (1956) *Sci Rep Tohoku Univ. Ser*, 5, 7, 21.  
 ——— (1965) *Sci Rep Tohoku Univ. Ser*, 5, 12, 1.

- Kato, Y, and Mori, Y (1968) *Rep. Ionos. Res. Japan*, **22**, 71  
Malurkar, S L (1954) *Indian J met Geophys*, **5**, 213  
Normand, C. (1907) *Terr magn atm. Electr.*, **12**, 15.  
Ryd, V H. (1917) *Publ Danush met Inst , Medd Nr* , 3.  
Sankar Narayan, P V (1956) *Kodakanal Bull* , No 144, 18  
Stoffregen, W (1956) *J atm terr Phys.*, **6**, 57.  
Van Zandt, T E (1960) *J geophys Res* , **65**, 2003

Printed in India

Geomagnetism

## MAGNETIC OBSERVATIONS AT HYDERABAD AND ETAYAPURAM DURING THE SOLAR ECLIPSE OF 16 FEBRUARY 1980

B. J. SRIVASTAVA, D. PANDURANGAM, T. S. SASTRY *and* HABIBA ABBAS

*National Geophysical Research Institute, Hyderabad-500 007, India*

*(Received 18 July 1981)*

Special magnetic observations of total intensity were continuously recorded at Hyderabad located just outside the track of totality with a Proton Precession Magnetometer (1nT/mm, 2cm/minute) on 15, 16 and 17 February 1980. These observations are analysed and studied along with records of the horizontal component taken at Hyderabad (0.99 obscuration), Etayapuram (0.82 obscuration) and Sabhawala (0.61 obscuration) magnetic observatories, on the eclipse day of 16 February 1980. Simultaneous records obtained at San Juan (U.S.A.) are also examined.

A moderate magnetic SC-storm commenced on 15 February at 1234 (SC amplitude in  $H$ , +6nT) and continued up to 16 February 2300 UT, with a range of 152nT in  $H$  and one K-index of 6 at Hyderabad. Both the horizontal component and the total intensity values at Hyderabad and the horizontal component at Etayapuram remained depressed by about 100nT on the day of eclipse as compared to the preceding day, and showed similar storm-time fluctuations superimposed thereon. Two sudden impulse events of global character were observed at 0902 UT and 1120 UT with  $H$ -amplitudes of  $-5$  and  $+4$ nT respectively at Hyderabad, at the commencement and the end of the eclipse.

A decrease of about 20nT in the horizontal component centred around the maximum phase, and about  $0.5'$  (6nT) in the westerly declination just after the maximum phase during the period of the eclipse at Etayapuram, located almost on the magnetic (dip) equator and under the influence of the equatorial electrojet, was apparently caused by the solar eclipse due to a decrease in the E-layer ionospheric conductivity and the Sq currents. At Hyderabad, a relatively smaller effect of 5nT was masked by the magnetic disturbance.

**Keywords:** Magnetic Intensity; SC-Storm; Ionospheric Conductivity; Electrojet; Sq Currents

### INTRODUCTION

THE ideal conditions for a clearcut demonstration of the Chapman-type reduction (1933) of about 28 per cent in the geomagnetic Sq variation at the time of a solar eclipse are: a magnetically quiet day, occurrence of the eclipse around local noon when the Sq attains its peak value, location of the observation site within the path of totality or closeby and a duration of several minutes for the totality. Chapman and Bartels (1940) pointed out that according to Chapman's theoretical discussion (1933), partial eclipses (with 70 per cent or more of the sun obscured at maximum phase) were as good as total eclipses for observation of their magnetic effects, in the shadow zone.

on the ground, implying thereby that totality in eclipses is of much less importance in geomagnetic than in astronomical studies. They also computed the effect of solar eclipses on the Sq current system, following the shutting off of the solar ultraviolet radiation by the moon, the consequent reduction in the ionospheric integrated conductivity (about 50 per cent in the E-layer) in the shadow zone, and the decrease of the Sq currents, resulting in a reduction of about 28 per cent in the geomagnetic Sq variation at the time of the eclipse. Since the Sq variations are abnormally large in the equatorial electrojet region as compared to low latitude stations lying outside the jet region, the eclipse reduction too would be expected to be quite large at the electrojet stations, even if the eclipse is not total.

Kato and Ossaka (1956) observed a clear and prominent geomagnetic effect decrease of 12nT in  $H$  in Ceylon (Sri Lanka) in the equatorial electrojet region on the occasion of the total solar eclipse of 20 June 1955, under very calm magnetic conditions. Although Srivastava and Sastri (1959) observed a decrease in the horizontal intensity at Phalodi in Rajasthan during the total solar eclipse of 30 June 1954, it could not be definitely ascribed to the eclipse due to slightly disturbed geomagnetic conditions prevailing at the time of the eclipse which occurred just before sunset.

The total solar eclipse of 16 February 1980, again provided an excellent opportunity for the study of its effect on the geomagnetic field in Peninsular India containing the track of totality, and the magnetic equator (equatorial electrojet region) in the extreme southern tip. Srivastava *et al.* (1980) gave a preliminary discussion of the magnetic observations made at Hyderabad and Etayapuram during the eclipse.

#### OBSERVATIONS

Special magnetic observations and continuous visual recording (speed 2cm/minute) of the total intensity  $F$  were carried out on 15, 16 and 17 February 1980, during the day hours at the Hyderabad Magnetic Observatory of NGRI, with a highly sensitive (1nT/mm) Proton Precession Magnetometer fabricated by the NGRI, besides the continuous photographic registration of the variations of  $H$ ,  $D$  and  $Z$  components using a set of normal La Cour variometers. The observations on 15 and 17 February were intended to serve as controls for the comparison of the observations recorded on the eclipse day of 16 February 1980. Simultaneous La Cour magnetograms obtained at the Etayapuram Magnetic Observatory of NGRI located almost on the magnetic (dip) equator in Tamil Nadu, and showing large geomagnetic variations due to the equatorial electrojet, were also analysed and studied for a possible eclipse reduction of the Chapman type. Magnetic records from the Sabhawala (Dehra Dun) Observatory operated by the Survey of India, in North India close to the Sq-focus, and also from the American Observatory at San Juan in the same latitude belt but in the opposite hemisphere which was free from the solar eclipse were also examined. Table I gives the coordinates of these observatories, the recording equipments and their sensitivities, the circumstances and the magnitude of the eclipse at each station as computed by Subrahmanyam and Rao (1979).

TABLE I\*

*Coordinates of the magnetic observatories, equipments used and their sensitivities and the circumstances of the solar eclipse of 16 February 1980*

Observatory	Geographic		Geomagnetic		Beginning of solar eclipse (UT)	Maximum phase of eclipse (UT)	Magni- tude at maxi- mum phase	Ending time of eclipse (UT)	Equipments and their sensitivities
	Lat	Long.	Lat.	Long.					
					h m	h m		h m	
Sabhawala	30°22'N	77°48'E	+ 20 8°	149 8°	09 09	10 18	0.61	11 20	Askania variometers, $H$ 3 2nT/mm, $D$ 0 5'/mm, $Z$ 3.4nT/mm, Paper speed 20 mm/hour.
Hyderabad	17°25'N	78°33'E	+ 7.6°	148 9°	08 58	10 17	0.99	11 26	La Cour variometers, $H$ 4.6nT/mm, $D$ 0.3'/mm, $Z$ 3 8nT/mm; Paper speed 15 mm/hour.
Etayapuram	09°10'N	78°01'E	— 0 6°	147 5°	08 51	10 11	0.82	11 21	La Cour variometers, $H$ 4.8nT/mm, $D$ 0.37'/ $Z$ 2.3nT/mm; Paper speed 15mm/hour.
San Juan (U S A)	18°07'N	293°51'E	+29.9°	3.2°		No Eclipse			Askania variometers, $H$ 1.7nT/mm, $D$ 0.5'/mm, $Z$ 3.8nT/mm; Paper speed 20mm/hour.

\*After Subrahmanyam and Rao (1979)

## DATA ANALYSIS AND ISOLATION OF ECLIPSE EFFECT

At the time of the solar eclipse of 16 February 1980, a magnetic storm was already in progress.

The storm of moderate intensity began with a sudden commencement on 15 February 1980 at 1234 UT (SC amplitude in  $H$  at Hyderabad being  $+6\text{nT}$ ) and continued up to 2300 UT on 16 February 1980, with a range of  $152\text{nT}$  in  $H$  and one K-index of 6 at Hyderabad. Both the horizontal component and the total intensity values at Hyderabad and the horizontal component at Etayyapuram remained depressed by about  $100\text{nT}$  on the day of the eclipse as compared to the preceding day and showed similar storm-time fluctuations superimposed thereon, except a characteristic decrease of about  $20\text{nT}$  at Etayyapuram during the period of the eclipse. Figs. 1, 2 & 3 give the plots of 15-minute values of  $F$  and  $H$  at Hyderabad and  $H$  at Etayyapuram on 15, 16, and 17 February.

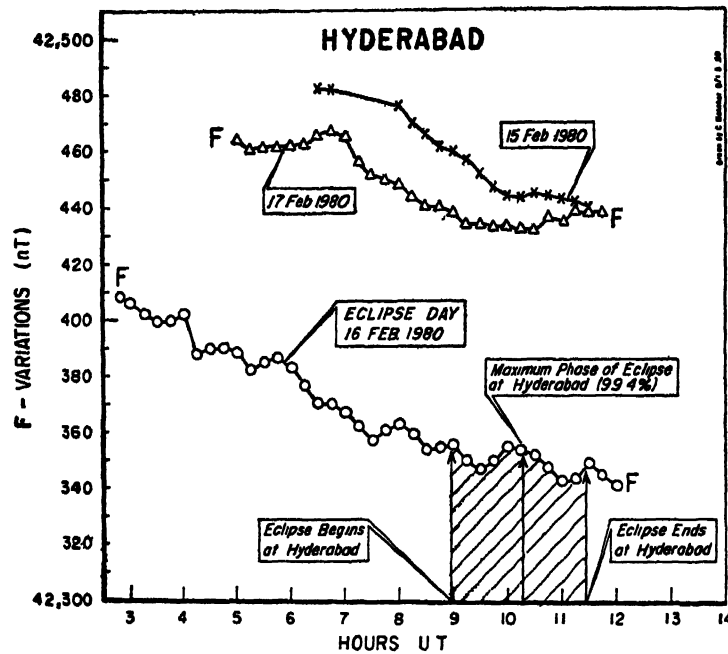


FIG 1 Plots of 15-minute values of the total geomagnetic intensity  $F$  at Hyderabad recorded with a Proton Precession Magnetometer on 15, 16 and 17 February 1980, during the day hours. The values on the eclipse day of 16 February 1980, were depressed by about  $100\text{nT}$  and showed storm-time oscillations.

Fig. 4 gives a plot of the 15-minute values of  $H$  on 16 February 1980, the day of the eclipse as recorded at Sabhawala (Dehra Dun), Hyderabad, Etayyapuram and San Juan. Storm-time fluctuations of global character were observed at all the stations, with the exception of an eclipse reduction of about  $20\text{nT}$  recorded only at Etayyapuram during the period of the eclipse.

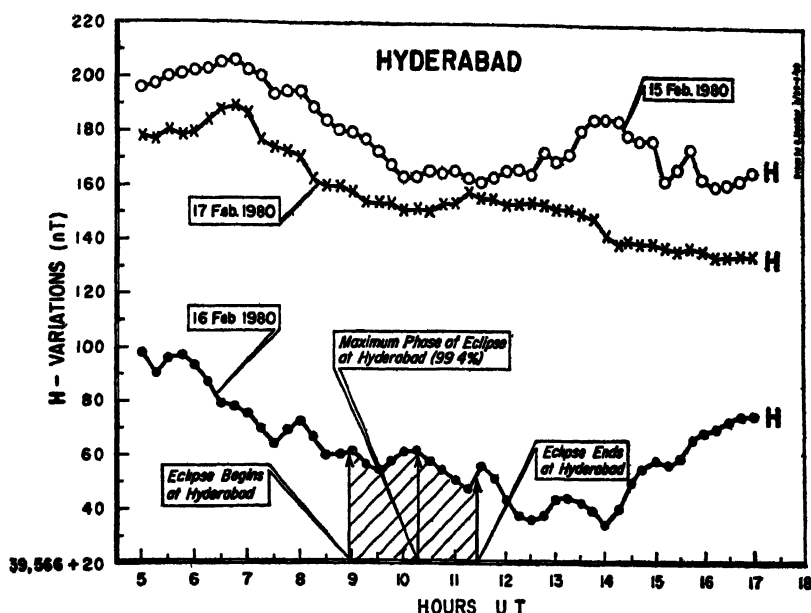


FIG. 2 Plots of 15-minute values of the horizontal intensity at Hyderabad on 15, 16 and 17 February 1980, scaled from the relevant magnetograms, during the day hours (05–17 UT). Note the depression of about 100 nT in the level of  $H$  on 16 February 1980, accompanied by storm-time fluctuations, due to the magnetic storm main phase. The effect of the solar eclipse (0.99) was vitiated by the fluctuations caused by the storm.

In order to confirm that the decrease in  $H$  observed at Etayyapuram during the eclipse was a real eclipse effect, without any contamination by the storm-time fluctuations or a counter-electrojet event, the following procedure was adopted. Departures of 15-minute values of  $H$  from the corresponding midnight value (average value for 1700 to 1800 hr UT) were computed both for Hyderabad and Etayyapuram on 16 February 1980, which gave a combination of  $S_q$  (ionospheric source) and storm-time fluctuations (magnetospheric source and ionospheric modifications). Since the storm-time fluctuations are of magnetospheric origin, with slight ionospheric modifications, their amplitudes at Hyderabad and Etayyapuram and other stations in Peninsular India, are expected to be of the same order. Hence, the differences between the corresponding departures of  $H$  at Etayyapuram and Hyderabad,  $\Delta H$  (ETT-HYB), were also computed from the 15-minute values for the hours of 01–14 UT, so as to remove the magnetospheric effect from the data and to get an idea of the ionospheric electrojet, the eclipse effect or counter-electrojet effect at Etayyapuram (Fig. 5). Rastogi (1975) used such differences between the  $S_q$  ( $H$ ) values at an equatorial electrojet station (Kodaikanal or Trivandrum) and a low latitude station (Alibag), to identify counter-electrojet events during intervals of time when  $\Delta H$  (KOD-ABG) decreased below its mean night-time value, i.e., it became negative.

Fig. 5 shows that no counter-electrojet event occurred at Etayyapuram on the day of the eclipse since no negative values of  $\Delta H$  (ETT-HYB) have been found. The decrease of about 15 nT around the maximum phase of the eclipse at Etayyapuram



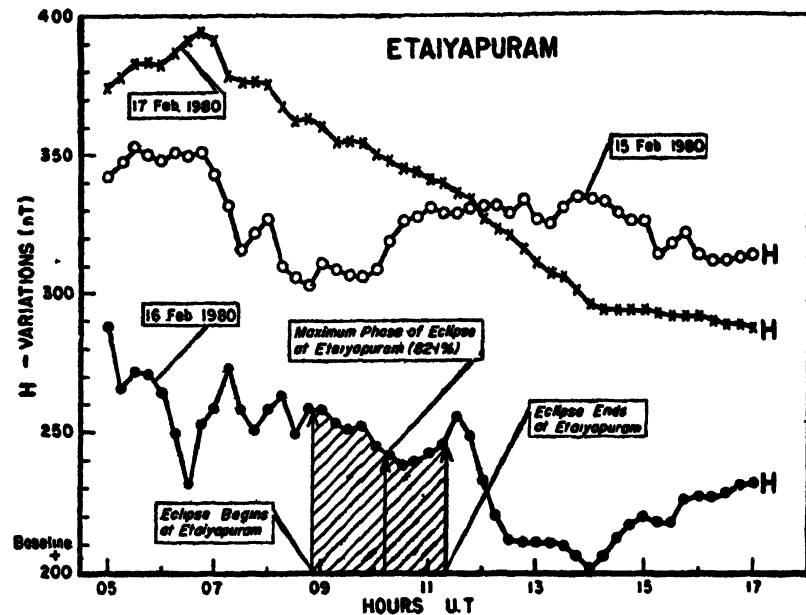


FIG. 3. Plots of 15-minute values of the horizontal intensity at the equatorial station of Etaiyapuram on 15, 16 and 17 February 1980, scaled from the relevant magnetograms during the day hours (05–17 UT). The level of  $H$  was again depressed by about 100 nT on 16 February 1980, due to the main phase of the magnetic storm, and showed storm-time fluctuations. Note the large decrease of about 20 nT around the maximum phase of the solar eclipse (0.82), caused by the eclipse

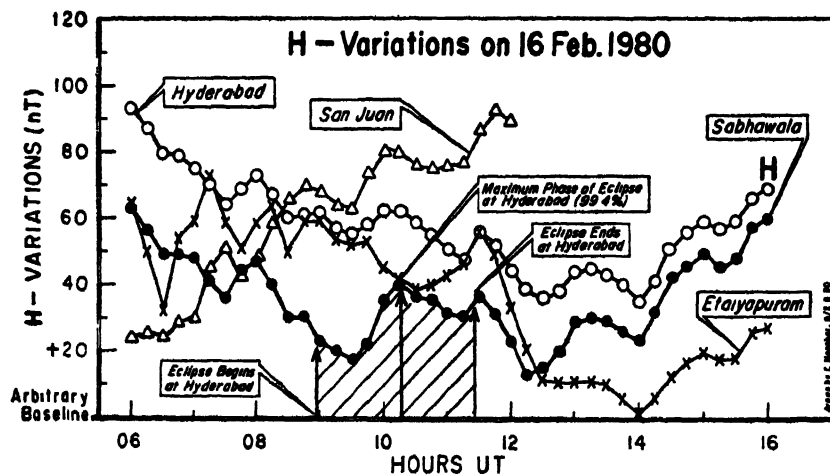


FIG. 4. Plots of 15-minute values of the horizontal intensity at Sabhawala, Hyderabad, Etaiyapuram (India) and San Juan (U.S.A.) on the eclipse day of 16 February 1980, scaled from the relevant magnetograms of the stations, showing similar storm-time fluctuations of global character during the period of the eclipse with the exception of Etaiyapuram. An eclipse reduction of about 20 nT can be clearly seen at Etaiyapuram during the eclipse.

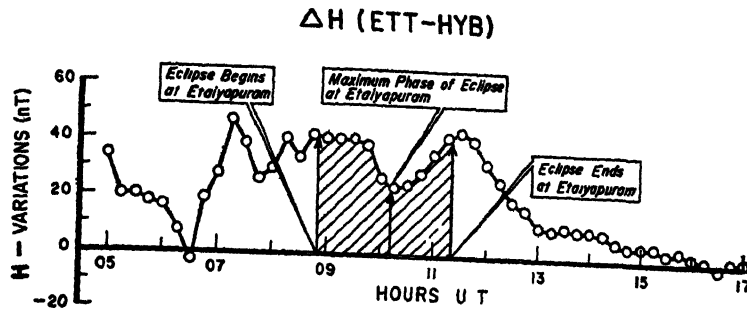


FIG. 5. Plots of 15-minute values of the differences of  $Sq(H)$  at Etaiyapuram and Hyderabad during the day hours on the eclipse day of 16 February 1980, showing clearly the difference between the eclipse reductions at Etaiyapuram and Hyderabad (15nT). It also shows the absence of a counter-electrojet event, during which the difference should be negative or below the night level

brings out the difference between the eclipse reduction in  $H$  at Etaiyapuram (20nT) and at Hyderabad (see Fig. 4). The eclipse reduction in  $H$  at Hyderabad thus turns out to be about 5nT. It will be seen from Figs. 2 and 3 that the  $Sq(H)$  corresponding to the eclipse hours on the control day of 17 February 1980, which was fairly quiet was about 20nT at Hyderabad and 60nT at Etaiyapuram. Thus the eclipse reduction in  $H$  at Hyderabad and Etaiyapuram works out to be 25 per cent and 33 per cent of the prevailing  $Sq(H)$  respectively, which is in good agreement with the theoretical results (28 per cent) of Chapman (1933).

Figs. 6 and 7 show the plots of 15-minute values of  $D$  at Hyderabad and Etaiyapuram respectively on 15, 16 and 17 February 1980, from 0500 to 1700hr UT as measured from the corresponding magnetograms of the two observatories.

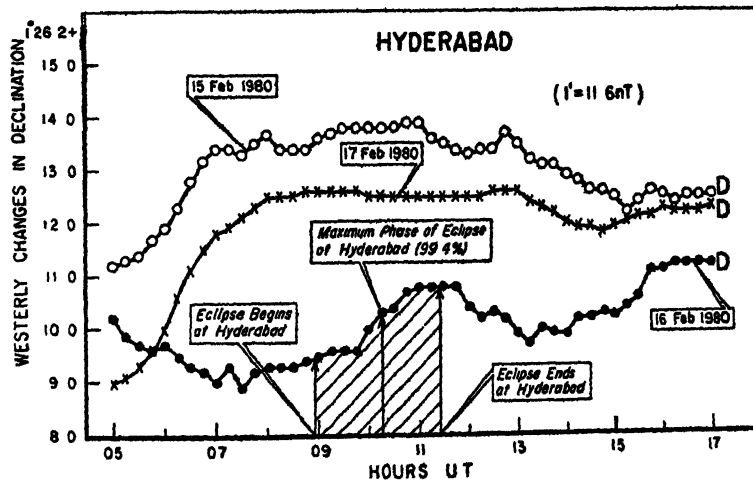


FIG. 6. Plots of 15-minute values of the westerly declination at Hyderabad on 15, 16 and 17 February 1980 scaled from the relevant magnetograms during the day hours (05–17 UT). Note the effect of the storm on 16 February 1980, and the westward swing observed during the eclipse

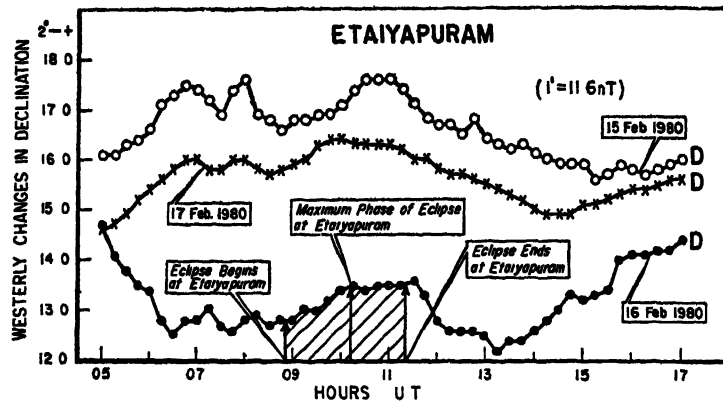


FIG. 7. Plots of 15-minute values of the westerly declination at Etaiyapuram on 15, 16 and 17 February 1980, scaled from the relevant magnetograms during the day hours (05–17 UT). The reduction of  $0.5'$  ( $6\text{ nT}$ ) in the westward swing observed during the eclipse, as compared to Hyderabad, was due to the solar eclipse

The storm effect can again be seen in the depressed levels of the westerly declination at both the stations on 16 February 1980, accompanied by similar storm-time oscillations. The westward swing of  $1.25'$  during the eclipse at Hyderabad reduced to  $0.75'$  at Etaiyapuram under the influence of the solar eclipse, thereby showing that the eclipse reduction at Etaiyapuram in the westward fluctuation was  $0.5'$  ( $6\text{ nT}$ ). Since the variations in the vertical component  $Z$  reflect a considerable amount of anomalous ground induction effects arising from crustal inhomogeneities, no attempt was made to study the eclipse effect in  $Z$ .

Of special significance were two sudden impulse events of global character recorded at the commencement and the end of the eclipse on 16 February 1980, at 0902 and 1120 UT with  $H$ -amplitudes of  $-5\text{ nT}$  and  $+4\text{ nT}$  respectively at Hyderabad. These formed part of the magnetic storm which was in progress on the day of the eclipse (Fig. 5), and were also observed simultaneously at Dixon Island, Sverdllovsk, Alma Ata, Tashkent, Furstenfeldbruck and San Juan. Such hydromagnetic signals are also associated with bursts of pulsation activity.

We have thus demonstrated how an eclipse effect can be isolated under geomagnetically disturbed conditions, following a method quite different from that of Stening *et al.* (1971), and further shown that these magnetic effects (reductions) are quite large in the equatorial electrojet region.

#### CONCLUDING REMARKS

Although a magnetic storm was in progress at the time of the solar eclipse of 16 February 1980, it was possible to identify and isolate an eclipse effect in the horizontal intensity and declination at the equatorial station of Etaiyapuram. The eclipse reduction in  $H$  at Etaiyapuram (0.82 obscuration) was about  $20\text{ nT}$  around the maximum phase, amounting to about 33 per cent decrease in the prevailing  $S_q$ , while at Hyderabad (0.99 obscuration) it was only about  $5\text{ nT}$ , a decrease of about 25 per

cent in the  $S_q$ , which is in good agreement with the theoretical results of 28 per cent reduction given by Chapman (1933). A reduction of about  $0.5'$  ( $6nT$ ) in the variation of westerly declination during the eclipse was also observed at Etayapuram

#### ACKNOWLEDGEMENTS

Grateful thanks are due to the Director, Geodetic and Research Branch, Survey of India, Dehra Dun, for copy of the magnetic record of Sabhawala, and to the World Data Centre A for Solar Terrestrial Physics, NOAA, Boulder, Colorado, U.S.A., for copies of the magnetograms for 16 February 1980, from other observatories around the world used in this investigation. We also thank Dr P. V. Sankar Narayan for valuable discussions, and Shri N. P. Rajendra Prasad for assistance in the observations with the Proton Precession Magnetometer. The paper is published with the kind permission of the Director, NGRI.

#### REFERENCES

- Chapman, S. (1933) The effect of a solar eclipse on the earth's magnetic field. *Terr. Mag.*, **38**, 175–183.
- Chapman, S., and Bartels, J. (1940) *Geomagnetism*, I and II. Clarendon Press, Oxford, 354, 794–798.
- Kato, Y., and Ossaka, J. (1956) The effect of the solar eclipse on the  $S_q$  current of the diurnal variation. *Sci. Rep. Tohoku Univ. Ser. No. 5, Geophys.*, **7**, Suppl., 21–29.
- Rastogi, R. G. (1975) On the simultaneous existence of eastward and westward flowing equatorial electrojet current. *Proc. Indian Acad. Sci.*, **81A**, 80–92.
- Srivastava, B. J., Pandurangam, D., Sastry, T. S., and Habiba Abbas (1980) A note on the geomagnetic observations made at Hyderabad and Etayapuram during the solar eclipse of 16 February 1980. In: *Observations of the Total Solar Eclipse of 16 February 1980—Preliminary Results*. INSA, New Delhi.
- Srivastava, B. J., and Sastri, N. S. (1959) On the variation in the horizontal intensity of the geomagnetic field at Phalodi (Rajasthan) during the solar eclipse of 30 June 1954. *Indian J. Met. Geophys.*, **10**, 73–84.
- Stening, R. J., Gupta, J. C., and van Beek, G. J. (1971) Magnetic observations in Canada during the solar eclipse of March 7, 1970. *Nat. Phys. Sci.*, **230**, 22–23.
- Subrahmanyam, P. V., and Rao, S. S. (1979) *Local Circumstances for the Total Solar Eclipse of February 16, 1980 for Indian locations*. Contr. No. 11 of Nizamiah and Japal-Rangapur Observatories. Department of Astronomy, Osmania University, Hyderabad, pp. 1–27.

Printed in India.

Geomagnetism

## GEOMAGNETIC FIELD OBSERVATIONS IN THE INDIAN ZONE DURING THE TOTAL SOLAR ECLIPSE OF 16 FEBRUARY 1980

R. G. RASTOGI, G. K. RANGARAJAN and A. K. AGARWAL

*Indian Institute of Geomagnetism, Colaba, Bombay-400 005, India*

*(Received 15 February 1982)*

The present paper examines the geomagnetic field observations in the Indian zone during the period of total solar eclipse of 16 February 1980. The eclipse day was highly disturbed and the magnetograms were affected both by non-ionospheric as well as non-Sq ionospheric currents. No definite eclipse induced effects in the geomagnetic field could be isolated when the magnetograms from Indian zone (65-80°E) are compared with the same from 100-150°E longitude zone.

**Keywords:** Geomagnetism; Solar Eclipse; Magnetogram; Non-Sq Ionospheric Currents

### INTRODUCTION

SOLAR quiet-day variation (Sq) of the geomagnetic field is largely due to the dynamo currents in the E-region and, therefore, it is natural to expect change in Sq whenever the dynamo system is altered. However, attempts to detect change in the geomagnetic field in the eclipse zone have only met with partial success (Rastogi, *see p 464*) mainly due to the following facts: (i) Geomagnetic eclipse effects will be clear only on magnetically quiet days whereas often the day of the eclipse is geomagnetically disturbed and (ii) the anticipated decrease in magnetic field is small though the E-region depletion of electron density is quite appreciable. Attempts have been made in recent years, to identify eclipse-induced geomagnetic field changes even during disturbed conditions (Stening *et al*, 1971; Lilley & Woods, 1978; and Rangarajan & Murty, 1981). A total eclipse of the sun, with its track of totality running almost parallel to the dip equator in the Indian zone, occurred on 16 February 1980.

In this note we utilize the original magnetograms obtained at a chain of magnetic observatories in the Indian zone (all stations are within  $\pm 5^\circ$  of 75°E meridian) for four days between 13 February and 17 February 1980. The stations considered include Gulmarg, Jaipur, Ujjain, Alibag, Hyderabad and Trivandrum. Actual magnetograms of Alibag for 4 days are shown in Fig 1.

### ANALYSIS AND RESULTS

The mean quiet-day variations in *H*-component during February 1980 at the Indian stations are shown in Fig. 2. It is seen that at Gulmarg the range of the diurnal varia-

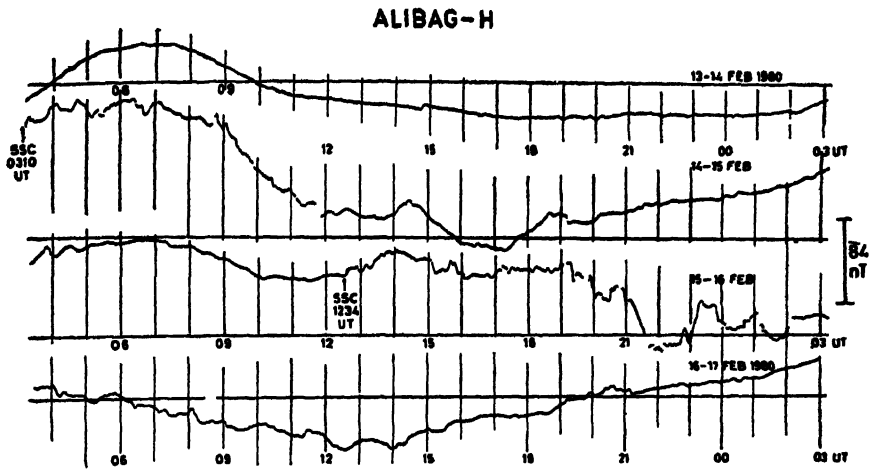


FIG. 1. Reduced magnetograms of Alibag  $H$  for four days between 13 and 17 February 1980

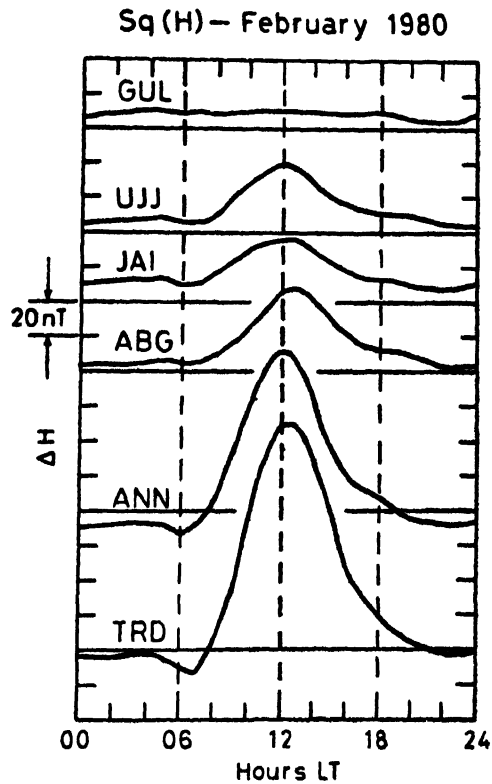


FIG 2 Average solar quiet day variation in  $H$  for February 1980 for some Indian stations

tion of  $S_q(H)$  is small indicative of the proximity of the station to the focus of the northern hemispheric  $S_q$  current system. This is consistent with the inferred position of focus for winter from latitudinal variations by Arora *et al* (1980).

During disturbances, the field variations of non-ionospheric origin are expected to have similar features and magnitudes at stations separated by small latitude spacings and in the same longitude zone, and therefore can mostly be eliminated by subtracting the recorded variations at Gulmarg from that of the other stations. In this process of subtraction, ionospheric part of the variations is expected to be retained (Kane, 1978). To test the validity, we obtained the difference in hourly values of  $H$  at Alibag and Gulmarg for each day of the month in February 1980. For all the days the maximum of the difference occurred within  $\pm 1$  hour of local noon but the difference curve for 16 February 1980 was distinctly odd. Also, synchronous with the maximum phase of the eclipse, a depression in the field could be noticed. The difference curves for some typical days are given in Fig. 3. Therefore, it was considered worthwhile to examine this feature in greater detail. The magnetograms were digitized at 3-minute intervals for the three days 13, 15 and 16 February 1980. 13th was a quiet day whereas the other two were marked by field fluctuations of disturbance origin. A sudden commencement was registered on the  $H$  trace at 0310 UT on 14 February and another at 1234 UT on 15 February (see Fig. 1).

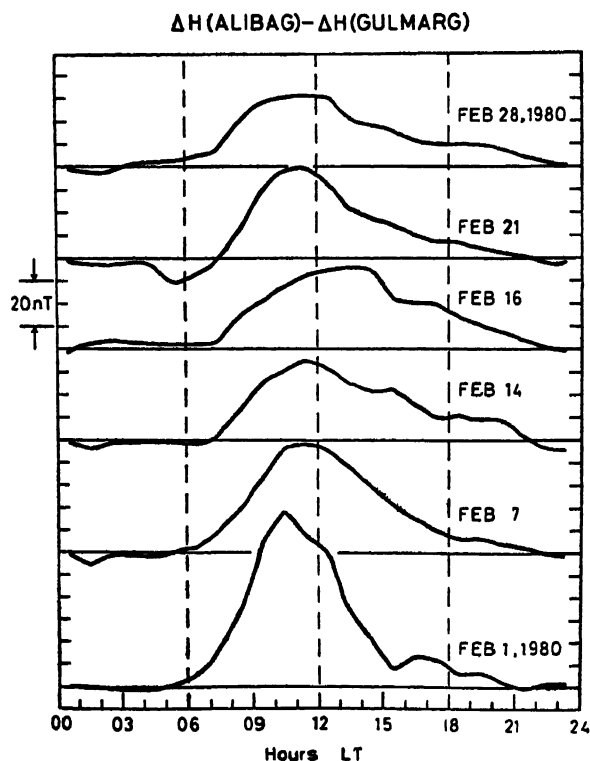


FIG. 3 Diurnal variation of the difference in mean hourly values of  $H$  at Alibag and Gulmarg for some typical days of the month of February 1980. Note the odd feature on the eclipse day.

Plots of the high-resolution difference (between station and Gulmarg) are given in Fig. 4. It is seen that on a magnetically quiet day the excess variation at both stations Alibag and Trivandrum are very smooth and systematic and depict behaviour expected of a local time dependent ionospheric-current-induced magnetic variations. On 15 February, the low latitude stations outside the electrojet belt, still depict the smooth diurnal variation and the difference curve for Tashkent and Gulmarg show the anticipated reversal in pattern. But, at Trivandrum in the electrojet region, the smooth variation is replaced by a two-humped structure indicative of the role played by electric fields in the jet region during disturbances (Rastogi, *see* p. 464).

On 16 February the quiet-day variation pattern is completely obscured at all the stations (*see* Fig. 1 for Alibag) suggesting that the entire variation is mainly due to disturbance only. The process of subtraction of Gulmarg data at each instant of time from other station, would therefore be expected to yield again features similar to that observed for 15 February 1980 except for the duration where the moon's shadow was sweeping over the station. Fig. 4 (top panel) shows that while Alibag and Jaipur do indeed show anticipated diurnal variation with maximum close to local noon, the phase reversal at Tashkent is absent. Hyderabad had a slightly different pattern and Trivandrum variations are characterized by high-frequency oscillations, even during periods before commencement of the eclipse. However, coincident with the eclipse interval, a clear deviation from the smooth decrease of the field could be noticed at all the stations Jaipur, Alibag, Trivandrum and to a small extent at Tashkent. Is this due to the solar eclipse? The answer could only be an ambiguous 'yes'. The ambiguity arises from several factors.

- (i) The eclipse effect decays exponentially as a function of distance away from the centre of totality and stations beyond about  $5^\circ$  is not expected to show any signature (Egedal, 1956, and Rastogi, 1981) but Jaipur being  $9^\circ$  away in latitude from path of totality does indeed show an appreciable deviation.
- (ii) If the depression in the field observed at Trivandrum is to be attributed to the eclipse effect, then similar depression occurring earlier to the onset of eclipse need also to be explained. If they are due to electric field changes in the equatorial region, then similar field was also the cause of depression during the eclipse period.
- (iii) Finally, for Tashkent where the obscuration of the sun was less than 15 per cent, there is still a tendency of the field to diminish in relation to its neighbourhood during the eclipse. Does it imply that the global Sq current, at least over the longitude zone of the moon's shadow path, reduces in strength for the duration of the eclipse? Or does it mean that the process of subtraction still leaves the effects of non Sq currents?
- (iv) In Fig. 5, we show the magnetic field variation on 16 February 1980 between 4 and 12 UT as recorded at pairs of station in nearly the same latitude but separated in longitude, which includes the hours of eclipse in the Indian zone. The eclipse effect being local time dependent, should be seen only at Indian zone and not at further east of Indian longitude stations. Thus there should



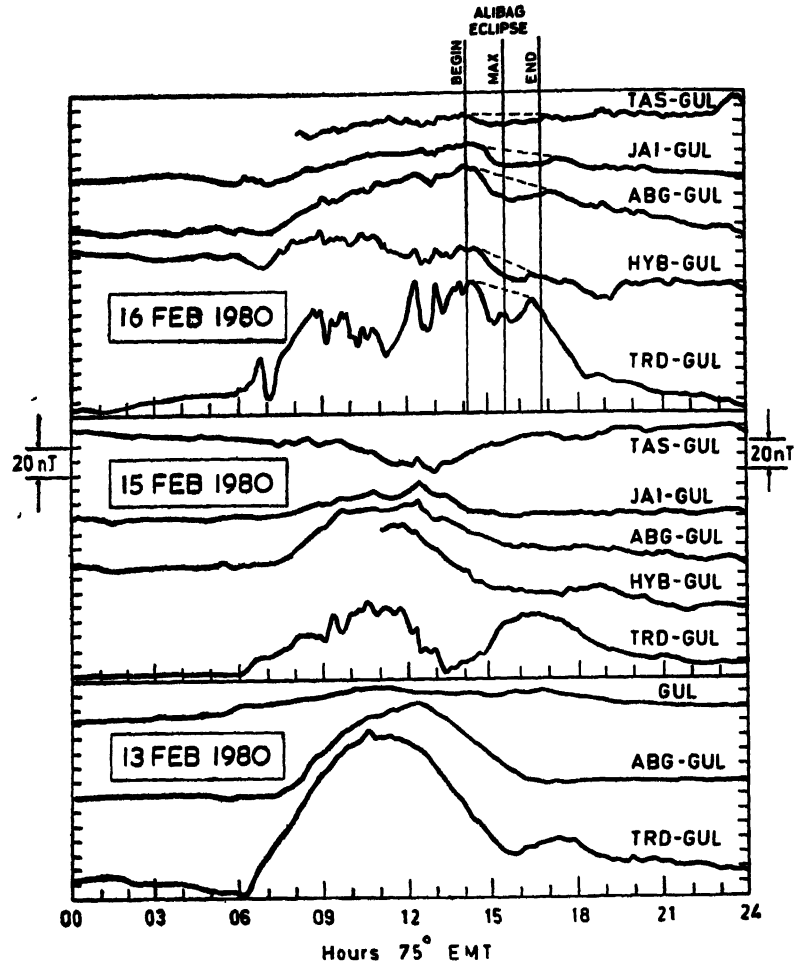


FIG 4 High-resolution difference curve (at 3min interval) between the  $H$  field at some stations in the Indian Zone and Gulmarg for three days 13, 15 and 16 February 1980

be no eclipse effects at Hong Kong (long.  $105^{\circ}\text{E}$ ), Kakioka (long.  $140^{\circ}\text{E}$ ) or Guam (long.  $145^{\circ}\text{E}$ ). On the other hand, field changes of non-ionospheric origin should occur at the same UT at all the stations. From Fig 5, we notice between 9 and 12 UT, a depression followed by a slow rise at Gulmarg, which occurs at the same UT at Hong Kong and can be seen even at Kakioka indicating this to be of non-ionospheric origin. If this variation has larger amplitude at Gulmarg, then one can see changes in the difference curves (Gulmarg minus station) coincident in time with the eclipse duration but not necessarily caused by the ionospheric changes due to the sun's obscuration. Thus the decrease of geomagnetic field component  $H$  at Indian stations with respect to the same Gulmarg though vary with the time of the eclipse in the Indian region near the

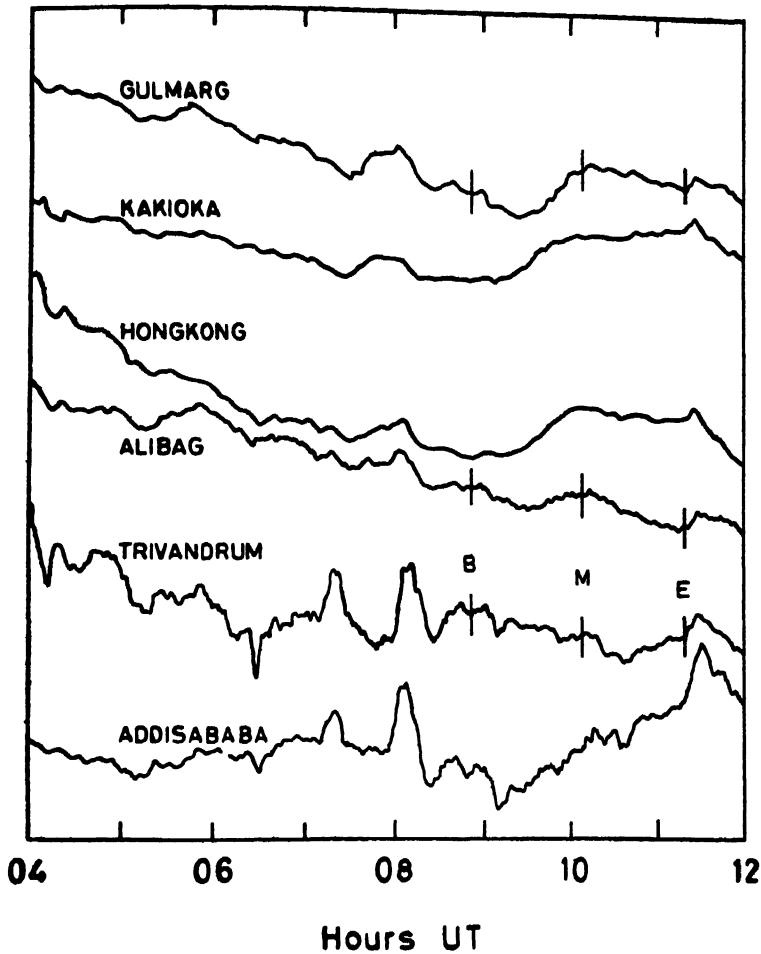


FIG 5  $H$  variation trace at pairs of stations in nearly the same latitude but well separated in longitude for 8 hours inclusive of eclipse duration on 16 February 1980

totality does not conclusively attribute due to loss of ionisation and thereby due to decrease of conductivity and hence due to the Sq current. Most probably these effects are due to some sort of non-Sq current regions during highly geomagnetic active periods. In the electrojet region, large short-period fluctuations are seen both at Trivandrum and at Addis Ababa centred on the eclipse duration in Indian zone. Many of these fluctuations appear to be only an enhancement of weak fluctuations observed simultaneously at other low latitude stations. These can be attributed to enhancement due to electrojet of sources universal in nature rather than localized eclipse effect. Any eclipse effect at Trivandrum, if present, seems to have been vitiated by large storm-time electric field fluctuations. For reference of their readers, details of the solar eclipse at few select stations are provided in Table I.

TABLE I

*Details of the solar eclipse at few select stations in Indian zone*

Station	Code	Geogr Lat	Geogr. Long	Dip	Begin	Max	End	Magnitude
IST								
Tashkent	TAS	41° 25' N	69° 12' E	61° N	—	—	—	0 15
Gulmarg	GUL	34° 03' N	74° 24' E	51° N	1440	1544	1642	0 47
Jaipur	JAI	26° 55' N	75° 48' E	40° N	1432	1546	1651	0 68
Ujjain	UJJ	23° 11' N	75° 47' E	33° N	1428	1545	1653	0 79
Alibag	ABG	18° 38' N	72° 52' E	25° N	1419	1540	1653	0 87
Hyderabad	HYD	17° 25' N	78° 33' E	20° N	1428	1547	1656	0 99
Trivandrum	TRD	8° 29' N	76° 57' E	1° S	1420	1540	1650	0 80

## REFERENCES

- Arora, B R, Rao, D R K, and Sastri, N S (1980) *Proc. Indian Acad. Sci*, **89**, 333.  
 Bossolaco, A, Elena, and Canena, A (1961) *Geofis pure appl (Milano)*, **48**, 102  
 Egedal, J (1956) *J. atm terr. Phys*, **6**, 228.  
 Kane, R. P. (1978) *J geophys Res* **83**, 5312  
 Lilley, F E M, and Woods, D V (1978) *J atm terr Phys*, **40**, 749  
 Rangarajan, G K., and Murty, A V. S (1981) *Curr. Sci*, **50**, 185  
 Rastogi, R. G (1981) *Indian J Radio Space Phys*, **10**, 1  
 ——— (1982) A review in the Present Bulletin  
 Stening, R J, Gupta, J. G, and van Beek, G J (1971) *Nat Phys Sci*, **230**, 22  
 Stoffregen, W. (1956) *J atm terr Phys*, **6**, 57

Printed in India

Geomagnetism

## MAGNETOMETER ARRAY STUDY AND TOTAL SOLAR ECLIPSE OF 16 FEBRUARY 1980

N K THAKUR, M. V. MAHASHABDE, B. R. ARORA and B P. SINGH

*Indian Institute of Geomagnetism, Colaba, Bombay-400 005, India*

and

B. J. SRIVASTAVA and S. N. PRASAD

*National Geophysical Research Institute,  
Uppal Road, Hyderabad-500 007, India*

*(Received 15 February 1982)*

During the period of total solar eclipse of 16 February 1980, in addition to the nine magnetic observatories over different parts of the country, the registration of transient magnetic variations was in progress by an array of 21 magnetometers in the Indian peninsula. The primary objective of this array study was to delineate the electrical conductivity structure through the electromagnetic induction effects. A few stations were so located that they could detect geomagnetic effect of solar eclipse. In spite of favourable geographical location, the possibility of detecting simple 'Chapman' effect was largely hindered because of the occurrence of a magnetic storm. As many of storm related effects propagate through ionosphere, it is likely that certain features of short-period fluctuations may be altered in the shadow region of total solar eclipse due to perturbation in ionospheric conductivity. The feasibility of detecting eclipse effect during magnetically disturbed conditions has been demonstrated by comparing simultaneous magnetic records in and outside the region of solar eclipse. Taking advantage of excellent network of magnetic observations during the period around 16 February 1980 over Indian peninsula, we have attempted to isolate magnetic effects associated with the eclipse.

Examination of the records of horizontal component at a number of stations situated on a line approximately at right angles to the path of totality indicates the presence of a depression on the field synchronous with the time of eclipse whose characteristics fairly resemble those expected from the Chapman theory. The critical examination of short-period fluctuations in  $H$  at other times coupled with the nature of variation in the vertical component, which is very prone to the local conductivity structure of the earth, clearly suggests that some of the spatial characteristics of the depression in the field observed at the time of eclipse may as well be due to the varying sub-surface geology. Yet another noteworthy event of unusual nature is a sharp fluctuation whose signature differs markedly to the north and south of the path of totality. Its amplitude increases with increasing distance from the path of totality, particularly in the electrojet belt. The possibility of its being associated with eclipse is discussed giving possible source mechanism.

**Keywords:** Magnetometer Array; Solar Eclipse; Complex Demodulation; Eclipse Effect

## INTRODUCTION

SINCE the beginning of the 20th century attempts have been made to discover geomagnetic field changes produced by solar eclipses. The observed results were not very convincing because of vague changes during eclipses and frequent overlapping with geomagnetic disturbances. Chapman (1933) discussed the eclipse effect theoretically, and Chapman and Bartels (1940) emphasized the need for further observations. Based on theoretical considerations, Chapman (1933) proposed an ionospheric current model during an eclipse, according to which a decrease of 28 per cent is expected in the  $S_q$  ( $H$ ) at the time of the eclipse. Nagata *et al.* (1955) used different ionospheric parameters and revised the Chapman model to account for the expected effect on all the components of the Earth's magnetic field.

Following Egedal and Ambolt (1955), Kato (1960) indicated a clearcut decrease in the horizontal field during an eclipse. Egedal and Ambolt (1955), Kato (1956, 1960 and 1965), Nagata *et al.* (1955), Stenning *et al.* (1971), Lilley and Woods (1977), Scheepers (1978) and Lilley and Woods (1978) discussed the eclipse effect on the geomagnetic field in detail.

An array of 21 magnetometers (Fig. 1) was in operation in southern India during

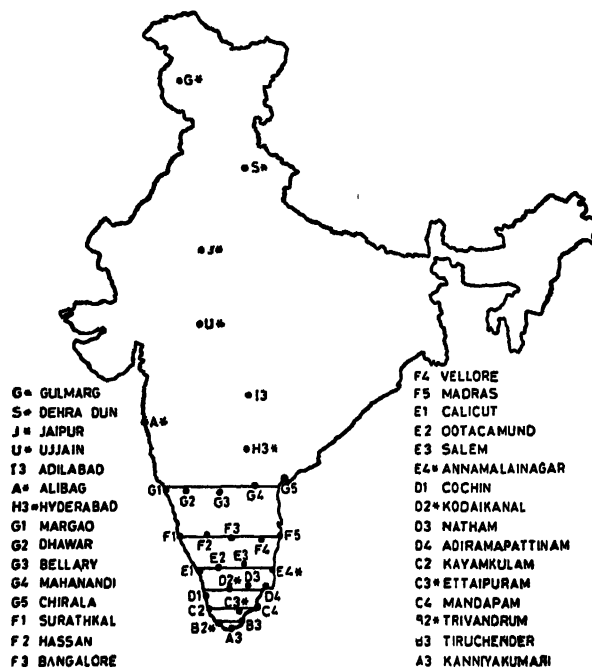
SOUTHERN MAGNETIC ARRAY STATIONS AND  
PERMANENT OBSERVATORIES OF INDIA

FIG 1 Map of India showing the locations of the 21 magnetometer array stations in South India and the permanent magnetic observatories\*.

the period December 1979 to March 1980. This gave us an opportunity to evaluate the eclipse effect on the geomagnetic field on 16 February 1980.

### RESULTS

With the proposed theories and observations, one would expect a clearcut decrease in the geomagnetic field. This effect could easily be evaluated and demonstrated, provided the eclipse day is quiet. Unfortunately, the day of the eclipse happened to be magnetically disturbed because of which it becomes difficult to isolate the eclipse effect. In such an eventuality one tries to study the behaviour of short-period events as has been done earlier (Stening *et al.*, 1971). We also selected five geomagnetic events which occurred prior to the onset of the eclipse, during the eclipse, and after the eclipse. All the amplitudes of the events in  $H$  were normalized, with respect to Hyderabad—a station away from tectonically active regions and located on the edge of totality. The amplitudes in  $Z$  being very susceptible to local geology and  $D$  amplitudes in the region being small, these were not analysed. Fig. 2 represents the normalized values at six stations situated on either side of the path of totality. To emphasize the observed effect, we also computed the complex demodulation (Banks, 1975) of these variations at the six stations including Hyderabad. These results are

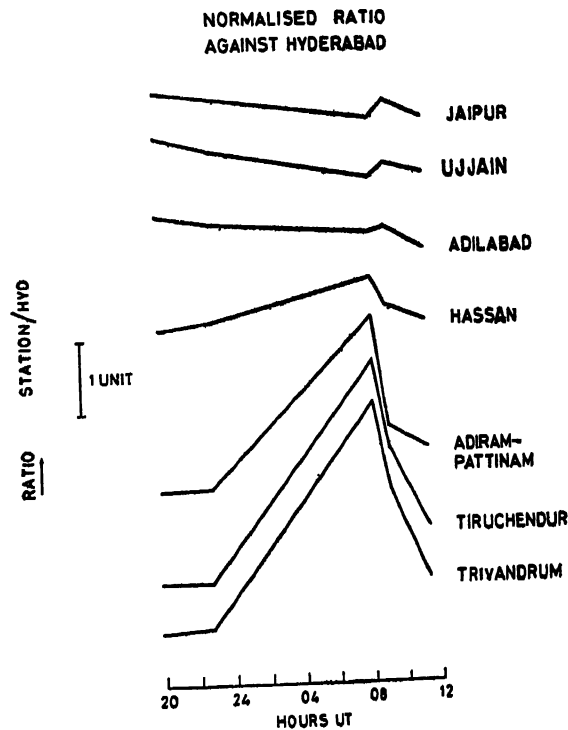


FIG 2 Plots of normalised values of  $H$ -amplitudes with respect to Hyderabad for selected short-period fluctuations on the eclipse day of 16 February 1980. Note the sharp fall in the ratio at the electrojet stations and increase in the ratio at the stations north of the path of totality.

presented in Fig. 3. The use of complex demodulation is to detect the presence of a hidden periodicity in a data series and to determine its frequency and phase, and variation of amplitude. We selected 23 minutes periodicity for our analysis, which showed a prominent spectral peak. The solar eclipse reduction in  $H$  can be clearly seen in Figs. 2 and 3.

#### DISCUSSION

Theories proposed so far predict 28 per cent decrease in the earth's magnetic field variation arising from solar quiet day current system, due to a reduction in the ionospheric conductivity at the time of the solar eclipse. These effects can be easily seen when the day of the solar eclipse is magnetically calm. Kato (1956, 1960) observed clearcut decreases in  $H$  for the solar eclipse in Ceylon on 20 June 1955 and at Sunwarrow Island on 12 October 1958 respectively. It is however observed that quiet conditions generally do not prevail during the occurrence of solar eclipses. One has therefore to search for an alternative method for the study of the effect of solar eclipses on disturbed days. Stening *et al.* (1971) considered the variation of short-period fluctuations and showed a reduction in the  $H$  amplitudes.

The studies carried out so far used only two or three stations' data to evaluate the solar eclipse effect. Chapman (1933) had also advocated that due weightage should be given to the internal currents induced by the external field. Any anomalous behaviour of induced internal currents may mislead in interpreting the observed results. An ideal way to study the solar eclipse effect is through an array of magnetometers spread over the eclipse region. An earlier attempt by Lilley and Woods (1976) by an array of magnetometers in Australia for the eclipse of 23 October 1976 indicated the effect of the solar eclipse. But subsequent remarks by Scheepers (1978) made Lilley & Woods (1978) to reinterpret their observed results. They have found that the observed effect near the path of totality was not due to the solar eclipse.

As the day of the eclipse (16 February 1980) was moderately disturbed (with one  $K_p$  index during the eclipse = 6), we attempted to evaluate the effect of eclipse in short-period events. The normalised ratio (Fig. 2) definitely indicates a fall in the amplitude especially at Hyderabad (99.4 per cent obscuration). To arrive at more conclusive results, a periodicity of around 23 minutes was subjected to complex demodulation. From Fig. 3, it can be clearly seen that a sharp fall in the amplitude of 23 minutes periodicity around the time of the greatest phase of the eclipse, does exist.

The present study thus clearly shows that the eclipse reduces the ionospheric conductivity and consequently causes a decrease in the  $H$  amplitudes of the geomagnetic fluctuations.

#### ACKNOWLEDGEMENTS

The authors thank the Directors of IIG and NGRI for support and encouragement of magnetometer array studies in India. They also thank Dr F. E. M. Lilley, ANU, Canberra, for the loan of the Australian magnetometers used for this study. Assistance in the field work rendered by Shri V. H. Badshah and Shri A. K. Phanse (IIG) and Dr A. V. Ramana Rao and Shri S. B. Gupta (NGRI), is gratefully acknowledged.

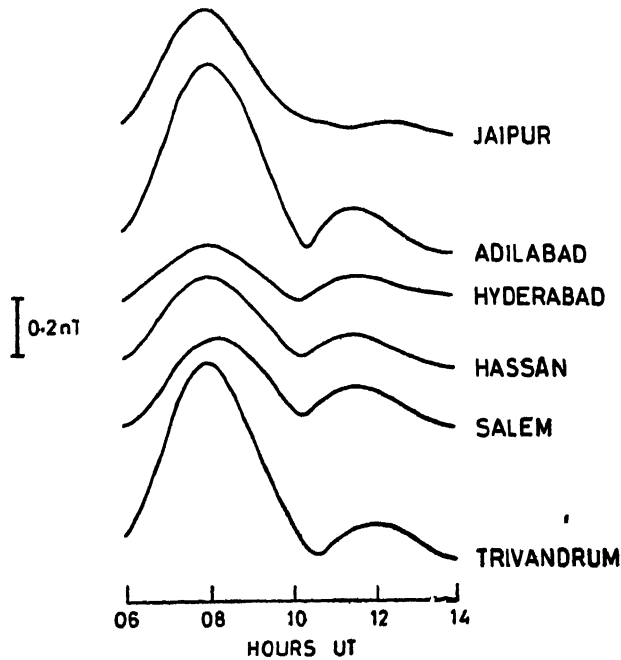
COMPLEX DEMODULATION OF  $H$   
FOR INDIAN STATIONS

FIG 3. Complex demodulation of  $H$ -variations (23-minute periodicity) at Indian stations during the solar eclipse of 16 February 1980

## REFERENCES

- Banks, R J (1975) *Geophys J R astr Soc*, **43**, 87–101  
 Chapman, S (1933) *Terr Mag*, **38**, 175–183  
 Chapman, S, and Bartles, J. (1940) *Geomagnetism*, 1 & 2 Clarendon Press, Oxford, 354, 794–798  
 Egedal, J, and Ambolt, N (1955) *J atm terr Phys*, **7**, 40  
 Kato, Y (1956) *Sci Rep Tohoku Univ Ser*, **5**, *Geophys*, **7** *Suppl*, 1–41  
 ——— (1960) *Sci Rep Tohoku Univ Ser*, **5**, *Geophys*, **11**, 1–10  
 ——— (1965) *Sci Rep Tohoku Univ Ser*, **5**, *Geophys*, **16**, 49–62.  
 Lilley, F E M, and Woods, D V (1977) *Nature*, **266**, 823  
 ——— (1978) *J atm terr Phys*, **40**, 749–754  
 Nagata, T, Nakata, Y, Rikitake, T, and Yacoyama, I (1955) *Rep Ionos. Res Japan*, **9**, 121–135  
 Stening, R J, Gupta, J C, and van Beek, G J (1971) *Nat. phys Sci*, **230**, 22–23  
 Scheepers, J L M (1978) *Nature*, **271**, 91



Printed in India.

**Overview (Rocket Experiment)**

**THE INDIAN ROCKET PROGRAMME FOR THE  
16 FEBRUARY 1980 SOLAR ECLIPSE**

B H. SUBBARAYA

*Physical Research Laboratory, Ahmedabad-380 009, India*

*(Received 31 July 1981)*

The importance of a solar eclipse for upper atmospheric studies and the great advantage of making *in-situ* measurements using rockets have been well recognised. Studies conducted during the previous eclipses have brought to focus several important problems in D-region chemistry, mesospheric and thermospheric structure, the thermal balance in the ionosphere, generation of gravity waves and changes in the electromagnetic structure of the upper atmosphere. The solar eclipse of 16 February 1980 was seen at 80 per cent obscuration level over the Thumba rocket range, 90 per cent obscuration level over the Sriharikota range and was nearly total over the new Balasore range. Recognising the great potential offered by this fortunate circumstance, the Indian scientific community set about organizing a consolidated rocket programme for this eclipse. The final approved rocket programme had of necessity to be a compromise between the scientific aspirations and the various practical and technological constraints such as the availability of rockets, indigenous scientific instrumentation capability, the fact that Balasore range was still new where the facilities had to be augmented for the conduct of scientific experiments, and that even though the Thumba range was well established and used to the undertaking of scientific campaigns, the Sriharikota range was relatively new and was not yet geared to the handling of scientific campaigns.

This review gives an account of the rocket programme that was undertaken in India for the 16 February 1980 solar eclipse, together with the scientific objectives of the programmes. Several institutions in India and a few scientists from abroad participated in the programme. A good portion of the rocket programme was successful and detailed results obtained from these experiments are presented in several contributed papers that follow.

**Keywords:** Indian Rocket Programme; Solar Eclipse; Mesospheric & Thermospheric Structure

**INTRODUCTION**

THE importance of a solar eclipse for atmospheric investigations has been well recognised for several decades (Beynon & Brown, 1956; and Anastassiades, 1970). In the earth's atmosphere, solar radiation plays a fundamental role in the photochemical and dynamical processes that take place, deciding the structure, composition and the dynamics of the atmosphere at all levels. Photodissociation of molecular oxygen provides not only the major energy source to the atmosphere at altitudes above about 90km, but also produces atomic oxygen which is the precursor

for a large number of photochemical reactions and processes. One of the major consequences of oxygen photodissociation is the production of ozone which has a fundamental role to play in the earth's atmosphere. Both atomic oxygen and ozone play important roles not only in the energetics of the earth's atmosphere but also in atmospheric chemistry by initiating and participating in a series of photochemical reactions. The series of photochemical reactions in the upper atmosphere is quite complex and a total solar eclipse offers a unique opportunity to study the upper atmosphere since in a relatively short interval of time, the solar radiation flux rapidly reduces to near zero values and then recovers to its original value. Since all this happens in a time interval much shorter than the normal 24 hours and since during these changes the solar zenith angle does not undergo a large variation the photochemical changes are much more enhanced than during the normal day-night cycle.

With the advent of *in situ* measuring techniques on board rockets and satellites, a solar eclipse has assumed an increased importance for study of the processes in the upper atmosphere. It has become possible to directly measure the concentrations at different levels in the atmosphere, not only of electrons and ions, but also make measurements on various photochemically important minor atmospheric constituents and the detailed changes of the composition in the atmosphere. A few eclipse campaigns have been conducted by various groups in the past and these have yielded several interesting results. The number of such campaigns has however been small. Low latitude studies have a special significance due to the fact that the effect of charge particle incidence is small. The solar eclipse of 16 February 1980 was seen as a total eclipse over some parts of India and was near total over the Thumba and SHAR rockets ranges (Table I). With the advances made in rocket instrumentation for upper atmospheric studies within the country, and the availability of three rocket ranges under the eclipse track the scientific community in India undertook a major rocket campaign to study several aspects of D-region chemistry, minor neutral constituents, E- and F-region irregularities, electrojet structure, and thermal structure of the ionosphere.

TABLE I

*Details of the eclipse track over the Indian rocket ranges*

	Time of first contact (IST)			Time of max eclipse (IST)			Eclipse magnitude (max)	Time of 4th contact (IST)		
Thumba (8°33'N, 76°52'E)	14h	19m	33s	15h	39m	51s	80.2%	16h	49m	55s
Shar (13°47'N, 80°15'E)	14h	29m	50s	15h	47m	34s	90.9%	16h	55m	44s
Balasore (21°30'N, 86°56'E)	14h	44m	20s	15h	56m	14s	97.6%	16h	59m	50s

## SCIENTIFIC OBJECTIVES OF THE ROCKET PROGRAMME

*D-Region Chemistry*

*Electron Loss Coefficient  $\psi$  and  $\lambda = N_-/N_e$  Variations During an Eclipse.* Previous eclipse studies (Ex Nov 1966 eclipse over Cassino, Brazil) have shown that the D-region electron densities decrease rapidly during an eclipse. The observed decreases require electron loss coefficients that are roughly ten times larger than the values estimated from other considerations (Belrose *et al*, 1972, and Mechtly *et al*, 1972). Measurement of positive ion densities during an eclipse, however, do not show an equally rapid decrease. It, therefore, appears that the negative ion to electron ratio  $\lambda = N_-/N_e$  changes during an eclipse. Large values of  $\lambda$  could lead to large values of the electron loss coefficient since  $\psi = (1 + \lambda)(\alpha_D + \lambda \alpha_i)$  where  $\alpha_D$  = dissociative recombination coefficient for electrons and  $\alpha_i$  = electron attachment loss coefficient. Simultaneous measurement of positive ion density and electron density during the eclipse were proposed to determine the actual values of  $\lambda$  during the eclipse.

*Mesospheric Structure.* There have been several attempts in the past to study the variations in atmospheric structure-densities and temperatures during an eclipse. At altitudes below about 80km the time constants of the atmosphere are large when compared to the eclipse duration. No significant variations in mesospheric structure are expected. However, ion composition measurements made during previous eclipses have given some surprising results.

The normal D-region ion composition is characterised by the dominance of water cluster ions below a certain level and the sudden transition from the cluster ions to molecular ions  $O_2^+$  and  $NO^+$  above this level. This level is near 82km for normal daytime conditions and 87km for night time conditions. The ion composition varies during an eclipse in a manner similar to that from day to night (Narcisi *et al*, 1969). The reaction schemes that convert  $O_2^+$  and  $NO^+$  into clusters are heavily temperature-dependent. The temperature dependence could be as large as  $T^{-5}$  (Chakrabarty & Chakrabarty, 1980). The large temperature gradient in the 80km (mesopause) region is used to explain the observed sudden transition from molecular ions to cluster ions under normal conditions. Changes in mesopause height and temperatures are considered to be responsible for the observed day to night changes in the transition level. The eclipse results of Narcisi *et al* (1969) suggest that during the eclipse the mesospheric temperatures undergo a variation similar to that from day to night. This intriguing aspect needs further investigation. An investigation of the mesospheric temperature variations during an eclipse was undertaken as part of the 16 February solar eclipse campaign. Measurements using both the Russian meteorological payloads as well as Lyman alpha absorption measurements to obtain  $O_2$ -concentration profiles and scale heights in the mesosphere.

*Ozone Concentration Profiles.* Ozone is an important minor constituent in the earth's upper atmosphere which is produced by the incidence of solar radiation on the atmosphere. However, the photochemistry at stratospheric and mesospheric altitudes which determines the equilibrium ozone concentrations is quite complex. It is well realised that at lower altitudes the photochemical time constants are large and the equilibrium ozone concentrations are determined by dynamical processes.

It is expected that at some altitude above about 40km photochemistry begins to dominate. In view of the fact that the photochemical schemes have been frequently revised in the past decade, it was considered fruitful to determine experimentally the ozone concentration profiles at different times during the eclipse and determine the level at which the photochemical time constant becomes comparable to the eclipse duration. A few measurements made during previous eclipses have yielded conflicting results and no definite conclusions could be drawn from these previous attempts.

#### *Dynamical Effects in the E- and F-Region*

**E-Region Irregularities** The 1966 Brazilian eclipse was observed to punch a hole in the ionosphere at the  $F_1$ -region altitudes. Subsequently, the hole was observed to drift vertically upwards with a velocity of 50m per second (Rishbeth, 1970). Whereas the direction of this drift is the same as the normal daytime drift which produces the equatorial anomaly, the magnitude is large, larger by about 60 per cent. This suggests an enhancement of the low latitude electric fields during an eclipse. The reduced electron density during an eclipse should produce a reduction in electrical conductivity. If electric currents are conserved, this would result in a localised enhancement of electric fields. Whereas direct measurement of equatorial electric fields by *in situ* probes is difficult, it should be possible to test this hypothesis by making measurements on the amplitude and spectrum of the electron density irregularities observed in the electrojet region. The local time of the eclipse was such that under normal conditions the electric fields are small and the two stream irregularities are not triggered (Prakash *et al*, 1980). If there is an enhancement in electric fields, such irregularities could be triggered. A programme of flying a magnetometer to measure the electrojet currents, an HF probe to measure the absolute value of electron densities in the E-region and a high frequency response Langmuir probe during the eclipse was undertaken to study the ambient electron density irregularities, their amplitudes and spectrum for exploring the possibility of enhancement of electric fields. The backscatter radar operating at Thumba would also give information on the electrojet irregularities and electric fields during the eclipse.

**Triggering of F-Region Irregularities** Spread-F is hypothesised to be triggered by the supersonic disturbances created in the medium by sunset (Klostermeyer, 1978). A total solar eclipse should also play a similar role. The fact that Spread-F has not been reported on ionograms during an eclipse could be related to the time constants involved—the growth and decay rates of the irregularities. After sunset, photoionisation continues to be absent and recombination effects prevail, while after the eclipse there is a recovery. Further, the groundbased ionosonde traditionally used to recognise Spread-F is sensitive only to a certain class of ionisation irregularities. *In-situ* measurements with a high frequency response Langmuir probe would enable a study of a much wider spectrum of irregularities and with greater sensitiveness than a groundbased ionosonde. It was, therefore, proposed to fly a high frequency response Langmuir probe on an RH-560 rocket from SHAR to detect the possible triggering of ionisation irregularities during an eclipse.

**Generation of Gravity Waves** It has been theoretically predicted that the transient nature of the solar radiation obscuration during an eclipse should generate gravity waves in the upper atmosphere (Chimonas & Hines, 1974). There is indirect evidence

to this effect in the travelling ionospheric disturbances detected at F-region heights from beacon studies and other ground based observations during some of the eclipses. Direct observational evidence for the same is, however, lacking. It was, therefore, proposed to make an attempt to test the hypothesis by direct measurements of winds in the upper atmosphere using the vapour release technique during the aftermath of an eclipse.

#### *Thermospheric Studies*

*Electron Heating and Cooling Rates.* Incoherent scatter radar studies of the thermal structure of the ionosphere during a solar eclipse showed a complex behaviour. Decrease in photoionisation during a solar eclipse results in a decrease in photo-electron flux and consequently a decreased heat input to the ambient electrons. The effect is drastic in the 150–200km region where  $T_e/T_i$  values were seen to decrease from the normal value of 2 to about 1.2 (Evans, 1965). This temperature decrease should have significant after-effects in the ionospheric structure such as enhanced diffusion from the topside. At low latitudes a thermal balance exists between the heat input to the ambient electrons by the suprathermal photo-electrons that are produced during ionisation of the atmospheric gas by solar radiation, and the heat loss due to collisional cooling of the heated electrons with neutrals. This situation is valid for all heights below about 400km (Geisler & Bowhill, 1965) and determines the equilibrium thermal structure of the ionosphere. Observations at low latitude should therefore enable a good check on the present day knowledge of the electron cooling rates in the ionosphere.

A programme was undertaken to make detailed measurements of the ionospheric structure during the eclipse by means of RH-560 rockets capable of reaching altitudes of about 350km. Measurements of electron density, electron temperature, ion temperature, suprathermal fluxes as well as measurements of positive ion composition were planned with Langmuir probe, electron temperature probe, ion trap, retarding potential analyser and ion mass spectrometer to make detailed calculations of ion chemistry as well as electron heating and cooling rates. Mass spectrometric measurements of ion composition were also expected to yield information on nitric oxide concentrations in the lower thermosphere. An experiment for measurements of nitric oxide concentrations in the mesosphere and lower thermosphere based on fluorescence measurements in the  $\gamma$ -bands was also planned in collaboration with the University of Tokyo as a supporting experiment on one of the succeeding days.

#### ROCKET PROGRAMME FOR THE SOLAR ECLIPSE OF 16 FEBRUARY 1980

To achieve the above scientific objectives, the following rocket programme was undertaken.

##### Thumba

- I. Centaur IIB rockets  
D-region studies, electrojet associated phenomena  
gravity wave generation
- II M-100 B rockets.  
Meteorological parameters.

Shar	:	RH-560 rockets Thermospheric studies—Composition. Thermal structure, Ionospheric irregularities.
Balasore	:	RH-200 Positive Ion densities in the stratosphere and mesosphere.

Details of the launching programme and the instrumentation used as well as the participating organisations are shown in Table II

TABLE II  
*Rocket launching programme*  
A. Thumba (8.5°N, 77°E)

<b>I. D-Region rockets</b>				
Centaur 05 60	D1	16 February 1980	1454hr IST	40% obscuration
„ 05 61	D2	16 February 1980	1522hr IST	70% obscuration
„ 05 64	D3	17 February 1980	1522hr IST	Certification
<i>Payloads</i>	<i>Parameter measured</i>		<i>Organisation</i>	<i>Scientists In-charge</i>
Gerdien Condenser	Total Positive Ion density N <sup>+</sup>		NPL	Dr M. N M Rao
Propagation experiment	Electron density Ne		NPL	Dr Y V. Somayajulu
Langmuir probe	Electron density profile and fine structure in electron density (Plasma instability) Ne Ne Ne		PRL	Dr S P. Gupta, Dr D. K. Chakrabarty
UV Photometer	Lyman alpha flux O <sub>2</sub> concentrations		PRL	Dr B H Subbaraya, Mr Shyam Lal
MUV Photometer	Ozone concentrations, Atmospheric Scattering in UV		PRL	Dr B H Subbaraya, Mr Shyam Lal
<b>II Electrojet Studies</b>				
Centaur 05 62		16 February 1980	1522hr	near maximum obscuration
Rb. magnetometer	Electrojet currents		PRL	Dr T. S G Sastry
HF probe	Electron density		VSSC	Dr Y. V. Somayajulu
(Rocket flight had to be cancelled due to last minute Launcher problems)				
<b>III Vapour Release</b>				
Centaur 05 63		16 February 1980	1852hr	evening twilight
Ba/Li vapour	Neutral atmospheric winds and wind shears Gravity waves generated by the eclipse and electric field measurements		PRL- VSSC	Dr R. Raghavarao Dr J N Desai Mr V. Babu
<b>IV Centaur 05 65</b>				
NO bands		17 February 1980		Morning twilight.
	Nitric Oxide concentrations		UTK, Japan	Dr Ogawa
Lyman alpha Photometer.	Lyman alpha flux and O <sub>2</sub> concentrations		NPL	Dr Y V Somayajulu
Ozone Photometer	Ozone concentration measurements		NPL	Dr S Sampath Mr A Banerjee

*Table Contd.*

V. *M-100B*

08 507	16 February 1980	1250hr	
08 508	"	1640hr	
Standard USSR Met. payload			Dr A. V. Fedynski, USSR.
Meteorological parameters			Dr V Narayanan, VSSC

## B SHAR (13 75°N, 85 25°E)

*Thermospheric and F-Region Studies**RH-560*

F-14	16 February 1980	1425hr IST	Control flight.
F-15	"	1545hr IST	near maximum obscuration (90 per cent)

<i>Payloads</i>	<i>Parameters measured</i>	<i>Institution</i>	<i>Scientists In-charge</i>
Langmuir probe	Electron density profile. Fine structure plasma instabilities	PRL	Dr S P. Gupta
Electron temperature probe	Te	UTK, Japan	Professor Hirao
Ion trap	Ni, Ti	NPL	Dr B C N. Rao
RPA	Supra thermal flux	NPL	Dr Y V Somayajulu
Ion Mass-Spectrometer	Positive Ion Composition	PRL	Dr J S Shirke Mr R Sridharan

Rocket F-15 malfunctioned at take-off and had to be command destructed.  
Only the control flight was successful and gave some data

## C. Balasore (21°30'N, 86°56'E)

*RH-200 — 2 Nos*

One on 16 February 1980 near totality

Second on 17 February 1980 Certification flight

<i>Payload</i>	Gerdien condenser	—	NPL	—	Dr M. N M Rao
----------------	-------------------	---	-----	---	---------------

The flight on the eclipse day was not successful

Only the certification flight was successful

## SOLAR AND GEOPHYSICAL DATA

The solar eclipse occurred under disturbed Geophysical conditions. There was a major geomagnetic storm with a sudden commencement at 0309hr UT on 14 February 1980 ending at 0315hr UT on 15 February 1980. This was followed by a second sudden commencement at 1230hr UT of 15 February 1980 and ending at 2200hr on 16 February 1980. The eclipse, therefore, occurred during the recovery phase of the storm. The solar and geophysical parameters for 16 February 1980 taken from the *Solar and Geophysical Data* issued by NOAA, USA are given below

$A_p = 40$	$\Sigma K_p$	=	37 <sub>+</sub>
Sunspot No = 163	$F_{10.7}$	=	200.2

The fact that the eclipse occurred under such disturbed conditions has made the interpretation of the data somewhat difficult to separate out the genuine eclipse effect

from that due to the storm. While a consolidation of the results from the various experiments that were successful is yet to be done, preliminary discussions of most of the results were presented during the Delhi symposium. These will appear as several contributed papers in this issue.

#### ACKNOWLEDGEMENTS

Planning and consolidation of rocket programme for the 16 February 1980 solar eclipse was aided by the efforts of several senior scientists in the country. Prominent among those to whom acknowledgements are due are Dr D Lal, S P Pandya, A. P. Mitra and R R Daniel. Detailed organisation of the rocket programme was facilitated by the efforts of scientists from the ISRO Headquarters as well as the engineers at TERLS and SHAR, special mention to be made of Messrs V Sudhakar and A. C. Bahl. Integration of rocket payloads was largely due to the enthusiastic co-operation of the staff of TERLS and the rocket launchings were facilitated by the IREX staff at the Thumba and SHAR ranges. A large number of engineers and technicians from the participating organisations, Physical Research Laboratory, Ahmedabad, National Physical Laboratory, New Delhi and Vikram Sarabhai Space Centre, Trivandrum worked beyond their normal capacity to bring to fruition the solar eclipse campaign. Finally, acknowledgements are due to the scientists from abroad, Professors Hirao and T Ogawa of the University of Tokyo, Japan and Professor Martelli of University of Sussex, U.K. as well as their associates who took active part in the Indian Solar eclipse campaign.

#### REFERENCES

- Anastassiades, M. Ed (1970) *Solar Eclipses and the Ionosphere*.  
 Belrose, J S, Ross, D B, and McNamara, A G (1972) *J atm terr Phys.*, **34**, 627  
 Beynon, W J G, and Brown, G M Ed (1956) *Solar Eclipses and the Ionosphere* Pergamon Press, London  
 Chakrabarty, D K, and Chakrabarty, P (1980) *Proc. Workshop Solar Terr Prediction, Boulder*, **IV**, G1  
 Chimonas, G, and Hines, C O (1974) In *The Upper Atmosphere in Motion, Geophys. Monogr.* **18**. American Geophysical Union  
 Evans, J V (1965) *J geophys Res*, **70**, 131-142  
 Geisler, J E, and Bowhill, S A (1965) *J atm terr Phys*, **27**, 1119-1146  
 Klostermeyer, J (1978) *J geophys Res*, **83**, 3753  
 Mechtly, E A, Sechrist, C F, and Smith, L G (1972) *J atm terr Phys*, **34**, 641  
 Narcisi, R S, Philbrick, C R, Bailey, A D, and Della Lucca (1969) *Aeronomy Rep* No 32, Univ Illinois, Urbana, Illinois, 355-363  
 Prakash, S, Gupta, S P, Subbaraya, B H, and Pandey, R (1980) In *Low Latitude Aeronomic Processes*, **8** (Ed A P Mitra), 3-16  
 Rushbeth, H (1970) In *Solar Eclipses and the Ionosphere* (Ed Anastassiades)



Printed in India.

**Rocket Experiment**

**STRATOSPHERIC AND MESOSPHERIC WINDS OVER THUMBA  
DURING THE SOLAR ECLIPSE OF 16 FEBRUARY 1980**

K. S. APPU *and* V. NARAYANAN

*Meteorological Section, TERLS/VSSC, Trivandrum-695 022, India*

*(Received 15 February 1982)*

During the solar eclipse of 16 February 1980, two M-100 rockets were launched from Thumba (8°32'N, 76°52'E) to study the eclipse effects on the equatorial stratospheric and mesospheric winds. The first launching was during pre-eclipse phase and the other was at the end phase of the eclipse. This study reveals that the solar eclipse makes no significant effect on both the zonal and meridional winds in the stratosphere and mesosphere over Thumba.

**Keywords:** Zonal Wind; Meridional Wind Circulation

**INTRODUCTION**

STUDIES on the response of the neutral atmosphere to the solar eclipse are very few. Earlier, rocket experiments were conducted using small meteorological rockets reaching a maximum altitude of about 60km in the eastern hemisphere (Ballard *et al.*, 1969, Quiroz & Henry, 1973; and Randhawa, 1974). Wind observations in the 80-100km region were made in South Antarctica using partial reflection method during the total solar eclipse of 23 October 1976 (Ball *et al.*, 1976). Different results are reported from these experiments on the wind circulation during solar eclipse.

In the meridional flow, while strong increase was observed around 58km at Wallops Island (Quiroz & Henry, 1973), no change was observed at Fort Sherman (Randhawa, 1974). At Fort Sherman, zonal wind flow had undergone a change from 15m/s before the eclipse to 9m/s near the maximum phase. Ball *et al.*, have concluded that eclipse did not produce any wind variations in the 80-100km region in sufficient magnitude to stand out from the naturally occurring wind variations.

The solar eclipse of 16 February 1980 gave an opportunity for the first time, to study the effect of solar eclipse on the neutral atmosphere over India. During this day two M-100B rockets were launched from Thumba. M-100B rockets are being launched regularly on Wednesdays from Thumba as a part of the Indo-Soviet collaborative programme on the studies of upper atmosphere. In this paper, stratospheric and mesospheric wind circulations obtained from the two special M-100B rocket soundings during the solar eclipse are discussed.

**EXPERIMENT**

At Thumba, the times of first contact, maximum phase and last contact were at 1420hr, 1540hr and 1650hr IST respectively. The maximum obscuration was 80 per

cent. The details of the two M-100B rocket experiments are given in Table-I. As there were other rocket soundings for ionospheric observations, the second M-100B rocket launching could be conducted only at the end phase of eclipse. In the M-100B rocket system, wind measurements are made by radar tracking of parachute for the region

TABLE I

*Details of the two M-100B rocket launchings conducted during the solar eclipse of 16 February 1980 at Thumba*

Time (hrs. IST)	Data available region (km)					
	Parachute wind			Chaff wind		
	from	to	Obscuration (%)	from	to	Obscuration (%)
1253	60	21	—	76	65	—
1635	60	22	16-8	78	65	17-10

below 60km and fibre glass chaff cloud for the 60-80km region. On the control day the chaff data obtained only above 65km. The wind measurement errors are 5m/s below 50km and 10m/s in the 60-80km region. The published wind data by the Central Aerological Observatory, USSR, have been utilised for the study.

## RESULTS

Fig. 1 depicts the wind profiles obtained from the launchings. As the changes in the circulation include the naturally occurring diurnal variations within the 4 hour period and eclipse induced effects, if any, the eclipse day data have been compared with the normal day changes in order to delineate the eclipse effect. On 10 April 1980 there were two M-100B rocket flights at 1130hr IST and 1530 hr IST, almost at the same intervals and timings as on the eclipse day. Data are available upto 40km on the 1530 flight. The stratospheric and mesospheric circulation during February through April 1980 was showing the typical spring circulation pattern. The stratospheric wind reversals took place during May only. So this day has been considered as the control day.

The deviations in zonal and meridional components (second observations minus first observations) have been found for the normal day and the eclipse day. Fig. 2 represents the vertical profiles of these deviations. Generally the wind variations observed on both the days are identical. So the weakening zonal flow and the strengthening of meridional flow observed on the eclipse day (Fig. 1) is a part of the diurnal circulation occurring in the afternoon during the 4 hour period.

M-100B rocket data are highly smoothed one. The spatial window above 50km is of the order of 5km. So the variations in a layer within this range cannot be consi-a

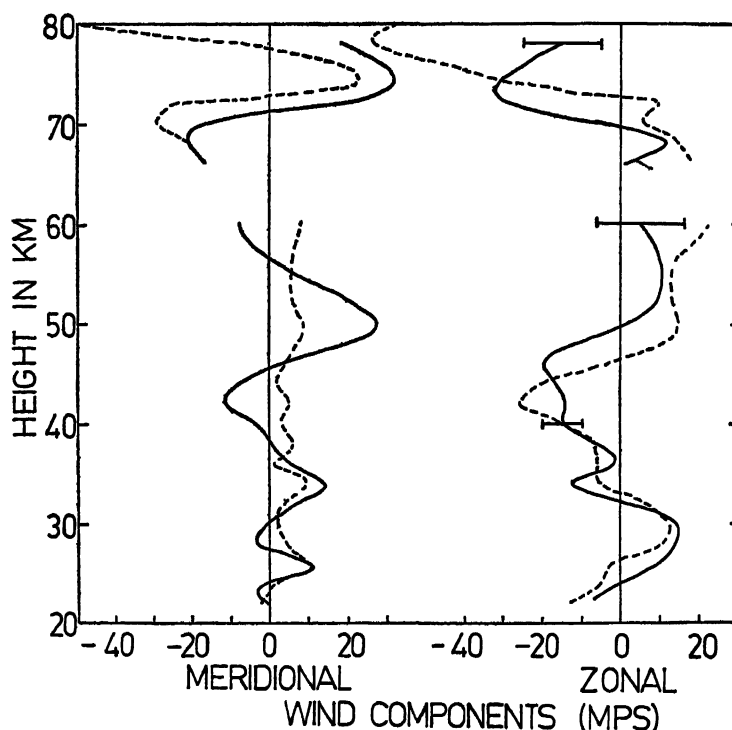


Fig 1 Vertical wind profiles of meridional and zonal components on the eclipse day. Dashed line for 1253hrs IST launching and solid line for the 1635hrs IST launching. Error bars are based on the measurements at different altitudes.

dered as real. The range of day-to-day variations in wind above 50–80km observed at Thumba is of the order of 10–20m/s (Narayanan, 1977) and the diurnal variation is 10–15m/s (Sasi & Reddy, 1977). The disparity in the meridional component observed at 50km (Fig. 2) cannot be treated as real variations caused by solar eclipse. Hence, considering the errors in the measurements and range of day-to-day variations as well as the vertical spatial window in the computations in the stratospheric and mesospheric region, the difference found between the two days (the eclipse day and control day) cannot be attributed confidently to real changes due to the eclipse.

#### CONCLUDING REMARKS

There are two limitations for the present study. (i) in M-100 rocket system small scale variations of the order of 5–10m/s cannot be considered as it falls in the range of inherent measurement error. (ii) there is only one observation during the eclipse and that too towards the end phase. Giving due consideration for the above limitations, it is tentatively concluded that the eclipse, during the end phase, makes no significant effect on both zonal and meridional winds in the equatorial stratosphere and mesosphere.

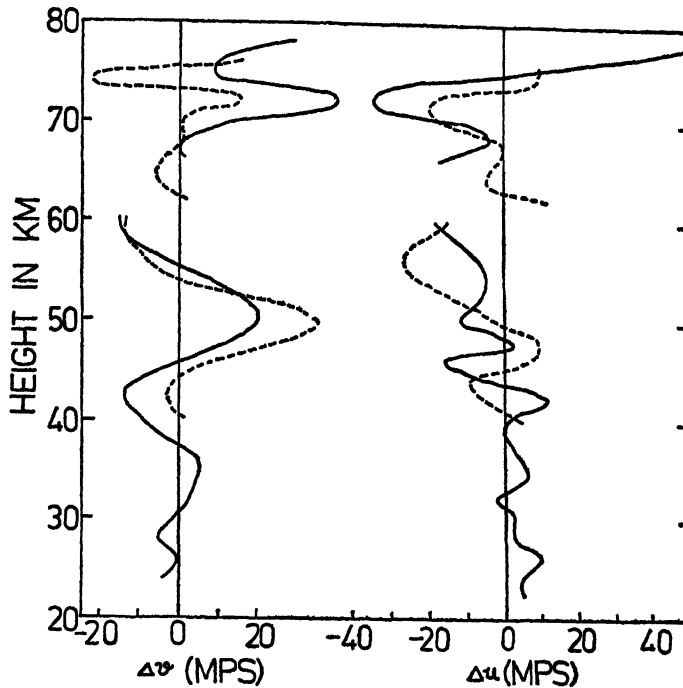


FIG 2 Vertical profiles of the deviations in meridional ( $\Delta V$ ) and zonal ( $\Delta U$ ) components. On the control day data is available up to 40km only

#### ACKNOWLEDGEMENTS

We are grateful to the State Committee of Hydrometeorology & Natural Resources Control (SCHNRC) of Moscow, for allotting two M-100B rockets for the solar eclipse study at Thumba. Thanks are also due to Dr C A Reddy and Dr V Krishnamurthy, Space Physics Division, Vikram Sarabhai Space Centre, for the valuable discussions.

#### REFERENCES

- Ball, S M, Stubbs, T J, and Vincent, R A (1980) Upper atmosphere wind observations over southern Australia during the total solar eclipse of 23 October 1976. *J. atm. terr. Phys*, **42**, 21-25
- Ballard, N N., Valenzuela, R, Isquardo, M, Randhawa, J S, Morla, R., Bottle, J R (1969) Solar eclipse temperature, wind and ozone in the stratosphere *J. geophys. Res*, **74**, 711-712
- Narayanan, V (1977) Preliminary results of the M-100 rocket diurnal launchings from Thumba. Space Sciences Symposium, January 18-21, 1977, VSSC, Trivandrum
- Quiroz, R S, and Henry, R M (1973) Stratospheric cooling and perturbations of the meridional flow during the solar eclipse of 7 March 1970 *J. atm. Sci*, **30**, 480-488
- Randhawa, J S (1974) Partial solar eclipse on temperature and wind in an equatorial atmosphere *J. geophys. Res*, **79**, 5052-5053
- Sasi, M N, and Reddy, C A (1977) A semi-empirical method for the study of diurnal and semi-diurnal oscillations in the rocket measured atmospheric winds and temperatures. *Indian J. Rad. Space Phys*, **6**, 274-278.

Printed in India.

**Rocket and Balloon Experiment**

**THERMAL STRUCTURE OF THE ATMOSPHERE—SURFACE TO  
MESOSPHERE—DURING THE SOLAR ECLIPSE OF 16 FEBRUARY  
1980**

K. S. APPU, B. V. KRISHNA MURTHY, V. NARAYANAN, C. A. REDDY  
*and*  
K. SEN GUPTA

*Vikram Sarabhai Space Centre, Trivandrum-695 022, India*

*(Received 15 February 1982)*

Temperature measurements were made from surface to 80km altitude by balloons and M-100 rockets from Trivandrum ( $8^{\circ}33'N$ ,  $76^{\circ}57'E$ ) before and during the solar eclipse of 16 February 1980. Analysis of the data show cooling near stratopause level and above, and warming in the lower stratosphere. Warming was also observed around 15km altitude. Balloon temperature measurements from Hyderabad showed a systematic cooling from 3 to 20km altitude.

**Keywords:** Atmospheric Thermal Structure; Mesosphere; Solar Eclipse; Stratopause

**INTRODUCTION**

At Trivandrum ( $8^{\circ}33'N$ ,  $76^{\circ}57'E$ ) temperature measurements from surface to 80km altitude were made during the total solar eclipse of 16 February 1980 which crossed the Indian subcontinent. At Trivandrum, the fractional area of the sun's disc covered at the maximum phase of the eclipse was 0.80.

Two M-100 rockets were launched on the day of eclipse, one before the eclipse at 1253hr IST and other during the eclipse at 1635hr. Using Rhenium-Tungsten wire as the temperature sensor, vertical temperature distributions were obtained from 21km to 80km.

Meteorological balloons were launched by Indian Meteorological Department as per our schedule from Hyderabad ( $17^{\circ}23'N$ ,  $78^{\circ}29'E$ ) and Trivandrum. The detailed schedule of balloon and M-100 rocket flights along with areas of the sun's disc covered are given in Table I.

**RESULTS AND DISCUSSION**

**(a) Rocket Observations**

Fig. 1 shows the two vertical temperature profiles obtained from the two launchings on the day of the eclipse. The main observed features are the following —

- i) Warming in 24 to 34km altitude region with maximum of  $10^{\circ}C$  at 30km;
- ii) Cooling above 38km with maximum cooling of  $14^{\circ}C$  at around 58km.

On 10 April 1980 there were two M-100 rocket launchings at 1130hr and 1534hr IST. As the observation time and the interval between the launchings on 10 April 1980

TABLE I

Date/Time (hr)	M-100 rockets		Balloons	
	Altitude range (km)	Obscuration (%)	Altitude range (km)	Obscuration (%)
<b>Trivandrum</b>				
15.2.80/1455	—	—	0-25	—
16.2.80/1215	—	—	0-22	—
„ /1253	21 to 76	—	—	—
„ /1530	—	—	0-22	79-67
„ /1635	21 to 76	17-8	—	—
<b>Hyderabad</b>				
16.2.80/1230	—	—	0-24	—
„ /1530	—	—	0-24	98-77

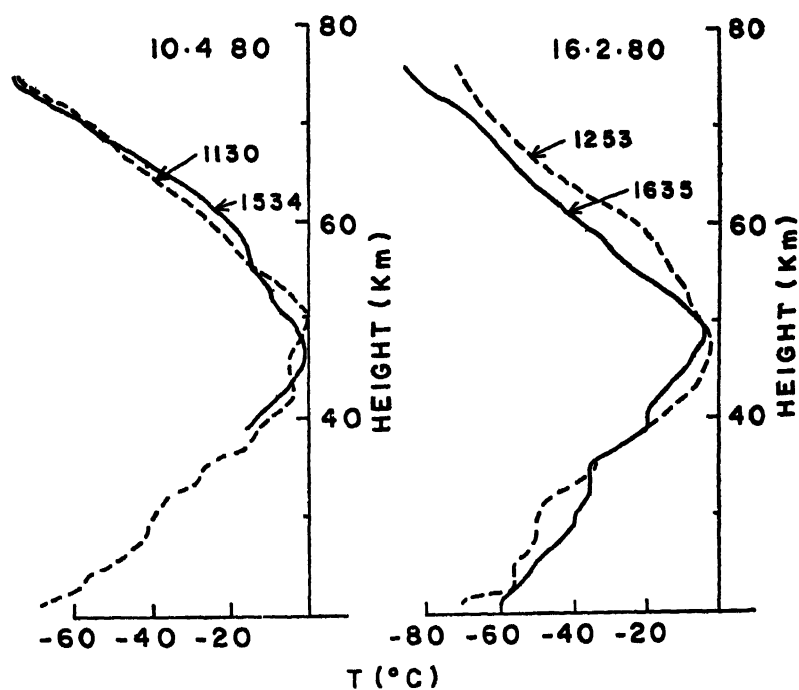


FIG 1 Vertical temperature profiles obtained from M-100B rocket launchings on 16.2.1980 and 10.4.1980 from Trivandrum

were almost the same as on the day of eclipse, those temperature profiles have been taken as reference to represent the amplitude of diurnal variation in the 4 hour interval 10 April 1980 temperature profiles are also plotted in Fig 1 For both the days i.e., 10 April 1980 and 16 February 1980, the temperature deviation ( $\Delta T$ )

between the observations (1530–1130hr) have been computed and are plotted in Fig. 2 as  $\Delta T$ -height profiles. On 10 April 1980 data are available only above 40km altitude. A best-fit curve for the  $\Delta T$  profile of eclipse day has been obtained and shown in the figure. A general cooling trend is clearly observed on that day above 38km altitude,

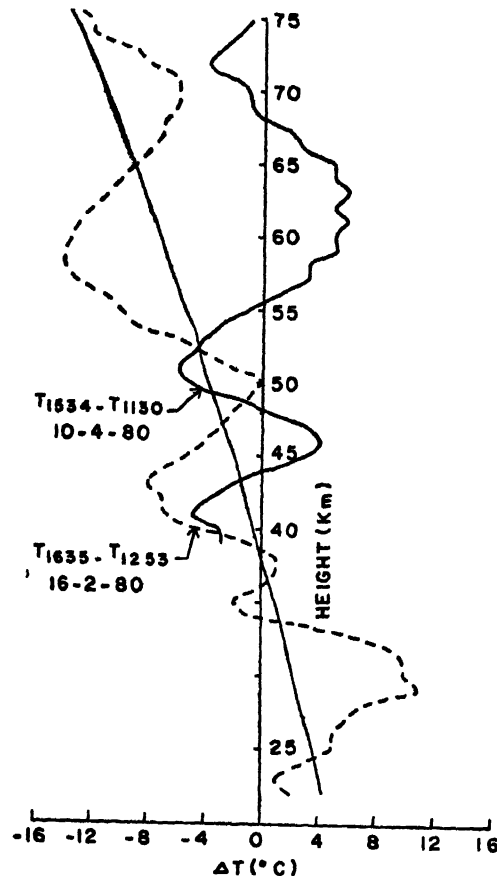


FIG. 2 Vertical profiles of the temperature deviations (rockets)

whereas on 10 April no such trend is found. The experiments conducted at Wallops Island during the total solar eclipse of 1970 (Quiroz & Henry, 1973) and partial solar eclipse at Fort Sherman in 1973 (Randhawa, 1974) have also revealed similar features like cooling near the stratopause level and warming by a few degrees near the end phase of the eclipse in a restricted layer in the lower stratosphere.

As our rocket observations were made during the last phase of the eclipse the extent of cooling during the maximum phase could not be obtained. The cooling observed in the temperature profile near stratopause region during the eclipse launch is as expected. The warming in the lower stratospheric region could be explained in terms of subsidence phenomenon due to a high degree of cooling around stratopause region. However, the extent of warming due to subsidence could not be estimated.

as the extent of cooling near stratopause during the maximum phase of the eclipse is not known.

(b) *Balloon Observations*

The difference between the temperature profiles obtained from balloon ascents during the eclipse and pre-eclipse periods are plotted in Fig. 3. The differences are plotted for both Trivandrum and Hyderabad. The data are available upto the altitude of 22km for Trivandrum and 24 km for Hyderabad. At Trivandrum no significant deviation in temperature is seen upto the altitude of 11km. But a significant warming

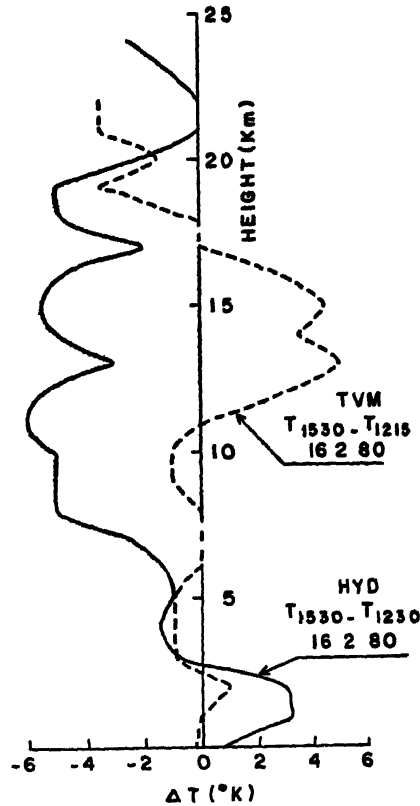


FIG 3 Vertical profiles of the temperature deviations (balloons)

is observed in 11 to 17km altitude region. Maximum warming is found to be of the order of 5  $^{\circ}\text{C}$  at 13km altitude, whereas at Hyderabad, as shown in Fig 3, a systematic cooling from 3 to 20km altitude is observed. In Fig 4, the difference between the temperature obtained from balloon flights of 16 February at 1500hr IST and that of the previous day at around the same time are plotted. It is interesting to note that the same amount of warming is noticed at 13km altitude on the day of eclipse. This confirms warming at 13km altitude region during the eclipse. No attempt is made here to explain the disparity observed in the temperatures at Trivandrum and Hydera-



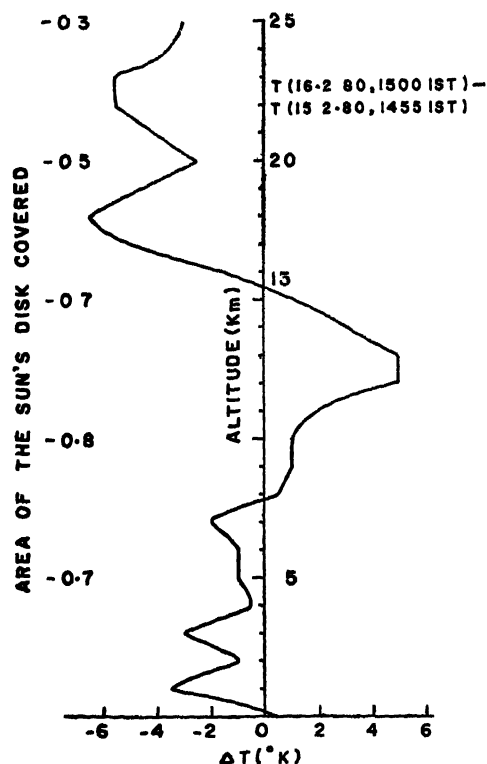


FIG. 4. Vertical profiles of the temperature deviations (balloons).

bad in the altitude region of 11 to 17km. However, it may be noted here that the eclipse was 80 per cent at Trivandrum whereas it was total at Hyderabad.

Though the temperature profiles obtained from M-100 rockets and balloon flights are available for some overlapping altitude regions, they cannot be compared as the flights are during the different phases of the eclipse.

#### ACKNOWLEDGEMENTS

The authors are grateful to the State Committee of Hydrometeorology and Natural Resources Control (SCHNRC) of Moscow for allotting two M-100B rockets for the solar eclipse experiments. Thanks are due to the India Meteorological Department for having special balloon ascents as per our schedule.

#### REFERENCES

- Quiroz, R. S., and Henry, R. M. (1973) Stratospheric cooling and perturbations of the meridional flow during the solar eclipse of 7 March 1970. *J. atm. Sci.*, **30**, 480-488.  
 Randhawa, J. S. (1974) Partial solar eclipse effects on temperature and wind in an equatorial atmosphere. *J. geophys. Res.*, **79**, 5052-5053.

Printed in India

Rocket Experiment

## D-REGION ELECTRON LOSS COEFFICIENTS DURING SOLAR ECLIPSE OF 16 FEBRUARY 1980

Y. V. SOMAYAJULU, K. S. ZALPURI *and* P. SUBRAHMANYAM

*Radio Science Division, National Physical Laboratory, New Delhi-110 012, India*

*(Received 15 February 1982)*

Three rocket flights were conducted from Thumba, India, at the geomagnetic equator as part of solar eclipse campaign of 16 February 1980. Each of the payloads included a propagation experiment to measure electron density by the absorption technique. In this paper, results obtained from two of the flights, one during the eclipse when obscuration was 70 per cent and other during normal time conditions but similar to eclipse time flight are presented. It has been found that electron density values during eclipse are in general low compared to normal time values. The difference being by about a factor of 2 at the height of minimum and by a factor of 2.7 at 90 km. The effective values of electron loss coefficients as derived from electron density values are found to be almost same as the normal time values particularly in the cluster ions dominated region.

**Keywords:** Rocket Experiment; Lower Ionosphere; Electron Density; Electron Loss Coefficient; Solar Eclipse

### INTRODUCTION

THREE Centaure-II rockets were flown from Thumba, India ( $8^{\circ}32'N$ ,  $76^{\circ}57'E$ ) as part of a campaign to study the effect of solar eclipse on the lower ionosphere. Each of the payloads included a propagation experiment to measure electron density by the absorption technique. The objective in carrying out this experiment was to deduce the electron loss coefficient in addition to study the change in electron concentration. The details of these flights are given in Table I. The third flight D3 conducted on 17 February 1980 was the control flight, representing normal full sun condition at the time of the D2 flight during the solar eclipse. Unfortunately due to technical problem, no useful data could be obtained from the first flight during eclipse, therefore in this paper results obtained from two rocket flights, one during the eclipse before the second contact and other from the control flights are presented.

### EXPERIMENTAL DETAILS & DATA ANALYSIS

The propagation experiment consisted in generating the ordinary and extraordinary modes alternatively on the ground using CW transmitter on two frequencies 1865 and 2610 kHz, the signals were received on the rocket and amplitude of the charac-

TABLE I

*Details of the rocket flights conducted from Thumba as part of solar eclipse campaign*

Flight No.	Date	Time IST	Solar Zenith Angle X	Percentage obscuration during eclipse
ISRO 5 60/D1	16 February 1980	1454	40 55°	40.2
ISRO 5 61/D2	"	1522	46.6°	70.5
ISRO 5.64/D3	17 February 1980	1522	46.7°	—

teristic waves received were telemetered to the ground. The ionospheric absorption suffered by the two modes respectively during passage through the ionosphere was derived from the variation of amplitude with rocket altitude. The experimental arrangement was such that the waves were propagated transverse to the geomagnetic field i.e., the transverse propagation; under these conditions at the equator, the two characteristic waves are linearly polarized.

The total absorption suffered thus deduced as a function of altitude was used to derive the ionospheric absorption by taking into account the contribution of free space absorption which is assumed to be zero at a reference altitude of 55km where ionospheric contribution to the total absorption is expected to be the least. The electron density values were then determined using generalized Sen and Wyller (1960) formulae. The details of the method are already described elsewhere (Somayajulu *et al.*, 1971). For collision frequency, a model based on Phelps (1960) was used

$$\nu_m = 9 \times 10^7 P \text{ Sec}^{-1} \text{ where } P \text{ is the pressure in mm of Hg}$$

For pressure, values based on CIRA (1972) model were used

## RESULTS AND DISCUSSION

The electron density profiles derived from the data for the two rocket flights, one during the eclipse D2 and other from the control flights D3 are shown in Fig 1. The estimated error limits of electron density are also shown in the same figure. These limits are based mainly on the scatter observed in the raw data inclusive of scaling errors. Quantitatively, the total errors in the measurement are estimated to be about 15 per cent in the altitude region 70–85km. Above this region, the accuracy in the measurement decreases with possibility of errors as large as 20 per cent at 90km.

It may be seen that the profile D3 obtained from the control flight reproduces the main features of a typical daytime electron density profile namely a gradual increase in the altitude region 70 to about 80km, a minimum or valley around 80km and a sharp increase above this altitude see, for example Somayajulu *et al.* (1973).

The electron density profile as obtained from D2 flight during eclipse shows an expected decrease in concentration, the difference being by a factor of 2 at the height of minimum and by about a factor of 2.7 at 90km. Also no appreciable change in the height of minimum during eclipse was found compared to normal time value.

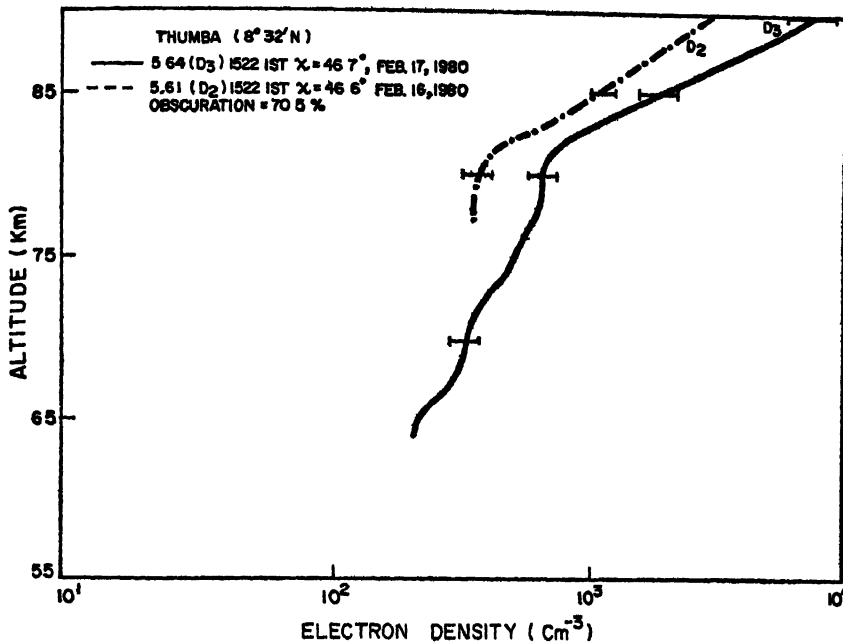


FIG 1 Electron density profiles as a function of altitude obtained from propagation experiment during normal and eclipse time (70 per cent obscuration)

This may be due to the fact that these observations were carried out during the eclipse when obscuration was only 70 per cent compared to those for totality in which case an upward shift in the height of minimum was observed in the range, 1.5 to 4.5 km (Mechtly *et al*, 1972).

The observed profiles are then utilized to derive the effective values of electron loss coefficient  $\alpha_{\text{eff}}$ . For the normal time flight, equilibrium conditions were assumed. In the altitude region above 70 km, where contribution from negative ions is negligible; the main loss mechanism is dissociative recombination with positive ions. Therefore, an  $\alpha$ -type of loss mechanism was considered and effective loss rate is taken as  $q/Ne^2$  where  $q$  is the production rate.

For the eclipse time conditions where due to partial or full cut-off of solar ionizing radiations, the production of electron decreases and hence, the equilibrium conditions cannot be assumed. In such a case, to determine  $\alpha_{\text{eff}}$  one should have an idea about the rate of change of electron density with time i.e.,  $dN/dt$  term. However, due to non-availability of data during the earlier phase of the eclipse, the electron values for D3 were reduced to those for the first contact on the assumptions (i) Equilibrium conditions at this time of first contact also exist (ii)  $\cos \chi$  variation for the production rate i.e.,  $q t = q_0 \cos \chi$ . The day to day variability in electron density in the D-region is small (Mitra & Somayajulu, 1979). Although the eclipse day and the day before were magnetically disturbed days with  $A_p$  values 40 and 33 respectively, the variations in electron density in the low latitude D-region are expected to be small. Belrose *et al* (1969) have shown that it takes 3 to 4 days for the effect of large geomagnetic disturbance with  $A_p$  values ranging between 40 and 60, to propagate from high latitudes

to midlatitudes. Accordingly for  $A_p$  values less than 40 as were observed for eclipse and preeclipse days, the effect of magnetic disturbance if at all any on the D-region ionization should take more than 4 days to propagate to low latitude region and hence can be neglected in the present case

Next consider the continuity equation for electrons as

$$\frac{dN}{dt} = q - \Psi N e^2 \quad \text{.. (1)}$$

where  $\Psi = (\alpha_{\text{eff}} + \lambda \alpha_i) (1 + \lambda)$  where  $\alpha_i$  is the ion-ion recombination rate and  $\lambda$  is the negative ions to electron density ratio.

For total eclipse conditions, it is believed that the negative ion concentration increases may be due to the absence of photodetachment process Chakrabarty and Mitra (1973) from theoretical considerations have shown that for total eclipse condition  $\lambda$  does not change much when only  $q$  term in continuity equation is changed. The values of  $\lambda$  they had obtained were 1.4 and  $4.4 \times 10^{-2}$  at 70 and 80 km respectively. However, if  $q$  is changed and the lumped detachment rate  $\gamma$  which takes into account the contributions from collisional as well as photodetachment from negative ions is taken equal to zero, the value of  $\lambda$  increases by an order of magnitude with values as high as  $7.7 \times 10^{-1}$  at 70 km and  $4.2 \times 10^{-2}$  at 80 km respectively.

The other important term contributing to the  $\alpha_{\text{eff}}$  values as determined from equation (1) is production term  $q$ . This term was calculated as follows taking into account contribution from various ionization sources.

1. Cosmic ray ionization of major neutral constituents. These rates were computed using CIRA (1972) model for major neutral constituents and considering formula as given by Velinov (1968)
2. Lyman- $\alpha$  ionizing minor neutral constituent nitric oxide. For the concentration of this constituent, we have taken an estimated profile of Mitra and Somayajulu (1979) which is based on rocket measurements from Thumba and satisfy the electron density and other constraints. For Lyman- $\alpha$  flux, a value of 4.0 ergs/cm<sup>2</sup> sec was adopted.
3. X-ray ionization of major neutral constituents in the wavelength band 1–8 Å. The integrated flux value in this wavelength band is available from satellite measurements (Solar Geophysical Data, 1980) corresponding to the time of flight of D2 and the same was adopted in this study. Due to non-availability of data from satellite measurements at the time of D3 flight, a typical value of X-ray flux of  $1 \times 10^{-3}$  ergs/cm sec was considered. These integrated flux values were resolved in a spectrum of individual wavelengths assuming the sun to be a grey body. The variation of production rates for eclipse time is assumed proportional to the visible portion of the solar disc.

Ionization of  $\text{O}_2$   $^1\Delta_g$  by solar radiations in the band 1027–1118 Å can also contribute to the total production rate though the contribution is small due to absorption of these radiations by carbon dioxide.

The production rates thus computed due to cosmic rays, Lyman- $\alpha$ , X-rays, for  $\text{O}_2$   $^1\Delta_g$  and total production rates as a function of altitude are shown in Fig. 2.

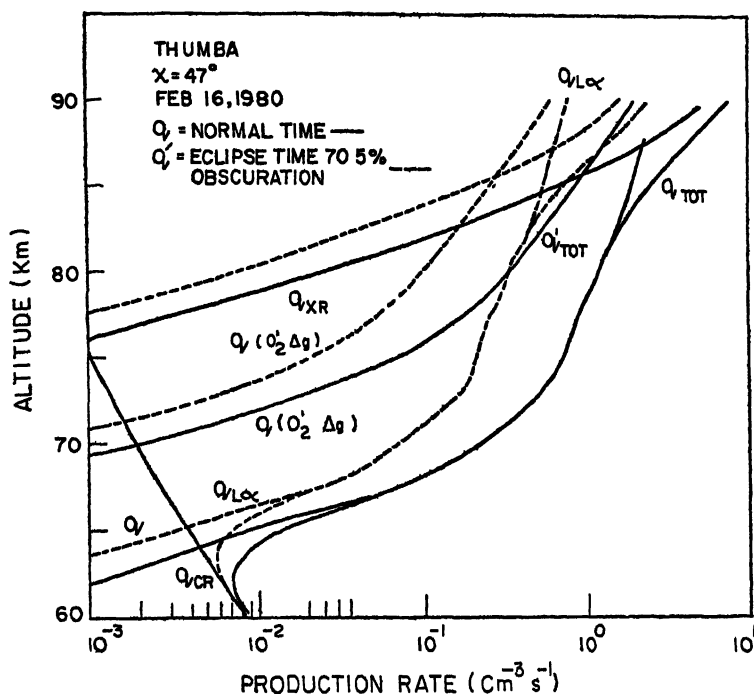


FIG. 2. Production rate profiles due to various sources of ionization both for normal and eclipse time conditions.

The variation of production rates for eclipse time is assumed proportional to the visible portion of the solar disc

The profiles of  $\alpha_{\text{eff}}$  thus derived are shown in Fig 3. For comparison the  $\alpha_{\text{eff}}$  profiles obtained by other workers and normal time (Aikin *et al*, 1972; Rowe, 1972, Johannessen, 1974, and Chakrabarty *et al*, 1978) and eclipse time (Mechtly *et al*, 1972) are also shown in the same figure.

It may be seen that the effective value of loss coefficient practically remains constant with a value  $5.8 \times 10^{-6} \text{ cm}^3 \text{ sec}^{-1}$  upto about 80 km, the region in which heavy clusters of positive ions dominate. Above this altitude the  $\alpha_{\text{eff}}$  values show a sharp decrease right upto 90 km reaching a value of about  $2.5 \times 10^{-7}$  which is close to the recommendation coefficient of  $\text{NO}^+$  and  $\text{O}_2^+$  ions dominating this region. The actual value of effective loss coefficient in this region in fact is controlled by the ratio  $[\text{NO}^+]/[\text{O}_2^+]$ .

The comparison of normal time profile of  $\alpha_{\text{eff}}$  for D3 with those obtained by other workers show in general good agreement both qualitatively as well as quantitatively. It may be seen that the derived profile in the cluster ions dominated region is within the range of  $\alpha_{\text{eff}}$  values suggested by Aikin *et al* (1972) and close to those obtained by Johannessen (1974) from ion composition data.

Comparison of eclipse time values derived from D2 data with those for normal time (D3) show that values for  $\alpha_{\text{eff}}$  are more or less the same below 85 km while above this altitude, the eclipse time values show increasing trend with the maximum

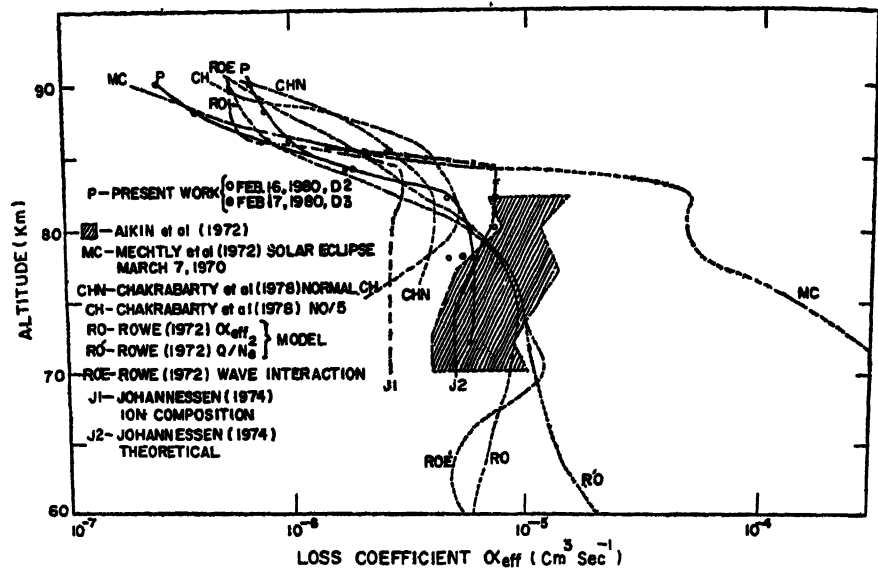


FIG 3. Electron loss coefficient  $\alpha_{eff}$  as a function of altitude derived from electron density observations. For comparison, profiles for normal and eclipse time due to other workers are also included

difference by a factor of 2.5 at 90km. It is felt that this difference could possibly be due to difference in  $[NO^+]/[O_2^+]$  ratio arising probably due to different X-ray flux on two days.

Mechtly *et al.* (1972) from their measurements during the total solar eclipse of 7 March 1970 had seen a virtual collapse of the D-region during totality. The profile of  $\alpha_{eff}$  derived by them show a sharp ledge around 82.5 km. Below this ledge, the  $\alpha_{eff}$  values show an increasing trend and become as high as by an order of magnitude contrary to normal time values or eclipse time values as obtained in this study. Such high values of  $\alpha_{eff}$  cannot be explained even theoretically. In fact, Mechtly *et al.* (1972) themselves felt that their estimated values of  $\alpha_{eff}$  are large by a factor of 8 or 10; probably as a result of equating the concentration of a single positive ion with the electron concentration rather than including more than one positive ion. It is, therefore, suggested to repeat such measurement in future eclipses.

### CONCLUSION

From the measurement of electron density values in the lower ionosphere during eclipse and normal time under similar conditions, it has been found that

- i) Electron density values during eclipse with 70 per cent obscuration are in general low compared to normal time values by about a factor of 2 at the height of minimum and by a factor of 2.7 at 90 km.
- ii) The effective values of electron loss coefficient  $\alpha_{eff}$  for the eclipse time were found to be almost same as the normal time values particularly below 85 km contrary to the high values reported earlier by Mechtly *et al.* (1972).

## ACKNOWLEDGEMENTS

The authors wish to thank personnels at TERLS and in particularly Mr V Sudhakar, Programme Manager, RSR and Mr M. D. Bhaskar, Head, ground support for their help and assistance in connection with payloads integration and launchings. Thanks are also due to Mr A Banerjee and Dr S Sampath for their help in fabrication of payloads. The technical help from Mr N. N. Kaul, Vishram Singh and Mr S. R. Bakshi and computational help from Mrs P. Chopra and Mr J. K. Gupta is also thankfully acknowledged.

## REFERENCES

- Aikin, A. C., Goldberg, R. A., Somayajulu, Y. V., and Avadhanulu, M. B. (1972) Electron and positive ion density altitude distribution in the equatorial D-region *J. atm. terr. Phys.*, **34**, 1483-1494
- Belrose, J. S., Hewitt, L. W., and Bunker, R. (1969) The partial reflection experiment as a tool for synoptic D-region research: and results of recent studies related to winter variability, 332-338.
- Chakrabarty, D. K., and Mitra, A. P. (1973) D-region during solar eclipse *RSD Rep.* No. 80 of National Physical Laboratory, New Delhi.
- Chakrabarty, D. K., Chakrabarty, P., and Witt, G. (1978) A theoretical attempt to explain some observed features of the D-region. *J. geophys. Res.*, **83**, 5763-5767
- CIRA (1972) *Cospar International Reference—Atmosphere.*
- Goldberg, R. A., and Aikin, A. C. (1971) Studies of positive ion composition in the equatorial D-region ionosphere *J. geophys. Res.*, **76**, 8352-8364
- Johannessen, A. (1974) Investigation of the positive ion composition in the upper mesosphere and lower thermosphere during daytime. *NDRE Rep.* No. 64, Norwegian Defence Research Establishment, Norway.
- Mechtly, E. A., Sechrist Jr., C. F., Smith, L. G. (1972) Electron loss coefficients for the D-region of the ionosphere from rocket measurements during the eclipses of March 1970 and November 1966 *J. atm. terr. Phys.*, **34**, 631-646
- Mitra, A. P., and Somayajulu, Y. V. (1979) A global model for D-region ionization *Space Res.*, **XIX**, 269-273
- Phelps (1960) Propagation constants for electromagnetic waves in weakly ionized air *J. appl. Phys.*, **31**, 1723, 1729
- Rowe, J. N. (1972) Model studies of the lower ionosphere *Sci. Rep.*, No. 406, of Penn State University, USA
- Sen, H. K., and Wyller, A. A. (1960) On the generalization of the Appleton-Hartree magnetoionic formulae *J. geophys. Res.*, **65**, 3931-3950
- Somayajulu, Y. V., Avadhanulu, M. B., Zalpuri, K. S., and Garg, S. C. (1971) Some preliminary results of rocket sounding of the D-region at the geomagnetic equator. *Space Res.*, **XI**, 1131-1137
- (1973) A study of the equatorial D-region *Space Res.*, **XIII**, 477-483
- Solar Geophysical Data* (1980) Issued by National Oceanic and Atmospheric Administration, Boulder, Colorado
- Velinov, P. (1968) On ionization in the ionospheric D-region by galactic cosmic rays *J. atm. terr. Phys.*, **30**, 1891-1905



Printed in India.

Rocket Experiment

## ON VARIATION OF $\lambda$ AND $\alpha_{\text{eff}}$ IN THE MESOSPHERE DURING THE SOLAR ECLIPSE OF 16 FEBRUARY 1980 OVER INDIA

S. P. GUPTA and D. K. CHAKRABARTY

*Physical Research Laboratory, Ahmedabad-380 009, India*

(Received 15 February 1982)

From the rocket measurements of electron density profiles at Thumba and Sriharikota the variation of  $\lambda$  (the ratio of negative ions to electron density) in the mesosphere during the solar eclipse of 16 February 1980 has been studied. It is found that the value of  $\lambda$  becomes almost 3 at 80km and at about 7 and 70km when the obscuration of the sun is 60 per cent. The implication of this variation of  $\lambda$  on the variation of  $\alpha_{\text{eff}}$  (the effective electron loss coefficient) during solar eclipse is examined and a discussion on the explanation of large value of  $\alpha_{\text{eff}}$  obtained by Mechtly *et al* (1972) and Belrose *et al* (1972) during 7 March 1970 eclipse is given in terms of heterogenous chemistry

**Keywords:** Solar Eclipse; Electron Density;  $\lambda$  and  $\alpha_{\text{eff}}$ ; Langmuir Probe

### INTRODUCTION

SEVERAL campaigns during solar eclipse have been conducted and examined in the past by various groups (Chakrabarty & Mitra, 1974). These have given many interesting results. Some of them are conclusive and some are not. Among those which are not conclusive are the variations of  $\lambda$  (the ratio of negative ions to electrons) and  $\alpha_{\text{eff}}$  (the effective electron loss coefficient) in the mesosphere. To study the variation of  $\lambda$ , simultaneous measurements of both electron density,  $N_e$ , and total positive ion density  $N^+$ , are required. The measurement of positive ion density being unreliable, uncertainty prevails in the estimation of  $\lambda$ . According to Danilov (1975), the experimental  $\lambda$  values during solar eclipse is somewhat contradictory, but values of  $\lambda > 1$  do exist at 80km during totality. From the simultaneous measurements of  $N_e$  and  $N^+$  in the previous eclipses, it has been seen that the value of  $\lambda$  during eclipse totality condition could be as large as 100 at 70km (Chakrabarty & Mitra, 1974). In case of  $\alpha_{\text{eff}}$ , Mechtly *et al* (1972), have found its value, to be  $\sim 10^{-4} \text{ cm}^3 \text{ s}^{-1}$  during the totality condition of solar eclipses of 12 November 1966 and 7 March 1970. While a value of  $\alpha_{\text{eff}}$ , as large as  $10^{-5} \text{ cm}^3 \text{ s}^{-1}$  is understandable, its value of the order of  $10^{-4} \text{ cm}^3 \text{ s}^{-1}$  is difficult to reconcile with the present knowledge of homogeneous ion chemistry. Under this background, the solar eclipse of 16 February 1980 provided an opportunity to examine the behaviour of these parameters during this natural phenomenon. This has been done from the electron density measurements made during this eclipse from two rocket launching stations of India viz, Thumba and Sriharikota. The results are described in this paper.

### EXPERIMENT AND DATA

Electron density has been measured during different phases of 16 February 1980 solar eclipse by using Langmuir probe. This instrument has been flown in rockets by PRL on a number of times and standardized to give electron density values with an accuracy of about 20 per cent (Prakash *et al*, 1974) in the D-region altitude. Four rockets were flown from Thumba (8°N, 76°E) of which one failed and two rockets were launched from Sriharikota (13°N, 80°E) of which one failed. The three electron density profiles we have chosen for this work are shown in Fig. 1 along with the details of the flight.

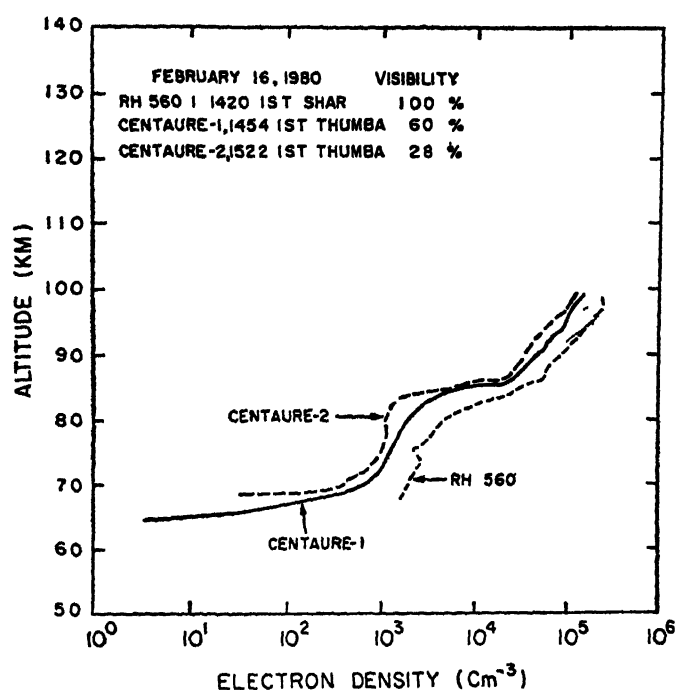


FIG. 1 Three rocket-borne electron density profiles of 16 February 1980 solar eclipse chosen for the present work

### VARIATION OF $\lambda$

The continuity equation of electron density distribution is given by

$$\frac{dNe}{dt} = \frac{q}{1+\lambda} - \alpha_{\text{eff}} Ne^2 \quad (1)$$

where  $q$  is the electron production rate and  $t$  is the time  $\alpha_{\text{eff}}$  can be written as.

$$\alpha_{\text{eff}} = \alpha_D + \lambda\alpha_i \quad (2)$$

where  $\alpha_D$  is the dissociative recombination coefficient between electrons and positive ions and  $\alpha_i$  is the ion-ion recombination coefficient. If one takes the widely used

values of  $\alpha_i = 10^{-7} \text{ cm}^3 \text{ s}^{-1}$  and of  $\alpha_D = 10^{-7} \text{ cm}^3 \text{ s}^{-1}$ , then as long as  $\lambda$  does not become about 100 (which holds good if one stays away from totality condition of a solar eclipse), then from eqn. (2)  $\alpha_{\text{eff}} = \alpha_D$  and eqn. 1 after rearrangement can be written as :

$$1 + \lambda = \frac{q}{\frac{dFe}{dt} + \alpha_D Ne^2} \quad \dots(3)$$

If '0' denotes the normal time and '1' denotes the eclipse time then from eqn. 3 one gets

$$\frac{1 + \lambda_1}{1 + \lambda_0} = \frac{F.L_0}{L_1} \quad \dots(4)$$

where  $F$  is the fraction of solar disc visible and

$$L = \frac{dNe}{dt} + \alpha_D Ne^2 \quad \dots(5)$$

Eqn. 4 will hold good in the region where the source of production is Lyman-alpha (between 70 and 80km). This equation has been used to compute the ratio  $(1 + \lambda_1)/(1 + \lambda_0)$  during the eclipse condition of 16 February 1980.  $dNe/dt$  values have been calculated after plotting  $Ne$  values of Fig 1 with time. The advantage of this method lies in the fact that this estimation is independent of the NO distribution where large amount of uncertainty exists. The values of  $(1 + \lambda_1)/(1 + \lambda_0)$  obtained in this way are shown in Fig. 2 for two altitudes viz, 70 and 80km. From this figure, the variation  $\lambda$  during eclipse can be found out if the values of  $\lambda_0$  are known. At 80km, one can take  $\lambda_0 \approx 0$ , then  $\lambda_1$  becomes 3.4 for 60 per cent obscuration of the sun at this altitude. At 70km, the widely used value of  $\lambda_0 = 1$ , then the value of  $\lambda_1$  at this altitude when the obscuration of the sun is 60 per cent becomes 6.7.

These values of  $\lambda$  are comparable with the values obtained by other workers. Willmore (1970) from the consideration of  $N^+$  (after applying several corrections) and  $Ne$  values during the solar eclipse of 20 May 1966 gives values of as 2.8 at 74km and 0.7 at 80km for an 84 per cent obscuration of the sun. Landmark *et al* (1970), during the same eclipse and same condition of obscuration give the value of  $1 + \lambda$  at 74km as 0.8 and 1.9 for before totality and after totality conditions respectively. They assumed the NO distribution given by Barth (1966). Chakrabarty and Chakrabarty (1977) after synthesis of all positive ion profiles and electron density profiles find the values of  $\lambda$  during totality condition of 7 March 1970 eclipse as 1 and 100 at 80 and 70km respectively.

#### VARIAION OF $\alpha_{\text{eff}}$

When the values of  $\lambda$  obtained above are substituted in eqn. 2, no variation of  $\alpha_{\text{eff}}$  is seen during eclipse at least upto an obscuration of 60 per cent of the solar disc. But Mechtly *et al* (1972) have obtained the value of  $\alpha_{\text{eff}}$  as  $10^{-4} \text{ cm}^3 \text{ s}^{-1}$  during eclipse totality condition at the same altitude. From eqn. 2, such a high value of  $\alpha_{\text{eff}}$  is possible only when  $\lambda = 1000$  which is unlikely. Thus it appears that from the homogeneous chemistry, it is difficult to explain the large value of  $\alpha_{\text{eff}}$  obtained by Mechtly *et al* (1972).

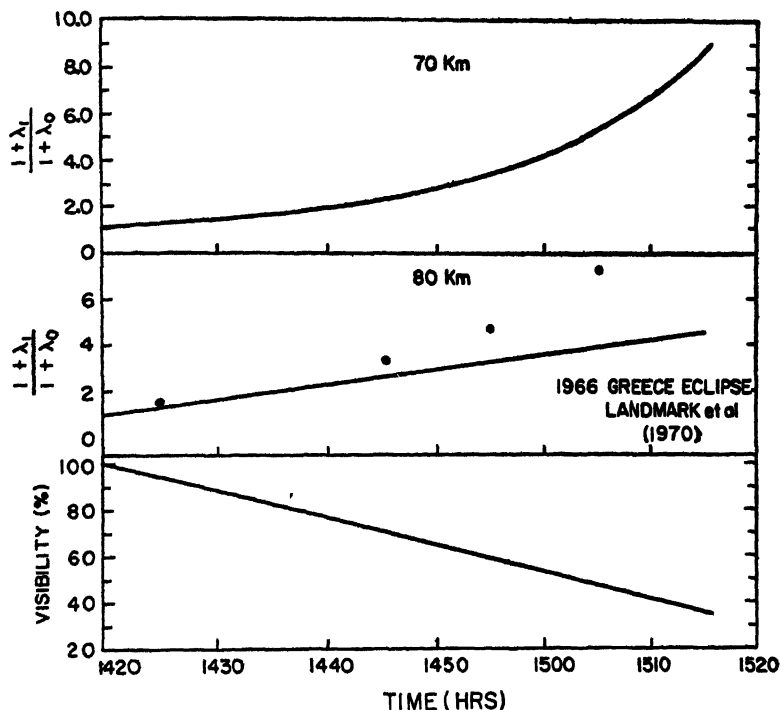


FIG. 2. Variation of the ratio of eclipse time and normal time  $1 + \lambda$  values at 70 and 80km derived from the electron density measurements of Fig 1. At the bottom, the visibility of solar disc with time during this eclipse is shown.

If one assumes that positive ions react with aerosols as it happens in the stratosphere (Chakrabarty & Chakrabarty, 1980) and writes the continuity equation of positive ion as follows

$$\frac{dN^+}{dt} = q - \alpha_D N^+ Ne - \alpha_i N^+ N^- - \beta Na N^+, \quad (6)$$

then considering the charge neutrality  $N^+ = Ne + N^-$  one gets for  $\alpha_{\text{eff}}$  the following equation

$$\alpha_{\text{eff}} = \alpha_D + \lambda \alpha_i + \frac{\beta Na}{Ne} \quad (7)$$

Here  $Na$  is the number density of aerosols and  $\beta$  is the coefficient of reaction between aerosols and positive ions. Since we do not know the variation  $Na$  during eclipse, the change in  $\alpha_{\text{eff}}$  during eclipse could be due to change in  $Ne$ . Since  $\alpha_D$  is of the order of  $10^{-6} \text{ cm}^3 \text{ s}^{-1}$  and  $\lambda \alpha_i$  is less than or equal to this value, from the value of Mechtly *et al* (1972) of  $\alpha_{\text{eff}}$ , we have from eqn (7),  $\frac{\beta Na}{Ne} 10^{-4} \text{ cm}^3 \text{ s}^{-1}$  for eclipse totality condition. Corresponding to this condition, if one takes  $Ne = 1 \text{ cm}^{-3}$ , then  $\beta Na = 10^{-4} \text{ s}^{-1}$ . For normal day time, around 75km, where  $Ne = 100 \text{ cm}^{-3}$ , the value of  $\frac{\beta Na}{Ne}$  ( $= 10^{-6} \text{ cm}^3 \text{ s}^{-1}$ ) will be an order of magnitude less than  $\alpha_D$  value ( $\lambda \alpha_i$ ).

is less than  $\alpha_D$ ). Thus, it is clear that as long as  $N_e$  is not less than  $10 \text{ cm}^{-3}$ , the contribution of  $\frac{\beta Na}{N_e}$  term in the value of  $\alpha_{\text{eff}}$  is not significant.

### CONCLUSION

From the time variation of electron density observed during the solar eclipse of 16 February 1980 over India, the variation of  $\lambda$  in the mesosphere is studied. It is seen that when the obscuration of the sun is 60 per cent the values of  $\lambda$  are about 3 and 7 at 80 and 70 km altitudes respectively. These values of  $\lambda$  when put in a homogeneous chemical scheme are not able to reproduce any variation of  $\alpha_{\text{eff}}$  during eclipse for which experimental evidences exist. The variation of  $\alpha_{\text{eff}}$  during eclipse could be obtained if one involves a process in which positive ions react with aerosols (heterogeneous scheme); and it is shown that this process becomes predominant over the process of dissociative recombination of positive ions with electrons only when electron density becomes less than about  $10 \text{ cm}^{-3}$ .

### REFERENCES

- Barth, C. A. (1966) Nitric oxide in the upper atmosphere *Ann. Geophys.*, **22**, 198.
- Belrose, J. S., Ross, D. B., and McNamara, A. G. (1972) Ionization changes in the lower ionosphere during the solar eclipse of 7 March 1970 *J. atm. terr. Phys.*, **34**, 627.
- Chakrabarty, D. K., and Mitra, A. P. (1974) D-region during solar eclipse. In *COSPAR Methods of Measurements and Results of Lower Ionosphere Structure* (Ed. K. Rawer), 183 Akademie-Verlag.
- Chakrabarty, D. K., and Chakrabarty, P. (1977) Role of atomic oxygen and ozone in the D-region during disturbed conditions *Space Res.*, **XVII**, 253.
- Chakrabarty, P., and Chakrabarty, D. K. (1980) The role of aerosols in relation to stratospheric modelling *Space Res.*, **XX**, 49.
- Danilov, A. D. (1975) Ionization-recombination cycle of the D-region *J. atm. terr. Phys.*, **37**, 885.
- Landmark, B., Haug, A., Thrane, E. V., Hall, J. E., Willmore, A. P., Jespersen, M., Pedersen, B. M., Anastassiades, M., Tsagakis, E., and Kane, J. A. (1970) Ionospheric observations during the annular solar eclipse of 20 May 1966-V. Interpretation of observed results *J. atm. terr. Phys.*, **32**, 1873.
- Mechty, E. A., Sechrist, C. F. Jr., and Smith, L. G. (1972) Electron loss coefficients for the D-region of the ionosphere from rocket measurements during the eclipses of March 1970 and November 1966 *J. atm. terr. Phys.*, **34**, 641.
- Prakash, S., Subbaraya, B. H., and Gupta, S. P. (1974) Some features of the equatorial D-region as revealed by the Langmuir probe experiments conducted at Thumba *COSPAR Methods of Measurements and Results of Lower Ionosphere Structure* (Ed. K. Rawer), 259 Akademie-Verlag.
- Willmore, A. P. (1970) Ionospheric observations during the annular solar eclipse of 20 May 1966-II. Positive ion probe observations. *J. atm. terr. Phys.*, **32**, 1855.

Printed in India

**Rocket Experiment**

**ROCKET MEASUREMENT OF PHOTOELECTRON FLUX DURING THE SOLAR ECLIPSE CAMPAIGN ON 16 FEBRUARY 1980 AT LOW LATITUDES**

B. C. N RAO, A. BANERJEE and Y. V. SOMAYAJULU

*Radio Science Division, National Physical Laboratory, New Delhi-110 012, India*

*(Received 15 February 1982)*

As part of the campaign of solar eclipse on 16 February 1980, two RH 560 rockets were launched from SHAR (13°47'N) which carried an NPL Retarding Potential Analyser (RPA) to measure suprathermal electrons. The first rocket was a control flight just before the start of the eclipse and the second one was launched during maximum obscuration (90 per cent). The control flight worked well and gave useful data. Since this is the first time that such rocket measurements of photoelectron flux at low latitudes were made, analysis of the data from the control flight on the eclipse day are presented in this paper. It shows that the integrated photoelectron energy spectrum exhibits a shape consistent with the mid-altitude measurements, but the computed flux values are significantly lower than those observed in mid-latitudes. Detailed results of photoelectron spectra as a function of altitude are analysed and described. At the apogee of around 330km, the differential flux for 10eV electrons is found to be about  $1.17 \times 10^4 \text{ cm}^{-2} \text{ s}^{-1} \text{ eV}^{-1} \text{ sr}^{-1}$ .

**Keywords:** Photoelectron Flux; Retarding Potential Analyser (RPA); Low Latitude; Altitude Distribution

**INTRODUCTION**

PHOTOELECTRONS play an important role in determining the thermal structure of the ionosphere and a number of studies have been made to estimate their fluxes theoretically and to measure them experimentally. The measurements were made with rockets (Doering *et al*, 1970, Maier & Rao, 1972; and Knudsen & Sharp, 1972), and satellites (Rao & Maier, 1970, and Doering *et al*, 1976). These have also been measured by incoherent scatter technique (Yngveeson & Perkins, 1968; and Evans & Gastman, 1970). It may be pointed out here that the rocket measurements which give the photoelectron spectrum as a function of height, have so far been made only at midlatitudes. The information at low latitudes is available only through the satellite measurements.

As a part of the campaign for the total solar eclipse on 16 February 1980, rocket measurements of photoelectrons are made with the retarding potential analyser at the low latitude station SHAR (India, 13°47'N). Out of the two RH-560 rockets launched, the control flight experiment worked well and gave useful data while the eclipse flight failed due to malfunctioning of the rocket. Hence, these measurements made during preeclipse period are analysed and presented in this paper. Further, these low latitude values are compared with similar rocket measurements made at midlatitudes.

## EXPERIMENT

Measurements were made with a planar retarding potential analyser (RPA). The sensor is a three grid structure mounted in a cylindrical housing. The aperture of the window had a 50mm diameter. The retarding grid was given a triangular sweep of 0 to - 32 volts in a time period of 1 sec.

The RPA was mounted on top of the RH-560 rocket looking upwards i.e., the sensor normal was coincident with the rocket spin axis. The rocket was launched on 16 February 1980 at 1420hr IST (solar zenith angle  $\lambda = 42^\circ$ ). The spin rate of the rocket varied between 5 to 6 rps in the altitude range of 150-330km. It may be pointed out that as the sensor was looking up from the top deck plate of the nose cone of the rocket, it was receiving the direct rays from the sun for most of the spin cycle and only for a fraction of the cycle it was able to record the atmospheric photoelectron flux. Thus there were only five to six points of recording in a single sweep of one second.

## RESULTS AND DISCUSSION

Good results have been obtained from about 150km to the apogee altitude of 330km. Three representative heights were chosen to illustrate the observations, 180km for a lower height, 250km as the height where the flux is maximum and the apogee height of 330km. It is found that the shape of the curves for different sweeps are roughly similar but their levels vary from one another. At 250km and 330km the variation from one curve to another seems to be larger than at lower altitude of 180km. The maximum currents for 180km, 250km and 330km are about  $1 \times 10^{-10}$ ,  $2.3 \times 10^{-10}$  and  $1.4 \times 10^{-10}$  amps respectively.

The above values of current can directly be converted into integral electron fluxes from a knowledge of the area of the aperture grid and the solid angle subtended by it. From the geometry of our sensor, it is found that it subtends a solid angle of about  $\pi$  steradians. Hence, the flux values are divided by  $\pi$  to get the flux per steradian. The effective transparency of grids is taken to be 0.8 on the basis of laboratory measured values of almost identical sensors at NASA Goddard Space Flight Centre. From the integral fluxes, the differential flux spectra are derived and shown in Fig. 1. In assigning the energy it is essential to know the rocket potential. However, this parameter is not measured by any experiment in this rocket flight. Hence, a value of -1 volt was assumed for rocket potential since several observations of other rocket flights have given values of this order in this height range. It may be mentioned that it is the major uncertainty in our estimate of the flux spectrum. The measurements need another correction for rocket shadowing of the photoelectrons as the sensor is not mounted in the optimum direction. The sensor axis is parallel to the rocket axis and at SHAR it makes an angle of about  $85^\circ$  (rocket attitude angle of elevation =  $82^\circ$ , azimuth =  $85^\circ$ , magnetic dip angle =  $10^\circ$ ) with the geomagnetic field lines. This situation is similar to the one discussed by Knudsen and Sharp (1972). It was shown there that under worst conditions when the angle is about  $90^\circ$  the measured fluxes are at least 50 per cent of what they would have been in the absence of vehicle shadowing. Hence, the measured values are increased by a factor of 2 to obtain the true flux. It may be noted that this factor is an upper limit.

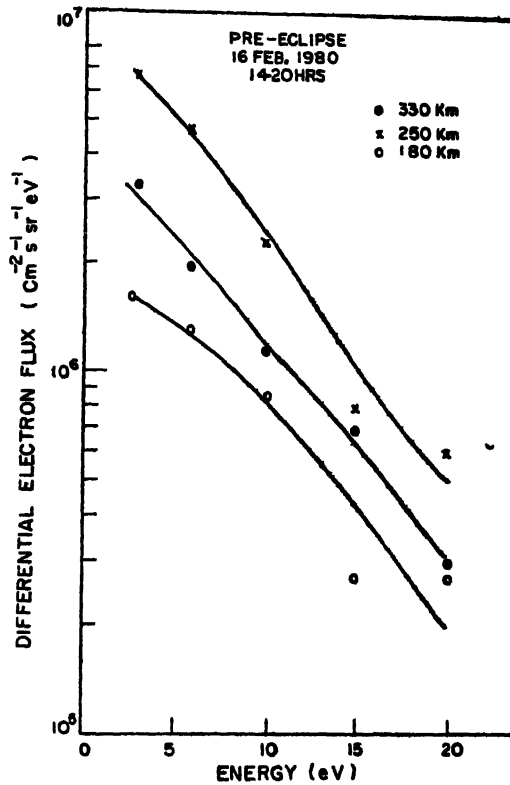


FIG. 1 Differential electron flux vs Energy for 180, 250 and 330km.

It may be seen from Fig. 1 that the spectra are almost similar in shape but differ in magnitude at different heights. Again the largest values are obtained for 250km. These observations are compared with the daytime observations of Doering *et al* (1970) at a midlatitude station, Wallops Island, on 31 July 1968 ( $\lambda = 60^\circ$ ). The present measurements over SHAR refer to higher solar activity and  $\lambda = 42^\circ$ . It is found that both of them show an increase of flux with altitude upto 250km. At their apogee height of 298km the values are almost same as at 250km whereas in our case the apogee height is 330km where the flux values are considerably smaller than at 250km. From our records we find that the maximum fluxes are occurring around 250km. The actual values at 250km are compared in Fig. 2. It can be seen that there is a difference of a factor of 3 to 6 between these two values at different energies. At a lower height of 180km there is a similar difference. If we compare with Knudsen and Sharp's (1972) observed spectrum at 180km (6 March 1970,  $\lambda = 47^\circ$ ), the differences increase.

It is generally assumed that the photoelectron flux is isotropic at lower heights below 200km where the magnetic field control is comparatively less. It is known from the theoretical works of Mariani (1964) and the experimental observations of Rao and Maier (1970) that the pitch angle distribution of the photoelectrons are anisotropic at higher altitudes. This may be resolved only by conducting some more rocket



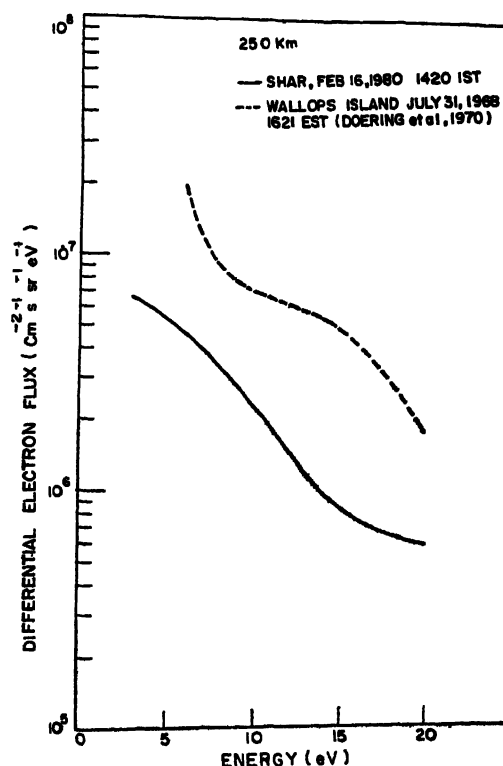


FIG 2 Comparison of differential electron flux at 250km between the results of Doering *et al.* (1970) and the present work

experiments with sensors mounted both parallel and perpendicular to the rocket axis. These experiments will also throw more light on the observed differences between the present results and those by other workers. On these flights a suitable probe will be included to measure the vehicle potential.

#### CONCLUSION

The photoelectron flux measurements over the low latitude station, SHAR, made for the first time are reported. These are found to be lower compared to the rocket measurements over the midlatitude station. It is concluded that further rocket investigations are necessary to resolve them.

#### ACKNOWLEDGEMENTS

The authors wish to thank Mr N N Kaul, Vishram Singh and S R Bakshi for the technical assistance in the fabrication of the payloads. Thanks are also due to Mrs P Chopra for technical and computational help. The assistance and kind co-operation extended by the integration laboratory of TERLS, Trivandrum in general and Mr V Sudhakar, Programme Manager, RSR/TERLS, in particular in different

stages of the testing and integration of the payloads are thankfully acknowledged. Lastly the authors like to express sincere appreciation for the excellent co-operation of the staff members of SHAR range, Sriharikota during the final assembly and launching operations of the rocket. The list will be incomplete if the authors fail to acknowledge the untiring efforts of Mr A. R. Sastri and Mr R. Sampath of TERLS right from the beginning of the integration till the launching.

## REFERENCES

- Doering, J. P., Fastie, W. C., and Feldman, P. D. (1970) Photoelectron excitation of  $N_2$  in the day airglow *J. geophys. Res.*, **75**, 4787.
- Doering, J. P., Peterson, W. K., Bostrom, C. O., and Potemera, T. A. (1976) High resolution daytime photoelectron energy spectra from AE-E *Geophys. Res. Lett.*, **3**, 129.
- Evans, J. V., and Gastman, I. J. (1970) Detection of conjugate photoelectrons at Millstone Hill *J. geophys. Res.*, **75**, 807.
- Knudsen, W. C., and Sharp, G. W. (1972) Eclipse and non-eclipse differential photoelectron flux *J. geophys. Res.*, **77**, 1221.
- Maier, E. J., and Rao, B. C. N. (1972) Rocket measurements of conjugate photoelectrons during the total solar eclipse of 7th March 1970 over Wallops Island. *J. atm. terr. Phys.*, **34**, 689.
- Mariani, F. (1964) Pitch-angle distribution of the photoelectrons and origin of the geomagnetic anomaly in the  $F_2$ -layer *J. geophys. Res.*, **69**, 556.
- Rao, B. C. N., and Maier, E. J. R. (1970) Photoelectron flux and protonospheric heating during the conjugate point sunrise *J. geophys. Res.*, **75**, 816.
- Yngveeson, K. O., and Perkins, F. W. (1968) Radar Thomson scatter studies of photoelectrons in the ionosphere and Landau damping. *J. geophys. Res.*, **73**, 97.



## AUTHOR INDEX

ABBAS, HABIBA	473	DEY, S. SEKHAR	302
ABHYANKAR, K. D	85,91	DUNHAM, D. W	70
ACHARYA, B. L.	388	DUNHAM, J. B.	70
ADIGA, B. B.	224	DÜRST, J.	53
AGARWAL, A. K.	482	DUTTA, R. N.	302
AGASHE, V. V.	284	EITZER, J. J.	89
AGGARWAL, S. K.	224	ESSEX, E. A.	444
AGRAWAL, M.	458	FELDMAN, WILLIAM C.	11
AGRAWAL, S. K.	280	FIALA, A. D.	70
AHUJA, HARBANS SINGH	125	GARG, S. C.	293
ALURKAR, S. K.	75	GERA, B. S.	224
ANGREJI, P. D.	57	GOEL, R. K.	263
APPU, K. S.	502, 506	GOYAL, S. SHEELA	420
ARGO, HAROLD V	11	GUPTA, K. Sen	506
ARORA, B. R.	489	GUPTA, R. K.	159
ASHOK, N. M.	57	GUPTA, S. P.	518
BABU, V. RAMESH	196	HAMID, A.	293
BALAN, N.	325, 406	HARVEY, J.	18
BALWALLI, R. R.	138	HAZRA, B. K.	217
BANERJEE, A.	523	JADHAV, D. B.	29, 260
BANSAL, T. C.	388	JAIN, C. L.	420
BANSHIDHAR	420	JAIN, R. M.	29, 260
BEAVERS, W. I.	89	JANI, K. G.	316
BECKERS, JACQUES M.	11	JOGULU, C.	400
BHANJA, R.	280	KAMBLE, V. B.	57
BHATNAGAR, A.	29, 260	KANKANE, R. K.	217
BHATT, H. C.	57	KAPOOR, RAMESH K.	224
BHATTACHARYYA, J. C.	1	KELLER, C. F.	33
BHONSLE, R. V.	75, 260	KHERA, M. K.	263
BRUNER, ELMO C.	11	KLOBUCHAR, J. A.	444
CALLA, O. P. N.	75	KOTADIA, K. M.	316
CARR, P. H.	89	KOTHARI, S. K.	420
CHADHA, R.	234	KULSHRESHTHA, S. M.	202
CHAKRABARTY, D. K.	518	KUMAR, U. V. GIRISH	380
CHAKRAVARTHY, R.	308	KUNHIKRISHNAM, P. K.	238
CHANDRA, H.	420, 427	LACEY, LEON B.	81
CHANDRASEKHAR, T.	57	LAKSHMI, D. R.	308
CHANDRASEKHARAN, C. K.	125, 143, 150, 202, 154	LAL, SHYAM	115
CHATTERJEE, KALIPADA	125, 143, 202, 254	LAROS, JOHN G.	11
CHATTERJEE, S. K.	302, 370	LIVINGSTON, W.	18
CHATURVEDI, U. K.	280	LOKNADHAM, B.	75
DAS, S. K.	202, 396	MAHASHABDE, M. V.	489
DAS GUPTA, A.	439	MAITRA, A.	439
DAS GUPTA, M. K.	302	MAKHDOUMI, B. A.	263
DATTA, G.	316	MATHUR, S.	458
DAVIES, KENNETH	342	MAUTER, H. A.	102
DAY, S. K.	439	MOHAMMED, P. M. PAKKIR	138
DE, A. K.	271	MOHANAKUMAR, K.	135, 209
DEGAONKAR, S. S.	75	MUKHERJEE, B. K.	168
DESAI, J. N.	57	MUKKU, VENKATANARAYANA REDDY	263
DESHPANDE, M. R.	420, 427	MURTHY, B. V. KRISHNA	238, 406, 506
DESIKAN, V.	150	MURTY, BH. V. RAMANA	168
DEVANARAYANAN, S.	135, 209	NARASIMHA, R.	175

NARAYANAN, V.	502, 506	SAHA, B.	302
NIRANJAN, K.	434	SAHA, S K.	302
NIZAMUDDIN, S.	263	SAHU, K. C.	57
NRU, D.	434	SAIN, MANGAL	308
PANDURANGAM, D.	473	SARDESAI, D. V.	458
PATEL, D. B.	316	SARKAR, A. B	143, 217
PATIL, D. D.	334	SASTRY, J. S.	196
PATHAK, P. P	263	SASTRY, T. S.	473
PHILBRICK, C R	444	SEHRA, J S	302
PRABHU, A.	175	SEN, A K.	302
PRASAD, C. R	175	SETHIA, G	420, 427
PRASAD, M V S. N	293	SEYKORA, E J.	64
PRASAD, S N.	489	SHARMA, M C.	131
PRATAF, R	260	SHELKE, R. N	29, 260
PURKAIT, N. N	396	SINGH, A K.	280
PUROHIT, S P.	29, 260	SINGH, B P.	489
RADHAKRISHNAN, E P.	325	SINGH, LAKHA	416
RAFIQUL, A R.	263	SINGHAL, S. P.	224
RAHALKAR, C. G	150	SIVARAMAN, M R	420
RAJARAM, GIRJA	334	SMARTT, R. N.	102
RAI, J.	263	SOMAYAJI, T. S N	375
RAI, R. K.	388, 458	SOMAYAJULU, Y. V.	416, 511, 523
RAINA, B N	263	SRIDHAR, A A	325
RAINA, M K.	234	SRINIVASAN, V	271
RAJ, P ERNEST	400	SRIVASTAVA, B N.	131
RAJU, G	75	SRIVASTAVA, B J	473, 489
RAJU, K. ANTHONY	91	SRIVASTAVA, G. P.	138, 150, 271
RAMAN, S SETHU	187	STREETE, JOHN L	81
RAMANA, K. V V	380	SUBBARAO, K. S V.	406
RAMANADHAM, R.	263	SUBBARAYA, B H	115, 494
RAMANAMURTY, Y V.	293	SUBRAHMANYAM, C V	370
RANA, S. S	75	SUBRAHMANYAM, P	511
RANGARAJAN, G K	482	SUBRAHMANYAM, P V	85
RANJAN, N	280	TANWAR, R S	131
RAO, A M	263	THAKUR, N. K.	489
RAO, B C N.	523	TREHAN, S K	302
RAO, B MADHUSUDHANA	400	TYAGI, T. R.	416
RAO, B V P S.	434	UPPAL, G. S	234
RAO, K. NARAHARI	175	USHA DEVI, K	325
RAO, K R	159	VADHER, N	420
RAO, M SRIRAMA	400	VAIDYA, D B.	57
RAO, P B	406	VARSHNEYA, N C	263
RAO, P V S RAMA	434	VATS, H O.	420, 427
RAO, T R	334	VENKATANARAYANA, R.	375
RASTOGI, R G	464, 482	VERMA, V P	254
RATHI, S M	284	VIJAYAKUMAR, P N	416
REDDY, B M	308	VIJAYVERGIA, S K.	388
REDDY, C. A	356, 506	VYAS, G D.	427
REDDY, C RAGHAVA	406	YAGNIK, H. K	388
REDDY, R SUSEEL	168	ZALPURI, K. S	511
SAHA, A. K	109, 370	ZIRKER, J B.	6, 102









